



รายงานวิจัยฉบับสมบูรณ์

โครงการ บทบาทของการได้รับไนตริกออกไซด์ต่อลักษณะของ
เซลล์มะเร็งปอดต้นกำเนิด

โดย

รศ.ภก.ดร. ปิติ จันทรวรโชติ

เดือน ปี ที่เสร็จโครงการ : มิถุนายน 2560

รายงานวิจัยฉบับสมบูรณ์

โครงการ บทบาทของการได้รับไนตริกออกไซด์ต่อลักษณะของ
เซลล์มะเร็งปอดต้นกำเนิด

รศ.ภก.ดร. ปิติ จันทรวัชรโชติ

ภาควิชาเภสัชวิทยาและสรีรวิทยา
คณะเภสัชศาสตร์ จุฬาลงกรณ์มหาวิทยาลัย

สนับสนุนโดยสำนักงานกองทุนสนับสนุนการวิจัยและจุฬาลงกรณ์มหาวิทยาลัย

(ความเห็นในรายงานนี้เป็นของผู้วิจัย สกว. ไม่จำเป็นต้องเห็นด้วยเสมอไป)

กิตติกรรมประกาศ

รายงานการวิจัยเรื่อง บทบาทของการได้รับไนตริกออกไซด์ต่อลักษณะของเซลล์มะเร็งปอดต้นกำเนิด (Role of nitric oxide exposure on lung cancer stem-like phenotypes) นี้สำเร็จลุล่วงไปได้ด้วยดี คณะผู้วิจัยขอกราบขอบพระคุณทุนอุดหนุนการวิจัยจากสำนักงานกองทุนสนับสนุนการวิจัย (สกว) ที่ให้การสนับสนุนทุนวิจัยเป็นเวลา 3 ปี

คณะผู้วิจัย

Project Code: RSA5780043

Project Title: Role of nitric oxide exposure on lung cancer stem-like phenotypes

Investigator: Associate professor Dr.Pithi Chanvorachote

E-mail Address: pithi_chan@yahoo.com

Project Period : June 16th 2014 to June 15th 2017

Nitric Oxide (NO) is a gaseous biological mediator that found in the cancer approximated area and may have a significant impact on cancer cell biology. As one important hallmark of cancer aggressiveness, stem cell-like property of cancer cells has garnered increasing attentions in the cancer-related field and accepted to be an important obstacle of success in cancer treatment. So far, the insight involving molecular basis of NO in regulation of cancer stem-like phenotypes in lung cancer is largely unknown. The present project aims to investigate the possible impact of NO treatment in long duration on the alterations of cancer stem cell-like phenotypes including the presence of cancer stem cell markers CD133 and ALDH, and stem cell-like and aggressive behaviors including tumorigenic activity, epithelial to mesenchymal transition (EMT), growth in anchorage-independent condition, anoikis resistant, chemotherapeutic resistant, migration and invasion, as well as investigate the underlying mechanisms involving up-stream signaling of survival pathways including Rac and Ras. Because the understanding of nature of the cancer cells in response to biological substance may lead to the better precision and efficiency in treating the disease, the information gained from this study could benefit the development of therapeutic approaches.

Keywords (3-5 words) nitric oxide, lung cancer, cancer stem cells

รหัสโครงการ: RSA5780043

ชื่อโครงการ: บทบาทของการได้รับไนตริกออกไซด์ต่อลักษณะของเซลล์มะเร็งปอดต้นกำเนิด

ชื่อนักวิจัย: รศ.ภก.ดร.ปิติ จันทรรวัชโชติ

E-mail Address: pithi_chan@yahoo.com

ระยะเวลาโครงการ: 16 มิถุนายน พ.ศ. 2557 ถึง 15 มิถุนายน พ.ศ. 2560

ไนตริกออกไซด์เป็นแก๊สชีวภาพที่พบได้ในมะเร็งและอาจจะมีผลต่อเซลล์มะเร็ง สิ่งสำคัญที่ก่อให้เกิดพฤติกรรมที่รุนแรงของการเกิดมะเร็งคือ เซลล์มะเร็งมีคุณสมบัติเป็นเซลล์มะเร็งต้นกำเนิดมากขึ้นทำให้เป็นอุปสรรคสำคัญในการรักษามะเร็ง ดังนั้นจึงศึกษาข้อมูลเชิงลึกเกี่ยวกับโมเลกุลพื้นฐานของไนตริกออกไซด์ในการควบคุมลักษณะของเซลล์มะเร็งต้นกำเนิดในมะเร็งปอดซึ่งยังไม่ทราบข้อมูลที่แน่ชัด การศึกษาในครั้งนี้จึงมีวัตถุประสงค์ในการตรวจหาผลของไนตริกออกไซด์ต่อการเปลี่ยนแปลงลักษณะการเกิดเซลล์มะเร็งต้นกำเนิดเมื่อได้รับไนตริกออกไซด์เป็นระยะเวลานาน เช่น การแสดงออกของโปรตีนบ่งชี้การเกิดเซลล์มะเร็งต้นกำเนิด CD133 และ ALDH และพฤติกรรมรุนแรงในการเกิดเซลล์มะเร็งต้นกำเนิด อาทิ การเปลี่ยนรูปร่างจากเซลล์อิมิพิสิเลียลไปเป็นมีเซนไคม์, การเจริญในสภาวะไร้การยึดเกาะ, ต้านการตายแบบอะนอยด์คิซิส, ตี้อต่อเคมีบำบัด, การเคลื่อนที่และการแพร่กระจายของเซลล์มะเร็ง และตรวจหากลไกที่เกี่ยวข้องกับวิถีการอยู่รอดของเซลล์ ซึ่งประกอบด้วย โปรตีน Rac และ Ras เพื่อให้เข้าใจธรรมชาติของเซลล์มะเร็งในการตอบสนองต่อสารชีวภาพที่อาจนำไปสู่ความแม่นยำและประสิทธิภาพในการรักษาโรค และข้อมูลที่ได้จากการศึกษาครั้งนี้จะเป็นประโยชน์ในการพัฒนาวิธีการรักษาต่อไปได้

(คำหลัก) ไนตริกออกไซด์, เซลล์มะเร็งปอด, เซลล์ต้นกำเนิดมะเร็งปอด

บทนำ

มะเร็งปอดเป็นสาเหตุหลักที่ทำให้เกิดการเสียชีวิตด้วยมะเร็ง (Lozano et al., 2012) ผู้ป่วยส่วนใหญ่จะเสียชีวิตด้วยกระบวนการแพร่กระจายของเซลล์มะเร็ง (metastasis) ซึ่งเป็นกระบวนการที่เซลล์มะเร็งแพร่กระจายไปยังส่วนต่างๆ ของร่างกาย จากข้อมูลทางคลินิกพบว่าการแพร่กระจายของเซลล์มะเร็งมีความสอดคล้องกับระดับไนตริกออกไซด์และเอนไซม์ไนตริกออกไซด์ซินเทสที่เพิ่มขึ้น ส่งผลให้เกิดพฤติกรรมความรุนแรงเพิ่มขึ้น และอัตราการอยู่รอดของผู้ป่วยมะเร็งปอดลดน้อยลง (Colakogullari et al., 2006; ESME et al., 2008; C.Y. Liu et al., 1998) จากการศึกษาที่ผ่านมาพบว่าไนตริกออกไซด์มีผลในการควบคุมพฤติกรรมของเซลล์มะเร็ง และกระตุ้นเซลล์มะเร็งปอดให้ดื้อต่อยาซิสพลาติน (Chanvorachote, 2006) และ Fas ligand ที่ถูกเหนี่ยวนำให้เกิดการตายแบบอะพอพอโทซิส (Chanvorachote, 2005) มากไปกว่านั้น ไนตริกออกไซด์ยังเพิ่มความสามารถในการแพร่กระจายของเซลล์มะเร็งปอดโดยยับยั้งการตายแบบอะนอยคิสในเซลล์ที่ไร้สภาวะการยึดเกาะ (Chanvorachote, 2009) แต่อย่างไรก็ตามยังไม่มีรายงานการวิจัยความสัมพันธ์ระหว่างไนตริกออกไซด์กับเซลล์มะเร็งปอดต้นกำเนิด ซึ่งเป็นสาเหตุหลักในการเกิดพฤติกรรมรุนแรงของเซลล์มะเร็ง เนื่องจากเซลล์มะเร็งที่แสดงลักษณะของเซลล์มะเร็งต้นกำเนิดจะเป็นสาเหตุหลักที่ทำให้เกิดการแพร่กระจายของเซลล์มะเร็ง ดื้อต่อเคมีบำบัดและการกลับมาเป็นซ้ำของโรค (Yang et al., 2009; Eramo et al., 2007; Li et al., 2007; Me et al., 2007) ดังนั้นจึงศึกษาปัจจัยความเป็นไปได้ในการเปลี่ยนเซลล์มะเร็งปกติให้เป็นเซลล์มะเร็งต้นกำเนิด รวมทั้งศึกษากลไกและข้อมูลเชิงลึกของชีววิทยาเซลล์มะเร็ง เพื่อเป็นประโยชน์ในการศึกษาการยับยั้งพฤติกรรมความรุนแรงของเซลล์มะเร็ง ซึ่งการวิจัยครั้งนี้จะศึกษาบทบาทของระดับของไนตริกออกไซด์ที่ไม่เป็นพิษต่อเซลล์ต่อการพัฒนาไปเป็นเซลล์มะเร็งต้นกำเนิดของเซลล์มะเร็งปอดเมื่อให้ไนตริกออกไซด์เป็นระยะเวลาสั้น เพื่อให้เข้าใจถึงชีววิทยาของเซลล์มะเร็ง และความเป็นไปได้ว่าไนตริกออกไซด์อาจจะมีบทบาทสำคัญในการควบคุมพฤติกรรมรุนแรงของการเกิดมะเร็งปอดได้

วิธีการทดลอง

1. การทดสอบความเป็นพิษ (Cytotoxicity Analysis) ;

ทดสอบความเป็นพิษของสารที่ทำให้เกิดไนตริกออกไซด์ ได้แก่ SNAP และ dipropylentriamine (DPTA) NONOate โดยใช้วิธีการทดสอบการอยู่รอดของเซลล์ (cell viability assay) และยืนยันผลโดยการทดสอบการเกิดการตายแบบอะพอพอโทซิสและการตายแบบเนโครซิส (apoptosis and necrosis evaluation assay) จากนั้นนำความเข้มข้นที่ไม่เป็นพิษต่อเซลล์ของไนตริกออกไซด์ไปใช้ในการศึกษาต่อไป

การทดสอบการอยู่รอดของเซลล์ (Cell Viability Assay)

เลี้ยงเซลล์ใน 96-well plates ที่ความหนาแน่นเซลล์เท่ากับ 1×10^4 cells/well บ่มที่อุณหภูมิ 37 องศาเซลเซียส เป็นเวลา 24 ชั่วโมง จากนั้นให้สาร DPTA NONOate ที่ความเข้มข้นต่างกัน และบ่มที่อุณหภูมิ 37 องศาเซลเซียส เป็นเวลา 24 ชั่วโมง หลังจากให้สาร DPTA NONOate แก่เซลล์ ทดสอบแล้ว นำเซลล์มาบ่มด้วยสาร MTT ความเข้มข้น 0.4 mg/ml เป็นเวลา 4 ชั่วโมง ที่อุณหภูมิ 37 องศาเซลเซียส จากนั้นนำส่วนของ supernatant ออก และใช้ DMSO ละลายผลึก formazan แล้วนำไปวัดความเข้มแสงที่ความยาวคลื่น 570 nm จากนั้นนำผลที่ได้มาคำนวณหาเปอร์เซ็นต์การอยู่รอดของเซลล์

การทดสอบการเกิดการตายแบบอะพอพโทซิสและการตายแบบเนโครซิส (Apoptosis and Necrosis Evaluation Assay)

คล้ายกับการทดสอบการมีชีวิตรอดของเซลล์ โดยเลี้ยงเซลล์ใน 96-well plates ที่ความหนาแน่นเซลล์เท่ากับ 1×10^4 cells/well บ่มที่อุณหภูมิ 37 องศาเซลเซียส เป็นเวลา 24 ชั่วโมง จากนั้นให้สาร DPTA NONOate ที่ความเข้มข้นต่างกัน และบ่มที่อุณหภูมิ 37 องศาเซลเซียส เป็นเวลา 24 ชั่วโมง หลังจากให้สาร DPTA NONOate แก่เซลล์ทดสอบแล้วบ่มเซลล์ด้วย Hoechst 33342 ความเข้มข้น 10 μ g/ml และ propidium iodide (PI) ความเข้มข้น 5 μ g/ml เป็นเวลา 5 นาที และถ่ายภาพฟลูออเรสเซนซ์ภายใต้กล้อง fluorescence microscope (Olympus IX51 with DP70)

2. การให้สารไนตริกออกไซด์เป็นระยะเวลานาน (Long-Term Nitric Oxide Treatment)

เลี้ยงเซลล์ใน 100 mm cell culture plates ที่ความหนาแน่น 5×10^5 cells โดยบ่มเซลล์ที่อุณหภูมิ 37 องศาเซลเซียส เป็นเวลา 4 ชั่วโมง เพื่อให้เซลล์เกาะ จากนั้นให้สาร DPTA NONOate ที่ความเข้มข้นไม่เป็นพิษต่อเซลล์ เทียบผลที่ได้กับ control ที่ไม่ได้รับสารไนตริกออกไซด์ โดยจะบ่มเป็นระยะเวลา 7 และ 14 วัน เพื่อนำไปทดสอบลักษณะการเกิดเซลล์มะเร็งต้นกำเนิด โดยที่ระยะเวลาที่บ่มนั้น เซลล์จะถูก sub-cultured และเติมสาร DPTA NONOate ทุกๆ 2 วัน

3. การศึกษาลักษณะของเซลล์มะเร็งต้นกำเนิด (Cancer Stem Cell-like Phenotype Analysis)

หลังจากให้สาร DPTA NONOate แก่เซลล์เป็นเวลา 7 และ 14 วันแล้วนำไปศึกษาลักษณะของเซลล์มะเร็งต้นกำเนิด

ศึกษารูปร่างและลักษณะของเซลล์ (Cell Morphology Characterization Assay)

ศึกษารูปร่างของเซลล์ที่ได้รับสารไนตริกออกไซด์เป็นระยะเวลา 7 และ 14 วันเทียบกับ control ที่ไม่ได้รับสารไนตริกออกไซด์ พร้อมทั้งถ่ายภาพรูปร่างลักษณะของเซลล์โดยการใช้ fluorescence microscope (Olympus IX51 with DP70)

ศึกษาการเพิ่มจำนวนของเซลล์ (Cell Proliferation Assay)

เลี้ยงเซลล์ที่ได้รับสารไนตริกออกไซด์มาแล้วเป็นระยะเวลา 7 และ 14 วัน รวมทั้ง control ใน 96-well plates ความหนาแน่นเซลล์เท่ากับ 1×10^3 cells/well ที่อุณหภูมิ 37 องศาเซลเซียส เป็นเวลา 24 และ 48 ชั่วโมง ตามลำดับ นำเซลล์มาบ่มด้วยสาร MTT ความเข้มข้น 0.4 mg/ml เป็นเวลา 4 ชั่วโมง ที่อุณหภูมิ 37 องศาเซลเซียส จากนั้นนำส่วนของ supernatant ออก และใช้ DMSO ละลายผลึก formazan แล้วนำไปวัดความเข้มแสงที่ความยาวคลื่น 570 nm จากนั้นนำผลที่ได้มาคำนวณหาเปอร์เซ็นต์การอยู่รอดของเซลล์

ศึกษาการเคลื่อนที่ของเซลล์ (Cell Migration Assay)

เลี้ยงเซลล์ที่ได้รับสารไนตริกออกไซด์มาแล้วเป็นระยะเวลา 7 และ 14 วัน รวมทั้ง control ใน 96-well plates ความหนาแน่นเซลล์เท่ากับ 2×10^4 cells/well ที่อุณหภูมิ 37 องศาเซลเซียส เป็นเวลา 24 ชั่วโมง จากนั้น scratch โดยการใช้นิพเพ็ตขนาด 20-200 μ l โดยเอา media เก่าออก พร้อมทั้งใส่ media ใหม่ 100 μ l จากนั้นดูการเคลื่อนที่ของเซลล์ที่เวลา 0, 24 และ 48 ชั่วโมง พร้อมทั้งถ่ายภาพภายใต้ fluorescence microscope (Olympus IX51 with DP70)

ศึกษาการแพร่กระจายของเซลล์มะเร็ง (Invasion assay)

การศึกษาการแพร่กระจายของเซลล์มะเร็ง จะเลี้ยงเซลล์ใน 24-well Transwell ที่มี filters ขนาด 8 μ m โดยก่อนเลี้ยงเซลล์ จะ coated plate ด้วย matrigel ปริมาณ 50 μ l จากนั้นใส่ RPMI media ที่มี 10% FBS ลงใน chamber ด้านล่าง และเลี้ยงเซลล์ที่ความหนาแน่น 3×10^5 cells ปริมาณ 100 μ l ลงใน chamber ด้านบน หลังจาก 24 ชั่วโมง จะดูด media และ matrigel ออก จากนั้น fixed เซลล์ด้วย 3.7% paraformaldehyde จากนั้นย้อมเซลล์ด้วย Hoechst 33342 และดูเซลล์ที่สามารถเคลื่อนที่ผ่าน matrigel ด้วย fluorescence microscope (Olympus IX51 with DP70)

ศึกษาการเจริญเติบโตของเซลล์ภายใต้สภาวะไร้การยึดเกาะ (Anchorage-Independent Growth Analysis)

เซลล์ที่ได้รับสารไนตริกออกไซด์เป็นระยะเวลา 7 และ 14 วัน รวมทั้ง control จะถูกทำให้เป็นเซลล์เดี่ยวและเลี้ยงใน 6-well plates ที่มี agar อยู่ โดยมีความหนาแน่นเซลล์เท่ากับ 5×10^3 cells/well จากนั้นบ่มเซลล์เป็นระยะเวลา 14 วัน เพื่อดูการเกิดโคโลนี

ศึกษาการมีชีวิตรอดและการเพิ่มจำนวนของเซลล์ในสภาวะไร้การยึดเกาะ (Anchorage-Independent Survival and Proliferation Assay)

หลังจากบ่มเซลล์เป็นเวลา 14 วัน เซลล์จะถูกนำมาวัดการอยู่รอดของเซลล์ด้วย Presto Blue™

ศึกษาการเกิดโคโลนีภายใต้สภาวะไร้การยึดเกาะ (Anchorage-Independent Colony Growth Assay)

หลังจากบ่มเซลล์เป็นเวลา 14 วัน จะถ่ายภาพการเกิดโคโลนีภายใต้กล้อง fluorescence microscope (Olympus IX51 with DP70) ขนาดของโคโลนีและจำนวนโคโลนีที่เกิดขึ้นจะถูกนำมาวิเคราะห์เพื่อหาความสัมพันธ์

4. พลาสมิดและการทรานสเฟกชัน (Plasmids and transfection).

พลาสมิดของโปรตีนที่สนใจที่เกี่ยวข้องกับการควบคุมพฤติกรรมความรุนแรงของเซลล์มะเร็ง เช่น เพิ่มจำนวนเซลล์มะเร็งต้นกำเนิด และเพิ่มการอยู่รอด จะประกอบด้วยโปรตีน Akt, FAK, Bcl-2, Mcl-1, Cav-1, และ iNOS เพื่อศึกษาผลของไนตริกออกไซด์ในการควบคุมการเป็นเซลล์มะเร็งต้นกำเนิด โดยทำให้โปรตีนที่สนใจมีการแสดงออกน้อยลง (ShRNA) ในพลาสมิดเพื่อยืนยันการแสดงออกของโปรตีนดังกล่าว นำเซลล์ที่จะ transfect มาเลี้ยงต่อใน 6-well plate ใน media ที่ไม่มี serum จนกระทั่งเซลล์เจริญเติบโตประมาณ 60-70% จากนั้นนำสาร Lipofectamine และ plasmids มาใช้ในการ transfect หลังจาก transfect ไปแล้ว 12 ชั่วโมง จะเปลี่ยน media เดิมออกแล้วเติม media ที่มี 5% FBS ลงไป เมื่อ transfect แล้ว 36 ชั่วโมง เซลล์จะถูกย่อยด้วย 0.03% trypsin และเลี้ยงเซลล์ใน 75-ml culture flasks เป็นเวลา 24 ถึง 28 วัน จากนั้นเลือกเซลล์ที่มีการเปลี่ยนแปลงยีนอย่างถาวรมารวมกันและดูการแสดงออกของโปรตีนด้วยวิธี Western blotting โดยเซลล์ที่นำมาใช้ทดสอบในวิธีนี้จะต้องเลี้ยงใน RPMI 1640 medium ที่ไม่มี antibiotic มาแล้วอย่างน้อย 2 passages

5. การวิเคราะห์โปรตีนด้วยวิธี western blot (Western Blot Analysis)

บ่มเซลล์ด้วย lysis buffer ที่ประกอบด้วย 2% Triton X-100, 1% sodium dodecyl sulfate (SDS), 100 mM NaCl, 10 mM Tris-HCl (pH 7.5), 1 mM EDTA, และ complete Mini cocktail protease inhibitor เป็นเวลา 45 นาที บนน้ำแข็ง จากนั้นนำเซลล์ที่ถูก lyse มาหาปริมาณโปรตีนที่ได้ โดยการใช้ BCA protein assay kit และปรับปริมาณโปรตีนให้เท่ากัน และทำการ denature โปรตีนด้วยการบ่มโปรตีนที่อุณหภูมิ 95 °C เป็นเวลา 5 นาที และนำโปรตีน 40 µg ไปโหลดใน 10% SDS-PAGE เพื่อให้เกิดการแยกของโปรตีน จากนั้น transfer โปรตีนลงบน nitrocellulose membranes และ block โปรตีนบน nitrocellulose membranes ด้วย 5% non-fat dry milk ที่ละลายใน TBST (25 mM Tris-HCl, pH 7.4, 125 mM NaCl, 0.1% Tween 20) เป็นเวลา 1 ชั่วโมง เมื่อ block โปรตีนเรียบร้อยแล้ว นำ membrane ไปบ่มด้วย primary antibodies ที่มีความจำเพาะต่อการเกิดเซลล์มะเร็งต้นกำเนิด เช่น โปรตีน ALDH และ CD133, และ β-actin เป็นเวลา 24 ชั่วโมง ที่อุณหภูมิ 4 °C รวมทั้ง primary antibodies อื่นๆ เช่น Akt, phosphorylated Akt, ERK, Phosphorylated ERK, FAK, phosphorylated FAK, Caveolin-1, Bcl-2, Bax, และ p53 เป็นเวลา 24 ชั่วโมง ที่อุณหภูมิ 4 °C เมื่อครบ 24 ชั่วโมงจะล้าง membrane ด้วย TBST 3 ครั้ง เป็นเวลา 10 นาที และบ่มด้วย horseradish peroxidase-labeled

secondary antibodies ต่อเป็นเวลา 2 ชั่วโมง ที่อุณหภูมิห้อง จากนั้นนำไปวัดด้วย chemiluminescent และวัดความเข้มของ band โปรตีนต่างๆเทียบกับโปรตีน β -actin

5. การวิเคราะห์อาร์เอ็นเอด้วยวิธีไมโครแอเรย์ (Microarray Analysis)

เซลล์ที่ได้รับสารไนตริกออกไซด์เป็นเวลา 14 วัน และ control จะถูกนำมาสกัด total RNA โดยการใช้สาร TRIzol[®] จากนั้นปริมาณ RNA ทั้งหมด และความบริสุทธิ์ของ RNA จะถูกวัดด้วยเครื่อง Thermo Scientific NanoDrop 2000 spectrophotometer ซึ่งค่าความสมบูรณ์ของ RNA (RNA integrity number, RIN) สามารถวัดได้โดยการใช้ Agilent's 2100 Bioanalyzer ก่อนจะวิเคราะห์ตัวอย่าง RNA ด้วยวิธีไมโครแอเรย์

6. การวิเคราะห์สถิติ (Statistical Analysis)

ข้อมูลทั้งหมดจะแสดงเป็น ค่า means \pm SD ซึ่งได้จากการทำการทดลองซ้ำสามการทดลองขึ้นไปและเปรียบเทียบกับ control โดยใช้ One-way analysis และ student's t test ในการวิเคราะห์ และมีค่าความเชื่อถือ $p < 0.05$

ผลการทดลอง

เนื่องจากความรู้ทางด้านมะเร็งในปัจจุบันแสดงให้เห็นว่าเซลล์มะเร็งต้นกำเนิด (Cancer stem cells) มีบทบาทสำคัญต่อการดำเนินไปของโรค การติดต่อยาเคมีบำบัด และการแพร่กระจายของเซลล์มะเร็งปอด แต่ความรู้ความเข้าใจในเรื่องการควบคุมและพฤติกรรมของเซลล์มะเร็งต้นกำเนิดในปัจจุบันยังคงจำกัด การเปลี่ยนแปลงที่ผันกลับได้อย่างรวดเร็วของเซลล์ที่มีลักษณะคล้ายเซลล์มะเร็งต้นกำเนิดภายในก้อนมะเร็ง อาจเกิดจากผลกระทบของสารชีวภาพที่พบในสภาวะแวดล้อมของก้อนมะเร็ง ส่งผลกระทบต่อเซลล์มะเร็งต้นกำเนิดหรือเซลล์มะเร็งธรรมดาให้มีความเป็นเซลล์ต้นกำเนิดเพิ่มขึ้นหรือลดลงได้ ความเข้าใจในกลไกระดับโมเลกุลและผลของสารแวดล้อมของก้อนมะเร็งต่อความเป็นเซลล์มะเร็งต้นกำเนิดอาจนำไปสู่การค้นพบเป้าหมายใหม่ในการออกฤทธิ์ของยาต้านมะเร็งที่มีประสิทธิภาพสูงได้ โครงการวิจัยนี้มีวัตถุประสงค์เพื่อ ศึกษาบทบาทของไนตริกออกไซด์ในระยะยาวต่อลักษณะของความเป็นเซลล์ต้นกำเนิดในเซลล์มะเร็งปอด และความรุนแรงของเซลล์มะเร็งที่จะส่งเสริมการแพร่กระจาย รวมถึงกลไกระดับโมเลกุลอันเป็นผลมาจากการที่เซลล์มะเร็งได้รับสารไนตริกออกไซด์

ไนตริกออกไซด์ เป็นสารชีวภาพที่มีความสำคัญต่อการส่งสัญญาณระหว่างเซลล์ซึ่งพบในปริมาณที่เพิ่มสูงขึ้นในมะเร็งหลายชนิดที่เซลล์มะเร็งได้รับในระยะเวลายาวส่งเสริมให้เซลล์มะเร็งปอดเกิดลักษณะเฉพาะและพฤติกรรมของเซลล์ที่สอดคล้องกับเซลล์มะเร็งต้นกำเนิดเพิ่มมากขึ้น กล่าวคือ เซลล์มะเร็งปอดที่ได้รับไนตริกออกไซด์จะมีกลไกการติดต่อการตายแบบอะนอยด์ซิส (anoikis resistance) เพิ่มการเจริญเติบโตของก้อนมะเร็ง (proliferation) เพิ่มการเคลื่อนที่ (migration) และเพิ่ม

การรุกรานแทรกตัวผ่านเนื้อเยื่อ (invasion) นอกจากนี้ยังพบว่าเซลล์มะเร็งดังกล่าวมีการแสดงออกของโปรตีนที่เป็นตัวบ่งชี้ของเซลล์มะเร็งต้นกำเนิด คือ CD133 และ ALDH1A1 เพิ่มมากขึ้นตามความเข้มข้นของไนตริกออกไซด์และระยะเวลาที่เซลล์สัมผัสกับสาร และยังพบการเพิ่มการแสดงออกของโปรตีนที่เป็นตัวบ่งชี้ของการเกิด epithelial to mesenchymal transition (EMT) คือ vimentin และ snail นอกจากนี้ ผลกระทบดังกล่าวสามารถเกิดขึ้นได้เหมือนกันทุกประการเมื่อใช้สารที่ให้ไนตริกออกไซด์อีกชนิดหนึ่งคือ S-nitroso-N-acetylpenicillamine (SNAP) และที่สำคัญผลทั้งหมดสามารถถูกยับยั้งได้เมื่อให้ 2-(4-carboxy-phenyl)-4, 4, 5, 5 tetramethylimidazole-1-oxy-3-oxide (PTIO) ซึ่งเป็นสารยับยั้งไนตริกออกไซด์ สารนี้จะยับยั้งพฤติกรรมที่แสดงถึงความรุนแรงในการแพร่กระจายของเซลล์ที่คล้ายเซลล์มะเร็งต้นกำเนิดและการแสดงออกของโปรตีนบ่งชี้สำหรับเซลล์ต้นกำเนิด การส่งเสริมให้เกิดฟีโนไทป์ของเซลล์มะเร็งต้นกำเนิดสามารถย้อนกลับได้เมื่อหยุดให้สารไนตริกออกไซด์เป็นระยะเวลา 7 วัน เมื่อศึกษากลไกในระดับโมเลกุลพบว่าการส่งเสริมพฤติกรรมที่แสดงถึงความรุนแรงของเซลล์มะเร็งต้นกำเนิดโดยไนตริกออกไซด์เกิดผ่านการกระตุ้นการทำงานของโปรตีน caveolin-1 (Cav-1) ซึ่งถูกทำให้มีการแสดงออกมากขึ้นหลังให้ไนตริกออกไซด์ การค้นพบนี้แสดงให้เห็นบทบาทใหม่ของไนตริกออกไซด์ในการควบคุมการเกิดฟีโนไทป์ของเซลล์มะเร็งต้นกำเนิด และความสำคัญของสารต่อพฤติกรรมที่แสดงถึงความรุนแรงในการแพร่กระจายของเซลล์มะเร็งผ่านการกระตุ้นโปรตีน Cav-1

นอกจากนี้ สารต่างๆ ที่เซลล์มะเร็งอาจจะได้รับและส่งผลกระทบต่อเซลล์ในทิศทางเดียว หรือตรงข้ามกับไนตริกออกไซด์ โดยใช้การทดลอง model เดียวกัน คือ ชาติตุเหล็ก ชาติตุสังกะสี สารซิโปรฟลอกซาซิน gignantol ไตรโคซาน ซิสพลาติน และ ouabain

ผู้วิจัยพบว่าการให้ชาติตุเหล็กในขนาดไม่เป็นพิษต่อเซลล์มะเร็งปอดส่งเสริมให้เกิดฟีโนไทป์และพฤติกรรมของเซลล์มะเร็งต้นกำเนิด คือ เพิ่มการเจริญเติบโตของก้อนมะเร็ง เพิ่มการเพิ่มจำนวน เพิ่มการเคลื่อนที่ และการแทรกตัวผ่านเนื้อเยื่อ โดยเพิ่มการแสดงออกของโปรตีนที่เป็นตัวบ่งชี้ของเซลล์ต้นกำเนิด ได้แก่ ACBG2 ผ่านการกระตุ้นการทำงานของโปรตีน Sox-9 ซึ่งการเพิ่มขึ้นของการส่งเสริมให้เกิดฟีโนไทป์และพฤติกรรมของเซลล์มะเร็งต้นกำเนิดดังกล่าวสัมพันธ์กับระดับอนุพันธ์ออกซิเจนชนิด Hydroxyl ที่เพิ่มขึ้น ในขณะเดียวกันผู้วิจัยยังพบว่าชาติตุสังกะสีเพิ่มการเกิด EMT คือเซลล์สามารถเกาะกันน้อยลง และมีการแสดงออกของโปรตีน N-cadherin vimentin snail และ slug เพิ่มขึ้น และมีการแสดงออกของโปรตีน E-cadherin ลดลง นอกจากนี้ชาติตุสังกะสียังเพิ่มการเคลื่อนที่และการแพร่กระจายของเซลล์มะเร็ง โดยเพิ่มการแสดงออกของโปรตีนที่เกี่ยวข้อง เช่น FAK, Rac1, และ RhoA ทั้งยังมีผลเพิ่มความสามารถของเซลล์มะเร็งในการเจริญเติบโตของก้อนมะเร็ง และชาติตุสังกะสีสามารถเหนี่ยวนำให้เกิด superoxide anion ภายในเซลล์อีกด้วย

ผู้วิจัยยังพบอีกว่าการสัมผัสยาซิโปรฟลอกซาซิน สามารถส่งเสริมให้เกิดฟีโนไทป์และพฤติกรรมของเซลล์มะเร็งต้นกำเนิดในเซลล์มะเร็งปอดได้เช่นกัน คือ เพิ่มการเจริญเติบโตของก้อนมะเร็ง และเพิ่มการแสดงออกของโปรตีนที่เป็นตัวบ่งชี้ของเซลล์ต้นกำเนิด ได้แก่ CD133, CD44, ABCG2 และ

ALDH1A1 รวมถึงเพิ่มการแสดงออกของโปรตีนที่เกี่ยวข้องกับการเพิ่มจำนวนและคงความเป็นเซลล์ต้นกำเนิด คือ Nanog และ Oct-4 การส่งเสริมพฤติกรรมที่แสดงถึงความรุนแรงของเซลล์มะเร็งต้นกำเนิด โดยยาซิโปรฟลอกซาซินเกิดผ่านการกระตุ้นการทำงานของโปรตีน Cav-1, Akt และ ERK กลไกที่ส่งเสริมให้เกิดฟีโนไทป์และพฤติกรรมของเซลล์มะเร็งต้นกำเนิดดังกล่าว สามารถยับยั้งโดยสาร gigantol ซึ่งเป็นสารสกัดจากกล้วยไม้ (*Dendrobium draconis*) โดยพบว่าสาร gigantol ยับยั้งการเกิดก้อนของเซลล์มะเร็งต้นกำเนิด และยับยั้งการแสดงออกของโปรตีนที่ CD133, ALDH1A1, Nanog และ Oct-4 โดยผ่านการลดการทำงานของโปรตีน Akt ผู้วิจัยได้ทำการศึกษากลไกอื่นๆ ที่ควบคุมการคงคุณสมบัติในการเป็นเซลล์ต้นกำเนิด โดยทำการศึกษาเบื้องต้นในเซลล์มนุษย์ปกติ (dermal papilla cell; DPC) หลังการให้ยาซิโปรฟลอกซาซิน พบว่าซิโปรฟลอกซาซินสามารถป้องกันการสูญเสียความเป็นเซลล์ต้นกำเนิดของ DPC ในระหว่างการเลี้ยงได้ โดยคงระดับการแสดงออกของโปรตีนที่เกี่ยวข้องกับความเป็นเซลล์ต้นกำเนิด โดยผ่านการกระตุ้นกลไก ATP-dependent tyrosine kinase/glycogen synthase kinase β และเพิ่มระดับการแสดงออกของโปรตีน Nanog และ Oct-4 นอกจากนี้ยังได้ศึกษาผลของสารไตรโคซานต่อการเกิด EMT จากการศึกษาพบว่าเซลล์มะเร็งที่ได้รับไตรโคซานจะมีการเกาะกันระหว่างเซลล์ลดลง และมีการแสดงออกของโปรตีน N-cadherin vimentin snail และ slug เพิ่มขึ้น พบว่าการเหนี่ยวนำให้เกิด EMT ด้วยไตรโคซานยังมีผลเพิ่มความสามารถของเซลล์มะเร็งในการเจริญเติบโตของก้อนมะเร็ง การเคลื่อนที่ และการรุกรานเนื้อเยื่อข้างเคียง โดยผ่านการกระตุ้นการทำงานของ FAK/Akt และ Rac1 ผู้วิจัยยังพบอีกว่าเซลล์ที่ได้รับยาซิสพลาตินขนาดต่ำมีการเพิ่มขึ้นของจำนวน filopodia ซึ่งการเพิ่มขึ้นดังกล่าวสัมพันธ์กับการเกิดการเคลื่อนที่ของเซลล์ที่มากขึ้น และการเพิ่มการแสดงออกของโปรตีน FAK/AKT, active Rho A-GTP และ active Rac-GTP ซิสพลาตินยังทำให้เกิดการเพิ่มขึ้นของอินทิกรินชนิด α_4 , α_v , β_1 และ β_5 อีกด้วย ซึ่งการแพร่กระจายดังกล่าวสามารถยับยั้งได้โดยสาร ouabain ซึ่งเป็นฮอร์โมนที่พบได้ในร่างกาย โดยพบว่า ouabain ยับยั้งการแสดงออกของโปรตีนอินทิกรินชนิด α_4 , α_5 , α_v , β_3 และ β_4 ในขณะที่เพิ่มการแสดงออกของอินทิกรินชนิด β_1 และ β_4 จากการเปลี่ยนรูปแบบการแสดงออกของอินทิกรินเมื่อเซลล์มะเร็งปอดได้รับ ouabain ดังกล่าว พบว่า ouabain ทำให้เซลล์มะเร็งปอดมีขนาดของก้อนมะเร็งเล็กลงอย่างชัดเจน และยับยั้งการเคลื่อนที่ของเซลล์มะเร็งปอดได้

ทั้งนี้ การค้นพบนี้แสดงให้เห็นถึงบทบาทใหม่ของไนตริกออกไซด์ในการควบคุมการเกิดฟีโนไทป์ของเซลล์มะเร็งต้นกำเนิด และความสำคัญของไนตริกออกไซด์ในการเพิ่มพฤติกรรมที่แสดงถึงความรุนแรงในการแพร่กระจายของเซลล์มะเร็ง และข้อมูลที่ได้ทำให้เพิ่มความเข้าใจที่ดีขึ้นในเรื่องของการปรับตัวของเซลล์มะเร็งภายหลังจากได้รับไนตริกออกไซด์ หรือหลังจากได้รับสารอื่นๆ คือ ชาติุเหล็ก ชาติุสังกะสี สารซิโปรฟลอกซาซิน gigantol ไตรโคซาน ซิสพลาติน และ ouabain ซึ่งจะเป็นประโยชน์ในการประกอบการพิจารณาในการรักษาและการใช้สารดังกล่าวในผู้ป่วยมะเร็งต่อไป

บทวิจารณ์

การเพิ่มขึ้นของไนตริกออกไซด์นั้น มักพบบริเวณรอบๆ ก้อนมะเร็งและอาจจะส่งผลต่อพฤติกรรมการเป็นมะเร็งของเซลล์มะเร็ง ไนตริกออกไซด์เป็นโมเลกุลที่สามารถแพร่ผ่านเข้าไปยังเนื้อเยื่อต่างๆได้ ดังนั้นจึงสามารถควบคุมพฤติกรรมของเซลล์มะเร็งได้หลายสาเหตุ การให้ไนตริกออกไซด์แก่เซลล์มะเร็งเป็นเวลานานสามารถเพิ่มการเคลื่อนที่ของเซลล์ผ่านทางวิถี FAK และ Akt โดยการเติมหมู่ฟอสเฟตให้กับ FAK ที่ตำแหน่ง Tyr 397 จะส่งผลให้เกิดการเคลื่อนที่ของเซลล์ ซึ่งการกระตุ้นของวิถีนี้ยังขึ้นอยู่กับระดับของ Cav-1 ภายในเซลล์ เคยมีรายงานว่า Cav-1 กระตุ้นการเคลื่อนที่ของเซลล์และการแพร่กระจายของเซลล์มะเร็ง โดยไนตริกออกไซด์สามารถกระตุ้นให้เกิดการเพิ่มการแสดงออกของโปรตีน Cav-1 ได้ นอกจากนี้เคยมีรายงานว่าไนตริกออกไซด์กระตุ้นให้เซลล์มะเร็งปอดติดต่อกับ Fas ligand และยา cisplatin และติดต่อกับการตายแบบอะนอยคิสในเซลล์มะเร็งปอดด้วย มีการศึกษาที่ผ่านมามีพบว่าเซลล์มะเร็งต้นกำเนิดเพิ่มความสามารถในการเคลื่อนที่ การแพร่กระจายของเซลล์มะเร็ง เพิ่มการเกิดก้อนมะเร็งและติดต่อกับการตายแบบอะนอยคิส ซึ่งไนตริกออกไซด์สามารถควบคุมการเกิดเซลล์มะเร็งต้นกำเนิดและพฤติกรรมความรุนแรงของเซลล์มะเร็งปอด โดยเพิ่มการแสดงออกของโปรตีนบ่งชี้การเกิดเซลล์มะเร็งต้นกำเนิด เช่น CD133 และ ALDH1A1 และเพิ่มพฤติกรรมความรุนแรงของเซลล์มะเร็ง ในขณะที่เดียวกัน Cav-1 อาจทำให้เกิดพฤติกรรมที่รุนแรงและติดต่อกับเคมีบำบัดในเซลล์มะเร็ง

การเกิดอนุมูลอิสระ ROS มีผลทำให้เซลล์มะเร็งสามารถเกิดการแพร่กระจายไปยังอวัยวะอื่นๆได้ อาทิเช่น เซลล์มะเร็งปอด (Chung-man *et al.*, 2001; Haigis *et al.*, 2012; Heath *et al.*, 2013) และเพิ่มปัจจัยเสี่ยงต่อพฤติกรรมที่รุนแรงของเซลล์มะเร็ง (Luanpitpong *et al.*, 2010) ซึ่งธาตุเหล็กสามารถทำให้เกิดการเพิ่มเซลล์มะเร็งต้นกำเนิด โดยเพิ่มขนาดและจำนวนของ tumor spheroids และเพิ่มการแสดงออกของ ABCG2 ซึ่งเป็นโปรตีนบ่งชี้ของการเกิดเซลล์มะเร็งต้นกำเนิด ในขณะที่เดียวกันยังเพิ่มจำนวนของเซลล์มะเร็งและเพิ่มการเคลื่อนที่ของเซลล์มะเร็ง เคยมีรายงานว่า SOX9 ทำหน้าที่เป็น oncogene ในมะเร็งหลายชนิด เช่น breast, colorectal, pancreatic, prostate, และ glioma (Lu *et al.*, 2008; Matheu *et al.*, 2012) ในทางตรงกันข้าม SOX9 ยังมีหน้าที่เป็น tumor suppressor ในมะเร็งกระเพาะปัสสาวะและมะเร็งผิวหนัง (Aleman *et al.*, 2008; Passeron *et al.*, 2009) ซึ่ง SOX9 ในมะเร็งปอดจะกระตุ้นให้เกิดการแพร่กระจายเซลล์มะเร็ง (Capaccione *et al.*, 2014; Luanpitpong *et al.*, 2016) ซึ่งให้เห็นว่าธาตุเหล็กกระตุ้นการทำงานของโปรตีน Sox-9 ซึ่งส่งเสริมให้เกิดฟีโนไทป์และพฤติกรรมของเซลล์มะเร็งต้นกำเนิด และยังมีความสัมพันธ์กับระดับอนุมูลอิสระออกซิเจนชนิด Hydroxyl ที่เพิ่มขึ้น

ธาตุสังกะสีมีความสัมพันธ์กับการเกิดมะเร็งปอดและมะเร็งชนิดอื่นๆ (Xie *et al.*, 2009; Demir *et al.*, 2014) โดยทำให้เกิดความเสียหายของโครโมโซมและเกิดการแตกหักของดีเอ็นเอของเซลล์มะเร็งปอด (Xie *et al.*, 2009) EMT มีความเกี่ยวข้องกับการแพร่กระจายตัวของเซลล์มะเร็ง โดยเซลล์จะสูญเสียการยึดเกาะ ทำให้เพิ่มการเคลื่อนที่ของเซลล์มะเร็งได้ (Craene and Rerx, 2013; Yang and Weinberg, 2008; Iwatsuki *et al.*, 2010; Thiery *et al.*, 2009) โดยโปรตีนบ่งชี้ที่เกี่ยวข้องกับ

เกิด EMT ของเซลล์มะเร็งต้นกำเนิด (Chiou *et al.*, 2010, Abdelalim and Tooyama, 2014) การศึกษาที่ผ่านมายังพบว่า phosphorylated Akt มีบทบาทสำคัญในการเกิด self-renewal ของ embryonic stem cells ผ่านทางโปรตีน Oct4 (Lin *et al.*, 2012; Wang *et al.*, 2013) นอกจากนี้ phosphorylated Akt ยังมีความสำคัญต่อการเพิ่มจำนวนและการเกิด pluripotency ของเซลล์มะเร็งต้นกำเนิดและการเกิด sphere formation (Matsubara *et al.*, 2013)

จากผลงานวิจัยที่ได้กล่าวมานี้ จะเห็นได้ว่าธาตุเหล็ก ธาตุสังกะสี สารซีโปรฟลอกซาซิน gigantol ไตรโคซาน ซิสฟลาติน และ ouabain สามารถนำมาประยุกต์ และนำความรู้มาพัฒนาเพื่อใช้เป็นสารในการรักษาและป้องกันการแพร่กระจายของเซลล์มะเร็งได้อย่างมีประสิทธิภาพ ในขณะเดียวกัน สารบางชนิดก็สามารถนำมาใช้เป็นข้อควรระวังให้กับผู้ป่วยมะเร็งได้ เนื่องจากเหนี่ยวนำให้เกิดการแพร่กระจายของเซลล์มะเร็งปอด

หนังสืออ้างอิง

- Abdelalim E.M. and Tooyama I. (2014) Knockdown of p53 suppresses Nanog expression in embryonic stem cells. *Biochemical and Biophysical Research Communications* 443(2):652–657.
- Aleman A, Adrien L, Lopez-Serra L, Cordon-Cardo C, Esteller M, Belbin TJ, Sanchez-Carbayo M. (2008) Identification of DNA hypermethylation of SOX9 in association with bladder cancer progression using CpG microarrays. *British Journal of Cancer*. 98: 466–473.
- Capaccione KM, Hong X, Morgan KM, Liu W, Bishop JM, Liu L, Markert E, Deen M, Minerowicz C, Bertino JR, Allen T, Pine SR. (2014) Sox9 mediates Notch1-induced mesenchymal features in lung adenocarcinoma. *Oncotarget* 5: 3636–3650.
- Chanvorachote P., Nimmannit U, Wang L, Stehlik C, Lu B, Azad N, and Rojanasakul Y. (2005) Nitric Oxide Negatively Regulates Fas CD95-induced Apoptosis through Inhibition of Ubiquitin-Proteasome-mediated Degradation of FLICE Inhibitory Protein. *Journal of Biological Chemistry*. 280, 42044-42050
- Chanvorachote P., Nimmannit U, Stehlik C, Wang L, Ongpipatanakul B, and Rojanasakul Y. (2006) Nitric Oxide Regulates Cell Sensitivity to Cisplatin-Induced Apoptosis through S-nitrosylation and Inhibition of Bcl-2 Ubiquitination, *Cancer Research*. 66, 6353-6360.
- Chanvorachote P., Nimmannit U, Lu Y, Talbott S, Jiang B, and Rojanasakul Y. (2009) Nitric Oxide Regulates Lung Carcinoma Cell Anoikis through Inhibition of Ubiquitin-Proteasomal Degradation of Caveolin-1. *Journal of Biological Chemistry*. 284, 28476-28484.
- Charafe-Jauffret E., Ginestier C., Iovino F., Wicinski J., Cervera N., Finetti P., et al. (2009) Breast cancer cell lines contain functional cancer stem cells with metastatic capacity and a distinct molecular signature, *Cancer Research*. 69(4):1302-1313.

- Chiou S.H., Wang M.L., Chou Y.T. et al. (2010) Coexpression of Oct4 and Nanog enhances malignancy in lung adenocarcinoma by inducing cancer stem cell-like properties and epithelial-mesenchymal transdifferentiation. *Cancer Research*, 70(24):10433–10444.
- Chung-man HJ, Zheng S, Comhair SA, Farver C, Erzurum SC. (2001) Differential expression of manganese superoxide dismutase and catalase in lung cancer. *Cancer Research* 61: 8578–8585.
- Craene BD, Berx G. (2013) Regulatory networks defining EMT during cancer initiation and progression. *Natural Reviews Cancer*. 13(2):97–110.
- Colakogullari, M., Ulukaya, E., Yilmaztepe, A., Ocakoglu, G., Yilmaz, M., Karadag, M., & Tokullugil, A (2006) Higher serum nitrate levels are associated with poor survival in lung cancer patients. *Clinical Biochemistry*, 39(9), 898–903.
- Demir E, Akca H, Kaya B, Burgucu D, Tokgun O, Turna F, et al. (2014) Zinc oxide nanoparticles: genotoxicity, interactions with UV-light and cell-transforming potential. *Journal of Hazard Mater*. 264:420–9. doi:10.1016/j.jhazmat.2013.11.043.
- Dubrovskaja A., Kim S., Salamone R.J., Walker J.R., Maira S.M., Garcia-Echeverria C., et al. (2009) The role of PTEN/Akt/PI3K signaling in the maintenance and viability of prostate cancer stem-like cell populations, *Proceedings of the National Academy of Sciences of United States of America* 106(1):268-273.
- Eramo, A., Lotti, F., Sette, G., Pillozzi, E., Biffoni, M., Di Virgilio, A., Conticello, C., et al. (2007). Identification and expansion of the tumorigenic lung cancer stem cell population. *Cell Death and Differentiation*, 15(3), 504–514.
- ESME, H., CEMEK, M., SEZER, M., SAGLAM, H., DEMIR, A., MELEK, H., & UNLU, M. (2008). High levels of oxidative stress in patients with advanced lung cancer. *Respirology*, 13(1), 112–116.
- Haigis MC, Deng CX, Finley LW, Kim HS, Gius D. (2012) SIRT3 is a mitochondrial tumor suppressor: a scientific tale that connects aberrant cellular ROS, the Warburg effect, and carcinogenesis. *Cancer Research* 72: 2468–2472.
- Heath JL, Weiss JM, Lavau CP, Wechsle DS. (2013) Iron deprivation in cancer-potential therapeutic implications. *Nutrients* 5: 2836–2859.
- Huang C.E., Hu F.W., Yu C.H. et al. (2014) Concurrent expression of Oct4 and Nanog maintains mesenchymal stem-like property of human dental pulp cells. *International Journal of Molecular Sciences*. 15(10):18623–18639.
- Iwatsuki M, Mimori K, Yokobori T, Ishi H, Beppu T, Nakamori S, et al. (2010) Epithelial–mesenchymal transition in cancer development and its clinical significance. *Cancer*

Science. 101(2):293–9. doi:10.1111/j.1349-7006.2009.01419.x.

- Jeter C.R., Liu B., Liu X. et al. (2011) NANOG promotes cancer stem cell characteristics and prostate cancer resistance to androgen deprivation. *Oncogene* 30(36):3833–3845.
- Leung E.L., Fiscus R.R., Tung J.W., Tin V.P., Cheng L.C., Sihoe A.D., et al. 2010) Nonsmall cell lung cancer cells expressing CD44 are enriched for stem cell-like properties, *PLoS One* 5(11):e14062.
- Li, C., Heidt, D. G., Dalerba, P., Burant, C. F., Zhang, L., Adsay, V., Wicha, M., et al. (2007). Identification of Pancreatic Cancer Stem Cells. *Cancer Research*, 67(3), 1030–1037.
- Lin Y., Yang Y., Li W. et al. (2012) Reciprocal regulation of Akt and Oct4 promotes the self-renewal and survival of embryonal carcinoma cells. *Molecular Cell* 48(4):627–640.
- Lozano, R., Naghavi, M., Foreman, K., Lim, S., Shibuya, K., Aboyans, V., Abraham, J., et al. (2012). Global and regional mortality from 235 causes of death for 20 age groups in 1990 and 2010: a systematic analysis for the Global Burden of Disease Study 2010. *The Lancet*, 380(9859), 2095–2128. Elsevier Ltd.
- Lu B, Fang Y, Xu J, Wang L, Xu F, Xu E, Huang Q, Lai M. (2008) Analysis of SOX9 expression in colorectal cancer. *Am J Clin Pathol* 130: 897–904.
- Luanpitpong S, Talbott SJ, Rojanasakul Y, Nimmannit U, Pongrakhananon V, Wang L, Chanvorachote P. (2010) Regulation of lung cancer cell migration and invasion by reactive oxygen species and caveolin-1. *The Journal of Biological Chemistry* 285: 38832–38840.
- Luanpitpong S, Li J, Manke A, Brundage K, Ellis E, McLaughlin S, Angsutararux P, Chanthra N, Voronkova M, Chen YC, Wang L, Chanvorachote P, Pei M, Issaragrisil S, Rojanasakul Y. SLUG is required for SOX9 stabilization and functions to promote cancer stem cells and metastasis in human lung carcinoma. *Oncogene* [Epub ahead of print].
- Ma, S., Chan, K. W., Hu, L., Lee, T. K. W., Wo, J. Y. H., Ng, I. O. L., Zheng, B. J., et al. (2007). Identification and Characterization of Tumorigenic Liver Cancer Stem/Progenitor Cells. *Gastroenterology*, 132(7), 2542–2556.
- Mani S.A., Guo W., Liao M.J., Eaton E.N., Ayyanan A., Zhou A.Y., et al. (2008) The epithelial-mesenchymal transition generates cells with properties of stem cells, *Cell* 133(4):704-715.
- Matheu A, Collado M, Wise C, Manterola L, Cekaite L, Tye AJ, Canamero M, Bujanda L, Schedl A, Cheah KS, Skotheim RI, Lothe RA, López de Munain A, Briscoe J, Serrano M, Lovell-Badge R. (2012) Oncogenicity of the developmental transcription factor Sox9.

Cancer Research 72: 1301–1315.

- Matsubara S., Ding Q., Miyazaki Y., Kuwahata T., Tsukasa K., and Takao S. (2013) mTOR plays critical roles in pancreatic cancer stem cells through specific and stemness-related functions. *Scientific Reports* 3:3230.
- Nieman MT, Prudof RS, Johnson KR, Wheelock MJ. (1999) N-cadherin promotes motility in human breast cancer cells regardless of their E-cadherin expression. *The Journal of Cell Biology*. 147(3):631–44.
- Park J.H., Han H.J. (2009) Caveolin-1 plays important role in EGF-induced migration and proliferation of mouse embryonic stem cells: involvement of PI3K/Akt and ERK, *American Journal of Physiology Cell Physiology*. 297(4):C935-C944.
- Passeron T, Valencia JC, Namiki T, Vieira WD, Passeron H, Miyamura Y, Hearing VJ. (2009) Upregulation of SOX9 inhibits the growth of human and mouse melanomas and restores their sensitivity to retinoic acid. *The Journal Clinical Investigation* 119(4): 954–963.
- Petersen A.M., Mirsepasi H., Halkjaer S.I., Mortensen E.M., Nordgaard-Lassen I., Krogh K.A. (2014) Ciprofloxacin and probiotic *Escherichia coli* Nissle add-on treatment in active ulcerative colitis: a double-blind randomized placebo controlled clinical trial, *Journal of Crohn's and Colitis* 8 (11):1498-1505.
- Saini H., Chhibber S., Harjai K. (2015) Azithromycin and ciprofloxacin: a possible synergistic combination against *Pseudomonas aeruginosa* biofilm-associated urinary tract infections, *International Journal of Antimicrobial Agents* 45(4):359-367.
- Thiery JP, Acloque H, Huang RY, Nieto MA. (2009) Epithelial–mesenchymal transitions in development and disease. *Cell*. 2009;139(5):871–90. doi:10.1016/j.cell.2009.11.007.
- Wang Y.D., Cai N., Wu X.L., Cao H.Z., Xie L.L., and Zheng P.S. (2013) OCT4 promotes tumorigenesis and inhibits apoptosis of cervical cancer cells by miR-125b/BAK1 pathway. *Cell Death and Disease*. 4(8):e760.
- Wei Y., Jiang Y., Zou F., Liu Y., Wang S., Xu N., et al. (2013) Activation of PI3K/Akt pathway by CD133-p85 interaction promotes tumorigenic capacity of glioma stem cells, *Proceedings of the National Academy of Sciences of United States of America* 110 (17) 6829e6834.
- Wheelock MJ, Shintani Y, Maeda M, Fukumoto Y, Johnson KR. (2008) Cadherin switching. *Journal of Cell Science*. 121(Pt 6):727–35. doi:10.1242/jcs.000455.
- Xenopoulos P., Kang M., Puliafio A., Di Talia S., and Hadjantonakis A.K. (2015) Heterogeneities in nanog expression drive stable commitment to pluripotency in the mouse blastocyst. *Cell Reports* 10(9):1508–1520.

- Xie H, Holmes AL, Young JL, Qin Q, Joyce K, Pelsue SC, et al. (2009) Zinc chromate induces chromosome instability and DNA double strand breaks in human lung cells. *Toxicol Appl Pharmacol.* 234(3):293–9. doi:10.1016/j.taap.2008.10.010.
- Yang W., Klamann L.D., Chen B., Araki T., Harada H., Thomas S.M., et al. (2006) An Shp2/SFK/Ras/Erk signaling pathway controls trophoblast stem cell survival, *Developmental Cell.* 10(3):317–327.
- Yang, G., Lu, X., Fu, H., Jin, L., Yao, L., & Lu, Z. (2009). Chemotherapy not only enriches but also induces cancer stem cells. *Bioscience Hypotheses*, 2(6), 393–395. Elsevier Ltd.
- Yang J, Weinberg RA. (2008) Epithelial–mesenchymal transition: at the crossroads of development and tumor metastasis. *Developmental Cell.* 14(6):818–29. doi:10.1016/j.devcel.2008.05.009.
- Yongsanguanchai N., Pongrakhananon V., Mutirangura A., Rojanasakul Y., Chanvorachote P. (2015) Nitric oxide induces cancer stem cell-like phenotypes in human lung cancer cells, *American Journal of Physiology Cell Physiology.* 308(2):C89-C100.
- Zhang X., Lou Y., Wang H. et al. (2015) Wnt signaling regulates the stemness of lung cancer stem cells and its inhibitors exert anticancer effect on lung cancer SPC-A1 cells. *Medical Oncology* 32(4).
- Zhao Q.W., Zhou Y.W., Li W.X., Kang B., Zhang X.Q., Yang Y., et al. (2015) Akt mediated phosphorylation of Oct4 is associated with the proliferation of stem like cancer cells, *Oncology Reports* 33(4):1621-1629.
- Zhu M., Yin F., Yang L. et al. (2014) Contribution of TIP30 to chemoresistance in laryngeal carcinoma. *Cell Death and Disease* 5(10);e1468.

Output จากโครงการวิจัยที่ได้รับทุนจาก สกว.

ผลงานวิจัยที่ได้รับการสนับสนุนจากโครงการ ได้รับการตีพิมพ์ในวารสารระดับนานาชาติ รวม 14 เรื่อง

1. Pithi Chanvorachote and Sudjit Luanpitpong*. Iron induces cancer stem cells and aggressive phenotypes in human lung cancer cells. *American Journal of Physiology-Cell Physiology.* 2016 May 1;310(9): C728-39. doi: 10.1152/ajpcell.00322.2015. Epub 2016 Feb 24.
2. Preeyaporn P Phiboonchaiyanan, Chayanin Kiratipaiboon, and Pithi Chanvorachote*, Ciprofloxacin mediates cancer stem cell phenotypes in lung cancer

cells through caveolin-1-dependent mechanism. *Chemico-Biological Interactions*. 2016 Apr 25;250: 1-11. doi: 10.1016/j.cbi.2016.03.005. Epub 2016 Mar 3.

3. Narumol Bhummaphan and Pithi Chanvorachote*. Gigantol Suppresses Cancer Stem Cell-Like Phenotypes in Lung Cancer Cells. *Evidence-Based Complementary and Alternative Medicine*. 2015 Aug. doi: 10.1155/2015/836564. Epub 2015 Aug 3.
4. Nuttida Yongsanguanchai , Varisa Pongrakhananon , Apiwat Mutirangura , Yon Rojanasakul, and Pithi Chanvorachote*. Nitric Oxide induces Cancer Stem Cell-like Phenotypes in Human Lung Cancer Cells. *American Journal of Physiology-Cell Physiology*. 2015 Jan 15;308(2): C89-100. doi: 10.1152/ajpcell.00187.2014. Epub 2014 Nov 19.
5. Thidarat Winithana, Somsong Lawanprasert, and Pithi Chanvorachote*. Triclosan potentiates epithelial-to-mesenchymal transition in anoikis-resistant human lung cancer cells. *Plos One*. 2014 Oct. doi: 10.1371/journal.pone.0110851.
6. Arpasinee Sanuphan, Preedakorn Chunhacha, Varisa Pongrakhananon, and Pithi Chanvorachote*. Long-Term Nitric Oxide Exposure Enhances Lung Cancer Cell Migration. *Biomed Research International*. 2013; 2013:186972. doi: 10.1155/2013/186972.
7. Chayanin Kiratipaiboon, Parkpoom Tengamnuay, and Pithi Chanvorachote*. Ciprofloxacin Improves the Stemness of Human Dermal Papilla Cells. *Stem Cells International*. 2016; 2016:5831276. doi: 10.1155/2016/5831276. Epub 2015 Nov 16.
8. Amatchai Maiuthed, and Pithi Chanvorachote*. Cisplatin at Sub-toxic Levels Mediates Integrin Switch in Lung Cancer Cells. *Anticancer Research*. 2014 Dec; 34(12): 7111-7.
9. Chuanpit Ninsontia, and Pithi Chanvorachote* Ouabain mediates integrin switch in human lung cancer cells. *Anticancer Research*. 2014 Oct; 34(10): 5495-502.
10. Vhudhipong Saisongkorh, Arnatchai Maiuthed, and Pithi Chanvorachote*. Nitric oxide increases the migratory activity of non-small cell lung cancer cells via AKT-mediated integrin αv and $\beta 1$ upregulation. *Cellular Oncology*. 2016 Oct; 39(5): 449-462.
11. Pithi Chanvorachote, Supakarn Chamni, Chuanpit Ninsontia, and Preeyaporn Plaimee Phiboonchaiyanan*. Potential anti-metastasis natural compounds for lung cancer. *Anticancer Research*. 2016 Nov, 36(11): 5707-5717.
12. Chuanpit Ninsontia, Preeyaporn Plaimee Phiboonchaiyanan, and Pithi Chanvorachote*. Zinc induces epithelial to mesenchymal transition in human lung

cancer H460 cells via superoxide anion-dependent mechanism. *Cancer Cell International*. 2016 Jun; 16(48): DOI 10.1186/s12935-016-0323-4.

13. Sudjit Luanpitpong, and Pithi Chanvorachote*. Nitric Oxide and Aggressive Behavior of Lung Cancer Cells. 2015 Sep; 35(9): 4585-4592

กิจกรรมอื่นๆ ที่เกี่ยวข้อง ได้แก่

- ผลงานอื่นๆ เช่น การไปเสนอผลงาน การได้รับเชิญไปเป็นวิทยากร
- การเชื่อมโยงทางวิชาการกับนักวิชาการอื่นๆ ทั้งในและต่างประเทศ
- การร่วมโครงการวิจัยกับ หน่วยวิจัยที่มีความเชี่ยวชาญทางด้านมะเร็งสูง ทั้งในประเทศและต่างประเทศ

1. Prof. Yon Rojanasakul

Cancer Center Research Programs, Westvirginia University, USA

2. Prof. Dr. rer. nat. Regine Schneider-Stock

Experimental Tumorpathology, University of Erlangen, Germany

3. ศาสตราจารย์ นายแพทย์ ดร. อภิวัฒน์ มุทิรางกูร

คณะแพทยศาสตร์ จุฬาลงกรณ์มหาวิทยาลัย

การเสนอผลงานในการประชุมระดับนานาชาติ

ผลงานนำเสนอ oral 3 เรื่องและนำเสนอ poster 1 เรื่อง โดยมีรางวัลการนำเสนอผลงานของนิสิตระดับปริญญาโท 2 รางวัล ดังนี้

1. รางวัลการนำเสนอผลงาน ประเภท oral 1 รางวัล

2. รางวัลการนำเสนอผลงาน ประเภท poster 1 รางวัล

การเชื่อมโยงกับต่างประเทศหรือรางวัลที่ได้รับ

หัวหน้าโครงการวิจัยได้รับ ทุนวิจัยระดับ Experienced Researcher จาก Alexander von Humboldt Foundation ประเทศสหพันธ์สาธารณรัฐเยอรมนี เป็นระยะเวลา รวม 10 เดือนซึ่งได้รับอนุญาตจากสำนักงานกองทุนสนับสนุนงานวิจัยให้ไปทำวิจัย โดยทำงานวิจัยร่วมกับ Prof. Dr. rer. nat. Regine Schneider-Stock, Experimental Tumorpathology, University of Erlangen, Germany โดยจะทำงานวิจัยเพื่อศึกษา cancer cell signal โดยการใช้ kinase array และศึกษาความสัมพันธ์ระหว่างเซลล์มะเร็งและเซลล์ต้นกำเนิดที่เป็นเซลล์ปกติ

ภาคผนวก

Research Article

Long-Term Nitric Oxide Exposure Enhances Lung Cancer Cell Migration

Arpasinee Sanuphan, Preedakorn Chunhacha,
Varisa Pongrakhananon, and Pithi Chanvorachote

Department of Pharmacology and Physiology, Faculty of Pharmaceutical Sciences and Cell-based Drug and Health Product Development Research Unit, Chulalongkorn University, Bangkok, Thailand

Correspondence should be addressed to Pithi Chanvorachote; pithi.chan@yahoo.com

Received 25 April 2013; Revised 27 June 2013; Accepted 28 June 2013

Academic Editor: Silvia Gregori

Copyright © 2013 Arpasinee Sanuphan et al. This is an open access article distributed under the Creative Commons Attribution License, which permits unrestricted use, distribution, and reproduction in any medium, provided the original work is properly cited.

Nitric oxide (NO) found in the vicinity of lung cancer cells may play a role in the regulation of cancer cell behaviors. To explore the possible effects of NO on cell motility, human lung cancer cells were exposed to nontoxic concentrations of NO for 0–14 days, and the migratory characteristics of the cells were determined. The present study found that long-term treatment with NO significantly enhanced cell migration in a dose- and time-dependent manner. Furthermore, we found that the increased migratory action was associated with the increased expression of caveolin-1 (Cav-1), which in turn activated the focal adhesion kinase (FAK) and ATP-dependent tyrosine kinase (Akt) pathways. Notably, the NO-treated cells exhibited an increased number of filopodia per cell, as well as an increase in the levels of cell division cycle 42 (Cdc42) protein. Together, these results indicate that extended NO exposure has a novel effect on cell migration through a Cav-1-dependent mechanism, a finding that strengthens our understanding of cancer biology.

1. Introduction

The cancer microenvironment has been reported to have a significant impact on cancer cells in many ways [1]. Indeed, in such an active environment, cell signaling molecules as well as mediators including proinflammatory cytokines and reactive species are found to be intensified [2]. Among them, the concentrations of nitric oxide (NO), a reactive nitrogen species synthesized by many cells, such as endothelial, immune, and tumor cells, are found to be dramatically increased in lung cancer environments [3, 4]. Excessive and uncontrolled NO production is associated with the pathogenesis of lung cancer [5]. Additionally, clinical observation has shown that NO levels in the lungs of lung cancer patients were increased in comparison to those of normal subjects [6, 7]. While cytokines have been shown to have significant effects on the behavior of cancer cells within microenvironment, the effects of long-term nitric oxide exposure on lung cancer cell motility remain unknown.

The ability of cancer cells to migrate is an important hallmark of successful metastasis [8]. The metastasis cascade is a multistep process that consists of five components: local migration and invasion, intravasation, circulation, extravasation, and colony formation at secondary sites [9]. Tumor cells need to be motile to invade tissues; this motility is achieved by changing their cell-cell adhesion properties and by reorganizing their cytoskeletons. These cellular mechanisms are regulated by various signaling molecules, including the Rho family of small GTPases, caveolin-1 (Cav-1), and focal adhesion kinase (FAK) [10, 11]. FAK is activated by an initial autophosphorylation at the Tyr 397 residue, and its activation is essential for the regulation of focal adhesion turnover and cell protrusion [12, 13]. Studies have reported that FAK mediates cells motility through the activation of the downstream Akt signaling pathway [14]. Furthermore, evidence has suggested that Cdc42 overexpression increased cell motility by inducing the formation of filopodia [11, 15, 16]. Recently, caveolin-1 (Cav-1), a 21–24 kDa integral membrane

protein, has garnered increasing attention as its role in the regulation of cancer cell behaviors has been revealed [17–26]. Increased Cav-1 expression was shown to be associated with enhanced progression of prostate, colon, and breast cancers [26, 27]. Likewise, elevated Cav-1 expression was associated with an increased metastasis capacity and poor survival in lung cancer patients [26, 28]. We investigated the role of long-term exposure to nontoxic doses of NO on lung carcinoma cell motility and examined the possible underlying mechanisms using pharmacological approaches. The findings of the present study aid in the better understanding of this microenvironment-related mediator and may help in the development of novel anticancer strategies.

2. Materials and Methods

2.1. Cells and Reagents. Human non-small-cell lung cancer cells (NCI-H460) were obtained from the American Type Culture Collection (ATCC) Manassas, VA, USA. Cells were cultured in RPMI 1640 medium supplemented with 5% fetal bovine serum, 2 mM L-glutamine, 100 IU/mL penicillin, and 100 µg/mL streptomycin (Gibco, MD, USA) in a humidified atmosphere of 5% CO₂ at 37°C. For long-term exposure experiments, cells were cultured in medium containing NO donor dipropyleneetriamine (DPTA) NONOate (0, 5, and 10 µM) for 7 and 14 days, respectively. The culturing medium was replaced by medium containing the freshly prepared NO donor every 2 days. The NO donor dipropyleneetriamine (DPTA) NONOate was purchased from Santa Cruz Biotechnology (Santa Cruz, CA, USA). The 3-(4,5-dimethylthiazol-2-yl)-2,5-diphenyltetrazolium bromide (MTT), Hoechst 33342, phalloidin tetramethylrhodamine B isothiocyanate, sulforhodamine B (SRB), bovine serum albumin (BSA), and dimethylsulfoxide (DMSO) were purchased from Sigma Chemical, Inc. (St. Louis, MO, USA). Antibodies for phosphorylated Akt (S473), Akt, phosphorylated FAK (Y397), FAK, Cdc42, Cav-1, β-actin, and peroxidase-conjugated secondary antibodies were obtained from Cell Signaling (Danvers, MA, USA). Lipofectamine 2000 and PrestoBlue were obtained from Invitrogen (Carlsbad, CA, USA).

2.2. Plasmids and Transfection. The Cav-1 expression plasmid was obtained from the American Type Culture Collection (ATCC) Manassas, VA, USA, and the Cav-1 short hairpin knockdown plasmid (shRNA-Cav-1) was obtained from Santa Cruz Biotechnology (Santa Cruz, CA, USA). Stable transfection of cells with the Cav-1 expression plasmid or the Cav-1 knockdown plasmid was achieved by culturing the cells until they reached approximately 60% confluence. Then, 15 µL lipofectamine 2000 reagent and 2 µg Cav-1 expression plasmid, shRNA-Cav-1, or control plasmid were used to transfect the cells in the absence of serum. After 12 h, the medium was replaced with fresh culture medium containing 5% FBS. Approximately 36 h after the beginning of the transfection, the cells were digested with 0.03% trypsin, and the cell suspensions were plated in 75 mL culture flasks and cultured for 20 to 30 days with antibiotic selection. The stable

transfectants were pooled, and the expression of the Cav-1 protein in the transfectants was confirmed by Western blotting. The cells were cultured in antibiotic-free RPMI 1640 medium for at least two passages before experiments were performed.

2.3. Cytotoxicity Assay. Cell viability was determined using the MTT assay. After treatment, the cells were treated with MTT (5.0 mg/mL in PBS) and incubated for 4 h at 37°C. Then, the MTT solution was removed, and 100 µL DMSO was added to dissolve the formazan crystal. The intensity of the formazan product was measured at 570 nm using a microplate reader (Anthros, Durham, NC, USA). The percentage of cell viability was calculated using the following formula:

$$\text{cell viability (\%)} = \frac{(\text{A570 of treatment} \times 100)}{\text{A570 of control}} \quad (1)$$

2.4. Cell Proliferation Assay. Cells were exposed to the NO donor at various concentrations and were subjected to the cell proliferation assay for 0, 24, and 48 h. Cells were seeded at a density of 5×10^3 cells/well in a 96-well plate. Cell proliferation was determined through incubation with PrestoBlue at a 1:10 dilution for 1 h, and the fluorescence intensity of the resazurin product (Resorufin) was measured at 530 nm (excitation wavelength) and 590 nm (emission wavelength).

2.5. Cell Migration. Cell migration was determined using a wound-healing assay. Cells were grown to a confluent monolayer in a 24-well plate, and then a scrape was made down the center of the well using a P200 micropipette tip. The well was then rinsed with phosphate-buffered saline (PBS) and replaced with RPMI medium. At the indicated times (0, 12, and 24 h), the wound spaces were imaged under a phase-contrast microscope (10X) (Olympus IX51 with DP70), and the wound spaces were measured on the image field at four points per field. Relative cell migration was calculated by dividing the percentage change in the wound space of the treated cells by that of the control cells in each experiment.

2.6. Invasion Assay. The invasion assay was performed using a Boyden chamber precoated with 50 µL 0.5% Matrigel (BD Biosciences, MA, USA) on the upper surface of the chamber [29]. Cells were seeded at a density of 3×10^4 cells/well in the upper chamber in serum-free conditions. RPMI medium containing 10% FBS was added to the lower chamber of the unit. After incubation for 24 h at 37°C, the cells in the upper chamber were removed with a cotton swab and the cells in the bottom unit were fixed with cold absolute methanol for 10 min and stained with 10 µg/mL Hoechst 33342 for 10 min. The cells were then visualized and scored under a fluorescence microscope (Olympus IX51 with DP70).

2.7. Morphological Characteristics of Cancer Cells. Cell morphology was investigated using phalloidin-rhodamine and sulforhodamine B staining assays. After NO exposure, the cells were fixed with 4% paraformaldehyde in PBS for 10 min

at 37°C, permeabilized with 0.1% Triton-X100 in PBS for 4 min, rinsed with PBS, and then blocked with 0.2% BSA for 30 min. The cells were then incubated with either a 1:100 dilution of phalloidin-rhodamine in PBS or 0.4% sulforhodamine B in 1% acetic acid for 15 min; the cells were then rinsed 3 times with PBS and mounted with 50% glycerol. The cell morphology was imaged using a fluorescence microscope (Olympus IX51 with DP70).

2.8. Western Blotting. After specific treatment, cells were incubated with lysis buffer containing 20 mM Tris-HCl (pH 7.5), 1% Triton X-100, 150 mM sodium chloride, 10% glycerol, 1 mM sodium orthovanadate, 50 mM sodium fluoride, 100 mM phenylmethylsulfonyl fluoride, and protease inhibitor cocktail (Roche Molecular Biochemicals) for 30 min on ice. The cell lysates were collected and determined for protein content using the BCA protein assay kit (Pierce Biotechnology, Rockford, IL, USA). Equal amounts of protein from each sample (40 µg) were denatured by heating at 95°C for 5 min with Laemmli loading buffer and loaded onto 10% SDS-polyacrylamide gel electrophoresis. After separation, proteins were transferred onto 0.45 µm nitrocellulose membranes (Bio-Rad). The transferred membranes were blocked in 5% nonfat dry milk in TBST (25 mM Tris-HCl (pH 7.5), 125 mM NaCl, and 0.05% Tween 20) for 30 min and incubated with the appropriate primary antibodies overnight at 4°C. Membranes were washed three times with TBST for 10 min and incubated with horseradish peroxidase- (HRP-) labeled secondary antibodies for 1 h at room temperature. The immune complexes were detected by chemiluminescence (Supersignal West Pico; Pierce, Rockford, IL, USA) and quantified using analyst/PC densitometry software (Bio-Rad).

2.9. Statistical Analysis. The mean data from independent experiments were normalized to the results of the control cells. The values are presented as the mean ± standard deviation (SD) from three or more independent experiments and were analyzed using one-way ANOVA with a post-hoc test (Tukey's test) at a significance level of $P < 0.05$ using SPSS version 16.0.

3. Results

3.1. Effect of NO Donor on the Viability of the Human Lung Cancer H460 Cell Line. We first characterized the effects of NO donor on the viability of the human lung cancer H460 cell line. The H460 cells were cultured in the presence and absence of DPTA NONOate (1–20 µM), a slow-releasing NO donor compound, for 24 h, and cell viability was determined. Figure 1(a) shows that when cells were treated with the NO donor, at concentrations ranging 1–10 µM, neither cytotoxicity nor proliferative effects were observed in the cells. A significant decrease in viability was first detected in cells treated with 20 µM DPTA NONOate; however, approximately 90% of the cells still remained viable. Accordingly, our results indicated that at the indicated doses, the NO donor did not cause a significant effect on cell viability up to 72 h of NO exposure (data not shown). To

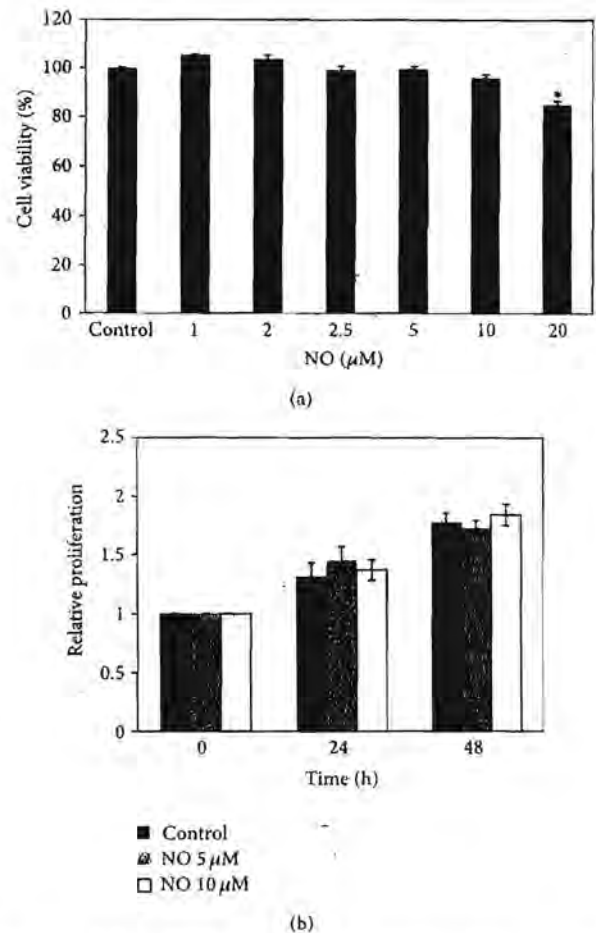


FIGURE 1; Effect of NO donor on cytotoxicity in lung carcinoma H460 cells. (a) Effect of DPTA NONOate on H460 cell viability. H460 cells were treated with various concentrations (0–20 µM) of DPTA NONOate for 24 h. The cell viability was analyzed using the MTT assay. (b) Proliferative effect of DPTA NONOate on H460 cells. Cell proliferation for 24 and 48 h was determined using PrestoBlue. The data are the mean ± SD ($n = 3$). * $P < 0.05$ versus the nontreated control.

investigate the effect of long-term NO treatment on cell proliferation, H460 cells were cultured in their optimal conditions supplemented with 5 or 10 µM NO donor, and their proliferative behavior was evaluated using PrestoBlue. As Figure 1(b) indicates, the NO-treated cells exhibited no significant changes in cell proliferation during the test period.

3.2. Long-Term NO Exposure Potentiates Migration and Invasion of H460 Cells. To investigate the effect of NO on cell migration, we performed scratch wound-healing assays. Cells were exposed to NO for 7 or 14 days and were subjected to the migration assay for 12 and 24 h. Figures 2(a) and 2(b) show that long-term treatment with the NO donor significantly enhanced the motility of the cells in dose- and time-dependent manners as compared with the H460 control cells. Treatment with 10 µM DPTA NONOate for 14 days

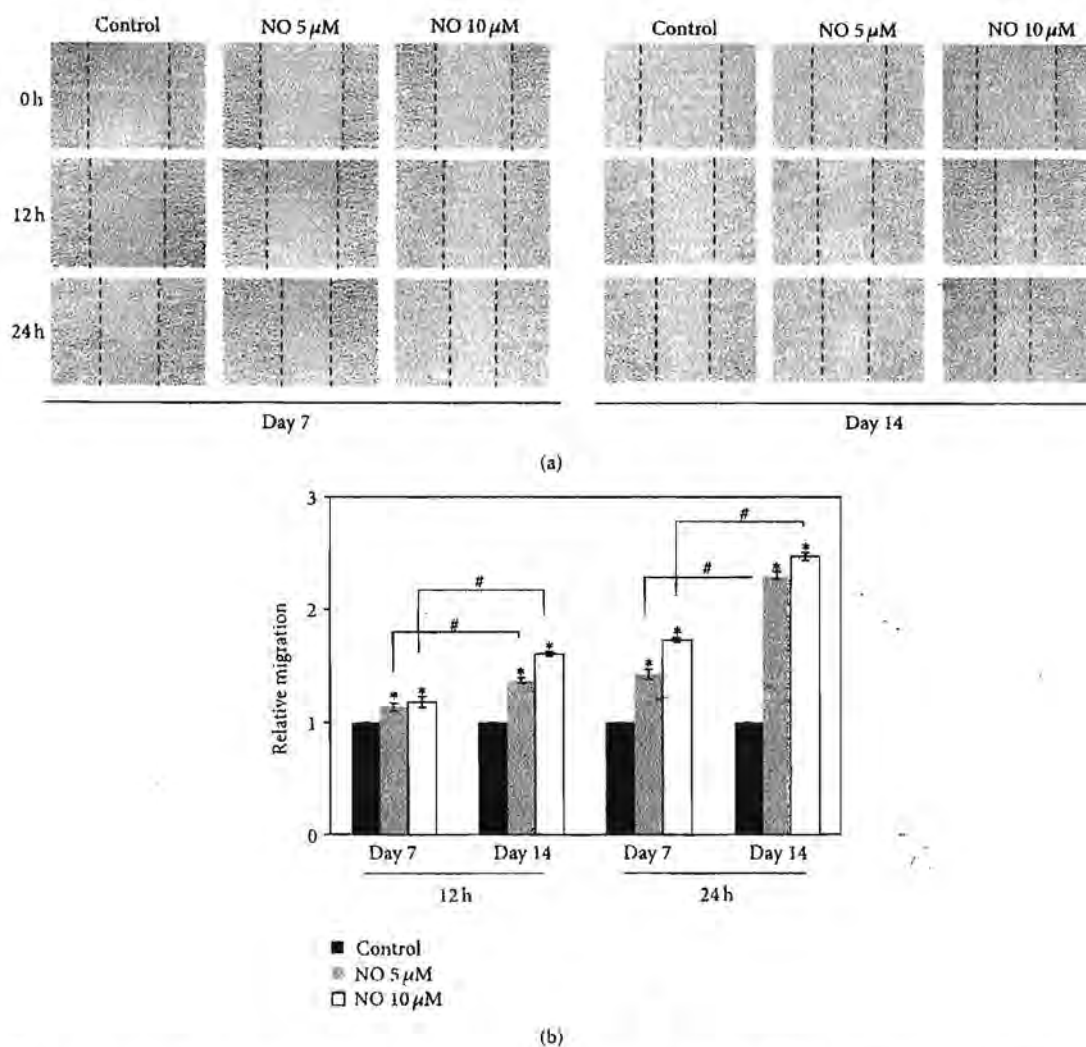


FIGURE 2: Effect of nitric oxide exposure on H460 cell migration. (a) Cells were exposed to NO donor at various concentrations for 7 or 14 days and subjected to a migration assay. Phase-contrast images were captured at 0, 12, and 24 h. (b) The relative cell migration was determined by comparing the relative change in wound space to the control cells. The data are the mean \pm SD ($n = 3$). * $P < 0.05$ versus the control cells, # $P < 0.05$ versus NO-treated cells at 7 days.

potentiated the migration of the cells approximately 2.5-fold as compared with the nontreated cells, as shown in Figure 2(b).

In addition, we investigated the effect of NO on H460 cell invasion using a precoated Matrigel Transwell unit, and we found that treatment with the NO donor at various concentrations (0, 5, and 10 μ M) for the indicated times significantly stimulated H460 cell invasion through the Matrigel, as shown in Figures 3(a) and 3(b).

3.3. NO Enhances Filopodia Formation in Lung Cancer Cells. Filopodia are generated through actin polymerization and rearrangement of actin filaments, and the formation of filopodia has been linked to increased tumor cell migration. To evaluate the effect of NO treatment on filopodia formation,

cells were exposed to NO as previously described, and the presence of filopodia was determined using a phalloidin-rhodamine staining assay. In addition to this staining, the cytoskeletal actin was also stained with sulforhodamine B dye. Figures 4(a) and 4(b) indicate that, when H460 cells were cultured in the presence of the NO donor, the cells exhibited an altered actin alignment and an increased number of filopodia.

3.4. The Long-Term NO Exposure Induces Cav-1-Dependent FAK and Akt Activation. Having demonstrated the potentiating effect of NO exposure on lung cancer cell motility, we next examined the underlying mechanism, focusing on the expression levels of the proteins known to play roles in cell migration. Cancer cells were treated with NO donor at

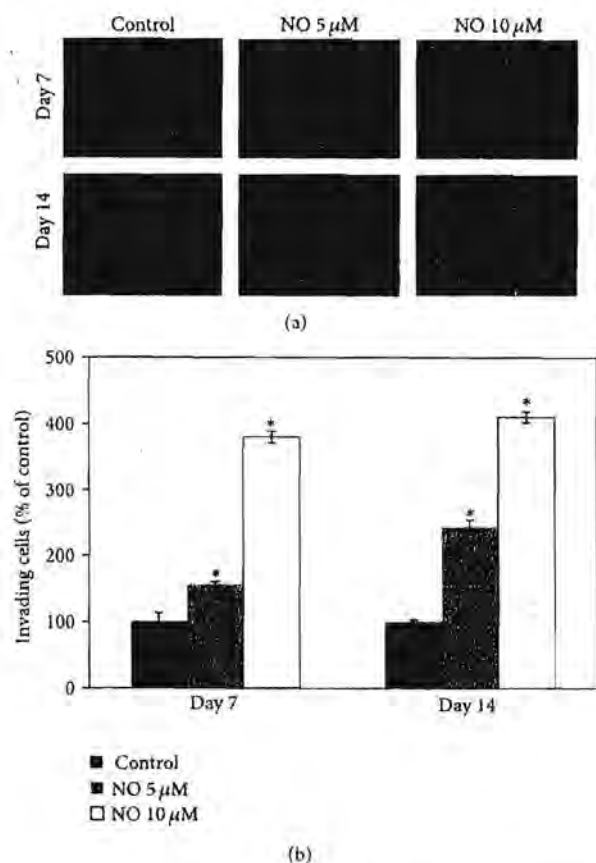


FIGURE 3: Effect of nitric oxide on H460 cell invasion. The invasion assay was performed using a Boyden chamber. (a) The cells that invaded the underside of the membrane were stained with 10 μ g/mL Hoechst 33342 for 10 min and visualized using a fluorescence microscope. (b) The relative cell invasion was determined as described in Materials and Methods. The data are the mean \pm SD ($n = 3$). * $P < 0.05$ versus the control cells.

different concentrations for 7 and 14 days and were analyzed by Western blotting. Expression levels of the migration-related proteins, namely, Cav-1, FAK, Akt, and Cdc42, were evaluated. Figures 5(a) and 5(b) show that NO exposure for 7 and 14 days significantly increased the levels of Cav-1, phosphorylated FAK (Tyr 397), phosphorylated Akt (Ser 473), and Cdc42, whereas NO exposure had no significant effect on the levels of total FAK and total Akt. Interestingly, the effects of NO on the mentioned proteins appeared to be dose- and time-dependent; cells treated with 10 μ M NO donor for 14 days exhibited the most pronounced changes in protein levels as compared to cells treated with 5 μ M NO donor or cells that were treated for a shorter period of time.

As Cav-1 has been shown to function as an adaptor protein that regulates the activities of other proteins as previously described [21], we tested whether the upregulation of the proteins mentioned previously was through Cav-1-dependent mechanism. Using gene manipulation approaches, Cav-1 overexpressed and knockdown cells were generated as

described in Materials and Methods. As expected, Western blot analysis of Cav-1 expression showed a substantial increase in Cav-1 protein level in the Cav-1-transfected cells, whereas a significant decrease in Cav-1 level was observed in the shRNA-Cav-1-transfected cells as compared with the control-transfected cells (Figure 6(a)). The Cav-1 overexpressing cells (H460/Cav-1), the Cav-1 knockdown cells (H460/ShCav-1), and the control H460 cells were cultured in the presence or absence of NO (5–10 μ M) for 14 days, and the levels of phosphorylated FAK (Tyr 397), phosphorylated Akt (Ser 473), and their total protein levels were determined. Figure 6(b) shows that the Cav-1 overexpressed cells (H460/Cav-1) exhibited a significantly increased level of phosphorylated FAK and phosphorylated Akt, whereas the total FAK and total Akt levels were not affected. In contrast, the NO-mediated FAK and Akt phosphorylation events were suppressed in the cells in which Cav-1 was knocked down (H460/ShCav-1 cells). These results indicate that long-term NO exposure in H460 cells induces FAK and Akt activation in a Cav-1-dependent manner.

4. Discussion

Worldwide, lung cancer is a leading cause of cancer-related death in both men and women [30], and approximately 90% of non-small-cell lung cancer deaths are attributed to cancer metastasis [28, 31]. Among the multiple steps of metastasis, migration of the cancer cells has been recognized as an important hallmark for the successful spread of cancer throughout the body [8, 9]. However, information regarding the key mediators that control the migratory activities of the cancer cells remains largely unknown. An increase in NO production has frequently been observed in the tissue surrounding the tumor and may be critical for some cancer cells behavior [3–7]. In addition, elevated NO production has been observed in the lung tissue of lung cancer patients in comparison with that of normal subjects [6, 7]. These findings have strengthened the idea that NO present in the lung cancer environment may affect the behavior of cancer cells.

NO is a gaseous molecule that is able to diffuse deeply into tissues; indeed, such a substance has been shown to regulate cell behaviors in many ways, including the relaxation of vascular smooth muscle [3, 32]. Controversial roles of NO have been reported for normal cell motility. NO was shown to inhibit vascular smooth muscle cell migration [32, 33]; however, the opposite effect was observed in the microglia cell model [32, 34]. Accordingly, both the inhibitory effect and promoting effect of NO on cancer cells have been reported [34, 35]. The variable effects of NO in tumors may depend on the localization of NO synthase and its activity, the concentration and duration of NO exposure, and the cellular sensitivity to NO [3–5, 32, 34, 36]. While the long-term effects of NO on lung cancer cell migration are still unknown, Hickok et al. showed that short-term treatment with an NO donor for 4, 6, and 24 h inhibited breast cancer cell migration through N-Myc downstream-regulated gene-1 (NDRG1) expression [35, 37]. However, in prostate cancer cells, NO was shown to potentiate cell motility [37, 38]. The

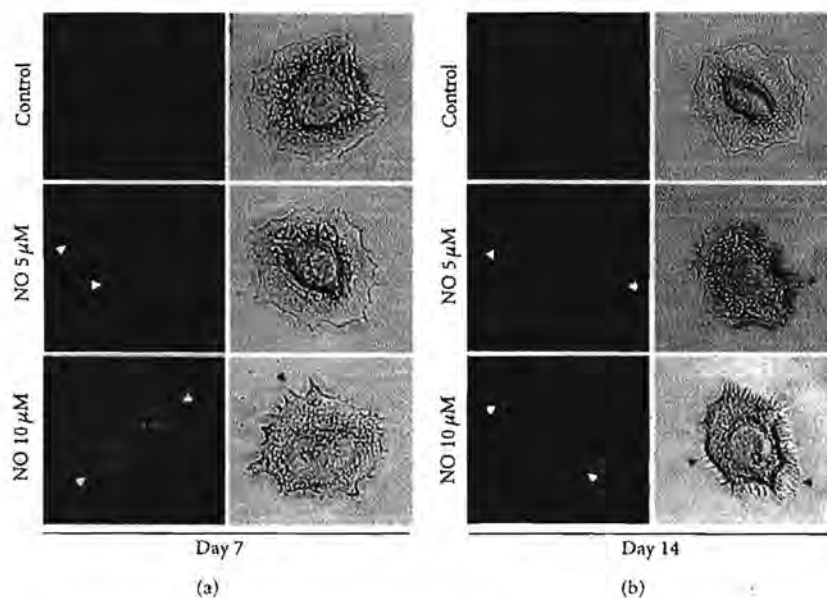


FIGURE 4: Filopodia formation in H460 cells treated with nitric oxide. H460 cells were treated with NO donor at concentrations of 0–10 μM for (a) 7 days and (b) 14 days. The cells were then stained with phalloidin-rhodamine and sulforhodamine B dye.

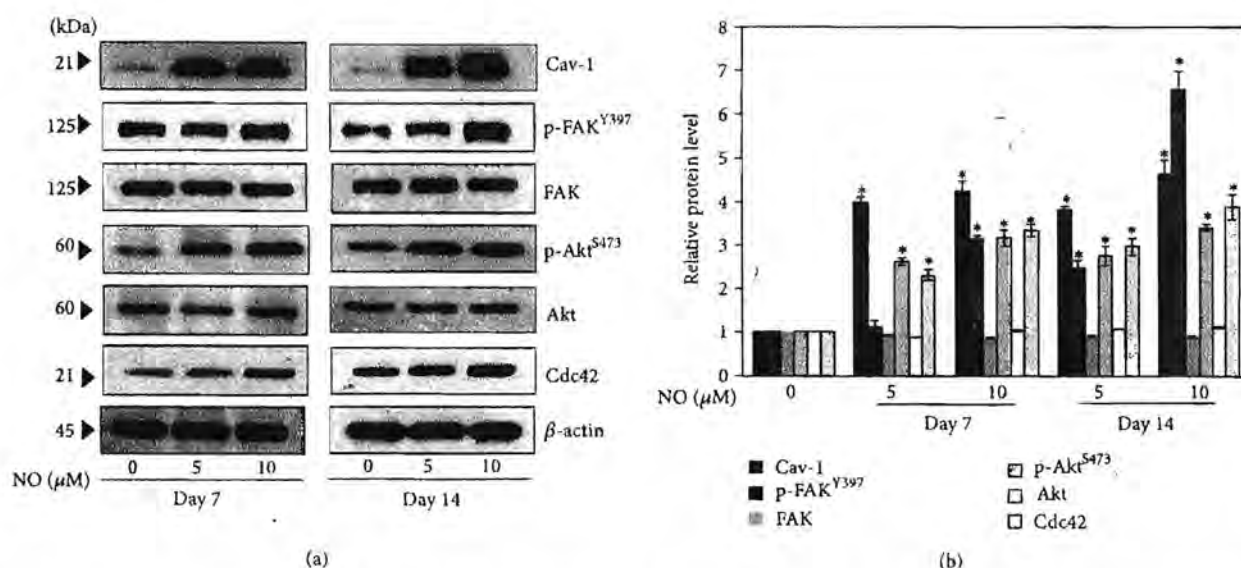


FIGURE 5: Nitric oxide exposure activates the FAK-Akt pathways. (a) NO-treated cells at 7 and 14 days were subjected to Western blotting, and the expression levels of phosphorylated FAK, total FAK, phosphorylated Akt, total Akt, Cdc42, and Cav-1 were determined. To confirm equal loading of the samples, the blots were reprobed with β -actin antibody. (b) The immunoblot signals were quantified by densitometry. The data are the mean \pm SD ($n = 3$). * $P < 0.05$ versus the nontreated control.

present study demonstrated the novel role of long-term NO exposure in the regulation of lung cancer cell migration that may be important for the fulfillment of cancer insights. Long-term exposure to NO enhances the cells motility via FAK- and Akt-dependent mechanisms. In addition, we provided evidence indicating that such an activation of the FAK-Akt pathway is dependent on the level of cellular Cav-1 (Figure 6).

Previous studies found that the phosphorylation of FAK at position Tyr 397 is critical for cell migration [12, 13].

Furthermore, FAK action on cell motility was shown to be involved with its downstream Akt [14, 39]. Our gene manipulation experiments further revealed the role of Cav-1 on FAK-Akt pathway. We found that phosphorylated FAK, as well as phosphorylated Akt, increased in response to long-term NO treatment of lung cell lines, and this response was limited in the Cav-1 knockdown cells. However, the upregulation of both phosphorylation events was shown to be intensified in the Cav-1 overexpressed cells (Figure 6). These

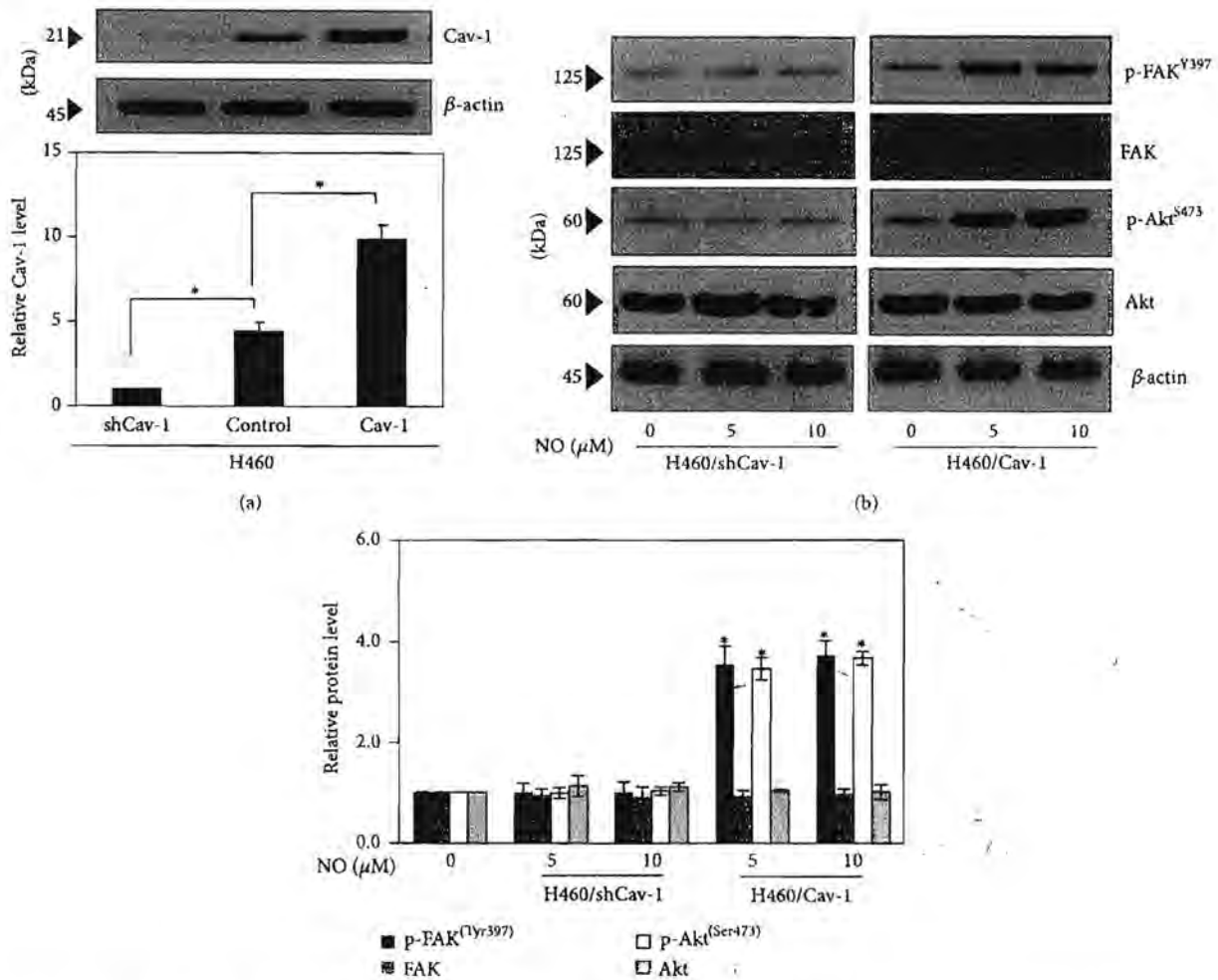


FIGURE 6: Nitric oxide mediated FAK-Akt activation via Cav-1-dependent mechanism. Stable Cav-1 overexpressed (H460/Cav-1) and Cav-1 knockdown (H460/ShCav-1) cell lines were established as indicated in Materials and Methods. (a) The expression level of Cav-1 protein in the control H460, H460/Cav-1, and H460/ShCav-1 cells was determined by Western blotting. (b) The cells were exposed to NO donor for 14 days, and the expression levels of phosphorylated FAK, total FAK, phosphorylated Akt, and total Akt were determined. The immunoblot signals were quantified by densitometry, and the mean data from the independent experiments were normalized to the control. The data are the mean \pm SD ($n = 3$). * $P < 0.05$ versus the control.

findings suggest that Cav-1 may have a novel influence on FAK-Akt-mediated cell migration in lung cancer cell models. Cav-1 is the principal component of caveolae membranes. Cav-1 has been reported to promote tumor cell migration and invasion, and an increase in Cav-1 expression is associated with tumor metastasis in lung cancer [17–27]. Consistent with its pro-survival role, Cav-1 positively regulated the growth of lung cancer H460 cells when these cells were treated with NO, as previously described [18]. Since an upregulation of NO, as well as Cav-1 protein, is associated with an aggressive status in lung cancer cells, therefore the results from this study may lead to a better understanding of lung cancer pathology.

Likewise, the small GTPase Cdc42 was shown to regulate actin filaments and the migration of tumor cells [10, 11]. In fibroblasts, Cdc42 induces the rapid formation and extension of filopodia, which are required for movement processes [11, 15, 16]. We investigated how NO exposure affected the

actin organization in lung cancer cells and found that NO upregulates Cdc42 protein and enhances the formation of filopodia in these cells. It is worth noting that we did not see a significant change in the level of Cdc42 following ectopic Cav-1 expression (data not shown), suggesting that the NO-mediated Cdc42 increase in this study was through a Cav-1-independent mechanism. Although further investigations may be needed to examine the underlying mechanisms by which NO controls Cdc42 and filopodia formation, this study first revealed the novel effect NO has on cancer cell migration through a Cdc42-dependent mechanism.

5. Conclusion

We demonstrated the possible role of long-term NO exposure on the metastatic behaviors of cancer cells, including

migration and invasion. NO exposure activated the FAK-Akt signaling pathway through a Cav-1-dependent mechanism and increased filopodia formation. Elevated NO levels have been observed in cancer environments; thus the knowledge gained from the present study may benefit our understanding of cancer biology and may be useful in the development of cancer therapies.

Abbreviations

Akt: ATP-dependent tyrosine kinase
 Cav-1: Caveolin-1
 Cdc42: Cell division cycle 42
 FAK: Focal-adhesion kinase
 NO: Nitric oxide
 MTT: 3-(4,5-Dimethylthiazol-2-yl)-2,5-diphenyltetrazolium bromide
 p-Akt: Phosphorylated Akt
 PBS: Phosphate-buffered saline
 p-FAK: Phosphorylated-FAK
 TBST: Tris-buffered saline with 0.1% Tween.

Conflict of Interests

The authors declare that there is no conflict of interests in this research.

Acknowledgments

This work was supported by grants from the Thailand Research Fund (P. Chanvorachote) and the Ratchadaphiseksomphot Endowment Fund, Chulalongkorn University (RE-S560530132-HR). The authors would like to thank Mr. Krich Rajprasit for his assistance in proof-reading.

References

- [1] D. Hanahan and R. A. Weinberg, "The hallmarks of cancer," *Cell*, vol. 100, no. 1, pp. 57-70, 2000.
- [2] G. Manda, M. T. Nechifor, and T.-M. Neagu, "Reactive oxygen species, cancer and anti-cancer therapies," *Current Chemical Biology*, vol. 3, no. 1, pp. 22-46, 2009.
- [3] A. Keibel, V. Singh, and M. C. Sharma, "Inflammation, microenvironment, and the immune system in cancer progression," *Current Pharmaceutical Design*, vol. 15, no. 17, pp. 1949-1955, 2009.
- [4] P. K. Lala and C. Chakraborty, "Role of nitric oxide in carcinogenesis and tumour progression," *Lancet Oncology*, vol. 2, no. 3, pp. 149-156, 2001.
- [5] F. Masri, "Role of nitric oxide and its metabolites as potential markers in lung cancer," *Annals of Thoracic Medicine*, vol. 5, no. 3, pp. 123-127, 2010.
- [6] F. A. Masri, S. A. A. Comhair, T. Koeck et al., "Abnormalities in nitric oxide and its derivatives in lung cancer," *American Journal of Respiratory and Critical Care Medicine*, vol. 172, no. 5, pp. 597-605, 2005.
- [7] H. Esme, M. Cemek, M. Sezer et al., "High levels of oxidative stress in patients with advanced lung cancer," *Respirology*, vol. 13, no. 1, pp. 112-116, 2008.
- [8] D. H. Geho, R. W. Bandle, T. Clair, and L. A. Liotta, "Physiological mechanisms of tumor-cell invasion and migration," *Physiology*, vol. 20, no. 3, pp. 194-200, 2005.
- [9] L. A. Mina and G. W. Sledge Jr., "Rethinking the metastatic cascade as a therapeutic target," *Nature Reviews Clinical Oncology*, vol. 8, no. 6, pp. 325-332, 2011.
- [10] M. Parri and P. Chiarugi, "Rac and Rho GTPases in cancer cell motility control," *Cell Communication and Signaling*, vol. 8, no. 23, pp. 1-14, 2010.
- [11] C. D. Nobes and A. Hall, "Rho, Rac, and Cdc42 GTPases regulate the assembly of multimolecular focal complexes associated with actin stress fibers, lamellipodia, and filopodia," *Cell*, vol. 81, no. 1, pp. 53-62, 1995.
- [12] B. Serrels, A. Serrels, V. G. Brunton et al., "Focal adhesion kinase controls actin assembly via a FERM-mediated interaction with the Arp2/3 complex," *Nature Cell Biology*, vol. 9, no. 9, pp. 1046-1056, 2007.
- [13] L. A. Cary, J. F. Chang, and J.-L. Guan, "Stimulation of cell migration by overexpression of focal adhesion kinase and its association with Src and Fyn," *Journal of Cell Science*, vol. 109, no. 7, pp. 1787-1794, 1996.
- [14] S. K. Mitra, D. A. Hanson, and D. D. Schlaepfer, "Focal adhesion kinase: in command and control of cell motility," *Nature Reviews Molecular Cell Biology*, vol. 6, no. 1, pp. 56-68, 2005.
- [15] W. E. Allen, G. E. Jones, J. W. Pollard, and A. J. Ridley, "Rho, Rac and Cdc42 regulate actin organization and cell adhesion in macrophages," *Journal of Cell Science*, vol. 110, no. 6, pp. 707-720, 1997.
- [16] K. Kaibuchi, S. Kuroda, and M. Amano, "Regulation of the cytoskeleton and cell adhesion by the Rho family GTPases in mammalian cells," *Annual Review of Biochemistry*, vol. 68, pp. 459-486, 1999.
- [17] T. M. Williams and M. P. Lisanti, "Caveolin-1 in oncogenic transformation, cancer, and metastasis," *American Journal of Physiology-Cell Physiology*, vol. 288, no. 3, pp. C494-C506, 2005.
- [18] P. Chanvorachote, U. Nimmannit, Y. Lu, S. Talbott, B.-H. Jiang, and Y. Rojanasakul, "Nitric oxide regulates lung carcinoma cell anoikis through inhibition of ubiquitin-proteasomal degradation of caveolin-1," *Journal of Biological Chemistry*, vol. 284, no. 41, pp. 28476-28484, 2009.
- [19] S. Luanpitpong, S. J. Talbott, Y. Rojanasakul et al., "Regulation of lung cancer cell migration and invasion by reactive oxygen species and caveolin-1," *Journal of Biological Chemistry*, vol. 285, no. 50, pp. 38832-38840, 2010.
- [20] P. Rungtabnapa, U. Nimmannit, H. Halim, Y. Rojanasakul, and P. Chanvorachote, "Hydrogen peroxide inhibits non-small cell lung cancer cell anoikis through the inhibition of caveolin-1 degradation," *American Journal of Physiology-Cell Physiology*, vol. 300, no. 2, pp. C235-C245, 2011.
- [21] K. Pongjit and P. Chanvorachote, "Caveolin-1 sensitizes cisplatin-induced lung cancer cell apoptosis via superoxide anion-dependent mechanism," *Molecular and Cellular Biochemistry*, vol. 358, no. 1-2, pp. 365-373, 2011.
- [22] P. Chunhacha, V. Pongrakhananon, Y. Rojanasakul, and P. Chanvorachote, "Caveolin-1 regulates Mcl-1 stability and anoikis in lung carcinoma cells," *American Journal of Physiology-Cell Physiology*, vol. 302, no. 9, pp. C1284-C1292, 2012.
- [23] T. Songserm, V. Pongrakhananon, and P. Chanvorachote, "Subtoxic cisplatin mediates anoikis resistance through hydrogen peroxide-induced caveolin-1 up-regulation in non-small cell

- lung cancer cells," *Anticancer Research*, vol. 32, no. 5, pp. 1659–1669, 2012.
- [24] H. Halim, S. Luanpitpong, and P. Chanvorachote, "Acquisition of anoikis resistance up-regulates caveolin-1 expression in human non-small cell lung cancer cells," *Anticancer Research*, vol. 32, no. 5, pp. 1649–1658, 2012.
- [25] W. Suchaoain and P. Chanvorachote, "Caveolin-1 attenuates hydrogen peroxide-induced oxidative damage to lung carcinoma cells," *Anticancer Research*, vol. 32, no. 2, pp. 483–490, 2012.
- [26] P. Chunhacha and P. Chanvorachote, "Roles of caveolin-1 on anoikis resistance in non small cell lung cancer," *International Journal of Physiology, Pathophysiology and Pharmacology*, vol. 4, no. 3, pp. 149–155, 2012.
- [27] C.-C. Ho, P.-H. Huang, H.-Y. Huang, Y.-H. Chen, P.-C. Yang, and S.-M. Hsu, "Up-regulated caveolin-1 accentuates the metastasis capability of lung adenocarcinoma by inducing filopodia formation," *American Journal of Pathology*, vol. 161, no. 5, pp. 1647–1656, 2002.
- [28] F. Sotgia, U. E. Martinez-Outschoorn, A. Howell, R. G. Pestell, S. Pavlides, and M. P. Lisanti, "Caveolin-1 and cancer metabolism in the tumor microenvironment: markers, models, and mechanisms," *Annual Review of Pathology: Mechanisms of Disease*, vol. 7, pp. 423–467, 2012.
- [29] V. P. Terranova, E. S. Hujanen, D. M. Loeb, G. R. Martin, L. Thornburg, and V. Glushko, "Use of a reconstituted basement membrane to measure cell invasiveness and select for highly invasive tumor cells," *Proceedings of the National Academy of Sciences of the United States of America*, vol. 83, no. 2, pp. 465–469, 1986.
- [30] D. M. Parkin, F. Bray, J. Ferlay, and P. Pisani, "Global cancer statistics, 2002," *CA: A Cancer Journal for Clinicians*, vol. 55, no. 2, pp. 74–108, 2005.
- [31] M. Paesmans, J. P. Sculier, P. Libert et al., "Prognostic factors for survival in advanced non-small-cell lung cancer: univariate and multivariate analyses including recursive partitioning and amalgamation algorithms in 1,052 patients," *Journal of Clinical Oncology*, vol. 13, no. 5, pp. 1221–1230, 1995.
- [32] S. Moncada and A. Higgs, "The L-arginine-nitric oxide pathway," *The New England Journal of Medicine*, vol. 329, no. 27, pp. 2002–2012, 1993.
- [33] R. Sarkar, E. G. Meinberg, J. C. Stanley, R. D. Gordon, and R. C. Webb, "Nitric oxide reversibly inhibits the migration of cultured vascular smooth muscle cells," *Circulation Research*, vol. 78, no. 2, pp. 225–230, 1996.
- [34] A. Chen, S. M. Kumar, C. L. Sahley, and K. J. Muller, "Nitric oxide influences injury-induced microglial migration and accumulation in the leech CNS," *Journal of Neuroscience*, vol. 20, no. 3, pp. 1036–1043, 2000.
- [35] A. Dhar, J. M. Brindley, C. Stark, M. L. Citro, L. K. Keefer, and N. H. Colburn, "Nitric oxide does not mediate but inhibits transformation and tumor phenotype," *Molecular Cancer Therapeutics*, vol. 2, no. 12, pp. 1285–1293, 2003.
- [36] D. Fukumura, S. Kashiwagi, and R. K. Jain, "The role of nitric oxide in tumour progression," *Nature Reviews Cancer*, vol. 6, no. 7, pp. 521–534, 2006.
- [37] J. R. Hickok, S. Sahni, Y. Mikhed, M. G. Bonini, and D. D. Thomas, "Nitric oxide suppresses tumor cell migration through N-Myc downstream-regulated gene-1 (NDRG1) expression: role of chelatable iron," *Journal of Biological Chemistry*, vol. 286, no. 48, pp. 41413–41424, 2011.
- [38] C. Polytarchou, M. Hatziapostolou, E. Poimenidi et al., "Nitric oxide stimulates migration of human endothelial and prostate cancer cells through up-regulation of pleiotrophin expression and its receptor protein tyrosine phosphatase $\beta/1$," *International Journal of Cancer*, vol. 124, no. 8, pp. 1785–1793, 2009.
- [39] J. Turečková, M. Vojtěchová, M. Krausová, E. Šloncová, and V. Korínek, "Focal adhesion kinase functions as an akt downstream target in migration of colorectal cancer cells," *Translational Oncology*, vol. 2, no. 4, pp. 281–290, 2009.

CALL FOR PAPERS | Stem Cell Physiology and Pathophysiology

Nitric oxide induces cancer stem cell-like phenotypes in human lung cancer cells

Nuttida Yongsanguanchai,¹ Varisa Pongrakhananon,^{2,3} Apiwat Mutirangura,⁴ Yon Rojanasakul,⁵ and Pithi Chanvorachote^{2,3}

¹Pharmaceutical Technology (International) Program, Chulalongkorn University, Bangkok, Thailand; ²Department of Pharmacology and Physiology, Faculty of Pharmaceutical Sciences, Chulalongkorn University, Bangkok, Thailand; ³Cell-Based Drug and Health Products Development Research Unit, Chulalongkorn University, Bangkok, Thailand; ⁴Center of Excellence in Molecular Genetics of Cancer and Human Diseases, Department of Anatomy, Faculty of Medicine, Chulalongkorn University, Bangkok, Thailand; ⁵School of Pharmacy, West Virginia University, Morgantown, West Virginia

Submitted 19 June 2014; accepted in final form 7 November 2014

Yongsanguanchai N, Pongrakhananon V, Mutirangura A, Rojanasakul Y, Chanvorachote P. Nitric oxide induces cancer stem cell-like phenotypes in human lung cancer cells. *Am J Physiol Cell Physiol* 308: C89–C100, 2015. First published November 19, 2014; doi:10.1152/ajpcell.00187.2014.—Even though tremendous advances have been made in the treatment of cancers during the past decades, the success rate among patients with cancer is still dismal, largely because of problems associated with chemo/radioresistance and relapse. Emerging evidence has indicated that cancer stem cells (CSCs) are behind the resistance and recurrence problems, but our understanding of their regulation is limited. Rapid reversible changes of CSC-like cells within tumors may result from the effect of biological mediators found in the tumor microenvironment. Here we show how nitric oxide (NO), a key cellular modulator whose level is elevated in many tumors, affects CSC-like phenotypes of human non-small cell lung carcinoma H292 and H460 cells. Exposure of NO gradually altered the cell morphology toward mesenchymal stem-like shape. NO exposure promoted CSC-like phenotype, indicated by increased expression of known CSC markers, CD133 and ALDH1A1, in the exposed cells. These effects of NO on stemness were reversible after cessation of the NO treatment for 7 days. Furthermore, such effect was reproducible using another NO donor, *S*-nitroso-*N*-acetylpenicillamine. Importantly, inhibition of NO by the known NO scavenger 2-(4-carboxy-phenyl)-4,4,5,5-tetramethylimidazole-1-*oxy*-3-oxide strongly inhibited CSC-like aggressive cellular behavior and marker expression. Last, we unveiled the underlying mechanism of NO action through the activation of caveolin-1 (Cav-1), which is upregulated by NO and is responsible for the aggressive behavior of the cells, including anoikis resistance, anchorage-independent cell growth, and increased cell migration and invasion. These findings indicate a novel role of NO in CSC regulation and its importance in aggressive cancer behaviors through Cav-1 upregulation.

cancer stem cells; nitric oxide; caveolin-1; CD133; ALDH1A1; non-small cell lung carcinoma

ACCORDING TO THE AMERICAN CANCER SOCIETY 2013 annual cancer statistics, lung cancer remains one of the most common malignancies and is the leading cause of cancer-related deaths worldwide (61). Increasing evidence has indicated the role of

cancer stem cells (CSCs) in cancer aggressiveness, chemoresistance, and relapse; they are being considered as the underlying causes of the high mortality rate of cancer (29, 47, 50, 55). The concept of a tumor having a heterogeneous cancer cell population with a subpopulation of cells possessing a high tumorigenic potential and stem-like property was first described in 1997 (5). This subpopulation is commonly known as tumor-initiating cells, tumor-propagating cells, or CSCs and has been identified in many types of cancer (16, 23, 40, 46, 56, 58, 63). CSCs have been suggested as the rationale behind chemo/radioresistance and cancer relapse (3, 4, 18, 39, 68) and have been a target of new cancer therapeutic strategies.

Nitric oxide (NO), a free radical gaseous molecule, is renowned for its involvement in various biological, physiological, and pathological processes (52). NO was initially identified as a transcellular messenger molecule synthesized by a family of enzymes called NO synthases (NOS), comprised of inducible NOS, endothelial NOS, and neuronal NOS, through the conversion of L-arginine in the presence of oxygen and NADPH (48, 51). A number of studies pointed out that all three isoforms of NOS are involved in the process of cancer development and progression (1, 25, 64, 66). Not only is NOS expression detectable in various cancers, but also the NO level is frequently upregulated in tumor areas (26, 36). Previous studies indicated that NO could render cells resistant to death induced by various stimuli (7, 8, 67). NO also regulates cancer cell migration and invasion (60), and increased NOS expression and activity have been reported in metastatic lung cancer cells (57). Clinical data further support the role of NO in lung cancer and metastasis. A high level of NO was observed in the lung of patients with lung cancer (43, 49), and a positive correlation has been reported between NO, its stable end-products nitrite and nitrate, and its generator NOS with advanced cancer staging and poor survival in patients with lung cancer (2, 15, 24). Animal studies further showed that genetic ablation of NOS suppressed lung tumor formation in mice (35). Together, these studies strongly support the role of NO in tumorigenesis and metastasis although the underlying mechanisms remain obscure.

We hypothesize that NO may mediate its procarcinogenic effects through CSCs because of their importance in cancer aggressiveness described above. We also hypothesize that NO

Address for reprint requests and other correspondence: P. Chanvorachote, Depts. of Pharmacology and Physiology, Faculty of Pharmaceutical Sciences, Chulalongkorn Univ., Pathumwan, Bangkok, Thailand 10330 (e-mail: pithi.c@chula.ac.th).

may mediate its effects through caveolin-1 (Cav-1) because its expression has been linked to cancer aggressiveness (11, 27, 28, 30, 42, 45, 59) and because NO has been shown to be a key regulator of Cav-1 in human lung cancer cells (7). Cav-1 is a scaffolding protein found in the cellular structure caveolae, which has been shown by our group and others to regulate the aggressiveness of cancer cells by increasing their motility and resistance to anoikis (11, 27, 28, 30, 42, 45, 59). It has also been shown to increase cell survival under nonadherent conditions via Mcl-1 stabilization (12) and upregulation of activated protein kinase B (Akt) (6). In this study, we used molecular and pharmacological approaches to investigate the role of NO in Cav-1 and CSC regulation and their impact on the invasive and anoikis properties of human lung cancer cells. We demonstrated for the first time that NO plays an important role in the CSC-like transformation of lung cancer cells. Cav-1 is upregulated during the transformation and is responsible for the anoikis resistance and invasive properties of the cells although it is not required for the stem-like phenotype.

MATERIALS AND METHODS

Cell culture and NO exposure. Human non-small cell lung cancer cell lines, NCI-H292 and NCI-H460, were obtained from the American Type Culture Collection (Manassas, VA). The cells were cultivated in Roswell Park Memorial Institute (RPMI) 1640 medium supplemented with 10% fetal bovine serum (FBS), 2 mM L-glutamine, and 100 U/ml penicillin and streptomycin. Cell cultures were maintained in a 37°C humidified incubator with 5% CO₂. Cells were routinely passaged at preconfluent density using a 0.25% trypsin solution with 0.53 mM EDTA. RPMI 1640 medium, FBS, L-glutamine, penicillin/streptomycin, phosphate-buffered saline (PBS), trypsin, and EDTA were purchased from GIBCO (Grand Island, NY). Cells were seeded into six-well plates at an initial plating density of 2×10^5 cells/well. Cells were allowed to adhere to the surface of the plates for 4 h, after which they were treated with the indicated concentrations of freshly prepared NO donor. The treated cells were subcultured and exposed to fresh NO every 3 days. The cells were subsequently collected at days 7 and 14 posttreatment for further analysis. The NO donor dipropyleneetriamine (DPTA) NONOate and NO scavenger 2-(4-carboxy-phenyl)-4,4,5,5-tetramethylimidazole-1-oxyl-3-oxide (PTIO) were obtained from Santa Cruz Biotechnology (Santa Cruz, CA), whereas another NO donor S-nitroso-N-acetylpenicillamine (SNAP) was obtained from Invitrogen (Carlsbad, CA).

Cytotoxicity and proliferation assays. For cytotoxicity assay, cells were seeded onto 96-well plates at a density of 1×10^4 cells/well and were allowed to incubate overnight. Cells were then treated with various concentrations of NO donor and analyzed for cell viability using 3-(4,5-dimethylthiazol-2-yl)-2,5-diphenyltetrazolium bromide (MTT) assay according to the manufacturer's protocol (Sigma Chemical, St. Louis, MO). The cytotoxicity index was calculated by dividing the absorbance of the treated cells by that of the control cells. For cell proliferation assay, cells were seeded onto 96-well plates at a density of 5×10^3 cells/well and were left to settle overnight. Cell proliferation was determined by PrestoBlue assay according to the manufacturer's protocol (Invitrogen).

Cell death assay. Nuclear costaining with Hoechst 33342 (Sigma Chemical) and propidium iodide (PI) (Sigma Chemical) was used to determine apoptotic and necrotic cell death. Cells were incubated with 10 μ M Hoechst 33342 and 5 μ M PI for 30 min at 37°C. They were visualized and imaged under a fluorescence microscope (Olympus IX51 with DP70).

Migration assay. Wound-healing assay was used to determine cell migration. Briefly, confluent monolayers of cells in a 96-well plate were wounded at the center of the well by a 200- μ l micropipette tip.

Four random fields of the wound space were examined and imaged under a phase-contrast microscope (Olympus IX51 with DP70) at various time points. Relative cell migration was quantified by dividing the percentage change of the wound space in treated cells to that of the control cells.

Invasion assay. The assay was performed in modified Boyden chambers with 8- μ m-pore filter inserts in 24-well plates (Corning Life Sciences, Corning, NY). The upper chamber of the inserts was coated with 50 μ l of 0.5% Matrigel from BD Biosciences (San Jose, CA), and 3×10^4 cells in serum-free medium were added on top. The lower chamber was filled with RPMI 1640 medium containing 10% FBS as a chemoattractant. After 24 h, the noninvading cells in the upper chamber were removed with a cotton swab, and the invading cells in the lower chamber were fixed with ice-cold methanol for 10 min and stained with 10 μ g/ml of Hoechst 33342 for 10 min. The stained cells were then visualized and scored under a fluorescence microscope (Olympus IX51 with DP70).

Anoikis assay. Cells were trypsinized into single-cell suspension before being seeded onto Costar six-well ultralow attachment plates (Corning Life Sciences). Suspended cells were incubated at 37°C and were harvested for analysis at various time points. Cell viability was assessed by MTT assay as described above.

Anchorage-independent growth assay. Anchorage-independent cell growth was determined by soft agar colony-formation assay. Soft agar was prepared by using a 1:1 mixture of RPMI 1640 medium containing 10% FBS and 1% agarose. The mixture was allowed to solidify in a 24-well plate to form a bottom layer, after which an upper cellular layer consisting of 3×10^3 cells/ml in the agarose gel with 10% FBS and 0.3% agarose was added. After the upper layer was solidified, RPMI medium containing 10% FBS was added to the system and incubated at 37°C. Colony formation was determined after 2 wk using a phase-contrast microscope (Olympus IX51 with DP70). Relative colony number and diameter were determined by dividing the values of the treated cells by those of the control cells.

Spheroid-formation assay. Spheroids were grown using an adjusted method from Kantara et al. (33). Approximately 5×10^3 cells/well were seeded onto a 12-well ultralow attachment plate using RPMI serum-free medium. Treated cells were treated every 3 days. Phase-contrast images of formed primary spheroids were taken at day 7 of treatment using a phase-contrast microscope (Olympus IX51 with DP70). Primary spheroids were resuspended into single cells, and again 5×10^3 cells/well were seeded onto a 12-well ultralow attachment plate using RPMI serum-free medium. Secondary spheroids were allowed to form for 30 days.

Western blot analysis. Cells were incubated on ice for 45 min with lysis buffer containing 20 mM Tris-HCl (pH 7.5), 1% Triton X-100, 150 mM NaCl, 10% glycerol, 1 mM Na₂VO₄, 50 mM NaF, 100 mM PMSF, and protease inhibitor mixture from Roche Molecular Biochemicals (Indianapolis, IN). Cell lysates were analyzed for protein content using BCA protein assay kit from Pierce Biotechnology (Rockford, IL). Equal amounts of denatured protein samples (40 μ g) were loaded onto 10% SDS-PAGE for ALDH1A1 and Cav-1 analysis or onto 7.5% SDS-PAGE for CD133 analysis before being transferred to 0.45- μ m nitrocellulose membranes (Bio-Rad, Hercules, CA). Transferred membranes were blocked with medium [25 mM Tris-HCl (pH 7.5), 125 mM NaCl, and 0.05% Tween 20 (TBST)] containing 5% nonfat dry milk powder for 30 min and incubated overnight with specific primary antibodies against CD133 (Cell Applications, San Diego, CA), ALDH1A1 (Santa Cruz Biotechnology), Cav-1 (Cell Signaling Technology, Beverly, MA), and β -actin (Santa Cruz Biotechnology). Membranes were washed three times with TBST and incubated with the following appropriate horseradish peroxidase-labeled secondary antibodies: anti-rabbit IgG (Cell Signaling Technology), anti-mouse IgG (Cell Signaling Technology), or anti-goat IgG (Santa Cruz Biotechnology), for 2 h at room temperature. The immune complexes were detected by SuperSignal West Pico chemiluminescent substrate (Pierce Biotechnology) and exposed to film.

Immunofluorescence. Cells were seeded onto six-well plates at a density of 5×10^5 cells/well and allowed to adhere for 24 h. The cells were fixed at room temperature for 10 min with 3.7% formaldehyde and blocked for 30 min in a solution containing 0.5% saponin, 1% FBS, and 1.5% goat serum. Cells were then incubated with CD133 (Cell Applications) primary antibody for 2 h before being washed and incubated with Alexa Fluor 488-conjugated goat anti-rabbit IgG (H+L) secondary antibody (Invitrogen) for 1 h. Hoechst 33342 was used to stain the cell nucleus. Immunofluorescence images were acquired via confocal laser-scanning microscopy (Zeiss LSM 510).

Flow-cytometry analysis. Treated and nontreated cells were collected using 1 mM EDTA at day 14 of treatment. Briefly, cells were fixed, blocked, and then incubated on ice with CD133 primary antibody for 1 h, followed by 30-min incubation with Alexa Fluor 488-conjugated goat anti-rabbit IgG (H+L) secondary antibody on ice with light omitted. Fluorescence intensity was scored by flow cytometry using a 488-nm excitation beam and a 519-nm band-pass filter (FACSort; Becton Dickinson, Rutherford, NJ). The mean fluorescence intensity was quantified by CellQuest software (Becton Dickinson).

Plasmid and transfection. Transfection of Cav-1 and its shRNA plasmids was performed as previously described (6) with the following modifications. Briefly, subconfluent (70%) monolayers of H292 and H460 cells were transfected with pEX_Cav-1-YFP (ATTC) or shRNA-Cav-1 (Santa Cruz Biotechnology) plasmid in serum-free RPMI 1640 medium using Lipofectamine 2000 reagent, according to the manufacturer's protocol (Invitrogen). After 2 h (H292) or 12 h (H460), the medium was replaced with RPMI 1640 containing 10% FBS. The cells were then cultured and selected for antibiotic resistance for 30 days to obtain stable transfectants. Expression of the targeted proteins was verified by Western blot assay. The cells were cultured in antibiotic-free RPMI 1640 medium for at least two passages before further experiments.

Statistical analysis. All treatment data were normalized to nontreated controls. Data are presented as the means \pm SD from at least four independent experiments. Statistical differences were determined using two-way ANOVA and a post hoc test at a significance level of $P < 0.05$.

RESULTS

Effect of DPTA NONOate on human lung cancer cell epithelial-mesenchymal transition. Elevated NO levels have been associated with cancer cell behaviors such as anoikis resistance, increased cell motility, and chemoresistance (8, 60, 67). To test whether NO might affect epithelial-mesenchymal transition (EMT) properties of lung cancer cells, we first determined the appropriate nontoxic concentrations of NO donor used in this study. Human lung cancer H292 and H460 cells were treated with various concentrations of DPTA NONOate (0–50 μ M), and cell viability was determined after 24 h by MTT assay. DPTA NONOate was relatively nontoxic at the doses below 30 μ M in H292 cells and below 15 μ M in H460 cells (data not shown). The low-dose DPTA treatments were stained by Hoechst 33342 and PI for apoptotic and necrotic cell death. The lack of DNA condensation/fragmentation and nuclear PI fluorescence indicated that cells do not undergo apoptosis or necrosis (data not shown). To determine the effect of NO donor treatment on cell morphology, H292 and H460 cells were treated with the nontoxic concentrations of DPTA NONOate, and cell morphology was examined microscopically. Figure 1, A and B, shows phase-contrast images of the treated cells on days 7 and 14 posttreatment. A gradual but clearly noticeable change in cell morphology toward the mesenchymal stem cell-like (spindle-like) phenotype was evident in both the treated H292 and H460 cells

compared with nontreated controls. The cell population lysates were probed for EMT markers, Vimentin and Snail, by Western blotting. Figure 1, C and D, shows that the NO donor induced Vimentin and Snail expression in a dose- and time-dependent manner. Approximately up to fourfold increases in both Vimentin and Snail protein levels were shown for H292 cells treated with 25 μ M DPTA for 14 days and approximately threefold for H460 cells treated with 10 μ M DPTA for 14 days. We then examined the effect of NO donor on cell migration and invasion by wound-healing assays and Boyden chamber invasion assays, respectively. Not only are EMT cells well known for their metastatic ability, but also previous studies have shown that CSCs possess increased cell motility for more efficient metastasis to secondary sites (10, 19, 29). Figure 1, E and F, shows that, in both cell lines, the motility rate of NO-treated cells was significantly increased relative to the nontreated controls. A 2.5-fold increase in the migration rate was observed in the H292 cells treated with 25 μ M DPTA for 14 days (Fig. 1E), and a 2.3-fold increase was observed in the H460 cells treated with 10 μ M DPTA for the same amount of time (Fig. 1F). Invasion assay similarly indicated the induction of cell invasivity in both H292 and H460 cells by the NO donor in a dose- and time-dependent manner (Fig. 1, G and H).

NO promotes CSC-like behaviors. Having shown the effect of NO donor treatment on EMT properties, we further investigated whether such treatment also affects CSC-like behaviors. H292 and H460 cells were treated with nontoxic concentrations of DPTA NONOate for 7 and 14 days, and cell behaviors including proliferation, anoikis resistance, colony and spheroid formation were examined. Stem cells are known to be slow proliferators. Figure 2, A and B, shows that the DPTA treatment resulted in a significant reduction in the proliferation rate of both H292 and H460 cells.

Resistance to anoikis or detachment-induced apoptosis are hallmarks of CSCs. Figure 2, C and D, illustrates the viability of H292 and H460 cells in response to cell detachment. Cells were first treated with NO donor for 7 and 14 days and analyzed for anoikis response at different time points. The results showed that the treated cells exhibited a significantly reduced anoikis response compared with the nontreated controls, suggesting the ability of NO to induce a CSC-like anoikis-resistant phenotype.

Finally, we tested whether NO can induce colony and spheroid formation, which is a distinguishing feature of CSCs. H292 and H460 cells were similarly treated with the NO donor and analyzed for colony formation on soft agar. Colony number and diameter were determined and expressed as relative values over nontreated control levels. Figure 2E displays the relative colony number and diameter of the treated and nontreated H292 cells. A significant (2.1-fold) increase in the number of colonies formed was recorded for the H292 cells treated with 10 μ M DPTA NONOate for 14 days, and a 2.5-fold increase and a 3.4-fold increase were observed for the cells treated for 7 and 14 days, respectively, with 25 μ M DPTA NONOate. For H460 cells, a significant increase in the colony number can only be seen at the high treatment dose of 10 μ M at day 7 (2.7-fold) and day 14 (3.3-fold) (Fig. 2F). However, both treated cell lines showed no significant difference in the colony diameter compared with controls. Representative images of the H292 and H460 colonies are shown in Fig. 2, G and H, with the circular photograph representing an $\times 1$ image and

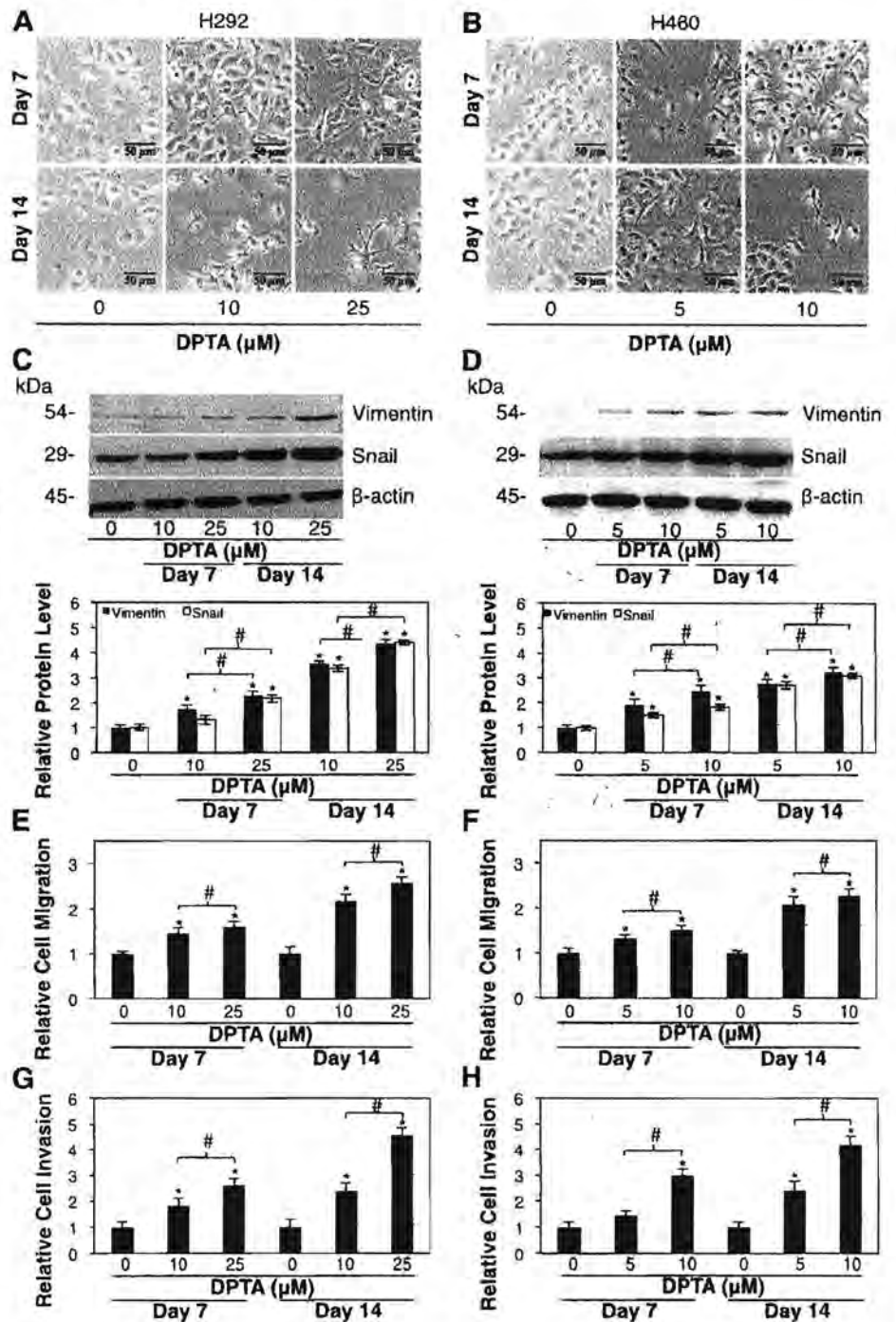


Fig. 1. Effect of nitric oxide (NO) donor on human lung cancer cell epithelial-mesenchymal transition (EMT). H292 (A) and H460 (B) cells were continuously treated with dipropyl-entriamine (DPTA) NONOate, and cell morphology was examined by phase-contrast microscopy after 7 and 14 days of treatment ($\times 10$). H292 (C) and H460 (D) cells were treated with DPTA NONOate (0–25 μM) for 7 and 14 days, and analyzed for EMT markers, Vimentin and Snail, by Western blotting. The blots were reprobated with β -actin to confirm equal loading of the samples. Blots were quantified by densitometry, and mean data from independent experiments were normalized and presented. Cell migration of H292 (E) and H460 (F) cells was determined by wound-healing assay. The wound spaces from random fields were measured and represented as relative migration to the control cells. Invasive behavior of H292 (G) and H460 (H) cells was evaluated by Transwell invasion assay. Invading cells attached to the lower side of the membrane filter were counted and represented as relative cell invasion to the control cells. Plots are means \pm SD ($n = 4$). $*P < 0.05$ vs. nontreated cells. $\#P < 0.05$ vs. DPTA NONOate-treated cells; scale bar = 50 μm .

the square representing an $\times 10$ image of the colonies. Figure 2, I and J, displays an $\times 4$ phase-contrast image of day 7 H292 and H460 primary spheroids, respectively. Cells were seeded at low density onto ultralow attach plates, and primary spheroids were allowed to form for 7 days. Control nontreated cells tend to survive through E-cadherin-mediated survival, whereas DPTA NONOate-treated cells can survive on their own as a single cell and slowly proliferate to form dense spheroids. The primary spheroids were then resuspended into single cells, and secondary spheroids were allowed to grow for 30 days in

RPMI serum-free medium. By day 30, the control nontreated spheroids were deformed and had already undergone apoptosis, whereas DPTA NONOate-treated spheroids still remained viable and intact (data not shown).

NO exposure induces CSC marker expression. We used two well-known CSC markers to verify the CSC-inducing effect of NO in H292 and H460 cells. The cells were cultivated in the presence or absence of DPTA NONOate for 7 and 14 days, and the expression levels of CD133 and ALDH1A1 were determined by Western blotting. Figure 3, A–D, shows that the NO

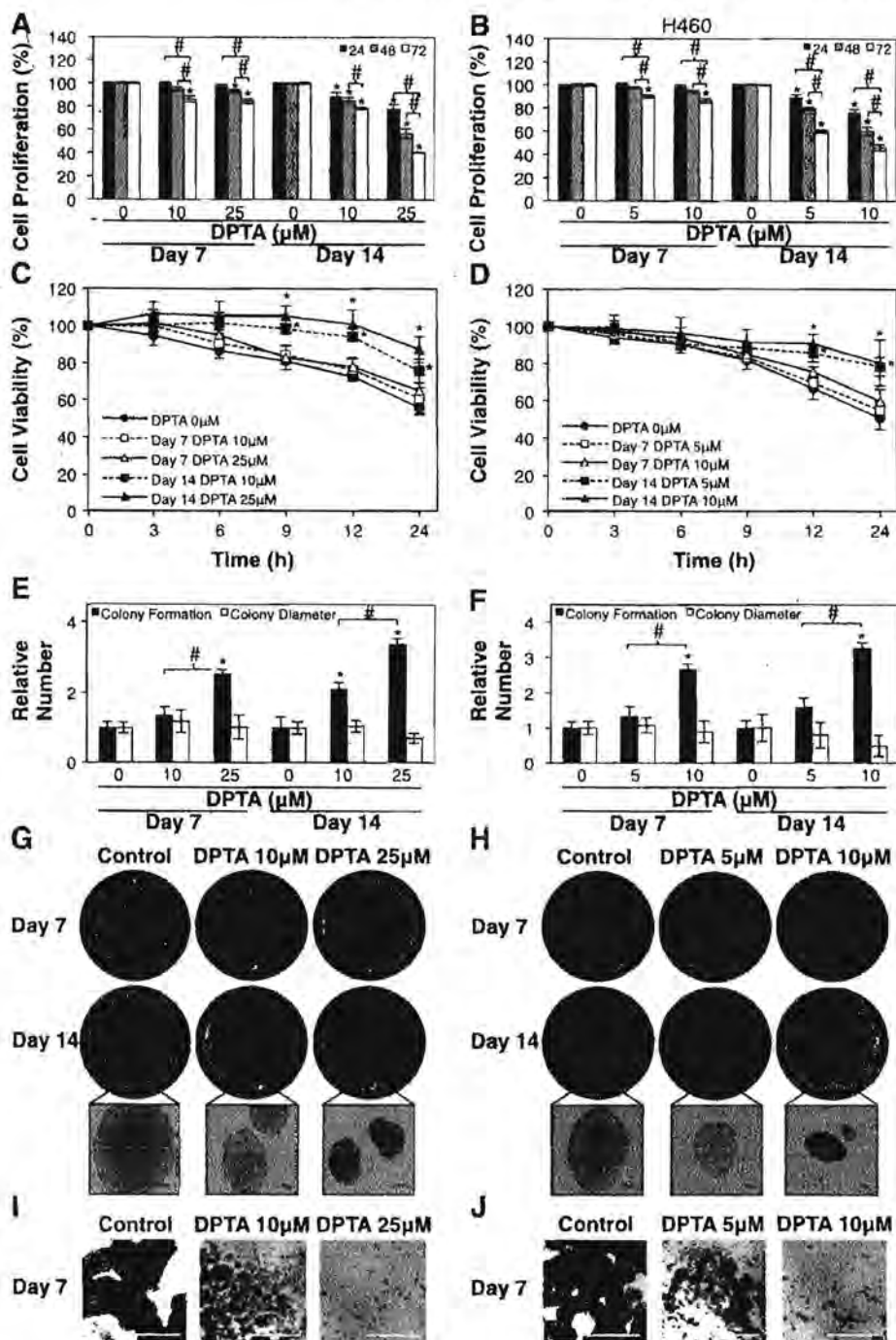
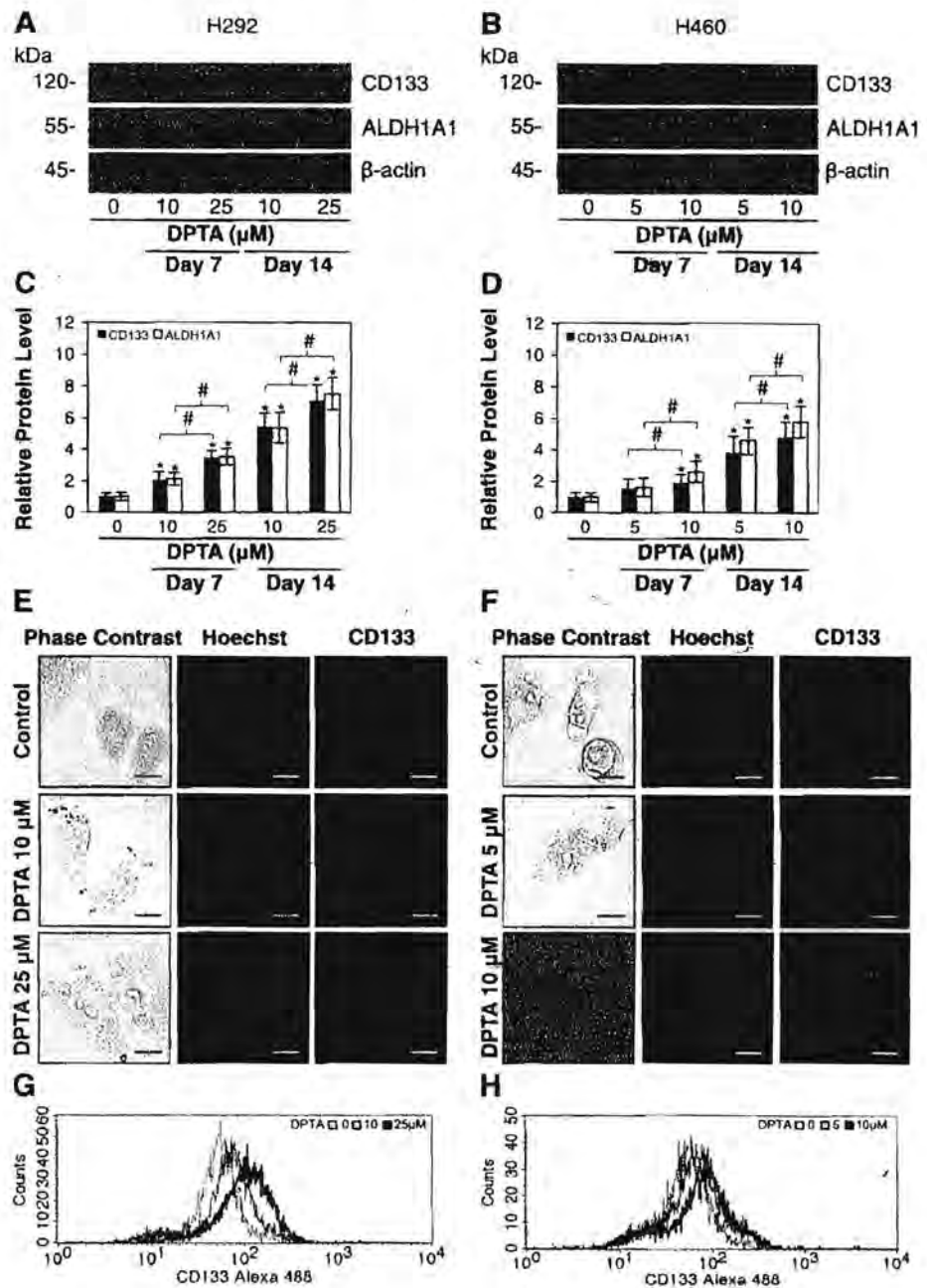


Fig. 2. NO donor enhances cancer stem cell (CSC)-like behaviors in lung cancer cells. H292 (A) and H460 (B) cells were treated with DPTA NONOate for 7 and 14 days and analyzed for cell proliferation at 24, 48, and 72 h by 3-(4,5-dimethylthiazol-2-yl)-2,5-diphenyltetrazolium bromide (MTT) assay. H292 (C) and H460 (D) cells were treated with DPTA NONOate for 7 and 14 days and analyzed for anoikis by measuring the viability of detached cells at various times by MTT assay. After being treated with DPTA NONOate (0–25 μM) for 7 and 14 days, H292 (E) and H460 (F) cells were suspended and subjected to colony-formation assay. Colony number and size were analyzed and calculated as relative to the control cells. Colony $\times 1$ and $\times 10$ images were captured after 2 wk of growth for H292 (G) and H460 cells (H). $\times 4$ Phase-contrast images of primary spheroids at day 7 were captured for treated and nontreated H292 (I) and H460 cells (J). All plots are means \pm SD ($n = 4$). $*P < 0.05$ vs. nontreated cells. $\#P < 0.05$ vs. DPTA NONOate-treated cells; scale bar = 200 μm .

donor induced CD133 and ALDH1A1 expression in a dose- and time-dependent manner. A 7.1-fold increase in CD133 and a 7.5-fold increase in ALDH1A1 expression were observed in the H292 cells treated with 25 μM DPTA NONOate for 14 days (Fig. 3C). In H460 cells, a 4.8-fold increase and a 5.8-fold increase in expression of the two CSC markers were observed after treatment with 10 μM DPTA NONOate for 14 days (Fig. 3D). To confirm the results, we performed immunofluorescence experiments assessing the expression of the CSC marker CD133 on the cells. H292 and H460 cells were treated with

NO donor for 14 days and analyzed for CD133 expression by immunofluorescence staining (Fig. 3, E and F). Consistent with the Western blot results, the immunofluorescence results indicate a dose-dependent increase in CD133 expression in both treated H292 and H460 cells. Furthermore, at day 14 treated and nontreated H292 and H460 cells were analyzed for CD133 cell surface intensity by flow cytometry, as shown in Fig. 3, G and H, respectively. CD133 on the cell surface intensifies dose dependently for both cell types. These results along with the findings on the NO effects on cell morphology and aggressive

Fig. 3. NO donor potentiates CSC markers in human lung cancer cells. H292 (A) and H460 (B) cells were treated with DPTA NONOate (0–25 μ M) for 7 and 14 days and analyzed for CSC markers, CD133 and ALDH1A1, by Western blotting. The blots were reprobed with β -actin to confirm equal loading of the samples. The immunoblot signals in H292 (C) and H460 (D) cells were quantified by densitometry, and mean data from independent experiments were normalized and presented. The bars are means \pm SD ($n = 8$). * $P < 0.05$ vs. nontreated cells. # $P < 0.05$ vs. DPTA NONOate-treated cells. The expression of CD133 in H292 (E) and H460 (F) cells was analyzed by fluorescence microscopy ($\times 40$). Cells were stained with Hoechst dye to aid visualization of the cell nucleus. The level of the cell surface expression of CD133 was measured by flow cytometry for treated and nontreated H292 (G) and H460 (H) cells at day 14 of treatment. Immunofluorescence and flow cytometry were performed using rabbit anti-CD133 monoclonal antibody followed by Alexa Fluor 488-labeled secondary antibody to visualize CD133 expression; scale bar = 10 μ m.



behaviors strongly support the role of NO in CSC-like properties of lung cancer cells.

Reversible effect of NO on CSC-like phenotypes. Having shown that NO drives the upregulation of CSC markers and promotes CSC-like behaviors, we next examined whether this effect of NO is reversible. The cells were first treated with 25 μ M (H292) or 10 μ M (H460) DPTA NONOate for 14 days, after which they were further cultured in the absence of NO donor for an additional 7 days and analyzed for CSC markers and cellular behaviors. Figure 4, A and B, shows that the cells with discontinued NO treatment were less resistant to anoikis, having their viability reverting to nearly the baseline level found in nontreated control cells. These cells also possessed

weaker colony-forming activity compared with the normal NO-treated cells (Fig. 4, C and D). Moreover, the expression of CSC markers, CD133 and ALDH1A1, on these cells was significantly reduced after the discontinuation of the NO donor (Fig. 4, E–H). Compared with the nontreated control cells, H292 cells treated with 25 μ M DPTA NONOate for 14 days exhibited a 6.6-fold and 6.9-fold increase, respectively, in the expression level of CD133 and ALDH1A1. After discontinuation of the NO donor, the CSC marker expression dropped to 4.2-fold and 3.3-fold over the control levels (Fig. 4G). A similar finding was observed in the H460 cells after the treatment and discontinuation of NO donor (Fig. 4H), supporting the generality of the effect of NO on CSC phenotypes.

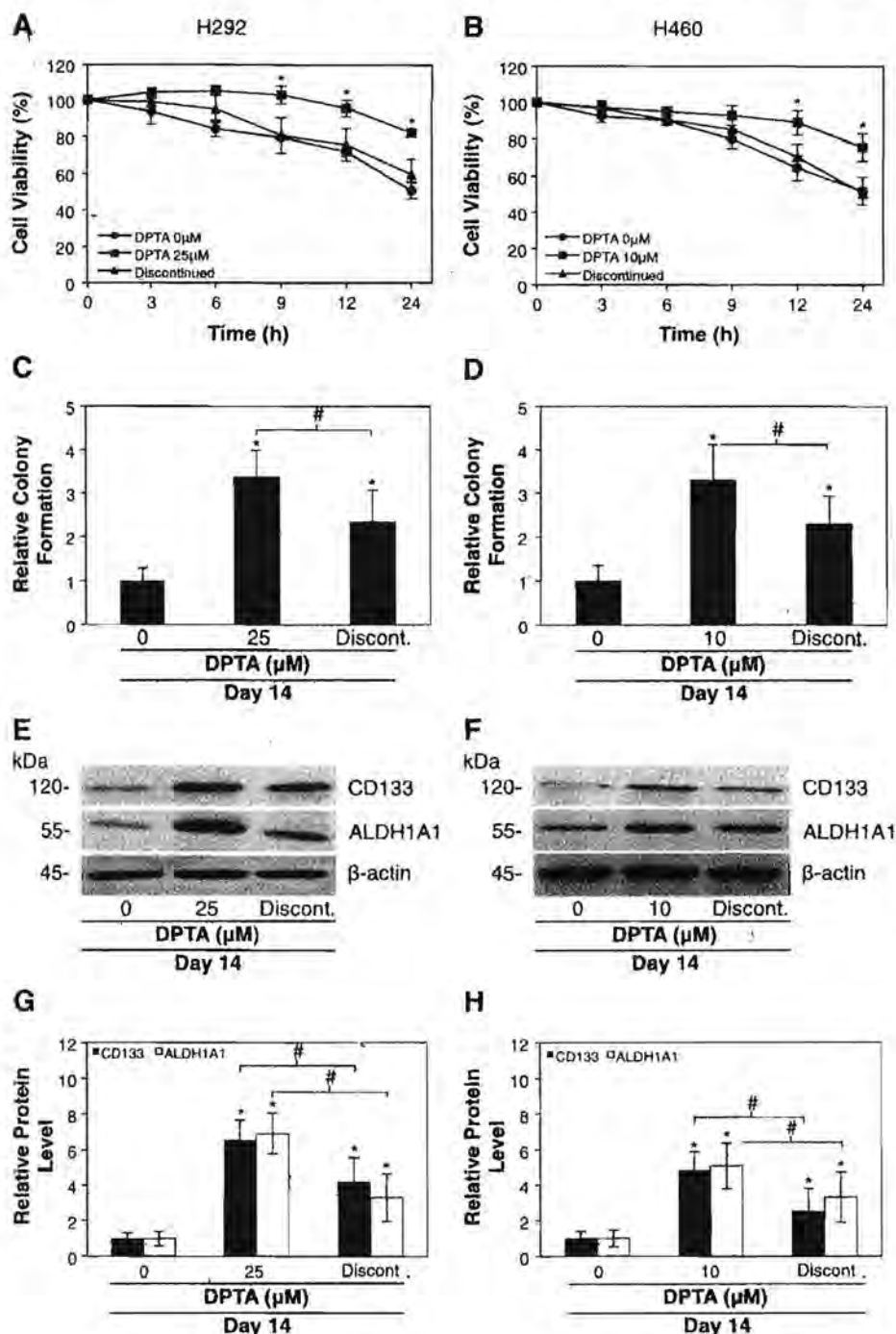


Fig. 4. The effect of NO on CSC-like phenotypes is reversible. After H292 and H460 cells were treated with 25 and 10 μM DPTA NONOate, respectively, for 14 days, the cells were further cultured in the absence of NO donor for 7 days. H292 (A) and H460 (B) cells were detached for 0–24 h. At indicated times, the detached cells were subjected to anoikis assay by measurement of cell viability using MTT assay. H292 (C) and H460 (D) cells were suspended and subjected to colony-formation assay. After 14 days, colony number was analyzed and calculated as relative to the control cells. H292 (E) and H460 (F) cells were collected, and CSC markers, CD133 and ALDH1A1, were analyzed by Western blotting. The blots were reprobed with β-actin to confirm equal loading. The immunoblot signals in H292 (G) and H460 (H) cells were quantified by densitometry, and mean data from independent experiments were normalized to the controls. The bars are means ± SD ($n = 4$ for A–D, $n = 8$ for G and H). * $P < 0.05$ vs. nontreated cells. # $P < 0.05$ vs. DPTA NONOate-treated cells.

Effects of NO donor (SNAP) and NO scavenger (PTIO) on CSC-like phenotypes. To confirm the effect of NO on CSC-like phenotypes, another NO donor SNAP and an NO scavenger PTIO were used. Cells were cultured in the presence or absence of NO modulators for 14 days, and CSC-like phenotypes were examined. Figure 5A shows that the SNAP-treated H292 cells displayed a dose-dependent increase in anoikis resistance compared with the nontreated control. In contrast, treatment of the cells with NO scavenger had a reversal effect (Fig. 5A), supporting the role of NO in the resistance process.

Consistent with this finding, a similar effect of NO donor and scavenger was observed in the H460 cells (Fig. 5B). Colony-formation studies also showed increased colony-forming activity of the SNAP-treated cells and decreased activity of the PTIO-treated cells, effects that were observed in both H292 and H460 cells (Fig. 5, C and D). Moreover, the SNAP-treated cells displayed an increased expression of the CSC markers, CD133 and ALDH1A1, whereas the PTIO-treated cells showed a reduced expression of the markers (Fig. 5, E–H). Figure 5, I and J, displays an $\times 4$ phase-contrast image of day

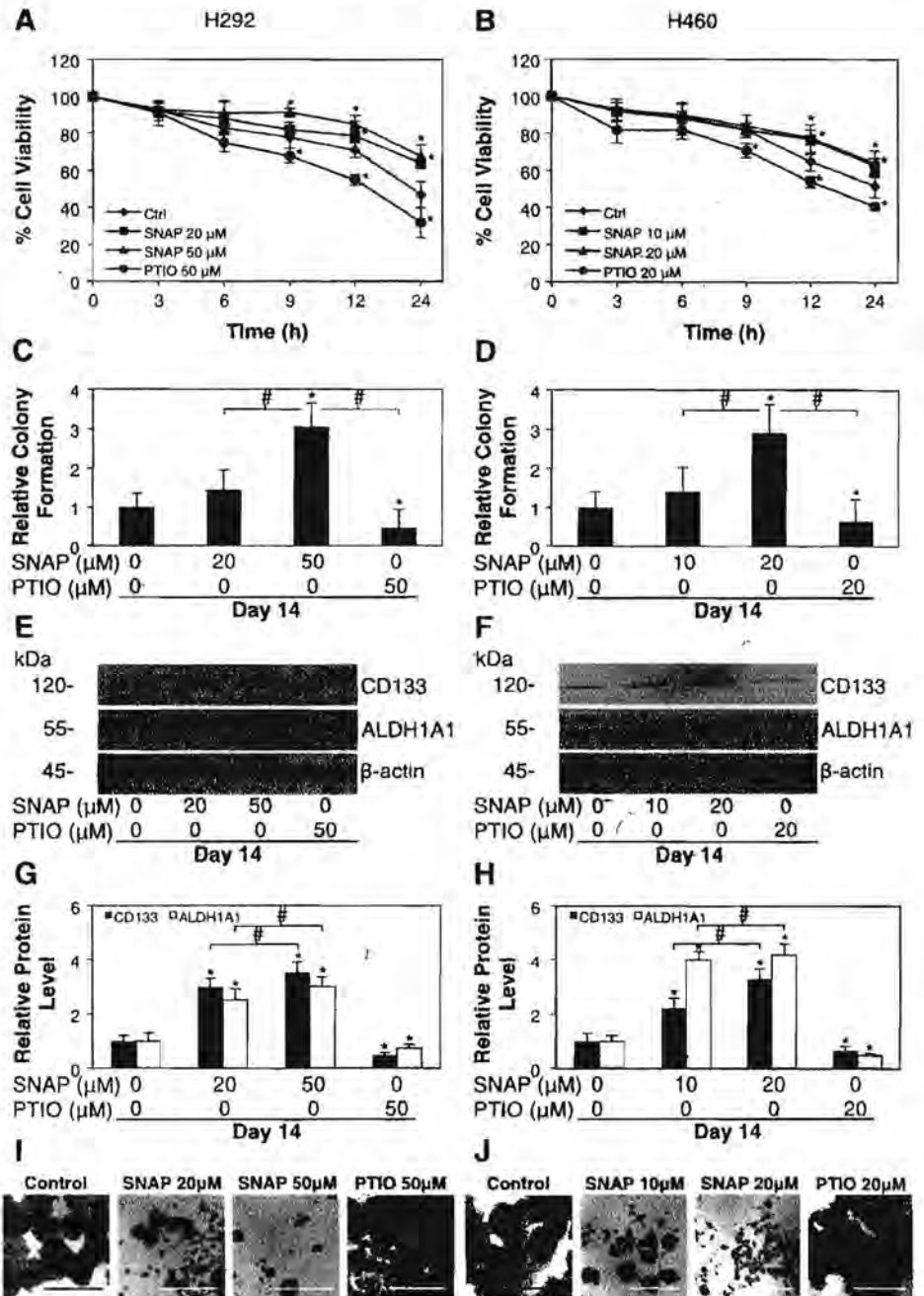


Fig. 5. Effect of NO donor *S*-nitroso-*N*-acetylpenicillamine (SNAP) and NO scavenger 2-(4-carboxy-phenyl)-4,4,5,5-tetramethylimidazole-1-*oxy*-3-*oxide* (PTIO) on CSC-like phenotypes. H292 (A) and H460 (B) cells were either left untreated as control (Ctrl) or treated with SNAP (10–50 μ M) or PTIO (20–50 μ M) for 14 days and analyzed for anoikis by measurement of the viability of detached cells by MTT assay. The treated and control H292 (C) and H460 (D) cells were suspended and subjected to colony-formation assay. The H292 (E) and H460 (F) cells were collected, and CSC markers, CD133 and ALDH1A1, were analyzed by Western blotting. The blots were reprobed with β -actin to confirm equal loading. The immunoblot signals in H292 (G) and H460 (H) cells were quantified by densitometry, and mean data from independent experiments were normalized to the controls. $\times 4$ Phase-contrast images of primary spheroids at day 7 were captured for treated and nontreated H292 (I) and H460 (J) cells. The bars are means \pm SD ($n = 4$). * $P < 0.05$ vs. nontreated control cells; # $P < 0.05$ vs. treated cells; scale bar = 200 μ m.

7 H292 and H460 spheroid formation, respectively. Similar to DPTA NONOate-treated cells, SNAP-treated cells formed dense circular spheroids, whereas control cells and PTIO-treated cells clump together to form huge irregular-shaped spheroids surviving through E-cadherin-mediated survival. Together, these results indicate the promoting role of NO in CSC-like properties of human lung cancer cells.

Cav-1 regulates aggressive behaviors of CSC-like cells but not CSC markers. Unveiling the key players underlying NO-mediated aggressive behaviors is of importance because of its potential applications in cancer therapy. *Cav-1* is known to be involved in various cancer cell behaviors including migration, invasion, and anoikis resistance (11, 27, 28, 30, 42, 45, 59) and

is subjected to NO regulation (7, 28). To explore the possible role of *Cav-1* in NO-mediated CSC-like behaviors, *Cav-1* expression was genetically modulated, and its effect on cellular behaviors in NO-treated cells was examined. Figure 6, A and B, shows that the *Cav-1* level was strongly upregulated in the NO-treated cells in a dose- and time-dependent manner, the effect that was found in both treated H292 and H460 cells. To test whether *Cav-1* is essential to the effect of NO on cellular behaviors, knockdown by *Cav-1* expression or enhancement by stable gene transfection and their effects on NO-induced cellular behaviors were determined. Figure 6, C and D, shows the effects of shRNA knockdown and gene overexpression on *Cav-1* protein expression. The genetically modified cells were

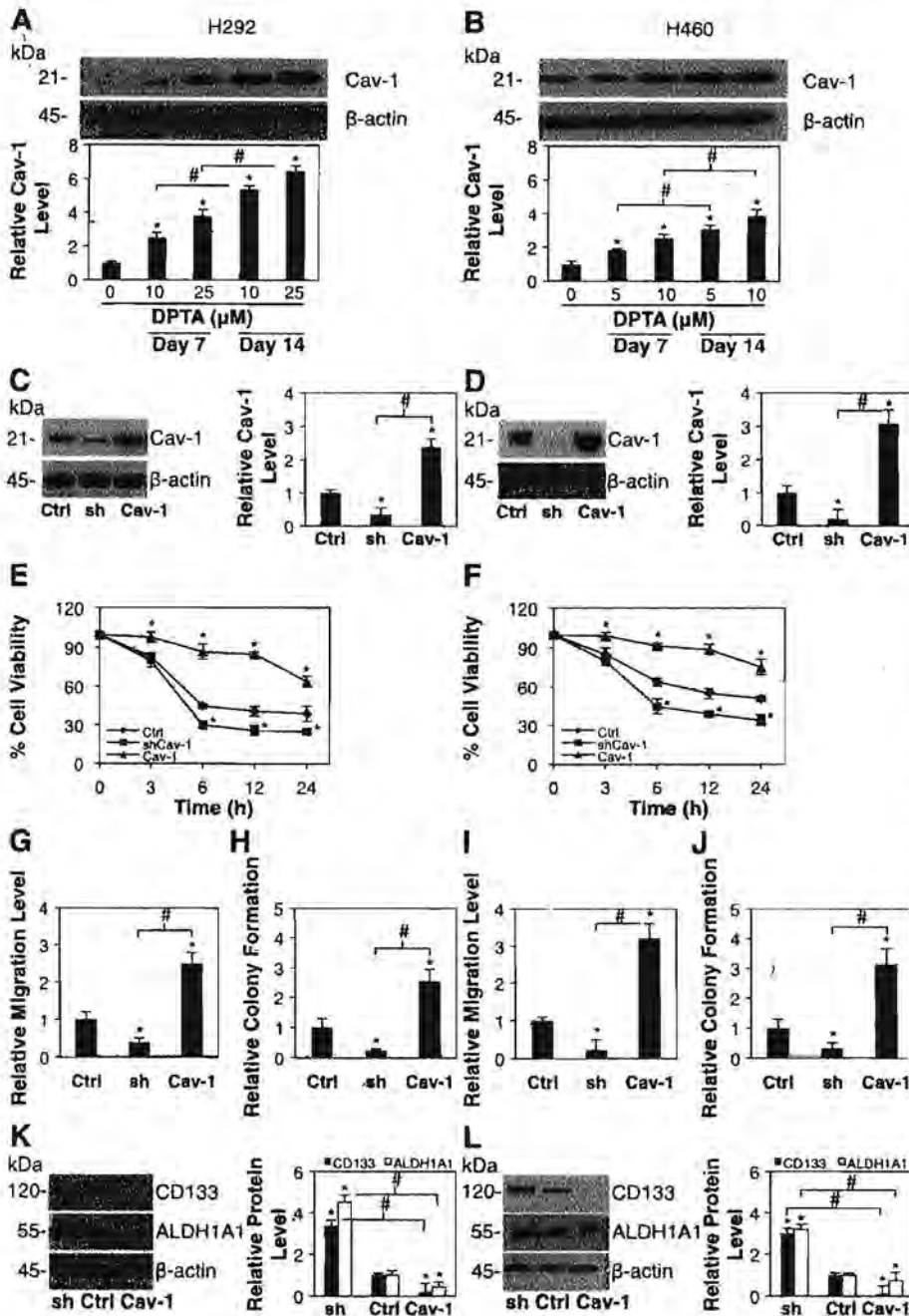


Fig. 6. Effect of caveolin-1 (Cav-1) on CSC-like behaviors. H292 (A) and H460 (B) cells were treated with 0–25 μM DPTA NONOate for 7 and 14 days. Cells were collected, and Cav-1 expression was determined by Western blotting. The blots were reprobbed with β-actin to confirm equal loading. The immunoblot signals were quantified by densitometry, and mean data from independent experiments were normalized to the controls. The bars are means ± SD (n = 4). *P < 0.05 vs. nontreated control cells. #P < 0.05 vs. treated cells at day 7. H292 (C) and H460 (D) cells were stably transfected with Cav-1-overexpressing plasmid (Cav-1), short hairpin (sh) knockdown plasmid, or control (Ctrl) plasmid, and Cav-1 expression in these cells was determined by Western blotting. Blots were reprobbed with β-actin as a loading control. Cav-1, sh, and Ctrl H292 and H460 cells were treated with 25 μM and 10 μM DPTA NONOate, respectively, for 14 days. H292 (E) and H460 (F) transfectants were detached, and cell viability was analyzed for anoikis assay. The motility of H292 (G) and H460 (I) transfectants was determined by wound-healing assay. The wound spaces from random fields were measured and represented as relative migration to the control cells. H292 (H) and H460 (J) transfectants were subjected to colony-formation assay. After 14 days, colony number was analyzed and calculated as relative to the control cells. H292 (K) and H460 (L) transfectants were collected, and CD133 and ALDH1A1 were analyzed by Western blotting. The blots were reprobbed with β-actin to confirm equal loading. The immunoblot signals were quantified by densitometry, and mean data from independent experiments were normalized to the controls. The bars are means ± SD (n = 4). *P < 0.05 vs. control transfected cells. #P < 0.05 vs. shCav-1-transfected cells.

treated with NO donor, and their cellular behaviors including anoikis, migration, invasion, and colony formation were examined. The results showed that Cav-1 knockdown cells were less resistant to anoikis and exhibited reduced cell motility and colony-forming activity compared with the vector-control cells, whereas the Cav-1-overexpressing cells showed opposite effects (Fig. 6, E–J). These results indicate that Cav-1 is required for the NO-mediated aggressive CSC-like behaviors.

Furthermore, we investigated the effect of Cav-1 knockdown and overexpression on CSC markers. Cells were treated with the NO donor for 14 days, and their expression levels of CD133 and ALDH1A1 were assessed by Western blotting. Our

results showed that the level of these CSC markers did not correlate with the level of Cav-1 (Fig. 6, K and L), suggesting a non-Cav-1-dependent mechanism of CSC marker upregulation in the NO-treated cells.

DISCUSSION

The concept of CSCs as a seed of malignant cells has garnered increasing attention and has been a subject of active research in recent years (14, 22, 54). Although detailed knowledge of this cell population remains obscure, the significant impact of this cell population in various forms of cancer has

increasingly been reported. CSCs have been identified by their putative markers such as ALDH and CD133 (19, 34, 62) and by their cellular traits such as spindle-shaped morphology, colony formation, and other aggressive behaviors (16, 23, 40, 46, 56, 58, 63).

NO is a key molecule produced from the crosstalk between cells and inflammation within the tumor microenvironment (13, 17, 20). Several studies have reported increased expression and activity of different forms of NOS in cancers (1, 64, 66). Interestingly, both pro- and antitumorigenic roles of NO have been described; however, it is generally accepted that the effect of NO on tumor progression is concentration dependent (21, 32, 53, 65). Previously, we have reported that NO promotes cell death resistance to Fas ligand (9) and cisplatin (8) in human lung cancer cells. In relevance to metastasis, we also found that NO mediates anoikis resistance of lung cancer cells (7). Together, these findings provide evidence supporting the role of NO in tumorigenesis and metastasis, consistent with the clinical observations showing a correlation between NO level and a high degree of tumor metastasis (45, 60). Several studies have demonstrated that CSCs possess an enhanced ability to migrate, invade, form tumors, and resist anoikis (16, 23, 40, 46, 56, 58, 63). However, the linkage between NO and aggressive cancer phenotypes in the context of CSCs has not been investigated. The present study demonstrated for the first time that NO regulates the stemness and aggressive behaviors of lung cancer cells. The NO donors DPTA NONOate and SNAP upregulate the expression of CSC markers, CD133 and ALDH1A1, and increase aggressive cellular behaviors, whereas the NO scavenger PTIO suppresses the markers and decreases aggressive behaviors (Fig. 5, E-G). These results suggest that NO may mediate its effects by regulating the stemness of cancer cells.

Cav-1 is a scaffold protein and essential constituent of caveolae, a flask-shaped invagination that occupies up to 20% of the cell membrane (41). Several lines of evidence have pointed out that Cav-1 may contribute to the aggressiveness and chemoresistance of human cancer cells, including lung carcinoma, ovarian carcinoma, colon adenocarcinoma, and breast adenocarcinoma cells (31, 37, 38). Cav-1 expression has been linked to increased cell motility and anoikis resistance (11, 12, 27, 28, 30, 42, 45, 59), two important features of metastatic cancer cells. In this study, we provide new evidence that NO increases the motility and resistance to anoikis of human lung cancer cells through a Cav-1-dependent mechanism. Cav-1 is upregulated in the NO-treated cells in a dose- and time-dependent manner (Fig. 6, A and B). Such upregulation is positively associated with the ability of the cells to migrate, invade, form colonies, and resist anoikis. Gene knock-down and overexpression studies confirm the positive regulatory role of Cav-1 in NO-mediated aggressive behaviors of lung cancer cells. This finding is, however, contradictory to the generally regarded role of Cav-1 as a tumor-suppressor protein (44). It is likely that Cav-1 may have multiple functions and may exert both positive and negative roles on cancer cell behaviors depending on the cancer stage, i.e., metastatic or nonmetastatic, tissue of origin, and tumor microenvironment, i.e., presence of nitrosative and oxidative stress. In the environment with a high NO level, Cav-1 is upregulated and prometastatic. Previous studies have also shown that NO stabilizes Cav-1 through a process of S-nitrosylation, which inhibits ubiquitin-proteasomal degradation of the protein (7).

Furthermore, Cav-1 can interact with Mcl-1 and improve its stability, leading to anoikis resistance of lung cancer cells (12).

The effect of NO on aggressive CSC-like behaviors was found to be reversible, which may explain the discrepancy of the NO effect on tumorigenesis. Discontinuation of NO exposure after a 2-wk treatment resulted in a reversal of the CSC-like effects of NO on cell anoikis, colony formation, cell invasion, and migration. It is worth noting that the level of NO in the tumor microenvironment varies depending on the expression of NOS and the activity of local and infiltrating immune cells. Therefore, the effect of NO on CSC-like behaviors may vary depending on the availability of NO and pathological conditions.

In summary, our data provide evidence that NO plays an important role in the regulation of CSC-like phenotypes of human lung cancer cells. NO induces an upregulation of CSC markers, CD133 and ALDH1A1, along with the increase in anoikis resistance, migration, invasion, and colony-formation activities. Such induction of the aggressive CSC-like behaviors is dependent on Cav-1 expression; however, the expression of CSC markers is independent or inversely dependent on the Cav-1 expression. Because increased NO production has been associated with several human cancers, NO may be one of the key regulators of CSCs and metastasis. This novel finding on the role of NO and Cav-1 in CSC regulation may have important implications in cancer chemotherapy and prevention.

ACKNOWLEDGMENTS

The authors thank The 90th Anniversary of Chulalongkorn University Fund (Ratchadaphiseksomphot Endowment Fund) and the Thailand Research Fund (RSA5780043).

GRANTS

This research is supported by The 90th Anniversary of Chulalongkorn University Fund (Ratchadaphiseksomphot Endowment Fund) and the Thailand Research Fund (RSA5780043).

DISCLOSURES

No conflicts of interest, financial or otherwise, are declared by the authors.

AUTHOR CONTRIBUTIONS

Author contributions: N.Y. performed experiments; N.Y. and P.C. analyzed data; N.Y., V.P., and P.C. interpreted results of experiments; N.Y. and V.P. prepared figures; N.Y. and P.C. drafted manuscript; N.Y., V.P., A.M., Y.R., and P.C. edited and revised manuscript; N.Y., V.P., A.M., Y.R., and P.C. approved final version of manuscript; P.C. conception and design of research.

REFERENCES

1. Ambs S, Merriam WG, Bennett WP, Felley-Bosco E, Ogunfusika MO, Oser SM, Klein S, Shields PG, Billiar TR, Harris CC. Frequent nitric oxide synthase-2 expression in human colon adenomas: implication for tumor angiogenesis and colon cancer progression. *Cancer Res* 58: 334-341, 1998.
2. Arias-Díaz J, Vara E, Torres-Melero J, García C, Baki W, Ramírez-Armengol JA, Balibrea JL. Nitrite/nitrate and cytokine levels in bronchoalveolar lavage fluid of lung cancer patients. *Cancer* 74: 1546-1551, 1994.
3. Bao S, Wu Q, McLendon RE, Hao Y, Shi Q, Hjelmeland AB, Dewhirst MW, Bigner DD, Rich JN. Glioma stem cells promote radioresistance by preferential activation of the DNA damage response. *Nature* 444: 756-760, 2006.
4. Bertolini G, Roz L, Perego P, Tortoreto M, Fontanella E, Gatti L, Pratesi G, Fabbri A, Andriani F, Tinelli S, Roz E, Caserini R, Lo Vullo S, Camerini T, Mariani L, Delia D, Calabro E, Pastorino U, Sozzi G. Highly tumorigenic lung cancer CD133+ cells display stem-like

- features and are spared by cisplatin treatment. *Proc Natl Acad Sci USA* 106: 16281–16286, 2009.
5. Bonnet D, Dick JE. Human acute myeloid leukemia is organized as a hierarchy that originates from a primitive hematopoietic cell. *Nat Med* 3: 730–737, 1997.
 6. Chanvorachote P, Chunhacha P. Caveolin-1 regulates endothelial adhesion of lung cancer cells via reactive oxygen species-dependent mechanism. *PLoS One* 8: e57466, 2013.
 7. Chanvorachote P, Nimmannit U, Lu Y, Talbott S, Jiang BH, Rojanasakul Y. Nitric oxide regulates lung carcinoma cell anoikis through inhibition of ubiquitin-proteasomal degradation of caveolin-1. *J Biol Chem* 284: 28476–28484, 2009.
 8. Chanvorachote P, Nimmannit U, Stehlik C, Wang L, Jiang BH, Ongpipatanakul B, Rojanasakul Y. Nitric oxide regulates cell sensitivity to cisplatin-induced apoptosis through S-nitrosylation and inhibition of Bcl-2 ubiquitination. *Cancer Res* 66: 6353–6360, 2006.
 9. Chanvorachote P, Nimmannit U, Wang L, Stehlik C, Lu B, Azad N, Rojanasakul Y. Nitric oxide negatively regulates Fas CD95-induced apoptosis through inhibition of ubiquitin-proteasome-mediated degradation of FLICE inhibitory protein. *J Biol Chem* 280: 42044–42050, 2005.
 10. Charafe-Jauffret E, Ginestier C, Iovino F, Wicinski J, Cervera N, Finetti P, Hur MH, Diebel ME, Monville F, Dutcher J, Brown M, Viens P, Kerri L, Bertucci F, Stassi G, Dontu G, Birnbaum D, Wicha MS. Breast cancer cell lines contain functional cancer stem cells with metastatic capacity and a distinct molecular signature. *Cancer Res* 69: 1302–1313, 2009.
 11. Chunhacha P, Chanvorachote P. Roles of caveolin-1 on anoikis resistance in non-small cell lung cancer. *Int J Physiol Pathophysiol Pharmacol* 4: 149–155, 2012.
 12. Chunhacha P, Pongrakhananon V, Rojanasakul Y, Chanvorachote P. Caveolin-1 regulates Mcl-1 stability and anoikis in lung carcinoma cells. *Am J Physiol Cell Physiol* 302: C1284–C1292, 2012.
 13. Clancy RM, Amin AR, Abramson SB. The role of nitric oxide in inflammation and immunity. *Arthritis Rheum* 41: 1141–1151, 1998.
 14. Clevers H. The cancer stem cell: premises, promises and challenges. *Nat Med* 17: 313–319, 2011.
 15. Colakogullari M, Ulukaya E, Yilmaztepe A, Ocakoglu G, Yilmaz M, Karadag M, Tokullugil A. Higher serum nitrate levels are associated with poor survival in lung cancer patients. *Clin Biochem* 39: 898–903, 2006.
 16. Collins AT, Berry PA, Hyde C, Stower MJ, Maitland NJ. Prospective identification of tumorigenic prostate cancer stem cells. *Cancer Res* 65: 10946–10951, 2005.
 17. Cook JA, Glus D, Wink DA, Krishna MC, Russo A, Mitchell JB. Oxidative stress, redox, and the tumor microenvironment. *Semin Radiat Oncol* 14: 259–266, 2004.
 18. Creighton CJ, Li X, Landis M, Dixon JM, Neumeister VM, Sjolund A, Rimm DL, Wong H, Rodriguez A, Herschkowitz JJ, Fan C, Zhang X, He X, Pavlick A, Gutierrez MC, Renshaw L, Larionov AA, Faratian D, Hilsenbeck SG, Perou CM, Lewis MT, Rosen JM, Chang JC. Residual breast cancers after conventional therapy display mesenchymal as well as tumor-initiating features. *Proc Natl Acad Sci USA* 106: 13820–13825, 2009.
 19. Croker AK, Goodale D, Chu J, Postenka C, Hedley BD, Hess DA, Allan AL. High aldehyde dehydrogenase and expression of cancer stem cell markers selects for breast cancer cells with enhanced malignant and metastatic ability. *J Cell Mol Med* 13: 2236–2252, 2009.
 20. Decker NK, Abdelmonem SS, Yaqoob U, Hendrickson H, Hormes J, Bentley M, Pitot H, Urrutia R, Gores GJ, Shah VH. Nitric oxide regulates tumor cell cross-talk with stromal cells in the tumor microenvironment of the liver. *Am J Pathol* 173: 1002–1012, 2008.
 21. Dhar A, Brindley JM, Stark C, Citro ML, Keefer LK, Colburn NH. Nitric oxide does not mediate but inhibits transformation and tumor phenotype. *Mol Cancer Ther* 2: 1285–1293, 2003.
 22. Dick JE. Stem cell concepts renew cancer research. *Blood* 112: 4793–4807, 2008.
 23. Eramo A, Lotti F, Sette G, Pillozzi E, Biffoni M, Di Virgilio A, Conticello C, Ruco L, Peschle C, De Maria R. Identification and expansion of the tumorigenic lung cancer stem cell population. *Cell Death Differ* 15: 504–514, 2008.
 24. Esme H, Cemek M, Sezer M, Saglam H, Demir A, Melek H, Unlu M. High levels of oxidative stress in patients with advanced lung cancer. *Respirology* 13: 112–116, 2008.
 25. Fujimoto H, Ando Y, Yamashita T, Terazaki H, Tanaka Y, Sasaki J, Matsumoto M, Suga M, Ando M. Nitric oxide synthase activity in human lung cancer. *Jpn J Cancer Res* 88: 1190–1198, 1997.
 26. Fukumura D, Kashiwagi S, Jain RK. The role of nitric oxide in tumour progression. *Nat Rev Cancer* 6: 521–534, 2006.
 27. Grande-Garcia A, Echarrri A, de Rooij J, Alderson NB, Waterman-Storer CM, Valdivielso JM, del Pozo MA. Caveolin-1 regulates cell polarization and directional migration through Src kinase and Rho GTPases. *J Cell Biol* 177: 683–694, 2007.
 28. Halim H, Luanpitpong S, Chanvorachote P. Acquisition of anoikis resistance up-regulates caveolin-1 expression in human non-small cell lung cancer cells. *Anticancer Res* 32: 1649–1658, 2012.
 29. Hermann PC, Huber SL, Herrler T, Aicher A, Ellwart JW, Guba M, Bruns CJ, Heeschen C. Distinct populations of cancer stem cells determine tumor growth and metastatic activity in human pancreatic cancer. *Cell Stem Cell* 1: 313–323, 2007.
 30. Ho CC, Huang PH, Huang HY, Chen YH, Yang PC, Hsu SM. Up-regulated caveolin-1 accentuates the metastasis capability of lung adenocarcinoma by inducing filopodia formation. *Am J Pathol* 161: 1647–1656, 2002.
 31. Ho CC, Kuo SH, Huang PH, Huang HY, Yang CH, Yang PC. Caveolin-1 expression is significantly associated with drug resistance and poor prognosis in advanced non-small cell lung cancer patients treated with gemcitabine-based chemotherapy. *Lung Cancer* 59: 105–110, 2008.
 32. Jenkins DC, Charles IG, Thomsen LL, Moss DW, Holmes LS, Baylis SA, Rhodes P, Westmore K, Emson PC, Moncada S. Roles of nitric oxide in tumor growth. *Proc Natl Acad Sci USA* 92: 4392–4396, 1995.
 33. Kantara C, O'Connell M, Sarkar S. Curcumin promotes autophagic survival of a subset of colon cancer stem cells, which are ablated by DCLK1-siRNA. *Cancer Res* 74: 2487–2498, 2014.
 34. Kim MP, Fleming JB, Wang H, Abbruzzese JL, Choi W, Kopetz S, McConkey DJ, Evans DB, Gallick GE. ALDH activity selectively defines an enhanced tumor-initiating cell population relative to CD133 expression in human pancreatic adenocarcinoma. *PLoS One* 6: e20636, 2011.
 35. Kisley LR, Barrett BS, Bauer AK, Dwyer-Nield LD, Barthel B, Meyer AM, Thompson DC, Malkinson AM. Genetic ablation of inducible nitric oxide synthase decreases mouse lung tumorigenesis. *Cancer Res* 62: 6850–6856, 2002.
 36. Lala PK, Orucevic A. Role of nitric oxide in tumor progression: Lessons from experimental tumors. *Cancer Metastasis Rev* 17: 91–106, 1998.
 37. Lavie Y, Fiucci G, Liscovitch M. Up-regulation of caveolae and caveolar constituents in multidrug-resistant cancer cells. *J Biol Chem* 273: 32380–32383, 1998.
 38. Lavie Y, Fiucci G, Liscovitch M. Upregulation of caveolin in multidrug resistant cancer cells: Functional implications. *Adv Drug Deliv Rev* 49: 317–323, 2001.
 39. Levina V, Marrangoni AM, DeMarco R, Gorelik E, Lokshin AE. Drug-selected human lung cancer stem cells: Cytokine network, tumorigenic and metastatic properties. *PLoS One* 3: e3077, 2008.
 40. Li C, Heidt DG, Dalerba P, Burant CF, Zhang L, Adsay V, Wicha M, Clarke MF, Simeone DM. Identification of pancreatic cancer stem cells. *Cancer Res* 67: 1030–1037, 2007.
 41. Li S, Couet J, Lisanti MP. Src tyrosine kinases, Galpha subunits, and H-Ras share a common membrane-anchored scaffolding protein, caveolin: Caveolin binding negatively regulates the auto-activation of Src tyrosine kinases. *J Biol Chem* 271: 29182–29190, 1996.
 42. Lin M, DiVito MM, Merajver SD, Boyanapalli M, van Golen KL. Regulation of pancreatic cancer cell migration and invasion by RhoC GTPase and Caveolin-1. *Mol Cancer* 4: 21, 2005.
 43. Liu CY, Wang CH, Chen TC, Lin HC, Yu CT, Kuo HP. Increased level of exhaled nitric oxide and up-regulation of inducible nitric oxide synthase in patients with primary lung cancer. *Br J Cancer* 78: 534–541, 1998.
 44. Lloyd PG, Hardin CD. Caveolae in cancer: Two sides of the same coin? Focus on "Hydrogen peroxide inhibits non-small cell lung cancer cell anoikis through the inhibition of caveolin-1 degradation". *Am J Physiol Cell Physiol* 300: C232–C234, 2011.
 45. Luanpitpong S, Talbott SJ, Rojanasakul Y, Nimmannit U, Pongrakhananon V, Wang L, Chanvorachote P. Regulation of lung cancer cell migration and invasion by reactive oxygen species and caveolin-1. *J Biol Chem* 285: 38832–38840, 2010.
 46. Ma S, Chan KW, Hu L, Lee TKW, Wo JYH, Ng IOL, Zheng BJ, Guan XY. Identification and characterization of tumorigenic liver cancer stem/progenitor cells. *Gastroenterology* 132: 2542–2556, 2007.

47. Marie-Egyptienne DT, Lohse I, Hill RP. Cancer stem cells, the epithelial to mesenchymal transition (EMT) and radioresistance: Potential role of hypoxia. *Cancer Lett* 341: 63–72, 2012.
48. Marletta MA. Nitric oxide synthase structure and mechanism. *J Biol Chem* 268: 12231–12234, 1993.
49. Masri FA, Comhair SAA, Koeck T, Xu W, Janocha A, Ghosh S, Dwelk RA, Golish J, Kinter M, Stuehr DJ, Erzurum SC, Aulak KS. Abnormalities in nitric oxide and its derivatives in lung cancer. *Am J Respir Crit Care Med* 172: 597–605, 2005.
50. Merlos-Suárez A, Barriga FM, Jung P, Iglesias M, Céspedes MV, Rossell D, Sevillano M, Hernando-Mombiona X, Silva-Diz V, Muñoz P, Clevers H, Sancho E, Mangués R, Batlle E. The intestinal stem cell signature identifies colorectal cancer stem cells and predicts disease relapse. *Cell Stem Cell* 8: 511–524, 2011.
51. Moncada S, Palmer JRM, Higgs AE. Biosynthesis of nitric oxide from L-arginine: A pathway for the regulation of cell function and communication. *Biochem Pharmacol* 38: 1709–1715, 1989.
52. Moncada S, Palmer R, Higgs EA. Nitric oxide: Physiology, pathophysiology, pharmacology. *Pharmacol Rev* 43: 109–142, 1991.
53. Muñtáné J, De la Mata M. Nitric oxide and cancer. *World J Hepatol* 2: 337–344, 2010.
54. O'Connor ML, Xiang D, Shigdar S, Macdonald J, Li Y, Wang T, Pu C, Wang Z, Qiao L, Duan W. Cancer stem cells: A contentious hypothesis now moving forward. *Cancer Lett* 344: 180–187, 2014.
55. Perona R, López-Ayllón BD, Castro Carpeño J, Belda-Iniesta C. A role for cancer stem cells in drug resistance and metastasis in non-small-cell lung cancer. *Clin Transl Oncol* 13: 289–293, 2011.
56. Ponti D, Costa A, Zaffaroni N, Pratesi G, Petrangolini G, Coradini D, Pilotti S, Pierotti MA, Daidone MG. Isolation and in vitro propagation of tumorigenic breast cancer cells with stem/progenitor cell properties. *Cancer Res* 65: 5506–5511, 2005.
57. Puhakka A, Kinnula V, Nöpänkangas U, Säily M, Koistinen P, Pääkkö P, Soini Y. High expression of nitric oxide synthases is a favorable prognostic sign in non-small cell lung carcinoma. *APMIS* 111: 1137–1146, 2003.
58. Ricci-Vitiani L, Lombardi DG, Pilozzi E, Biffoni M, Todaro M, Peschle C, De Maria R. Identification and expansion of human colon-cancer-initiating cells. *Nature* 445: 111–115, 2007.
59. Rungtabnapa P, Nimmannit U, Halim H, Rojanasakul Y, Chanvorachote P. Hydrogen peroxide inhibits non-small cell lung cancer cell anoikis through the inhibition of caveolin-1 degradation. *Am J Physiol Cell Physiol* 300: C235–C245, 2011.
60. Sanuphan A, Chunhacha P, Pongrakhananon V, Chanvorachote P. Long-term nitric oxide exposure enhances lung cancer cell migration. *Biomed Res Int* 2013: 186972, 2013.
61. Siegel R, Naishadham D, Jemal A. Cancer statistics. *CA Cancer J Clin* 63: 11–30, 2013.
62. Silva IA, Bai S, McLean K, Yang K, Griffith K, Thomas D, Ginestier C, Johnston C, Kueck A, Reynolds RK, Wicha MS, Buckanovich RJ. Aldehyde dehydrogenase in combination with CD133 defines angiogenic ovarian cancer stem cells that portend poor patient survival. *Cancer Res* 71: 3991–4001, 2011.
63. Singh SK, Clarke ID, Terasaki M, Bonn VE, Hawkins C, Squire J, Dirks PB. Identification of a cancer stem cell in human brain tumors. *Cancer Res* 63: 5821–5828, 2003.
64. Thomsen LL, Lawton FG, Knowles RG, Beestley JE, Riveros-Moreno V, Moncada S. Nitric oxide synthase activity in human gynecological cancer. *Cancer Res* 54: 1352–1354, 1994.
65. Thomsen LL, Miles DW. Role of nitric oxide in tumour progression: Lessons from human tumours. *Cancer Metastasis Rev* 17: 107–118, 1998.
66. Thomsen LL, Miles DW, Happerfield L, Bobrow LG, Knowles RG, Moncada S. Nitric oxide synthase activity in human breast cancer. *Br J Cancer* 72: 41–44, 1995.
67. Wongvaranon P, Pongrakhananon V, Chunhacha P, Chanvorachote P. Acquired resistance to chemotherapy in lung cancer cells mediated by prolonged nitric oxide exposure. *Anticancer Res* 33: 5433–5444, 2013.
68. Zhang Y, Wang Z, Yu J, Shi JZ, Wang C, Fu WH, Chen ZW, Yang J. Cancer stem-like cells contribute to cisplatin resistance and progression in bladder cancer. *Cancer Lett* 322: 70–77, 2012.

Nitric oxide increases the migratory activity of non-small cell lung cancer cells via AKT-mediated integrin αv and $\beta 1$ upregulation

Vhudhipong Saisongkorh^{1,2} · Arnatchai Maiuthed^{1,2} · Pithi Chanvorachote^{1,2}

Accepted: 21 June 2016 / Published online: 4 July 2016
© International Society for Cellular Oncology 2016

Abstract

Background Previously, nitric oxide (NO) has been found to affect the metastatic behavior of various types of cancer. In addition, it has been found that alterations in integrin expression may have profound effects on cancer cell survival and migration. Here, we aimed at assessing the effects of non-toxic concentrations of NO on human non-small cell lung cancer (NSCLC) cells, including the expression of integrins and the migration of these cells.

Methods The cytotoxic and proliferative effects of NO on human NSCLC-derived H460, H292 and H23 cells were tested by MTT assay. The migration capacities of these cells was evaluated by wound healing and transwell migration assays. The expression of integrins and migration-associated proteins was determined by Western blot analyses.

Results We found that NO treatment caused a significant increase in the expression of integrin αv and $\beta 1$ in all three NSCLC-derived cell lines tested. Known migration-associated proteins acting downstream of these integrins, including focal adhesion kinase (FAK), active RhoA (Rho-GTP) and active cell division control 42 (Cdc42-GTP), were found to be significantly activated in response to NO. In addition, we found that NO-treated cells showed an increased motility and that this motility was associated with a significant increase in the number of filopodia per cell. We also found that

NO-treated cells exhibited increased active protein kinase G (PKG), protein kinase B (AKT) and FAK expression levels. Using a pharmacological approach, we found that the integrin-modulating effect of NO is most likely brought about by a PKG/AKT-dependent mechanism, since the observed changes in integrin expression were abolished by AKT inhibitors, but not by FAK inhibitors.

Conclusion Our data suggest a novel role of NO in the regulation of integrin expression and, concomitantly, the migratory capacity of NSCLC cells.

Keywords Nitric oxide · Integrin · Migration · Lung cancer

1 Introduction

Micro-environmental factors may have profound effects on cancer cells, including their metastatic behavior [1–3]. Since metastasis is one of the most crucial factors determining the survival of cancer patients, ample attempts have been made to identify key molecular mediators that control metastasis. Non-small cell lung cancer (NSCLC) is a highly metastatic malignancy, and the disease is estimated to be the leading cause of cancer-related death [4–8]. The endogenous gas nitric oxide (NO) is known to play a role in the progression of different types of cancer [9] and it has been found that the expression of several forms of NO synthases (NOSs) is strongly upregulated in, among others, NSCLC cells [10]. In addition, it has been found that NO levels in the lungs of patients with lung cancer are higher than those in non-cancer subjects [11]. Previously, we and others have found potentiating effects of NO on the survival [12], the acquisition of cancer stem cell-like characteristics [13] and chemotherapy resistance [14] of NSCLC cells. In addition, it has been reported by others that excessive and uncontrolled NO production

✉ Pithi Chanvorachote
pithi_chan@yahoo.com

¹ Department of Pharmacology and Physiology, Faculty of Pharmaceutical Sciences, Chulalongkorn University, Pathumwan, Bangkok 10330, Thailand

² Cell-based Drug and Health Products Development Research Unit, Faculty of Pharmaceutical Sciences, Chulalongkorn University, Bangkok, Thailand

is positively correlated with the metastatic behavior of various types of cancer [10, 15].

An essential early step in cancer cell dissemination is the turnover of cell-extracellular matrix (ECM) adhesion molecules, which results in cancer cell migration. New interactions between migrating cancer cells and the ECM are generated in the front, and disassembled in the rear, in response to stimulating micro-environmental factors. The key proteins governing cell adhesion are integrins, which comprise a diverse family of transmembrane glycoprotein receptors that mediate dynamic interactions between the ECM and the actin cytoskeleton during cell motility [16]. Additionally, integrin interactions with ECM components are known to generate several signals controlling cell survival and motility [17, 18]. In terms of motility, integrins activate the FAK/Src pathway, which leads to increases in the activity of Rho GTPase family members, including active RhoA (Rho-GTP), active Rac1 (Rac-GTP) and active cell division control 42 (Cdc42-GTP) [16], resulting in cytoskeletal dynamic shifts, the formation of lamellipodia and the formation of filopodia, respectively [19]. Accumulating evidence suggests that the motile behavior of cancer cells is accompanied by switches in cellular integrin patterns, with some integrins decreasing and others increasing [20]. Specifically, increases in integrins αv , $\alpha 5$, $\beta 1$ and $\beta 3$ have been shown to enhance the migration and metastasis of cancer cells [21–24].

So far, the effect of NO on the regulation of integrin expression in lung cancer cells and its contribution to their motility has remained largely unknown. Here, we investigated the role of NO in the regulation of integrins and cell migration in human NSCLC-derived cells (H460, H292 and H23). Using molecular and pharmacological approaches, we found that NO plays an important role in NSCLC cell migration by increasing the expression of specific integrins. In addition, we found that the NO-induced integrin expression switches in these cells are mediated primarily by an AKT-dependent mechanism.

2 Materials and methods

2.1 Cells and reagents

Human non-small cell lung cancer (NSCLC)-derived cell lines H460, H292 and H23 were obtained from the American Type Culture Collection (ATCC®, Manassas, VA, USA). The cells were cultured in RPMI1640 medium supplemented with 10 % fetal bovine serum (FBS), 2 mM L-glutamine and 100 units/ml of each penicillin and streptomycin (Gibco, MD, USA) at 37 °C with 5 % CO₂ in a humidified incubator. NO donor dipropylentriamine (DPTA NONOate) was purchased from Santa Cruz Biotechnology (Santa Cruz,

CA, USA). 3-(4,5-dimethylthiazol-2-yl)-2,5-diphenyltetrazoliumbromide (MTT), dimethyl sulfoxide (DMSO), Hoechst 33342, propidium iodide (PI), Phalloidin-Rhodamine and bovine serum albumin (BSA) were purchased from Sigma Chemical, Inc. (St. Louis, MO, USA). Perifosine (AKT inhibitor), FAK inhibitor14 (FAK inhibitor) and antibodies directed against integrin αv , $\alpha 5$, $\beta 1$, $\beta 3$, PKG, p-AKT (Thr308), AKT, p-FAK (Tyr397), FAK and β -actin, and its respective secondary antibodies were purchased from Cell Signaling (Danvers, MA, USA). Antibodies directed against Rho-GTP, Rac-GTP and Cdc42-GTP were purchased from NewEast Bioscience (King of Prussia, PA, USA).

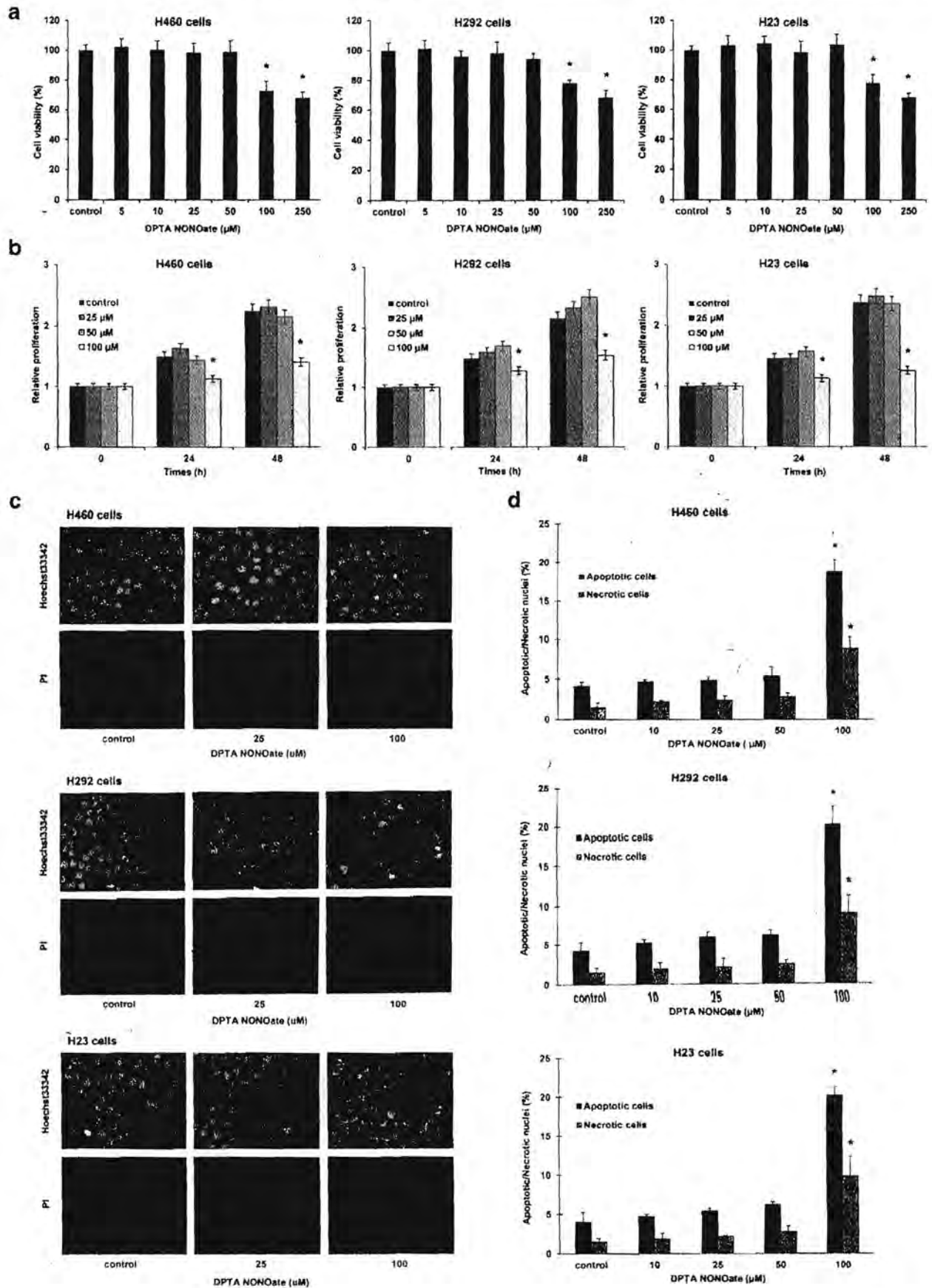
2.2 Cytotoxicity assay

Cell viability was determined by MTT assay. Human NSCLC-derived cells (H460, H292 and H23) were seeded at a density of 1×10^4 cells/well in 96-well plates and treated with NO donor (0–250 μ M) for 24 h. Next, the cells were incubated with MTT (400 μ g/ml) for 4 h at 37 °C, after which the supernatant solution was removed and 100 μ l DMSO was added to dissolve the crystal formazan product. The resulting formazan intensities were measured by spectrophotometry at 570 nm using a microplate reader (Anthros, Durham, NC, USA). The percentage of cell viability was calculated as absorbance of NO-treated cells relative to non-treated cells.

2.3 Proliferation assay

To evaluate proliferative effects, human NSCLC-derived cells (H460, H292 and H23) were seeded at a density of 2×10^3 cells/well in 96-well plates and treated with NO donor (0–100 μ M) for 0, 24 and 48 h. Next, cell proliferation was determined through incubation with MTT (400 μ g/ml) for 4 h at 37 °C, after which the optical densities (OD) of the formazan products were measured at 570 nm using a microplate reader (Anthros, Durham, NC, USA). The proliferation rates were determined using the following equation: $OD_{\text{at indicated time}} / OD_{\text{at time 0}}$. The relative proliferation rates were determined by comparing the proliferation rates of treated cells with those of untreated control cells.

Fig. 1 Effect of nitric oxide on cytotoxicity. Human NSCLC-derived cell lines (H460, H292 and H23 cells) were treated with NO donor (0–250 μ M) for 24 h. **a** Cell viabilities analyzed by MTT assay. **b** Relative proliferation rates at 0, 24 and 48 h. **c** Apoptotic and necrotic cell death after NO treatment examined by Hoechst 33342/PI co-staining. **d** Percentages of apoptotic and necrotic nuclei in NO-treated cells. Data represent mean \pm SD ($n = 3$). * $p < 0.05$ versus non-treated control



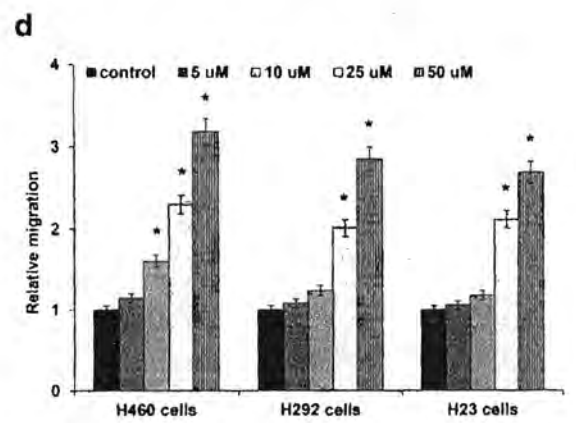
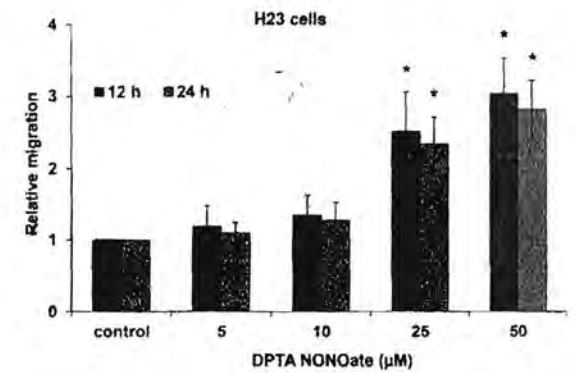
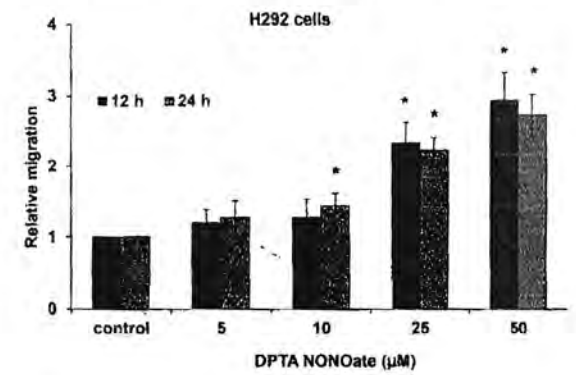
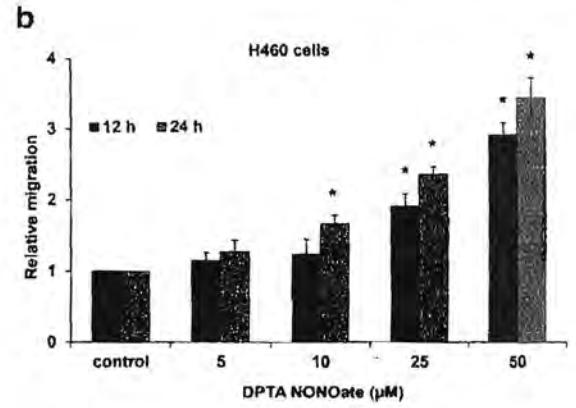
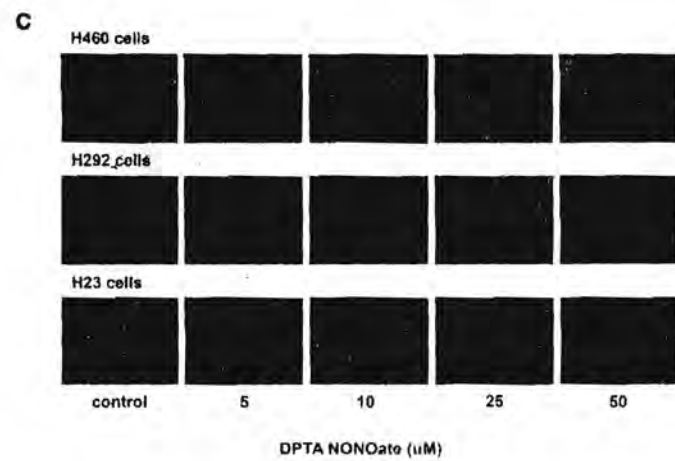
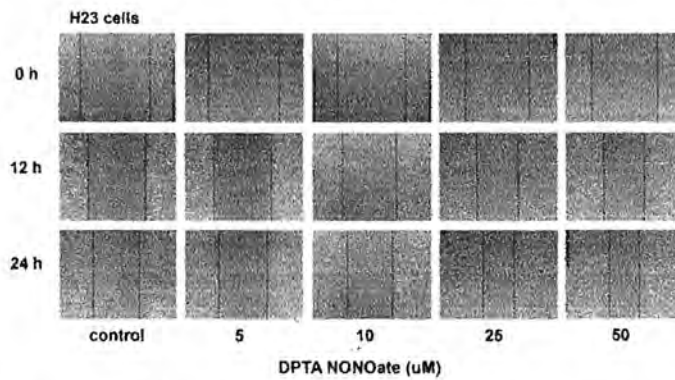
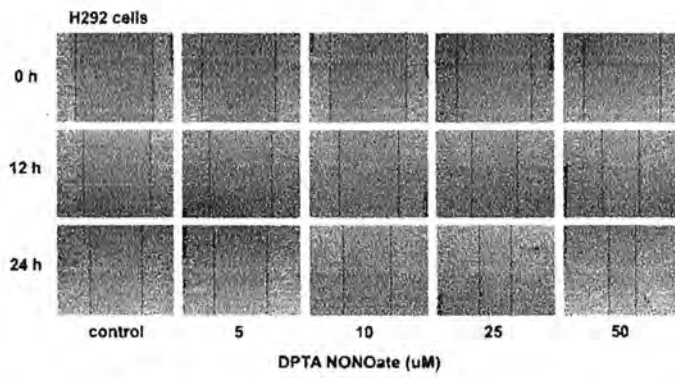
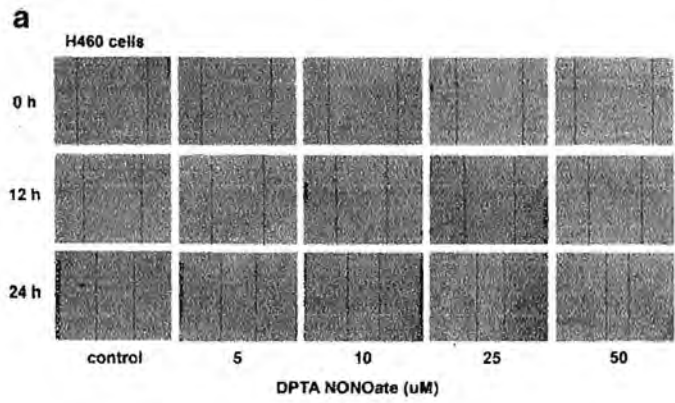


Fig. 2 Nitric oxide enhances human NSCLC cell migration. Human NSCLC-derived cell lines (H460, H292 and H23 cells) were treated with NO donor (0–50 μ M) for 24 h. After treatment, the migratory abilities were assessed by wound healing and transwell migration assays. **a** Phase-contrast images (20 \times) captured at 0, 12 and 24 h. **b** Relative migrations determined by comparing wound spaces to those of non-treated controls. **c** Cells migrated into the lower transwell chamber stained with Hoechst 33342 and visualized by fluorescence microscopy (20 \times). **d** Relative migrations determined by comparisons to non-treated controls. Data represent mean \pm SD ($n = 3$). * $p < 0.05$ versus non-treated control

2.4 Nuclear staining assay

Human NSCLC-derived cells (H460, H292 and H23) were seeded in 96-well plates at a density 1×10^4 cells/well, incubated overnight, and treated with NO donor (0–100 μ M) for 24 h. Next, the cells were rinsed in phosphate-buffered saline (PBS) and subsequently incubated with 10 μ g/ml Hoechst 33342 and 5 μ g/ml propidium iodide (PI) for 30 min. Nuclear condensation and DNA fragmentation of apoptotic cells and PI-positive necrotic cells were visualized and scored using a fluorescence microscope (Olympus IX5; 40 \times) equipped with a DP70 digital camera system (Olympus, Tokyo, Japan).

2.5 Wound healing assay

For the wound healing assay, human NSCLC-derived cells (H460, H292 and H23) were seeded in 96-well plates at a density of 3×10^4 cells/well and treated with NO donor (0–50 μ M) for 24 h. Next, the monolayer cells were allowed to migrate after scratching 'wounds' with a P200 micropipette tip. Detached cells were removed by rinsing once with PBS, after which RPMI1640 serum free medium was added. At indicated time points (0, 12 and 24 h), phase contrast images of the wound spaces were captured under a bright field microscope (20 \times) and the wound spaces were measured using Olympus DP controller software. The relative migrations were calculated by dividing the percentages change in space of the NO-treated cells by those of the non-treated cells in each experiment.

2.6 Transwell migration assay

After NO treatment, transwell migration assays were performed using a Boyden chamber (BD Bioscience, MA, USA). To this end, human NSCLC-derived cells (H460, H292 and H23) were seeded at a density 3×10^4 cells/well in the upper chamber supplemented with RPMI1640 serum free medium, while RPMI-1640 complete medium containing 10 % FBS was added to the lower chamber compartment. After incubation for 24 h at 37 $^{\circ}$ C, the non-migrating cells in the upper chamber were gently removed with a cotton swab,

whereas the cells that had migrated to the lower compartment were fixed with cold absolute methanol for 10 min and stained with 10 μ g/ml Hoechst 33342 for 10 min. Finally, these cells were visualized and captured using a fluorescence microscope (Olympus IX5; 20 \times).

2.7 Morphology change assay

To characterize the effect of NO on cell morphology, NO-treated NSCLC (H460) cells were fixed with 4 % paraformaldehyde for 10 min after which the cell membranes were permeabilized by 0.1 % Triton-X for 5 min. Next, the cells were rinsed with PBS and blocked for unspecific binding with 0.2 % BSA in PBS for 30 min, incubated with a 1:100 dilution of phalloidin-rhodamine in PBS for 30 min, rinsed in PBS three times and mounted in 50 % glycerol/PBS. Cell morphology changes were visualized and captured using a fluorescence microscope (Olympus IX5; 40 \times).

2.8 Western blot analysis

After NO treatment, NSCLC-derived cells (H460, H292 and H23) were incubated with lysis buffer containing 20 mM Tris-HCl (pH 7.5), 1 % Triton X-100, 150 mM sodium chloride, 10 % glycerol, 1 mM sodium orthovanadate, 50 mM sodium fluoride, 100 mM phenylmethylsulfonyl fluoride and protease inhibitor cocktail (Roche Molecular Biochemical) for 30 min on ice. The cellular lysates were collected and their protein content was determined using a BCA protein assay kit (Pierce Biotechnology, Rockford, IL, USA). Equal amounts of protein from each sample were separated by SDS-PAGE and transferred to 0.45 μ m nitrocellulose membranes (Bio-Rad). The resulting blots were blocked for 1 h with 5 % non-fat dry milk in TBST (Tris-buffer saline with 0.1 % Tween containing 25 mM Tris-HCl (pH 7.5), 125 mM NaCl and 0.1 % Tween 20) and incubated with the appropriate primary antibodies at 4 $^{\circ}$ C overnight. After three washes in TBST, the blots were incubated with horseradish peroxidase (HRP)-conjugated secondary antibodies for 2 h at room temperature. Finally, protein bands were detected using an enhancement chemiluminescence substrate (Supersignal West Pico; Pierce, Rockford, IL, USA) and quantified using the analyst/PC densitometry software package (Bio-Rad).

2.9 Statistical analysis

Data from three or more independent experiments are presented as mean \pm standard deviation (SD). Multiple comparisons for significant differences between multiple groups were performed using analysis of variance (ANOVA), followed by individual comparisons with Scheffe's post-hoc test. Statistical significance was considered at $p < 0.05$.

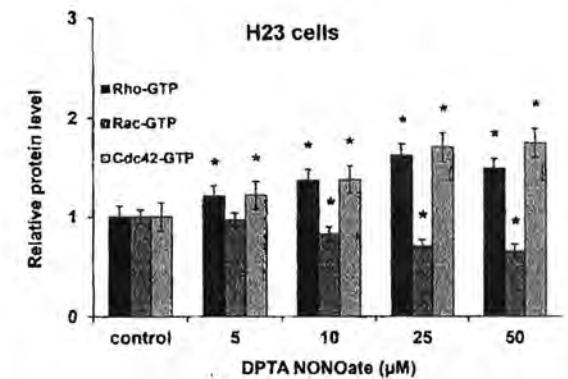
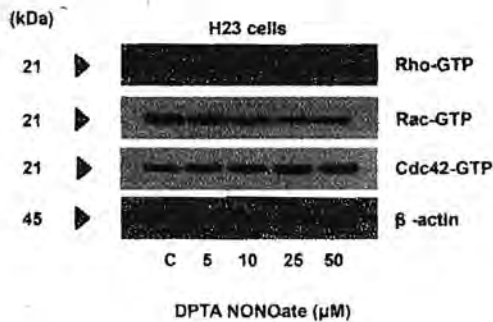
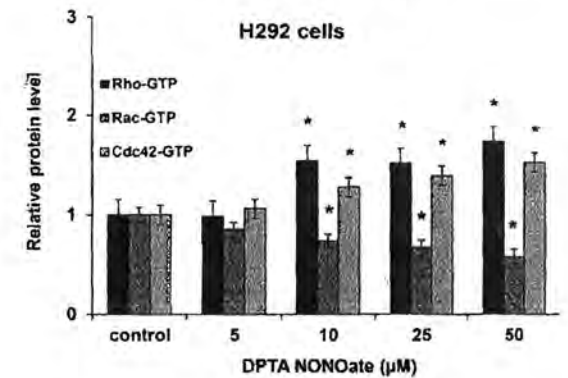
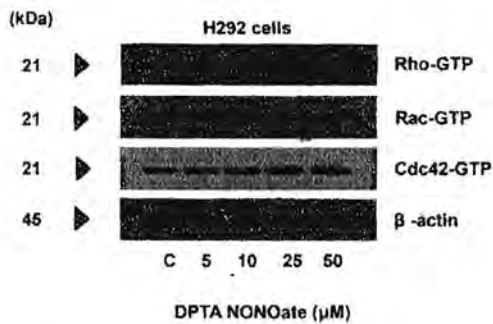
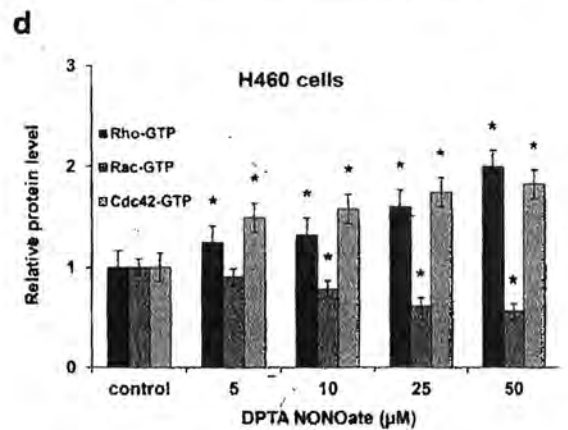
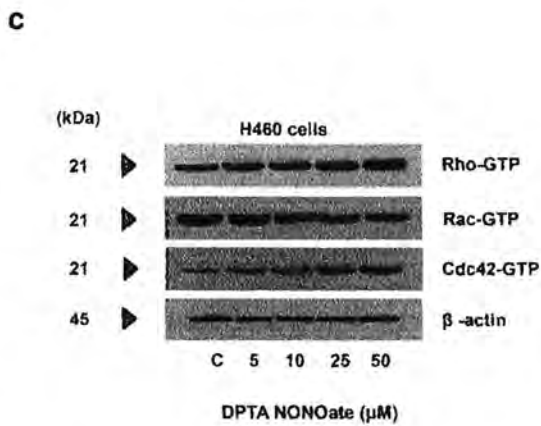
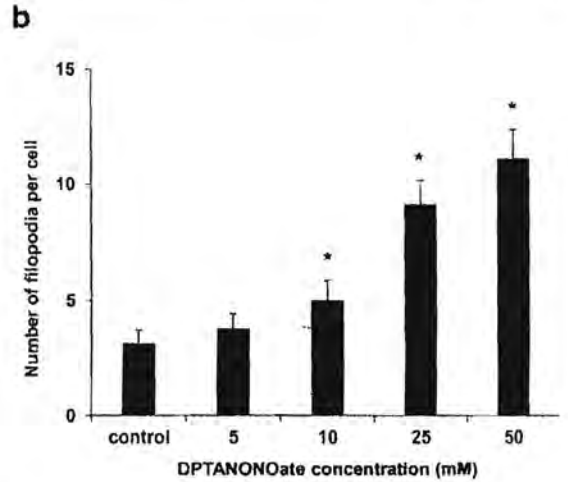
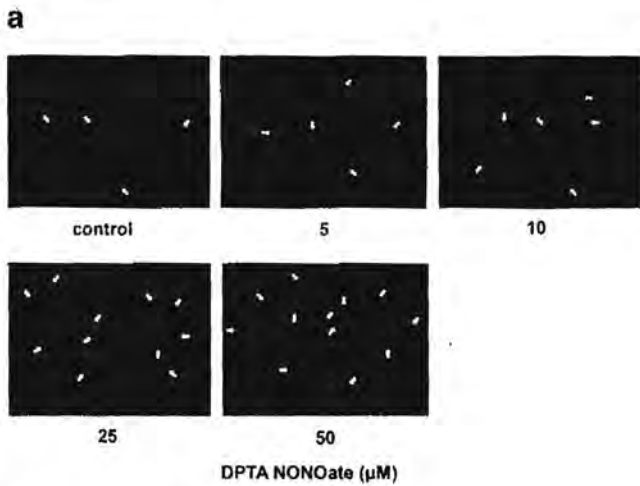


Fig. 3 Nitric oxide activates migration-associated proteins. Human NSCLC-derived cell lines (H460, H292 and H23 cells) were treated with NO donor (0–50 μ M) for 24 h. After treatment (a) Filopodia of H460 cells were stained with phalloidin-rhodamine and visualized by fluorescence microscopy (40 \times). (b) The numbers of filopodia per cell were analyzed and compared to the non-treated control. (c) The expression levels of Rho GTPase proteins in H460, H292 and H23 cells were determined by Western blotting and (d) relative protein levels were quantified by densitometry. Data represent mean \pm SD ($n = 3$). * $p < 0.05$ versus non-treated control

3 Results

3.1 Effect of nitric oxide on the viability of human NSCLC cells

To obtain the appropriate doses of the nitric oxide (NO) donor to be used, we first determined the viabilities of NO-treated human NSCLC-derived H460, H292 and H23 cells. To this end, the cells were treated with various concentrations (0–250 μ M) of NO donor for 24 h after which the respective cell viabilities were determined by MTT assay. We found that NO donor concentrations of 0–50 μ M had neither cytotoxic nor proliferative effects on the cells tested (Fig. 1a–b). A significant decrease in cell viability was first observed in cells treated with 100 μ M NO donor. To confirm the non-cytotoxic concentration of NO, the occurrence of apoptotic and necrotic cells was determined by nuclear staining. We found that neither apoptotic nor necrotic cells appeared in cultures treated with 0–50 μ M NO donor, whereas 100 μ M NO donor treatment led to a significant increase in apoptotic and necrotic cells compared to the non-treated control cells (Fig. 1c–d).

3.2 Nitric oxide increases the migration of human NSCLC cells

Wound healing assays and transwell migration assays were performed to determine the effect of NO on lung cancer cell migration. For the wound healing assays, human NSCLC-derived H460, H292 and H23 cells were exposed to non-toxic concentrations of NO donor (0–50 μ M) for 24 h. Then the cells were subjected to the wound healing assay and allowed to migrate for 24 h. By doing so, we found that NO treatment significantly enhanced the motility of all NSCLC cells tested in a dose-dependent manner (Fig. 2a–b). The subsequent transwell migration assay results confirmed that NO increased the migration capacity of all cells tested, i.e., the cells migrated through the filter membrane to the lower chamber compartment after treatment with NO for 24 h. The migration of the H460, H292 and H23 cells showed a dose-dependent pattern. Significant values were first observed in 10, 25 and 25 μ M NO-treated H460, H292 and H23 cells, respectively (Fig. 2c–d). Taken

together, these results indicate that NO enhances the migratory behavior of human NSCLC cells. The susceptibility of the cells tested varied somewhat, possibly due to differences in cell biological characteristics.

3.3 Nitric oxide increases filopodia formation and migration-associated protein expression

Filopodia are known to play an essential role in cellular movement and, as such, they are used as indicators of motile cells. Filopodia at the protrusion areas, i.e., the fronts of the cells, have been found to contain integrins and other molecules facilitating anchorage formation [25, 26]. To test whether NO can mediate filopodia formation, NSCLC H460 cells were treated with NO donor as previously described, after which the presence of filopodia was determined using a phalloidin-rhodamine staining method. By doing so, we found that NO-treated cells indeed exhibited significant increases in filopodia numbers at the protrusion edges of the cells (Fig. 3a–b).

In addition, we aimed to confirm the effect of NO on cell migration by assessing the expression of migration-associated proteins. To this end, human NSCLC-derived H460, H292 and H23 cells were treated with NO donor after which the Rho-GTP, Rac-GTP and Cdc42-GTP protein levels were determined by Western blotting. We found that treatment of the cells with NO caused significant increases in the Rho-GTP and Cdc42-GTP protein levels, whereas the Rac-GTP protein level was found to be slightly decreased (Fig. 3c–d).

3.4 Nitric oxide mediates integrin expression switching

Integrin expression switching is generally accepted as a determining factor in cell motility [16, 20, 27]. In particular, increased expression of specific integrins, including α v, α 5, β 1 and β 3, has been shown to enhance the motility of cancer cells [21–24]. Therefore, we set out to investigate the effect of NO on integrin expression. To this end, NSCLC-derived H460, H292 and H23 cells were cultured in the presence of NO donor (0–50 μ M) for 24 h, after which the expression of integrins α v, α 5, β 1 and β 3 was determined by Western blotting. We found that NO treatment led to dramatic increases in the expression of integrins α v and β 1 in all three cell lines, whereas the expression of integrin β 3 was only found to be slightly increased in the H292 and H23 cells (Fig. 4). NO treatment had no significant effect on integrin α 5. Based on the presumption that augmentation of specific integrins, especially α v, α 5, β 1 and β 3, is associated with a high migratory activity, we conclude from our results that NO induces the migration of NSCLC cells, at least in the part by increasing the expression of integrins α v and β 1.

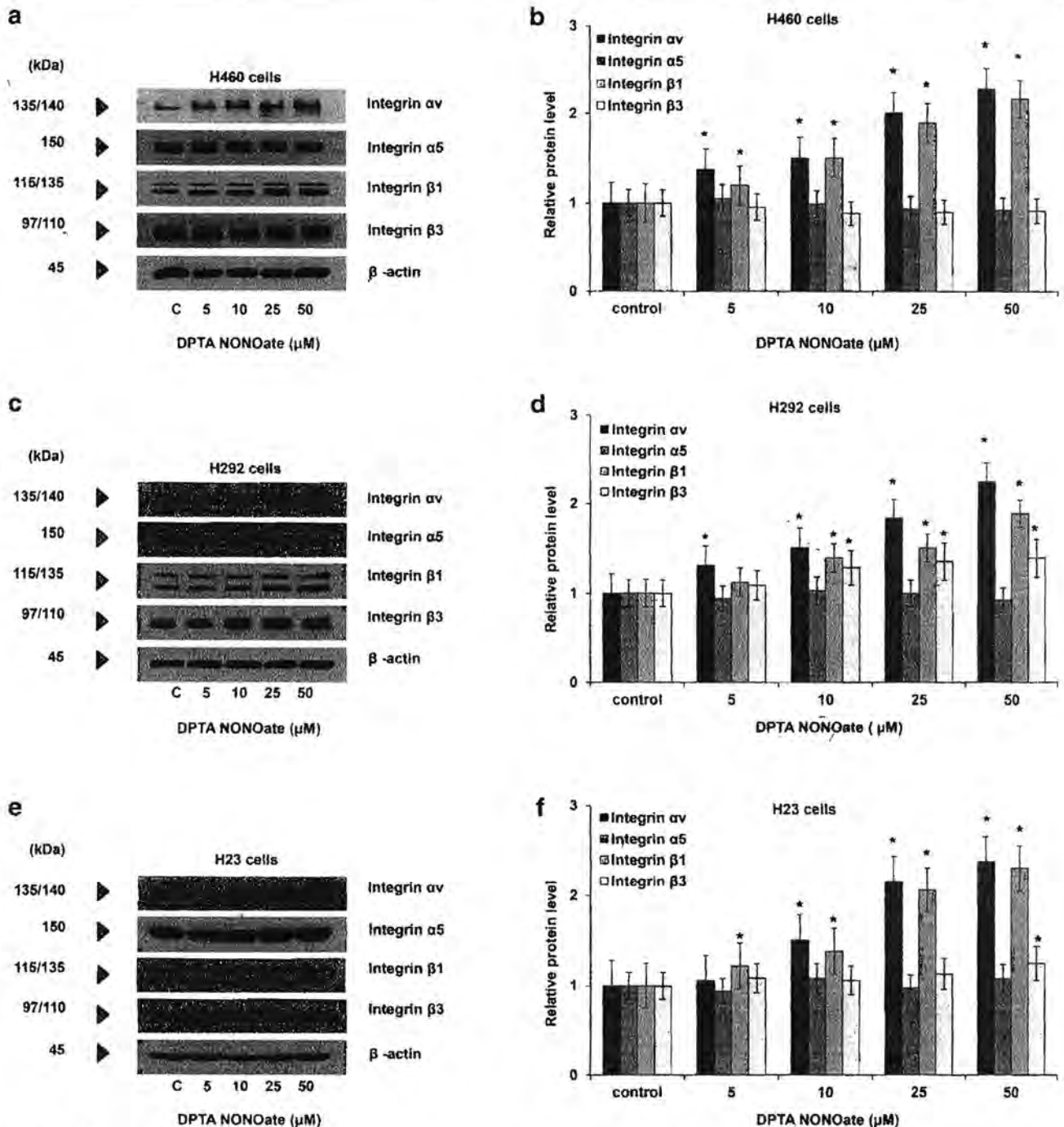


Fig. 4 Effects of nitric oxide on integrin expression. Human NSCLC-derived cell lines (H460, H292 and H23 cells) were treated with NO donor (0–50 μM) for 24 h. After treatment, (a, c, e) the integrin

expression levels (αv , $\alpha 5$, $\beta 1$ and $\beta 3$) were determined by Western blotting. (b, d, f) Relative protein levels quantified by densitometry. Data represent mean \pm SD ($n = 3$). * $p < 0.05$ versus non-treated control

3.5 Nitric oxide induces integrin αv and $\beta 1$ expression via a PKG/AKT-dependent mechanism

Active PKG is known to act as a target of cGMP induced by NO [28]. Also, AKT has been shown to act as a downstream phosphorylation target of PKG [29]. In order to unravel the mechanism by which NO regulates

integrin expression, the activation of PKG, AKT and FAK in response to NO treatment was assessed in NSCLC-derived H460, H292 and H23 cells. Through Western blot analysis we found that NO treatment led to a significant increase in active PKG and in p-AKT/AKT and p-FAK/FAK ratios in a dose-dependent manner in these cells (Fig. 5).

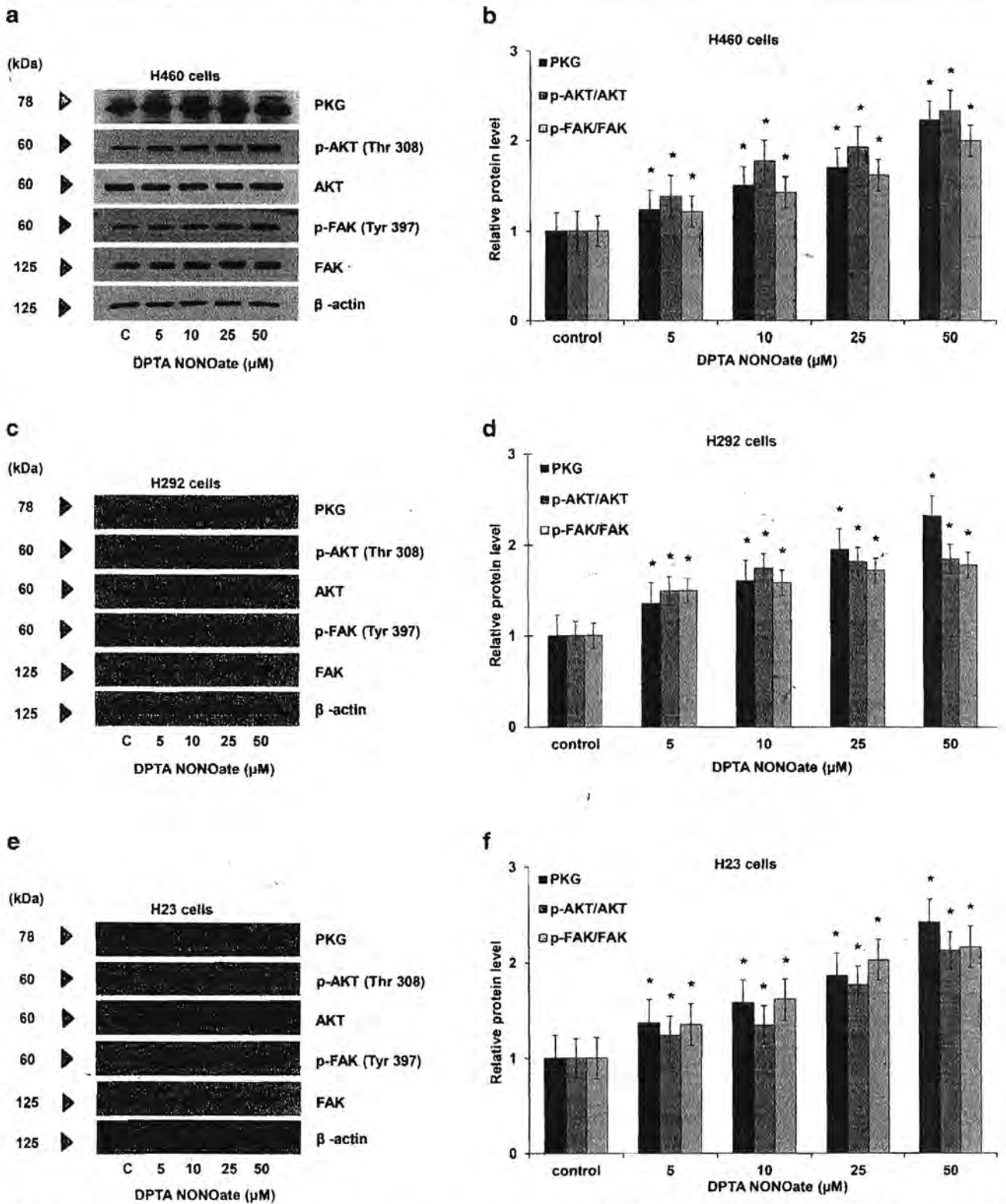


Fig. 5 Nitric oxide activates PKG, AKT and FAK signaling proteins. Human NSCLC-derived cell lines (H460, H292 and H23 cells) were treated with NO donor (0–50 μ M) for 24 h. After treatment (**a**, **c**, **e**) the expression levels of PKG, p-AKT, AKT, p-FAK and FAK were

determined by Western blotting. (**b**, **d**, **f**) Relative protein levels quantified by densitometry. Data represent mean \pm SD ($n = 3$). * $p < 0.05$ versus non-treated control

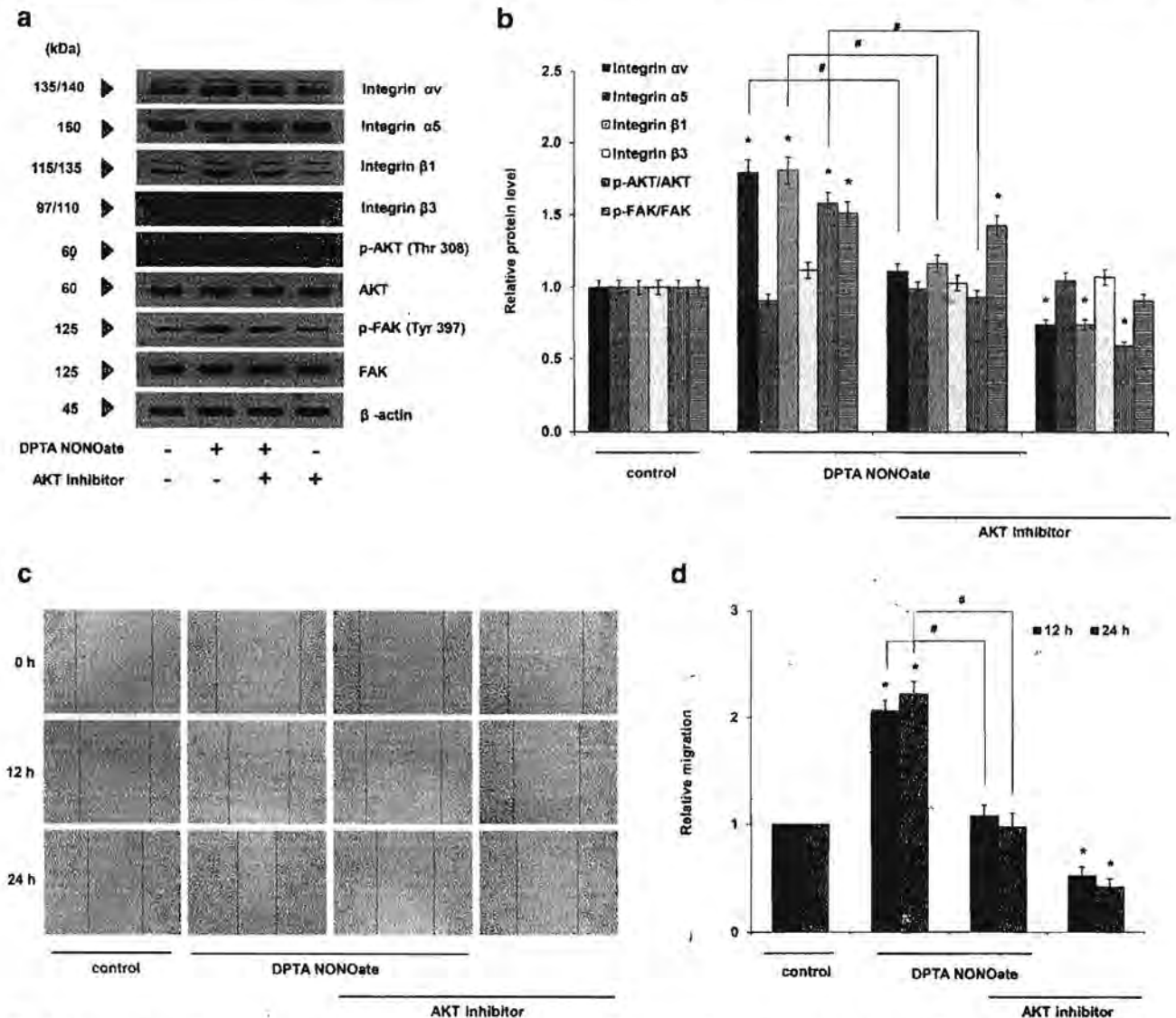


Fig. 6 Nitric oxide mediates integrin expression switching and enhances NSCLC cell migration via an AKT-dependent mechanism. NSCLC H460 cells were treated with or without NO donor (25 μ M) and AKT inhibitor (5 μ M) for 24 h. After treatment (a) the integrin expression levels (α v, α 5, β 1, β 3) and those of related proteins were determined by Western

blotting. b Relative protein levels quantified by densitometry. c Phase contrast images of wound healing captured at 0, 12 and 24 h. d Relative migration determined by comparing wound spaces to those of controls. Data represent mean \pm SD ($n = 3$). * $p < 0.05$ versus non-treated control, # $p < 0.05$ versus NO-treated control

As AKT and FAK have in the past been shown to control the expression of integrins [30–32], we next used AKT and FAK inhibitors to assess their regulatory effects in NSCLC-derived cells. First, we applied the AKT inhibitor (perifosine 5 μ M) to H460 cells to test its effect on the expression of the integrins α v and β 1. We found that treatment of these cells with NO significantly increased the expression of both integrins (Fig. 6), and that the AKT inhibitor concomitantly inhibited the activation of AKT mediated by NO. Interestingly, we found that the AKT inhibitor also diminished the effect of NO on integrin α v and β 1 expression induction, suggesting that NO mediates these integrin alterations via an AKT-dependent mechanism. It is worth noting that treatment

of the H460 cells with the AKT inhibitor also diminished the effect of NO on FAK activation, implying that the FAK signal in this condition was also mediated through an AKT-dependent mechanism. In addition, we found that the AKT inhibitor abolished the migration-enhancing effect of NO.

Whereas we found that FAK inhibitor 14 (10 μ M) significantly suppressed FAK activity, no significant effect was observed on the NO-mediated integrin expression switch (Fig. 7). Additionally, we found that the activation of AKT in response to NO was not affected by the FAK inhibitor. Interestingly, however, we also found that the FAK inhibitor significantly decreased the migratory response of H460 cells to NO. Taken together, we conclude that our data indicate that

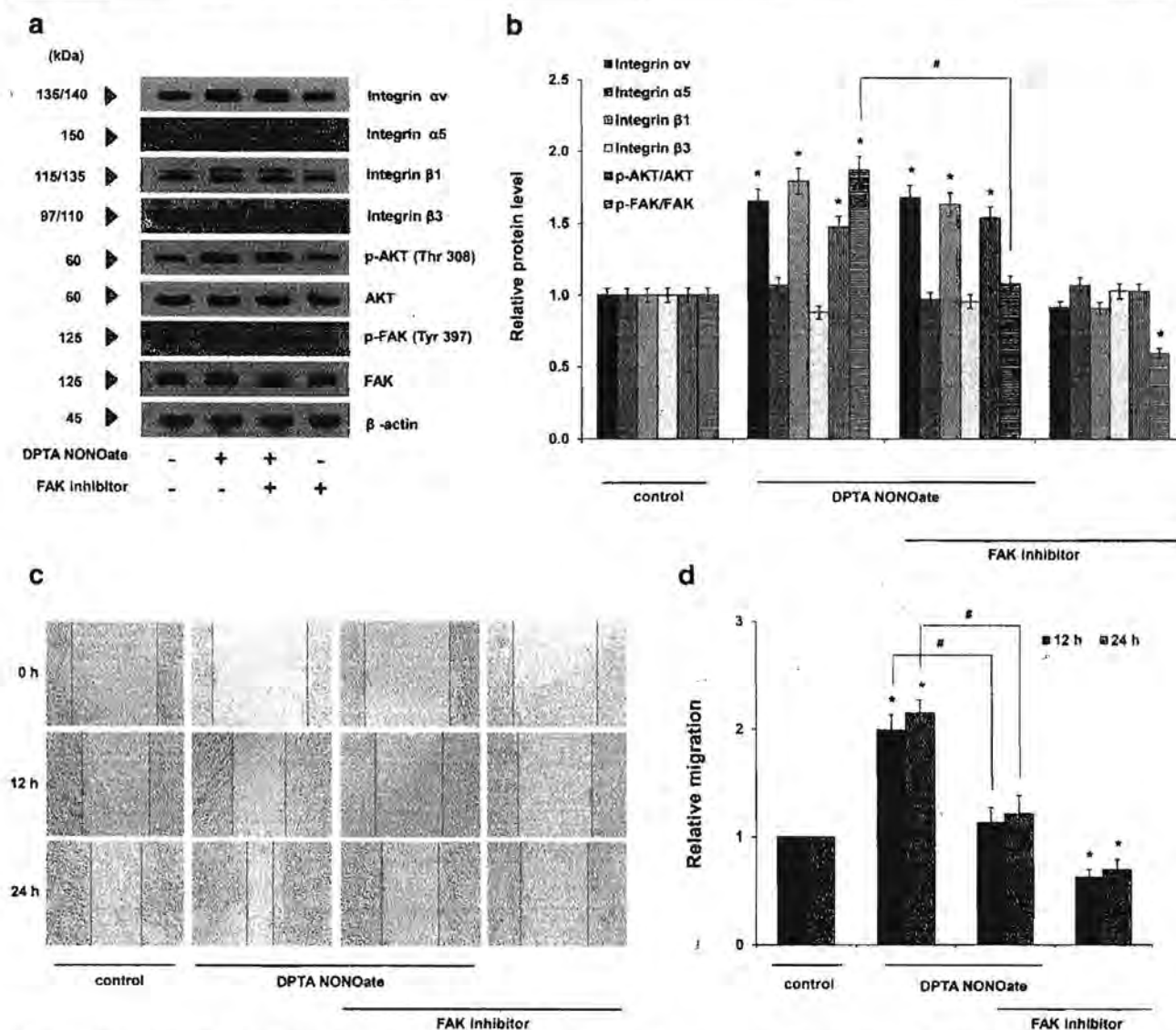


Fig. 7 Integrin signaling induced by nitric oxide mediates H460 cell migration through FAK. NSCLC H460 cells were treated with or without NO donor (25 μ M) and FAK inhibitor (10 μ M) for 24 h. After treatment (a) the integrin expression levels (αv , $\alpha 5$, $\beta 1$, $\beta 3$) and those of related proteins were determined by Western blotting. b Relative protein

levels quantified by densitometry. c Phase contrast images of wound healing captured at 0, 12 and 24 h. d Relative migration determined by comparing wound spaces to those of controls. Data represent mean \pm SD ($n = 3$). * $p < 0.05$ versus non-treated control, # $p < 0.05$ versus NO-treated control

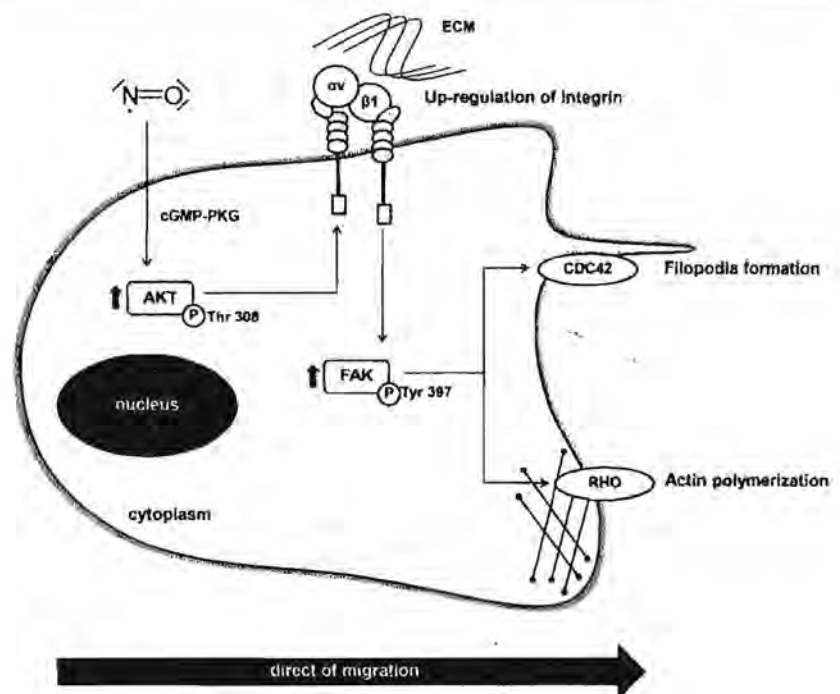
NO mediates integrin expression induction through an AKT-dependent mechanism and that FAK acts downstream to the NO/PKG/AKT cascade in controlling NSCLC cell migration.

4 Discussion

In this study we show that NO, an endogenous gas, functions as an integrin expression modulator in NSCLC cells. Our results additionally suggest that increases in the expression of integrins αv and $\beta 1$ augments the migratory activity of H460, H292 and H23 cells via AKT activation that, in turn, results from PKG activation, a known molecular target of NO.

NO is synthesized through NOS, which is abundantly present in lung cancer tissues [11]. Also, tumor-associated immune cells have been found to induce high micro-environmental NO levels [33, 34]. Some studies have indicated that NO may be cytotoxic to cancer cells since NO can directly induce oxidative stress and DNA damage signals that may result in apoptosis [35]. However, more recent studies have shown that NO at physiological or lower levels is non-cytotoxic, and may even potentiate cellular functions [36]. In case of lung cancer, NO has been found to attenuate its response to cisplatin [14, 37] and to Fas ligand-induced apoptosis [38]. Additionally, NO has been found to mediate anoikis resistance through Caveolin-1 up-regulation [12, 39]. Integrin switching or

Fig. 8 Schematic overview of nitric oxide mediated integrin switching via an AKT-dependent mechanism. Nitric oxide increases p-AKT, which induces expression upregulation of integrins αv and $\beta 1$. High integrin levels recruit and activate FAK to mediate effector molecules such as Cdc42-GTP and Rho-GTP, thereby promoting the migratory process in NSCLC cells



alterations in integrin patterns on the surface of cancer cells has been shown to positively influence their migration and invasion [19, 20]. Integrins are transmembrane glycoprotein receptors that transmit signals from the ECM to intracellular signaling pathways. They regulate a number of cellular processes including survival, proliferation, adhesion and motility [16, 27]. Some integrins, including integrins αv and $\beta 1$, have been shown to potentiate the motility of cells [21, 24, 40]. In conformity with these data, we found that increases in NO-mediated integrin expression levels correlated with increases in the migration of NSCLC cells.

Based on its importance in both cell migration and proliferation, AKT has been denoted as a critical target for anticancer therapy. AKT signaling has been linked to chemotherapy resistance and cancer metastasis [41]. In lung cancer, the PI3K pathway upstream of AKT has been found to be frequently deregulated due to genetic instability resulting in increases in PI3K and, subsequently, AKT signaling [42]. Enhanced activation of AKT has frequently been encountered in NSCLC cells, and has been shown to be correlated with chemo- and radiotherapy resistance [43]. Activated AKT in primary NSCLC tumors has been suggested to act as a poor prognostic factor [41]. In addition to these findings, we here provide data indicating that NO-induced alterations in integrin expression are AKT dependent. We found that treating NSCLC cells with NO resulted in PKG activation, which in turn resulted in AKT activation. Conversely, we found that AKT inhibition resulted in suppression of NO-mediated integrin expression changes in these lung cancer cells, pointing at the importance of the AKT pathway in regulating integrin expression.

In cellular protrusions FAK is activated through phosphorylation at its Tyr 397 position. Active p-FAK stimulates downstream pathways resulting in actin polymerization and filopodia formation [44]. In addition, several GTPases have been found to regulate migration-associated cytoskeleton dynamics. Cdc42-GTP, for example, promotes filopodia formation and extends forward protrusions. Likewise, Rho-GTP regulates stress fiber accumulation and controls rearward contractions, whereas Rac-GTP regulates actin rearrangements and induces lamellipodia formation [20]. Here, we found that these GTPases are also involved in NSCLC motility and that Cdc42-GTP and Rho-GTP are significantly increased in NO-treated NSCLC cells. Consistent with previously reported findings, we noted that upregulation of Cdc42-GTP in NO-treated NSCLC cells correlated with increases in the numbers of filopodia.

In conclusion, we show here for the first time that NO induces the expression of integrin αv and $\beta 1$ in human NSCLC cells through PKG/AKT signaling (Fig. 8). As integrin expression switching has been found to correlate with chemotherapy resistance, enhanced metastasis and a poor prognosis in many cancers, the findings reported here may be instrumental for uncovering the role of NO in imposing an aggressive behavior upon lung cancer cells, at least in part through integrin expression regulation.

Acknowledgments This study was funded by the Thailand Research Fund (RSA5780043). The funders had no role in the study design, the data collection and analysis, the decision to publish or the preparation of the manuscript.

Compliance with ethical standards

Conflict of interest The authors declare that they have no competing interests.

References

1. A. Khosravi, S. Shahrabadi, M. Shahjehani, N. Saki, The bone marrow metastasis niche in retinoblastoma. *Cell. Oncol.* **38**, 253–263 (2015)
2. J. A. Joyce, J. W. Pollard, Microenvironmental regulation of metastasis. *Nat. Rev. Cancer* **9**, 239–252 (2009)
3. S. Wan, Y. Liu, Y. Weng, W. Wang, W. Ren, C. Fei, Y. Chen, Z. Zhang, T. Wang, J. Wang, BMP9 regulates cross-talk between breast cancer cells and bone marrow-derived mesenchymal stem cells. *Cell. Oncol.* **37**, 363–375 (2014)
4. A. Koren, E. Sodja, M. Rijavec, M. Jez, V. Kovac, P. Korosec, T. Cufar, Prognostic value of cytokeratin-7 mRNA expression in peripheral whole blood of advanced lung adenocarcinoma patients. *Cell. Oncol.* **38**, 387–395 (2015)
5. E. Prodromaki, A. Korpetinou, E. Giannopoulou, E. Vlotinou, μ . Chatziathanasiadou, N. Papachristou, C. Scopa, H. Papadaki, H. Kalofonos, D. Papachristou, expression of the microRNA regulators Drossha, dicer and Ago2 in non-small cell lung carcinomas. *Cell. Oncol.* **38**, 307–317 (2015)
6. C. Zeng, W. Fan, X. Zhang, RRM1 expression is associated with the outcome of gemcitabine-based treatment of non-small cell lung cancer patients—a short report. *Cell. Oncol.* **38**, 319–325 (2015)
7. Z. B. Cincin, M. Unlu, B. Kiran, E. S. Bireller, Y. Baran, B. Cakmakoglu, Anti-proliferative, apoptotic and signal transduction effects of hesperidin in non-small cell lung cancer cells. *Cell. Oncol.* **38**, 195–204 (2015)
8. R. L. Siegel, K. D. Miller, A. Jemal, Cancer statistics. *CA Cancer J. Clin.* **65**, 5–29 (2015)
9. L. C. Jadeski, K. O. Hum, C. Chakraborty, P. K. Lala, Nitric oxide promotes murine mammary tumour growth and metastasis by stimulating tumour cell migration, invasiveness and angiogenesis. *Int. J. Cancer* **86**, 30–39 (2000)
10. D. Fukumura, S. Kashiwagi, R. K. Jain, The role of nitric oxide in tumour progression. *Nat. Rev. Cancer* **6**, 521–534 (2006)
11. C. Liu, C. Wang, T. Chen, H. Lin, C. Yu, H. Kuo, Increased level of exhaled nitric oxide and up-regulation of inducible nitric oxide synthase in patients with primary lung cancer. *Brit. J. Cancer* **78**, 534 (1998)
12. P. Chanvorachote, U. Nimmanit, Y. Lu, S. Talbot, B.-H. Jiang, Y. Rojanasakul, Nitric oxide regulates lung carcinoma cell anoikis through inhibition of ubiquitin-proteasomal degradation of caveolin-1. *J. Biol. Chem.* **284**, 28476–28484 (2009)
13. N. Yongsanguanchai, V. Pongrakhananon, A. Mutirangura, Y. Rojanasakul, P. Chanvorachote, Nitric oxide induces cancer stem cell-like phenotypes in human lung cancer cells. *Am. J. Physiol. - Cell Ph* **308**, C89–C100 (2015)
14. P. Chanvorachote, U. Nimmanit, C. Stehlik, L. Wang, B.-H. Jiang, B. Ongpipatanakul, Y. Rojanasakul, Nitric oxide regulates cell sensitivity to cisplatin-induced apoptosis through S-nitrosylation and inhibition of Bcl-2 ubiquitination. *Cancer Res.* **66**, 6353–6360 (2006)
15. X. Weiming, L. Z. Liu, M. Loizidou, M. Ahmed, I. G. Charles, The role of nitric oxide in cancer. *Cell Res.* **12**, 311–320 (2002)
16. A. Huttenlocher, A. R. Horwitz, Integrins in cell migration. *Cold Spring Harb. Perspect. Biol.* **3**, a005074 (2011)
17. S. P. Holly, M. K. Larson, L. V. Parise, Multiple roles of integrins in cell motility. *Exp. Cell Res.* **261**, 69–74 (2000)
18. D. G. Stupack, D. A. Cheresh, Get a ligand, get a life: integrins, signaling and cell survival. *J. Cell Sci.* **115**, 3729–3738 (2002)
19. J. D. Hood, D. A. Cheresh, Role of integrins in cell invasion and migration. *Nat. Rev. Cancer* **2**, 91–100 (2002)
20. H. Truong, E. H. Danen, Integrin switching modulates adhesion dynamics and cell migration. *Cell Adhes. Migr.* **3**, 179–181 (2009)
21. N. C. Wong, B. M. Mueller, C. F. Barbas, P. Ruminiski, V. Quaranta, E. C. Lin, J. W. Smith, αv integrins mediate adhesion and migration of breast carcinoma cell lines. *Clin. Exp. Metastasis* **16**, 50–61 (1998)
22. R. Hosotani, M. Kawaguchi, T. Masui, T. Koshiba, J. Ida, K. Fujimoto, M. Wada, R. Doi, M. Imamura, Expression of integrin $\alpha v \beta 3$ in pancreatic carcinoma: relation to MMP-2 activation and lymph node metastasis. *Pancreas* **25**, e30–e35 (2002)
23. P. T. Caswell, H. J. Spence, M. Parsons, D. P. White, K. Clark, K. W. Cheng, G. B. Mills, M. J. Humphries, A. J. Messent, K. I. Anderson, Rab25 associates with $\alpha 5 \beta 1$ integrin to promote invasive migration in 3D microenvironments. *Dev. Cell* **13**, 496–510 (2007)
24. D. Wang, S. Müller, A. R. Amin, D. Huang, L. Su, Z. Hu, M. A. Rahman, S. Nannapaneni, L. Koenig, Z. Chen, The pivotal role of integrin $\beta 1$ in metastasis of head and neck squamous cell carcinoma. *Clin. Cancer Res.* **18**, 4589–4599 (2012)
25. H. Guillou, A. Depraz-Depland, E. Planus, B. Vianay, J. Chaussy, A. Grichine, C. Albiges-Rizo, M. R. Block, Lamellipodia nucleation by filopodia depends on integrin occupancy and downstream Rac1 signaling. *Exp. Cell Res.* **314**, 478–488 (2008)
26. R. Mayor, C. Carmona-Fontaine, Keeping in touch with contact inhibition of locomotion. *Trends Cell Biol.* **20**, 319–328 (2010)
27. W. Guo, F. G. Giancotti, Integrin signalling during tumour progression. *Nat. Rev. Mol. Cell Biol.* **5**, 816–826 (2004)
28. S. H. Francis, J. L. Busch, J. D. Corbin, cGMP-dependent protein kinases and cGMP phosphodiesterases in nitric oxide and cGMP action. *Pharmacol. Rev.* **62**, 525–563 (2010)
29. S. H. Lee, J. S. Byun, P. J. Kong, H. J. Lee, D. K. Kim, H. S. Kim, J.-H. Sohn, J. J. Lee, S. Y. Lim, W. Chun, Inhibition of eNOS/sGC/PKG pathway decreases Akt phosphorylation induced by Kainic acid in mouse hippocampus. *Korean J. Physiol. Pharmacol.* **14**, 37–43 (2010)
30. D. J. Sieg, C. R. Hauck, D. Ilic, C. K. Klingbeil, E. Schaefer, C. H. Damsky, D. D. Schlaepfer, FAK integrates growth-factor and integrin signals to promote cell migration. *Nat. Cell Biol.* **2**, 249–256 (2000)
31. S. K. Mitra, D. D. Schlaepfer, Integrin-regulated FAK–Src signaling in normal and cancer cells. *Curr. Opin. Cell Biol.* **18**, 516–523 (2006)
32. M. S. Roberts, A. J. Woods, T. C. Dale, P. van der Shuijs, J. C. Norman, Protein kinase B/Akt acts via glycogen synthase kinase 3 to regulate recycling of $\alpha v \beta 3$ and $\alpha 5 \beta 1$ integrins. *Mol. Cell Biol.* **24**, 1505–1515 (2004)
33. P. K. Lala, C. Chakraborty, Role of nitric oxide in carcinogenesis and tumour progression. *Lancet Oncol.* **2**, 149–156 (2001)
34. P. Allavena, A. Sica, G. Solinas, C. Porta, A. Mantovani, The inflammatory micro-environment in tumor progression: the role of tumor-associated macrophages. *Crit. Rev. Oncol. Hematol.* **66**, 1–9 (2008)
35. M. Valko, C. Rhodes, J. Moncol, M. Izakovic, M. Mazur, Free radicals, metals and antioxidants in oxidative stress-induced cancer. *Chem. Biol. Interact.* **160**, 1–40 (2006)
36. A. Sanuphan, P. Chunhacha, V. Pongrakhananon, P. Chanvorachote, Long-term nitric oxide exposure enhances lung cancer cell migration. *Biomed. Res. Int.* **2013**, 186972 (2013). doi:10.1155/2013/186972
37. P. Wongvaranon, V. Pongrakhananon, P. Chunhacha, P. Chanvorachote, Acquired resistance to chemotherapy in lung

- cancer cells mediated by prolonged nitric oxide exposure. *Anticancer Res.* **33**, 5433–5444 (2013)
38. P. Chanvorachote, U. Nimmannit, L. Wang, C. Stehlik, B. Lu, N. Azad, Y. Rojanasakul, Nitric oxide negatively regulates Fas CD95-induced apoptosis through inhibition of ubiquitin-proteasome-mediated degradation of FLICE inhibitory protein. *J. Biol. Chem.* **280**, 42044–42050 (2005)
39. P. Chunchacha, P. Chanvorachote, Roles of caveolin-1 on anoikis resistance in non small cell lung cancer. *Int. J. Physiol. Pathophysiol. Pharmacol.* **4**, 149–155 (2012)
40. A. Maiuthed, P. Chanvorachote, Cisplatin at sub-toxic levels mediates integrin switch in lung cancer cells. *Anticancer Res.* **34**, 7111–7117 (2014)
41. E. G. Sarris, M. W. Saif, K. N. Syrigos, The biological role of PI3K pathway in lung cancer. *Pharmaceuticals* **5**, 1236–1264 (2012)
42. J. Luo, B. D. Manning, L. C. Cantley, Targeting the PI3K-Akt pathway in human cancer: rationale and promise. *Cancer Cell* **4**, 257–262 (2003)
43. J. Brognard, A. S. Clark, Y. Ni, P. A. Dennis, Akt/protein kinase B is constitutively active in non-small cell lung cancer cells and promotes cellular survival and resistance to chemotherapy and radiation. *Cancer Res.* **61**, 3986–3997 (2001)
44. S. K. Mitra, D. A. Hanson, D. D. Schlaepfer, Focal adhesion kinase: in command and control of cell motility. *Nat. Rev. Mol. Cell Biol.* **6**, 56–68 (2005)

ANTICANCER RESEARCH

International Journal of Cancer Research and Treatment

ISSN: 0250-7005 (print)
ISSN: 1791-7530 (online)

Editorial Office: International Institute of Anticancer Research,
DELINASIOS G.J. & CO G.P., Kapandriti, POB 22, Attiki 19014,
Greece. Fax: 0030-22950-53389; Tel: 0030-22950-52945
e-mail: journals@iiar-anticancer.org

Dear Sir/Madam:

Enclosed are the galley proofs of your article for ANTICANCER RESEARCH.

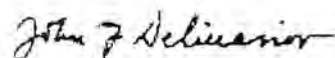
We would like to call your attention to the following:

1. Please read thoroughly, correct, and return the proofs to the Editorial Office **within 24 hours**.
2. Proofs should be returned preferably **by e-mail** or **fax**. Delays in the return of these proofs will necessitate the publication of your paper in a later issue of the journal.
3. Please read the entire manuscript carefully to verify that no changes in meaning have been introduced into the text through language improvements or editorial corrections.
4. Corrections should be limited to typographical errors.
5. Should you require reprints, PDF file, online open access, issues or special author rate subscriptions, please fill the attached reprint order form.
6. If you opt for online open access publication of your paper, it will instantly upon publication be available to read and reproduce free of charge.
7. Should you require information about your article (publication date, volume, page numbers, etc) please call: +30-22950-52945 or send an e-mail to journals@iiar-anticancer.org.
8. Please provide your complete address (not P.O.B.), telephone and fax numbers for the delivery of reprints and issues.
9. Please feel free to contact us with any queries that you may have (Tel./Fax: +30-22950-53389 or +30-22950-52945, e-mail: journals@iiar-anticancer.org).

Thank you for taking the time to study these guidelines.

I greatly appreciate your cooperation and your valuable contribution to this journal.

Yours sincerely,



J.G. Delinasios
Managing Editor

Enclosures

| |
|--------------------------------------------------------------------------------------------------------------------------------------------------------------------------------------------------------------------|
| <p>19430-L Please mark the appropriate section for this paper</p> <p><input type="checkbox"/> Experimental</p> <p><input type="checkbox"/> Clinical</p> <p><input type="checkbox"/> Epidemiological</p> |
|--------------------------------------------------------------------------------------------------------------------------------------------------------------------------------------------------------------------|

Review

Nitric Oxide and Aggressive Behavior of Lung Cancer Cells

SUDJIT LUANPITPONG¹ and PITHI CHANVORACHOTE²

¹*Siriraj Center of Excellence for Stem Cell Research, Faculty of Medicine Siriraj Hospital, Mahidol University, Bangkok, Thailand;*

²*Department of Pharmacology and Physiology, Faculty of Pharmaceutical Sciences, Chulalongkorn University, Bangkok, Thailand*

Abstract. Nitric oxide (NO) is an important cell signaling molecule of which level is frequently elevated in many tumors including lung. Cellular phenotypes and behaviors are influenced by NO found in proximity to tumor, namely the tumor microenvironment. In lung cancer, a high level of NO is linked to advanced stage and poor survival of patients. This review describes the promotory role of NO in aggressive behavior of lung cancer cells with a focus on apoptosis and anoikis resistance, cell migration and invasion and cancer stem cells, all of which are key determinants of cancer relapse and metastasis. We specifically address the effects of NO on the modulations of structure, stability, function and activity of key proteins, and discuss how these changes could affect aggressive behavior. Such knowledge will encourage additional experimental and clinical investigations that contribute to the understanding on molecular basis of cancer pathophysiology which could lead to targeted cancer therapy.

Lung cancer is one of the most common cancers and the leading cause of cancer-related death worldwide that kills more than one million people each year (1). Major hurdles for lung cancer treatment are the poor responses to chemotherapy and late diagnosis at locally advanced or metastatic stage (2-4). Increasing evidence has indicated that nitric oxide (NO) signaling is implicated in the pathophysiology of many types of cancer, particularly in tumorigenesis and cancer progression in various tissues, including the brain, breast, prostate, pancreas and lung (5, 6).

Correspondence to: Pithi Chanvorachote, Department of Pharmacology and Physiology, Faculty of Pharmaceutical Sciences, Chulalongkorn University, Bangkok 10330, Thailand. Tel: +66 22188344, Fax: +66 22188340, e-mail: pithi_chan@yahoo.com

Key Words: Nitric oxide, lung cancer, metastasis, apoptosis, migration, cancer stem cells, review.

A relatively short-lived free radical, NO is renowned for its role as a messenger or effector signaling molecule, is generated endogenously from the metabolism of L-arginine to L-citrulline through a complex reaction catalyzed by various NADPH-dependent enzymes called nitric oxide synthase (NOS) (7). NOS exists in three isoforms, each with a distinct function and working conditions: neuronal NOS (nNOS or NOS1), inducible NOS (iNOS or NOS2) and endothelial NOS (eNOS or NOS3) (8). Up-regulation of NOS and elevated NO activity is frequently detected in tumor microenvironments (9, 10). NO can be derived from tumor cells themselves and from neighboring cells. Due to its lipophilic nature, NO from neighboring cells, e.g. endothelial cells in the microvasculature or immune cells and stromal cells in tumors, can freely diffuse across cellular membranes and ultimately affect tumor phenotypes and behavior (9, 11). Depending mainly on the concentration and duration of NO exposure, NO appears to exert dichotomous roles in cancer (promotory or inhibitory), a relatively low (micromolar range), but sustained level of NO generally promotes tumors (12, 13).

In patients with lung cancer, a high level of exhaled NO and its metabolites nitrite and nitrotyrosine, as well as the serum nitrite/nitrate, an estimate of in vivo NO, were observed compared with healthy controls (14-16). It was further demonstrated that the high level of serum nitrite/nitrate was associated with advanced-stage lung cancer and poor survival rate of patients (16), suggesting that NO might be involved in aggressive tumor phenotypes and metastasis. In this review, we summarize the current findings and understanding of NO in aggressive phenotypes of human lung cancer and discuss its effect on key proteins in relation to chemotherapeutic resistance and each step of metastasis.

Chemotherapy Resistance in Lung Cancer

Chemotherapy is a major treatment modality for cancer, including lung cancer (2). Intrinsic chemotherapy resistance

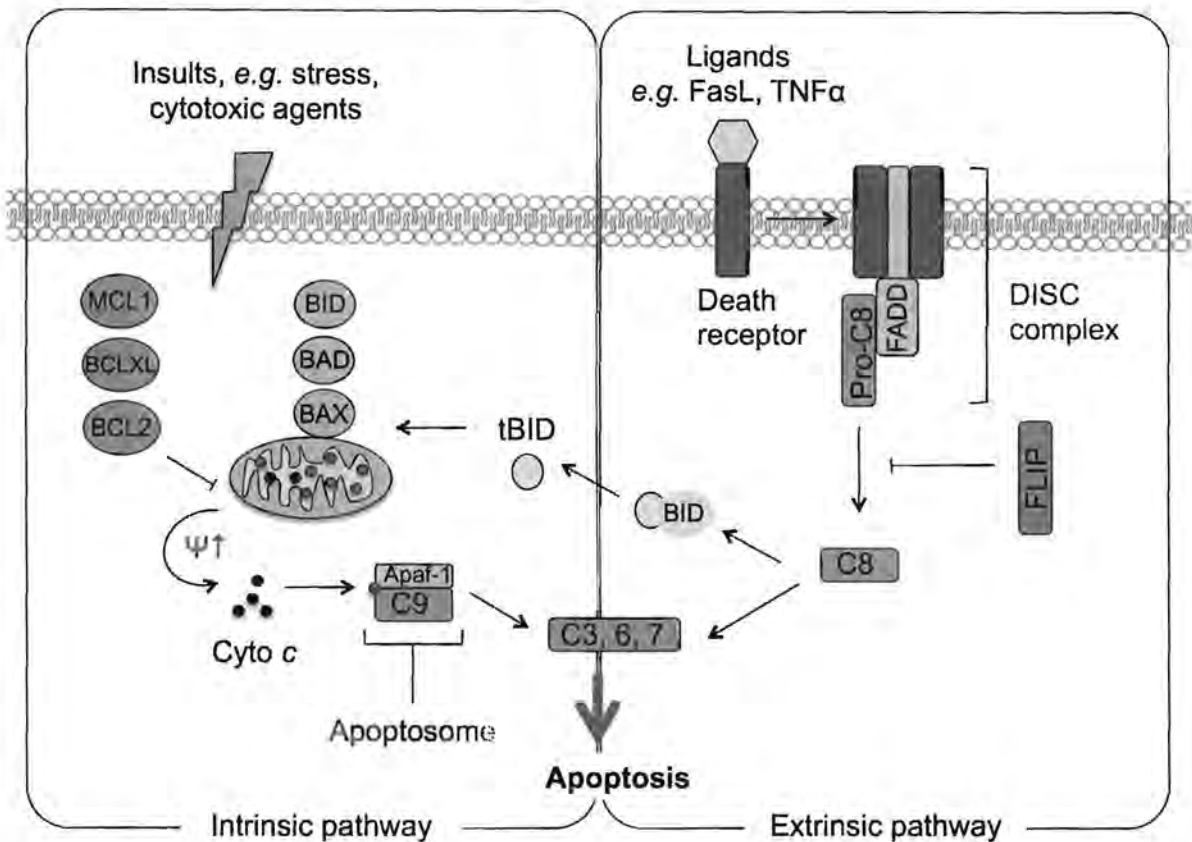


Figure 1. Schematic overview of the major pathways of apoptosis. An intrinsic pathway of apoptosis is induced by various insults such as cytotoxic agents and cellular stress that lead to an alteration in mitochondrial membrane potential (ψ), which is regulated by B-cell lymphoma 2 (BCL2) family proteins, a release of cytochrome c (Cytoc c) and an activation of caspase (C)-9. On the other hand, the extrinsic pathway of apoptosis involves the binding of death receptors to their respective ligands and an activation of caspase (C)-8, a process which can be inhibited by FLICE-inhibitory protein (FLIP). In addition, BH3 interacting-domain death agonist (BID) can be cleaved by caspase-8 and transduces these death signals to the intrinsic pathway.

is often observed in non-small cell lung cancer (NSCLC) cells, while acquired resistance over the course of treatment is often reported in small-cell lung cancer (SCLC) (17). Most, if not all, chemotherapeutic agents induce cancer cell death through the induction of apoptosis (18, 19). Thus, the apoptotic machinery is important in dictating the success of chemotherapy, failure to induce apoptosis leads to chemotherapy resistance (20). NO has been shown to possess both pro- and anti-apoptotic activities, depending on the cellular context, redox status and dosage of NO (21). NO at high concentrations induces apoptosis via oxidative stress and caspase activation (22, 23). On the other hand, accumulating evidence has indicated that the physiological level of NO inhibits apoptosis in several cell types, including lung cancer cells, as detailed below.

NO and apoptosis resistance. Apoptosis is a process of programmed cell death that may be initiated either through

the intrinsic mitochondrial pathway or extrinsic death receptor pathway (Figure 1). In general, the intrinsic pathway is activated in response to a variety of death signals, e.g. DNA damage, oxidative or nitrosative stress and cytotoxic agents, leading to the permeabilization of outer membrane of mitochondria, which is controlled by the balance of the pro-apoptotic (e.g. BCL2-associated X (BAX), Bcl-2 homologous killer (BAK), Bcl-2-associated death promoter (BAD) and BH3 interacting-domain death agonist (BID)) and anti-apoptotic (e.g. B-cell lymphoma 2 (BCL2), B-cell lymphoma-extra large (BCL-xL) and myeloid leukemia cell differentiation protein (MCL1)) BCL2 family proteins, and subsequent release of cytochrome c (24). The released cytochrome c binds to caspase adaptor molecule apoptotic protease activating factor 1 (APAF1) and recruits initiator caspase-9, forming a complex called the apoptosome that promotes activation of effector caspases (e.g. caspase-3, capase-6 and caspase-7) to induce apoptosis. The extrinsic

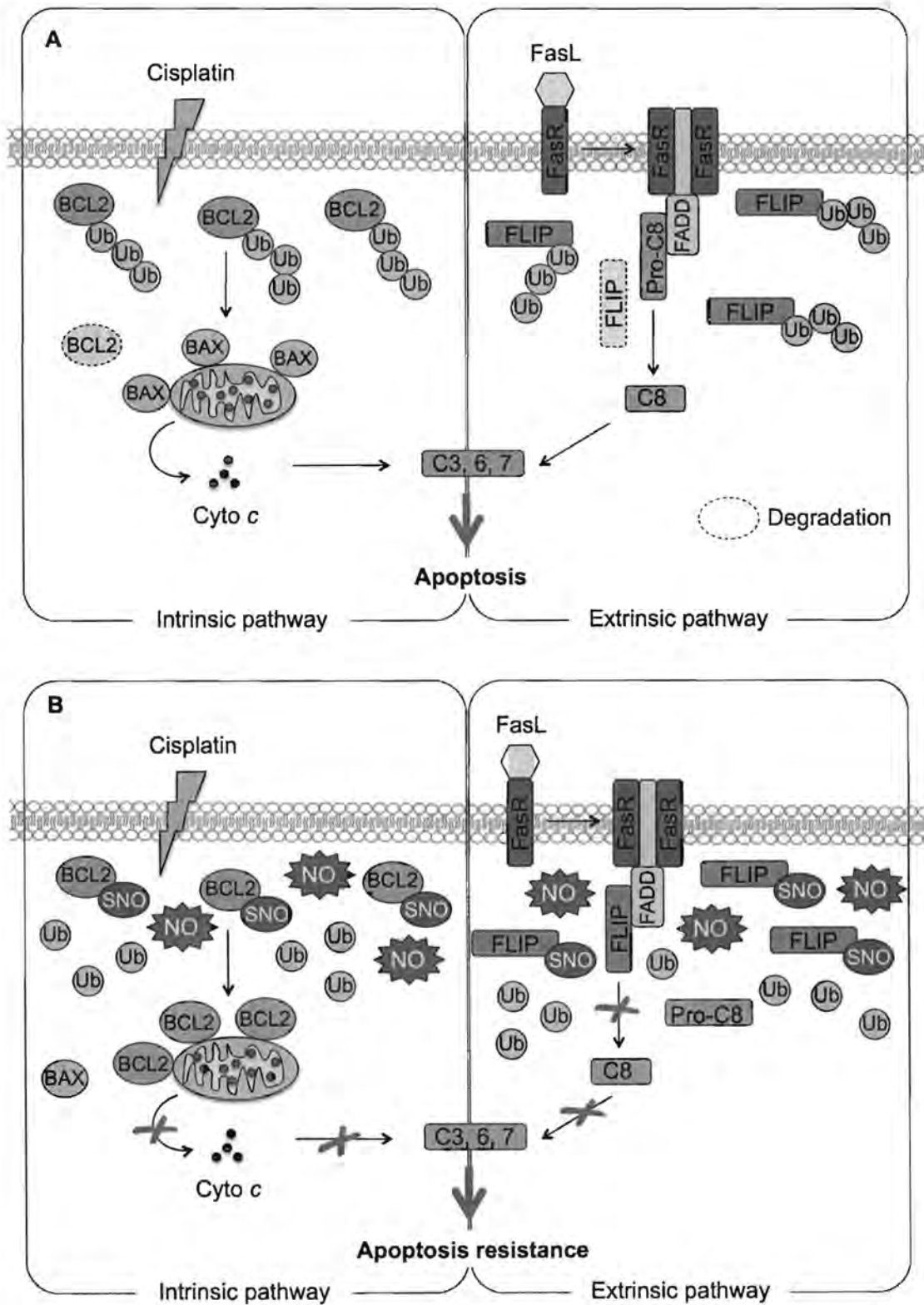


Figure 2. Schematic representation of the regulatory effects of NO on intrinsic and extrinsic apoptosis pathways. A: Cisplatin and Fas ligand (FasL)-mediated apoptosis through the ubiquitin (Ub)-proteasomal degradation of B-cell lymphoma 2 (BCL2) and FLICE-inhibitory protein (FLIP), respectively. B: S-Nitrosylation (SNO) of BCL2 and FLIP by NO prevents its ubiquitin-proteasomal degradation and inhibits cellular apoptosis.

pathway is activated through the binding of death-inducing ligands such as Fas (CD95), tumor necrosis factor- α (TNF α) or TNF-related apoptosis-inducing ligand (TRAIL) to their respective cell surface death receptors, resulting in the recruitment and activation of initiator caspase-8 to death-inducing signaling complex (DISC), which subsequently activates effector caspases to cleave cellular substrates (25).

NO was shown to suppress apoptosis induced by various agents through both intrinsic and extrinsic pathways. In the intrinsic pathway, NO was shown to render lung cancer cells to resistance to apoptosis induced by cisplatin chemotherapy through mechanisms that involves BCL2 up-regulation by preventing its degradation through ubiquitin-proteasome pathway that is mediated by *S*-nitrosylation a major post-translational protein modification resulting from a coupling of nitroso moiety to reactive cysteine thiol (SH), of BCL2 (Figure 2) (26). In the extrinsic pathway, *S*-nitrosylation of FLIP (FLICE-inhibitory protein) is an important mechanism rendering FLIP resistant to ubiquitination and proteasomal degradation by Fas death ligand and ultimately inhibits apoptosis (Figure 2) (27). It has been shown that defects in Fas-mediated apoptosis affects not only immune cells, but also the responses of tumor cells to chemotherapy and irradiation. Recently, *S*-nitrosylation of FLIP was additionally revealed to link to nuclear factor kappa-light-chain-enhancer of activated B cells (NF κ B) activation through the disruption of FLIP/ retinoic acid inducible gene-1 (RIP1) complex and RIP1 redistribution to cell membrane. Impairment of RIP1 translocation impaired anti-apoptotic function of FLIP, indicating that *S*-nitrosylation of FLIP is necessary to confer apoptosis resistance (28). Since increase expression of BCL2, FLIP and NO are frequently observed in chemotherapy-resistant lung cells, *S*-nitrosylation of BCL2 and FLIP could be a key mechanism of chemotherapy resistance.

Regarding the adaptive responses of lung cancer cells to chemotherapy, our group found that relatively long-term (7-14 days) exposure of the cells to NO resulted in significant up-regulation of survival-related proteins including ATP-dependent tyrosine kinase (AKT), caveolin-1 (CAV1) and anti-apoptotic BCL2 (29). Up-regulation of AKT and BCL2 was further found to render lung cancer cells to apoptosis resistance induced by various chemotherapeutic agents, including cisplatin, etoposide and doxorubicin, while up-regulation of CAV1 was related only to doxorubicin and etoposide resistance.

Cancer Metastasis

Cancer metastasis is a multistep process of which a restricted proportion of tumor cells spread from the primary tumor to form a secondary tumor at distant sites. It is the leading cause of cancer-related death and is a prime target for cancer therapy (30). To metastasize, tumor cells must sequentially

follow the principal steps: (i) cell detachment from the primary tumor; (ii) local invasion of host stroma into the lymphatic and blood circulation (intravasation); (iii) survival of cells in the circulation (anoikis resistance); (iv) adhesion of cells to capillary walls; (v) cell invasion and penetration out of the circulation (extravasation); and colonization and formation of secondary tumors (31, 32). NO has been shown to be involved in all of the essential steps of lung cancer metastasis as detailed below.

NO and anoikis. During metastasis, the loss of cell interaction with neighboring cells and the extracellular matrix (ECM) triggers apoptotic cell death called anoikis, which is an important biological mechanism inhibiting cancer cell dissemination (33). Thus, anoikis resistance may facilitate distant metastasis. This consensus is supported by clinical evidence demonstrating a strong correlation between circulating tumor cells with anoikis resistance in advanced cancer and poor survival of patients (34, 35).

Numerous direct and indirect studies suggested that increased NO production suppresses anoikis through the alteration of pro-survival signals, apoptosis-regulatory signals, certain membrane microdomains, and oncogenes. With regard to pro-survival signals, NO regulates PI3K/AKT and suppresses anoikis through mechanisms that likely involve *S*-nitrosylation of phosphatase and tensin homolog deleted on chromosome 10 (PTEN) (36). *S*-Nitrosylation of PTEN also induce its ubiquitination and subsequent degradation, leading to the loss of PTEN that is known to confer anoikis resistance on lung carcinoma (37).

As a form of apoptosis, anoikis is regulated through the common pathways of apoptosis, which include the intrinsic mitochondrial and extrinsic death receptor pathways. As mentioned above, NO affected anti-apoptotic protein FLIP and BCL2 stability through its *S*-nitrosylation. Overexpression of FLIP and BCL2 was reported to render cells resistant to anoikis (38, 39) and is commonly observed in lung carcinoma (40, 41), suggesting the role of NO in anoikis resistance through these proteins.

CAV1, an essential constituent of cell membrane invaginations, has been implicated in metastasis and poor prognosis of lung cancer (42). Our studies have shown that the level of CAV1 in lung carcinoma H460 cells gradually decreased in a time-dependent manner after cell detachment and that ectopic expression of CAV1 prevented anoikis through the stabilization of anti-apoptotic protein MCL1 (43). CAV1 interacts with MCL1 and interferes with its degradation, which occurs during anoikis, through ubiquitin-proteasomal pathway. NO is a critical regulator of CAV1 stability and anoikis resistance. We showed that NO induced *S*-nitrosylation of CAV1, which subsequently prevented its proteasomal degradation and induction of anoikis under cell-detachment conditions (Figure 3) (44).

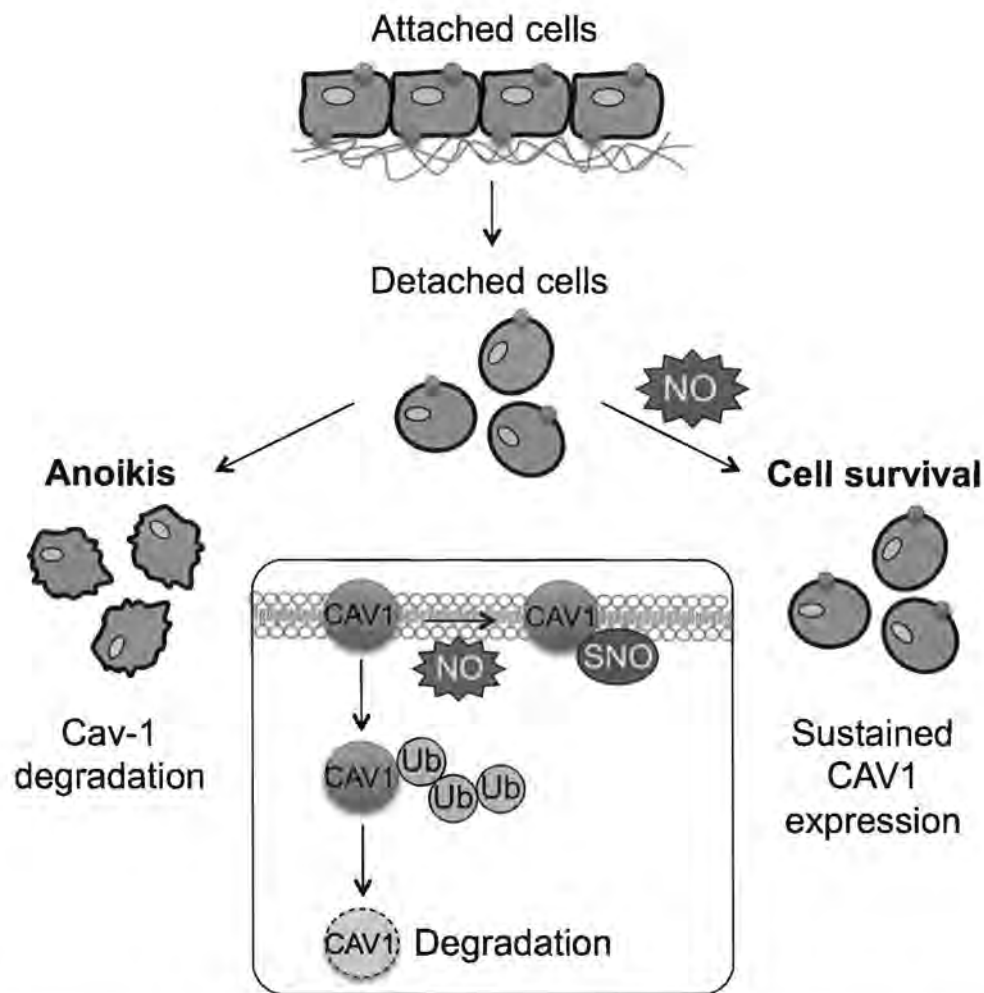


Figure 3. Schematic representation of the regulatory role of NO in resistance to anoikis. The majority of tumor cells undergo detachment-induced apoptosis (anoikis). S-Nitrosylation (SNO) of caveolin-1 (CAV1) by NO prevents its ubiquitin-proteasomal degradation and renders cells anoikis-resistant.

NO and cell migration and invasion. The ability of lung cancer cells to migrate and invade allows them to change their position within tissues and into other tissues. Cell migration and invasion are thereby critical steps of cancer metastasis. To intravasate into and extravasate out of lymphatic and blood circulation, primary tumor cells must migrate and invade through the epithelial basement membrane, surrounding stromal structures consisting of the ECM, and vascular basement membrane (45). Only a small fraction of primary cells become invasive and eventually metastasize at any given time, and NO has been shown to affect such fraction through regulation of multiple proteins. We focus on the promoting effects of micromolar levels of NO on cell motility.

An elevated level of CAV1 expression is reported to correlate well with enhanced invasive ability of lung carcinoma. Redistribution of CAV1 to lung cancer cells led

to the formation of filopodia, a spike-like projection enriched with F-actin filaments at the leading edge of cells that facilitates cell movement (42). We found that prolonged exposure of lung cancer H460 cells to NO altered cell morphology, e.g. cell enlargement, and cell migration in accordance with an increase in filopodia formation and CAV1 expression (46). We further revealed that CAV1 mediates focal adhesion kinase (FAK) and its downstream AKT pathways, affecting lung cancer cell protrusion and migration.

Prolonged NO exposure also activated epithelial-mesenchymal transition (EMT) in various lung cancer cell lines, namely H292, H23, A549 and H460 (47). EMT is a multistep cellular process that allows epithelial cells, which normally interact with the basement membrane, to undergo changes leading to a mesenchymal phenotype, which lacks membrane bounding and allows enhanced cell migration and

invasion (48). EMT is characterized by the progressive loss of epithelial markers, such as vimentin, tight junction protein 1 (ZO1) and E-cadherin, and gain of mesenchymal markers, such as zinc finger protein SNAI2 (SLUG), zinc finger protein SNAI1 (SNAIL), N-cadherin and β -catenin. Prolonged NO exposure induced dramatic increase in vimentin and SNAIL, independently of CAV1, suggesting the additional mechanism of NO-mediated cell motility.

Cancer Stem Cells

Cancer stem cells (CSCs; also known as tumor-initiating cells) are defined as a rare subpopulation of tumor cells that are capable of self-renewal and generate a progeny of differentiated cells that constitute a large majority of cells in the tumor (49). The existence of CSCs has been identified in many types of cancer, including that of the brain, breast, colon, prostate and lung (50). Currently, CSCs are being considered as the underlying causes of chemo/radioreistance, cancer relapse and high mortality rate of lung cancer, due to their reported role in aggressive behavior of human cancer cells and tumorigenesis (51, 52). Hallmarks of CSCs include unlimited cell proliferation, evasion of apoptosis, increased cell migration and invasion, and capability of initiating tumor formation.

NO and CSCs. The role of NO in CSCs has been suggested in breast cancer in that NO induced CD44 expression and signal transducer and activator of transcription 3 (STAT3) activation, indicative of breast CSCs (53). The previous findings that NO increased lung cancer aggressiveness, together with its suggested role in breast CSCs, led to the hypothesis that NO may mediate its lung procarcinogenic effects through CSCs. Our findings revealed that prolonged NO exposure induced two well-known lung markers of CSCs, namely CD133 and aldehyde dehydrogenase 1 family, member A1 (ALDH1A1) in multiple lung cancer cell lines, *e.g.* H460 and H292, in a dose- and time-dependent manner in agreement with the greater anchorage-dependent growth, spheroid formation and anoikis resistance, indicating the induction of CSC-like behavior by NO (54). Such effects of NO, however, were reversible after cessation of NO treatment. Furthermore, CAV1 was found to be critical in NO-mediated aggressiveness of CSCs, although its level did not correlate well with CD133 and ALDH1A1. CAV1 has been shown to interact and regulate the transporter ATP-binding cassette sub-family G member 2 (ABCG2) another potential marker of lung CSCs (55, 56). Thus, it is plausible that CAV1 might regulate NO-mediated CSCs through ABCG2.

Concluding Remarks

Accumulating evidence has demonstrated the tumor-promoting role of NO in various types of cancer, including of the lung,

spanning from tumor initiation of cellular transformation to tumor progression through the metastatic cascade and resistance to radio/chemotherapy. In this review, we summarize the role of NO and its key target proteins in relation to chemotherapeutic and anoikis resistance, and cell migration and invasion of lung cancer cells. Understanding the roles of NO in such aggressive behavior of lung cancer cells is important because they are key determinants of cancer metastasis and relapse that remain therapeutic challenges. Ultimately, we summarize the relatively novel findings on the implication of NO in lung CSC regulation, which could be the underlying causes of all NO-mediated aggressive behavior. NO seems to manifest its effects through key target proteins through the post-translational protein modification of *S*-nitrosylation. *S*-Nitrosylation controls the function and activity of numerous tumor-associated proteins and its dysregulation could lead to cancer pathology, inspiring the new idea of targeted cancer treatment based on *S*-nitrosylation.

Author disclosure statement

No potential competing financial interests were disclosed.

Acknowledgements

This work is supported by the Thailand Research Fund (RSA5780043). The Authors wish to thank Mr. Krich Ratprasit

References

- Esposito L, Conti D, Ailavajhala R, Khalil N and Giordano A: Lung cancer: are we up to the challenge? *Curr Genomics* 11: 513-518, 2010.
- Chang A: Chemotherapy, chemoresistance and the changing treatment landscape for NSCLC. *Lung Cancer* 71: 3-10, 2011.
- Crino L, Weder W, van Meerbeeck J and Felip E: Early stage and locally advanced (non- metastatic) non-small-cell lung cancer: ESMO Clinical Practice Guidelines for diagnosis, treatment and follow-up. *Ann Oncol* 21: V103-V115, 2010.
- Riihimaki M, Hemminki A, Fallah M, Thomsen H, Sundquist K, Sundquist J and Hemminki K: Metastatic sites and survival in lung cancer. *Lung Cancer* 86: 78-84, 2014.
- Hickok JR and Thomas DD: Nitric oxide and cancer therapy: the emperor has NO clothes. *Curr. Pharm. Des.* 16: 381-391, 2010.
- Choudhari SK, Chaudhary M, Bagde S, Gadgil AR and Joshi V: Nitric oxide and cancer: a review. *World J. Surg. Oncol* 11: 118, 2013.
- Palmer RM, Ferrige AG and Moncada S: Nitric oxide release accounts for the biological activity of endothelium-derived relaxing factor. *Nature* 327: 524-526, 1987.
- Knowles RG: Nitric oxide synthases. *Biochem. Soc. Trans* 24: 875-878, 1996.
- Fukumura D, Kashiwagi S and Jain RK: The role of nitric oxide in tumour progression. *Nat. Rev. Cancer* 6: 521-534, 2006.
- Lala PK and Orucevic A: Role of nitric oxide in tumor progression: lessons from experimental tumors. *Cancer Metastasis Rev* 17: 91-106, 1998.

- 11 Tse GM, Wong FC, Tsang AK, Lee CS, Lui PC, Lo AW, Law BK, Scolyer RA, Karim RZ and Putti TC: Stromal nitric oxide synthase (NOS) expression correlates with the grade of mammary phalloides tumour, *J. Clin. Pathol* 58: 600-604, 2005.
- 12 Mocellin S, Bronte V, Nitti D: Nitric oxide a double-edged sword in cancer biology: searching for therapeutic opportunities, *Med. Res. Rev.* 2007, 27, 317-352, 2007.
- 13 Ridnour LA, Thomas DD, Donzell D, Espey MG, Roberts DD, Wink DA and Isenberg JS: The biphasic nature of nitric oxide in carcinogenesis and tumour progression, *Lancet Oncol* 2: 149-156, 2001.
- 14 Liu CY, Wang CH, Chen TC, Lin HC, Yu CT and Kuo HP: Increased level of exhaled nitric oxide and up-regulation of inducible nitric oxide synthase in patients with primary lung cancer, *Br. J. Cancer* 78: 534-541, 1998.
- 15 Masri FA, Comhair SAA, Koeck T, Xu W, Janocha A, Ghosh S, Dweik RA, Golish J, Kinter M, Stuehr DJ, Erzurum SC and Aulak KS: Abnormalities in nitric oxide and its derivatives in lung cancer, *Am. J. Respir. Crit. Care Med* 172: 597-605, 2005.
- 16 Colakogullari M, Ulukaya E, Yilmaztepe A, Ocakoglu G, Yilmaz M, Karadag M and Tokullugil A: Higher serum nitrate levels are associated with poor survival in lung cancer patients, *Clin. Biochem* 39: 898-903, 2006.
- 17 Shanker M, Willcuts D, Roth JA and Ramesh R: Drug resistance in lung cancer, *Lung Cancer Targets Therapy J*: 23-29, 2010.
- 18 Bold RJ, Termuhlen PM and McConkey DJ: Apoptosis, cancer and cancer therapy, *Surg. Oncol* 6: 133-142, 1997.
- 19 Hannun YA: Apoptosis and the dilemma of cancer chemotherapy, *Blood* 89: 1845-1853, 1997.
- 20 Pommier Y, Sordet O, Antony S, Hayward RL and Kohn KW: Apoptosis defects and chemotherapy resistance: molecular interaction maps and networks, *Oncogene* 23: 2934-2949, 2004.
- 21 Kolb JP: Mechanisms involved in pro- and anti-apoptotic role of NO in human leukemia, *Leukemia* 14: 1685-1694, 2000.
- 22 Klein JA and Ackerman SL: Oxidative stress, cell cycle, and neurodegeneration, *J. Clin. Investig* 111: 785-793, 2003.
- 23 Umansky V, Ushmorov A, Ratter F, Chlichlia K, Bucur M, Lichtenauer A and Rocha M: Nitric oxide-mediated apoptosis in human breast cancer cells requires changes in mitochondrial functions and is independent of CD95 (APO1/Fas), *Int. J. Oncol* 16: 109-117, 2000.
- 24 Tait SWG and Green DR: Mitochondria and cell death: outer membrane permeabilization and beyond, *Nat. Rev. Mol. Cell Biol* 11: 621-632, 2010.
- 25 Guicciardi ME and Gores GJ: Life and death by death receptors, *FASEB J* 23: 1625-1637, 2009.
- 26 Chanvorachote P, Nimmannit U, Stehlik C, Wang L, Ongpipatanakul B and Rojanasakul Y: Nitric oxide regulates cell sensitivity to cisplatin-induced apoptosis through S-nitrosylation and inhibition of BCL2 ubiquitination, *Cancer Res* 66: 6353-6360, 2006.
- 27 Chanvorachote P, Nimmannit U, Wang L, Stehlik C, Lu B, Azad N and Rojanasakul Y: Nitric oxide negatively regulates Fas CD95-induced apoptosis through inhibition of ubiquitin-proteasome-mediated degradation of FLICE inhibitory protein, *J. Biol. Chem* 280: 42044-42050, 2005.
- 28 Talbott SJ, Luanpitpong S, Stehlik C, Azad N, Iyer AK, Wang L and Rojanasakul Y: S-nitrosylation of FLICE-inhibitory protein determines its interaction with RIP1 and activation of NF- κ B, *Cell Cycle* 13: 1948-1957, 2014.
- 29 Wongvaranon P, Pongrakhananon V, Chunhacha P and Chanvorachote P: Acquired chemotherapeutic resistance in lung cancer cells dediated by prolonged nitric oxide exposure, *Anticancer Res* 33: 5433-5444, 2013.
- 30 Steeg PS and Theodorescu D: Metastasis: a therapeutic target for cancer, *Nat. Clin. Pract. Oncol* 5: 206-219, 2008.
- 31 Fidler I: The pathogenesis of cancer metastasis: the 'seed and soil' hypothesis revisited, *Nat. Rev. Cancer* 3: 453-458, 2003.
- 32 Talmadge JE and Fidler IJ: AACR Centennial Series: the biology of cancer metastasis: historical perspective, *Cancer Res* 70: 5649-5669, 2010.
- 33 Frisch SM and Sreaton RA: Anoikis mechanisms, *Curr. Opin. Cell Biol* 14: 563-568, 2002.
- 34 Cristofanilli M, Budd GT, Ellis MJ, Stopeck A, Matera J, Miller MC, Reuben JM, Doyle GV, Allard J and Terstappen LW: Circulating tumor cells, disease progression, and survival in metastatic breast cancer, *N. Engl. J. Med* 351: 781-791, 2004.
- 35 Moreno JG, Miller MC, Gross S, Allard WJ, Gomella LG and Terstappen LW: Circulating tumor cells predict survival in patients with metastatic prostate cancer, *Urology* 65: 713-718, 2005.
- 36 Numajiri N, Takasawa K, Nishiya T, Tanaka H, Ohno K, Hayakawa W, Asada M, Matsuda H, Azumi K, Kamata H, Nakamura T, Hara H, Minami M, Lipton SA and Uehara T: On-off system for PI3-kinase-AKT signaling through S-nitrosylation of phosphatase with sequence, *Proc. Natl. Acad. Sci. USA* 108: 10349-10354, 2011.
- 37 Mccarroll JA, Gan PP, Erlich RB, Liu M, Dwarte T, Sagnella S, Akerfeldt M, Yang L, Parker AL, Chang MH, Shum MS, Byrne FL and Kavallaris M: TUBB3/ β III-tubulin acts through the PTEN/AKT signaling axis to promote tumorigenesis and anoikis resistance in non-small cell lung cancer, *Cancer Res* 75(2): 415-425, 2015.
- 38 Mawji IA, Simpson CD, Hurren R, Gronda M, Williams MA, Filmus J, Jonkman J, Da Costa RS, Wilson BC, Thomas MP, Reed JC, Glinsky GV and Schimmer AD: Critical role of Fas-associated death domain-like interleukin-1-converting enzyme-like inhibitory protein in anoikis resistance and distant tumor formation, *J Natl Cancer Inst* 99: 811-822, 2007.
- 39 Pongrakhananon V, Nimmannit U, Luanpitpong S, Rojanasakul Y and Chanvorachote P: Curcumin sensitizes non-small cell lung cancer cell anoikis through reactive oxygen species-mediated BCL2 downregulation, *Apoptosis* 15: 574-585, 2010.
- 40 Riley JS, Hutchinson R, McArt DG, Crawford N, Holohan C, Paul I, Van Schaebybroeck S, Salto-Tellez M, Johnston PG, Fennell DA, Gately K, O'Bryne K, Cummins R, Kay E, Hamilton P, Stasik I and Longley DB: Prognostic and therapeutic relevance of FLIP and procaspase-8 overexpression in non-small cell lung cancer, *Cell Death and Disease* 4: e951, 2013.
- 41 Laudanski J, Chydzewski L, Niklinska, WE, Kretowska M, Furman M, Sawicki B and Niklinski J: Expression of BCL2 protein in non-small cell lung cancer: correlation with clinicopathology and patient survival, *Neoplasma* 46: 25-30, 1999.
- 42 Hu CC, Huang PH, Huang HY, Chen YH, Yang PC and Hsu SM: Up-regulated caveolin-1 accentuates the metastasis capability of lung adenocarcinoma by inducing filopodia formation, *Am. J. Pathol* 161: 1647-1656, 2002.
- 43 Chunhacha P, Pongrakhananon V, Rojanasakul Y and Chanvorachote P: Caveolin-1 regulates MCL1 stability and anoikis in lung carcinoma cells, *Am. J. Physiol. Cell. Physiol* 302: C1284-C1892, 2012.

- 44 Chanvorachote P, Nimmannit U, Lu Y, Talbott S, Jiang B and Rojanasakul Y: Nitric oxide regulates lung carcinoma cell anoikis through inhibition of ubiquitin-proteasomal degradation of caveolin-1, *J. Biol. Chem* 284: 28476-28484, 2009.
- 45 Bravo-Cordero JJ, Hodgson L and Condeelis J: directed cell invasion and migration during metastasis. *Curr. Opin. Cell Biol* 24: 277-283, 2012.
- 46 Sanuphan A, Chunhacha P, Pongrakhananon V and Chanvorachote P: Long-term nitric oxide exposure enhances lung cancer cell migration. *Biomed Res Int*: 186972, 2013.
- 47 Chanvorachote P, Pongrakhananon V and Chunhacha P: Prolonged nitric oxide exposure enhances enhanced anoikis resistance and migration through epithelial-mesenchymal transition and caveolin-1 up-regulation. *Biomed Res Int*: 941359, 2014.
- 48 Kalluri R and Weinberg RA: The basics of epithelial-mesenchymal transition, *J Clin Invest* 119: 1420-1428, 2009.
- 49 Ailles LE and Weissman IL: Cancer stem cells in solid tumors, *Curr. Opin. Biotechnol* 18: 460-466, 2007.
- 50 Ho MM, Ng AV, Lam S and Hung JY: Side population in human lung cancer cell lines and tumors is enriched with stem-like cancer cells, *Cancer Res* 67: 4827-4833, 2007.
- 51 Levina V, Marrangoni AM, DeMarco R, Gorelik E and Lokshin A.E: Drug-selected human lung cancer stem cells: cytokine network, tumorigenic and metastatic properties. *PLoS One* 3: e3077, 2008.
- 52 Perona R, López-Ayllón BD, Castro Carpeño J and Belda-Iniesta C: A role for cancer stem cells in drug resistance and metastasis in non-small-cell lung cancer. *Clin. Transl. Oncol* 13: 289-293, 2011.
- 53 Switzer CH, Glynn SA, Cheng RYS, Ridnour LA, Green JE, Ambs S and Wink DA: S-Nitrosylation of EGFR and SRC activates an oncogenic signaling network in human basal-like breast cancer. *Mol. Cancer Res* 10: 1203-1215, 2012.
- 54 Yongsanguanchai N, Pongrakhananon V, Mutirangura A, Rojanasakul Y and Chanvorachote P: Nitric oxide induces cancer stem cell-like phenotypes in human lung cancer cells. *Am J Physiol Cell Physiol* 308(2): C89-100, 2015.
- 55 Herzog M, Storch CH, Gut P, Kotlyar D, Fullekrug J, Ehehalt R, Haefeli WE and Weiss J: Knockdown of caveolin-1 decreases activity of breast cancer resistance protein (BCRP/ABCG2) and increases chemotherapeutic sensitivity. *Naunyn-Schmied Arch. Pharmacol* 383: 1-11, 2011.
- 56 Luanpitpong S, Wang L, Stueckle TA, Tse W, Chen YC and Rojanasakul Y: Caveolin-1 regulates lung cancer stem-like cell induction and p53 inactivation in carbon nanotube-driven tumorigenesis. *Oncotarget* 5: 3541-3554, 2014.

Received April 29, 2015

Revised June 7, 2015

Accepted June 9, 2015

ANTICANCER RESEARCH

International Journal of Cancer Research and Treatment

ISSN: 0250-7005 (print)
ISSN: 1791-7530 (online)

Editorial Office: International Institute of Anticancer Research,
DELINASIOS G.J. & CO G.P., Kapandriti, P.O.B. 22, Attiki 19014, Greece
Fax: +30-22950-53389; Tel: +30-22950-52945; e-mail: journals@iiar-anticancer.org

Please type or print the requested information on the reprint order form and return it to the Editorial Office by fax or e-mail. Fees for reprints, PDF file, online open access and subscriptions must be paid for in advance. If your paper is subject to charges for excess pages or color plates, please add these charges to the payment for reprints. The reprints are not to be sold.

PRICE LIST FOR REPRINTS WITHOUT COVER

| Page length | Online | | Number of copies requested (prices are in Euro) | | | | | | | | | |
|-------------|-------------------------|---------------------|-------------------------------------------------|-----|-----|-----|------|------|------|------|------|------|
| | Open Access Fee* (Euro) | PDF File Fee (Euro) | 50 | 100 | 200 | 300 | 400 | 500 | 1000 | 1500 | 2000 | 3000 |
| 1-4pp | 400 | 175 | 140 | 285 | 337 | 388 | 453 | 504 | 851 | 1135 | 1470 | 2038 |
| 5-8 | 600 | 225 | 150 | 388 | 453 | 530 | 595 | 672 | 1083 | 1445 | 1832 | 2554 |
| 9-12 | 700 | 277 | 160 | 504 | 569 | 659 | 737 | 827 | 1341 | 1780 | 2219 | 3096 |
| 13-16 | 800 | 354 | 180 | 659 | 737 | 840 | 943 | 1046 | 1625 | 2141 | 2657 | 3676 |
| 17-20 | 900 | 419 | 200 | 788 | 879 | 982 | 1098 | 1227 | 1883 | 2451 | 3044 | 4244 |

***Online open access of an article published in 2015 is accompanied by a complimentary online subscription to ANTICANCER RESEARCH.**

For reprints with cover: Please add EURO 80.00 per 100 copies.

Postage: Please add 5% on the reprint prices.

Reprint Order Form

Of my paper No. **19430** comprising **8** printed pages, entitled «**Nitric Oxide and Aggressive Behavior of...**» accepted for publication in ANTICANCER RESEARCH Vol. **35** No. **9**

- I require a total of _____ copies at EURO:
- I do not require reprints.
- Please send me a PDF file of the article at EURO:
- Please provide Online Open Access of the article at the Stanford University Highwire Press website (at Euro) immediately upon publication, and enter my complimentary online subscription to ANTICANCER RESEARCH.
- Please send me a copy of the issue containing my paper at EURO 45.00.
- Please enter my personal subscription to ANTICANCER RESEARCH at the special Author's price of EURO 390.00 (print; online) (Year: 2015).
- A check for the above amounts payable to DELINASIOS G.J. & CO G.P., is enclosed.
- Please send an invoice to (Billing Name and Address):
VAT number (For EC countries):
Name:
Address: _____ Signature:
Country: _____ City:
Postal code: _____ e-mail:
Tel: _____ Fax:
- Please send reprints to (Complete Address and Tel. no.):

ANTICANCER RESEARCH

International Journal of Cancer Research and Treatment

ISSN: 0250-7005 (print) ISSN: 1791-7530 (online)

June 9, 2015

Dr. Pithi Chanvorachote,

Re: Your manuscript No. 19430 entitled «Nitric Oxide and Aggressive Behavior of...»

Dear Dr

Referring to your above manuscript for publication in AR, please allow us to use this form letter in reply:

1. *Referee's recommendations:*

- Urgent to be published immediately.
- Accepted in the presented form.
- Accepted with minor changes.
- Accepted with grammatical or language corrections.
- Remarks: **No Running Title. Please provide.**

2. *Excess page charges.*

- Your article has approx. **8** printed pages and is in excess of the allotted number by approx. **xx** printed pages. The charges are EURO € **xxxx** per excess page, totalling EURO € **xxxx**
We ask you to confirm acceptance of these charges.
- Your article includes **3** pages with color figures. The charges are EURO € **650** per color page, totalling EURO € **975 (-50% Discount)**
- Our invoice will be sent by e-mail to the corresponding author.

3. Your article will appear in Volume **35**, Issue No. **9, 2015**

4. Please order your reprints, pdf or online open access, now. This will facilitate our prompt planning of future issues and rapid publication of your article. Reprints will be delivered by rapid one-day delivery within one month from publication.

We would appreciate your prompt reply.

With many thanks,

Yours sincerely,



J.G. Delinasios
Managing Editor

EDITORIAL OFFICE: INTERNATIONAL INSTITUTE OF ANTICANCER RESEARCH
DELINASIOS G.J. & CO G.P., Kapandriti, P.O.B. 22, Attiki 19014, Greece. Tel.: 0030-22950-52945;
Tel & Fax:0030-22950-53389; e-mail: journals@iiar-anticancer.org

CALL FOR PAPERS | *Cell and Molecular Processes in Cancer Metastasis*

Iron induces cancer stem cells and aggressive phenotypes in human lung cancer cells

Pithi Chanvorachote^{1,2} and Sudjit Luanpitpong^{2,3}

¹Department of Pharmacology and Physiology, Faculty of Pharmaceutical Sciences, Chulalongkorn University, Bangkok, Thailand; ²Cell-based Drug and Health Products Development Research Unit, Chulalongkorn University, Bangkok, Thailand; and ³Siriraj Center of Excellence for Stem Cell Research, Faculty of Medicine Siriraj Hospital, Mahidol University, Bangkok, Thailand

Submitted 9 November 2015; accepted in final form 17 February 2016

Chanvorachote P, Luanpitpong S. Iron induces cancer stem cells and aggressive phenotypes in human lung cancer cells. *Am J Physiol Cell Physiol* 310: C728–C739, 2016. First published February 24, 2016; doi:10.1152/ajpcell.00322.2015.—Evidence has accumulated in support of the critical impact of cancer stem cells (CSCs) behind the chemotherapeutic failure, cancer metastasis, and subsequent disease recurrence and relapse, but knowledge of how CSCs are regulated is still limited. Redox status of the cells has been shown to dramatically influence cell signaling and CSC-like aggressive behaviors. Here, we investigated how subtoxic concentrations of iron, which have been found to specifically induce cellular hydroxyl radical, affected CSC-like subpopulations of human non-small cell lung carcinoma (NSCLC). We reveal for the first time that subchronic iron exposure and higher levels of hydroxyl radical correlated well with increased CSC-like phenotypes. The iron-exposed NSCLC H460 and H292 cells exhibited a remarkable increase in propensities to form CSC spheroids and to proliferate, migrate, and invade in parallel with an increase in level of a well-known CSC marker, ABCG2. We further observed that such phenotypic changes induced by iron were not related to an epithelial-to-mesenchymal transition (EMT). Instead, the sex-determining region Y (SRY)-box 9 protein (SOX9) was substantially linked to iron treatment and hydroxyl radical level. Using gene manipulations, including ectopic SOX9 overexpression and SOX9 short hairpin RNA knockdown, we have verified that SOX9 is responsible for CSC enrichment mediated by iron. These findings indicate a novel role of iron via hydroxyl radical in CSC regulation and its importance in aggressive cancer behaviors and likely metastasis through SOX9 upregulation.

cancer stem cells; lung cancer; iron; hydroxyl radical; SOX9

IRON IS A CRUCIAL ELEMENT TO normal cell metabolism and biosynthesis, necessary for cell growth and proliferation. In cancers, iron homeostasis has been tilted in various tumor cells towards an increase in intracellular iron availability (22). Iron enables the functions of several vital enzymes, including mitochondrial enzymes that are involved in the production of cellular energy and detoxifying enzymes such as glutathione peroxidase and catalase, which are responsible for the antioxidant machinery of the cells (50). On the other hand, iron has been widely known as a redox-modulating molecule, owing to its high reactivity to easily gain and lose electrons. The free

intracellular ferrous iron (Fe^{2+}) can generate hydroxyl radical (OH^\cdot), a highly reactive oxygen species (hROS), via the Fenton reaction through its reacting with hydrogen peroxide (H_2O_2), especially when excess iron is available (9). Not only could it damage the nearby biomolecules, e.g., lipids and DNA, which can result in mutations that lead to the development of cancer, OH^\cdot could also act as a signaling molecule in certain cellular pathways. We have previously shown that an increased cellular OH^\cdot by iron can accelerate the migratory and invasive capabilities of lung cancer cells (33), pointing out the role of this specific reactive oxygen species (ROS) in the regulation of aggressive cancer cell behaviors, which could be linked to tumor progression and metastasis.

Lung cancer is the leading cause of cancer-related death that kills more than one million people worldwide each year (47). Increasing evidence has highlighted the role of cancer stem cells (CSCs) presenting in lung tumors in chemoresistance, cancer metastasis, and subsequent disease recurrence and relapse (30, 36, 43). Thus, it is believed that CSCs are the underlying cause of the high mortality rate, making them a dominant target of novel cancer therapeutic strategies. We hypothesized that iron may affect CSCs and their aggressive phenotypes through its ability to modify redox status of the cells. Several mechanisms of CSC regulation have been proposed; most of these are common regulatory pathways critical for normal developmental process. For instance, an epithelial-to-mesenchymal transition (EMT), a highly conserved cellular process that transforms epithelial cells into mesenchymal cells, has perhaps received the most attention since EMT is a common occurrence in metastasis of lung and other tumors (41, 51), although certain studies have shown that cancer stemness and EMT are not always associated (8, 17, 36). Likewise, sex-determining region Y-box (SOX) family is being recognized (12, 15); SOX9 in particular is important in the lungs as it involves in tracheal differentiation and formation and has been shown to be upregulated in advanced lung carcinoma (25, 36, 52). In this study, we investigated the role of iron (ferrous sulfate, FeSO_4) via OH^\cdot formation in EMT activation and SOX9 expression and CSC phenotype. Using gene expression and knockdown strategies as well as pharmacological inhibitors, we demonstrated the important role of SOX9 in CSC acquisition and maintenance of the lung cancer cells induced by iron, thus revealing the existence of a novel mechanism of iron and ROS-mediated CSC regulation, which could be important in carcinogenesis and metastasis.

Address for reprint requests and other correspondence: S. Luanpitpong, Siriraj Center of Excellence for Stem Cell Research, Faculty of Medicine Siriraj Hospital, Mahidol University, Bangkoknoi, Bangkok 10700, Thailand (e-mail: suidjit@gmail.com).

Table 1. Intracellular iron (Fe^{2+}) in $FeSO_4$ -exposed lung carcinoma cells for 24 h

| | Iron (Fe^{2+}) Content, pg/cell | |
|-----------------------------------|-------------------------------------|------------------|
| | H460 | H292 |
| Nontreatment | 0.2728 ± 0.0121 | 0.2439 ± 0.0069 |
| $FeSO_4$ 75 μ M | 0.4045 ± 0.0015* | 0.2874 ± 0.0066 |
| $FeSO_4$ 150 μ M | 0.4285 ± 0.0072* | 0.4451 ± 0.0145* |
| $FeSO_4$ 150 μ M + DFX 0.5 mM | 0.3261 ± 0.0072† | 0.2802 ± 0.0178† |

* $P < 0.05$ vs. nontreated control. † $P < 0.05$ vs. $FeSO_4$ -exposed cells at 150 μ M.

MATERIALS AND METHODS

Cell culture and iron exposure. Human non-small cell lung cancer (NSCLC) NCI-H460 and NCI-H292 cell lines were obtained from the American Type Culture Collection (ATCC, Manassas, VA). The cells were cultured in Roswell Park Memorial Institute (RPMI) 1640 medium supplemented with 10% fetal bovine serum (FBS), 2 mM L-glutamine, and 100 U/ml penicillin and 100 μ g/ml streptomycin (GIBCO, Grand Island, NY) and were maintained in a 37°C humidified incubator with 5% CO_2 . Cells were seeded onto six-well plates at an initial plating density of 2×10^5 cells/well and were treated with

the indicated concentrations of freshly prepared $FeSO_4$ (Sigma-Aldrich, St. Louis, MO) every 3 days. For subchronic exposure, which is referred to as an in vitro exposure for a period of three or more days (53), the cells were subsequently collected at 3 and 7 days posttreatment for further analysis. Deferoxamine (DFX; Sigma) was used as an iron chelator, while sodium formate (NaFM; Sigma) and dimethylthiourea (DMTU; Sigma) were used as a scavenger of OH^\cdot . Intracellular iron (Fe^{2+}) content in $FeSO_4$ -exposed cells as evaluated by Iron Assay Kit (Abcam, Cambridge, UK) is shown in Table 1.

Cytotoxicity and proliferation assays. Cells were seeded onto 96-well plates at a density of 1.5×10^4 cells/well and were treated with various concentrations of $FeSO_4$ and analyzed for cell viability using MTT (3-(4,5-dimethylthiazol-2-yl)-2,5-diphenyltetrazolium bromide) assay. Cells were incubated with 500 μ g/ml of MTT for 4 h at 37°C, and the intensity of formazan product was measured at 550 nm using a microplate reader (Synergy H1, BioTek, Winooski, VT). Relative cell viability was calculated by dividing the absorbance of the treated cells by that of the control cells. Cell proliferation was confirmed by cell counting using a Scepter automated cell counter (EMD Millipore, Billerica, MA).

OH \cdot detection. Generation of hROS was determined according to the method previously described using 3'-p-(hydroxyphenyl) fluorescein (HPF; Sigma) as a probe (34). Briefly, cells were incubated with the probe (10 μ M) for 1 h at 37°C in Hanks' buffered salt solution

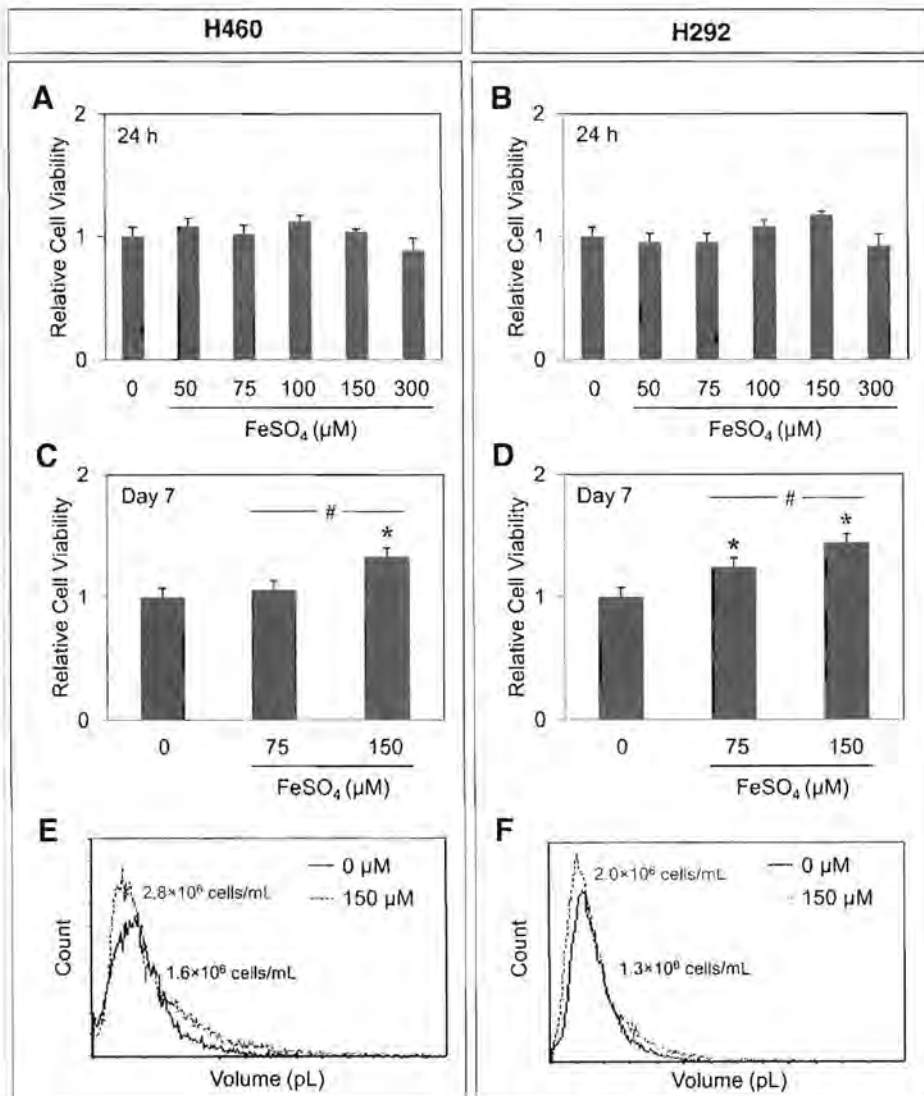


Fig. 1. Subchronic exposure to iron donor induces human lung cancer cell proliferation. A and B: non-small cell lung cancer (NSCLC) H460 (A) and H292 (B) cells were treated with various concentrations (0–300 μ M) of iron donor ferrous sulfate ($FeSO_4$) for 24 h and cell viability was evaluated by MTT (3-(4,5-dimethylthiazol-2-yl)-2,5-diphenyltetrazolium bromide) assay to identify their subtoxic concentrations. C and D: NSCLC H460 (C) and H292 (D) cells were subchronically exposed to various subtoxic concentrations (0–150 μ M) of $FeSO_4$ for 7 days and cell proliferation was evaluated by MTT assay. E and F: representative histograms of cell volume distribution comparing subchronic iron-exposed H460 (E) and H292 (F) cells for 7 days with the nontreated control cells using an automated cell counter. Data are means \pm SD ($n = 4$). * $P < 0.05$ vs. nontreated control. # $P < 0.05$ vs. $FeSO_4$ -exposed cells at 75 μ M.

(HBSS) and analyzed for fluorescence intensity using a fluorescence plate reader at 485-nm excitation and 520-nm emission (Synergy H1). For electron spin resonance (ESR) measurements, cells were incubated with 5,5-dimethyl-1-pyrroline-*N*-oxide (DMPO, 10 mM) for 10 min at 37°C in the presence or absence of OH⁻ modulators. ESR signals were measured using a Bruker EMX spectrometer (Bruker Instruments, Billerica, MA) and a flat cell assembly. Hyperfine couplings were measured (to 0.1 G) directly from magnetic field separation using potassium tetraperoxochromate and 1,1-diphenyl-2-picrylhydrazyl as reference standards. An Acquisit program (Bruker Instruments) was used for data acquisition and analysis.

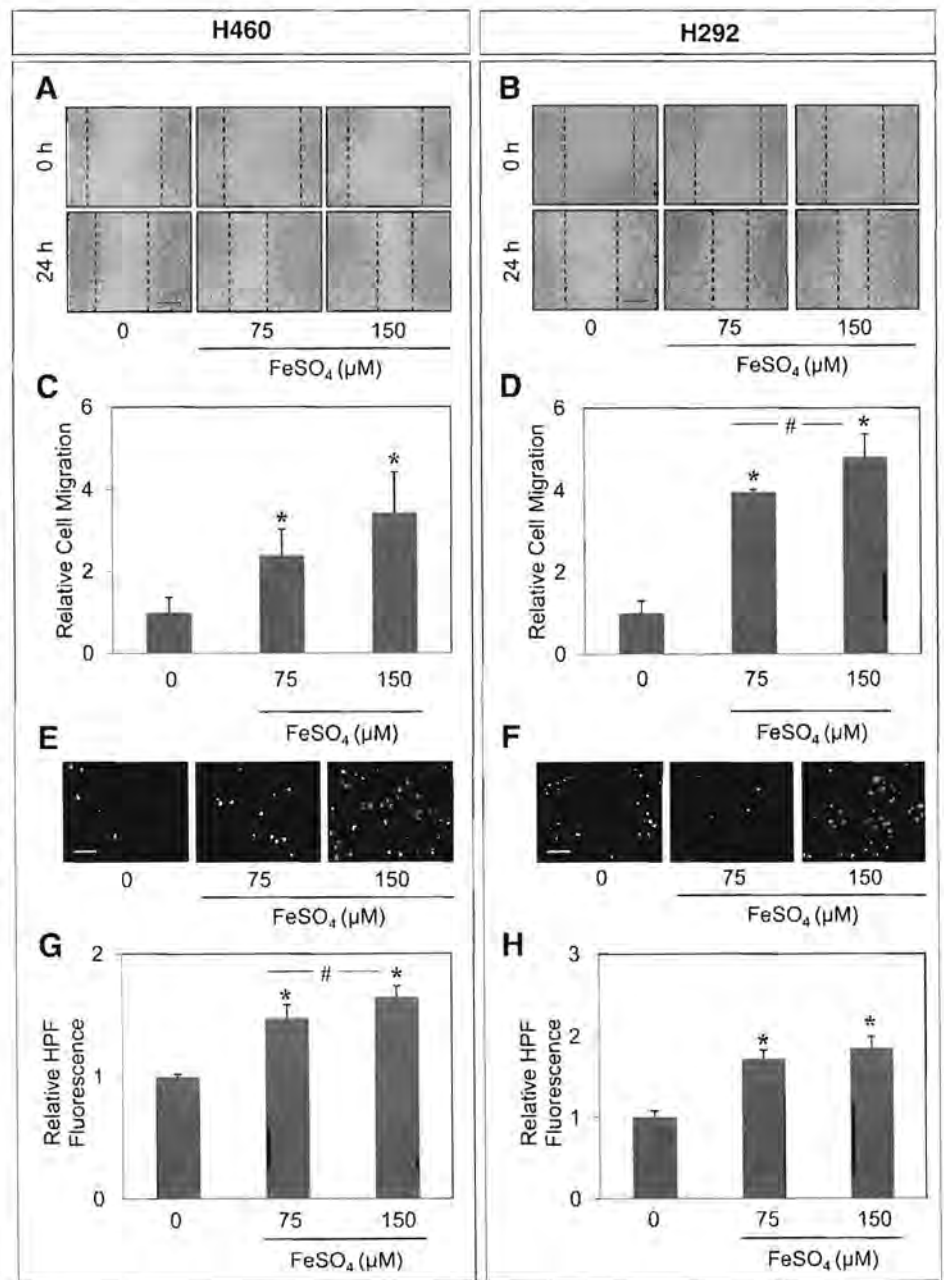
Migration assay. Wound-healing assay was used to determine cell migration. Briefly, confluent monolayers of cells in a 24-well plate were wounded at the center of the well by a 200 μ l micropipette tip. Six random fields of the wound space were examined and imaged under a phase contrast microscope (Eclipse Ti-U with NiS-Elements, Nikon, Tokyo, Japan) at various time points. Relative cell migration

was quantified by dividing the percentage change of the wound space in treated cells to that of the control cells.

Invasion assay. Cell invasion was determined using a 24-well Transwell unit with polycarbonate (PVDF) filters (8 μ m pore size). The membrane was coated with a mixture of laminin (50 μ g/ml), type IV collagen (50 μ g/ml), and gelatin (2 mg/ml in 10 mM glacial acetic acid). Cells at a density of 1×10^4 cells/well were seeded into the upper chamber of the Transwell unit in serum-free medium. The lower chamber of the unit was added with a medium containing 10% FBS. Cells were allowed to invade for 24 h, after which the cells on the upper side of membrane were removed with a cotton swab. Cells that invaded the underside of the membrane were stained with 10 μ g/ml Hoechst 33342 for 10 min and visualized under a fluorescence microscope (Eclipse Ti-U).

Tumor sphere assay. Tumor sphere assay was performed under nonadherent and serum-free conditions as previously described as stem cell-selective conditions (16, 30). Briefly, cells were resuspended

Fig. 2. Subchronic exposure to iron donor induces human lung cancer migration and invasion and highly reactive oxygen species (hROS) generation. *A* and *B*: confluent monolayers of subchronic iron-exposed H460 (*A*) and H292 (*B*) cells, using FeSO₄ (0–150 μ M) for 7 days, were wounded and the cells were allowed to migrate for 24 h. Wound space was visualized under a phase contrast microscope. Scale bar, 250 μ m. *C* and *D*: quantitative analysis of the changes in wound space of iron-exposed H460 (*C*) and H292 (*D*) cells over control cells. *E* and *F*: cell invasion was determined by Transwell assay after the iron-exposed H460 (*E*) and H292 (*F*) cells and control cells were allowed to invade for 24 h. Invaded cells were stained with Hoechst 33342 (10 μ g/ml) to aid the visualization of the cells. Scale bar, 100 μ m. *G* and *H*: NSCLC H460 (*G*) and H292 (*H*) cells were treated with various concentrations (0–150 μ M) of FeSO₄ for 1 h and cellular hROS generation was determined by fluorescent plate reader using 3'-*p*-(hydroxyphenyl) fluorescein (HPF) as a fluorescent probe. Data are means \pm SD ($n = 4$). * $P < 0.05$ vs. nontreated control. # $P < 0.05$ vs. FeSO₄-exposed cells at 75 μ M.



in 0.8% methylcellulose (MC)-based serum-free medium (Stem Cell Technologies, Vancouver, BC, Canada) supplemented with 20 ng/ml epidermal growth factor (BD Biosciences, San Jose, CA), basic fibroblast growth factor, and 4 mg/ml insulin (Sigma) and plated at 500 cells in an ultra-low attachment 96-well plates. Cells were then cultured for 2 wk and were visualized under a phase contrast microscope (Eclipse Ti-U).

Western blot analysis. Cells were incubated on ice for 45 min with lysis buffer containing 20 mM Tris-HCl (pH 7.5), 1% Triton X-100, 150 mM NaCl, 10% glycerol, 1 mM Na₃VO₄, 50 mM NaF, 100 mM PMSF, and cocktail protease inhibitor mixture (Roche Molecular Biochemicals, Indianapolis, IN). Cell lysates were analyzed for protein content using BCA protein assay kit from Pierce Biotechnology (Rockford, IL). Equal amounts of denatured protein samples (50 µg) were loaded onto 7.5–12% SDS-PAGE before transferring onto 0.45 µm PVDF membranes (Bio-Rad, Hercules, CA). Transferred membranes were blocked for 1 h in 5% nonfat dry milk in TBST (25 mM Tris-HCl, pH 7.5, 125 mM NaCl, and 0.05% Tween 20) and incubated overnight with specific primary antibodies against

ABCG2 (Cell Signaling Technology; CST, Beverly, MA), CD133 (Cell Applications, San Diego, CA), EMT (CST), SOX9 (EMD Millipore), and β-actin (Santa Cruz Biotechnology). Membranes were washed three times with TBST and incubated with appropriate horseradish peroxidase (HRP)-labeled secondary antibodies for 2 h at room temperature. The immune complexes were detected by Immobilon chemiluminescent substrate (EMD Millipore) and digital imager (ImageQuant LAS, GE Healthcare, Pittsburgh, PA).

Side population analysis. Cells were labeled with 5 µg/ml Hoechst 33342 in Dulbecco's modified Eagle's medium-F-12 medium containing 2% FBS in the presence or absence of 25 µM ABCG2 inhibitor fumitremorgin C (FTC; EMD Biosciences, San Diego, CA) at 37°C for 90 min. Side population (SP) analysis was performed using BD FACSAria cell sorter (BD Biosciences, Franklin Lakes, NJ) using UV laser and Hoechst Blue (450/20) and Red (675 LP) filters. SP fraction was calculated based on the disappearance of SP cells in the presence of FTC.

Gene expression analysis by RT-qPCR. Total RNA was prepared using TRIzol reagent (Invitrogen, Carlsbad, CA). cDNA was prepared

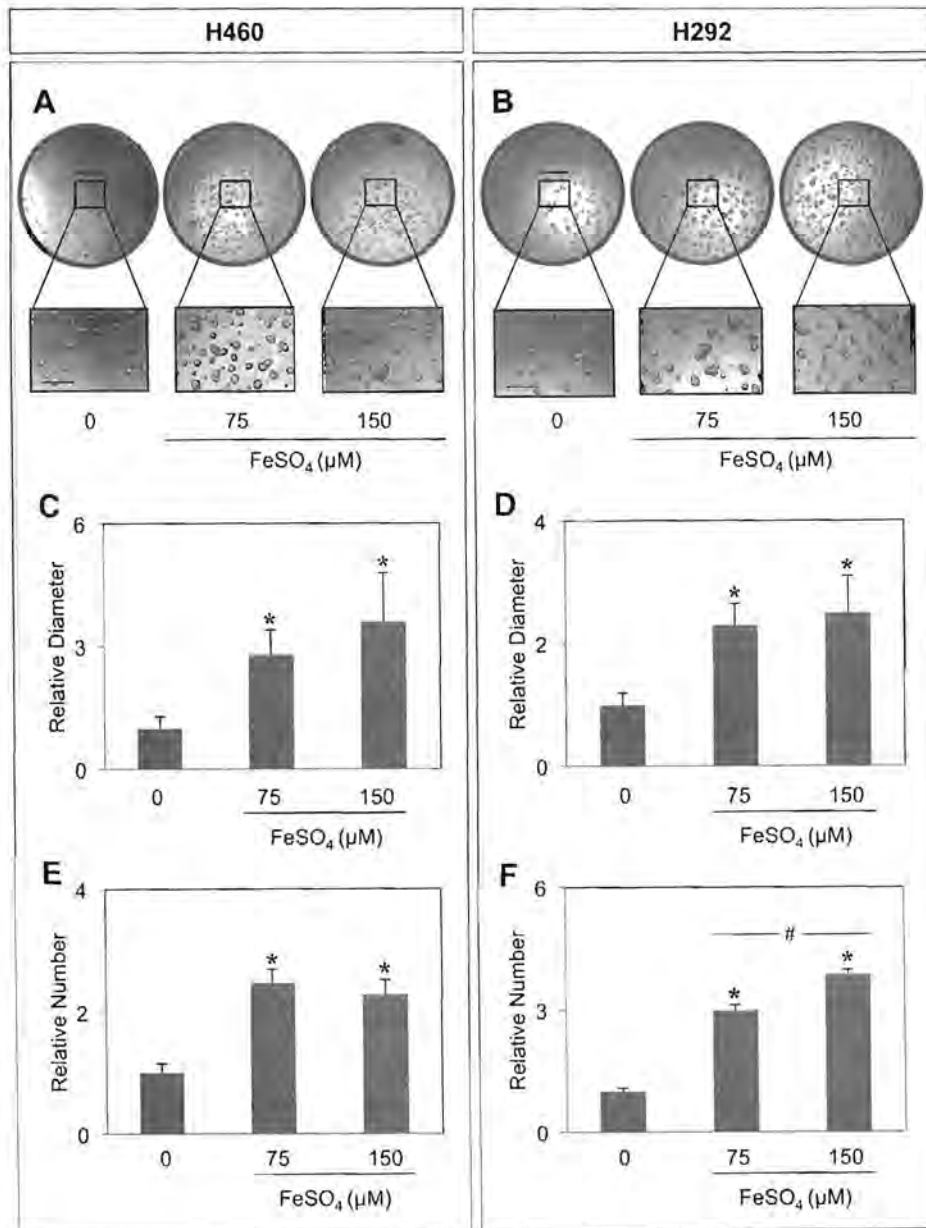


Fig. 3. Subchronic exposure to iron donor enhances lung tumor sphere formation. *A* and *B*: subchronic iron-exposed H460 (*A*) and H292 (*B*) cells, using FeSO₄ (0–150 µM) for 7 days, were analyzed for tumor sphere formation. Cells were cultured under nonattached and serum-starved conditions in methylcellulose-based medium, and tumor spheroids were visualized under a phase contrast microscope after 2 wk of culture. Scale bars, 500 µm (*top*) and 250 µm (*bottom*). *C–F*: quantitative analysis of tumor spheroids of H460 (*C* and *E*) and H292 (*D* and *F*) cells in size and number. Data are means ± SD (*n* = 4). **P* < 0.05 vs. nontreated control. #*P* < 0.05 vs. FeSO₄-exposed cells at 75 µM.

using 2 μg of RNA and reverse transcribed using SuperScript III First-Strand Synthesis System and Oligo(dT) primers (Invitrogen). qPCR analysis was carried out on 7500 Fast Real-time PCR machine (Applied Biosystems, Foster City, CA) using Power SYBR Green PCR Master Mix (Applied Biosystems). The PCR reaction consisted of 1 \times SYBR Green PCR master mix, 200 nM forward and reverse primers, and 1 μl of template cDNA. The total volume was adjusted to 20 μl with nuclease-free water. Initial enzyme activation was performed at 95°C for 10 min, followed by 40 cycles of denaturation at 95°C for 15 s and primer annealing/extension at 60°C for 1 min. Melting curve analysis was performed to determine primer specificity. The relative expression of each gene was normalized against the housekeeping gene glyceraldehyde 3-phosphate dehydrogenase (GAPDH) product.

Plasmid and transfection. Cells were transfected with SOX9 (Origene, Rockville, MD) or green fluorescent protein (GFP; Invitrogen) using Lipofectamine 2000 reagent, according to the manufacturer's protocol (Invitrogen) in RPMI medium in the absence of serum and antibiotics. After 12 h of incubation, the medium was replaced with complete culture medium containing 10% FBS. The cells were then cultured and selected for G418 (400 $\mu\text{g}/\text{ml}$) resistance for 30 days to obtain stable transfectants. Expression of SOX9 was verified by Western blot assay. The cells were cultured in antibiotic-free RPMI 1640 medium for at least two passages before further experiments were performed.

Lentivirus production and inhibition of SOX9 by RNA interference. Lentiviral plasmids carrying short hairpin (sh) RNA sequence against human SOX9 were obtained from Addgene (Cambridge, MA; plasmid 40644) (20), and shSOX9 lentivirus production was performed using HEK293T packaging cells (ATCC) in conjugation with pCMV.dR8.2 dvpr lentiviral packaging and pCMV-VSV-G envelope plasmids (Addgene, plasmids 8454 and 8455) (48). Cells were incubated with shSOX9 viral particles in the presence of hexadimethrine bromide for

36 h and were cultured and selected for puromycin (1 $\mu\text{g}/\text{ml}$) resistance for 30 days. The infected cells were analyzed for SOX9 expression prior to use by Western blotting.

Statistical analysis. Data are means \pm SD from at least three independent experiments. Statistical analysis was performed by one-way ANOVA and Turkey's post hoc test at a significance level of $P < 0.05$.

RESULTS

Effect of iron on viability and aggressive behaviors of human lung cancer cells. Elevated intracellular iron has been shown to generate OH^\cdot via the Fenton reaction that may be toxic to the cells. To test whether iron might affect a lung CSC subpopulation, we first determined the appropriate noncytotoxic concentrations of iron donor, FeSO_4 . Human lung cancer H460 and H292 cells were treated with various concentrations of FeSO_4 (0–300 μM) and cell viability was determined after 24 h by MTT assay. FeSO_4 was relatively nontoxic at all of the tested doses in H460 and H292 cells (Fig. 1, A and B). The absence of apoptotic and necrotic cell death was confirmed by Hoechst 33342 and propidium iodide (PI) costaining (data not shown). As we sought to determine the dynamics of lung CSCs and aggressive phenotypes, we performed subchronic iron exposure in this study. Excessive cell growth and increased cell motility are important behaviors determining the capability of tumor cells to disseminate and metastasize (5, 19). Figure 1, C and D, shows that subchronic treatment of FeSO_4 (0–150 μM) for 7 days promoted lung tumor cell growth as determined by MTT assay, the results of which were verified by automated cell count as shown in Fig. 1, E and F. Wound healing assay

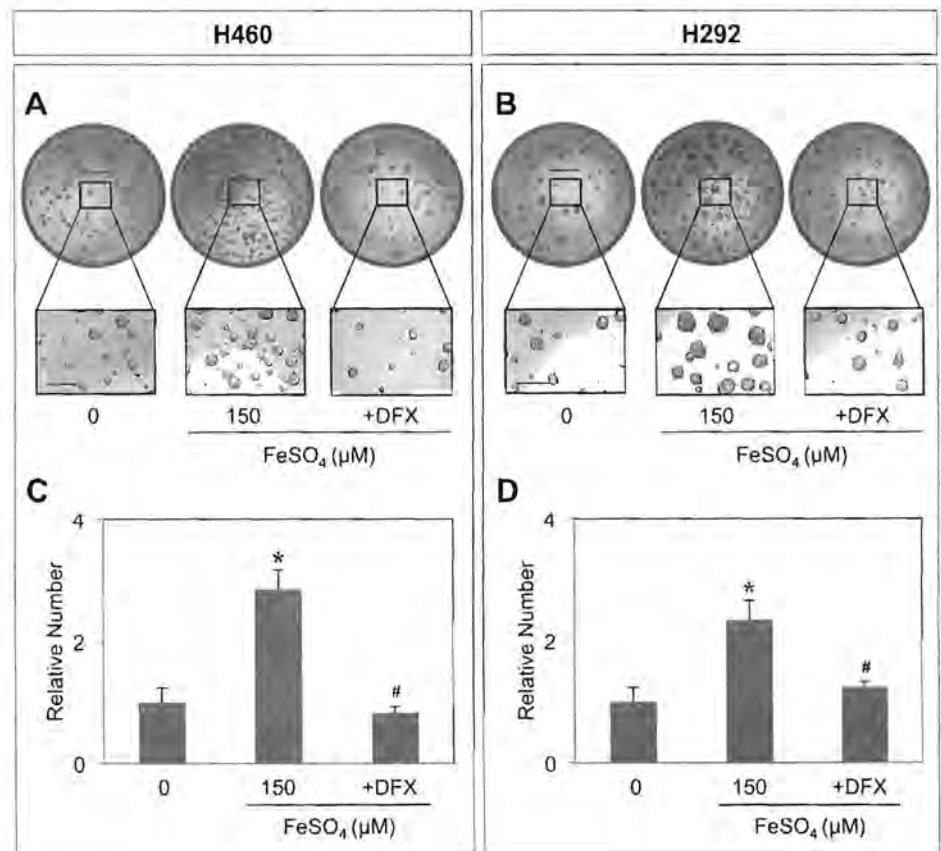


Fig. 4. Effects of iron chelator on iron-induced cancer stem cell (CSC) sphere formation. A and B: subchronic iron-exposed H460 (A) and H292 (B) cells, using FeSO_4 (150 μM) for 7 days with or without iron chelator deferoxamine (DFX; 0.25 mM), were cultured under nonattached, serum-starved conditions in methylcellulose-based medium. Tumor spheroids were visualized under a phase contrast microscope after 2 wk of culture. Scale bars, 500 μm (top) and 250 μm (bottom). C and D: quantitative analysis of tumor spheroids of H460 (C) and H292 (D) cells. Data are means \pm SD ($n = 3$). * $P < 0.05$ vs. nontreated control. # $P < 0.05$ vs. FeSO_4 -exposed cells at 150 μM .

indicated a remarkable increase in cell motility of subchronic (7 days) iron-exposed H460 and H292 cells; a much smaller wound was observed in the iron treatment group (Fig. 2, A and B). Quantitative analysis of the changes in wound space after 24 h is shown in Fig. 2, C and D. Transwell invasion assay similarly indicated an increase in cell invasiveness in iron-exposed cells (Fig. 2, E and F).

The major species of ROS include superoxide (O_2^-), H_2O_2 , and OH^\cdot . To ensure that the indicated nontoxic concentrations of $FeSO_4$, e.g., at up to 150 μM , were sufficient to generate OH^\cdot in H460 and H292 cells, intracellular ROS in response to $FeSO_4$ was determined using HPF as a specific fluorescent probe. HPF is a cell-permeable probe that is highly sensitive towards hROS such as OH^\cdot , while much less sensitive towards other ROS such as H_2O_2 and O_2^- (46). Figure 2, G and H, shows that $FeSO_4$ (75–150 μM) significantly induced hROS, likely OH^\cdot , within 1 h after posttreatment in both cells.

Iron induces CSC spheroid formation and biomarkers. A fundamental property of CSCs is the ability to self-renew and

generate differentiated progeny (2, 14). Capability of tumor cells to form three-dimensional spheroids under nonattached and serum-starved conditions of tumor sphere formation assay was shown to be a gold standard for evaluation of CSCs and their self-renewal (31, 36). As CSCs are known to contribute to aggressive phenotypes of human cancer cells, we hypothesized that subchronic iron exposure may affect CSCs. Figure 3, A and B, shows that subchronic iron-exposed H460 and H292 cells formed larger and higher numbers of floating spherical colonies compared with passage-matched nontreated controls. Quantitative analysis of lung spheroids in size and number is shown in Fig. 3, C and D, and Fig. 3, E and F, respectively. These results indicated: 1) the existence of lung CSCs in H460 and H292 cell lines; and 2) the acquisition and maintenance of lung CSCs in response to subchronic iron treatment in a dose-dependent manner. All H460 and H292 cells that were passaged from first-generation tumor spheres preserved the ability to form second-generation spheres (data not shown), thus confirming their self-renewal and repopulation capability.

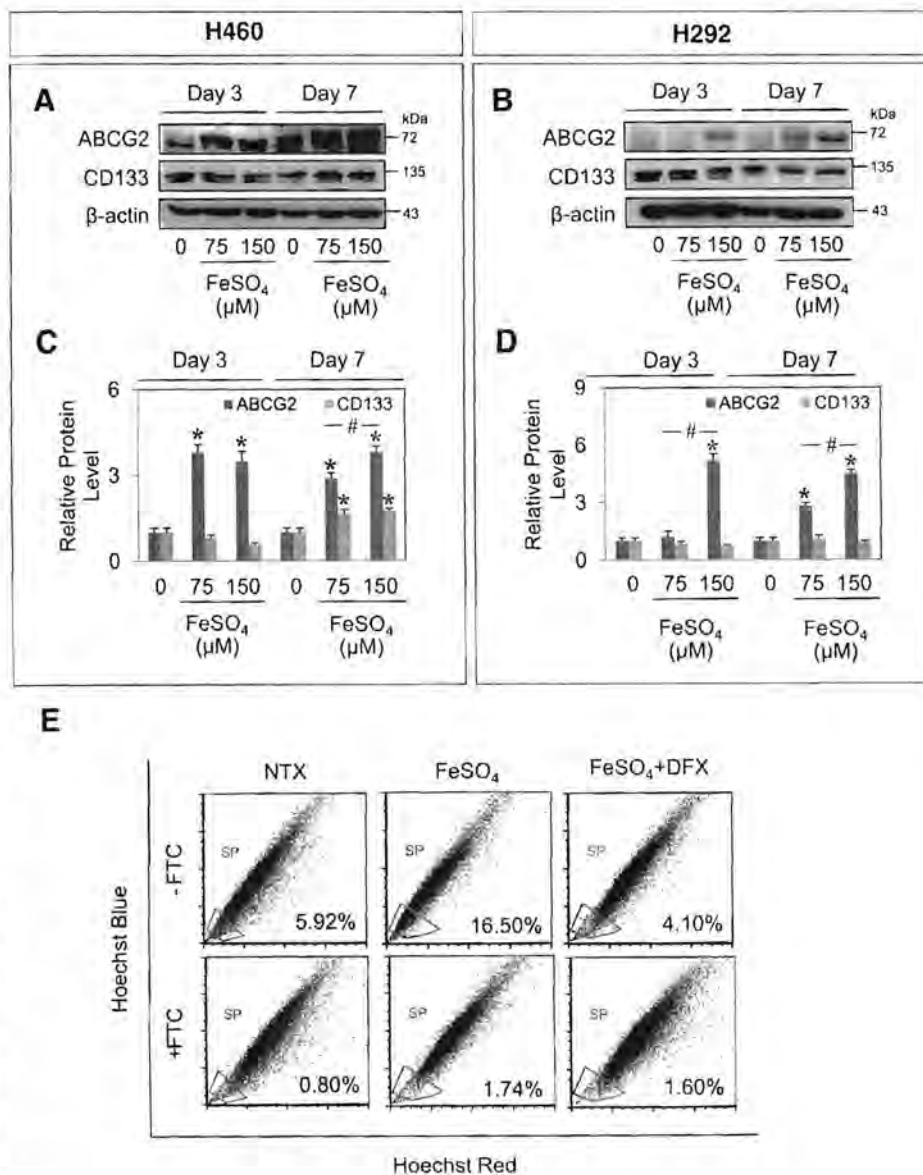


Fig. 5. Effects of subchronic iron exposure on CSC biomarkers of human lung cancer cells. A and B: subchronic iron-exposed H460 (A) and H292 (B) cells, using $FeSO_4$ (0–150 μM) for 3–7 days, were evaluated for lung CSC biomarkers ABCG2 and CD133 using Western blotting. Blots were reprobed with β -actin to confirm equal loading of samples. C and D: densitometry analysis of Western blot bands from three independent experiments, one of which is shown here, after normalization to the results obtained in nontreated cells. E: analysis of side population (SP) in iron-exposed H460 cells, using 150 μM $FeSO_4$ for 3 days, in the presence or absence of iron chelator DFX and ABCG2-specific inhibitor fumitremorgin C (FTC) by FACS. SP cells (box) were determined by their disappearance in the presence of FTC and are shown as percentage of pool population. Data are means \pm SD ($n = 3$). * $P < 0.05$ vs. nontreated control (NTX). # $P < 0.05$ vs. $FeSO_4$ -exposed cells at 75 μM .

Addition of the iron chelator DFX inhibited the effect of iron on spheroid formation, thus assuring the involvement of iron in the process (Fig. 4, A–D).

To confirm the induction of lung CSCs by iron and to track CSC dynamics, time and dose profiles of the levels of two well-known lung CSC biomarkers, ABCG2 and CD133 (7, 23), were generated. H460 and H292 cells were subchronically treated with FeSO₄ (0–150 μM) for 3 or 7 days, and the expression of ABCG2 and CD133 was evaluated by Western blotting. Figure 5, A–D, shows that FeSO₄ gradually increased ABCG2 levels in H460 and H292 cells in a dose- and time-dependent manner, while it had minimal effect on CD133 levels. Notably, the iron induction of CSC markers occurred rapidly within 3 days after exposure of higher-dose iron (150 μM FeSO₄). Side population (SP) analysis, which has been identified as a common phenotype of CSCs based on their distinct low Hoechst staining pattern from high ABCG2 expression (23, 35), revealed that a proportion of SP cells was ~6% in control cells and 15% in FeSO₄-exposed cells (Fig. 5E). These results together with the above findings on CSC-like aggressive behaviors of iron-exposed cells strongly support the role of iron in CSC acquisition and maintenance of lung cancer cells.

Effect of iron on EMT. Activation of EMT is an essential developmental process that enables reprogramming of epithelial cells towards a mesenchymal phenotype to enhance intrinsic cell motility, which is required during gastrulation and organogenesis (27, 49). In normal adult tissues, EMT was shown to be involved in wound repair and tissue regeneration. In cancers, tumor cells that underwent EMT have been shown to acquire aggressive phenotypes and EMT has been further associated with CSC regulation (37, 39). Having demonstrated that iron induced lung CSCs, we next evaluated for EMT-like cell morphology and profiled EMT regulatory proteins in iron-exposed cells at 3 or 7 days by Western blotting. The results revealed that FeSO₄ treatment had minimal effect on H460 and H292 lung cell morphology (Fig. 6, A and B) in agreement with the observed nonsignificant changes in expression levels of epithelial markers (for example, E-cadherin) and mesenchymal markers (slug, vimentin, and β-catenin) upon FeSO₄ treatment (Fig. 6, C and D). Further, gene expression analysis revealed the minimal and mostly insignificant changes of EMT markers in response to the treatment for up to 7 days (Fig. 6, E and F). Altogether, these results suggest that EMT was not critical in the regulatory role of iron in lung CSCs in the tested system.

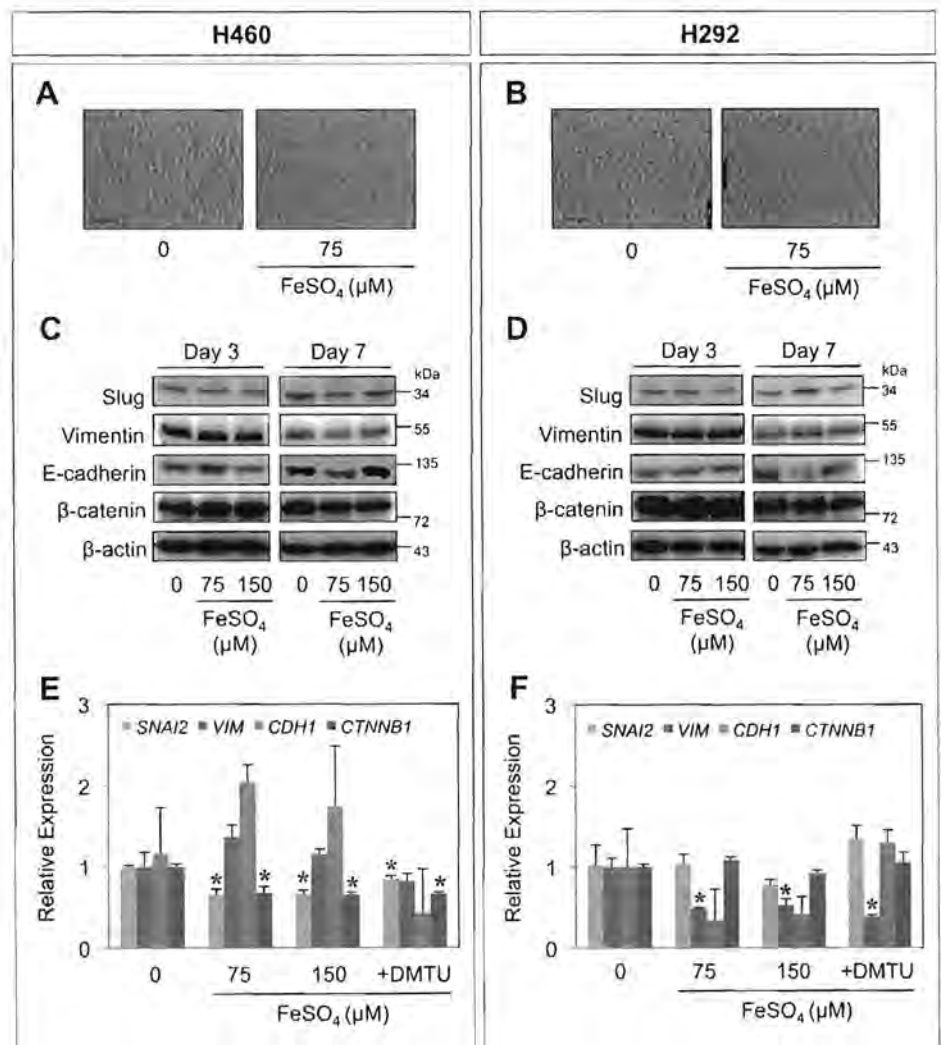


Fig. 6. Effects of subchronic iron exposure on epithelial-to-mesenchymal transition (EMT) of human lung cancer cells. A and B: cell morphology of subchronic iron-exposed H460 (A) and H292 (B) cells, using FeSO₄ (0–150 μM) for 7 days, was visualized under a phase contrast microscope. Scale bar, 200 μm. C and D: Western blot analysis of epithelial marker E-cadherin and mesenchymal markers, including slug, vimentin, and β-catenin. E and F: gene expression analysis of epithelial marker *CDH1* and mesenchymal markers, including *SNAI2*, *VIM*, and *CTNNB1*, at 7 days postexposure. DMTU, dimethylthiourea. Data are means ± SD (n = 3). *P < 0.05 vs. nontreated control.

Effect of iron on SOX9 expression. Increasing evidence has pointed to the involvement of SOX family proteins in regulation of many aggressive cancers, for instance, SOX2 in prostate cancer, SOX10 in melanoma, and SOX9 in lung adenocarcinoma (12, 25, 45). Additionally, we have previously shown that SOX9 regulates lung CSCs and promotes lung metastasis in vivo (36). We hypothesized that SOX9 may be regulated by iron, which may represent a key mechanism of CSC regulation by iron. To test this possibility, H460 and H292 cells were subchronically treated with FeSO₄ (0–150 μM) for 3 or 7 days and their effect on SOX9 was determined by Western blotting. Figure 7, A–D, shows that SOX9 levels increased in response to FeSO₄ in a dose- and time-dependent manner in both cells. To confirm the role of SOX9 in lung CSCs, the cells were stably transfected with SOX9 or GFP control plasmid and their effects on SOX9 expression and tumor sphere formation assay were determined. Western blot analysis revealed a substantial increase in the expression of SOX9-overexpressing cells (Fig.

7, E and F). Figure 7, G and H, reveals that SOX9-overexpressing cells exhibited larger and greater number of tumor spheroids compared with control cells, thus validating the promoting role of SOX9 in the CSC acquisition in H460 and H292 cells.

OH⁻ mediates iron-induced CSCs through SOX9-dependent mechanism. The presence of iron is known to generate OH⁻ formation via the Fenton reaction. To substantiate the involvement of OH⁻ in iron promoting effect on lung CSCs, intracellular OH⁻ was manipulated using pharmacological inhibitors of OH⁻ and ESR measurements were performed using DMPO as a spin-trapping reagent to aid the detection of short-lived oxygen free radicals. In response to FeSO₄ treatment, an ESR signal consisting of a 1:2:2:1 quartet which is a characteristic of DMPO-OH⁻ adduct was observed (Fig. 8A). Addition of OH⁻ inhibitor NaFM and DMTU to the iron-treated H460 cells inhibited the ESR signal (Fig. 8, A and B), indicating the scavenging of OH⁻ under the test condition. Next, cells were

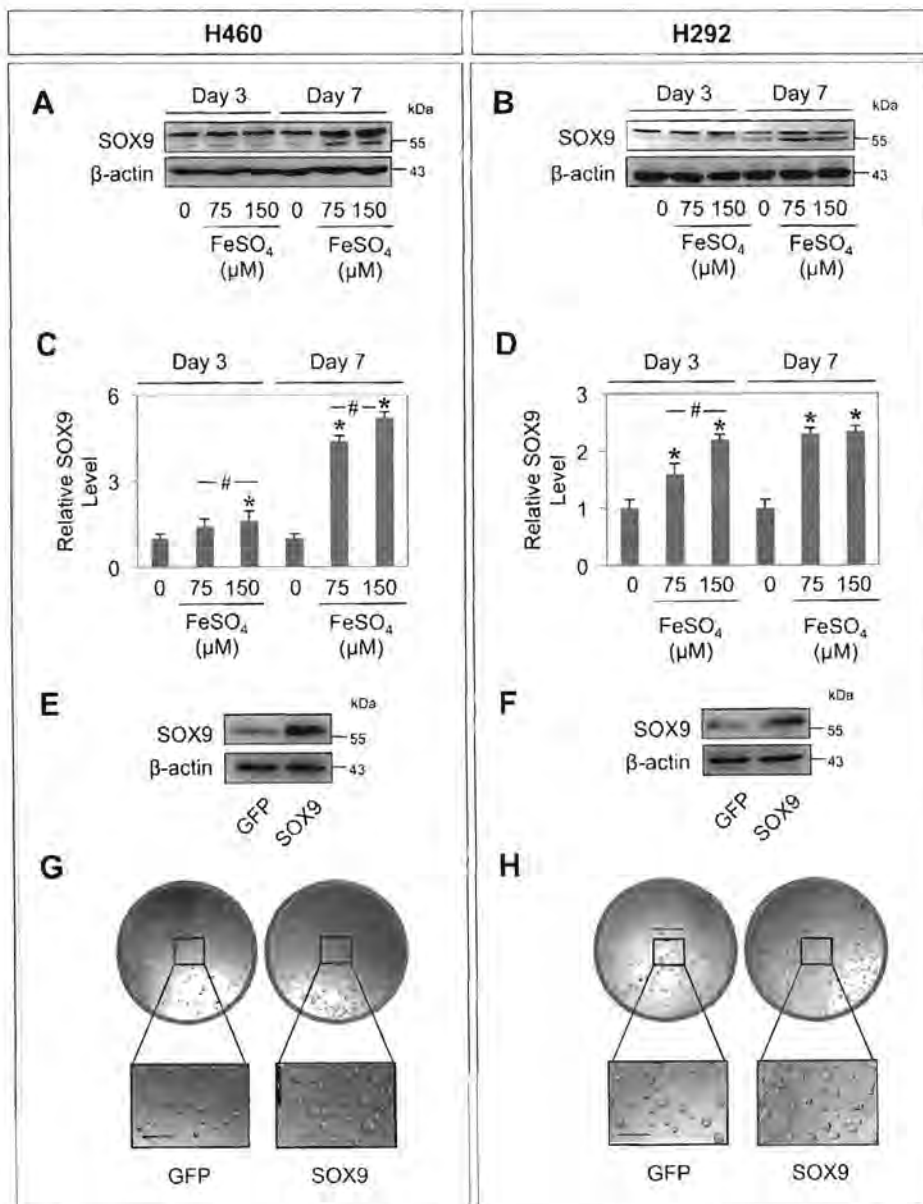
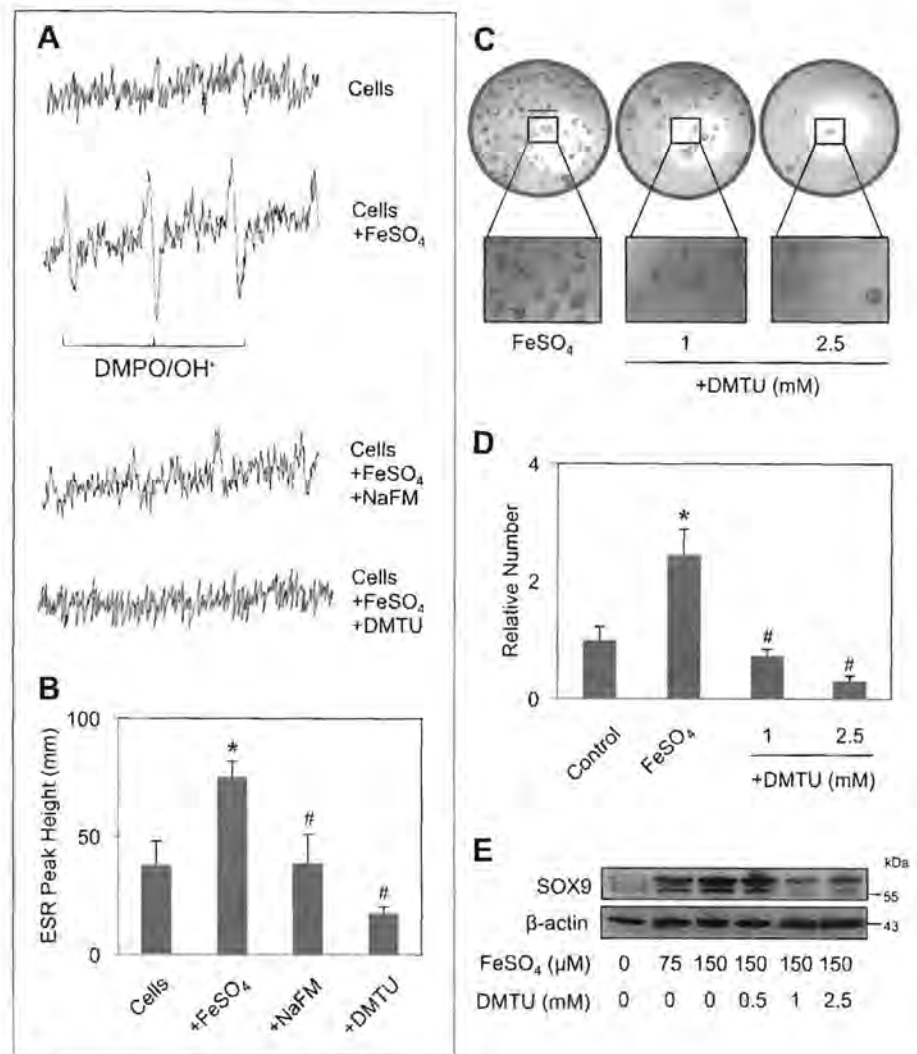


Fig. 7. Effect of subchronic iron exposure on sex-determining region Y (SRY)-box 9 (SOX9) expression of human lung cancer cells. A and B: subchronic iron-exposed H460 (A) and H292 (B) cells, using FeSO₄ (0–150 μM) for 3–7 days, were evaluated for SOX9 expression using Western blotting. Blots were reprobed with β-actin to confirm equal loading of samples. C and D: densitometry analysis of Western blot bands from three-independent experiments, one of which is shown here, after normalization to the results obtained in nontreated cells. E and F: NSCLC H460 (E) and H292 (F) cells were stably transfected with SOX9 or green fluorescent protein (GFP) control plasmid, and their SOX9 expression was determined by Western blotting. G and H: effects of SOX9 overexpression on tumor sphere formation. SOX9 and GFP-transfected H460 (G) and H292 (H) cells were cultured under nonattached and serum-starved conditions in methylcellulose-based medium, and tumor spheroids were visualized under a phase contrast microscope after 2 wk of culture. Scale bars, 500 μm (top) and 250 μm (bottom). Data are means ± SD (n = 4). *P < 0.05 vs. nontreated control. #P < 0.05 vs. FeSO₄-exposed cells at 75 μM.

Fig. 8. Effects of hydroxyl radical (OH^\cdot) scavenger on iron-induced OH^\cdot generation, lung tumor sphere formation, and SOX9 overexpression. **A:** NSCLC H460 cells were incubated in PBS containing the spin trapper 5,5-dimethyl-1-pyrroline-*N*-oxide (DMPO; 10 mM) with or without iron donor FeSO_4 (75 μM) and OH^\cdot scavenger sodium formate (NaFM; 2.5 mM) or DMTU (2.5 mM). Electron spin resonance (ESR) spectra were then recorded 10 min after the addition of the test agents. The spectrometer settings were as follows: receiver gain at 2.5×10^4 , time constants at 0.04 s, modulation amplitude at 1.0 G, scan time at 42 s, and magnetic field at $3,475 \pm 100$ G. **B:** analysis of ESR measurements. **C:** subchronic iron-exposed H460 cells, using FeSO_4 (75 μM) for 7 days in the presence or absence of OH^\cdot scavenger DMTU (1–2.5 mM), were cultured under nonattached and serum-starved conditions in methylcellulose-based medium, and tumor spheroids were visualized under a phase contrast microscope after 10 days of culture. Scale bars, 300 μm (top) and 150 μm (bottom). **D:** quantitative analysis of tumor spheroids. **E:** Western blot analysis of SOX9 expression in subchronic iron-exposed H460 cells, using FeSO_4 (0–150 μM) for 7 days, in the presence or absence of OH^\cdot scavenger DMTU (0.5–2.5 mM). Data are means \pm SD ($n = 4$). * $P < 0.05$ vs. nontreated control. # $P < 0.05$ vs. FeSO_4 -exposed cells.



subchronically treated with FeSO_4 for 7 days in the presence or absence of various concentrations of DMTU (0–2.5 mM) and the formation of tumor spheroids was determined. Figure 8, C and D, shows that tumor sphere induction by iron was inhibited by the addition of DMTU in a dose-dependent manner, indicating the role of OH^\cdot in acquisition of CSCs after iron treatment. Western blot analysis of SOX9 further demonstrated that its level was suppressed under FeSO_4 and DMTU cotreatment, thus strengthening the conclusion that the effect of iron was mediated by OH^\cdot formation.

To further confirm the role of SOX9 in lung CSC induction by iron, SOX9 expression was inhibited by RNA interference using shRNA against *SOX9* (shSOX9). NSCLC H460 cells were treated with shSOX9 viral particles or control shRNA particles (shCon), and iron exposure experiments were performed. Figure 9, B and C, shows that FeSO_4 inductive effect on lung CSCs was substantially lower in shSOX9 knockdown cells, in close association with SOX9 expression levels (Fig. 9A), indicating the critical role of SOX9 in iron effect. Altogether, our results demonstrated that the effect of iron was mediated by OH^\cdot formation through a mechanism that involved SOX9 regulation.

DISCUSSION

Tumor heterogeneity comprises many different populations, including the majority normal tumor cells, CSCs (also known as tumor-initiating cells) and neighboring cells, such as immune cells, cancer-associated fibroblasts and endothelial cells, that provide the tumor microenvironment (2, 44). Growing evidence supports that a CSC subpopulation is the root of tumor growth and progression and that persistent CSCs surviving conventional chemo- and/or radiotherapy are behind disease relapse and recurrence. Several studies have shown that conventional therapy not only spares CSCs, but also enriches them, and that this was linked to subsequent poor survival of patients (1, 7, 30). It is mandatory to determine the regulatory mechanisms of CSCs to understand their aggressive behaviors and identify the potential novel targets of cancer therapy.

Increased oxidative stress and ROS production in the tumor microenvironment were implicated in carcinogenesis and metastasis of several cancers, including lung (11, 21, 23). Differential effects of specific ROS, namely, superoxide (O_2^-), H_2O_2 , and OH^\cdot , on cell migration and invasion, which are initial steps of cancer metastasis, were reported by our group, i.e., O_2^- and H_2O_2 suppressed migration and invasion, while

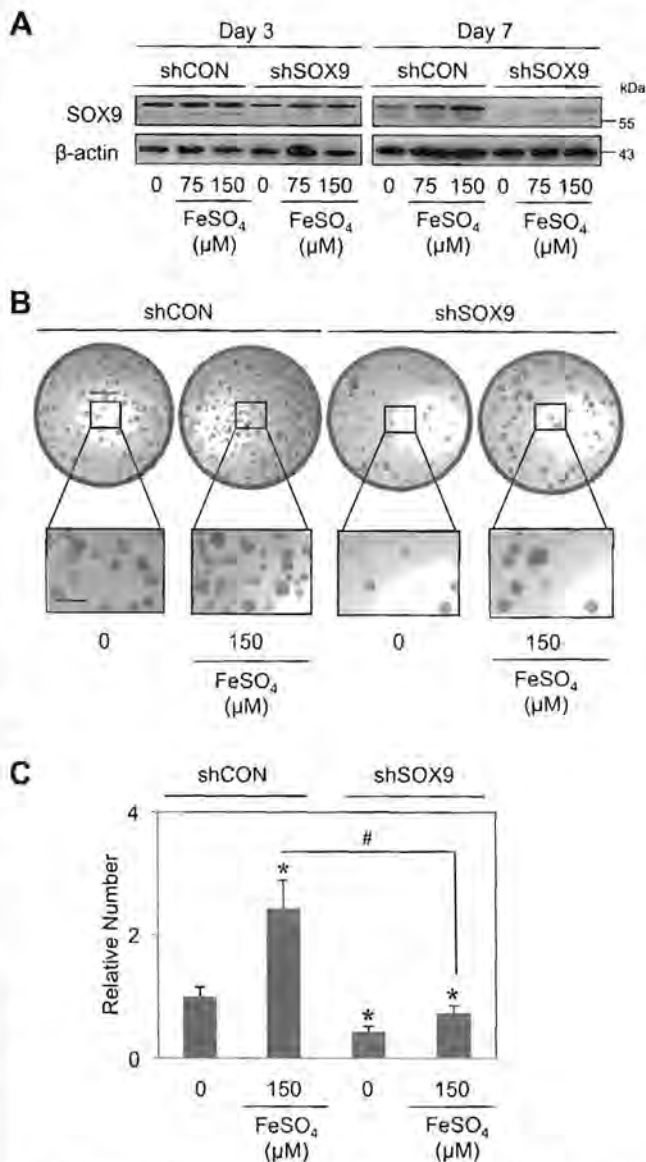


Fig. 9. Effects of SOX9 knockdown on iron-induced SOX9 expression and lung tumor sphere formation. SOX9 knockdown experiments were performed in NSCLC H460 cells using shRNA (shSOX9) viral particles or control short hairpin RNA (shCON) particles. **A**: subchronic iron-exposed shSOX9 and shCON cells, using FeSO₄ (0–150 μM) for 3–7 days, were evaluated for SOX9 expression using Western blotting. Blots were reprobed with β-actin to confirm equal loading of samples. **B**: subchronic iron-exposed shSOX9 and shCON cells, using FeSO₄ (0–150 μM) for 7 days, were cultured under nonattached and serum-starved conditions in methylcellulose-based medium, and tumor spheroids were visualized under a phase contrast microscope after 2 wk of culture. Scale bars, 300 μm (top) and 150 μm (bottom). **C**: quantitative analysis of tumor spheroids in number. Data are means ± SD (n = 4). *P < 0.05 vs. nontreated control. #P < 0.05 vs. FeSO₄-exposed shCON cells.

OH[•] promoted it, suggesting a linkage of OH[•] formation and increased risk of tumor aggressiveness (33). In normal stem cells, redox status appeared to dictate their self-renewal and differentiation (26). However, effects of specific ROS on normal stem cells and CSCs remain elusive. In this study, we revealed for the first time that the change in redox status of NSCLC by iron donor FeSO₄ towards OH[•] generation augmented their aggressive behaviors, in part, through the enrichment of CSC phenotype. Subchronic iron-exposed H460 and

H292 cells acquired a greater proportion of CSC subpopulation compared with nontreated cells, as demonstrated by the larger size and number of tumor spheroids under CSC-selective conditions and the upregulation of CSC marker ABCG2 (Figs. 3–5), in parallel with increased cell proliferation and motility (Figs. 1 and 2), the effects of which were inhibited by iron chelator DFX (Fig. 4) and OH[•] scavenger DMTU (Fig. 8), indicating the regulatory role of OH[•]. Our findings are supported by several studies that demonstrated iron deprivation by various methods, e.g., using iron chelators or targeting transferrin receptor with antibodies, as a potential strategy for cancer therapy (9, 22, 50). For instance, a decrease in tumor engraftment with iron chelator deferasirox treatment was observed in a mouse model of acute myeloid leukemia, suggesting a possible linkage of iron to leukemia CSCs although with no known mechanisms (29). Additionally, the following clinical observations suggest a possible involvement of iron in pathogenesis of several chronic lung diseases: 1) increased risk of pulmonary fibrosis in patients with iron overload syndromes, e.g., idiopathic pulmonary hemosiderosis (IPH) (13); 2) iron accumulation in lung allografts after transplantation, which places them at increased risk of subsequent fibrosis and organ failure (6); and 3) disruption of iron homeostasis in lung tissues of cystic fibrosis patients, as indicated by increased expression of ferritin, iron importer divalent metal transporter (DMT1), and iron exporter ferroportin 1 (FPN1) (18). Remarkably, epidemiological studies suggest that the presence of iron in asbestos fibers, which likely leads to a local iron overload, is important for asbestos-induced mesothelioma and lung carcinoma (24, 40). SOX9 was originally known for its functions in embryonic development, specifically chondrogenesis, bone formation, and testis and lung development (4, 28). It has garnered increasing attention both in functions and as a prognostic factor in cancers. SOX9 has been reported to act as an oncogene in several cancers, including breast, colorectal, pancreatic, prostate, and glioma (32, 38). On the other hand, it has been shown to act as a tumor suppressor in bladder cancer and melanoma (3, 42). Recently, we and others have demonstrated the importance of SOX9 in lung cancer, that is SOX9 promoted lung cancer cell invasion and inhibition of SOX9 abolished lung CSCs in vitro (10, 36) and tumor cell growth and experimental metastasis in vivo (25, 36). Overexpression of SOX9 was found in the majority of lung adenocarcinoma of patient samples, particularly in their advanced stage (25, 36). Here, we showed that SOX9 upregulation was responsible for lung CSC promotion by subchronic iron exposure in NSCLC cells, which was mediated by OH[•] generation (Fig. 8). Our finding is in agreement with the previous study that reported an upregulation of SOX9 in human retinal pigment epithelial cells in response to 1-wk iron overload dominated by ferric ammonium citrate (250 μM) (54).

A recent study by Capaccione et al. (10) indicated that SOX9 was a Notch-1 target gene in human lung cancer and that overexpression of SOX9 could reverse mesenchymal phenotype induced by Notch-1 back to epithelial phenotype, a similar process to EMT. Although we found herein that subchronic iron exposure mediated SOX9 upregulation (Figs. 7–9), we observed minimal effect of iron on EMT as demonstrated by an insignificant change of cellular phenotypes and epithelial and mesenchymal markers (Fig. 6). These inconsistent findings

might be due to the particular mechanisms of iron and cellular oxidative stress on SOX9 that bypassed EMT, which require further investigation.

In conclusion, our study provides compelling evidence that iron and OH⁻ regulation of lung CSCs and tumor aggressiveness is mediated, at least in part, through SOX9 upregulation, which could be important in understanding tumor progression and metastasis. These new findings suggest a linkage between aberrant iron homeostasis, elevated OH⁻ formation, and increased risk of tumor formation and metastasis and further strengthen the potential application of iron deprivation in cancer therapy and the clinical significance of SOX9 as a key determinant and prognosis factor of advanced lung carcinoma.

ACKNOWLEDGMENTS

We acknowledge Professors Yon Rojanasakul and Surapol Issaragrisil for technical assistance and comments on the manuscript.

GRANTS

This research is supported by a grant from the Thailand Research Fund (RSA5780043).

DISCLOSURES

No conflicts of interest, financial or otherwise, are declared by the author(s).

AUTHOR CONTRIBUTIONS

P.C. and S.L. conception and design of research; P.C. and S.L. performed experiments; P.C. and S.L. analyzed data; P.C. and S.L. interpreted results of experiments; P.C. and S.L. prepared figures; P.C. and S.L. drafted manuscript; P.C. and S.L. approved final version of manuscript; S.L. edited and revised manuscript.

REFERENCES

- Abubaker K, Latifi A, Luwor R, Nazaretian S, Zhu H, Quinn MA, Thompson EW, Findlay JK, Ahmed N. Short-term single treatment of chemotherapy results in the enrichment of ovarian cancer stem cell-like cells leading to an increased tumor burden. *Mol Cancer* 12: 24, 2013.
- Ailles LE, Weissman IL. Cancer stem cells in solid tumors. *Curr Opin Biotechnol* 18: 460–466, 2007.
- Aleman A, Adrien L, Lopez-Serra L, Cordon-Cardo C, Esteller M, Belbin TJ, Sanchez-Carbayo M. Identification of DNA hypermethylation of SOX9 in association with bladder cancer progression using CpG microarrays. *Br J Cancer* 98: 466–473, 2008.
- Asou Y, Nifuji A, Tsuji K, Shinomiya K, Olson EN, Koopman P, Noda M. Coordinated expression of scleraxis and Sox9 genes during embryonic development of tendons and cartilage. *J Orthop Res* 20: 827–833, 2002.
- Bacac M, Stamenkovic I. Metastatic cancer cell. *Annu Rev Pathol* 3: 221–247, 2008.
- Baz MA, Ghio AJ, Roggli VL, Tapon VF, Piantadosi CA. Iron accumulation in lung allografts after transplantation. *Chest* 112: 435–439, 1997.
- Bertolini G, Roz L, Perego P, Tortoreto M, Fontanella E, Gatti L, Pratesi G, Fabbri A, Andriani F, Tinelli S, Roz E, Caserini R, Lo Vullo S, Camerini T, Mariani L, Delia D, Calabro E, Pastorino U, Sozzi G. Highly tumorigenic lung cancer CD133+ cells display stem-like features and are spared by cisplatin treatment. *Proc Natl Acad Sci USA* 106: 16281–16286, 2009.
- Biddle A, Liang X, Gammon L, Fazil B, Harper LJ, Emich H, Costea DE, Mackenzie IC. Cancer stem cells in squamous cell carcinoma switch between two distinct phenotypes that are preferentially migratory or proliferative. *Cancer Res* 71: 5317–5326, 2011.
- Bystrom LM, Guzman ML, Rivella S. Iron and reactive oxygen species: friends or foes of cancer cells? *Antioxid Redox Signal* 20: 1917–1924, 2014.
- Capaccione KM, Hong X, Morgan KM, Liu W, Bishop JM, Liu L, Markert E, Deen M, Minerowicz C, Bertino JR, Allen T, Pine SR. Sox9 mediates Notch1-induced mesenchymal features in lung adenocarcinoma. *Oncotarget* 5: 3636–3650, 2014.
- Chung-man HJ, Zheng S, Comhair SA, Farver C, Erzurum SC. Differential expression of manganese superoxide dismutase and catalase in lung cancer. *Cancer Res* 61: 8578–8585, 2001.
- Cronin JC, Watkins-Chow DE, Incao A, Hasskamp JH, Schonewolf N, Aoude LG, Hayward NK, Bastian BC, Dummer R, Loftus SK, Pavan WJ. SOX10 ablation arrests cell cycle, induces senescence, and suppresses melanomagenesis. *Cancer Res* 73: 5709–5718, 2013.
- Cutz E. Idiopathic pulmonary hemosiderosis and related disorders in infancy and childhood. *Perspect Pediatr Pathol* 11: 48–81, 1987.
- Dalerba P, Cho RW, Clarke MF. Cancer stem cells: models and concept. *Annu Rev Med* 58: 267–284, 2007.
- Dong C, Wilhelm D, Koopman P. SOX genes and cancer. *Cytogenet Genome Res* 105: 442–447, 2004.
- Dontu G, Abdallah WM, Foley JM, Jackson KW, Clarke MF, Kammaura MF, Wicha MS. In vitro propagation and transcriptional profiling of human mammary stem/progenitor cells. *Genes Dev* 17: 1253–1270, 2003.
- Gavert N, Vivanti A, Hazin J, Brabletz T, Ben-Ze'ev A. L1-mediated cancer cell metastasis does not require changes in EMT and cancer stem cell markers. *Mol Cancer Res* 9: 14–24, 2011.
- Ghio AJ, Roggli VL, Soukup JM, Richards JH, Randell SH, Muhlebach MS. Iron accumulates in the lavage and explanted lungs of cystic fibrosis patients. *J Cyst Fibros* 12: 390–398, 2013.
- Goi T, Fujioka M, Satoh Y, Tabata S, Koneri K, Nagano H, Hirono Y, Katayama K, Hirose K, Yamaguchi A. Angiogenesis and tumor proliferation/metastasis of human colorectal cancer cell line sw620 transfected with endocrine glands-derived-vascular endothelial growth factor, as a new angiogenic factor. *Cancer Res* 64: 1906–1910, 2004.
- Guo W, Keckesova Z, Donaher JL, Shibue T, Tischler V, Reinhardt F, Itzkovitz S, Noske A, Zurrer-Hardi U, Bell G, Tam WL, Mani SA, van Oudenaarden Weinberg RA. Slug and Sox9 cooperatively determine the mammary stem cell state. *Cell* 148: 1015–1028, 2012.
- Haigis MC, Deng CX, Finley LW, Kim HS, Gius D. SIRT3 is a mitochondrial tumor suppressor: a scientific tale that connects aberrant cellular ROS, the Warburg effect, and carcinogenesis. *Cancer Res* 72: 2468–2472, 2012.
- Heath JL, Weiss JM, Lavau CP, Wechsle DS. Iron deprivation in cancer-potential therapeutic implications. *Nutrients* 5: 2836–2859, 2013.
- Ho MM, Ng AV, Lam S, Hung JY. Side population in human lung cancer cell lines and tumors is enriched with stem-like cancer cells. *Cancer Res* 67: 4827–4833, 2007.
- Jiang L, Nagai H, Ohara H, Hara S, Tachibana M, Hirano S, Shinohara Y, Kohyama N, Akatsuka S, Toyokuni S. Characteristics and modifying factors of asbestos-induced oxidative DNA damage. *Cancer Sci* 99: 2142–2151, 2008.
- Jiang SS, Fang WT, Hou YH, Huang SF, Yen BL, Chang JL, Li SM, Liu HP, Liu YL, Huang CT, Li YW, Jang TH, Chan SH, Yang SJ, Hsiung CA, Wu CW, Wang LH, Chang IS. Upregulation of SOX9 in lung adenocarcinoma and its involvement in the regulation of cell growth and tumorigenicity. *Clin Cancer Res* 16: 4363–4373, 2010.
- Juntilla MM, Patil VD, Calamito M, Joshi RP, Birnbaum MJ, Koretzky GA. AKT1 and AKT2 maintain hematopoietic stem cell function by regulating reactive oxygen species. *Blood* 115: 4030–4038, 2010.
- Kalluri R, Weinberg RA. The basics of epithelial-mesenchymal transition. *J Clin Invest* 119: 1420–1428, 2009.
- Kanai Y, Hiramatsu R, Matoba S, Kidokoro T. From SRY to SOX9: mammalian testis differentiation. *J Biochem* 138: 13–19, 2005.
- Kim JL, Kang HN, Kung MH, Yoo YA, Kim JS, Choi CW. The oral iron chelator deferasirox induces apoptosis in myeloid leukemia cells by targeting caspase. *Acta Haematol* 126: 241–245, 2011.
- Levina V, Marrangoni AM, DeMarco R, Gorelik E, Lokshin AR. Drug-selected human lung cancer stem cells: cytokine network, tumorigenic and metastatic properties. *PLoS One* 3: e3077, 2008.
- Levina V, Marrangoni A, Wang T, Parikh S, Su Y, Herberman R, Lokshin A, Gorelik E. Elimination of human lung cancer stem cells through targeting of the stem cell factor-c-kit autocrine signaling loop. *Cancer Res* 70: 338–46, 2010.
- Lü B, Fang Y, Xu J, Wang L, Xu F, Xu E, Huang Q, Lai M. Analysis of SOX9 expression in colorectal cancer. *Am J Clin Pathol* 130: 897–904, 2008.
- Luanpitpong S, Talbott SJ, Rojanasakul Y, Nimmannit U, Pongrakhananon V, Wang L, Chanvorachote P. Regulation of lung cancer cell migration and invasion by reactive oxygen species and caveolin-1. *J Biol Chem* 285: 38832–38840, 2010.

34. Luanpitpong S, Nimmannit U, Chanvorachote P, Leonard SS, Pongrakhananon V, Wang L, Rojanasakul Y. Hydroxyl radical mediates cisplatin-induced apoptosis in human hair follicle dermal papilla cells and keratinocytes through Bcl-2-dependent mechanism. *Apoptosis* 16: 769–782, 2011.
35. Luanpitpong S, Wang L, Stueckle TA, Tse W, Chen YC, Rojanasakul Y. Caveolin-1 regulates lung cancer stem-like cell induction and p53 inactivation in carbon nanotube-driven tumorigenesis. *Oncotarget* 5: 3541–3554, 2014.
36. Luanpitpong S, Li J, Manke A, Brundage K, Ellis E, McLaughlin S, Angsutararux P, Chanthra N, Voronkova M, Chen YC, Wang L, Chanvorachote P, Pei M, Issaragrisil S, Rojanasakul Y. SLUG is required for SOX9 stabilization and functions to promote cancer stem cells and metastasis in human lung carcinoma. *Oncogene* [Epub ahead of print].
37. Mani SA, Guo W, Liao MJ, Ng E, Ayyanan A, Zhou AY, Brooks M, Reinhard F, Zhang CC, Shipitsin M, Campbell LL, Polyak K, Briskin C, Yang J, Weinberg RA. The epithelial-mesenchymal transition generates cells with properties of stem cells. *Cell* 133: 704–715, 2008.
38. Matheu A, Collado M, Wise C, Manterola L, Cekaite L, Tye AJ, Canamero M, Bujanda L, Schedl A, Cheah KS, Skotheim RI, Lothe RA, López de Munain A, Briscoe J, Serrano M, Lovell-Badge R. Oncogenicity of the developmental transcription factor Sox9. *Cancer Res* 72: 1301–1315, 2012.
39. May CD, Sphyris N, Evans KW, Werden SJ, Guo W, Mani SA. Epithelial-mesenchymal transition and cancer stem cells: A dangerously dynamic duo in breast cancer progression. *Breast Cancer Res* 13: 202, 2011.
40. McDonald A, McDonald J, Pooley F. Mineral fibre content of lung in mesothelial tumours in North America. *Ann Occup Hyg* 26: 417–422, 1982.
41. Nurwidya F, Takahashi F, Murakami A, Takahashi K. Epithelial mesenchymal transition in drug resistance and metastasis of lung cancer. *Cancer Res Treat* 44: 151–156, 2012.
42. Passeron T, Valencia JC, Namiki T, Vieira WD, Passeron H, Miyamura Y, Hearing VJ. Upregulation of SOX9 inhibits the growth of human and mouse melanomas and restores their sensitivity to retinoic acid. *J Clin Invest* 119: 954–963, 2009.
43. Perona R, Lopez-Ayllon BD, Castro Carpeno J, Belda-Iniesta C. A role for cancer stem cells in drug resistance and metastasis in non-small-cell lung cancer. *Clin Transl Oncol* 13: 289–293, 2011.
44. Quail DF, Joyce JA. Microenvironmental regulation of tumor progression and metastasis. *Nat Med* 19: 1423–1437, 2013.
45. Rybak AP, Tang D. SOX2 plays a critical role in EGFR-mediated self-renewal of human prostate cancer stem-like cells. *Cell Signal* 25: 2734–2742, 2013.
46. Setsukinai K, Urano Y, Kakinuma K, Majima HJ, Nagano T. Development of novel fluorescence probes that can reliably detect reactive oxygen species and distinguish specific species. *J Biol Chem* 278: 3170–3175, 2003.
47. Siegel R, Naishadham D, Jemal A. Cancer statistics, 2013. *CA Cancer J Clin* 63: 11–30, 2013.
48. Stewart SA, Dykxhoorn DM, Palliser D, Mizuno H, Yu EY, An DS, Sabatini DM, Chen IS, Hahn WC, Sharp PA, Weinberg RA, Novina CD. Lentivirus-delivered stable gene silencing by RNAi in primary cells. *RNA* 9: 493–501, 2003.
49. Thiery JP, Acloque H, Huang RY, Nieto MA. Epithelial-mesenchymal transitions in development and disease. *Cell* 139: 871–890, 2009.
50. Torti SV, Torti FM. Iron and cancer: more ore to be mined. *Nat Rev Cancer* 13: 342–355, 2013.
51. Tsai JH, Yang J. Epithelial-mesenchymal plasticity in carcinoma metastasis. *Genes Dev* 27: 2192–2206, 2013.
52. Turcatel G, Rubin N, Menke DB, Martin G, Shi W, Warburton D. Lung mesenchymal expression of Sox9 plays a critical role in tracheal development. *BMC Biol* 11: 117, 2013.
53. Westerink RH, Vijverberg HP. Vesicular catecholamine release from rat PC12 cells on acute and subchronic exposure to polychlorinated biphenyls. *Toxicol Appl Pharmacol* 183: 153–159, 2002.
54. Wolkow N, Li Y, Maminishkis A, Song Y, Alekseev O, Iacovelli J, Song D, Lee JC, Dunaief JL. Iron upregulates melanogenesis in cultured retinal pigment epithelial cells. *Exp Eye Res* 128: 92–101, 2014.

PRIMARY RESEARCH

Open Access



Zinc induces epithelial to mesenchymal transition in human lung cancer H460 cells via superoxide anion-dependent mechanism

Chuanpit Ninsontia^{1,2}, Preeyaporn Plaimee Phiboonchaiyanan^{1,2} and Pithi Chanvorachote^{1,2*}

Abstract

Background: Epithelial to mesenchymal transition (EMT) has been shown to be a crucial enhancing mechanism in the process of cancer metastasis, as it increases cancer cell capabilities to migrate, invade and survive in circulating systems. This study aimed to investigate the effect of essential element zinc on EMT characteristics in lung cancer cells.

Methods: The effect of zinc on EMT was evaluated by determining the EMT behaviors using migration, invasion and colony formation assay. EMT markers were examined by western blot analysis. Reactive oxygen species (ROS) were detected by specific fluorescence dyes and flow cytometry. All results were analyzed by ANOVA, followed by individual comparisons with post hoc test.

Results: The present study has revealed for the first time that the zinc could induce EMT and related metastatic behaviors in lung cancer cells. Results showed that treatment of the cells with zinc resulted in the significant increase of EMT markers N-cadherin, vimentin, snail and slug and decrease of E-cadherin proteins. Zinc-treated cells exhibited the mesenchymal-like morphology and increased cancer cell motility with significant increase of activated FAK, Rac1, and RhoA. Also, tumorigenic abilities of lung cancer cells could be enhanced by zinc. Importantly, the underlying mechanism was found to be caused by the ability of zinc to generate intracellular superoxide anion. Zinc was shown to induce cellular superoxide anion generation and the up-regulation of EMT markers and the induced cell migration and invasion in zinc-treated cells could be attenuated by the treatment of MnTBAP, a specific superoxide anion inhibitor.

Conclusion: Knowledge gains from this study may highlight the roles of this important element in the regulation of EMT and cancer metastasis and fulfill the understanding in the area of cancer cell biology.

Keywords: Zinc, Epithelial-to-mesenchymal transition, Superoxide anion, Lung cancer, Metastasis, Reactive oxygen species

Background

Metastatic potential of lung cancer cells has been accepted to be an important cause of high rate of death worldwide [1]. Knowledge indicates that the process of cancer cell transition from epithelial to mesenchymal phenotypes or epithelial to mesenchymal transition

(EMT) plays a dominant role in facilitating metastasis and progression in many types of cancer [2–4]. EMT-phenotypic cancer cells elicit highly metastatic potentials, such as aggressive migratory, invasive and increased tumorigenicity [2–5]. During EMT, epithelial cells undergo remarkable morphological conversion from stone-like epithelial morphology to elongated-like mesenchymal morphology and the crucial hallmarks of EMT are the loss of E-cadherin, a cellular junction protein typically expressed in epithelial cells, and the increase of mesenchymal markers (e.g. N-cadherin, vimentin, snail and

*Correspondence: pithi_chan@yahoo.com

¹ Department of Pharmacology and Physiology, Faculty of Pharmaceutical Sciences, Chulalongkorn University, Pathumwan, Bangkok 10330, Thailand

Full list of author information is available at the end of the article



© 2016 The Author(s). This article is distributed under the terms of the Creative Commons Attribution 4.0 International License (<http://creativecommons.org/licenses/by/4.0/>), which permits unrestricted use, distribution, and reproduction in any medium, provided you give appropriate credit to the original author(s) and the source, provide a link to the Creative Commons license, and indicate if changes were made. The Creative Commons Public Domain Dedication waiver (<http://creativecommons.org/publicdomain/zero/1.0/>) applies to the data made available in this article, unless otherwise stated.

slug) [2–5]. Zinc is a trace element implicated in many important cellular processes including structural, functional and signaling of the cells [6, 7]. Zinc is detected in plasma at the concentrations ranging from 10 to 18 μM [6, 7] and the concentration of zinc in plasma or tissues is found to be elevated in pathological condition of cancer [8–11]. Importantly, evidence indicates that several zinc influx transporters such as Zrt/Irt-like protein (ZIP) 6 [12], ZIP7 [13] and ZIP10 [14] were shown to be up-regulated in cancer cells and their high levels correlate with aggressive behaviors and poor prognosis. Such data has suggested the roles of zinc in regulation of cancer cell biology. However, effects of zinc on the EMT process of cancer cells are largely unknown.

Recently, the involvement of ROS in EMT process has been continuously revealed [15–17]. Together with the fact that zinc has been shown to regulate cellular redox status of the cells [18–20], it is possible that zinc may affect the cancer cell behaviors via ROS-dependent mechanism. Indeed, the exogenous zinc has a capability to induce ROS production via NADPH oxidase and mitochondria-dependent mechanism [18–20]. Zinc exposure was found to induce translocation of NADPH oxidase subunits to plasma membrane, which is the signature event for NADPH oxidase activation and such an event was inhibited by the addition of NADPH oxidase inhibitor [7, 19, 20]. Together, we hypothesize that zinc may affect the process of EMT in lung cancer cells. Also, we attempt to clarify the mechanisms involved in zinc-induced EMT. The findings from this study could help fulfill the understanding in tumor cell biology and could provide important information useful for zinc management in cancer patients.

Methods

Cells and reagents

Human lung cancer epithelial H460 cell was obtained from the American Type Culture Collection (ATCC, Manassas, VA). H460 cell was cultured in RPMI 1640 medium in a 5 % CO_2 environment at 37 °C. The media was supplemented with 2 mM L-glutamine, 10 % fetal bovine serum and 100 units/ml of penicillin/streptomycin (Gibco, Gaithersburg, MA, USA). Zinc sulfate, dimethyl sulfoxide (DMSO), 2,7-dichlorofluorescein diacetate (DCFH₂-DA), dihydroethidium (DHE), hydroxyphenyl fluorescein (HPF), DMNQ (2,3-dimethoxy-1,4-naphthoquinone), 3-(4,5-Dimethylthiazol-2-yl)-2,5-diphenyltetrazolium bromide (MTT) and Hoechst 33342 were obtained from Sigma Chemical, Inc. (St. Louis, MO, USA). Mn (III) tetrakis (4-benzoic acid) porphyrin chloride (MnTBAP) was obtained from Calbiochem (San Diego, CA, USA). Antibodies for N-cadherin, E-cadherin, vimentin, snail, slug, phosphorylated

FAK (Y397), FAK, and β -actin and peroxidase-labeled secondary antibodies were obtained from Cell Signaling Technology, Inc. (Denver, MA). Mouse monoclonal antibodies for active Rho-GTP and Rac1-GTP were obtained from NewEast Biosciences (Malvern, PA, USA). Immobilon Western chemiluminescent HRP substrate was obtained from Millipore, Corp (Billerica, MA, USA) and Thermo Fisher Scientific Inc. (Rockford, IL, USA).

Cytotoxicity assay

Cell viability was determined by MTT colorimetric assay. Briefly, cells in 96-well plate were incubated with 500 $\mu\text{g}/\text{ml}$ of MTT for 4 h at 37 °C. The supernatant was then removed and dimethylsulfoxide (DMSO) was added to dissolve the formazan product. The intensity was spectrophotometrically measured at 570 nm using an ELISA reader (Anthros, Durham, NC, USA). All analyses were performed in at least three independent replicate cultures. The optical density ratio of treated to non-treated control cells was calculated and presented in terms of relative cell viability.

Apoptosis assay

Apoptotic cell death was detected by Hoechst 33342 staining. After specific treatments, cells were stained with 10 μM of the Hoechst 33342 for 30 min at 37 °C. The apoptotic cells having condensed chromatin and/or fragmented nuclei stained by Hoechst 33342 were visualized and scored under a fluorescence microscope (Olympus IX51 with DP70).

Cell morphology characterization

Cell morphology was investigated by seeding the cells at a density of 5×10^4 cells/well onto a 12-well plate for 48 h. The cells were treated with various concentrations of zinc sulfate for 24 h. The cells were then washed with PBS, fixed with 4 % paraformaldehyde in PBS for 10 min at 37 °C, rinsed three times with PBS, and mounted with 50 % glycerol. Cell morphology was then assessed by a phase contrast microscope (Eclipse Ti-U, Nikon, Tokyo, Japan).

Immunofluorescence

Cells were seeded at a density of 1×10^5 cells/well onto coverslips in six-well plate and incubated overnight. After the treatment, the cells on coverslips were fixed with 4 % paraformaldehyde for 30 min and permeabilized with 0.1 % Triton-X for 20 min. Thereafter, the cells were incubated with 3 % bovine serum albumin (BSA) for 30 min to prevent nonspecific binding. The cells were washed and incubated with rabbit anti-Vimentin antibody for 1 h at room temperature. Primary antibody was removed and the cells were washed and subsequently incubated with

Alexa Fluor 488 (Invitrogen) conjugated goat anti-rabbit IgG (H + L) secondary antibody for 1 h at room temperature. Samples were washed with PBS then visualized and imaged by fluorescence microscope (Olympus IX 51 with DP70, Olympus America Inc., Center valley, PA).

Western blot analysis

After specific treatments, cells were incubated in lysis buffer containing 20 mM Tris-HCl (pH 7.5), 1 % Triton X-100, 150 mM sodium chloride, 10 % glycerol, 1 mM sodium orthovanadate, 50 mM sodium fluoride, 100 mM phenylmethylsulfonyl fluoride, and a protease inhibitor cocktail (Roche Molecular Biochemicals) for 90 min on ice. The cell lysates were collected, and the protein content was determined using the BCA protein assay kit (Thermo scientific, IL, USA). Equal amounts of proteins from each sample (60 µg) were denatured by heating at 95 °C for 5 min with Laemmli loading buffer and subsequently loaded onto a 10 % SDS-PAGE. After separation, proteins were transferred onto 0.45 µM nitrocellulose membranes (Bio-Rad, Hercules, CA). The transferred membranes were blocked for 1 h in 5 % nonfat dry milk in TBST (25 mM Tris-HCl pH 7.5, 125 mM NaCl, and 0.05 % Tween 20) and incubated with the appropriate primary antibodies at 4 °C overnight. Then, the membranes were washed twice with TBST for 10 min and incubated with horseradish peroxidase-labeled isotype-specific secondary antibodies for 2 h at room temperature. The immune complexes were detected by enhancement with chemiluminescence substrate (Supersignal West Pico; Pierce, Rockford, IL) and quantified the level of proteins using image software.

Migration assay

Migration was determined by wound healing and transwell assays. For the wound healing assay, a monolayer of cells was cultured in a 96-well plate, and a wound space was made with a 1-mm-wide tip. After rinsing with PBS, the cell monolayers were incubated with the indicated treatments and allowed to migrate for 24 h. Micrographs were taken under a phase contrast microscope (Olympus DP70, Melville, NY), and the wound spaces were measured using Olympus DP controller software. Quantitative analysis of cell migration was performed using an average wound space from those random fields of view, and the percentage of change in the wound space was calculated using the following formula: % change = (average space at time 0 h) - (average space at time 24 h)/(average space at time 0 h) × 100. Relative cell migration was calculated by dividing the percentage change in the wound space of treated cells by that of the control cells in each experiment. For the transwell assay, the cells were seeded at a density of 5×10^4 cells/well onto the upper chamber of

a transwell (8 µm pore size) in a 24-well plate in serum-free medium and incubated with various concentrations of zinc. RPMI medium containing 10 % FBS was added to the lower chamber. Following the incubation, the non-migrated cells in the upper chamber were removed by cotton-swab wiping, and the cells that migrated to the underside of the membrane were stained with 10 µg/ml of Hoechst 33342 for 10 min and visualized and scored under a fluorescence microscope (Olympus IX51 with DP70).

Invasion assay

An invasion assay was performed using a 24-well transwell unit with polycarbonate (PVDF) filters (8 µm pore size). The membrane was coated with 0.5 % matrigel on the upper surface of the chamber overnight at 37 °C in a humidified incubator. The cells were plated at a density of 2×10^4 cells per well into the upper chamber of the transwell unit in serum-free medium. Medium containing 10 % FBS was added to the lower chamber of the unit. After incubation with specific test agents for 24 h at 37 °C, the medium in the upper chamber was aspirated, and the cells on the upper side of the membrane were removed with a cotton swab. The cells that invaded to the underside of the membrane were stained with 10 µg/ml of Hoechst 33342 for 10 min, visualized and scored under a fluorescence microscope (Olympus IX51 with DP70).

In vitro 3D tumorigenesis assay

In vitro 3D tumorigenesis was performed in a matrigel-coated 96-well plate. A plate was coated with 0.5 % agarose and left for solidification. The cells were suspended in culture medium containing 4 % matrigel and various concentrations of zinc, and plated at a density of 3×10^2 cells/well onto a agarose-coated plate. Medium containing various concentrations of zinc were replaced every 3 days. After 10 days, the cells were visualized and scored by image analyzer under microscope (Olympus IX51 with DP70). Whole area of each well was captured in one picture and the colonies with more than 25 µm of diameter were quantified.

ROS detection

Intracellular ROS were determined by fluorescence microplate reader and by flow cytometry using the ROS-specific probe, superoxide anions, hydrogen peroxide and hydroxyl radicals were determined by DHE, DCFH₂-DA and HPF, respectively. For fluorescence microplate reader, cells were seeded overnight in 96-well plate. Before zinc treatment cells were incubated with 10 µM of dihydroethidium (DHE), dichlorofluorescein diacetate (DCFH₂-DA) or hydroxyphenyl fluorescein (HPF) for 30 min at 4 °C, after which they were washed and

treated with various concentrations of zinc (0–50 μ M) for 1 and 3 h. After incubation, the fluorescence intensity was immediately analyzed by fluorescence microplate reader (SpectraMax M5, Molecular Devices Corp., Sunnyvale, CA, USA) using a 488-nm excitation beam and a 610-nm band-pass filter for DHE, using a 480-nm excitation beam and a 530-nm band-pass filter for detecting DCF fluorescence or using a 490-nm excitation beam and a 515-nm band-pass filter for HPF. For flow cytometry, cells were seeded overnight in six-well plate. Before zinc treatment cells were incubated with 10 μ M of DHE, DCFH₂-DA or HPF for 30 min at 4 °C, after which they were washed and treated with 50 μ M of zinc for 1 and 3 h. After incubation, cells were washed, re-suspended in phosphate-buffered saline (PBS), and immediately analyzed for fluorescence intensity by FACScan flow cytometer (Beckton Dickinson, Rutherford, NJ) using a 488-nm excitation beam and a 610-nm band-pass filter for DHE, using a 480-nm excitation beam and a 530-nm band-pass filter for detecting DCF fluorescence or using a 490-nm excitation beam and a 515-nm band-pass filter for HPF. Mean fluorescence intensity was quantified by CellQuest software (Becton–Dickinson) analysis of the recorded histograms. Relative fluorescence was calculated as a ratio of the treated to the non-treated control fluorescence intensity.

Statistical analysis

All treatment data were normalized to non-treated controls. Data are expressed as the mean \pm SD from three or more independent experiments. Multiple comparisons were examined for significant differences of multiple groups, using analysis of variance (ANOVA), followed by individual comparisons with post hoc test. Statistical significance was set at $p < 0.05$.

Results

Effects of zinc on viability of human lung cancer H460 cells

In order to investigate the effect of zinc on EMT phenotypes in human lung cancer cells, we first evaluated the non-cytotoxic concentrations of zinc. Cells were cultured in the presence or absence of zinc (0–100 μ M) for 24 h, and cell viability was determined by MTT assay at 24 h. The results indicated that treatment of the cells with zinc at the concentrations ranging from 5 to 50 μ M caused no significant cytotoxicity (Fig. 1a). The significant decrease in cell viability was first detected in response to 100 μ M of zinc treatment with approximately 86 % of the cells remaining viable.

Proliferative effect of zinc at above concentrations was further evaluated by treating the cells with zinc for 0–72 h. Figure 1b indicates that zinc at the concentrations

of 0–50 μ M had no inductive effect on cell proliferation. To confirm the effect of zinc on cell toxicity, cells were similarly treated with zinc for 24 h, and apoptosis was evaluated by Hoechst 33342 staining assay. Figure 1c, d show that apoptotic cells containing condensed and/or fragmented nuclei were not detectable in response to zinc treatment at the concentrations of 5–50 μ M.

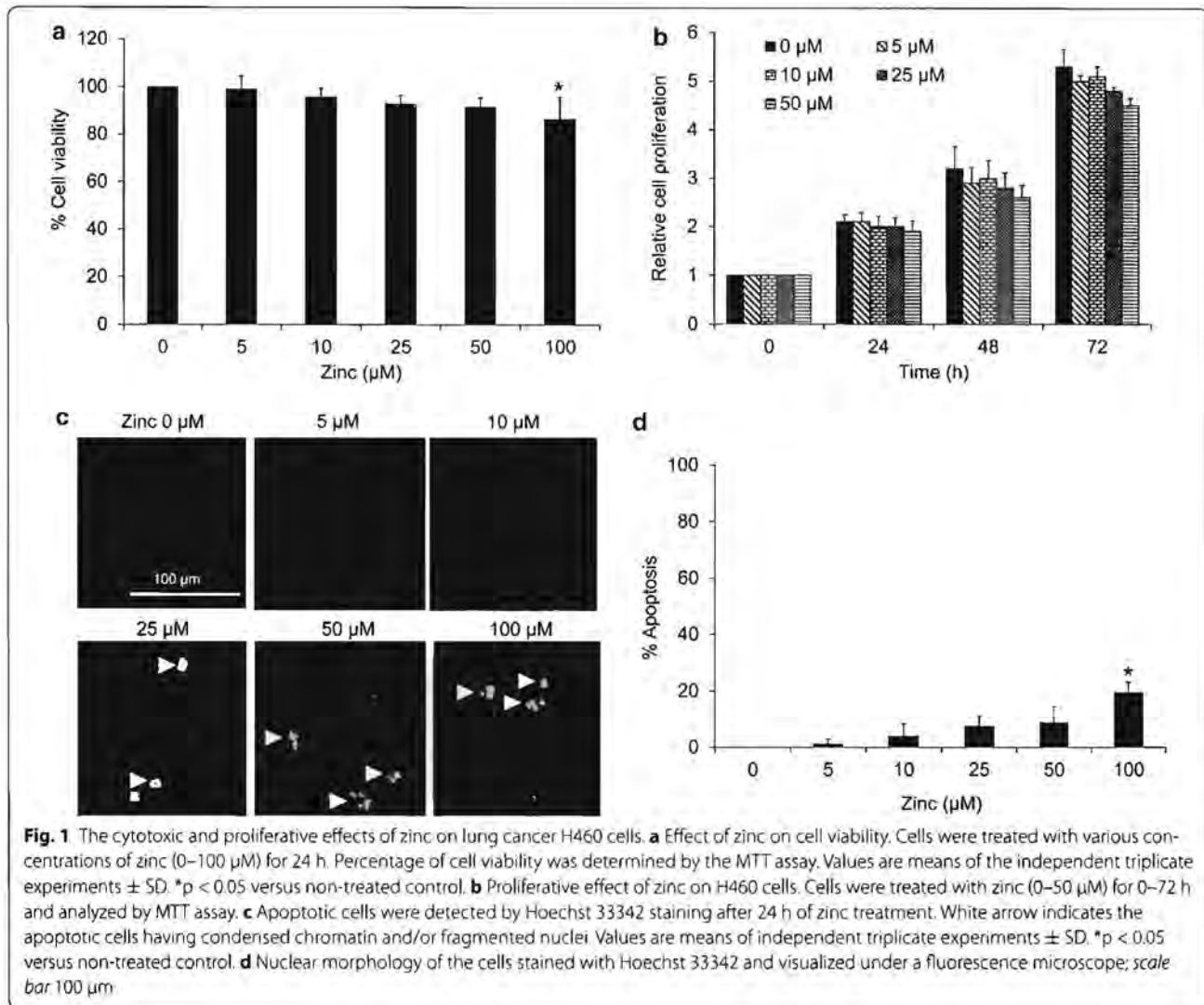
Zinc induces epithelial to mesenchymal transition in human lung cancer H460 cells

The effect of zinc on EMT in H460 cells was next investigated. The alteration of cell morphology as well as hallmarks of EMT were used to monitor the effect of zinc on EMT process in lung cancer cells. Cells were treated with zinc at non-toxic concentrations for 24 h. The morphology of the cells was captured and presented in Fig. 2a. The results showed that the zinc-treated cells exhibited morphology of mesenchymal-like cells with the elongated shape and loss of cell polarity. These results also suggested that the mesenchymal-like morphology is somehow dose-dependent as the more elongated cells could be found in the cells treated with high concentrations of zinc. In addition, the expression of mesenchymal marker vimentin was significantly increased in response to zinc treatment (Fig. 2b).

The switch of E-cadherin to N-cadherin and increase of EMT proteins including vimentin, slug, and snail have been shown to be important hallmarks of EMT in cancer cells [2–5]. We next determined such cellular EMT markers in the lung cancer cells treated with zinc by western blot analysis. Obviously, treatment of the cells with zinc could reduce E-cadherin in a dose-dependent manner. Together with the fact that the significant increase of N-cadherin was found when treating the cells with 5–50 μ M of zinc, these data strongly indicated that zinc could be able to mediate E-cadherin to N-cadherin switching in these cells. In addition, the upstream transcription factors of EMT namely snail and slug were determined in the zinc-treated cells. These factors were shown to bind to E-box elements in the promoter region of E-cadherin, resulting in the transcriptional repression of E-cadherin and induction of mesenchymal markers [2–4]. Figure 2c, d indicate that zinc significantly increased the levels of slug and snail. Also, the EMT protein vimentin was found to be induced by zinc. Taken together, our results suggested that zinc could induce EMT in lung cancer cells.

Zinc facilitates H460 cell migration and invasion

One important phenotype of EMT cells is the increase in cell motility. Studies have demonstrated that EMT could enhance aggressiveness of tumor cells by increasing



their ability to migrate and invade [2–4]. To evaluate the effect of zinc on cancer cell motility, cells were left untreated or pretreated with zinc at non-toxic concentrations for 24 h and subjected to migration and invasion assays as described in "Methods" section. Wound healing migratory assay showed that zinc significantly facilitated migratory activity of the cells with the relative cell migration increased approximately 1.3- to 1.8-fold in comparison to that of non-treated control cells (Fig. 3a, b). Also, the transwell migration assay was performed to confirm the migratory effect of zinc. Figure 3c shows that zinc treatment significantly increased the number of cells passed through the membrane of well, suggesting that such element induced cell migration.

Next, we performed experiments to test the ability of the cancer cells in invading through matrigel. The

transwell was pre-coated with matrigel and the zinc-treated cells were seeded on top. The cells were allowed to invade for 24 h and the invaded cells at the lower part of the membrane were determined. Figure 3d shows that zinc significantly promoted the invasion of H460 cells in a dose-dependent manner.

Enhanced tumor cell migration and invasiveness are shown to be down-stream behaviors of FAK signal [21–24]. We next determined the effect of zinc treatment on motility regulatory proteins including FAK, activated (phosphorylated at Try397) FAK, active forms of RAC1, and RhoA by western blot analysis. The results showed that treatment of the cells with 0–50 μM of zinc for 24 h dramatically increased the activation of FAK (Fig. 3e, f). Also, its down-stream functioning proteins active Rac1 and RhoA were found to increase, accordingly. These

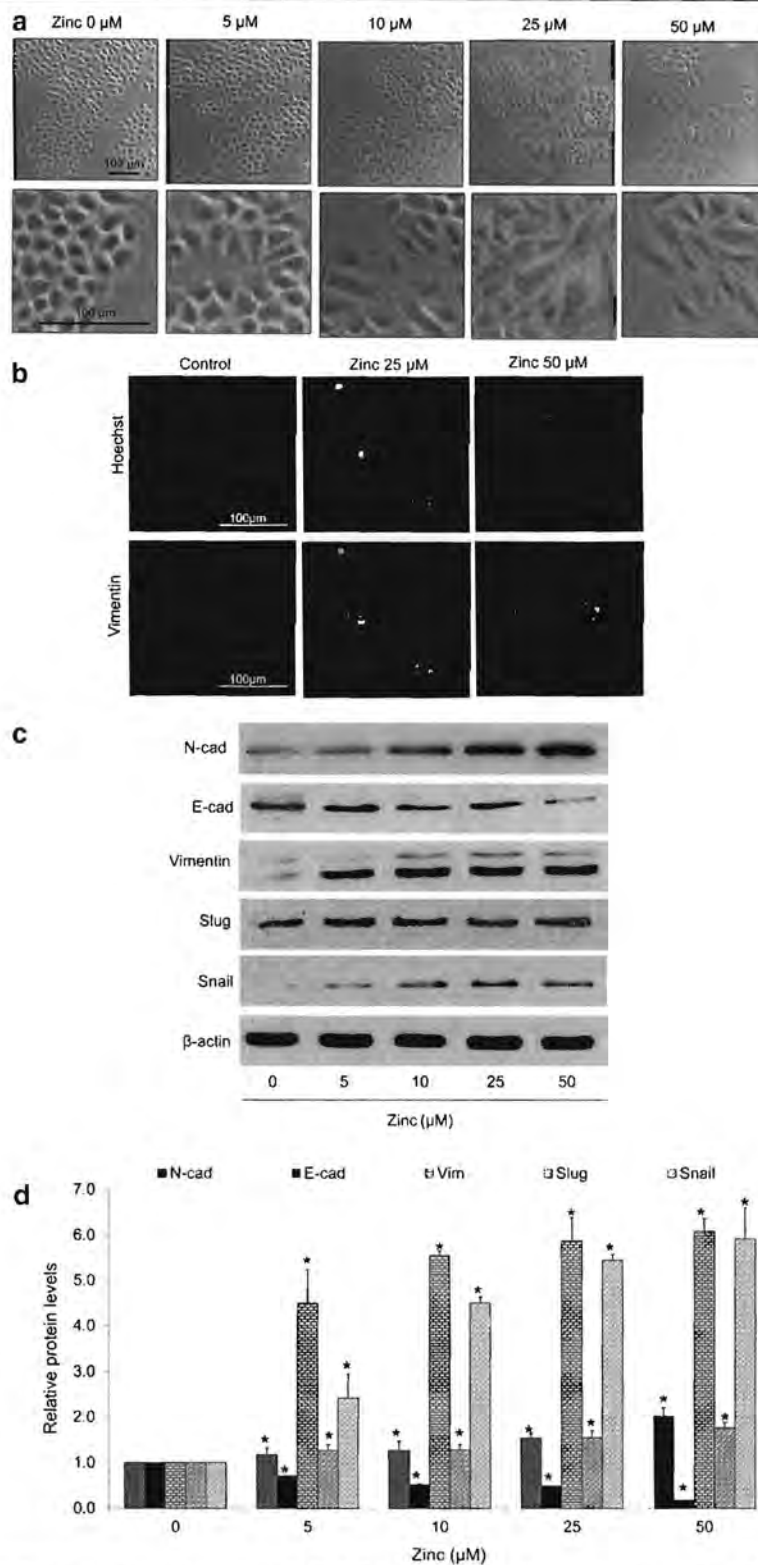
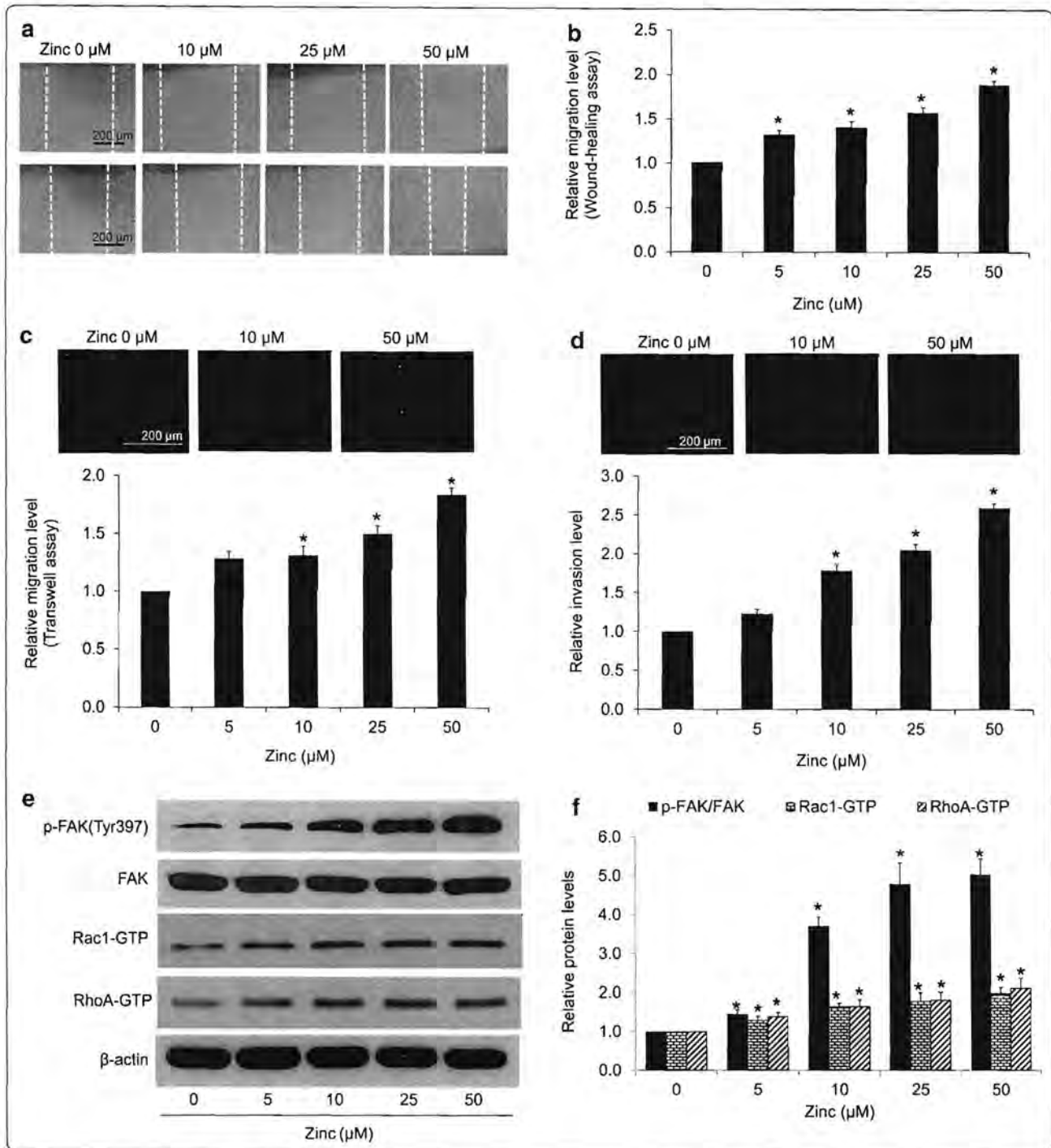


Fig. 2 Effect of zinc on epithelial to mesenchymal transition (EMT). Cells were treated with various concentrations of zinc (0–50 μM) for 24 h. **a** Cells morphology was examined by phase-contrast microscope; *scale bar* 100 μm . **b** Expression of vimentin was analyzed by immunofluorescence staining; *scale bar* 100 μm . **c** The expression levels of EMT protein markers were determined by western blotting. The blots were re-probed with β -actin to confirm equal loading of the samples. **d** The blots were quantified by densitometry and mean data from three independent experiments were normalized to the results. The *bars* are the mean \pm SD of independent triplicate experiments. * $p < 0.05$ versus untreated control



results suggested that zinc treatment increase EMT-associated cell behaviors through FAK-dependent pathway.

Zinc enhances tumorigenicity in human lung cancer H460 cells

Having shown that zinc could enhance cell migration and invasion, we next tested whether zinc may augment

the ability of cancer cell to initiate a new tumor. It is well known that the EMT process facilitate tumor formation at the metastatic site [25–27] and this potential is responsible for cancer progression [25–27]. Previous studies have shown that in vitro 3D tumorigenesis assay reflexes ability of the cancer cells in in vivo cancer condition [28]. Cells were left un-treated or pre-treated with various

(See figure on previous page.)

Fig. 3 Effect of zinc on lung cancer cell migration and invasion. Cells were pre-treated with zinc (0–50 μM) for 24 h. The treated cells were subjected to migration and invasion assays. **a** For wound healing assay, the confluent monolayers of the cells were wounded by using a 1 mm-wide tip and cultured with the medium containing indicated treatments. After 24 h of incubation, wound spaces were analyzed and represented as a relative migration level. **b** The relative migration level was determined by comparing the relative change of zinc-treated cells to untreated control cells. Values are means of independent triplicate experiments \pm SD. * $p < 0.05$ versus untreated control. **c** For transwell migration assay, migratory cells were stained with Hoechst 33342 for 30 min, determined under a fluorescence microscope and represented as average number of migratory cells in each field relatively to control cells. **d** Cell invasion was evaluated using a transwell coated with matrigel as described under “Methods” section. After 24 h, the cells that invaded across the membrane were stained with Hoechst 33342 for 30 min and visualized under a fluorescence microscope. Value was represented as average number of invaded cells in each field relatively to control. Values are means of independent triplicate experiments \pm SD. * $p < 0.05$ versus untreated control. **e** The expression levels of motility-regulatory proteins were determined by western blotting. The blots were re-probed with β -actin to confirm equal loading of the samples. **f** The blots were quantified by densitometry and mean data from three independent experiments were normalized to the results. The bars are the mean \pm SD of independent triplicate experiments. * $p < 0.05$ versus untreated control

concentrations of zinc (0–50 μM) for 24 h and subjected to tumorigenesis assay as described in “Methods” section. After 10 days of 3D culturing, the colony number and diameter were determined. Figure 4 shows that zinc treatment enhances tumorigenic ability of the lung cancer cells as indicated by the significant increase in the number and size of colonies in zinc-treated groups. The number of colonies increased approximately 1.38- and 1.76-fold in response to zinc at 25 and 50 μM , respectively (Fig. 4b).

Zinc induces intracellular superoxide anion generation in H460 cells

Studies have demonstrated the roles of ROS on cancer EMT phenotypes [15–17]. Because zinc has been previously shown to affect the redox balance of the cells and exhibit the pro-oxidant activity in normal and cancer

cells [7, 18–20], we next evaluated whether the effect of zinc in regulation of EMT in these lung cancer cells is through ROS-dependent mechanism. To examine the specific ROS levels induced by zinc, cells were incubated with various ROS specific probes as mentioned in “Methods” section for 30 min before treatment with 0–50 μM zinc and intracellular ROS levels were determined by flow cytometry and fluorescence microplate reader. Figure 5a, d show that zinc significantly increased cellular superoxide anion, while it had minimal effect on hydrogen peroxide (Fig. 5b, e) and hydroxyl radical (Fig. 5c, f). Consistent with microplate reader determination, flow cytometric analysis revealed that intracellular superoxide anion significantly increased up to twofold in response to zinc treatment (Fig. 5g) and zinc had no detectable effect on hydrogen peroxide and hydroxyl radical (Fig. 5h, i). We further confirmed the superoxide

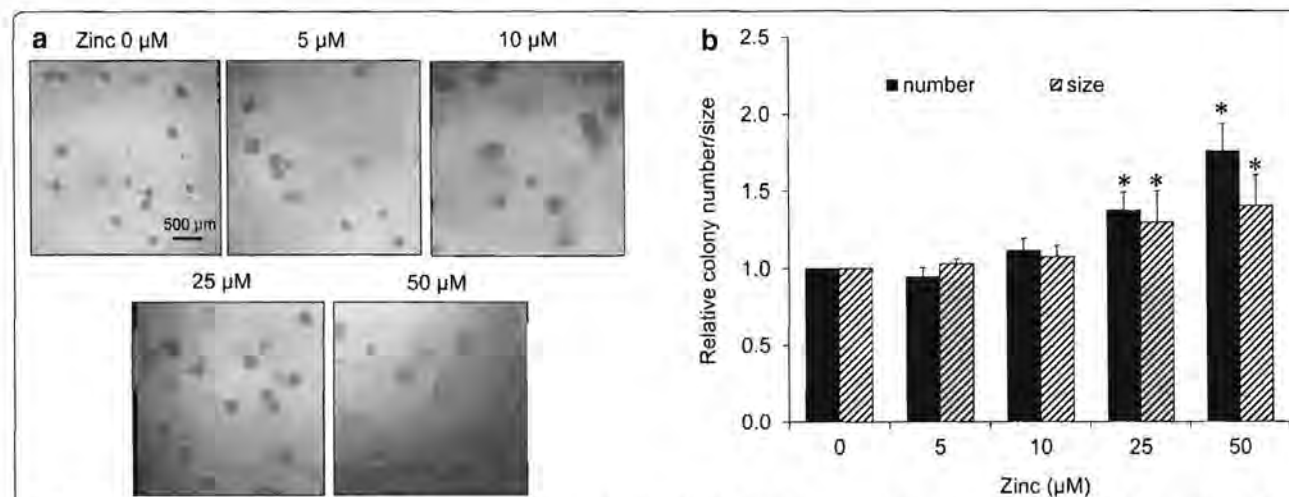


Fig. 4 Zinc enhances tumorigenic potential of H460 lung cancer cells. **a** H460 cells were pre-treated with zinc (0–50 μM) for 24 h. The treated cells were subjected to 3D tumorigenesis assay. The cells were suspended in RPMI medium containing 4 % matrigel and zinc (0–50 μM) and plated onto agarose-coated plate. After 10 days, colonies were visualized under microscope; scale bar 500 μm . **b** Value was represented as average diameter and number of colonies in each field relatively to control cells using image analyzer. Values are means of independent triplicate experiments \pm SD. * $p < 0.05$ versus untreated control

anion-inducing effect of zinc using specific superoxide anion inhibitor MnTBAP. Results indicated that treatment with the zinc caused the superoxide anion up-regulation in the cells and such event could be abolished by the addition of MnTBAP, confirming that the major ROS induced by zinc treatment in our system was superoxide anion (Fig. 5j, k).

Zinc mediates EMT phenotypes in lung cancer cells through superoxide anion-dependent mechanism

In order to investigate the role of superoxide anion on EMT induction, cell morphology, EMT markers, migratory behaviors, and colony formation were evaluated in the cells treated with zinc and specific inhibitor of superoxide anion. Cells were cultured in the presence or absence of MnTBAP for 1 h prior to zinc treatment and EMT phenotypes were determined. Also, to clarify role of superoxide anion, the superoxide anion inducer DMNQ was used. The results show that treatment of the cells with DMNQ or zinc alone was able to switch the morphology of lung cancer cells from epithelial to fibroblast-like mesenchymal feature (Fig. 6a). Addition of MnTBAP to the zinc-treated cells could be able to attenuate such morphologic transformation.

Immunocytochemistry showed the increased vimentin found in DMNQ- and zinc- treated cells. And the increased vimentin signal induced by zinc was suppressed by the addition of MnTBAP (Fig. 6b). Consistently, the results of western blot analysis revealed that EMT markers including N-cadherin, vimentin, snail, and slug were found to be significantly increased in response to DMNQ and zinc treatment and such phenomenon could be reversed by the addition of MnTBAP (Fig. 6c, d).

As DMNQ was used as a superoxide anion donor, the intracellular superoxide anion generated by DMNQ was determined. Cells were incubated with DHE as mentioned in "Methods" section for 30 min and treated with 5 μ M of DMNQ. DHE intensity was determined by flow cytometry. The result indicated the 1.5-fold superoxide induction in DMNQ-treated cells as shown in Fig. 6e.

The migration and invasion of the cells were further evaluated. The results were consistent with the expression levels of EMT proteins that DMNQ and zinc could be able to induce cell migration and invasion and such

inductions could be abolished by superoxide anion inhibitor (Fig. 7a–d). Also, the colony size and number which were increased in response to zinc treatment were found to be significantly attenuated by the treatment of MnTBAP (Fig. 7e, f). Taken together, these results pointed out that zinc induces EMT process, migratory behaviors, and tumorigenic potential in the lung cancer cells via superoxide anion-dependent mechanism.

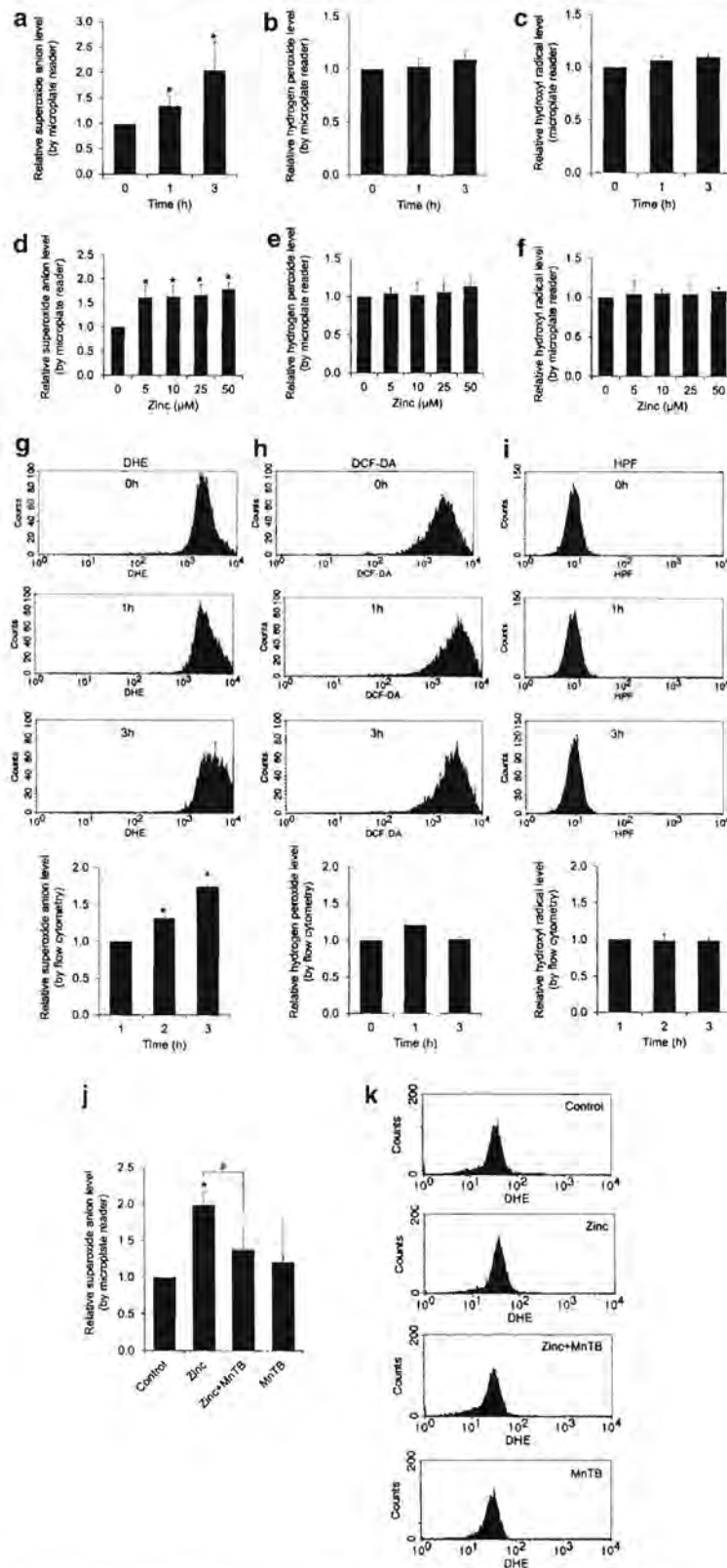
Discussion

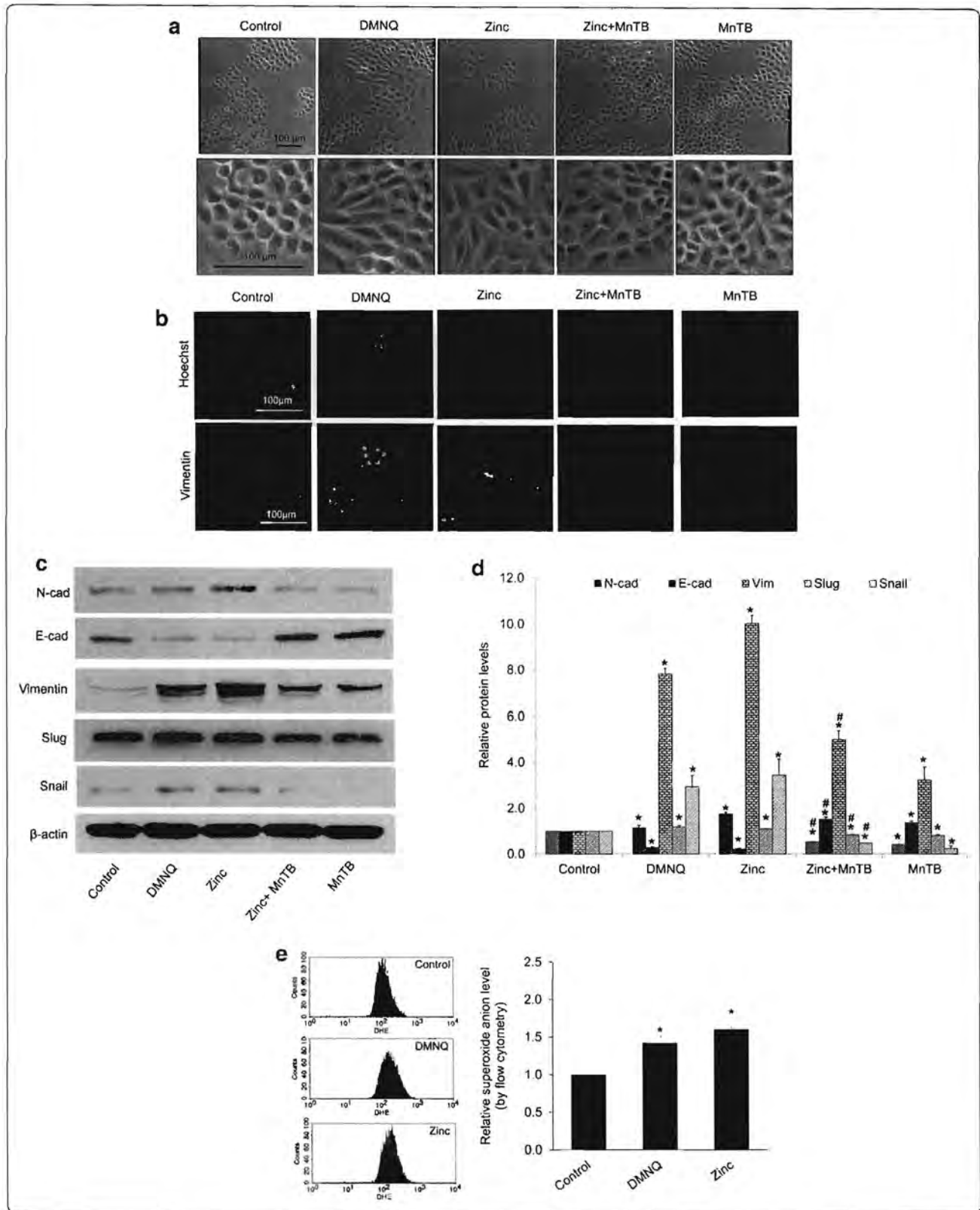
Accumulating data have guided for a long time that zinc, an essential element composition of numerous proteins [6–8, 29], may play important parts on the basis of cancer cell biology. The plasma zinc level was found to be significantly elevated in certain cancer tissues [8–11]. Zinc-containing compounds seem to be associated with carcinogenesis in lung cancer other cancers [30, 31]. In detail, zinc chromate was found to increase cytotoxicity, chromosome damage and DNA double strand breaks in human lung epithelial cells, suggesting the roles of zinc-containing compounds in cell toxicity and carcinogenesis [30]. Besides, the increase of zinc influx transporters such as ZIP6 [12], ZIP7 [13] and ZIP10 [14] has been linked to the aggressive behaviors and poor prognosis of breast cancer [12–14, 32].

Until recently, the knowledge of zinc on the molecular mechanisms of cancer metastasis is still not fully understood especially those regulating EMT. EMT is considered a critical augmenting process of cancer metastasis as it facilitates cancer dissemination in many ways [2–4]. In the process of EMT, cellular phenotypes are altered together with the distinguished expressions of protein markers being changed from epithelial toward mesenchymal types [2–5]. The process facilitates the loss of cell adhesion, increases motility, and survival in detached condition [2–5]. During EMT, an elongated fibroblast-like morphology of the cells is frequently observed. However, indicators like the switching between E-cadherin and N-cadherin, as well as EMT transcription factors snail and slug are more acceptable as hallmarks of EMT [2–5]. In particular, lung cancer H460 cells were shown to undergo EMT in response to various stimuli [33, 34]. EMT features of H460 cells were characterized by (i) the change of cell morphology from epithelial to

(See figure on next page.)

Fig. 5 Zinc induces intracellular superoxide anion generation in H460 cells. **a–i** The cells were incubated with specific ROS probes, namely, DHE, DCFH₂-DA, or HPF at 4 °C for 30 min prior to the treatment with zinc (0–50 μ M) for 0–3 h and the fluorescence intensity was analyzed by a microplate reader and flow cytometry. Mean intensity was normalized to untreated control cells and represented as relative ROS levels. Values are means of independent triplicate experiments \pm SD. * p < 0.05 versus untreated control. **j–k** The cells were incubated with DHE at 4 °C for 30 min prior to pre-treatment with 50 μ M MnTBAP (superoxide anion inhibitor) for 1 h in the presence or absence of zinc (50 μ M) for 3 h and the fluorescence intensity was analyzed by a microplate reader and flow cytometry. Mean intensity was normalized to untreated control cells and represented as relative ROS levels. Values are means of independent triplicate experiments \pm SD. * p < 0.05 versus untreated control





(See figure on previous page.)

Fig. 6 Effect of superoxide anion on EMT. **a** H460 cells were incubated with 5 μ M DMNQ (superoxide anion inducer) or 50 μ M MnTBAP (superoxide anion inhibitor), in the presence or absence of zinc (50 μ M) for 24 h prior to morphology examination using phase contrast microscope; *scale bar* 100 μ m. **b** Cells were treated with 5 μ M DMNQ or 50 μ M MnTBAP in the presence or absence of zinc (50 μ M) for 24 h. Expression of vimentin were analyzed by immunofluorescence staining; *scale bar* 100 μ m. **c** Cells were treated with 5 μ M DMNQ or 50 μ M MnTBAP, in the presence or absence of zinc (50 μ M) for 24 h. The cells were collected and analyzed for EMT markers by western blotting. The blots were re-probed with β -actin to confirm equal loading. **d** The immunoblot signals were quantified by densitometry and mean data from independent experiments were normalized to the results. The *bars* are the mean \pm SD of independent triplicate experiments. * p < 0.05 versus untreated control cells. * p < 0.05 versus 50 μ M zinc-treated cells. **e** Cells were incubated with DHE at 4 $^{\circ}$ C for 30 min prior to the treatment of DMNQ (5 μ M) or zinc (50 μ M), and the fluorescence intensity was analyzed by flow cytometry at 3 h. Mean intensity was normalized to untreated control cells and represented as relative superoxide anion levels. Values are means of independent triplicate experiments \pm SD. * p < 0.05 versus untreated control

fibroblast-like mesenchymal shape, (ii) the increased EMT markers N-cadherin, vimentin, snail, and slug, together with the reduction of epithelial marker E-cadherin, and (iii) EMT behaviors, including increased migration, invasion and tumorigenic potential [33–38]. In consistent with such studies, our results showed that zinc-treated lung cancer cells displayed the elongated mesenchymal-like shape with the significant increase of EMT markers namely N-cadherin, vimentin, snail and slug (Fig. 2). Also, we found that the E-cadherin was dramatically reduced in response to zinc treatment.

Previous studies indicated that EMT facilitates the cell motility by decreasing cell–cell interaction via E-cadherin, while increases in N-cadherin-mediated steady-state of active Rac1 [21, 22]. Similar to N-cadherin, Vimentin was shown to increase FAK and Rac1 activities [23, 24]. We found that zinc could induce EMT, resulting in the increase of cancer cell migration and invasion. The proteins regulating cell motility like FAK, RhoA and Rac1 were found to be activated in response to such up-stream signals (Fig. 3). Also, the EMT event was shown to be a key factor that enhances ability of cancer cells to metastasis by increasing the survival after cell detachment and ability to form tumors [34, 39]. It has been previously reported that the ability of cancer cells in forming new tumor can be enhanced by EMT as a result from snail augmentation [25–27]. We have supported this fact by the demonstration that treatment of the cells with zinc induced EMT with significant increase of snail increased number and size of

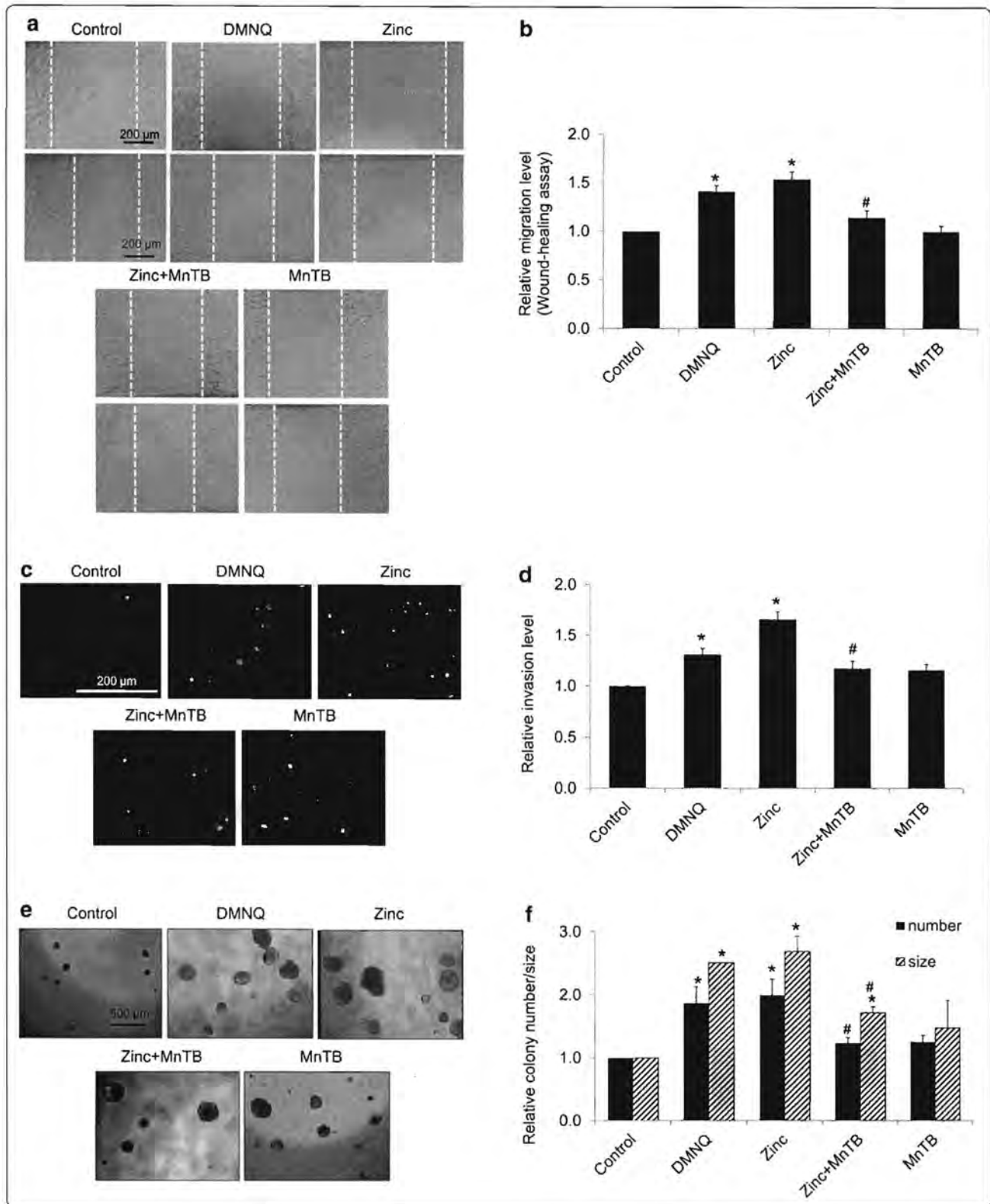
tumor colonies in 3D culturing anchorage-independent condition (Fig. 4).

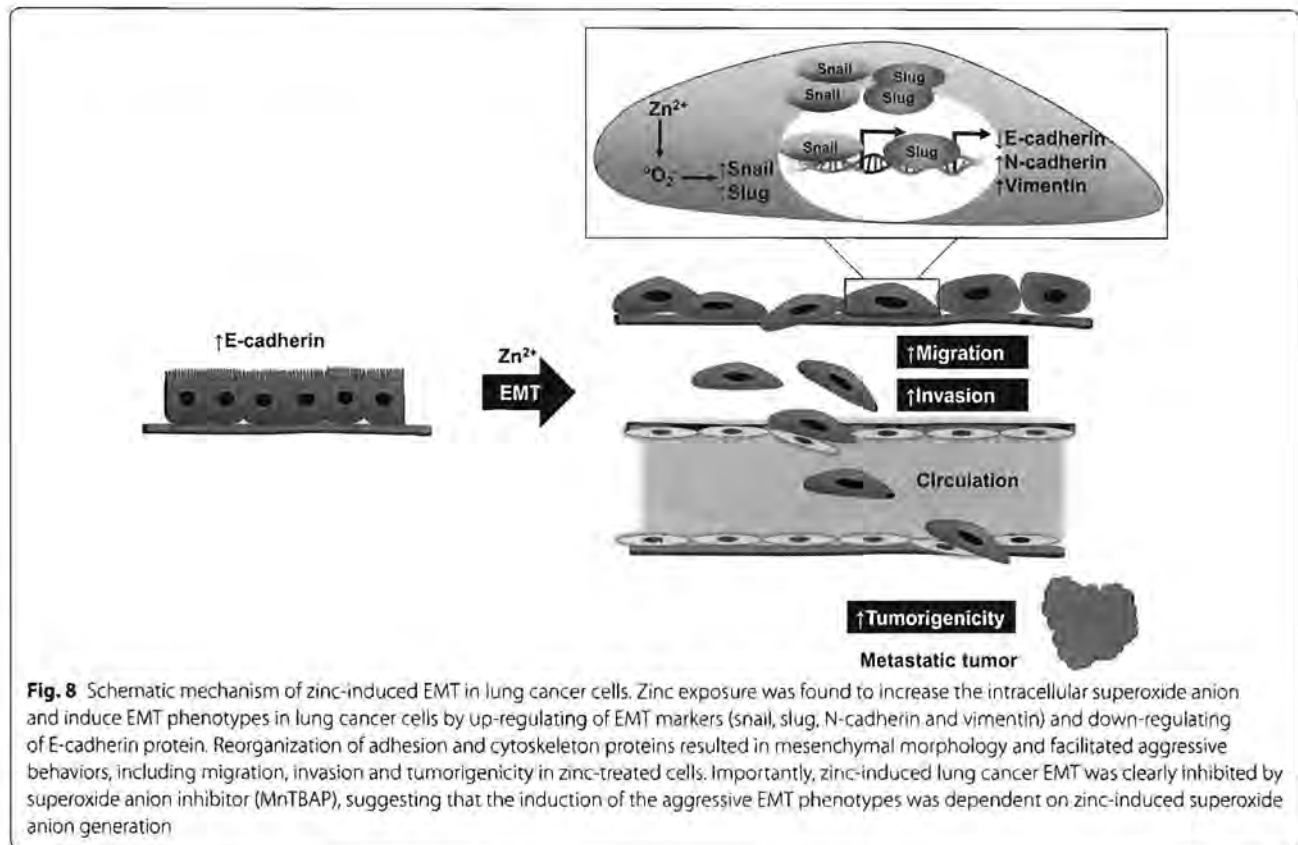
In the previous work, we have reported that the widely used chemical agent triclosan could be able to enhance EMT and aggressive behaviors in anoikis-resistant lung cancer cells [34]. However, role of endogenous element zinc on such effects has not been clarified. This current study has reported for the first time that zinc significantly induced EMT and tumorigenic potential in lung cancer cells through the enhancement of cellular superoxide anion level. Superoxide anion has been implicated in various biological and pathological processes [40–42]. Evidence has shown that the level of superoxide anion is frequently upregulated in cancer cells and regulates cancer cell proliferation, migration and metastasis [42–46]. Interestingly, we have first revealed the role of such a specific ROS in regulation of EMT in cancer cells, as the EMT could be induced by addition of superoxide anion generator (Figs. 6, 7). The EMT mediated by zinc treatment was abolished by the superoxide anion inhibitor. These findings not only provide the evidence of endogenous element in regulation of cancer biology, but also add the fact involving specific ROS roles on EMT process of cancer cells. The involvement of ROS signaling on cancer metastasis and EMT has garnered increasing attentions [15–17, 47]. The EMT-related transcription factor snail was shown to be sensitive to the balance of cellular ROS status [47, 48].

Interestingly, zinc was previously addressed to have the potential to interfere with redox status of the cells by

(See figure on next page.)

Fig. 7 Zinc promotes EMT-related cancer aggressive behaviors of H460 cells through superoxide anion-dependent mechanism. **a** For cell migration, cells were incubated with 5 μ M DMNQ (superoxide anion inducer) or 50 μ M MnTBAP (superoxide anion inhibitor), in the presence or absence of zinc (50 μ M) for 24 h before the assay. After 24 h of incubation, wound spaces were analyzed and represented as a relative migration level. **b** The relative cell migration was determined by comparing the relative change of those in untreated cells. **c–d** For invasion, cells were incubated with 5 μ M DMNQ or 50 μ M MnTBAP in the presence or absence of zinc (50 μ M) for 24 h and cells invasion was evaluated using a transwell coated with matrigel as described under "Methods" section. Value was represented as average number of invaded cells in each field relatively to control. **e** For tumorigenicity, cells were incubated with 5 μ M DMNQ or 50 μ M MnTBAP in the presence or absence of zinc (50 μ M) for 24 h prior to grow in matrigel. After 10 days, colonies were visualized under microscope; *scale bar* 500 μ m. **f** Value was represented as average diameter and number of colonies in each field relatively to control cells using image analyzer. Values of all experiments are means of independent triplicate experiments \pm SD. * p < 0.05 versus untreated control. * p < 0.05 versus 50 μ M zinc-treated cells





inducing oxidative stress [18–20]. In neurons, intracellular zinc is shown to trigger the ROS production during the process of neuron damage [49, 50]. Besides, the elevation of intracellular zinc was shown to induce superoxide anion production from the function of 12-lipoxygenase (12-LOX) enzyme [49, 50]. Interestingly, zinc was demonstrated to promote Hep-2 cancer cell apoptosis by stimulating oxidative stress [18]. Our results showed that zinc could increase superoxide anion in the human lung cancer cells (Fig. 5). The superoxide anion in such cases was suggested to be generated through NADPH oxidase system [19, 20]. Although studies have indicated that hydrogen peroxide can also mediate EMT in human malignant mesothelioma and human ovarian cancer cells [51, 52], treatment of the zinc in our system caused no effect on the cellular level of hydrogen peroxide (Fig. 5). We further investigated the role of superoxide anion on EMT using the superoxide anion inducer DMNQ. DMNQ is known to induce superoxide anion generation via NADPH oxidase activity [53, 54]. We found that treatment of the cells with DMNQ significantly increased the protein hallmarks of EMT as well as metastatic potentials (Figs. 6, 7). Such roles of superoxide anion on EMT were linked with the results of zinc, suggesting that zinc mediates the EMT

phenotypes via the production of cellular superoxide anion. These results were confirmed by the ROS inhibitory experiment. Addition of MnTBAP in the zinc-treated cells was shown to abolish superoxide anion induction as well as EMT phenotypes in response to zinc treatment (Figs. 6, 7), strongly indicating that the effect of zinc on EMT was regulated via superoxide-dependent mechanism.

Conclusions

In summary, our finding provided the evidence that zinc played a key role in the regulation of EMT and metastatic behaviors. Such inductions of the aggressive EMT phenotypes were dependent on zinc-induced superoxide anion generation as indicated in the summarized schematic figure (Fig. 8). This information helps fulfill the knowledge regarding the role of zinc in tumor cell biology.

Abbreviations

DCFH₂-DA: 2,7-dichlorofluorescein diacetate; DHE: dihydroethidium; DMNQ: 2,3-dimethoxy-1,4-naphthoquinone; EMT: epithelial to mesenchymal transition; FAK: focal adhesion kinase; HPF: hydroxyphenyl fluorescein; MnTBAP: Mn (III) tetrakis (4-benzoic acid) porphyrin chloride; NADPH: nicotinamide adenine dinucleotide phosphate; Rac1: Ras-related C3 botulinum toxin substrate 1; RhoA: Ras homolog gene family member A; ROS: reactive oxygen species; ZIP: Zrt/Irt-like protein.

Authors' contributions

PC conceived the study. PC designed the experiments. CN and PP performed the experiments. PC and CN analyzed and interpreted the data. PC contributed reagents/materials/analysis tools. CN drafted the manuscript. PC and CN revised the manuscript critically before submission. All authors read and approved the final manuscript.

Author details

¹ Department of Pharmacology and Physiology, Faculty of Pharmaceutical Sciences, Chulalongkorn University, Pathumwan, Bangkok 10330, Thailand. ² Cell-based Drug and Health Products Development Research Unit, Faculty of Pharmaceutical Sciences, Chulalongkorn University, Bangkok, Thailand.

Acknowledgements

This study was funded by The Thailand Research Fund through The Royal Golden Jubilee Ph.D. program (Grant No. PHD/0004/2556) and Grants (RSA5780043). The funders had no role in study design, data collection and analysis, decision to publish, or preparation of the manuscript.

Competing interests

The authors declare that they have no competing interests.

Received: 8 March 2016 Accepted: 6 June 2016

Published online: 17 June 2016

References

- Siegel R, Ma J, Zou Z, Jemal A. Cancer statistics, 2014. *CA Cancer J Clin*. 2014;64(1):9–29. doi:10.3322/caac.21208.
- Craene BD, Berx G. Regulatory networks defining EMT during cancer initiation and progression. *Nat Rev Cancer*. 2013;13(2):97–110.
- Yang J, Weinberg RA. Epithelial–mesenchymal transition: at the crossroads of development and tumor metastasis. *Dev Cell*. 2008;14(6):818–29. doi:10.1016/j.devcel.2008.05.009.
- Iwatsuki M, Mimori K, Yokobori T, Ishi H, Beppu T, Nakamori S, et al. Epithelial–mesenchymal transition in cancer development and its clinical significance. *Cancer Sci*. 2010;101(2):293–9. doi:10.1111/j.1349-7006.2009.01419.x.
- Thiery JP, Acloque H, Huang RY, Nieto MA. Epithelial–mesenchymal transitions in development and disease. *Cell*. 2009;139(5):871–90. doi:10.1016/j.cell.2009.11.007.
- Hajo H, Wolfgang M. The regulatory and signaling functions of zinc ions in human cellular physiology. In: Cellular and molecular biology of metals. Boca Raton: CRC Press; 2010. p. 181–212.
- Wu W, Bromberg PA, Samet JM. Zinc ions as effectors of environmental oxidative lung injury. *Free Radic Biol Med*. 2013;65:57–69. doi:10.1016/j.freeradbiomed.2013.05.048.
- Nimmanon T, Taylor K. Zinc signaling and cancer. In: Fukuda T, Kambe T, editors. Zinc signals in cellular functions and disorders. Berlin: Springer; 2014. p. 285–313.
- Kollmeier H, Seemann J, Wittig P, Rothe G, Witting C. Zinc concentrations in human tissues. Liver zinc in carcinoma and severe liver disease. *Pathol Res Pract*. 1992;188(7):942–5. doi:10.1016/s0344-0338(11)80255-4.
- Wright EB, Dormandy TL. Liver zinc in carcinoma. *Nature*. 1972;237(5351):166.
- Margalioth EJ, Schenker JG, Chevion M. Copper and zinc levels in normal and malignant tissues. *Cancer*. 1983;52(5):868–72.
- Hogstrand C, Kille P, Ackland Margaret L, Hiscox S, Taylor Kathryn M. A mechanism for epithelial–mesenchymal transition and anoikis resistance in breast cancer triggered by zinc channel ZIP6 and STAT3 (signal transducer and activator of transcription 3). *Biochem J*. 2013;455(Pt 2):229–37. doi:10.1042/BJ20130483.
- Taylor KM, Hiscox S, Nicholson RI, Hogstrand C, Kille P. Protein kinase CK2 triggers cytosolic zinc signaling pathways by phosphorylation of zinc channel ZIP7. *Sci Signal*. 2012;5(210):11. doi:10.1126/scisignal.2002585.
- Kagara N, Tanaka N, Noguchi S, Hirano T. Zinc and its transporter ZIP10 are involved in invasive behavior of breast cancer cells. *Cancer Sci*. 2007;98(5):692–7. doi:10.1111/j.1349-7006.2007.00446.x.
- Wu W-S, Wu J-R. The role of ROS signaling in tumor progression. In: Wu W-S, Hu C-T, editors. Signal transduction in cancer metastasis. Cancer metastasis—biology and treatment. Berlin: Springer; 2010. p. 103–18.
- Wang Z, Li Y, Sarkar FH. Signaling mechanism(s) of reactive oxygen species in epithelial–mesenchymal transition reminiscent of cancer stem cells in tumor progression. *Curr Stem Cell Res Ther*. 2010;5(1):74–80.
- Wu W-S. The signaling mechanism of ROS in tumor progression. *Cancer Metastasis Rev*. 2006;25(4):695–705. doi:10.1007/s10555-006-9037-8.
- Rudolf E, Rudolf K, Cervinka M. Zinc induced apoptosis in HEP-2 cancer cells: the role of oxidative stress and mitochondria. *BioFactors*. 2005;23(2):107–20.
- Rudolf E. Depletion of ATP and oxidative stress underlie zinc-induced cell injury. *Acta Medica (Hradec Kralove)*. 2007;50(1):43–9.
- Noh KM, Koh JY. Induction and activation by zinc of NADPH oxidase in cultured cortical neurons and astrocytes. *J Neurosci*. 2000;20(23):RC111.
- Nieman MT, Prudoff RS, Johnson KR, Wheelock MJ. N-cadherin promotes motility in human breast cancer cells regardless of their E-cadherin expression. *J Cell Biol*. 1999;147(3):631–44.
- Wheelock MJ, Shintani Y, Maeda M, Fukumoto Y, Johnson KR. Cadherin switching. *J Cell Sci*. 2008;121(Pt 6):727–35. doi:10.1242/jcs.000455.
- Havel LS, Kline ER, Salgueiro AM, Marcus AI. Vimentin regulates lung cancer cell adhesion through a VAV2-Rac1 pathway to control focal adhesion kinase activity. *Oncogene*. 2015;34(15):1979–90. doi:10.1038/onc.2014.123.
- Mendez MG, Kojima S, Goldman RD. Vimentin induces changes in cell shape, motility, and adhesion during the epithelial to mesenchymal transition. *FASEB J*. 2010;24(6):1838–51. doi:10.1096/fj.09-151639.
- Hwang WL, Yang MH, Tsai ML, Lan HY, Su SH, Chang SC, et al. SNAIL regulates interleukin-8 expression, stem cell-like activity, and tumorigenicity of human colorectal carcinoma cells. *Gastroenterology*. 2011;141(1):279–91. doi:10.1053/j.gastro.2011.04.008.
- Voon DC, Wang H, Koo JK, Chai JH, Hor YT, Tan TZ, et al. EMT-induced stemness and tumorigenicity are fueled by the EGFR/Ras pathway. *PLoS One*. 2013;8(8):e70427. doi:10.1371/journal.pone.0070427.
- Zhou W, Lv R, Qi W, Wu D, Xu Y, Liu W, et al. Snail contributes to the maintenance of stem cell-like phenotype cells in human pancreatic cancer. *PLoS One*. 2014;9(1):e87409. doi:10.1371/journal.pone.0087409.
- Kimlin LC, Casagrande G, Virador VM. In vitro three-dimensional (3D) models in cancer research: an update. *Mol Carcinog*. 2013;52(3):167–82. doi:10.1002/mc.21844.
- Lansdown AB, Mirastschijski U, Stubbs N, Scanlon E, Agren MS. Zinc in wound healing: theoretical, experimental, and clinical aspects. *Wound Repair Regen*. 2007;15(1):2–16. doi:10.1111/j.1524-475X.2006.00179.x.
- Xie H, Holmes AL, Young JL, Qin Q, Joyce K, Pelsue SC, et al. Zinc chromate induces chromosome instability and DNA double strand breaks in human lung cells. *Toxicol Appl Pharmacol*. 2009;234(3):293–9. doi:10.1016/j.taap.2008.10.010.
- Demir E, Akca H, Kaya B, Burgucu D, Tokgun O, Turna F, et al. Zinc oxide nanoparticles: genotoxicity, interactions with UV-light and cell-transforming potential. *J Hazard Mater*. 2014;264:420–9. doi:10.1016/j.jhazmat.2013.11.043.
- Levenson CW, Somers RC. Nutritionally regulated biomarkers for breast cancer. *Nutr Rev*. 2008;66(3):163–6. doi:10.1111/j.1753-4887.2008.00020.x.
- Lin LC, Hsu SL, Wu CL, Hsueh CM. TGFbeta can stimulate the p38/Jbeta-catenin/PPARgamma signaling pathway to promote the EMT, invasion and migration of non-small cell lung cancer (H460 cells). *Clin Exp Metastasis*. 2014;31(8):881–95. doi:10.1007/s10585-014-9677-y.
- Winitthana T, Lawanprasert S, Chanvorachote P. Triclosan potentiates epithelial-to-mesenchymal transition in anoikis-resistant human lung cancer cells. *PLoS One*. 2014;9(10):e110851. doi:10.1371/journal.pone.0110851.
- Gomez-Casal R, Bhattacharya C, Ganesh N, Bailey L, Basse P, Gibson M, et al. Non-small cell lung cancer cells survived ionizing radiation treatment display cancer stem cell and epithelial–mesenchymal transition phenotypes. *Mol Cancer*. 2013;12(1):94. doi:10.1186/1476-4598-12-94.
- Kim IG, Kim SY, Choi SI, Lee JH, Kim KC, Cho EW. Fibulin-3-mediated inhibition of epithelial-to-mesenchymal transition and self-renewal of ALDH+ lung cancer stem cells through IGF1R signaling. *Oncogene*. 2014;33(30):3908–17. doi:10.1038/onc.2013.373.
- Fernando RI, Litzinger M, Trono R, Hamilton DH, Schlom J, Palena C. The T-box transcription factor Brachyury promotes epithelial–mesenchymal transition in human tumor cells. *J Clin Invest*. 2010;120(2):533–44. doi:10.1172/jci38379.

38. Yao W, Liu Y, Zhang Z, Li G, Xu X, Zou K, et al. ALX1 promotes migration and invasion of lung cancer cells through increasing snail expression. *Int J Clin Exp Pathol*. 2015;8(10):12129–39.
39. Chunchacha P, Sriuranpong V, Chanvorachote P. Epithelial–mesenchymal transition mediates anoikis resistance and enhances invasion in pleural effusion-derived human lung cancer cells. *Oncol Lett*. 2013;5(3):1043–7. doi:10.3892/ol.2013.1108.
40. Brandes RP. Role of NADPH oxidases in the control of vascular gene expression. *Antioxid Redox Signal*. 2003;5(6):803–11. doi:10.1089/152308603770380115.
41. Buetler TM, Krauskopf A, Ruegg UT. Role of superoxide as a signaling molecule. *Physiology*. 2004;19(3):120–3.
42. Yang JQ, Buettner GR, Domann FE, Li Q, Engelhardt JF, Weydert CD, et al. v-Ha-ras mitogenic signaling through superoxide and derived reactive oxygen species. *Mol Carcinog*. 2002;33(4):206–18.
43. Lopez-Lazaro M. Excessive superoxide anion generation plays a key role in carcinogenesis. *Int J Cancer*. 2007;120(6):1378–80. doi:10.1002/ijc.22493.
44. Banskota S, Regmi SC, Kim JA. NOX1 to NOX2 switch deactivates AMPK and induces invasive phenotype in colon cancer cells through overexpression of MMP-7. *Mol Cancer*. 2015;14:123. doi:10.1186/s12943-015-0379-0.
45. Suh Y-A, Arnold RS, Lassegue B, Shi J, Xu X, Sorescu D, et al. Cell transformation by the superoxide-generating oxidase Mox1. *Nature*. 1999;401(6748):79–82.
46. Safford SE, Oberley TD, Urano M, St Clair DK. Suppression of fibrosarcoma metastasis by elevated expression of manganese superoxide dismutase. *Cancer Res*. 1994;54(16):4261–5.
47. Lee SS, Tsai CH, Yu CC, Chang YC. Elevated snail expression mediates tumor progression in areca quid chewing-associated oral squamous cell carcinoma via reactive oxygen species. *PLoS One*. 2013;8(7):e67985. doi:10.1371/journal.pone.0067985.
48. Cichon MA, Radisky DC. ROS-induced epithelial-mesenchymal transition in mammary epithelial cells is mediated by NF- κ B-dependent activation of snail. *Oncotarget*. 2014;5(9):2827–38.
49. Aizenman E, Stout AK, Hartnett KA, Dineley KE, McLaughlin B, Reynolds LJ. Induction of neuronal apoptosis by thiol oxidation: putative role of intracellular zinc release. *J Neurochem*. 2000;75(5):1878–88.
50. Zhang Y, Wang H, Li J, Jimenez DA, Levitan ES, Aizenman E, et al. Peroxynitrite-induced neuronal apoptosis is mediated by intracellular zinc release and 12-lipoxygenase activation. *J Neurosci*. 2004;24(47):10616–27. doi:10.1523/jneurosci.2469-04.2004.
51. Kim MC, Cui FJ, Kim Y. Hydrogen peroxide promotes epithelial to mesenchymal transition and stemness in human malignant mesothelioma cells. *Asian Pac J Cancer Prev*. 2013;14(6):3625–30.
52. Cheng JC, Klausen C, Leung PC. Hydrogen peroxide mediates EGF-induced down-regulation of E-cadherin expression via p38 MAPK and snail in human ovarian cancer cells. *Mol Endocrinol*. 2010;24(8):1569–80. doi:10.1210/me.2010-0034.
53. Watanabe N, Forman HJ. Autooxidation of extracellular hydroquinones is a causative event for the cytotoxicity of menadione and DMNQ in A549-S cells. *Arch Biochem Biophys*. 2003;411(1):145–57.
54. Ishihara Y, Shiba D, Shimamoto N. Enhancement of DMNQ-induced hepatocyte toxicity by cytochrome P450 inhibition. *Toxicol Appl Pharmacol*. 2006;214(2):109–17. doi:10.1016/j.taap.2005.12.003.

Submit your next manuscript to BioMed Central
and we will help you at every step:

- We accept pre-submission inquiries
- Our selector tool helps you to find the most relevant journal
- We provide round the clock customer support
- Convenient online submission
- Thorough peer review
- Inclusion in PubMed and all major indexing services
- Maximum visibility for your research

Submit your manuscript at
www.biomedcentral.com/submit



Research Article

Ciprofloxacin Improves the Stemness of Human Dermal Papilla Cells

Chayanin Kiratipaiboon,¹ Parkpoom Tengamnuay,² and Pithi Chanvorachote^{3,4}

¹Pharmaceutical Technology (International) Program, Faculty of Pharmaceutical Sciences, Chulalongkorn University, Bangkok 10330, Thailand

²Department of Pharmaceutics and Industrial Pharmacy, Faculty of Pharmaceutical Sciences, Chulalongkorn University, Bangkok 10330, Thailand

³Department of Pharmacology and Physiology, Faculty of Pharmaceutical Sciences, Chulalongkorn University, Bangkok 10330, Thailand

⁴Cell-Based Drug and Health Product Development Research Unit, Faculty of Pharmaceutical Sciences, Chulalongkorn University, Bangkok 10330, Thailand

Correspondence should be addressed to Pithi Chanvorachote; pithi_chan@yahoo.com

Received 12 January 2015; Revised 18 March 2015; Accepted 19 March 2015

Academic Editor: Kenichi Tamama

Copyright © 2015 Chayanin Kiratipaiboon et al. This is an open access article distributed under the Creative Commons Attribution License, which permits unrestricted use, distribution, and reproduction in any medium, provided the original work is properly cited.

Improvement in the expansion method of adult stem cells may augment their use in regenerative therapy. Using human dermal papilla cell line as well as primary dermal papilla cells as model systems, the present study demonstrated that ciprofloxacin treatment could prevent the loss of stemness during culture. Clonogenicity and stem cell markers of dermal papilla cells were shown to gradually decrease in the culture in a time-dependent manner. Treatment of the cells with nontoxic concentrations of ciprofloxacin could maintain both stem cell morphology and clonogenicity, as well as all stem cells markers. We found that ciprofloxacin exerted its effect through ATP-dependent tyrosine kinase/glycogen synthase kinase 3β dependent mechanism which in turn upregulated β -catenin. Besides, ciprofloxacin was shown to induce epithelial-mesenchymal transition in DPCs as the transcription factors ZEB1 and Snail were significantly increased. Furthermore, the self-renewal proteins of Wnt/ β -catenin pathway, namely, Nanog and Oct-4 were significantly upregulated in the ciprofloxacin-treated cells. The effects of ciprofloxacin in preserving stem cell features were confirmed in the primary dermal papilla cells directly obtained from human hair follicles. Together, these results revealed a novel application of ciprofloxacin for stem cell maintenance and provided the underlying mechanisms that are responsible for the stemness in dermal papilla cells.

1. Introduction

Based on the fact that dermal papilla cells (DPCs) interaction with epithelial stem cells can induce generation of new hair follicles [1–3], the cell therapy using DPCs has emerged as a potentially new approach for hair transplantation [4, 5]. DPCs have been intensively investigated to possess many advantages for cell therapy approaches. However, many studies also demonstrated the loss of their stemness and inductive activity during the *in vitro* passages [4, 6–8].

The hair follicle is composed of epithelial and mesenchymal compartments. DPCs, the major cell population existing in the mesenchymal compartments, are located at the base

of the hair follicle and function as a signaling center in the hair follicle morphogenesis and growth cycle [9]. These cells instruct the epithelial stem cells through specific signals to proliferate and differentiate into multiple layers of the growing hair shaft [1–3]. Interestingly, DPCs have been characterized as multipotent stem cells and the stemness of such cells is tightly associated with the ability to induce hair follicle formation. With comprehensive knowledge of the stem cell biology, the evidence suggested that CD133, a protein marker of human stem cells, contributes to the hair inductive property of DPCs in transgenic mice [10, 11]. In addition, an ablation of stem cell-related transcription factors including Sox2 in DPCs leads to the impairment of the hair shaft

outgrowth [12]. Although the molecular features that regulate stemness as well as hair inductive function in these specialized DPCs are still largely unknown, the Wnt/ β -catenin signaling appears to lend strong support to hair follicle morphogenesis and regeneration [13–15]. Indeed, β -catenin was shown to regulate crucial signaling pathways in hair follicle formation in response to several stimuli, including fibroblast growth factor (FGF) and insulin-like growth factor (IGF) [13]. In transgenic mice model, the suppression of β -catenin in the DPCs resulted in the inhibition of hair follicle formation [13], as epithelial-mesenchymal transition (EMT) lately has been shown to play an important role in the stem cell behaviors and the activation of Wnt/ β -catenin signaling was shown to activate the transition of the epithelial cells toward mesenchymal stem cells. Together with the concept that transcription factors presenting in the cell undergoing EMT like Snail were found to be important for the accomplishment of stem cell functions [16–18], it is likely that these β -catenin and EMT could impact the stemness and stem cell activity in the DPCs.

Ciprofloxacin (CIP) has been used as an antibiotic prophylaxis for the prevention of bacterial infection in patients receiving stem cell transplant and in stem cell research [19, 20]. Also, this considerably safe drug is widely used in the treatment of certain infection in cell culture [21]. So far, the molecular basis of CIP on human cell biology has not been fully investigated, especially in the area of stem cell research. The present study therefore aimed to elucidate the possible role of CIP for its possible effect on the stemness of DPCs using human dermal papilla cell line and primary human dermal papilla cells as models.

2. Material and Methods

2.1. Cells and Reagents. Immortalized dermal papilla cells (DPCs) were obtained from Applied Biological Materials Inc. (Richmond, BC, Canada). The cells were cultured in Prigrow III medium (Richmond, BC, Canada) supplemented with 10% fetal bovine serum (FBS) and 100 units/mL of penicillin/streptomycin (Life technologies, MD, USA) at 37°C in a 5% CO₂ atmosphere. For primary human DPCs, they were obtained from PromoCell (Heidelberg, Germany). The cells were cultured in medium containing bovine pituitary extract 4 μ L/mL, fetal calf serum 0.05 mL/mL, basic fibroblast growth factor 1 ng/mL, recombinant human insulin 5 μ g/mL and phenol red 0.62 ng/mL from PromoCell (Heidelberg, Germany), and 100 units/mL of penicillin/streptomycin at 37°C in a 5% CO₂ atmosphere. Ciprofloxacin (CIP) and dimethylsulfoxide (DMSO) were purchased from Sigma (St. Louis, MO, USA). Hoechst 33342 and propidium iodide (PI) were obtained from Molecular Probes Inc. (Eugene, OR, USA). 3-(4,5-Dimethylthiazol-2-yl)-2,5-diphenyltetrazolium bromide (MTT) and Alexa Fluor 488/594 conjugated secondary antibody were from Invitrogen (Carlsbad, CA, USA). Rabbit monoclonal antibodies for integrin β 1, phosphorylated ATP-dependent tyrosine kinase (Akt, Ser 473), Akt, phosphorylated glycogen synthase kinase3 β (GSK3 β , Ser 9), GSK3 β , ZEB1, Nanog, Oct-4, Slug, Snail, Vimentin, N-cadherin, phosphorylated extracellular signal-regulated kinase (Erk),

Erk, β -actin, and peroxidase conjugated anti-rabbit IgG were obtained from Cell Signaling (Denver, MA, USA). Rabbit CD133 antibody was bought from Cell Applications Inc. (San Diego, CA, USA). Rabbit procollagen type I antibody, goat aldehyde dehydrogenase 1A1 antibody (ALDH1A1), and peroxidase conjugated anti-goat IgG were obtained from Santa Cruz Biotechnology Inc. (Dallas, Texas, USA). Immobilon Western Chemiluminescent HRP substrate was from Millipore Corp. (Billerica, MA) and Thermo Fisher Scientific Inc. (Rockford, IL).

2.2. Cell Viability Assay. MTT viability assay was used to evaluate cell viability. Cells were seeded at a density of 1×10^4 cells/well and cultivated for 12 h in 96-well plate. Afterward, the cells were incubated with various concentrations of CIP (0–10 μ g/mL) for 24 h. The cells were then incubated with 5 mg/mL MTT for 4 h at 37°C. Then, the supernatant was removed and replaced with 100 μ L of DMSO to dissolve the formazan crystal. The intensity of MTT product was measured at 570 nm using a microplate reader (Anthos, Durham, NC). Cell viability was calculated by the following formula and presented as a percentage to untreated control value

$$\text{Cell viability (\%)} = \frac{\text{A570 of treatment}}{\text{A570 of control}} \times 100. \quad (1)$$

2.3. Nuclear Staining Assay. Hoechst 33342 and PI costaining was used to detect apoptotic and necrosis cell death. Cells were seeded at a density of 1×10^4 cells/well and cultivated for 12 h. Subsequently, the cells were treated with various concentrations of CIP (0–10 μ g/mL) for further 24 h. After treatments, the cells were stained with 10 μ M of Hoechst and 5 μ g/mL of PI for 30 min at 37°C and visualized by fluorescence microscope (Olympus IX 51 with DP70, Olympus America Inc., Center valley, PA).

2.4. Cell Morphology and Aggregation Behavior Evaluation. DP cells were seeded at a density of 6×10^3 cells/well onto 24-well plate and incubated for 12 h. The cells were treated with various concentrations of CIP (0–10 μ g/mL) for 72 h, and cell morphology was observed at 0, 24, 48, and 72 h. The aggregation behavior of the cells was determined at 72 h. Morphology and aggregation behaviors of cells were photographed by a phase-contrast microscope (Olympus IX51 with DP70, Olympus America Inc., Center valley, PA).

2.5. Cell Cycle Analysis. Cells were seeded at a density of 3×10^4 cells/well onto 6-well plate and incubated overnight. The cells were cultured in the presence or absence of CIP (10 μ g/mL) for 72 h. After indicated treatment, the cells were incubated in the absence of growth factors for 24 h. The cells were then incubated with complete media for 12 h, trypsinized and fixed with 70% absolute ethanol at –20°C overnight. The cells were washed with cold PBS and incubated in PI solution containing 0.1% Triton-X, 1 μ g/mL RNase, and 1 mg/mL propidium iodide at 37°C for 30 min. The cells at the early passages (passages 2–3) without serum-starvation were used as an untreated control at 0 h. DNA in whole cells

was stained with PI, and cell cycle profile was analyzed using flow cytometry (FACSort, Becton Dickinson, Rutherford, NJ, USA).

2.6. Immunofluorescence. Cells were seeded at a density of 3×10^4 cells/well onto coverslips in 6-well plate and incubated overnight. The cells were cultured in the presence or absence of ciprofloxacin ($10 \mu\text{g}/\text{mL}$) for 72 h. The cells at the early passages were used as an untreated control at 0 h. The coverslips were fixed with 4% paraformaldehyde for 20 min and permeabilized with 0.1% Triton-X for 10 min at room temperature. Thereafter, the coverslips were incubated with 3% bovine serum albumin (BSA) for 30 min at room temperature to prevent nonspecific binding. The coverslips were washed and incubated with CD133 or procollagen type I rabbit monoclonal antibodies at 1:100 dilution overnight at 4°C . After primary antibody incubation, the coverslips were washed with PBS and subsequently incubated with Alexa Fluor 488 or 594 conjugated secondary antibodies for 1 h at room temperature. Samples were examined with Confocal Laser Scanning Microscopy (Zeiss LSM 510) to analyze expression of CD133 and procollagen type I.

2.7. Western Blot Analysis. Cells were seeded at a density of 5×10^4 cells/well onto 6-well plate for 12 h and cultured in the presence of various concentrations of CIP (2.5 – $10 \mu\text{g}/\text{mL}$) for 72 h. After washing the cells with PBS, cell lysates were prepared by incubating the cells in ice-cold lysis buffer containing 20 mM Tris-HCl (pH 7.5), 0.5% Triton X, 10% glycerol, 150 mM sodium chloride, 50 mM sodium fluoride, 1 mM sodium orthovanadate, 1 mM phenylmethylsulfonyl fluoride, and commercial protease inhibitor cocktail (Roche Molecular Biochemicals) for 45 min on ice. Subsequently, cell lysates were collected and determined for protein content by the Bradford method (Bio-Rad, Hercules, CA). Equal amounts of proteins of each sample ($50 \mu\text{g}$) were boiled in Laemmli loading buffer at 95°C for 5 min. The proteins were subsequently loaded on 10% SDS-polyacrylamide electrophoresis. After separation, proteins were transferred onto $0.45 \mu\text{m}$ nitrocellulose membranes (Bio-Rad). Following blocking with 5% nonfat milk in TBST [25 mM Tris-HCl (pH 7.5), 0.05% Tween-20, and 125 mM NaCl] for 2 h, membranes were then incubated with appropriate primary antibodies for 10 h at 4°C . Membranes were washed three times with TBST for 15 min and incubated with horseradish peroxidase-coupled secondary antibodies for 1 h at room temperature. The immune complexes were detected with Chemiluminescence substrate (SuperSignal West Pico, Pierce, Rockford, IL) and quantified using analyst/PC densitometry software (Bio-Rad).

2.8. Statistical Analysis. Data were obtained from at least four independent experiments and presented as means \pm standard deviation (SD). Statistical analysis was performed using one-way ANOVA with post hoc test at a significance level (α) of 0.05. These analyses were performed using SPSS Version 19 (SPSS Inc., Chicago, IL).

3. Results

3.1. Effect of CIP on Viability of DPCs. To study the role of CIP on the stem cell property of DPCs, we first characterized cell viability and cell death response to CIP treatment in DPCs using MTT and Hoechst 33342/propidium iodide (PI) costaining assays. Treatment of the cells with CIP at the concentrations of 0 – $10 \mu\text{g}/\text{mL}$ for 24 h caused no significant change in cell viability compared with control levels (Figure 1(a)). Consistent with the Hoechst/PI apoptosis assay, our results indicated that the treatment drug at such concentrations caused neither apoptosis nor necrosis detected by Hoechst and PI, respectively (Figure 1(b)). This information may help to clarify that the following effects of CIP on DPCs were not a consequence of cytotoxic effect or cell stress.

3.2. CIP Maintains Stem Cell-Like Characteristics in DPCs. DPCs have been reported to function as multipotent stem cells and the stemness of DPCs was linked to their ability to induce hair follicles [10–12]. However, DPCs lose their hair follicle inductive ability during culture [4, 6–8]. We found that, after culturing the DPCs for 5 days, the shape and appearance of DPCs are spontaneously altered toward fibroblast-like morphology. The primitive DPCs usually appearing as spindle-shaped cells changed to flat multipolar cells with elongated shapes (Figure 2(a)). Besides, the DPCs at the beginning showed an aggregative growth pattern in culture and such pattern was lost during the extended time of culturing. In order to test whether CIP affects the change in morphology of these DPCs, the cells were treated with CIP at the concentrations of 0 – $10 \mu\text{g}/\text{mL}$ for 0 – 72 h, and morphology of the cells as well as aggregative pattern was determined. Figure 2(a) shows that most of untreated control cells exhibited fibroblast-like morphology at 48 and 72 h. Meanwhile, the morphology of CIP treated cells remained unaltered (Figure 2(a)). Because the hair follicle inductive property of the DPCs has been shown to relate with their aggregate behaviors [22], we further investigated the effect of CIP treatments on the aggregative growth pattern of the cells. The DPCs at early passages (passages 2–3) were cultured in the presence or absence of CIP for 72 h and the aggregate size and number were determined. Figures 2(b), 2(c), and 2(d) show that CIP at the concentration of 5 and $10 \mu\text{g}/\text{mL}$ significantly increased the size as well as the number of cell aggregation in comparison to those of untreated control at 72 h.

As mesenchymal cells have been shown to be slow-cycling cells, we next investigated the effect of CIP on the proliferation and the cell cycle distribution of DPCs. The DPCs were cultured in the presence or absence of CIP for 72 h and subjected to cell cycle evaluation. The cells were incubated in the absence of growth factors for 24 h. Then, the cells were incubated with complete media for 12 h and the cell cycle progression was analyzed by PI and flow cytometer. Also, the DPCs at the early passages without serum-starvation were used as a control. Figures 2(e) and 2(f) show that, at 12 h after the cells receive growth factors, the untreated control cells at 72 h proceeded to M phase of the cell cycle. Importantly, treatment of the cells with $10 \mu\text{g}/\text{mL}$ CIP attenuated the cell cycle progression as the cells cannot enter

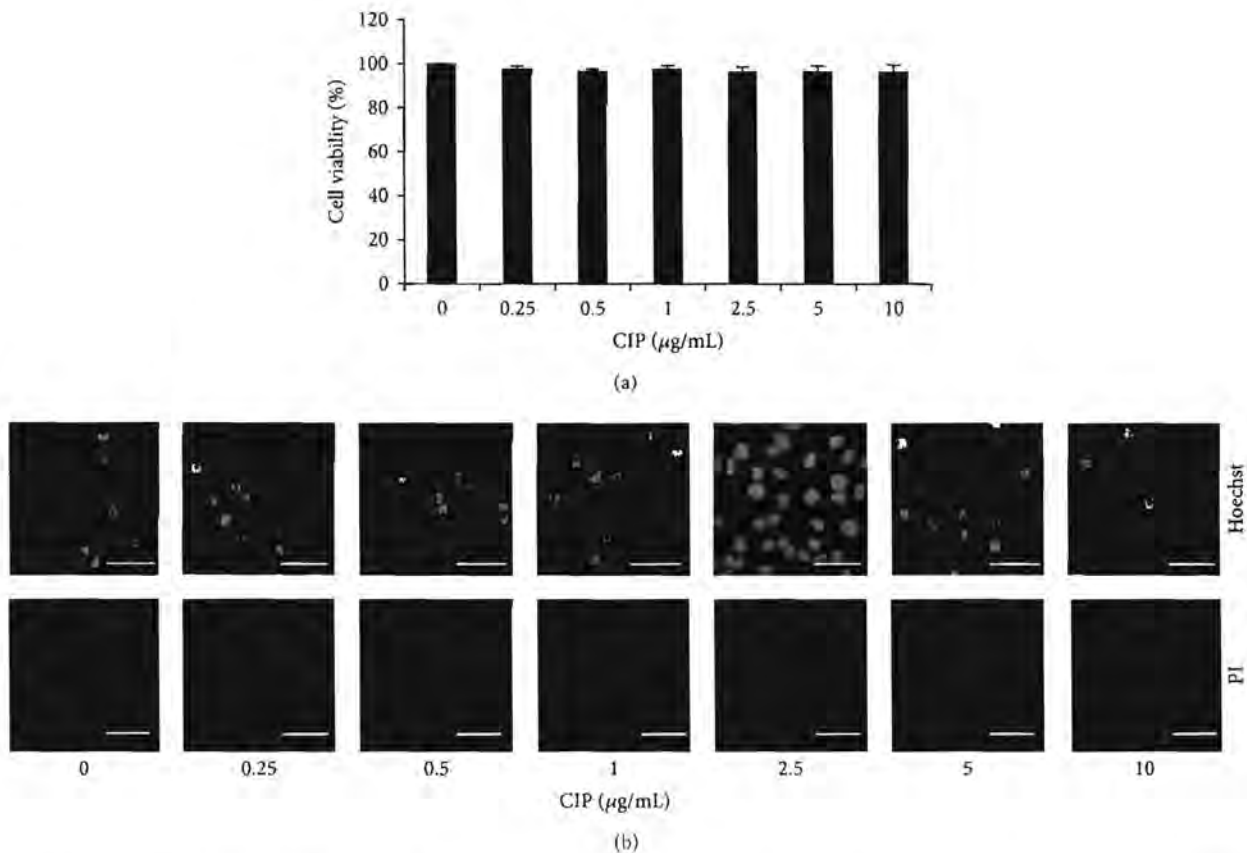


FIGURE 1: Cytotoxicity of CIP on DPCs. (a) Cells were treated with CIP (0–10 $\mu\text{g/mL}$) for 24 h. Cytotoxicity was determined by MTT assay. (b) After indicated treatment for 24 h, mode of cell death was examined by Hoechst 33342/PI costaining assay. Scale bar is 100 μm . The data represent the means of four independent samples \pm SD.

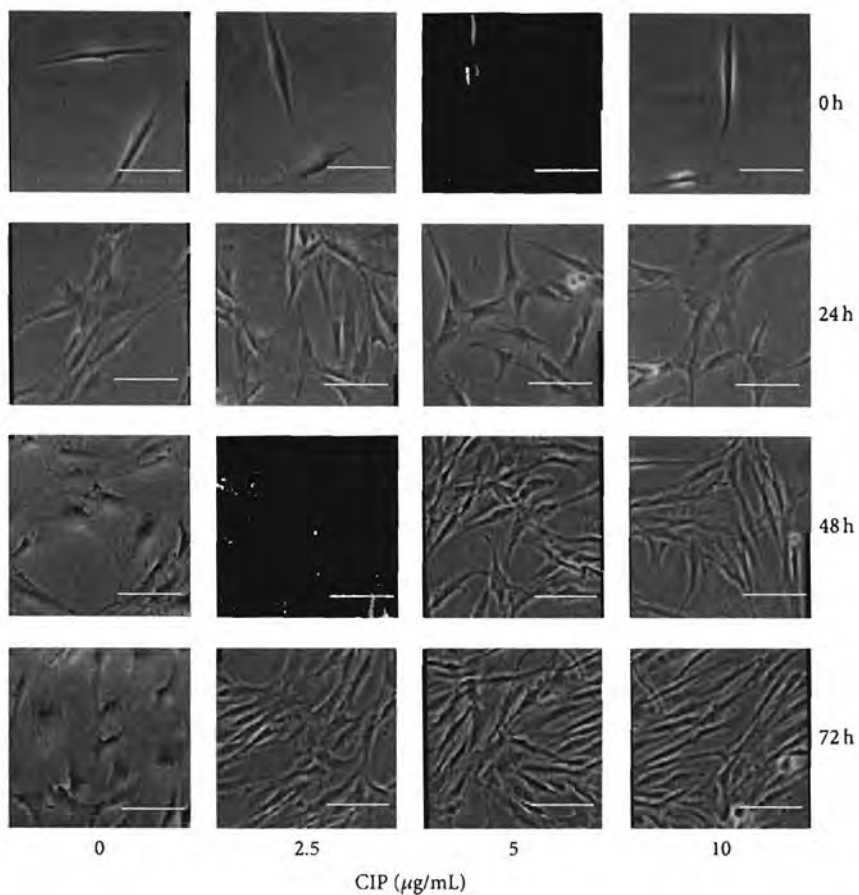
to M phase. Further, the cell cycle distribution was quantified as described in Section 2.5. The results confirmed the above findings that the treatment of the cells with CIP significantly decreased the cell population in G2/M phase (Figures 2(e) and 2(f)).

3.3. CIP Prevents the Downregulation of Stem Cell Markers in DPCs. Having shown that culture of the DPCs caused the spontaneous decline of stem cell-like phenotypes, we next clarify the mentioned conception by detecting stem cell markers in such cells. Because the CD133 and procollagen type I expressions have been recognized as the dermal papilla cell and fibroblast indicators, respectively [11, 23, 24], we analyzed the expression of such proteins in the DPCs treated with CIP at the concentrations of 10 $\mu\text{g/mL}$ for 72 h and the control cells. Immunocytochemistry showed that the expression of CD133 with CIP was suppressed in the DPCs cells after being cultivated for 72 h in comparison to that of control cells (DPCs at the early passages at 0 h, Figure 3(a)). Treatment of the cells with CIP could dramatically prevent such a loss of CD133 expression in the cells (Figure 3(a)). These results suggested that CIP preserve the stemness of DPCs during culture. Also, the expression level of fibroblast marker procollagen type I was significantly increased in

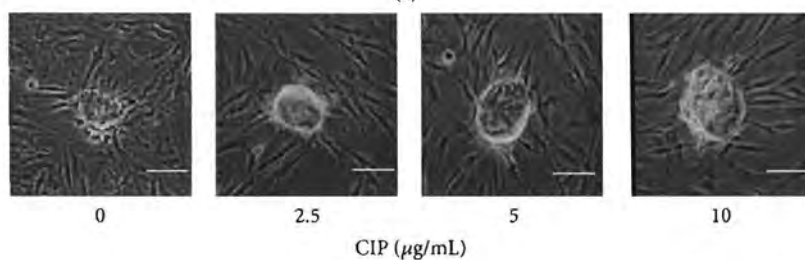
the untreated DPCs cells at 72 h, whereas the increase in fibroblast marker could be prevented by CIP at the concentration of 10 $\mu\text{g/mL}$ (Figure 3(a)).

We further exploited the information to show that CIP prevents the loss of stemness in cultured DPCs. By utilizing CD133, integrin $\beta 1$, and ALDH1A1 as dermal papilla markers and procollagen type I as a fibroblast marker, the cells cultured in the presence or absence of CIP were analyzed for the proteins by western blot analysis. Figure 3(b) shows that the expression of procollagen type I was upregulated in a time-dependent manner, whereas treatment with CIP could prevent the increase of such a protein. As expected, all mesenchymal related proteins including CD133, integrin $\beta 1$, and ALDH1A1 were gradually decreased in the untreated control cells in a time-dependent fashion and treatment of the cells with CIP inhibited the reduction of the protein markers (Figure 3(b)). We also performed the dose-dependent experiment to assure the effect of the drug on DPCs stemness. The results indicated that CIP increased the stem cell markers in these cells while it decreased fibroblast marker in a dose-dependent manner (Figure 3(c)).

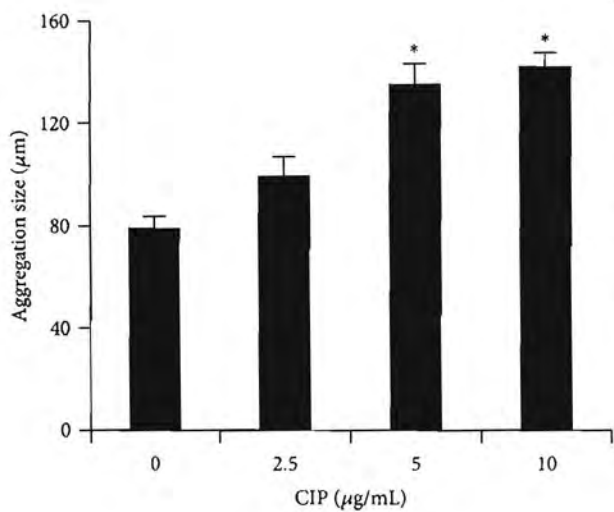
3.4. CIP Activates Wnt/ β -Catenin Signaling and Epithelial-Mesenchymal Transition (EMT) in DPCs. Activation of



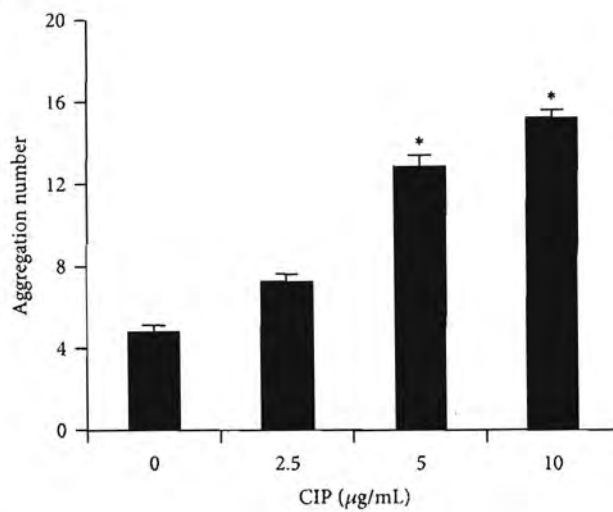
(a)



(b)



(c)



(d)

FIGURE 2: Continued.

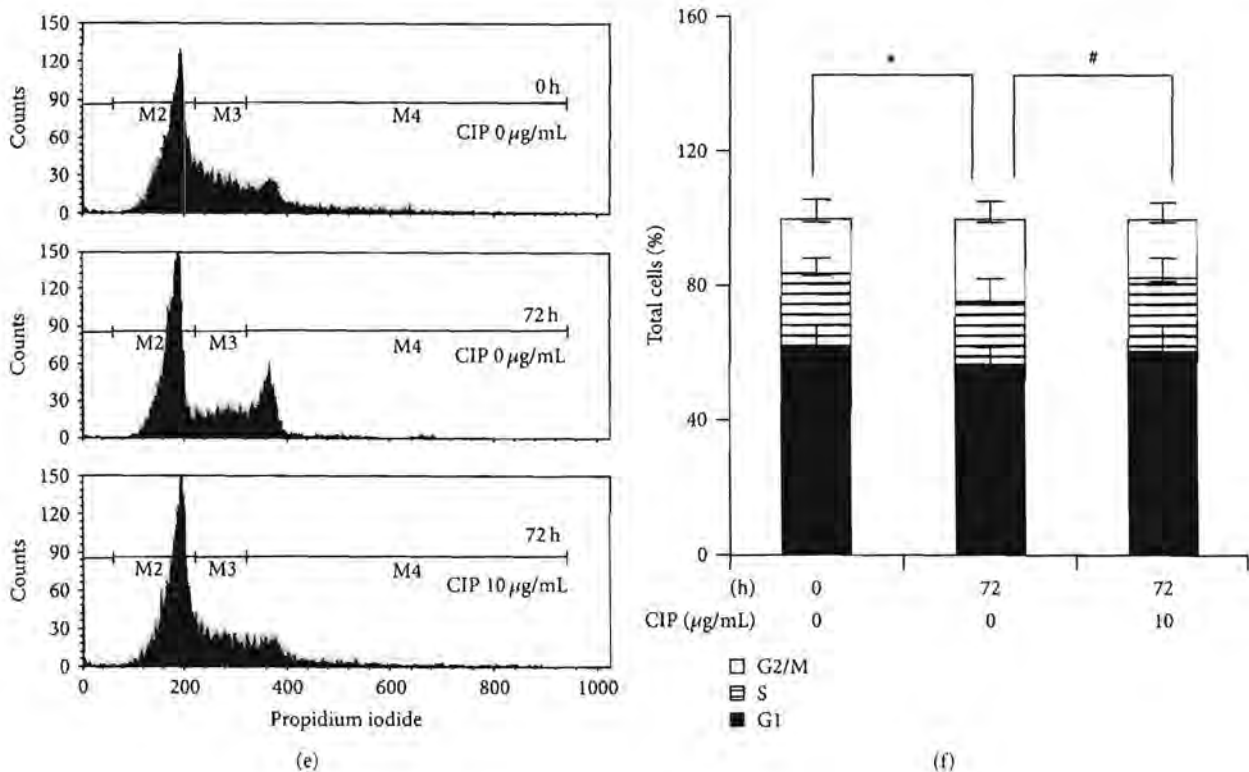
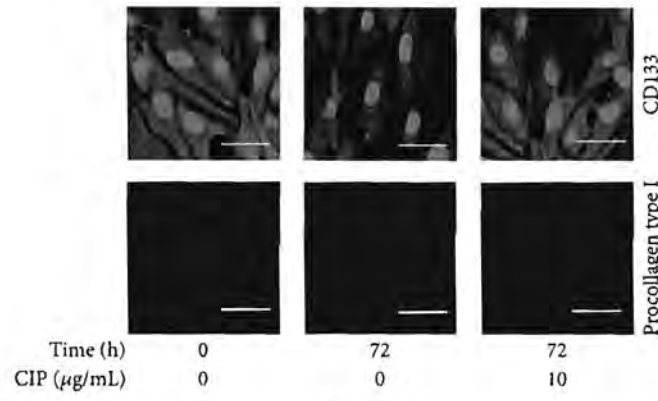


FIGURE 2: Effects of CIP on stem cell-like characteristics in DPCs. (a) Cells were treated with CIP (0–10 µg/mL) for various times (0–72 h). After indicated treatment, morphology of DPCs was observed. Scale bar is 100 µm. (b) Aggregation behavior of cells was determined after indicated treatment for 72 h. Scale bar is 100 µm. ((c)-(d)) Aggregation size and aggregation number were determined by image analyzer. The data represent the means of four independent samples ± SD. **P* < 0.05 versus untreated control. ((e)-(f)) Cells were cultured in the presence or absence of CIP (10 µg/mL) for 72 h and serum-starved for 24 h. After serum-starvation, cells were incubated with complete media for 12 h. The cells at the early passages (passages 2–3) without serum-starvation were also used as an untreated control at 0 h. Cell cycle distribution was determined by PI staining and flow cytometry. The data represent the means of four independent samples ± SD. **P* < 0.05 versus untreated control at 0 h; #*P* < 0.05 versus untreated control at 72 h.

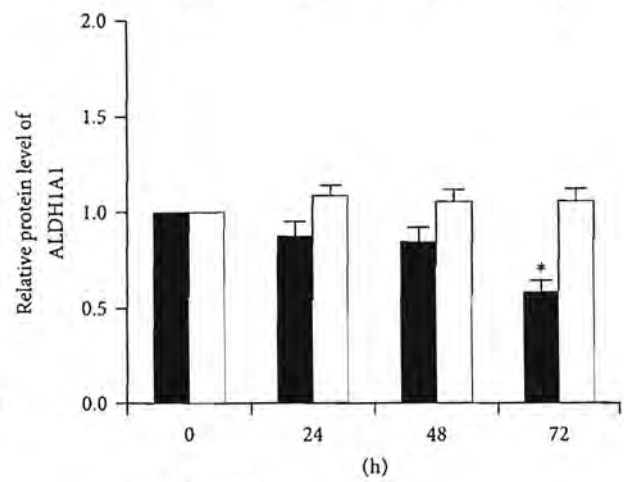
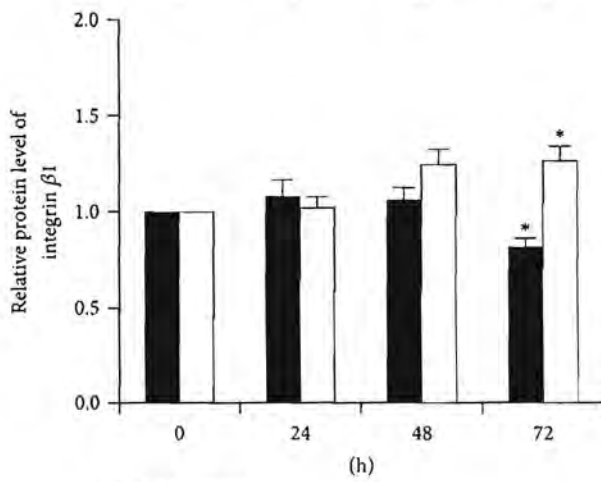
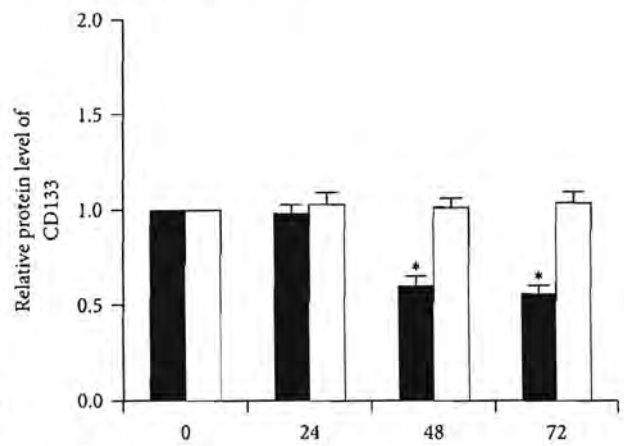
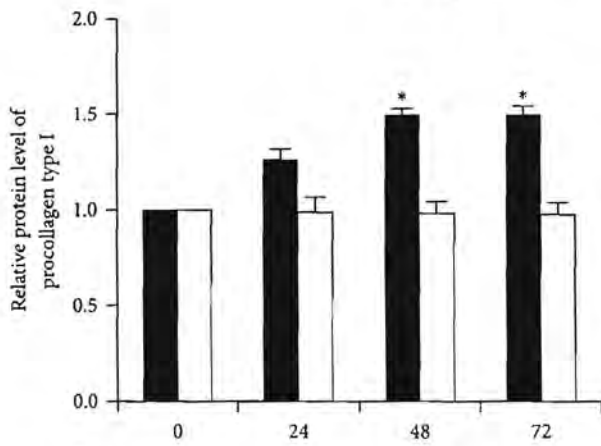
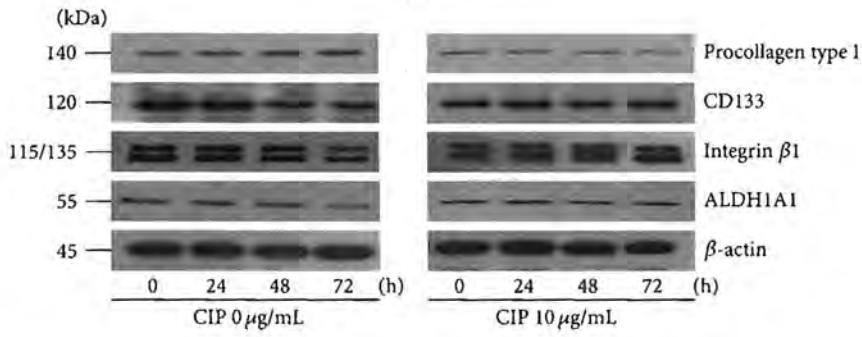
Wnt/ β -catenin signaling was shown to play a critical role in stem cell maintenance [25–27] and hair regeneration [13–15]. In addition, the hair follicle inductive effect in cultured DPCs could be prolonged by exposing the cells to Wnt/ β -catenin activator [14, 15]. Based on these data, it is promising that CIP may exert its positive role in stemness in DPCs through this pathway. The signaling proteins related to Wnt/ β -catenin including activated Akt (phosphorylated Akt at Ser 473), total Akt, inactivated glycogen synthase kinase3 β (phosphorylated GSK3 β at Ser 9), parental GSK3 β , and β -catenin were determined by western blot analysis.

The results showed that activated Akt was significantly enhanced by treatment of the cells with CIP at 2.5–10 µg/mL in a dose-dependent manner (Figure 4(a)). Consequently, the downstream GSK3 β was inactivated by the treatment of CIP as indicated by an increase in phosphorylated GSK3 β (Figure 4(a)). As GSK3 β was shown to inhibit the degradation process of β -catenin, we found corresponding results that phosphorylated GSK3 β leads to an increase of cellular β -catenin in CIP treated DPCs (Figure 4(a)). These data suggested that CIP maintains stemness in DPCs at least in part by increased cellular β -catenin via Akt/GSK3 β pathway.

Recently, the process of the cell transition from epithelial-mesenchymal phenotypes (EMT) has garnered increased attention in cell biology as it is linked with the stem cell-like properties in various cells [16–18]. Furthermore, the transcription factors upregulated during EMT like Snail were shown to maintain the stem cell-like phenotypes in many cells [16–18]. In order to clarify whether this EMT plays a part in stem cell maintenance of CIP, the EMT-activating transcription factors including ZEB1, Slug, and Snail were determined in the CIP treated cells by western blotting. After incubation with CIP for 72 h, the cellular levels of ZEB1 and Snail were significantly upregulated; however, we found only minimal change in case of Slug (Figure 4(b)). Moreover, we have determined the levels of downstream gene targets of Snail including N-cadherin and vimentin [28, 29]. The results indicated that such proteins are significantly upregulated in the CIP-treated cells (Figure 4(c)). It is worth noting herein that p-Erk (Thr 202/Tyr 204), an activation downstream target of Snail [30], was also found to be increased in CIP-treated cells. Taken together, our results revealed the novel molecular mechanism by which CIP mediates the stem cell-like phenotypes in the DPCs through β -catenin and EMT.



(a)

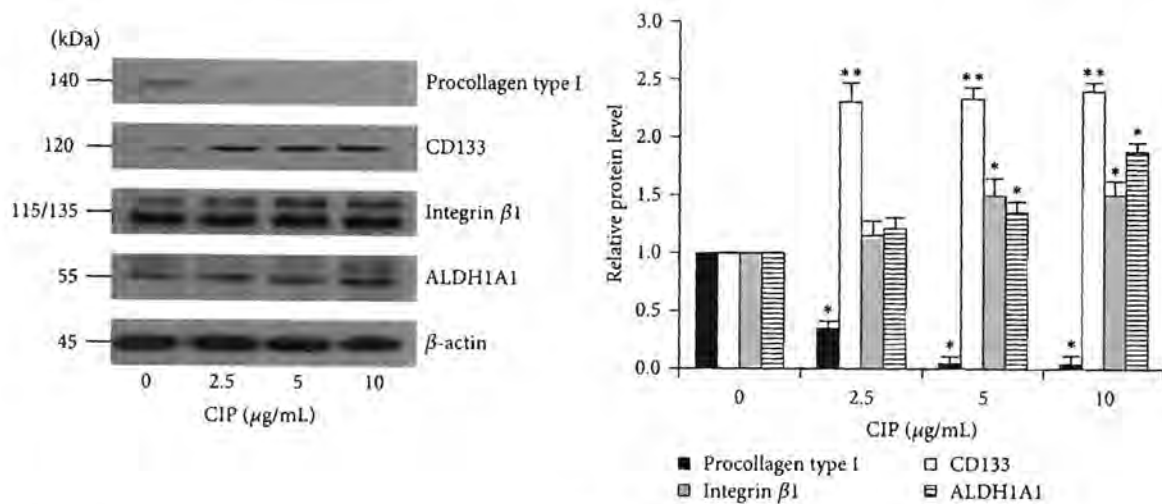


■ CIP 0 $\mu\text{g/mL}$
□ CIP 10 $\mu\text{g/mL}$

■ CIP 0 $\mu\text{g/mL}$
□ CIP 10 $\mu\text{g/mL}$

(b)

FIGURE 3: Continued.



(c)

FIGURE 3: Effects of CIP on stem cell markers in DPCs. (a) Cells were cultured in the presence or absence of CIP (10 μ g/mL) for 72 h. The cells at the early passages were used as an untreated control at 0 h. Expression of CD133 and procollagen type I were analyzed by immunofluorescence staining. Scale bar is 50 μ m. (b) Time-dependent effects of CIP treatment on the expression of stem cell markers were determined. Cells were cultured in the presence or absence of CIP (10 μ g/mL) for 0–72 h. The levels of procollagen type I, CD133, integrin β 1, and ALDH1A1 were determined by western blot analysis. Blots were reprobed with β -actin to confirm equal loading. The immunoblot signals were quantified by densitometry and the mean data from independent experiments were normalized to the results. The data represent the means of four independent samples \pm SD. * P < 0.05 versus untreated control at 0 h. (c) Cells were treated with CIP (0–10 μ g/mL) for 72 h. After indicated treatment, levels of procollagen type I, CD133, integrin β 1, and ALDH1A1 were analyzed by western blot. β -actin was served as the loading control. The immunoblot signals were quantified by densitometry and the mean data from independent experiments were normalized to the results. The data represent the means of four independent samples \pm SD. * P < 0.05 and ** P < 0.01 versus untreated control.

3.5. CIP Increases the Self-Renewal Transcription Factors in DPCs. Self-renewal is an important signature of stem cells [31–33]. To provide supportive data on the effects of CIP on DPCs stemness, critical transcription factors that maintain pluripotency and self-renewal in stem cells, including Nanog and Oct-4, were determined [34, 35]. After treatment of the cells with 5 and 10 μ g/mL of CIP (Figure 4(b)), the cells exhibited dramatic increases of Nanog and Oct-4 in a dose-dependent manner, suggesting that the treatments induced the self-renewal machinery in these cells.

3.6. CIP Maintains the Stem Cell-Like Phenotypes of Primary Human DPCs. To determine the extent to which primary human DPCs will respond to the CIP treatment by the same manner, we treated the isolated human DPCs with 0–10 μ g/mL CIP and evaluated stem cell characteristics, accordingly. Figures 5(a) and 5(b) indicate that treatment of the cells with 0–10 μ g/mL CIP caused no direct cytotoxicity in these cells. We next tested the signature characteristics of stem cells to assess whether CIP sustained the stemness in these primary cells. The cells were cultured in the presence or absence of CIP for 72 h and the expression of stem cells as well as fibroblast markers was determined as described previously. Western blot analysis revealed that the levels of CD133, integrin β 1, and ALDH1A1 were significantly increased in response to CIP treatment in a dose-dependent manner, whereas the expression of procollagen type I was significantly suppressed (Figure 5(c)). Furthermore, the Wnt/ β -catenin

and EMT were evaluated by western blotting. Figure 5(d) shows that treatment of the cells with CIP significantly increased the level of activated Akt level, inactivated GSK3 β , and β -catenin. Besides, the EMT transcription factors ZEB1 and Snail were found to be upregulated in response to the treatment (Figure 5(e)). Taken together, these data supported our earlier findings that CIP maintains the stemness of DPCs via β -catenin and EMT.

4. Discussion

DPCs have been shown to exhibit phenotypic plasticity by differentiating to different cell types [36]. Interestingly, multipotency of DPCs is accepted to be an important factor determining an ability to induce hair follicle formation [10–12]. Although advancement in research facilitates the culture of these specialized cells, previous study has shown that the hair inducing property of DPCs is gradually declined during culture [4, 6, 7]. In an attempt to evaluate the possible ways to maintain the DPCs signature *in vitro*, we have discovered for the first time that CIP was able to prevent the loss of DPCs stemness during culture. Treatment of the DPCs with nontoxic concentration of CIP prevented the spontaneous alteration of cell morphology toward fibroblast-like cells (Figure 2(a)). Also, our immunocytochemistry as well as protein analysis revealed that the cultured DPCs decreased the stem cell markers, and that could be prevented by an addition of CIP (Figures 3(a) and 3(b)). In addition, we found

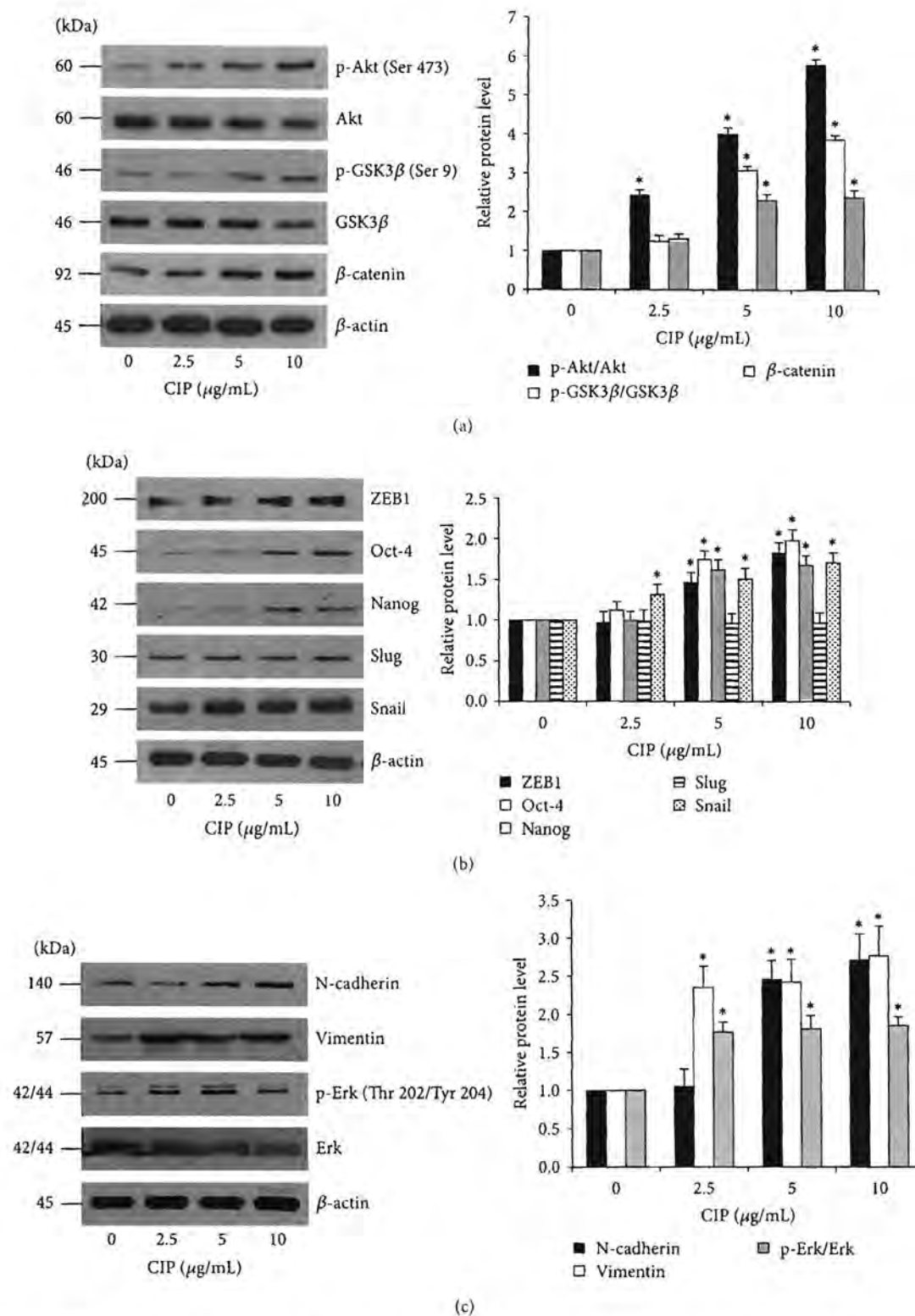
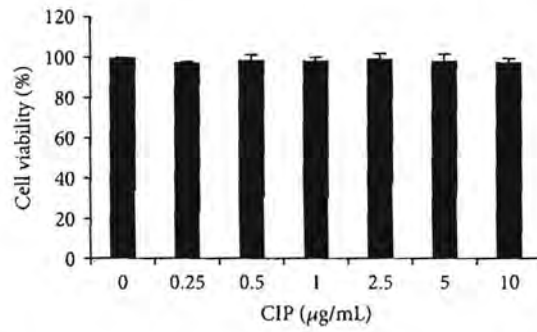
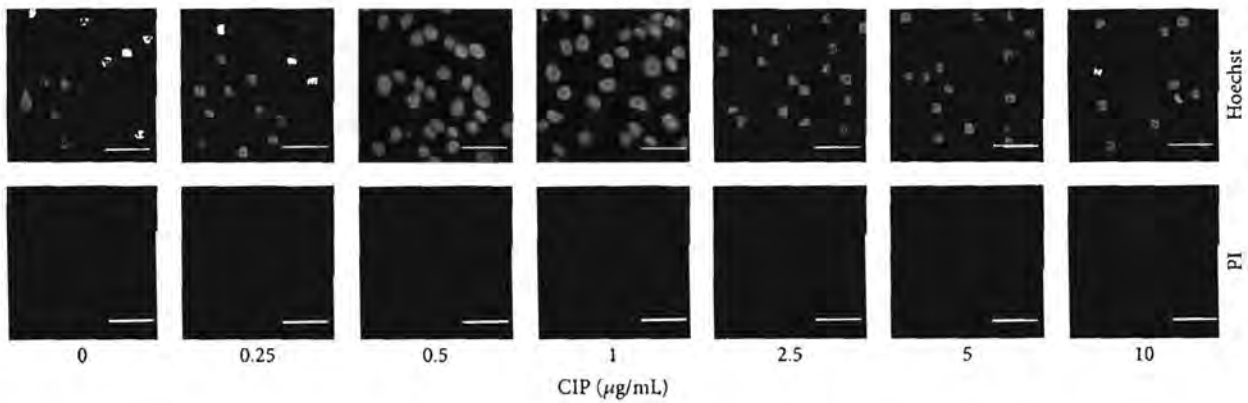


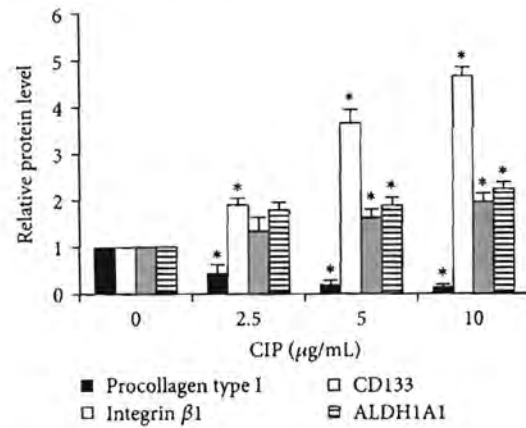
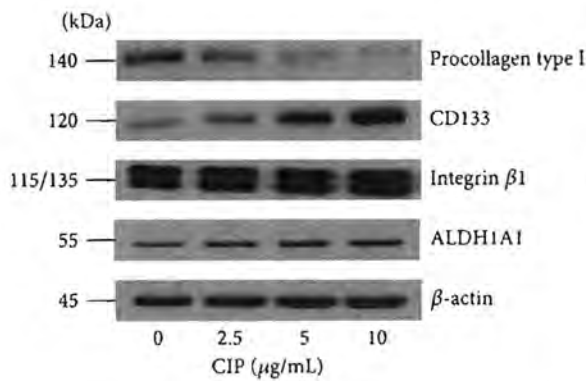
FIGURE 4: Effects of CIP on Wnt/β-catenin signaling, EMT, and self-renewal transcription factors in DPCs. (a) Cells were treated with CIP (1–10 μg/mL) for 72 h. After indicated treatment, the levels of Wnt/β-catenin signaling (Akt, p-Akt (Ser 473), GSK3β, p-GSK3β (Ser 9), and β-catenin) were analyzed by western blot analysis. The immunoblot signals were quantified by densitometry and mean data from independent experiments were normalized to the results. (b) EMT and self-renewal transcription factors (ZEB1, Oct-4, Nanog, Slug, and Snail) were determined by western blot analysis. (c) Downstream targets of Snail including N-cadherin, vimentin, total Erk, and p-Erk (Thr 202/Tyr 204) were analyzed by western blot analysis. β-actin was used as the loading control. The western blot signals were quantified by densitometry and mean data from independent experiments were normalized to the results. The data represent the means of four independent samples ± SD. **P* < 0.05 versus untreated control.



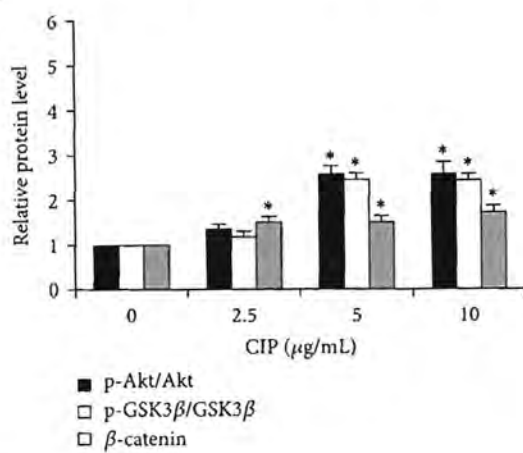
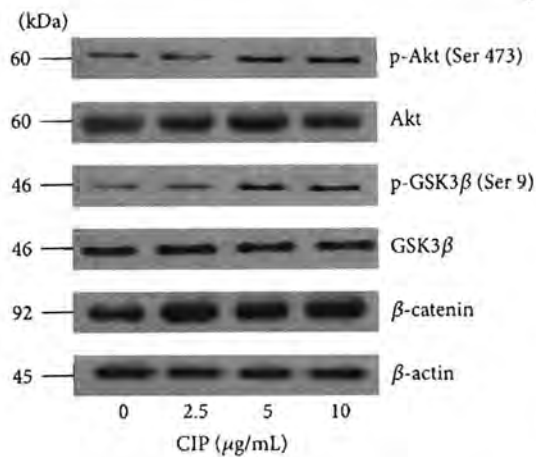
(a)



(b)



(c)



(d)

FIGURE 5: Continued.

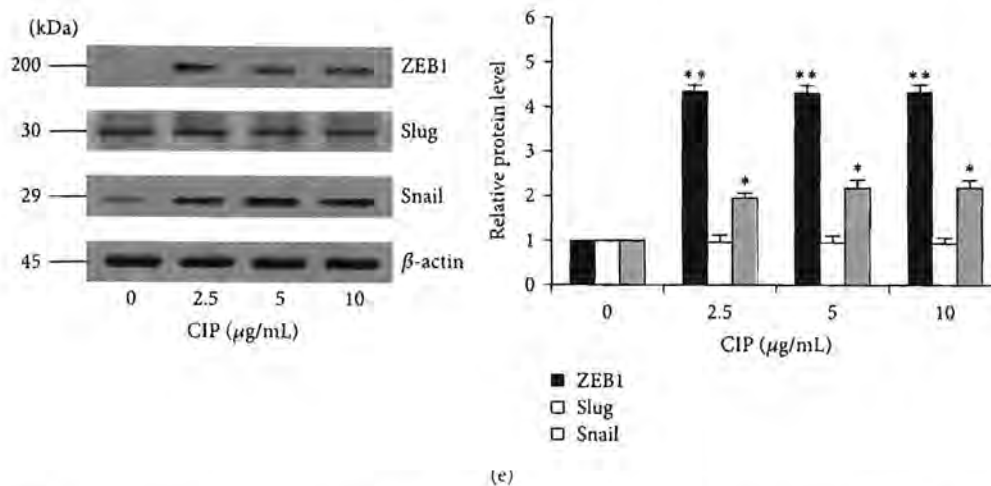


FIGURE 5: Effects of CIP on stem cell-like phenotypes in primary human DPCs. (a) Cells were treated with CIP (0–10 μ g/mL) for 24 h. Cytotoxicity was determined by MTT assay. The data represent the means of four independent triplicate samples \pm SD. (b) After indicated treatment, mode of cell death was examined by Hoechst 33342/PI costaining assay. Scale bar is 100 μ m. ((c)–(e)) Cells were treated with CIP (0–10 μ g/mL) for 72 h. After indicated treatment, the levels of stem cell markers (procollagen type I, CD133, integrin β 1, and ALDH1A1), Wnt/ β -catenin signaling (Akt, p-Akt, GSK3 β , p-GSK3 β , and β -catenin), and EMT transcription factors (ZEB1, Slug, and Snail) were determined by western blot analysis, respectively. β -actin was served as the loading control. The immunoblot signals were quantified by densitometry and mean data from independent experiments were normalized to the results. The data represent the means of four independent samples \pm SD. * $P < 0.05$ and ** $P < 0.01$ versus untreated control.

the increase of procollagen type I in the DPCs, suggesting that the DPCs can instinctively differentiate to fibroblast-like cells (Figure 3(b)). This observation is in agreement with the previous reports indicating that DPCs differentiate toward fibroblast-like cells [23, 24].

Regarding stem cell research, CD133, a transmembrane glycoprotein, has been widely used as a standard biomarker of stem cells [37]. We found that DPCs at the early passages exhibited high level of CD133; however, the expression of this protein was found to decline in a time-dependent manner during the time of cultivation, indicating that the cells have lost their stemness. Together with other stem cell markers, CIP was shown to sustain stemness of DPCs as indicated by the steady level of CD133, ALDH1A, and integrin β 1 (Figure 3(b)). Besides, the presence of ALDH1A, a detoxifying enzyme highly expressed in stem cells, was shown to regulate stem cell function [38]. Thus the increase of the proteins in response to CIP treatment could support our finding that CIP maintains the stemness of the cells.

In the past decade, considerable progress has been obtained in elucidating stem cell signaling pathways, in particular Wnt/ β -catenin that is critical for maintaining stem cell features as well as function [25–27]. Previously, studies reported that an ablation of β -catenin in DPCs causes the suppression of hair growth and regeneration [13]. The β -catenin functions as a cotranscription factor of T-cell factor/lymphoid enhancing factor (TCF/LEF) and consequently regulates expression of proteins facilitating stem cell functions [39]. The cellular level of β -catenin is tightly controlled by GSK3 β . The phosphorylation of β -catenin by the function of GSK3 β resulted in ubiquitination and proteasomal

degradation of β -catenin. The activated Akt is shown to inhibit such a function of GSK3 β by phosphorylating the GSK3 β at serine 9 [39]. Therefore, the activation of Akt increases cellular level of β -catenin. As a consequence, β -catenin accumulates in cytoplasm and translocates into nucleus leading to stimulation of target genes. Here, we showed that the levels of activated Akt and inactivated GSK3 β were upregulated consistently with the increase of β -catenin in CIP treated cells (Figures 4(a) and 5(d)). These results suggested that the stemness sustaining effect of CIP is due to the activation of Akt/ β -catenin pathway.

Indeed, the DPCs require stemness in terms of molecular signals rather than pluripotency for the production of cytokines and growth factors functioning in the keratinocyte recruitment and proliferation. In this regard, activation of Wnt/ β -catenin signaling was shown to induce hair follicle formation and hair growth through stem cell signals that drive cytokine synthesis [7, 13, 40, 41]. For the focus points of this study, the upregulation of stemness signals including β -catenin, Nanog, Oct4, Slug, and Snail described the mechanism of ciprofloxacin in driving the DPCs to functioning in enhancing the growth of hair (Figures 4 and 5).

Recent evidences have suggested that β -catenin interacts with many signaling pathways involved in pluripotency and EMT [25–27, 35, 42]. Furthermore, Wnt/ β -catenin signaling activation was shown to increase the expression of EMT proteins and pluripotent activating transcription factors [43–47]. Consistent with previous reports that the transcription factors Snail and ZEB1 play an important role in EMT process [16, 18], we found significant increase of such proteins in the DPCs treated with CIP (Figures 4(b) and 5(e)), and

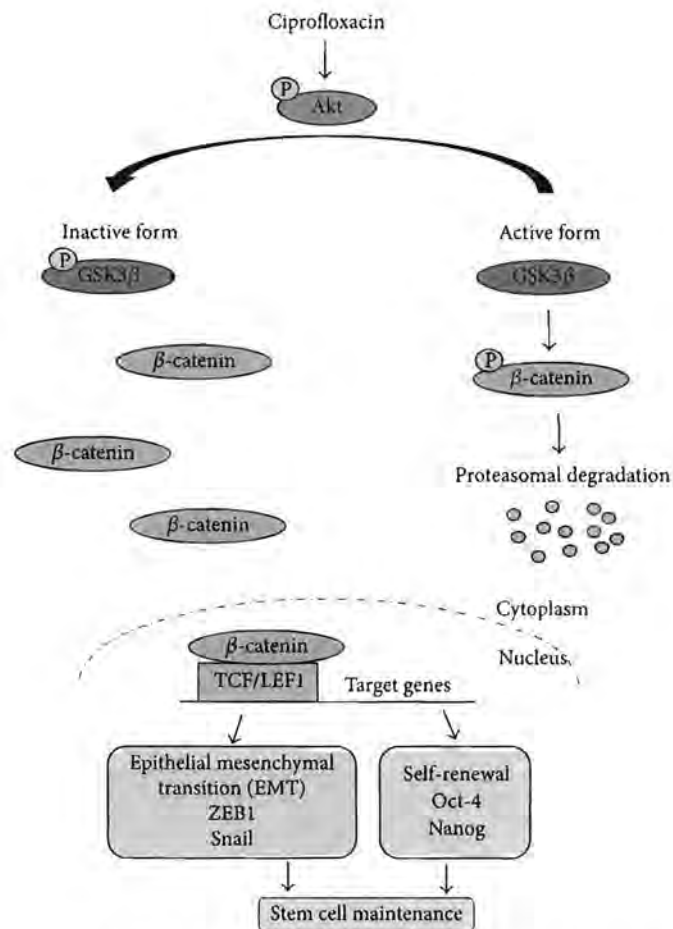


FIGURE 6: Schematic diagram summarizes the effects of CIP for improvement of the stemness in human DPCs. CIP improved the stemness of human DPCs through Akt activation which accounts for GSK3 β inactivation, resulting in the increase of cellular β -catenin. As a consequence, β -catenin accumulates in cytoplasm and translocates into nucleus leading to stimulation of target genes, including transcription factors associated with EMT and self-renewal that might exert the stemness sustaining effect of CIP.

the increase of EMT markers was found to be corresponding to the stem cell-like morphology and aggregative behavior. Our findings also lend strong support to the view that Akt/GSK3 β -dependent β -catenin upregulation is important for the DPCs to maintain their stemness. We unveiled that the transcription factors which are downstream targets of Wnt/ β -catenin, namely, Nanog and Oct4, were upregulated in the CIP-treated cells.

In closing, we systemically evaluated the positive role of CIP treatment for the maintenance of stemness in cultured DPCs. We identified a novel finding on the stemness regulatory effect of CIP in DPCs, that is, through Akt/GSK3 β -dependent β -catenin signal resulting in an upregulation of transcription factors associated with EMT and self-renewal (Figure 6). This information may open the door to further investigations and make this new application of the drug in culture be useful for the cell therapeutic approaches.

Abbreviations

DPCs: Dermal papilla cells
GSK3 β : Glycogen synthase kinase3 β

Akt: ATP-dependent tyrosine kinase
EMT: Epithelial-mesenchymal transition
FGF: Fibroblast growth factor
IGF: Insulin-like growth factor
CIP: Ciprofloxacin
TCF: T-cell factor
LEF: Lymphoid enhancing factor.

Conflict of Interests

The authors declare that there is no conflict of interests regarding the publication of this paper.

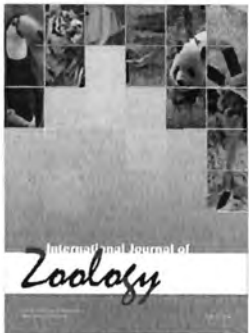
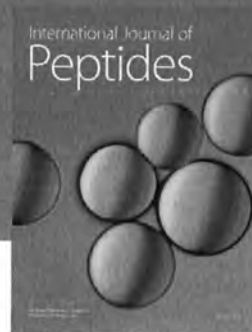
Acknowledgments

This research has been supported by the Ratchadaphiseksomphot Endowment Fund of Chulalongkorn University (CU-57-003-HR) and The Thailand Research Fund through a Research and Researchers for Industries program. The funders had no role in study design, data collection and analysis, decision to publish, or preparation of the paper.

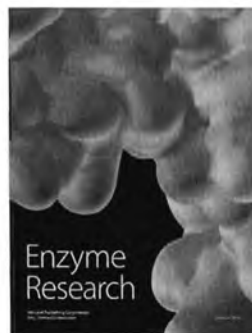
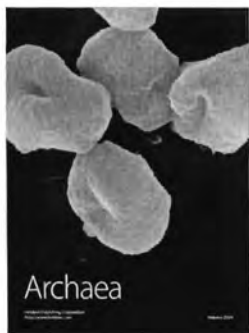
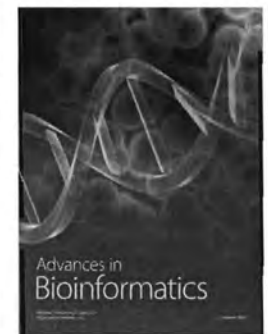
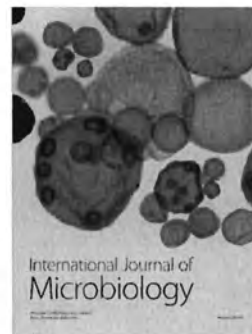
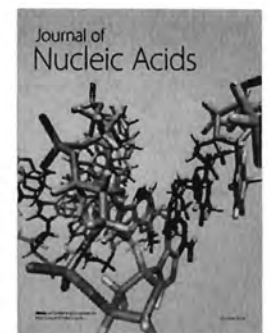
References

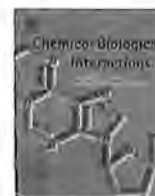
- [1] G. Cotsarelis, "Epithelial stem cells: a folliculocentric view," *The Journal of Investigative Dermatology*, vol. 126, no. 7, pp. 1459–1468, 2006.
- [2] M. R. Schneider, R. Schmidt-Ullrich, and R. Paus, "The hair follicle as a dynamic miniorgan," *Current Biology*, vol. 19, no. 3, pp. R132–R142, 2009.
- [3] K. S. Stenn and R. Paus, "Controls of hair follicle cycling," *Physiological Reviews*, vol. 81, no. 1, pp. 450–481, 2001.
- [4] C. A. B. Jahoda, K. A. Horne, and R. F. Oliver, "Induction of hair growth by implantation of cultured dermal papilla cells," *Nature*, vol. 311, no. 5986, pp. 560–562, 1984.
- [5] J. Teumer and J. Cooley, "Follicular cell implantation: an emerging cell therapy for hair loss," *Seminars in Plastic Surgery*, vol. 19, no. 2, pp. 193–200, 2005.
- [6] K. A. Horne, C. A. B. Jahoda, and R. F. Oliver, "Whisker growth induced by implantation of cultured vibrissa dermal papilla cells in the adult rat," *Journal of Embryology and Experimental Morphology*, vol. 97, pp. 111–124, 1986.
- [7] R. R. Driskell, A. Giangreco, K. B. Jensen, K. W. Mulder, and F. M. Watt, "Sox2-positive dermal papilla cells specify hair follicle type in mammalian epidermis," *Development*, vol. 136, no. 16, pp. 2815–2823, 2009.
- [8] J. H. Shim, T. R. Lee, and D. W. Shin, "Novel in vitro culture condition improves the stemness of human dermal stem/progenitor cells," *Molecules and Cells*, vol. 36, no. 6, pp. 556–563, 2013.
- [9] T. J. van Raay, K. B. Moore, I. Iordanova et al., "Frizzled 5 signaling governs the neural potential of progenitors in the developing *Xenopus* retina," *Neuron*, vol. 46, no. 1, pp. 23–36, 2005.
- [10] A. N. Ziegler, J. S. Schneider, M. Qin et al., "IGF-II promotes stemness of neural restricted precursors," *Stem Cells*, vol. 30, no. 6, pp. 1265–1276, 2012.
- [11] Y. Ito, T. S. Hamazaki, K. Ohnuma, K. Tamaki, M. Asashima, and H. Okochi, "Isolation of murine hair-inducing cells using the cell surface marker prominin-1/CD133," *Journal of Investigative Dermatology*, vol. 127, no. 5, pp. 1052–1060, 2007.
- [12] L. Armstrong, O. Hughes, S. Yung et al., "The role of PI3K/AKT, MAPK/ERK and NFkappabeta signalling in the maintenance of human embryonic stem cell pluripotency and viability highlighted by transcriptional profiling and functional analysis," *Human Molecular Genetics*, vol. 15, no. 11, pp. 1894–1913, 2006.
- [13] D. Enshell-Seijffers, C. Lindon, M. Kashiwagi, and B. A. Morgan, "Beta-catenin activity in the dermal papilla regulates morphogenesis and regeneration of hair," *Developmental Cell*, vol. 18, no. 4, pp. 633–642, 2010.
- [14] J. Kishimoto, R. E. Burgeson, and B. A. Morgan, "Wnt signaling maintains the hair-inducing activity of the dermal papilla," *Genes & Development*, vol. 14, no. 10, pp. 1181–1185, 2000.
- [15] H. Shimizu and B. A. Morgan, "Wnt signaling through the β -catenin pathway is sufficient to maintain, but not restore, anagen-phase characteristics of dermal papilla cells," *Journal of Investigative Dermatology*, vol. 122, no. 2, pp. 239–245, 2004.
- [16] S. A. Mani, W. Guo, M.-J. Liao et al., "The epithelial-mesenchymal transition generates cells with properties of stem cells," *Cell*, vol. 133, no. 4, pp. 704–715, 2008.
- [17] W. Guo, Z. Keckesova, J. L. Donaher et al., "Slug and Sox9 cooperatively determine the mammary stem cell state," *Cell*, vol. 148, no. 5, pp. 1015–1028, 2012.
- [18] Y. Shimono, M. Zabala, R. W. Cho et al., "Downregulation of miRNA-200c links breast cancer stem cells with normal stem cells," *Cell*, vol. 138, no. 3, pp. 592–603, 2009.
- [19] K. A. Sepkowitz, "Antibiotic prophylaxis in patients receiving hematopoietic stem cell transplant," *Bone Marrow Transplantation*, vol. 29, no. 5, pp. 367–371, 2002.
- [20] I. Gabanyi, F. H. Lojudice, P. M. Kossugue, E. Rebelato, M. A. Demasi, and M. C. Sogayar, "VP22 herpes simplex virus protein can transduce proteins into stem cells," *Brazilian Journal of Medical and Biological Research*, vol. 46, no. 2, pp. 121–127, 2013.
- [21] J. M. Mowles, "The use of ciprofloxacin for the elimination of mycoplasma from naturally infected cell lines," *Cytotechnology*, vol. 1, no. 4, pp. 355–358, 1988.
- [22] A. Osada, T. Iwabuchi, J. Kishimoto, T. S. Hamazaki, and H. Okochi, "Long-term culture of mouse vibrissa dermal papilla cells and de novo hair follicle induction," *Tissue Engineering*, vol. 13, no. 5, pp. 975–982, 2007.
- [23] J. A. McDonald, T. J. Broekelmann, M. L. Matheke, E. Crouch, M. Koo, and C. Kuhn III, "A monoclonal antibody to the carboxyterminal domain of procollagen type I visualizes collagen-synthesizing fibroblasts. Detection of an altered fibroblast phenotype in lungs of patients with pulmonary fibrosis," *The Journal of Clinical Investigation*, vol. 78, no. 5, pp. 1237–1244, 1986.
- [24] Y. Riaz, H. T. Cook, A. Wangoo, B. Glenville, and R. J. Shaw, "Type 1 procollagen as a marker of severity of scarring after sternotomy: effects of topical corticosteroids," *Journal of Clinical Pathology*, vol. 47, no. 10, pp. 892–899, 1994.
- [25] J. Li, J. Li, and B. Chen, "Oct4 was a novel target of Wnt signaling pathway," *Molecular and Cellular Biochemistry*, vol. 361, no. 1–2, pp. 233–240, 2012.
- [26] B. J. Merrill, "Wnt pathway regulation of embryonic stem cell self-renewal," *Cold Spring Harbor Perspectives in Biology*, vol. 4, Article ID a007971, pp. 1–17, 2012.
- [27] T. Miki, S. Y. Yasuda, and M. Kahn, "Wnt/beta-catenin signaling in embryonic stem cell self-renewal and somatic cell reprogramming," *Stem Cell Reviews and Reports*, vol. 7, no. 4, pp. 836–846, 2011.
- [28] L. D. M. Derycke and M. E. Bracke, "N-cadherin in the spotlight of cell-cell adhesion, differentiation, invasion and signalling," *The International Journal of Developmental Biology*, vol. 48, no. 5–6, pp. 463–476, 2004.
- [29] D. Olmeda, M. Jordá, H. Peinado, Á. Fabra, and A. Cano, "Snail silencing effectively suppresses tumour growth and invasiveness," *Oncogene*, vol. 26, no. 13, pp. 1862–1874, 2007.
- [30] A. Barrallo-Gimeno and M. A. Nieto, "The Snail genes as inducers of cell movement and survival: Implications in development and cancer," *Development*, vol. 132, no. 14, pp. 3151–3161, 2005.
- [31] C. Blanpain, W. E. Lowry, A. Geoghegan, L. Polak, and E. Fuchs, "Self-renewal, multipotency, and the existence of two cell populations within an epithelial stem cell niche," *Cell*, vol. 118, no. 5, pp. 635–648, 2004.
- [32] S. He, D. Nakada, and S. J. Morrison, "Mechanisms of stem cell self-renewal," *The Annual Review of Cell and Developmental Biology*, vol. 25, pp. 377–406, 2009.
- [33] S. P. Medvedev, A. I. Shevchenko, and S. M. Zakain, "Molecular basis of mammalian embryonic stem cell pluripotency and self-renewal," *Acta Naturae*, vol. 2, no. 3, pp. 30–46, 2010.
- [34] Y.-H. Loh, Q. Wu, J.-L. Chew et al., "The Oct4 and Nanog transcription network regulates pluripotency in mouse embryonic stem cells," *Nature Genetics*, vol. 38, no. 4, pp. 431–440, 2006.
- [35] T. Su, S. Dan, and Y. Wang, "Akt-Oct4 regulatory circuit in pluripotent stem cells," *Chinese Science Bulletin*, vol. 59, no. 10, pp. 936–943, 2014.

- [36] G. D. Richardson, E. C. Arnott, C. J. Whitehouse et al., "Plasticity of rodent and human hair follicle dermal cells: implications for cell therapy and tissue engineering," *Journal of Investigative Dermatology Symposium Proceedings*, vol. 10, no. 3, pp. 180–183, 2005.
- [37] Z. Li, "CD133: a stem cell biomarker and beyond," *Experimental Hematology & Oncology*, vol. 2, no. 1, pp. 1–8, 2013.
- [38] B. P. Levi, Ö. H. Yilmaz, G. Duyster, and S. J. Morrison, "Aldehyde dehydrogenase 1a1 is dispensable for stem cell function in the mouse hematopoietic and nervous systems," *Blood*, vol. 113, no. 8, pp. 1670–1680, 2009.
- [39] S. Fukumoto, C.-M. Hsieh, K. Maemura et al., "Akt participation in the Wnt signaling pathway through Dishevelled," *The Journal of Biological Chemistry*, vol. 276, no. 20, pp. 17479–17483, 2001.
- [40] R. R. Driskell, V. R. Juneja, J. T. Connelly, K. Kretschmar, D. W.-M. Tan, and F. M. Watt, "Clonal growth of dermal papilla cells in hydrogels reveals intrinsic differences between Sox2-positive and -Negative cells in vitro and in vivo," *Journal of Investigative Dermatology*, vol. 132, no. 4, pp. 1084–1093, 2012.
- [41] C. Clavel, L. Grisanti, R. Zemla et al., "Sox2 in the dermal papilla niche controls hair growth by fine-tuning BMP signaling in differentiating hair shaft progenitors," *Developmental Cell*, vol. 23, no. 5, pp. 981–994, 2012.
- [42] K. Kim, Z. Lu, and E. D. Hay, "Direct evidence for a role of beta-catenin/LEF-1 signaling pathway in induction of EMT," *Cell Biology International*, vol. 26, no. 5, pp. 463–476, 2002.
- [43] M. F. Cole, S. E. Johnstone, J. J. Newman, M. H. Kagey, and R. A. Young, "Tcf3 is an integral component of the core regulatory circuitry of embryonic stem cells," *Genes & Development*, vol. 22, no. 6, pp. 746–755, 2008.
- [44] E. Lambertini, T. Franceschetti, E. Torreggiani et al., "SLUG: a new target of lymphoid enhancer factor-1 in human osteoblasts," *BMC Molecular Biology*, vol. 11, article 13, 12 pages, 2010.
- [45] L. Pereira, F. Yi, and B. J. Merrill, "Repression of Nanog gene transcription by Tcf3 limits embryonic stem cell self-renewal," *Molecular and Cellular Biology*, vol. 26, no. 20, pp. 7479–7491, 2006.
- [46] D. ten Berge, W. Koole, C. Fuerer, M. Fish, E. Eroglu, and R. Nusse, "Wnt signaling mediates self-organization and axis formation in embryoid bodies," *Cell Stem Cell*, vol. 3, no. 5, pp. 508–518, 2008.
- [47] K. Wu, J. Fan, L. Zhang et al., "PI3K/Akt to GSK3 β / β -catenin signaling cascade coordinates cell colonization for bladder cancer bone metastasis through regulating ZEB1 transcription," *Cellular Signalling*, vol. 24, no. 12, pp. 2273–2282, 2012.



Hindawi
Submit your manuscripts at
<http://www.hindawi.com>





Ciprofloxacin mediates cancer stem cell phenotypes in lung cancer cells through caveolin-1-dependent mechanism



Preeyaporn Plaimee Phiboonchaiyanan^{a, b}, Chayanin Kiratipaiboon^b,
Pithi Chanvorachote^{a, b, *}

^a Department of Pharmacology and Physiology, Faculty of Pharmaceutical Sciences, Chulalongkorn University, Bangkok, Thailand

^b Cell-Based Drug and Health Product Development Research Unit, Faculty of Pharmaceutical Sciences, Chulalongkorn University, Bangkok, Thailand

ARTICLE INFO

Article history:

Received 28 December 2015

Received in revised form

25 February 2016

Accepted 2 March 2016

Available online 3 March 2016

Keywords:

Cancer stem cells

Ciprofloxacin

Non-small cell lung cancer

Caveolin-1

ABSTRACT

Cancer stem cells (CSCs), a subpopulation of cancer cells with high aggressive behaviors, have been identified in many types of cancer including lung cancer as one of the key mediators driving cancer progression and metastasis. Here, we have reported for the first time that ciprofloxacin (CIP), a widely used anti-microbial drug, has a potentiating effect on CSC-like features in human non-small cell lung cancer (NSCLC) cells. CIP treatment promoted CSC-like phenotypes, including enhanced anchorage-independent growth and spheroid formation. The known lung CSC markers; CD133, CD44, ABCG2 and ALDH1A1 were found to be significantly increased, while the factors involving in epithelial to mesenchymal transition (EMT); Slug and Snail, were depleted. Also, self-renewal transcription factors Oct-4 and Nanog were found to be up-regulated in CIP-treated cells. The treatment of CIP on CSC-rich populations obtained from secondary spheroids resulted in the further increase of CSC markers. In addition, we have proven that the mechanistic insight of the CIP induced stemness is through Caveolin-1 (Cav-1)-dependent mechanism. The specific suppression of Cav-1 by stably transfected Cav-1 shRNA plasmid dramatically reduced the effect of CIP on CSC markers as well as the CIP-induced spheroid formation ability. Cav-1 was shown to activate protein kinase B (Akt) and extracellular signal-regulated kinase (ERK) pathways in CSC-rich population; however, such an effect was rarely found in the main lung cancer cells population. These findings reveal a novel effect of CIP in positively regulating CSCs in lung cancer cells via the activation of Cav-1, Akt and ERK, and may provoke the awareness of appropriate therapeutic strategy in cancer patients.

© 2016 Elsevier Ireland Ltd. All rights reserved.

1. Introduction

Ciprofloxacin (CIP), a member of antibiotic drug in fluoroquinolone family, has been widely used in several clinical aspects such as urinary tract infection and inflammatory bowel disease [1,2]. Also, it is used to manage the chemotherapy-associated febrile neutropenia in cancer patients [3]. Recently, it has been reported that CIP is able to show an anti-tumor effect in various human cancer cell lines [4–8]. Moreover, a proliferative inhibition effect of CIP was observed in the human colonic and non-small cell lung

cancers (NSCLC) [4–6], and cytotoxicity and apoptosis induction abilities were found in the human prostate and pancreatic cancers [7,8]. However, the potential of CIP in potentiating cancer aggressiveness is largely unknown.

Approximately 80% of all lung malignancies were claimed to be NSCLC. This type of lung cancer frequently relapses with the median progression time at approximately 5–24 months [9]. Recent evidence has suggested that cancer stem cells (CSCs), a subpopulation of cancer cells with high aggressive behavior, are responsible for the cancer progression and relapse [10–12]. CSCs were reported to be less responsive to chemotherapy and could be identified in NSCLC population [13,14]. Likewise, clinical data indicated that lung cancer patients exhibiting high level of CSC markers are related to low recurrence-free survival [15,16]. According to several studies, CSCs can initiate tumor development and have the ability to maintain tumor growth through the specific properties including self-renewal, tumorigenic and multilineage potentials [17–19].

* Corresponding author. Department of Pharmacology and Physiology, Faculty of Pharmaceutical Sciences, Chulalongkorn University, Phatumwan, Bangkok 10330, Thailand.

E-mail addresses: pithi.c@chula.ac.th, pithi_chan@yahoo.com (P. Chanvorachote).

CSCs can be identified by expression of their specific surface markers, such as CD133, CD44, aldehyde dehydrogenase (ALDH) and some others [17]. ALDH is a detoxified-enzyme and responsible for therapeutic resistance [20]. In addition, CSCs can be recognized by an elevated expression of ATP-Binding Cassette (ABC) transporter superfamily which relates to a high level of drug resistance. ABC is activated in response to environmental factors and functions to control the chemical homeostasis [21]. Additionally, CSCs express some genes known to govern the stem cell functions including Octamer-binding transcription factor 4 (Oct-4), Nanog and sex determining region Y-box 2 (Sox-2) which are found to be overexpressed in the CSCs in many types of cancers [19,22–27]. Previous reports showed that within NSCLC population, there was a subpopulation of CD44 positive cells possessing active pluripotency genes including Oct-4, Nanog and Sox-2. These cells were reported to be cisplatin-resistant, have the ability to form spheroid, and cause tumor growth in mice and *in vitro* [26]. Further evidences have suggested the association of CSC phenotype and survival pathway namely protein kinase B (Akt) signaling. CD133 positive CSCs that were isolated from glioblastoma [28] and prostate cancers [29] exhibited increased phospho-Akt levels associating with the maintenance of CSC-like phenotype. Moreover, Akt was reported to phosphorylate transcription factor of the stem cell, Oct-4, and further to increase the proliferation of CSCs [30]. Caveolin-1 (Cav-1), a scaffolding protein of cell membrane called caveolae, was shown to potentiate cancer cell aggressiveness. Cav-1 was shown to regulate aggressive behaviors of lung cancer cell by increasing cell migration, invasion, anoikis resistance and anchorage-independent growth [31–33]. Additionally, Cav-1 was shown to induce the expression of activated Akt in NSCLC cells [34].

Studies suggested that CSC population might be increased in response to cancer microenvironment factors [35]. In NSCLC, nitric oxide was shown to induce CSC-like phenotypes [31]. Also, the cancer cells can be induced to gain more stemness phenotype or can be transformed into stem cell-like cancer cells [31]. If this is the case, targeted elimination of CSCs may not be sufficient for cancer therapy. The better understanding in CSC biology and identifying new influencing factors in controlling CSC population may be beneficial for the supportive care and development of strategy for cancer treatment. Therefore, the aim of this study is to investigate the effect of CIP on CSCs in human NSCLC cells.

2. Materials and methods

2.1. Cell culture and CIP treatment

Human NSCLC cell lines (NCI-H460) were obtained from the American Type Culture Collection (Manassas, VA). Immortalized human dermal papilla cells (DPCs) were obtained from Applied Biological Materials Inc. (Richmond, BC). H460 cells were cultured in Roswell Park Memorial Institute (RPMI) 1640 medium supplemented with 10% fetal bovine serum (FBS), 2 mM L-glutamine and 100 U/mL penicillin and 100 µg/mL streptomycin. DPCs were cultured in Prigrow III medium (Richmond, BC, Canada) supplemented with 10% FBS, 2 mM L-glutamine and 100 U/mL of penicillin and 100 µg/mL streptomycin. Cells were cultivated in a 37 °C humidified incubator with 5% CO₂ and were routinely subcultured using a 0.25% trypsin solution with 0.53 mM EDTA. RPMI 1640 medium, FBS, L-glutamine, penicillin/streptomycin, phosphate-buffered saline (PBS), trypsin and EDTA were bought from GIBCO (Grand Island, NY). CIP were obtained from Sigma (St. Louis, MO). Cells were seeded into 6-well plates at density of 5×10^4 cells/well and allowed to adhere to the plates overnight. At 24 h of plating, cells were treated with the indicated concentrations of CIP everyday. Every 2 days, cells were subcultured. The

cells were collected for further analysis at days 1, 3 and 7 after treatment.

2.2. Cell viability assay

MTT viability assay was used to measure cell viability. Cells were plated onto 96-well plates at density 1×10^4 cells/well for viability assay. The cells were allowed to adhere for 24 h and further treated with various concentrations of CIP (0–10 µg/mL). At 24 of CIP exposure, cell viability was analyzed using 3-(4,5-dimethylthiazol-2-yl)-2,5-diphenyltetrazolium bromide (MTT) assay according to the manufacturer's protocol (Sigma Chemical, St. Louis, MO). Cell viability was calculated by dividing the absorbance of the treated cells by the control cells and presented as a percentage to untreated control value.

2.3. Cell death assay

Hoechst 33342 (Molecular Probes Inc., Eugene, OR) and PI (Molecular Probes Inc.) co-staining was used to determine apoptotic and necrosis cell death [36]. After the treatments, cells were stained with 10 µM of Hoechst and 5 µg/mL of PI for 30 min at 37 °C, then cells were visualized and imaged by fluorescence microscope (Olympus IX 51 with DP70, Olympus America Inc., Center valley, PA).

2.4. Anchorage-independent growth assay

Anchorage-independent cell growth was investigated by soft agar colony-formation assay. The bottom layer of 0.5% agarose was prepared by using a 1:1 mixture of RPMI 1640 medium containing 10% FBS and 1% agarose. After that the bottom layer was allowed to solidify for 30 min. An upper cellular layer consisting of 0.3% agarose gel with 10% FBS and containing 1×10^3 cells/ml was added. After the upper layer was solidified, RPMI medium containing 10% FBS was added over upper layer and incubated at 37 °C for 14 days. Colony formation was observed and imaged using a phase-contrast microscope (Olympus IX51 with DP70). Relative colony number and size were calculated by dividing the values of the treated cells by the control cells.

2.5. Spheroid-formation assay

Spheroids culture assay used in this study was slightly modified from Kantara et al. and Yongsanguanchai et al. [31,37]. When CIP treatment was completed, cells were detached into single cells using 1 mM EDTA and 2.5×10^3 cells/well were grown in 24-well ultralow-attached plate. RPMI serum-free medium was used to culture spheroids. At day 7 of primary spheroid culture, primary spheroids were resuspended into single cells using 1 mM EDTA, and again 2.5×10^3 cells/well were seeded onto a 24-well ultralow-attached plate. Secondary spheroids were allowed to form for 21 days. Phase-contrast images of the secondary spheroids were taken at days 7, 14 and 21 of the treatment under a phase-contrast microscope (Olympus IX51 with DP70).

2.6. Migration assay

Cell migration was investigated by wound-healing assay. Confluent monolayers of cells were wounded at the center of the 96-well plate by a 200-µL micropipette tip. Five random fields of the wound space were observed and imaged under a phase-contrast microscope (Olympus IX51 with DP70) at 24 and 48 h after plated. Relative migration level was calculated by dividing the percentage change of the wound space in CIP-treated cells to the non-treated cells.

2.7. Western blot analysis

When the treatment was completed, cells were washed with PBS. The cell lysates were prepared by incubating the cells in ice-cold lysis buffer containing 20 mM TrisHCl (pH 7.5), 0.5% Triton X, 10% glycerol, 150 mM sodium chloride, 50 mM sodium fluoride, 1 mM sodium orthovanadate, 1 mM phenylmethylsulfonyl fluoride and protease inhibitor cocktail (Roche Molecular Biochemicals, Indianapolis, IN) for 45 min on ice. Protein content was then analyzed using BCA protein assay kit from Pierce Biotechnology (Rockford, IL). Equal amounts of proteins (40 μ g) were boiled in Laemmli loading buffer at 95 °C for 5 min. The proteins were loaded onto 10% SDS-polyacrylamide electrophoresis for separation, and transferred onto 0.45 μ m nitrocellulose membranes (Bio-Rad, Hercules, CA). The membranes were blocked with 5% skim milk in TBST (25 mM TrisHCl (pH 7.5), 0.05% Tween-20, and 125 mM NaCl) and incubated overnight at 4 °C with specific primary antibodies. Primary antibody for CD133 was bought from Cell Applications Inc. (San Diego, CA). Antibodies for CD44, ABCG2, Cav-1, Oct-4, Nanog, Sox-2, Akt, p-Akt (Ser 473), ERK, p-ERK (Thr 202/Tyr 204), Slug, Snail and β -actin were obtained from Cell Signaling (Denver, MA). ALDH1A1 antibody was purchased from Santa Cruz Biotechnology Inc. (Dallas, TX). Membranes were washed three times with TBST and incubated with horseradish peroxidase-coupled secondary antibodies for 2 h at room temperature. Peroxidase conjugated anti-rabbit IgG and anti-mouse IgG were obtained from Cell Signaling (Denver, MA, USA). Peroxidase conjugated anti-goat IgG was obtained from Santa Cruz Biotechnology Inc. The immune complexes were detected with chemiluminescent substrate (SuperSignal West Pico, Pierce, Rockford, IL) and exposed to film. The data were quantified using analyst/PC densitometry software (Bio-Rad).

2.8. Plasmid and transfection

Transfection of shRNA-Cav-1 plasmid was performed as previously reported [31]. Briefly, subconfluent (70%) monolayers of H460 cells were transfected with shRNA-Cav-1 (Santa Cruz Biotechnology Inc.) plasmid in serum-free RPMI 1640 medium using Lipofectamine 2000 reagent, according to the manufacturer's protocol (Invitrogen, Eugene, OR) for 12 h. The medium was then replaced with RPMI 1460 containing 10% FBS. To obtain stable transfectants, the cells were cultured and selected for antibiotic resistance for 30 days. Expression of the Cav-1 proteins was verified by Western blot assay. The cells were prepared for further experiments by culturing in antibiotic-free RPMI 1640 medium for at least two passages.

2.9. Flow cytometry analysis

After the treatment, the cells were collected, washed and blocked. Then the cells were incubated on ice with mouse anti-CD44 antibody for 1 h. The primary antibody was removed and the cells were incubated on ice for 30 min with Alexa Fluor 647-conjugated goat anti-mouse IgG (H+L) secondary antibody (Life Technologies, Eugene, OR) for CD44. Fluorescence intensity was detected by flow cytometry using a 647-nm excitation beam and a 668-nm band-pass filter (FACSort; Becton Dickinson, Rutherford, NJ). The mean fluorescence intensity was quantified by CellQuest software (Becton Dickinson).

2.10. Statistical analysis

The treatment data were normalized with the non-treated controls group. The results were expressed as the mean

values \pm standard deviation (SD) from at least three independent experiments. The statistical comparisons were carried out using one-way ANOVA with post hoc test (SPSS, SPSS Inc., Chicago, IL, USA). Statistical significance was accepted within the 95% confidence limit ($p < 0.05$).

3. Results

3.1. Effect of ciprofloxacin on cell behaviors related to cancer stem cell and epithelial-mesenchymal transition

CSCs have been identified inside tumors and suggested as the rationale behind cancer recurrence [10–12,15]. To study the role of CIP on the CSC properties, we first investigated the appropriate non-cytotoxic concentrations of CIP used in this study in human lung epithelial carcinoma H460 cells. Cells were treated with various concentrations of CIP (0–10 μ g/mL), and cell survival was determined after 24 h by MTT assay. CIP was relatively non-toxic at doses 0.5–5 μ g/mL (Fig. 1a). At the 10 μ g/mL of CIP treatment, a significant decrease in cell viability was observed with ~85% of the cells remained viable. To study the role of CIP in apoptosis induction, cells were similarly treated with CIP, then apoptotic and necrotic cell death were determined after 24 h by Hoechst 33342 and PI staining assay, respectively. Consistent with the cell viability assay, lack of chromatin condensation and nuclear fluorescence were observed at the doses 0.5–5 μ g/mL indicating the cells that did not undergo apoptosis or necrosis (Fig. 1b). The treatment dose of 10 μ g/mL caused an increase in cell apoptosis over control level, as indicated by an increased nuclear fluorescence staining and chromatin condensation/fragmentation.

CSCs have been identified by their cellular traits such as spheroid and colony formation [17,31,38]. As the ability of the cancer cells to form spheroids together with grow and survive in an anchorage-independent condition has been widely accepted as a hallmark of CSCs, we therefore investigated the role of CIP on these behaviors. Cells were treated with the non-cytotoxic concentrations of CIP for 7 days and analyzed for colony formation on soft agar. Colony number and diameter were determined and expressed as relative values over non-treated control levels. Fig. 1d displays the relative colony number and diameter of the treated and non-treated cells at day 14. A significant increase in the number of colonies formed was recorded for 2.5 and 5 μ g/mL of the treatments (Fig. 1c, d). However, the treated cells showed no significant difference in the colony diameter compared with control.

To confirm the aforementioned effect of CIP on CSCs, the lung cancer cells were similarly treated with the CIP and analyzed for spheroid formation. Cells were pretreated with the non-cytotoxic concentration of CIP for 7 days, and were subjected to spheroid formation assay in ultralow-attached plates. The treated cells were seeded at low density in RPMI serum-free medium, and primary spheroids were allowed to form for 7 days. The primary spheroids were then resuspended into single cells, and secondary spheroids were allowed to grow for 21 days. Treatment of CIP significantly increased cell ability to form spheroids which was first detected at day 14 (Fig. 1e). At day 21, spheroid numbers were counted and expressed as relative values over non-treated control levels. CIP treatment significantly increased in the spheroid number in dose-dependent manner (Fig. 1f). These results indicate the role of CIP in induction of CSC-like behaviors in lung cancer cells.

Because previous studies have shown that CSCs fundamentally elicited the process of the cell transition from epithelial to mesenchymal (EMT) character that consequently enhanced their ability to metastasize to distant sites, and the induction of EMT has been reported to increase the stem cell-like phenotype [31,39,40]. Therefore, we further investigated the effect of CIP on EMT by

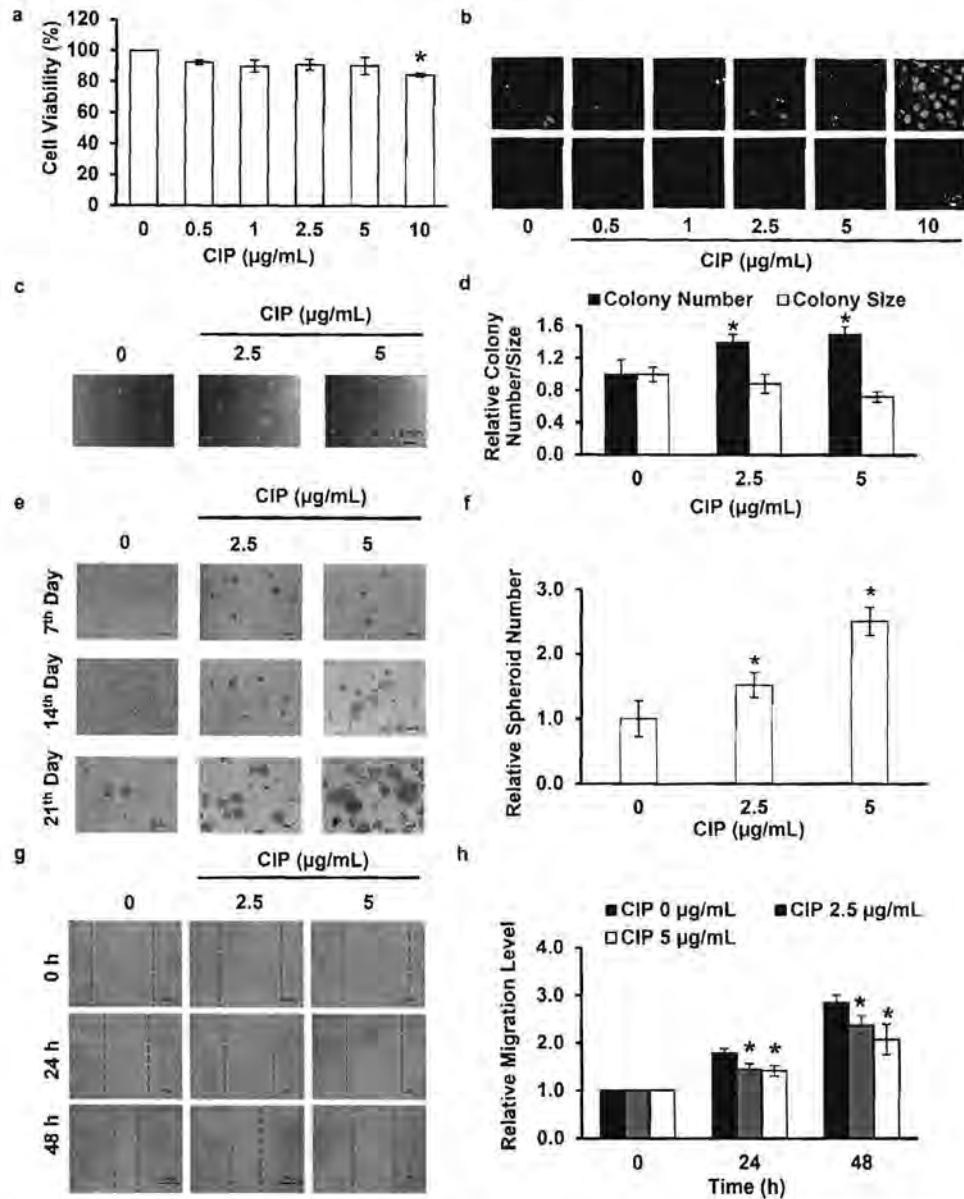


Fig. 1. Effect of CIP on cell viability, CSC-like behaviors, and EMT. Subconfluent (90%) monolayers of H460 cells were treated with CIP (0.5–10 µg/mL) at 37 °C for 24 h. **a**, effect of CIP on cell survival determined by MTT assay. **b**, effect of CIP on cell apoptosis and necrosis determined by Hoechst 33342 and PI assay. The cells were untreated or treated with CIP (0.5–5 µg/mL) for 7 days and analyzed for CSC-like behaviors. **c**, **d** effect of CIP determined by colony-formation assay. **e**, **f** effect of CIP determined by spheroid formation assay. **g**, **h** effect of CIP detected by wound healing assay. Triplicate samples were averaged for each group. Error bars show SD of triplicate experiments ($n = 9$). * $p < 0.05$ versus non-treated cells.

determining EMT behavior, such as cell migration. The cells were treated with the non-cytotoxic concentrations of CIP for 7 days and subjected to wound healing assay for 24 h and 48 h. Fig. 1g and h indicate that the CIP-treated cells exhibited less motility behavior in comparing to that of the control cells. A significant decrease in the migration level was shown at the doses 2.5 and 5 µg/mL of CIP treatment for 24 and 48 h. These results indicate the role of CIP in regulation of CSC induction despite a reduction of EMT.

3.2. Ciprofloxacin increases cancer stem cell markers in lung cancer and dermal papilla cells

Having shown that CIP enhanced CSC phenotypes in lung cancer cells, we next confirmed such observation by using well-known lung CSC markers [13]. Cells were treated with CIP in dose-and

time-dependent experiments and the expression level of CD133, CD44, ABCG2 and ALDH1A1 were determined by Western blotting. Fig. 2a and Fig. 2b show that CIP treatment at *day 3* and *7* caused an increase in CD133, CD44, ABCG2 and ALDH1A1 expression over the control level. By *day 7*, the expression of those proteins increased in the CIP treated groups compared with those of non-treated control group (Fig. 2c, d). These results along with the finding on the CIP effect on CSC behaviors strongly support the role of CIP in inducing CSC-like properties of lung cancer cells.

Because the self-renewal is an important signature of CSCs [41], we next determined whether the treatment of CIP could affect the self-renewal-related proteins in the lung cancer cells. Transcription factors that have been shown to maintain pluripotency and self-renewal in CSCs [19,22–26], including Oct-4, Nanog and Sox-2 were investigated in the CIP-treated and non-treated cells by

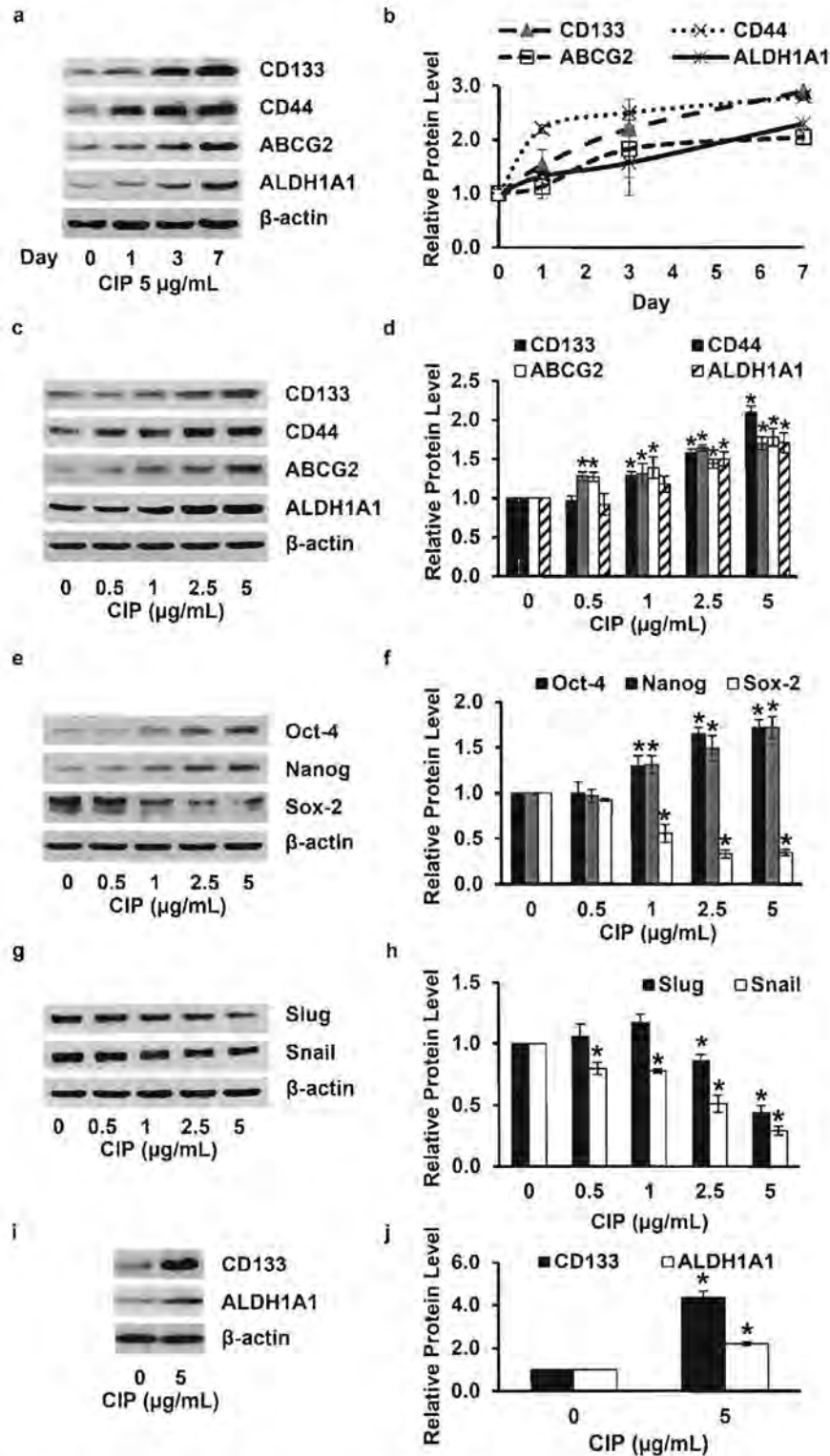


Fig. 2. Ciprofloxacin induces CSC marker and self-renewal transcription factor expression. **a, b** subconfluent monolayers of H460 cells were treated with CIP (5 μ g/mL) for 1, 3 and 7 days, then cell extracts were prepared and analyzed for CD133, CD44, ABCG2 and ALDH1A1 by immunoblotting. The blots were re-probed with β -actin antibody to confirm equal loading of samples. The immunoblot signals were quantified by densitometry, and mean data from independent experiments were normalized to the result obtained from the cells in an absence of CIP (control). **c, d** effect of CIP on CSC marker expression. Cells were treated with various doses of CIP (0.5, 1, 2.5 and 5 μ g/mL) for 7 days. Cell lysates were prepared and analyzed for CD133, CD44, ABCG2 and ALDH1A1 by immunoblotting. Densitometry was done to determine the relative levels of CSC marker after re-probing with β -actin antibody. **e, f** effect of CIP on CSC transcription factor expression. **g, h** dose dependent effect of CIP on EMT transcription factor expression. Cells were treated with various doses of CIP for 7 days. Cell lysates were prepared and analyzed for Oct-4, Nanog, Sox-2, Slug and Snail expression by immunoblotting. **i, j** effect of CIP on CSC marker expression in DPCs. Cells were treated with CIP (5 μ g/mL) for 3 days. Cell lysates were prepared and analyzed for CD133 and ALDH1A1 expression by immunoblotting. Densitometry was done to determine the relative levels of CSC marker after re-probing with β -actin antibody. Columns, mean ($n = 4$); bars, SD. *, $p < 0.05$ versus non-treated control.

Western blot analysis. Fig. 2e and f show that the CIP increased Oct-4 and Nanog expressions in a dose-dependent manner, while Sox-2 expression was decreased in response to CIP treatment. These results suggest that the treatment of CIP was able to increase the self-renewal machinery in lung cancer cells by up-regulating such transcription factors.

We next tested whether the treatment of the cells with CIP could affect the transcription factors that are related to EMT process. The transcription factors that are up-regulated during EMT such as Slug and Snail [42] were investigated in the CIP-treated and non-treated cells by Western blot analysis. Fig. 2g and h show that CIP treatment at day 7 caused a decrease in Slug and Snail.

Having shown that CIP enhanced stemness in lung cancer cells, we further confirmed such observation in the well-known multipotent stem cells, human dermal papilla cells (DPCs). Cells were treated with CIP and the expression level of CD133 and ALDH1A1 were determined by Western blotting. Fig. 2i and j show that CIP treatment caused an increase in CD133 and ALDH1A1 expression over the control level. These results in DPCs strongly support the role of CIP in enhancement of CSC-like properties in lung cancer cells.

3.3. Ciprofloxacin induces cancer stem cell phenotypes via caveolin-1-dependent mechanism

Revealing the key players underlying CIP-mediated CSC-like phenotypes is of importance. Cav-1 is known to associate with aggressive lung cancer cell behaviors [31–34,43,44], even though its regulatory role on stem cell biology is still unknown. To study the possible role of Cav-1 in CIP-induced CSC-like phenotype, we investigated the Cav-1 expression in response to CIP treatment by immunoblotting. Fig. 3a to d show that the Cav-1 strongly up-regulated in the CIP-treated cells in both dose- and time-dependent manners.

Furthermore, the knockdown of Cav-1 by stable transfection of Cav-1-shRNA plasmid resulted in significant decrease in Cav-1 (Fig. 3e, f), and abolishment of CSC induction caused by CIP treatment (Fig. 3g, h). It is worthy noting herein that in the absence of CIP, shRNA Cav-1 transfection significantly down-regulated the CSC markers including CD133, CD44, ABCG2 and ALDH1A1. To confirm, Cav-1 knockdown cells and vector transfected control cells were subjected to spheroid formation assay in the absence or presence of CIP. Fig. 3i and j show that Cav-1 knockdown cells exhibited almost no ability of to form spheroid. As expected, the spheroid formation were also significantly decreased in Cav-1 knockdown cells after treatment with CIP when compare to control cells (Fig. 3i, j). These results suggest that the induction effect of CIP on stemness of lung cancer cells was through Cav-1 pathway.

3.4. Ciprofloxacin enhances stemness in cancer stem cell-rich population through Cav-1 and Akt

Besides showing the effect of CIP on the total population of lung cancer cells which majorly composes of non-CSC population and a minor of CSC population [45,46], we next tested the effect of CIP treatment on CSC-rich population. The CSC-rich population was established by growing the cells in a single-cell suspended condition to form primary and secondary spheroids. By day 7 of secondary spheroids, the cells were collected and characterized for stem cell markers. Fig. 4a and b shows that the expressions of CD133, CD44, ABCG2 and ALDH1A1 were dramatically increased in comparison to that of the wild type total cells.

CSC-rich population was treated with CIP at 5 µg/mL for 7 days and the expressions of CD133, CD44, ABCG2 and ALDH1A1 were determined by Western blot analysis. Fig. 4c and d show that CIP

treatment caused the increase in CD133, CD44, ABCG2 and ALDH1A1 expressions over the control level. Also, the immunocytochemistry experiments assessing the expression of CD44 detected by flow cytometry showed that CIP treatment exhibited an increase in cell surface expression of CD44 (Fig. 4e, f). Next, the self-renewal transcription factors in CSC-rich population were determined. In the presence of CIP, the expressions level of Oct-4 and Nanog were increased (Fig. 4g, h); but the treatment decreased the expression level of Sox-2. CSC-rich group treated with CIP was further determined for EMT markers including Slug and Snail by Western blotting assay. Fig. 4i and j show that the CIP treatment resulted in a significant decrease of Slug and Snail expression. These results support with our earlier data showing the inhibition of CIP on EMT phenotype which further confirmed the independence of EMT process in CIP-induced CSC-like phenotype.

Because previous reports revealed the critical roles of Akt and ERK in CSC phenotype induction and maintenance [28–30,47], additionally Cav-1 was shown to increase Akt and ERK survival activities [48,49], we next investigated the effect of CIP on Akt and ERK pathways. The effect of CIP on Cav-1 expression in CSC-rich population was then characterized. Fig. 5a and b show that CIP treatment significantly induced Cav-1 expression over control level. We next investigated the effect of CIP on Akt and ERK expressions in total population and CSC-rich population. CSC-rich and the wild type total population were treated with CIP and the expression level of total Akt, activated Akt (phosphorylated Akt at Ser 473), total ERK and activated ERK (phosphorylated ERK at Thr 202/Try 204) were investigated by Western blot analysis. Fig. 5c and d show that the CIP induced activated Akt and activated ERK expression only in CSC-rich population. Interestingly, in the wild type population, CIP treatment showed a negative effect on Akt and no effect on ERK. These data suggest the potentiating role of CIP in regulating CSC-like phenotypes, at least in part, by the induction of Cav-1, Akt- and ERK-dependent pathways in CSCs.

4. Discussion

The CSCs theory has a primary reason for the relapse and resistance of cancer after therapy [10–16,39,50,51]. Therefore, CSCs have recently gained an increasing attention in cancer research field. CSCs have ability to generate new tumor through their stem cell properties, importantly self-renewal potential and differentiation into multiple cell lineages [17–19]. CSCs of lung cancer are well recognized by their specific markers such as CD133, CD44, ABCG2 and ALDH1A1 together with the CSC aggressive behaviors including spheroid and colony formation [13,17,21,31]. CIP, a known topoisomerase-II inhibitor, is an FDA-approved anti-microbial drug [1,2]. CIP is frequently used for the treatment of febrile neutropenia-caused by chemotherapy [3]. Because the information regarding the effect of CIP on CSC biology is rarely known, we have revealed for the first time that CIP positively regulates the stemness and CSC aggressive behaviors of lung cancer cells. CIP increased spheroid and colony formation in an anchorage-independent manner (Fig. 1c–f), along with up-regulated the expressions of the known CSC markers (Fig. 2a–d, Fig. 2i, j and Fig. 4c–f). Additionally, the self-renewal proteins, namely, Oct-4 and Nanog were significantly up-regulated in the CIP-treated cells (Fig. 2e, f and Fig. 4g, h). Indeed, Oct-4, a member of the POU domain transcription factor family, is a specific protein regulating mammalian development [25,27,52]. Likewise, Nanog also plays a critical role in regulating the pluripotent of inner cell mass during embryonic development [53]. As the augmented expression of Oct-4 and Nanog were previously demonstrated in NSCLC to accentuate the ability of cells to form spheroid, increase tumorigenicity in mice, and cause drug resistant [26]. The induction of these transcription

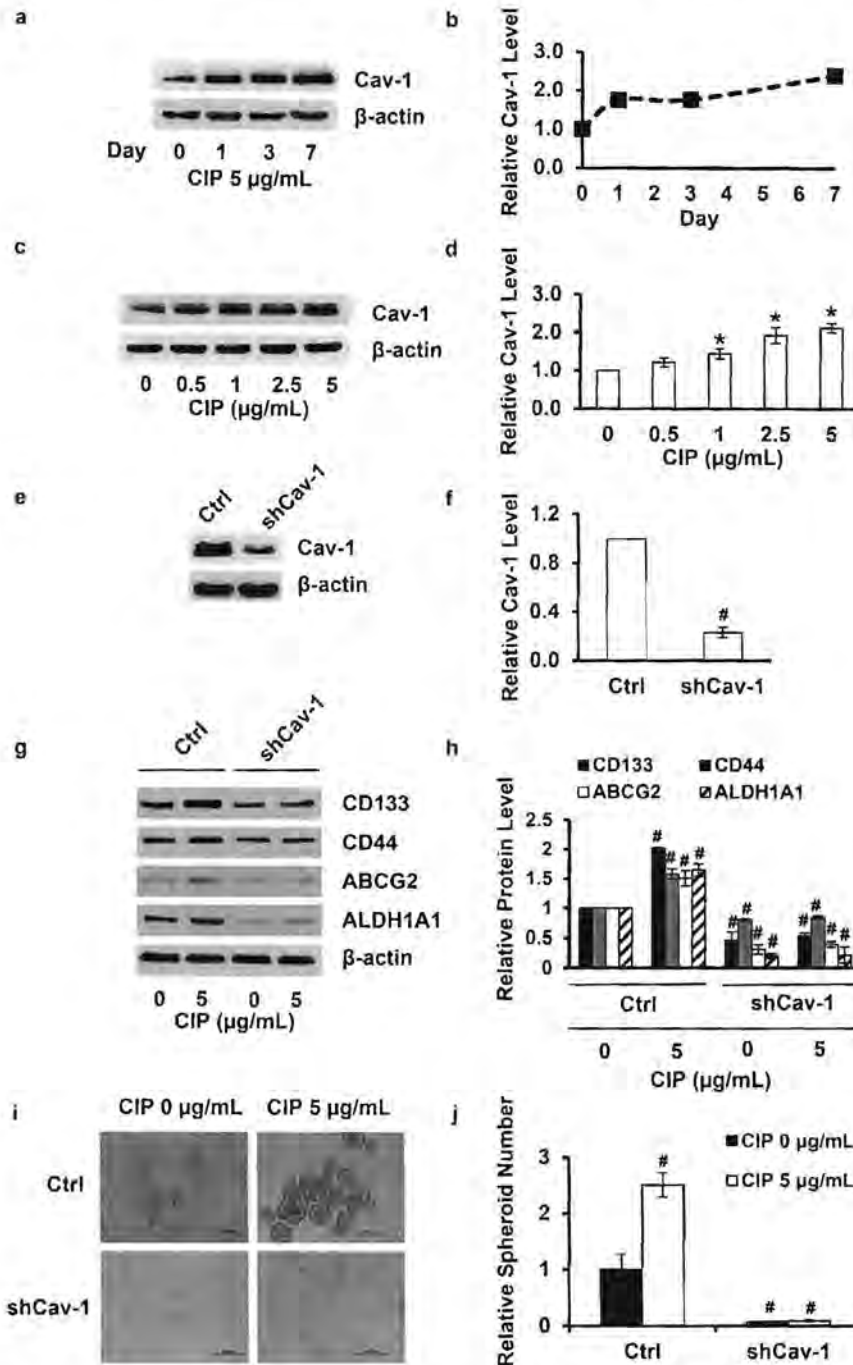


Fig. 3. Caveolin-1 regulates CSC marker expression in CIP treatment. **a, b** subconfluent monolayers of H460 cells were treated with CIP (5 μg/mL) for 1, 3 and 7 days, and cell extracts were prepared and analyzed for Cav-1 by immunoblotting. The blots were reprobed with β-actin antibody to confirm equal loading of samples. The immunoblot signals were quantified by densitometry, and mean data from independent experiments were normalized to the result obtained in cells in the absence of CIP. **c, d** dose effect of CIP on Cav-1 expression. Cells were treated with varying doses of CIP (0.5, 1, 2.5 and 5 μg/mL) for 7 days. Cell lysates were prepared and analyzed for Cav-1 by immunoblotting. Densitometry was done to determine the relative levels of CSC marker after reprobing with β-actin antibody. **e, f** H460 cells were stably transfected with short hairpin (sh) knockdown plasmid of Cav-1 (shCav-1), or control (Ctrl) plasmid, and Cav-1 expression in these cells was determined by Western blotting. Blots were reprobed with β-actin as a loading control. The immunoblot signals were quantified by densitometry, and mean data from independent experiments were normalized to the result obtained from the cell transfected with control plasmid. **g, h** transfected and control plasmid cells were treated with CIP (5 μg/mL) for 7 days, and cell lysates were prepared and analyzed for CD133, CD44, ABCG2 and ALDH1A1 by immunoblotting. The blots were reprobed with β-actin to confirm equal loading. The immunoblot signals were quantified by densitometry, and mean data from independent experiments were normalized to the controls. **i, j** transfected and control plasmid cells were treated with CIP (5 μg/mL) for 7 days, and cells were allowed to form secondary spheroid for 21 days. Columns, mean (n = 4); bars, SD. *, p < 0.05 versus non-treated control. #, p < 0.05 versus non-treated control plasmid.

factors along with CSC phenotypes, may support the possible role of CIP treatment in potentiating stemness of lung cancer cells.

Sufficient evidence has indicated the role of Cav-1 protein on aggressiveness and chemoresistance in several cancers [54,55],

including lung cancer [31–33,43]. Cav-1 over-expression and caveolar structure maintained pluripotency marker expression in mouse embryonic stem cells, including Oct-4, Sox-2, FoxD3 and Rex1 [56]. Previous study showed that nitric oxide exposure to lung

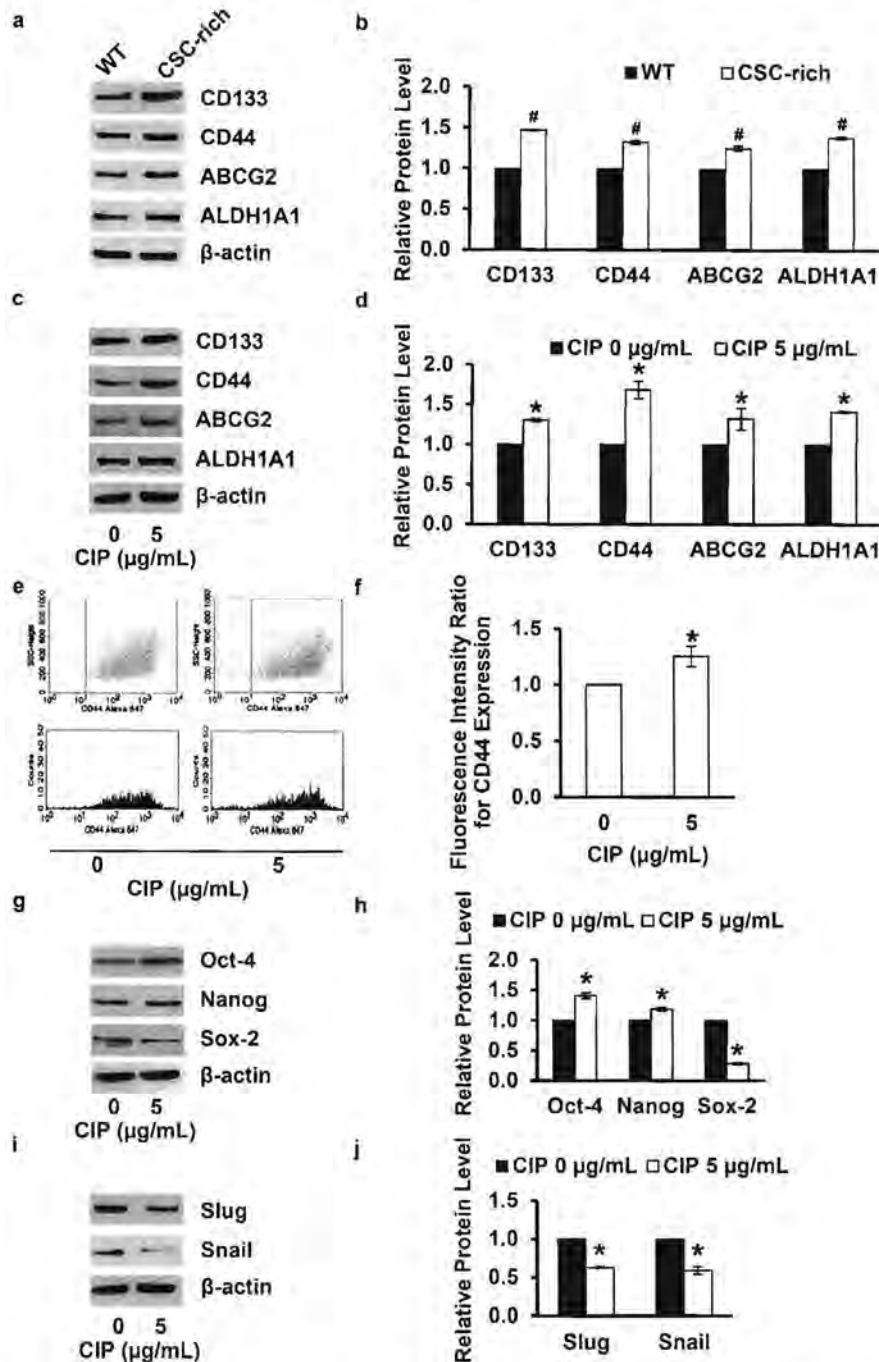


Fig. 4. Ciprofloxacin induces CSC markers and self-renewal transcription factors in CSC-rich population. a, b characterization of CSC-rich population derived from secondary spheroid, as described in Materials and Methods. Cell lysate of the parental wild type cells (WT) and CSC-rich cells were prepared and analyzed for CD133, CD44, ABCG2 and ALDH1A1 by immunoblotting. The blots were reprobbed with β -actin antibody to confirm equal loading of samples. The immunoblot signals were quantified by densitometry, and mean data from independent experiments were normalized to the result obtained with the WT cells. c, d effect of CIP on stem cell marker expression. CSC-rich population was treated with CIP (5 μ g/mL) for 7 days, and cell extracts were prepared and analyzed for CD133, CD44, ABCG2 and ALDH1A1 by immunoblotting. Densitometry was done to determine the relative levels of CSC marker after reprobbed with β -actin antibody. e, f The level of the cell surface expression of CD44 was measured by flow cytometry for treated and non-treated CSC-rich population at day 7 of CIP treatment. Flow cytometry was performed using mouse anti-CD44 monoclonal antibody followed by Alexa Fluor 647-labeled secondary antibody to visualize CD44 expression. g, h effect of CIP on self-renewal transcription factor expression. i, j effect of CIP on EMT transcription factor expression. CSC-rich population was treated with CIP (5 μ g/mL) for 7 days, and cell extracts were prepared and analyzed for Oct-4, Nanog, Sox-2, Slug and Snail expressions by immunoblotting. Columns, mean (n = 4); bars, SD. *, $p < 0.05$ versus non-treated control. #, $p < 0.05$ versus non-treated wild type control.

cancer cells promoted CSC-like phenotype through Cav-1 augmentation [31]. *In-vivo* study of a carbon nanotube-induced carcinogenesis. Cav-1 was identified as a key protein for defining the lung CSC formation. Cav-1 was up-regulated in lung CSCs and further induced tumorigenesis and metastasis via p53

dysregulation [57]. These findings suggested that Cav-1 is the specific marker for CSCs and influences self-renewal property and multi-differentiation of CSCs. In this study, Cav-1 is up-regulated in response to CIP-treated cells in both total and CSC-rich population (Fig. 3a–d and Fig. 5a, b). The Cav-1 knockdown experiment

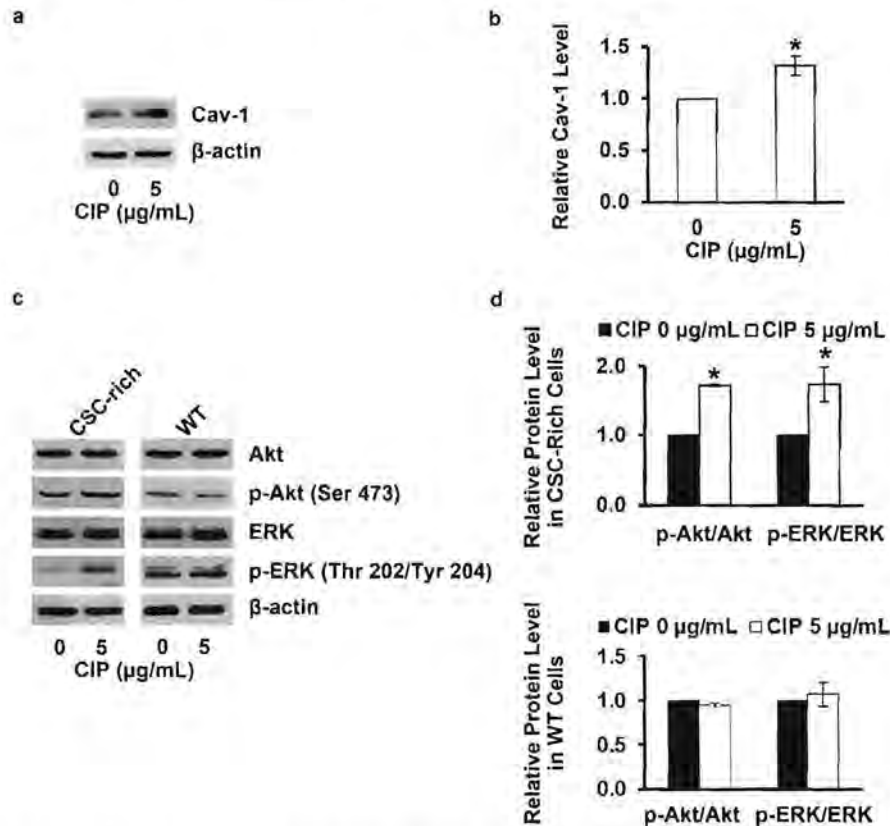


Fig. 5. Ciprofloxacin up-regulates Cav-1 and the upstream transcription factors in CSC-rich population. CSC-rich population and wild type control (WT) population were treated with CIP (5 $\mu\text{g/mL}$) for 7 days, and cell extracts were prepared and analyzed for Cav-1 and upstream transcription factor expression by immunoblotting. a, b effect of CIP on Cav-1 expression in CSC-rich cells. c, d effect of CIP on survival proteins, total Akt, activated Akt (phosphorylated Akt at Ser 473), total ERK and activated ERK (phosphorylated ERK at Thr 202/Tyr 204), expressions in CSC-rich and WT groups. The blots were re-probed with β -actin antibody to confirm equal loading of samples. The immunoblot signals were quantified by densitometry, and mean data from independent experiments were normalized to the result obtained from the absence of CIP. Columns, mean ($n = 4$); bars, SD. *, $p < 0.05$ versus non-treated control.

provides evidence indicating that CIP increased stemness of the cells is through Cav-1-dependent mechanism (Fig. 3g–j), as the CSC-potentiating effect of CIP was abolished in Cav-1 knockdown cells.

We provided further details of the mechanistic fundamental of CIP on stemness regulation. According to the reports, CSC phenotypes were shown to be dependent on the activation status of Akt and ERK [28–30,47]. CD133 positive cells isolated from glioblastoma [28] and prostate cancer [29] were shown to have an increased p-Akt levels. An inhibition of Akt activity resulted in a decrease in the level of Oct-4 and an attenuation of stem cell proliferation [30]. Moreover, previous studies demonstrated that ERK maintains pluripotency of stem cell survival in trophoblast cells [47]. Our current data showed that CIP increased Akt and ERK phosphorylation (Fig. 5c, d) only in CSC-rich population, suggesting the specificity of CIP on the regulation of CSCs. In embryonic stem cells, epidermal growth factor was shown to stimulate cell proliferation via Cav-1 activation [58]. According to the study, Cav-1 was linked to PI3K/Akt-ERK pathway and had an essential role in cell proliferation [58]. It has been previously reported that Cav-1 directly interacts and inhibits serine/threonine protein phosphatases PP1 and PP2A through scaffolding domain binding site interactions [48]. This leads to an increased phosphorylation of specific PPA/PP2A substrates, including phosphorylated Akt. These results were confirmed in mutant Cav-1 with the scaffolding domain deleted cells and plasmid vector expressing wild type Cav-1 cells. The deletion of Cav-1 scaffolding domain decreases phosphorylated Akt compared to the wild type

Cav-1 [48]. Together with our finding indicating that CIP up-regulated Cav-1 (Fig. 5a, b) and Akt/ERK activation (Fig. 5c, d), CIP may increase CSC phenotypes via Cav-1-Akt/ERK dependent pathway.

CSCs were reported to increase EMT characteristic that eventually enhanced their ability to metastasis [31,39]. Induction of EMT has been reported to increase the stem cell-like phenotype in certain cells [40]. Surprisingly, we found that CIP treatment significantly suppressed cell migration (Fig. 1f, h) and down-regulated EMT markers (Fig. 2g, h and Fig. 4i, j). Consistent with our findings, the activation of EMT while suppressing CSC characters were observed in some conditions [59–63].

It was known that CIP has the ability to accumulate in serum after an oral and an intravenous (i.v.) administrations [64,65]. CIP concentration in serum after a single oral administration of 750 mg was reported to be 4.3 $\mu\text{g/mL}$ [64]. For a high-dose treatment (800 mg every 12 h for 8 days, i.v.), CIP can reach a serum concentration of 13 $\mu\text{g/mL}$ [65]. In order to mimic the concentration of CIP in serum, CIP at range 0.5–10 $\mu\text{g/mL}$ were used in this study. Therefore, CIP concentrations used in this study are comparable with the range of serum concentrations during the clinical use. This indicates that the prescribed CIP to cancer patient can increase the risk of CSC induction.

5. Conclusion

In closing, we systemically evaluated the positive role of CIP treatment for the stemness induction in lung cancer cells. We have

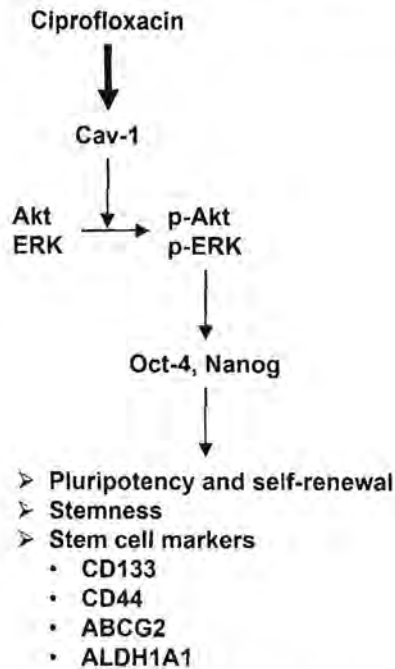


Fig. 6. Schematic diagram summarizes the effects of CIP for induction of the CSC-like phenotypes in CSC-rich lung cancer cells. The present study reveals that CIP has an ability to induce CSC markers including CD133, CD44, ABCG2 and ALDH1A1 through Cav-1 dependent pathway. Activation of Cav-1 accounts for Akt and ERK activation, resulting in the increase of pluripotency and self-renewal transcription factor expressions, Oct-4 and Nanog, that may exert the CSC-like phenotype induction effect of CIP. Arrow indicates activation.

identified a novel finding on the stemness regulatory effect of CIP that it is through Cav-1 and the downstream Akt and ERK pathways (Fig. 6). These results also provide the initial evidence for provoking further investigations that may lead to the awareness of CIP used in cancer patients.

Conflict of interest

The authors declare that there is no conflict of interests regarding the publication of this manuscript.

Acknowledgments

This research is supported by 1) Rachadapisek Sompote Fund for Postdoctoral Fellowship, Chulalongkorn University and 2) the Thailand Research Fund (RSA5780043), and Mr. Krich Rajprasit.

Transparency document

Transparency document related to this article can be found online at <http://dx.doi.org/10.1016/j.cbi.2016.03.005>.

References

- [1] A.M. Pteisen, H. Mirsepasi, S.I. Halkjaer, E.M. Mortensen, I. Nordgaard-Lassen, K.A. Kroghelt, Ciprofloxacin and probiotic *Escherichia coli* Nissle add-on treatment in active ulcerative colitis: a double-blind randomized placebo controlled clinical trial, *J. Crohns Colitis* 8 (11) (2014) 1498–1505.
- [2] H. Saini, S. Chhibber, K. Harjai, Azithromycin and ciprofloxacin: a possible synergistic combination against *Pseudomonas aeruginosa* biofilm-associated urinary tract infections, *Int. J. Antimicrob. Agents* 45 (4) (2015) 359–367.
- [3] N. Pherwani, J.M. Ghayad, L.M. Holle, E.L. Kurpiuk, Outpatient management of febrile neutropenia associated with cancer chemotherapy: risk stratification and treatment review, *Am. J. Health Syst. Pharm.* 72 (8) (2015) 619–631.
- [4] L.A. Bourikas, G. Kolios, V. Valatas, G. Notas, I. Drygiannakis, I. Pelagiadis, et al.,

- Ciprofloxacin decreases survival in HT 29 cells via the induction of TGF- β 1 secretion and enhances the anti-proliferative effect of 5-fluorouracil, *Br. J. Pharmacol.* 157 (3) (2009) 362–370.
- [5] E.R. Mondal, S.K. Das, P. Mukherjee, Comparative evaluation of anti-proliferative activity and induction of apoptosis by some fluoroquinolones with a human non-small cell lung cancer cell line in culture, *Asian Pac. J. Cancer Prev.* 5 (2) (2004) 196–204.
- [6] T. Kloskowski, N. Gurtowska, J. Olkowska, J.M. Nowak, J. Adamowicz, J. Tworzywicz, et al., Ciprofloxacin is a potential topoisomerase II inhibitor for the treatment of NSCLC, *Int. J. Oncol.* 41 (6) (2012) 1943–1949.
- [7] A.C. Pinto, J.N. Moreira, S. Simoes, Ciprofloxacin sensitizes hormone-refractory prostate cancer cell lines to doxorubicin and docetaxel treatment on a schedule-dependent manner, *Cancer Chemother. Pharmacol.* 64 (3) (2009) 445–454.
- [8] V. Yadav, P. Varshney, S. Sultana, J. Yadav, N. Saini, Moxifloxacin and ciprofloxacin induces S-phase arrest and augments apoptotic effects of cisplatin in human pancreatic cancer cells via ERK activation, *BMC Cancer* 15 (2015) 581.
- [9] A. Ashworth, G. Rodrigues, G. Boldt, D. Palma, Is there an oligometastatic state in non-small cell lung cancer? A systematic review of the literature, *Lung Cancer* 82 (2) (2013) 197–203.
- [10] A. Merlos-Suarez, F.M. Barriga, P. Jung, M. Iglesias, M.V. Cespedes, D. Rossell, et al., The intestinal stem cell signature identifies colorectal cancer stem cells and predicts disease relapse, *Cell Stem Cell* 8 (5) (2011) 511–524.
- [11] P.C. Hermann, S.L. Huber, T. Herrler, A. Aicher, J.W. Ellwart, M. Guba, et al., Distinct populations of cancer stem cells determine tumor growth and metastatic activity in human pancreatic cancer, *Cell Stem Cell* 1 (3) (2007) 313–323.
- [12] C.Y. Yang, C.H. Lin, J.K. Jiang, Early relapse in a rectal cancer patient: possible implication of circulating cancer stem cell, *J. Surg. Oncol.* 102 (2) (2010) 196–197.
- [13] F.F. Sun, Y.H. Hu, L.P. Xiong, X.Y. Tu, J.H. Zhao, S.S. Chen, et al., Enhanced expression of stem cell markers and drug resistance in sphere-forming non-small cell lung cancer cells, *Int. J. Clin. Exp. Pathol.* 8 (6) (2015) 6287–6300.
- [14] R. Perona, J. Lopez-Ayllon, B. Fau – de Castro Carpeno, C. de Castro Carpeno, J. Fau – Belda-Iniesta, C. Belda-Iniesta, A role for cancer stem cells in drug resistance and metastasis in non-small-cell lung cancer, *Clin. Transl. Oncol.* 13 (5) (2011) 289–293.
- [15] J. Liu, Z. Xiao, S.K. Wong, V.P. Tin, K.Y. Ho, J. Wang, et al., Lung cancer tumorigenicity and drug resistance are maintained through ALDH(hi)CD44(hi) tumor initiating cells, *Oncotarget* 4 (10) (2013) 1698–1711.
- [16] H. Qu, R. Li, Z. Liu, J. Zhang, R. Luo, Prognostic value of cancer stem cell marker CD133 expression in non-small cell lung cancer: a systematic review, *Int. J. Clin. Exp. Pathol.* 6 (11) (2013) 2644–2650.
- [17] C. Peitzsch, I. Kurth, L. Kunz-Schughart, M. Baumann, A. Duhrovská, Discovery of the cancer stem cell related determinants of radioresistance, *Radiother. Oncol.* 108 (3) (2013) 378–387.
- [18] A. Kreso, E. Dick, Evolution of the cancer stem cell model, *Cell Stem Cell* 14 (3) (2014) 275–291.
- [19] S. Slawek, K. Szmyt, M. Fularz, J. Dziudzi, M. Boruczkowski, J. Sikora, et al., Pluripotency transcription factors in lung cancer—a review, *Tumour Biol.* (2015), <http://dx.doi.org/10.1007/s13277-015-4407-x>.
- [20] J.E. Russo, J. Hilton, Characterization of cytosolic aldehyde dehydrogenase from cyclophosphamide resistant L1210 cells, *Cancer Res.* 48 (11) (1988) 2963–2968.
- [21] A.-M. Bleau, D. Hambardzumyan, T. Ozawa, E.I. Fomchenko, J.T. Huse, C.W. Brennan, et al., PTEN/PI3K/Akt pathway regulates the side population phenotype and ABCG2 activity in glioma tumor stem-like cells, *Cell Stem Cell* 4 (3) (2009) 226–235.
- [22] T. Nagata, Y. Shimada, S. Sekine, R. Hori, K. Matsui, T. Okumura, et al., Prognostic significance of NANOG and KLF4 for breast cancer, *Breast Cancer* 21 (1) (2014) 96–101.
- [23] J. Shan, J. Shen, L. Liu, F. Xia, C. Xu, G. Duan, et al., Nanog regulates self-renewal of cancer stem cells through the insulin-like growth factor pathway in human hepatocellular carcinoma, *Hepatology* 56 (3) (2012) 1004–1014.
- [24] Y. Atlasi, S.J. Mowla, S.A. Ziaee, A.R. Bahrami, OCT-4, an embryonic stem cell marker, is highly expressed in bladder cancer, *Int. J. Cancer* 120 (7) (2007) 1598–1602.
- [25] C. Samardzija, M. Quinn, J.K. Findlay, N. Ahmed, Attributes of Oct4 in stem cell biology: perspectives on cancer stem cells of the ovary, *J. Ovarian Res.* 5 (1) (2012) 37.
- [26] E.L. Leung, R.R. Fiscus, J.W. Tung, V.P. Tin, L.C. Cheng, A.D. Sihoe, et al., Non-small cell lung cancer cells expressing CD44 are enriched for stem cell-like properties, *PLoS One* 5 (11) (2010) e14062.
- [27] M.F. de Resende, L.T. Chinen, S. Vieira, J. Jampietro, F.P. da Fonseca, J. Vassallo, et al., Resonance of OCT4 isoform expression in prostate cancer, *Tumour Biol.* 34 (5) (2013) 2665–2673.
- [28] Y. Wei, Y. Jiang, F. Zou, Y. Liu, S. Wang, N. Xu, et al., Activation of PI3K/Akt pathway by CD133-p85 interaction promotes tumorigenic capacity of glioma stem cells, *Proc. Natl. Acad. Sci. U. S. A.* 110 (17) (2013) 6829–6834.
- [29] A. Dubrovská, S. Kim, R.J. Salamone, J.R. Walker, S.M. Maira, C. Garcia-Echeverria, et al., The role of PTEN/Akt/PI3K signaling in the maintenance and viability of prostate cancer stem-like cell populations, *Proc. Natl. Acad. Sci. U. S. A.* 106 (1) (2009) 268–273.
- [30] Q.W. Zhao, Y.W. Zhou, W.X. Li, B. Kang, X.Q. Zhang, Y. Yang, et al., Akt-mediated phosphorylation of Oct4 is associated with the proliferation of stemlike cancer

- cells, *Oncol. Rep.* 33 (4) (2015) 1621–1629.
- [31] N. Yongsanguanchai, V. Pongrakhananon, A. Mitfirangura, Y. Rojanasakul, P. Chanvorachote, Nitric oxide induces cancer stem cell-like phenotypes in human lung cancer cells, *Am. J. Physiol. Cell Physiol.* 308 (2) (2015) C89–C100.
- [32] P. Chunhacha, P. Chanvorachote, Roles of caveolin-1 on anoikis resistance in non small cell lung cancer, *Int. J. Physiol. Pathophysiol. Pharmacol.* 4 (3) (2012) 149–155.
- [33] H. Halim, P. Chanvorachote, Long-term hydrogen peroxide exposure potentiates anoikis resistance and anchorage-independent growth in lung carcinoma cells, *Cell Biol. Int.* 36 (11) (2012) 1055–1066.
- [34] P. Chanvorachote, P. Chunhacha, Caveolin-1 regulates endothelial adhesion of lung cancer cells via reactive oxygen species-dependent mechanism, *PLoS One* 8 (2) (2013) e57466.
- [35] J.A. Cook, D. Cius, D.A. Wink, M.C. Krishna, A. Russo, J.B. Mitchell, Oxidative stress, redox, and the tumor microenvironment, *Semin. Radiat. Oncol.* 14 (3) (2004) 259–266.
- [36] S. Huerta, E.J. Goulet, S. Huerta-Yepez, E.H. Livingston, Screening and detection of apoptosis, *J. Surg. Res.* 139 (1) (2007) 143–156.
- [37] C. Kantara, M. O'Connell, S. Sarkar, S. Moya, R. Ullrich, P. Singh, Curcumin promotes autophagic survival of a subset of colon cancer stem cells, which are ablated by DCLK1-siRNA, *Cancer Res.* 74 (9) (2014) 2487–2498.
- [38] S.H. Chiou, C.C. Yu, C.Y. Huang, S.C. Lin, C.J. Liu, T.H. Tsai, et al., Positive correlations of Oct-4 and nanog in oral cancer stem-like cells and high grade oral squamous cell carcinoma, *Clin. Cancer Res.* 14 (13) (2008) 4085–4095.
- [39] E. Charafe-Jauffret, C. Ginestier, F. Iovino, J. Wicinski, N. Cervera, P. Finetti, et al., Breast cancer cell lines contain functional cancer stem cells with metastatic capacity and a distinct molecular signature, *Cancer Res.* 69 (4) (2009) 1302–1313.
- [40] S.A. Mani, W. Guo, M.J. Liao, E.N. Eaton, A. Ayyanan, A.Y. Zhou, et al., The epithelial-mesenchymal transition generates cells with properties of stem cells, *Cell* 133 (4) (2008) 704–715.
- [41] S. He, D. Nakada, S.J. Morrison, Mechanisms of stem cell self-renewal, *Annu. Rev. Cell Dev. Biol.* 25 (2009) 377–406.
- [42] S.A. Mani, W. Guo, M.-J. Liao, E.N. Eaton, A. Ayyanan, A.Y. Zhou, et al., The epithelial-mesenchymal transition generates cells with properties of stem cells, *Cell* 133 (4) (2008) 704–715.
- [43] T.Y. Luan, T.N. Zhu, Y.J. Cui, G. Zhang, X.J. Song, D.M. Gao, et al., Expression of caveolin-1 is correlated with lung adenocarcinoma proliferation, migration, and invasion, *Med. Oncol.* 32 (7) (2015) 207.
- [44] P. Chunhacha, V. Pongrakhananon, Y. Rojanasakul, P. Chanvorachote, Caveolin-1 regulates Mcl-1 stability and anoikis in lung carcinoma cells, *Am. J. Physiol. Cell Physiol.* 302 (9) (2012) C1284–C1292.
- [45] W.W. Hwang-Versluis, W.-H. Kuo, P.-H. Chang, C. C. Pan, H.-H. Wang, S.-T. Tsai, et al., Multiple lineages of human breast cancer stem/progenitor cells identified by profiling with stem cell markers, *PLoS ONE* 4 (12) (2009) e8377.
- [46] C.E. Meacham, S.J. Morrison, Tumour heterogeneity and cancer cell plasticity, *Nature* 501 (7467) (2013) 328–337.
- [47] W. Yang, L.D. Klamon, B. Chen, T. Araki, H. Harada, S.M. Thomas, et al., An Shp2/SFK/Ras/Erk signaling pathway controls trophoblast stem cell survival, *Dev. Cell.* 10 (3) (2006) 317–327.
- [48] L. Li, C.H. Ren, S.A. Tahir, C. Ren, T.C. Thompson, Caveolin-1 maintains activated Akt in prostate cancer cells through scaffolding domain binding: site interactions with and inhibition of serine/threonine protein phosphatases PP1 and PP2A, *Mol. Cell Biol.* 23 (24) (2003) 9389–9404.
- [49] R.L. Kortum, M.R. Fernandez, D.L. Costanzo-Garvey, H.J. Johnson, K.W. Fisher, D.J. Volle, et al., Caveolin-1 is required for kinase suppressor of Ras 1 (KSR1)-mediated extracellular signal-regulated kinase 1/2 activation, R-RasV12-induced senescence, and transformation, *Mol. Cell Biol.* 34 (18) (2014) 3461–3472.
- [50] S. Vinogradov, X. Wei, Cancer stem cells and drug resistance: the potential of nanomedicine, *Nanomedicine (Lond)* 7 (4) (2012) 597–615.
- [51] N.A. Lobo, Y. Shimono, D. Qian, M.F. Clarke, The biology of cancer stem cells, *Annu. Rev. Cell Dev. Biol.* 23 (2007) 675–699.
- [52] M. Pesce, X. Wang, D.J. Wolgemuth, H.R. Schöler, Differential expression of the Oct-4 transcription factor during mouse germ cell differentiation, *Mech. Dev.* 71 (1–2) (1998) 89–98.
- [53] I. Chambers, D. Colby, M. Robertson, J. Nichols, S. Lee, S. Tweedie, et al., Functional expression cloning of Nanog, a pluripotency sustaining factor in embryonic stem cells, *Cell* 113 (5) (2003) 643–655.
- [54] L.B. Auzair, V.K. Vincent-Chong, W.M. Ghani, T.G. Kallarakkal, A. Ramanathan, C.E. Lee, et al., Caveolin 1 (Cav-1) and actin-related protein 2/3 complex, subunit 1B (ARPC1B) expressions as prognostic indicators for oral squamous cell carcinoma (OSCC), *Eur. Arch. Otorhinolaryngol.* (2015) 1–9.
- [55] W.-R. Liu, L. Jin, M.-X. Tian, X.-F. Jiang, L.-X. Yang, Z.-B. Ding, et al., Caveolin-1 promotes tumor growth and metastasis via autophagy inhibition in hepatocellular carcinoma, *Clin. Res. Hepatol. Gastroenterol.* (2015 Jul 20), <http://dx.doi.org/10.1016/j.clinre.2015.06.017> pii: S2210-7401(15)00153-9.
- [56] M.Y. Lee, J.M. Ryu, S.H. Lee, J.H. Park, H.J. Han, Lipid rafts play an important role for maintenance of embryonic stem cell self-renewal, *J. Lipid Res.* 51 (8) (2010) 2082–2089.
- [57] S. Luanpitpong, L. Wang, T.A. Stueckle, W. Tse, Y.C. Chen, Y. Rojanasakul, Caveolin-1 regulates lung cancer stem-like cell induction and p53 inactivation in carbon nanotube-driven tumorigenesis, *Oncotarget* 5 (11) (2014) 3541–3554.
- [58] J.H. Park, H.J. Han, Caveolin-1 plays important role in EGF-induced migration and proliferation of mouse embryonic stem cells: involvement of PI3K/Akt and ERK, *Am. J. Physiol. Cell Physiol.* 297 (4) (2009) C935–C944.
- [59] H.Y. Jung, J. Yang, Unraveling the TWIST between EMT and cancer stemness, *Cell Stem Cell.* 16 (1) (2015) 1–2.
- [60] J.M. Schmidt, E. Panzilius, H.S. Bartsch, M. Immler, J. Beckers, V. Kari, et al., Stem-cell-like properties and epithelial plasticity arise as stable traits after transient twist1 activation, *Cell Rep.* 10 (2) (2015) 131–139.
- [61] B. Beck, G. Lapouge, S. Korive, B. Drogar, K. Deaedelaere, S. Delafaille, et al., Different levels of twist1 regulate skin tumor initiation, stemness, and progression, *Cell Stem Cell.* 16 (1) (2015) 67–79.
- [62] K. Jain, A. Basu, Protein kinase C epsilon promotes EMT in breast cancer, *Breast cancer (Auckl)* 8 (2014) 61–67.
- [63] G. Rajendran, D. Dutta, J. Hong, A. Paul, B. Saha, B. Mahato, et al., Inhibition of protein kinase C signaling maintains rat embryonic stem cell pluripotency, *J. Biol. Chem.* 288 (34) (2013) 24351–24362.
- [64] P.P. How, J.H. Fischer, J.A. Arruda, A.H. Lau, Effects of lanthanum carbonate on the absorption and oral bioavailability of ciprofloxacin, *Clin. J. Am. Soc. Nephrol. CJASN* 2 (6) (2007) 1235–1240.
- [65] T.R. Utrup, E.W. Mueller, D.P. Healy, R.A. Callcut, J.D. Peterson, W.E. Hurford, High-dose ciprofloxacin for serious gram-negative infection in an obese, critically ill patient receiving continuous venovenous hemodiafiltration, *Ann. Pharmacother.* 44 (10) (2010) 1660–1664.

Research Article

Gigantol Suppresses Cancer Stem Cell-Like Phenotypes in Lung Cancer Cells

Narumol Bhummaphan¹ and Pithi Chanvorachote^{1,2}

¹Cell-Based Drug and Health Product Development Research Unit, Faculty of Pharmaceutical Sciences, Chulalongkorn University, Bangkok 10330, Thailand

²Department of Pharmacology and Physiology, Faculty of Pharmaceutical Sciences, Chulalongkorn University, Bangkok 10330, Thailand

Correspondence should be addressed to Pithi Chanvorachote; pithi.chan@yahoo.com

Received 29 March 2015; Revised 16 July 2015; Accepted 21 July 2015

Academic Editor: Shrikant Anant

Copyright © 2015 N. Bhummaphan and P. Chanvorachote. This is an open access article distributed under the Creative Commons Attribution License, which permits unrestricted use, distribution, and reproduction in any medium, provided the original work is properly cited.

As cancer stem cells (CSCs) contribute to malignancy, metastasis, and relapse of cancers, potential of compound in inhibition of CSCs has garnered most attention in the cancer research as well as drug development fields recently. Herein, we have demonstrated for the first time that gigantol, a pure compound isolated from *Dendrobium draconis*, dramatically suppressed stem-like phenotypes of human lung cancer cells. Gigantol at nontoxic concentrations significantly reduced anchorage-independent growth and survival of the cancer cells. Importantly, gigantol significantly reduced the ability of the cancer cells to form tumor spheroids, a critical hallmark of CSCs. Concomitantly, the treatment of the compound was shown to reduce well-known lung CSCs markers, including CD133 and ALDH1A1. Moreover, we revealed that gigantol decreased stemness in the cancer cells by suppressing the activation of protein kinase B (Akt) signal which in turn decreased the cellular levels of pluripotency and self-renewal factors Oct4 and Nanog. In conclusion, gigantol possesses CSCs suppressing activity which may facilitate the development of this compound for therapeutic approaches by targeting CSCs.

1. Introduction

Recent researches in the field of cancer have shown that, within the malignant tumor as well as in the blood of advanced stage cancer patients, there are special cancer cells called cancer stem cells (CSCs) [1]. Such CSCs have been shown to reproduce themselves and sustain the tumor [2, 3]. Moreover, researchers accept that these CSCs account for most aggressive behaviors of the disease including chemotherapeutic resistance, metastasis, and cancer relapse [4–6]. The concept that CSCs are a critical factor driving cancer cell aggressiveness and metastasis has led to the intensive investigations of the novel therapeutic strategies as well as drugs targeting the CSCs [4, 5].

CSCs have been shown to maintain their stemness through the sustained level of several transcription factors as well as the stem cell-related signals. In lung cancer, the

expression of Nanog and octamer-binding transcription factor 4 (Oct4) was shown to enhance malignancy through the CSCs induction [7, 8]. Oct4 and Nanog and their activation targets are found to be overexpressed in the CSCs in many types of cancers [9–13] and their expressions associate with the pathogenesis, tumor development, and progression of cancers. The function of Nanog was shown to involve the self-renewal property of the stem cells [14, 15]. Likewise, the activation of Oct4 gene or Oct4 transfection has been shown to promote dedifferentiation and CSCs-like phenotypes [16, 17]. Although the defined upstream molecular mechanisms of such stem cell mediators remain underinvestigated, signal of Akt serine/threonine protein kinase has been widely accepted to play an important role in regulating the self-renewal as well as other stem cell-like phenotypes in CSCs [18, 19]. In non-small-cell lung cancer, Akt signaling was reported to involve with the self-renewal of stem-like cells [20–23]. The

phosphorylated Akt was shown to phosphorylate the Oct4 which resulted in the increase of tumorigenic potential [24]. Also, Nanog was shown to be a downstream target of the Akt pathway [25, 26].

In line with the previous studies indicating the anticancer [27] and antimigration [27] activities of gigantol, a bibenzyl compound isolated from the Thai orchid, *Dendrobium draconis*, we aimed to investigate its possible effect on inhibition of CSCs phenotypes as well as related molecular signals in lung cancer cells. The findings gained from the present study may encourage the development and further investigation on gigantol for its use for cancer therapeutic approaches.

2. Materials and Methods

2.1. Chemicals and Antibodies. Gigantol was isolated from *Dendrobium draconis* as previously described, and its purity was determined using HPLC and NMR spectroscopy with more than 95% purity was used in this study [28]. 3-(4,5-Dimethylthiazol-2-yl)-2,5-diphenyltetrazolium bromide (MTT), Hoechst 33342, propidium iodide (PI), bovine serum albumin (BSA), and dimethyl sulfoxide (DMSO) were purchased from Sigma chemical, Inc. (St. Louis, MO). The following were purchased: CD133 (cat. number CA1217) (Cell Applications, San Diego, CA), ALDH1A1 (cat. number SC-22589) (Santa Cruz Biotechnology), total Akt (cat. number 9272) (Cell signaling Technology), phosphorylated Akt (Ser473) (cat. number 4060) (Cell signaling Technology), Oct4 (cat. number 2750) (Cell signaling Technology), Nanog (cat. number 4903) (Cell signaling Technology), α -tubulin (cat. number 2144) (Cell signaling Technology), β -actin (cat. number SC-130656) (Santa Cruz Biotechnology), peroxidase-labeled secondary antibodies: anti-rabbit IgG (cat. number 7074) (Cell-signaling Technology) or anti-mouse (cat. number 7076) (Cell-signaling Technology), and Perifosine (Cell-signaling Technology).

2.2. Cell Culture. Human non-small-cell lung cancer cell lines, NCI-H460, and human keratinocyte HaCaT cells were obtained from the American Type Culture Collection (Manassas, VA). NCI-H460 was cultivated in Roswell Park Memorial Institute (RPMI) 1640 medium supplemented with 10% fetal bovine serum (FBS), 2 mM L-glutamine, and 100 U/mL penicillin and streptomycin. HaCaT cells were cultivated in Dulbecco's Modified Eagle Medium (DMEM) supplemented with 10% fetal bovine serum (FBS), 2 mM L-glutamine, and 100 U/mL penicillin and streptomycin. Cell cultures were maintained in a 37°C humidified incubator with 5% CO₂. Cells were routinely passaged at preconfluent density using a 0.25% trypsin solution with 0.53 mM EDTA. RPMI 1640 medium, FBS, L-glutamine, penicillin/streptomycin, phosphate-buffered saline (PBS), trypsin, and EDTA were purchased from GIBCO (Grand Island, NY).

2.3. Cytotoxicity Assays. For cytotoxicity assays, cells were seeded onto 96-well plates at a density of 1×10^4 cells/well and were allowed to incubate overnight. Cells were then

treated with various concentrations of gigantol and analyzed for cell viability using 3-(4,5-dimethylthiazol-2-yl)-2,5-diphenyltetrazolium bromide (MTT) assay according to the manufacturer's protocol. The cytotoxicity index was calculated by dividing the absorbance of the treated cells by that of the control cells [27, 29].

2.4. Cell Death Assay. Nuclear costaining with Hoechst 33342 and propidium iodide (PI) was used to determine apoptotic and necrotic cell death. Cells were incubated with 10 μ M Hoechst 33342 and 5 μ M PI for 30 min at 37°C. They were visualized and imaged under a fluorescence microscope (Olympus IX51 with DP70) [27, 30].

2.5. Anchorage-Independent Growth Assay. Anchorage-independent growth cell growth was determined by soft agar colony-formation assay. Soft agar was prepared by using a 1:1 mixture of RPMI 1640 medium containing 10% FBS and 1% agarose. The mixture was allowed to solidify in a 24-well plate to form a bottom layer, after which an upper cellular layer consisting of 3×10^3 cells/mL in the agarose gel with 10% FBS and 0.3% agarose was added. After the upper layer was solidified, RPMI medium containing 10% FBS was added to the system and incubated at 37°C. Colony formation was determined after 2 weeks using a phase-contrast microscope (Olympus IX51 with DP70). Relative colony number and area were determined by dividing the values of the treated cells by those of the control cells.

2.6. Spheroid Formation Assay. Approximately 2.5×10^3 cells/well were seeded onto a 24-well ultralow attachment plate using RPMI serum-free medium. Treated cells were treated every 3 days. Phase-contrast images of formed primary spheroids were taken at day 7 of treatment using a phase-contrast microscope (Olympus IX51 with DP70). Primary spheroids were resuspended into single cells, and again 2.5×10^3 cells/well were seeded onto a 24-well ultralow attachment plate using RPMI serum-free medium. Secondary spheroids were allowed to form for 30 days [6, 31].

2.7. Western Blot Analysis. Cells were incubated on ice for 45 min with lysis buffer containing 20 mM Tris-HCl (pH 7.5), 1% Triton X-100, 150 mM NaCl, 10% glycerol, 1 mM Na₃VO₄, 50 mM NaF, 100 mM PMSF, and protease inhibitor mixture from Roche Molecular Biochemicals (Indianapolis, IN). Cell lysates were analyzed for protein content using BCA protein assay kit from Pierce Biotechnology (Rockford, IL). Equal amounts of denatured protein samples (60 μ g) were loaded onto 10% SDS-PAGE for CD133 and ALDH1A1 analysis and equal amounts of denatured protein samples (100 μ g) were loaded onto 10% SDS-PAGE for Akt, phosphorylated Akt, Oct4, and Nanog analysis before being transferred to 0.45- μ m nitrocellulose membranes (Bio-Rad, Hercules, CA). Transferred membranes were blocked with medium (25 mM Tris-HCl (pH 7.5), 125 mM NaCl, and 0.05% Tween 20 (TBST)) containing 5% nonfat dry milk powder for 30 min and incubated overnight with specific primary antibodies against CD133, ALDH1A1, Akt, phosphorylated Akt

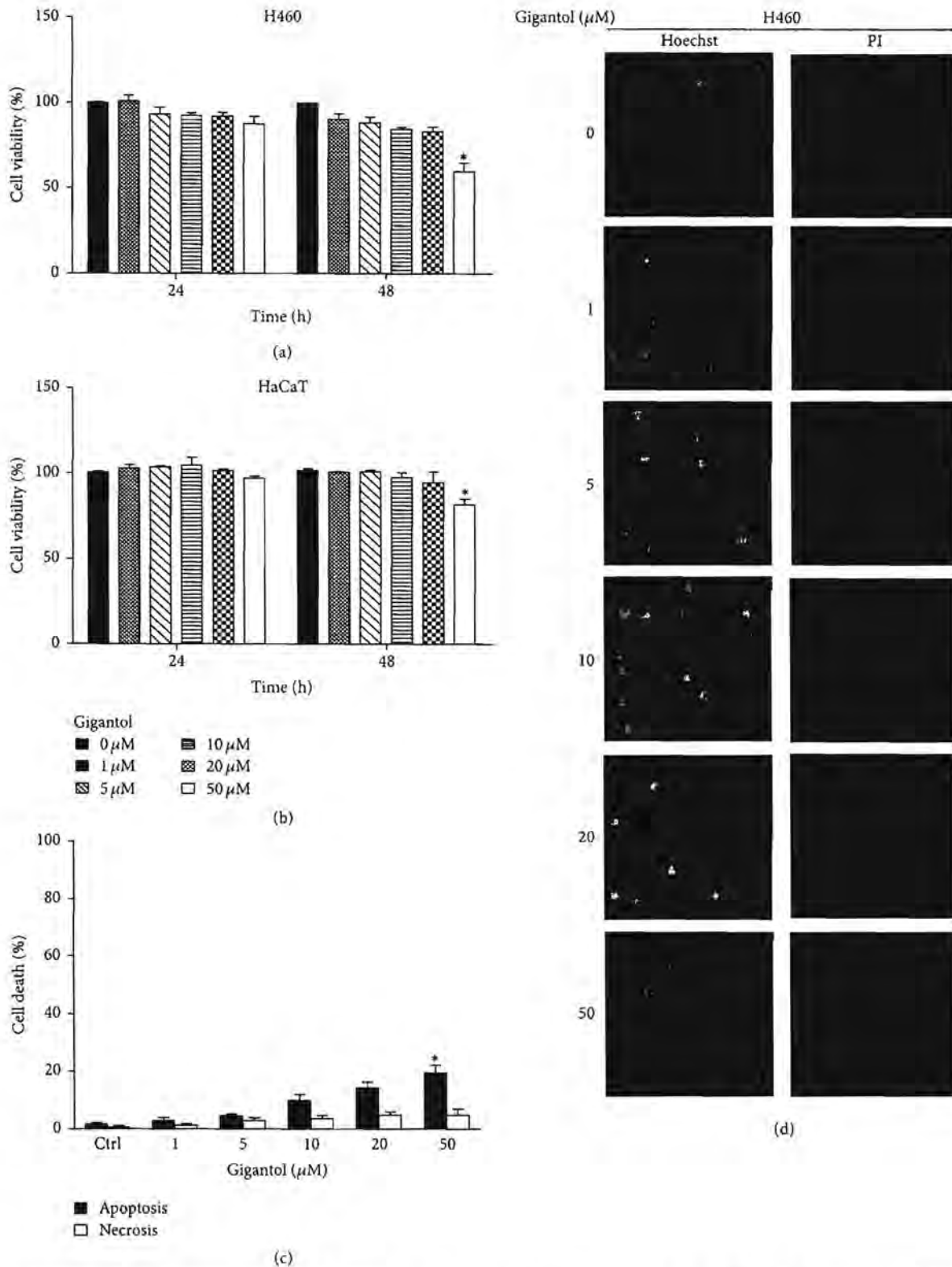


FIGURE 1: Cytotoxic effect of gigantol on human lung cancer H460 cells. (a) H460 cells and (b) HaCaT cells were treated with various concentrations of gigantol (0–50 μM) for 24 and 48 h. Cell viability was determined by a 3-(4,5-dimethylthiazol-2-yl)-2,5-diphenyltetrazolium bromide (MTT) assay. The viability of untreated cells was represented as 100%. ((c) and (d)) H460 cells were treated with gigantol (0–50 μM) for 48 h. Apoptotic and necrotic cell death were evaluated using Hoechst 33342/PI staining and calculated as a percentage compared with nontreated control cells. All plots are means ± SD (n = 3). *P < 0.05 versus nontreated cells.

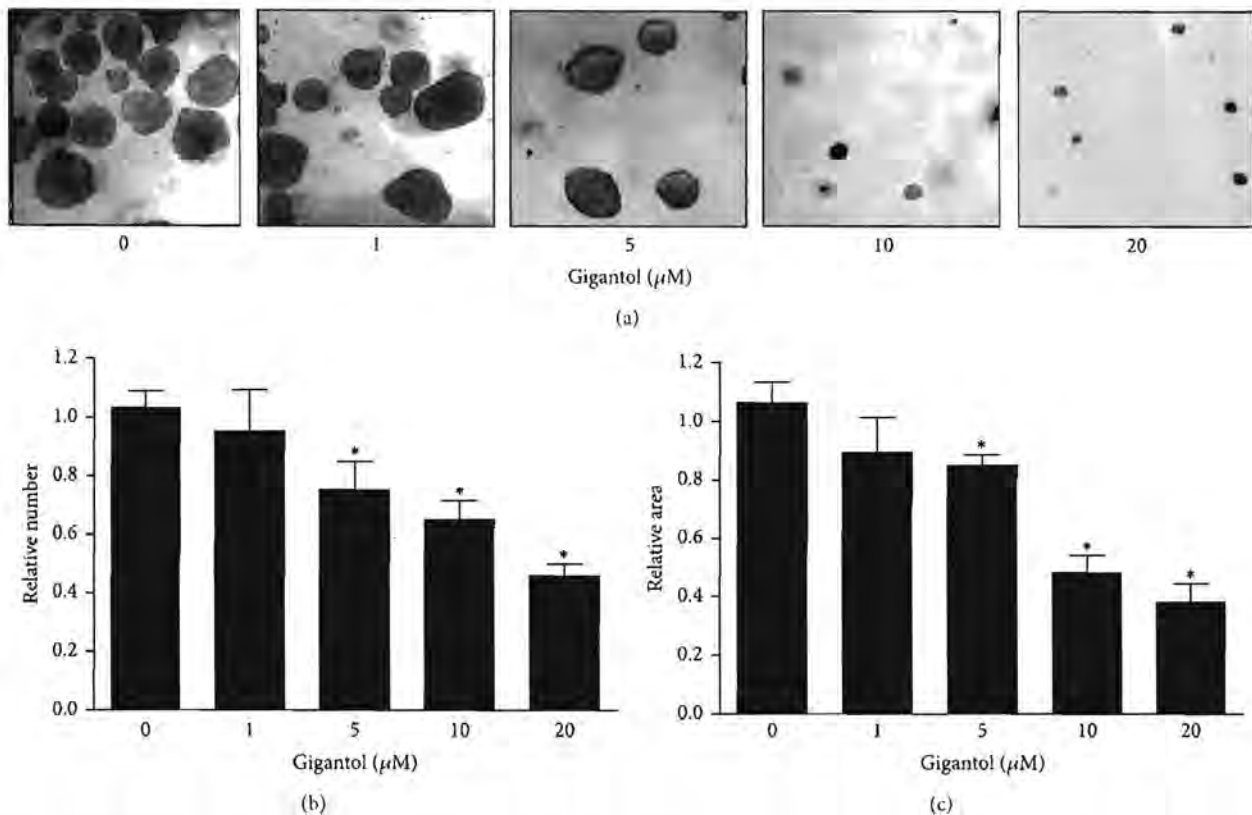


FIGURE 2: Gigantol inhibits anchorage-independent growth of human lung cancer H460 cells. (a) After being treated with gigantol (0–20 μM) for 48 h, H460 cells were suspended and subjected to anchorage-independent growth assay. (b) Colony number and size were analyzed and calculated as relative values to the control cells. Colony 4x images were captured after day 10. All plots are means \pm SD ($n = 3$). * $P < 0.05$ versus nontreated cells.

(Ser473), Oct4, Nanog, α -tubulin, and β -actin. Membranes were washed three times with TBST and incubated with the following appropriate horseradish peroxidase-labeled secondary antibodies: anti-rabbit IgG or anti-mouse, for 2 h at room temperature. The immune complexes were detected by SuperSignal West Pico chemiluminescent substrate (Pierce Biotechnology) and exposed to film.

2.8. Statistical Analysis. All treatments data were normalized to nontreated controls. Data are presented as the means \pm SD from at least three independent experiments. Statistical differences were determined using two-way ANOVA and a post hoc test at a significance level of $P < 0.05$.

3. Results

3.1. Cytotoxicity of Gigantol on Lung Cancer H460 and Normal Keratinocyte HaCaT Cells. Previous studies found that CSCs within tumors drive tumor growth and recurrence [2]. To test whether gigantol has an effect on CSCs phenotypes, we first characterized the noncytotoxic concentrations of the tested compound. Human lung cancer cells and normal keratinocyte stem cells were treated with various concentrations of gigantol (0, 1, 5, 10, 20, and 50 μM), and cell viability was determined after 24 and 48 h by MTT viability assay. Gigantol

was considered nontoxic at the doses below 20 μM for both the lung cancer H460 and keratinocyte cells (Figures 1(a) and 1(b)). In addition, analysis of the mode of cell death (apoptosis and necrosis) using Hoechst33342/propidium iodide staining assay showed that treatment of the compound at 0–20 μM caused neither apoptosis nor necrosis to H460 cells. The significant increase of apoptosis was only found in the H460 cells treated with 50 μM gigantol (Figures 1(c) and 1(d)).

3.2. Gigantol Suppresses CSC-Like Phenotypes. As the ability of the cancer cells to form spheroids as well as growth and survival in anchorage-independent condition has been widely accepted as a hallmark of CSCs, we next tested the effect of gigantol on such behaviors. H460 cells were treated with noncytotoxic concentrations of gigantol (0–20 μM) for 48 h, and the cells were subjected to anchorage-independent growth and spheroid formation assays. For anchorage-independent growth, the colony number and colony size were determined and presented as relative values in comparison to those of nontreated control. Figure 2(a) shows that treatment of the cells with gigantol resulted in the significant decrease of colony number and colony size in a dose-dependent manner. A significant suppression was first detected at 5 μM of gigantol with approximately 30% reduction in terms of colony number and 20% reduction in terms of size.

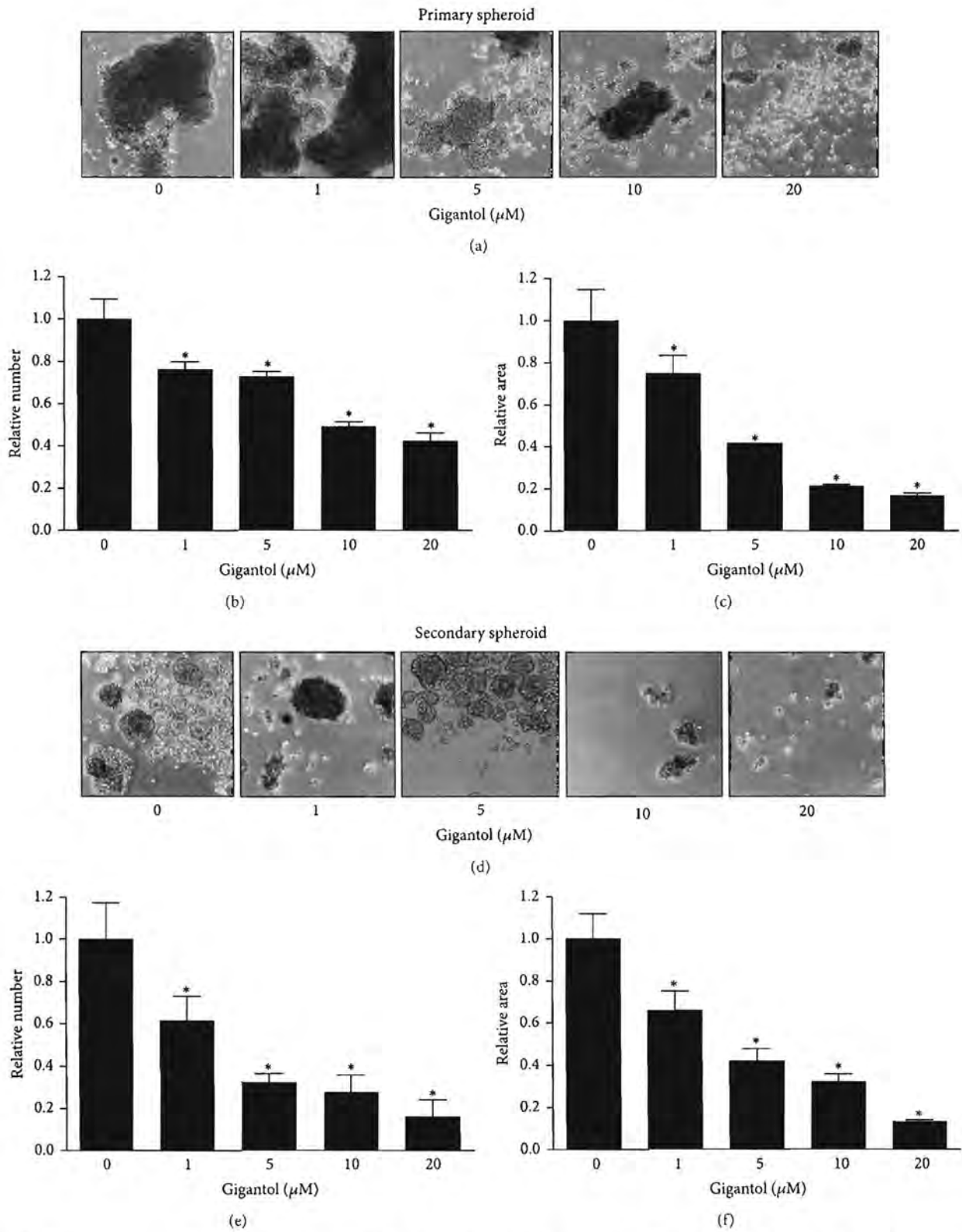


FIGURE 3: Gigantol suppresses CSC-like phenotypes. (a) After being treated with gigantol (0–20 μM) for 48 h, H460 cells were suspended and subjected to spheroid formation assay. (b) 4x phase-contrast images of primary spheroids at day 7 were captured for treated and nontreated cells. (c) The primary spheroids were resuspended into single cells, and secondary spheroids were allowed to grow for 30 days. (d) 4x phase-contrast images of secondary spheroids at day 30 were presented. All plots are means \pm SD ($n = 3$). * $P < 0.05$ versus nontreated cells.

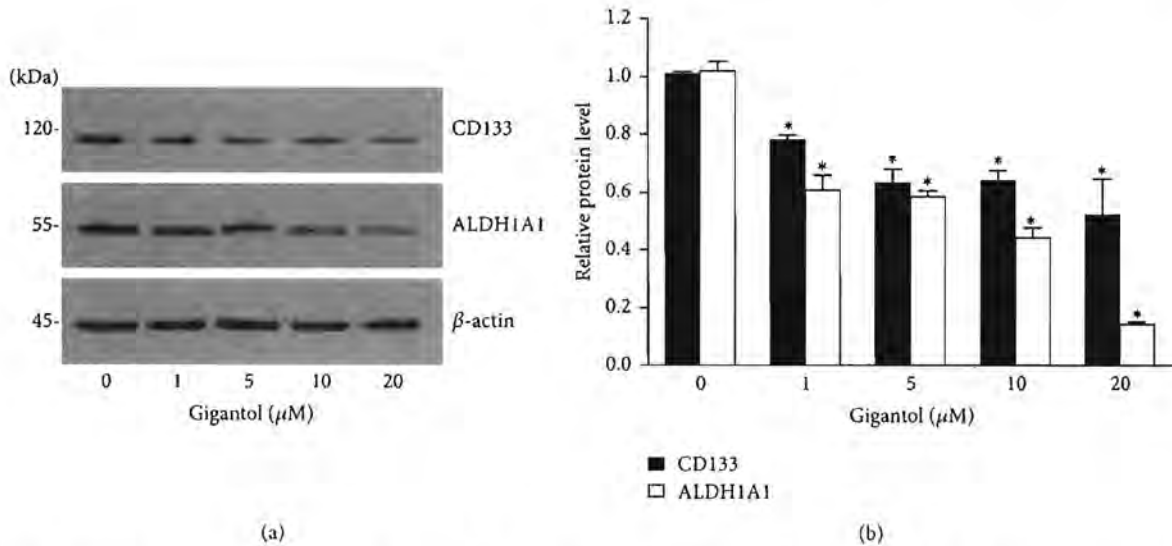


FIGURE 4: Gigantol reduces CSC markers. (a) After H460 cells were treated with gigantol (0–20 μ M) for 48 h, cells were collected, and CSC markers, CD133 and ALDH1A1, were analyzed by Western blotting. The blots were reprobbed with β -actin to confirm equal loading. (b) Band density was quantified by densitometry, and mean data from independent experiments were normalized to the controls. The bars are means \pm SD ($n = 3$). * $P < 0.05$ versus nontreated cells.

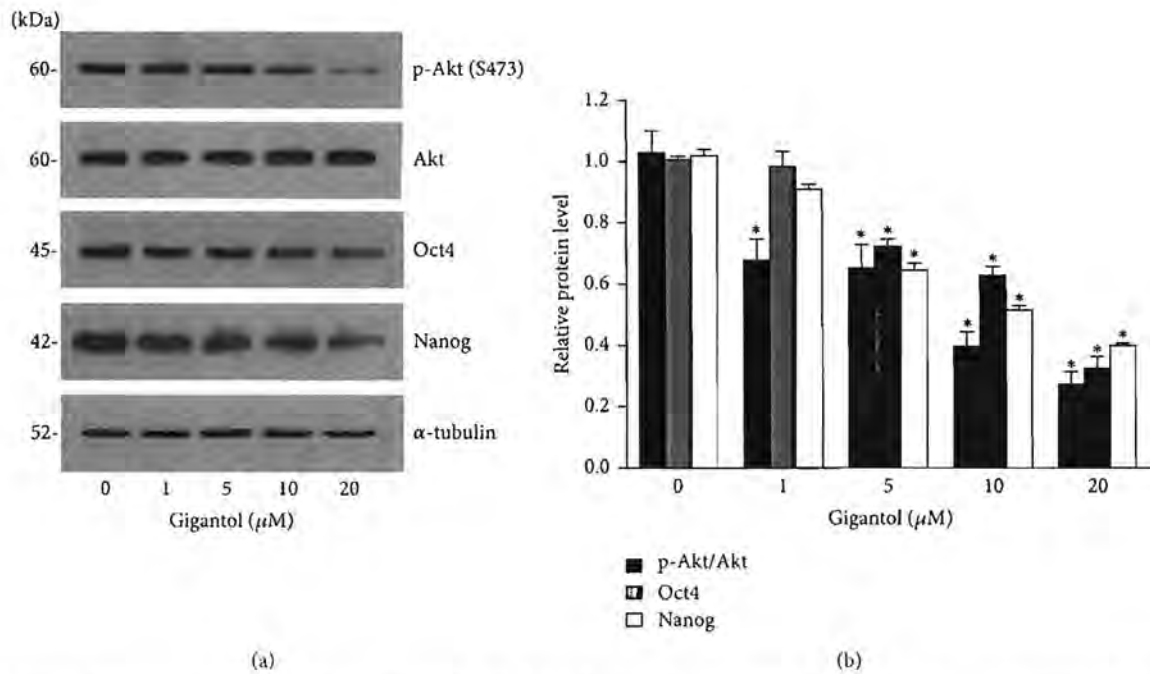


FIGURE 5: Gigantol suppresses Oct4 and Nanog through Akt-dependent mechanism. (a) After H460 cells were treated with gigantol (0–20 μ M) for 48 h, cells were collected, and the cellular levels of self-renewal pluripotency transcription factor, Oct4 and Nanog, were analyzed by Western blotting. The blots were reprobbed with α -tubulin to confirm equal loading. (b) Signals were quantified by densitometry, and mean data from independent experiments were normalized to the controls. The bars are means \pm SD ($n = 3$). * $P < 0.05$ versus nontreated cells.

To confirm the above effect of gigantol on CSCs, the lung cancer cells were similarly treated and subjected to the spheroid formation assay. Cells were pretreated with gigantol for 48 h, detached, resuspended, and seeded at low density onto ultralow attachment plates. The primary spheroids were allowed to form for 7 days (Figure 3(a)). The primary

spheroids were then detached and resuspended. The secondary spheroids were allowed to grow for 30 days in RPMI serum-free medium (Figure 3(d)). In the nontreated control cells, the cells have an ability to form aggregates and spheroids in the primary detection. Although the number and size of spheroids were found to be significantly diminished in

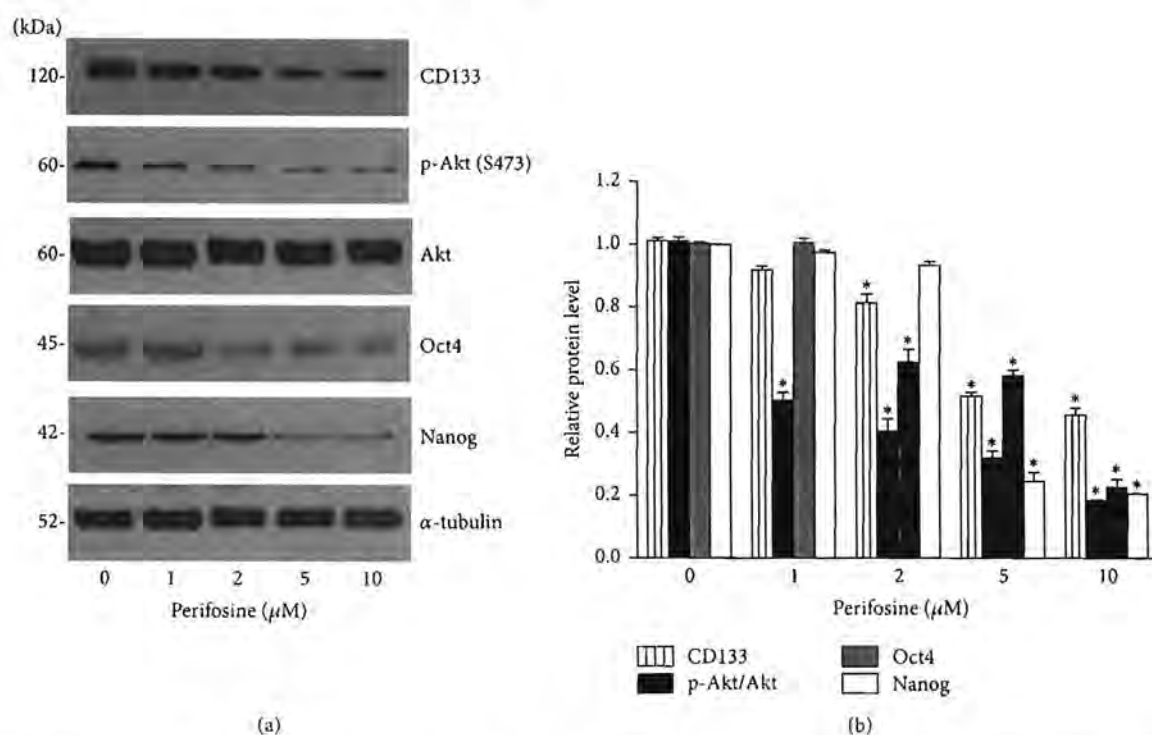


FIGURE 6: Akt inhibitor perifosine suppresses CD133, Oct4, and Nanog. (a) H460 cells were treated with perifosine (0–10 μ M) for 48 h. Cells were collected and CSCs marker CD133 and the cellular levels of self-renewal pluripotency transcription factors, Oct4 and Nanog, were analyzed by Western blotting. The blots were reprobated with α -tubulin to confirm equal loading. (b) Signals were quantified by densitometry, and mean data from independent experiments were normalized to the controls. The bars are means \pm SD ($n = 3$). * $P < 0.05$ versus nontreated cells.

the secondary spheroids, there are a number of spheroids remaining in such a condition referring to the presence of CSCs in H460 populations. Interestingly, treatment of the cells with nontoxic concentrations of gigantol dramatically reduced both number and size of tumor spheroids (Figure 3), suggesting that the compound has a suppressing effect on the CSCs populations in these cells.

3.3. Gigantol Reduces CSC Markers. Having shown that gigantol suppressed the CSCs phenotypes in the lung cancer cells, we next confirmed such observation by determining the well-known lung CSC markers. The cells were cultivated in the presence or absence of gigantol for 48 h, and the expression levels of CD133 and ALDH1A1 were determined by Western blotting. Figure 4 shows that treatment of the cells with gigantol significantly suppressed CD133 and ALDH1A1 expressions in a dose-dependent manner, confirming that gigantol suppresses CSCs phenotypes in lung cancer cells.

3.4. Gigantol Suppresses Oct4 and Nanog Reduction through Akt-Dependent Mechanism. The activity of phosphorylated Akt has been shown to link with the proliferation and self-renewal properties of normal and cancer stem cells [12, 24, 32–35]. Evidence has suggested that Akt activity resulted in the increase of cellular levels of self-renewal pluripotency transcription factor Oct4 and Nanog [25, 36, 37]. We further

tested whether gigantol suppressed the CSCs through such a pathway. Cells were treated with the nontoxic concentrations of gigantol for 48 h, and phosphorylated Akt, total Akt, Oct4, and Nanog were determined by Western blotting. Figure 5 shows that the treatment of the cells with gigantol caused decrease of phosphorylated Akt in a dose-dependent manner, whereas total Akt was not altered in comparison to those of nontreated control. Also, its downstream transcription factors including Oct4 and Nanog were found to be significantly reduced following the reduction of phosphorylated Akt. Previous study showed that perifosine (known as Akt inhibitor) reduced the number of mammospheres [38]. To confirm that gigantol regulates Nanog and Oct4 mediated by Akt-dependent mechanism, we used perifosine to study. H460 cells were treated with noncytotoxic concentrations of perifosine (0–10 μ M) for 48 h, and the stem cell-regulating proteins were analyzed using Western blot analysis. Figure 6 shows that treatment of the cells with perifosine significantly reduced phosphorylated Akt with only minimal change of total Akt. Importantly, such an Akt inhibitor significantly suppressed CD133 expression in a dose-dependent manner. Also, the downstream transcription factors including Oct4 and Nanog were found to decrease as a consequence of phosphorylated Akt reduction. Therefore, our results have demonstrated that gigantol possesses the CSCs reducing effect and could be beneficial for the treatment of lung cancer by targeting CSCs.

4. Discussion

Lung cancer has been recognized as a major cause of cancer-related death because of high incidence and relapse [39]. Recent studies have shown that the CSCs presenting in the lung cancer may facilitate the malignancy and progression of the disease [7]. Important hallmarks of CSCs are abilities to resist chemotherapeutic drugs, spread, and generate the new tumors [4, 40]. In searching for the potential compounds targeting CSCs, many researchers have focused on the compounds that can suppress stem cell-related pathways. The phosphorylated Akt, a well-known survival and proliferating signal, has been long shown to play an important role in regulating stemness in many cell models [18, 41]. In case of drug development, DC120, a novel Akt inhibitor, was shown to suppress nasopharyngeal carcinoma cancer stem-like cells [42]. Also, the short hairpin RNA of Akt is able to suppress the proliferation and self-renewal of lung cancer stem cells [18]. These data highlight the possibility that compounds inhibiting Akt pathway and related downstream stem cell pathways may benefit the treatment of lung cancer.

We have demonstrated herein for the first time that gigantol, a pure compound isolated from *Dendrobium draconis*, exhibited CSCs suppressing activity in human lung cancer cells. Treatment of the cancer cells with gigantol resulted in the decrease of CSCs indicated by the reduction of cancer cell growth in an anchorage-independent condition as well as the decrease of spheroid formation (Figures 2 and 3). As CD133 and ALDH1A1 have been widely accepted as stem cell marker in lung cancer [6, 43–46], we evaluated the expression of both proteins and found that both proteins were significantly downregulated in gigantol-treated cells. Also, gigantol was shown to suppress stemness through the inhibition of Akt-dependent Oct4 and Nanog reduction (Figure 5). Oct4 and Nanog are the transcription factors frequently found in the stem cells and their functions contribute to the self-renewal and pluripotency of stem cells. Previous studies showed that high expression or ectopic forced expression of Oct4 and Nanog in lung cancer cells transforms the lung cancer cells to CSC-like phenotypes [7, 35, 47, 48]. The high expression level of Nanog in many cancers is also recognized as an indicator of a poor prognosis [49]. Evidence suggested that Oct4 and Nanog are involved in the maintenance of pluripotency and self-renewal in CSCs. Overexpression of Oct4 and Nanog enhanced colony-forming efficiency and promoted the differentiation properties [35, 50]. The knockdown of both transcription factors was reported to decrease proliferation and invasion and reverse the epithelial-mesenchymal transition (EMT) of CSCs [7, 51]. In terms of upstream signaling pathway, Akt has been shown to modulate stem cell homeostasis in the differentiation process of embryonal carcinoma cells (ECCs). Previous studies revealed that phosphorylated Akt plays the critical role in the self-renewal of embryonic stem cells through Oct4 [24, 52]. In addition, phosphorylated Akt is important for the proliferation and maintenance of pluripotency of CSCs as well as sphere formation [53].

In conclusion, we reported a novel finding on the effect of gigantol in suppression of stemness and other CSC-like phenotypes in human lung cancer cells. We have demonstrated

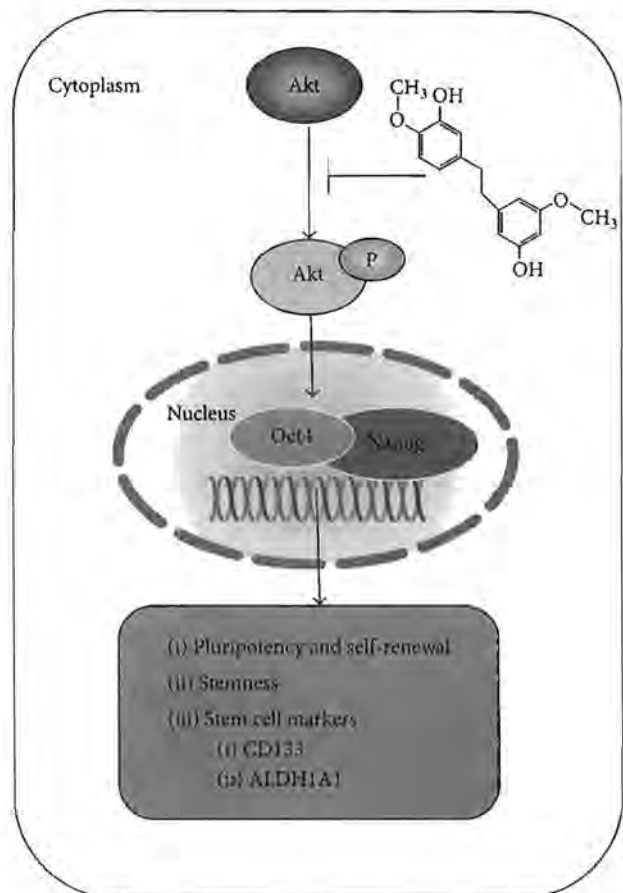


FIGURE 7: The scheme represents the effect of gigantol on human lung cancer cells. The present study reveals that gigantol has an ability to reduce CSCs markers including CD133 and ALDH1A1 in the cancer cells by suppressing the activation of protein kinase B (Akt) signal which in turn decreased the cellular levels of pluripotency and self-renewal factors Oct4 and Nanog.

that the compound suppresses CSCs features by suppressing the Akt signal leading to the decrease of stem cell factors Oct4 and Nanog (Figure 7). Because CSCs have been tightly linked to the progression of cancer, aggressiveness, and metastasis, the findings of this study could be beneficial to the development of this compound to be useful for cancer therapeutic approaches.

Conflict of Interests

The authors declare that there is no conflict of interests regarding the publication of this paper.

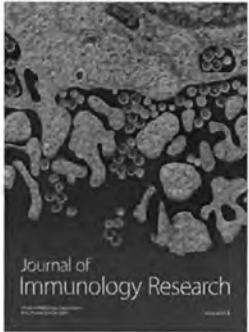
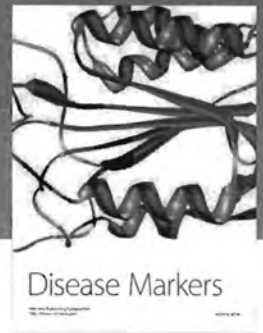
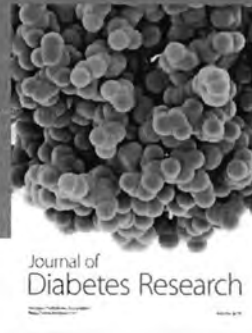
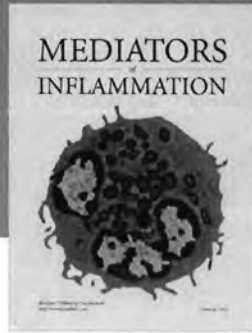
Acknowledgment

This work was supported by Thailand Research Fund (RSA5780043). The authors would like to thank Professor Boonchoo Sritularak and Professor Krich Rajprasit.

References

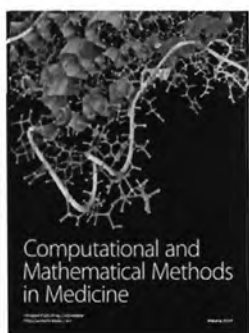
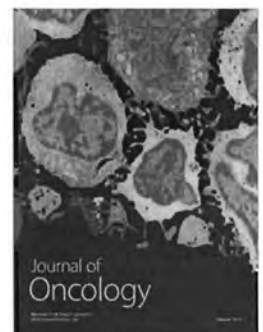
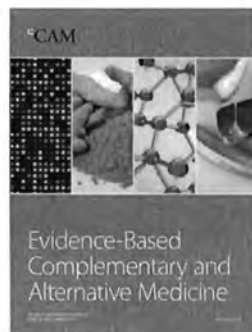
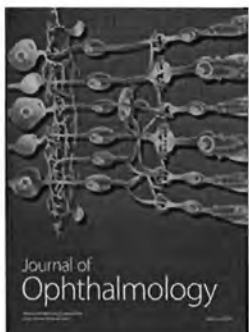
- [1] B. Bao, A. Ahmad, A. S. Azmi, S. Ali, and F. H. Sarkar, "Overview of cancer stem cells (CSCs) and mechanisms of their regulation: implications for cancer therapy," in *Current Protocols in Pharmacology*, S. J. Enna, Ed., Unit 14.25, pp. 1–14, John Wiley & Sons, 2013.
- [2] F. Li, B. Tiede, J. Massagué, and Y. Kang, "Beyond tumorigenesis: cancer stem cells in metastasis," *Cell Research*, vol. 17, no. 1, pp. 3–14, 2007.
- [3] L. Cheng, A. V. Ramesh, A. Flesken-Nikitin, J. Choi, and A. Y. Nikitin, "Mouse models for cancer stem cell research," *Toxicologic Pathology*, vol. 38, no. 1, pp. 62–71, 2010.
- [4] S. Vinogradov and X. Wei, "Cancer stem cells and drug resistance: the potential of nanomedicine," *Nanomedicine*, vol. 7, no. 4, pp. 597–615, 2012.
- [5] N. A. Lobo, Y. Shimono, D. Qian, and M. F. Clarke, "The biology of cancer stem cells," *Annual Review of Cell and Developmental Biology*, vol. 23, pp. 675–699, 2007.
- [6] N. Yongsanguanchai, V. Pongrakhananon, A. Mutirangura, Y. Rojanasakul, and P. Chanvorachote, "Nitric oxide induces cancer stem cell-like phenotypes in human lung cancer cells," *The American Journal of Physiology—Cell Physiology*, vol. 308, no. 2, pp. C89–C100, 2014.
- [7] S.-H. Chiou, M.-L. Wang, Y.-T. Chou et al., "Coexpression of Oct4 and Nanog enhances malignancy in lung adenocarcinoma by inducing cancer stem cell-like properties and epithelial-mesenchymal transdifferentiation," *Cancer Research*, vol. 70, no. 24, pp. 10433–10444, 2010.
- [8] K.-H. Wang, A.-P. Kao, C.-C. Chang, T.-C. Lin, and T.-C. Kuo, "Upregulation of *Nanog* and *Sox-2* genes following ectopic expression of Oct-4 in amniotic fluid mesenchymal stem cells," *Biotechnology and Applied Biochemistry*, 2015.
- [9] T. Nagata, Y. Shimada, S. Sekine et al., "Prognostic significance of NANOG and KLF4 for breast cancer," *Breast Cancer*, vol. 21, no. 1, pp. 96–101, 2014.
- [10] J. Shan, J. Shen, L. Liu et al., "Nanog regulates self-renewal of cancer stem cells through the insulin-like growth factor pathway in human hepatocellular carcinoma," *Hepatology*, vol. 56, no. 3, pp. 1004–1014, 2012.
- [11] S. M. Kumar, S. Liu, H. Lu et al., "Acquired cancer stem cell phenotypes through Oct4-mediated dedifferentiation," *Oncogene*, vol. 31, no. 47, pp. 4898–4911, 2012.
- [12] C. Samardzija, M. Quinn, J. K. Findlay, and N. Ahmed, "Attributes of Oct4 in stem cell biology: perspectives on cancer stem cells of the ovary," *Journal of Ovarian Research*, vol. 5, pp. 1757–2215, 2012.
- [13] Y. Atlasi, S. J. Mowla, S. A. M. Ziaee, and A.-R. Bahrami, "OCT-4, an embryonic stem cell marker, is highly expressed in bladder cancer," *International Journal of Cancer*, vol. 120, no. 7, pp. 1598–1602, 2007.
- [14] J. Zhang, L. A. Espinoza, R. J. Kinders et al., "NANOG modulates stemness in human colorectal cancer," *Oncogene*, vol. 32, no. 37, pp. 4397–4405, 2013.
- [15] C.-C. Tsai, P.-F. Su, Y.-F. Huang, T.-L. Yew, and S.-C. Hung, "Oct4 and nanog directly regulate dnmt1 to maintain self-renewal and undifferentiated state in mesenchymal stem cells," *Molecular Cell*, vol. 47, no. 2, pp. 169–182, 2012.
- [16] A. Liu, X. Yu, and S. Liu, "Pluripotency transcription factors and cancer stem cells: small genes make a big difference," *Chinese Journal of Cancer*, vol. 32, no. 9, pp. 483–487, 2013.
- [17] K. H. Noh, B. W. Kim, K.-H. Song et al., "Nanog signaling in cancer promotes stem-like phenotype and immune evasion," *The Journal of Clinical Investigation*, vol. 122, no. 11, pp. 4077–4093, 2012.
- [18] A. G. Jiang, H. Y. Lu, G. Zhang, L. X. Zhang, and X. Y. Gao, "Short hairpin RNA targeting AKT1 and PI3K/p85 suppresses the proliferation and self-renewal of lung cancer stem cells," *Molecular Medicine Reports*, vol. 12, no. 1, pp. 363–370, 2015.
- [19] W. S. Kim, Y. Zhu, Q. Deng et al., "Erythropoiesis from human embryonic stem cells through erythropoietin-independent AKT signaling," *Stem Cells*, vol. 32, no. 6, pp. 1503–1514, 2014.
- [20] Y. Lin, Z. Yang, A. Xu et al., "PIK3R1 negatively regulates the epithelial-mesenchymal transition and stem-like phenotype of renal cancer cells through the AKT/GSK3 β /CTNMB1 signaling pathway," *Scientific Reports*, vol. 5, article 8997, 2015.
- [21] A. Dubrovska, S. Kim, R. J. Salamone et al., "The role of PTEN/Akt/PI3K signaling in the maintenance and viability of prostate cancer stem-like cell populations," *Proceedings of the National Academy of Sciences of the United States of America*, vol. 106, no. 1, pp. 268–273, 2009.
- [22] R. Gargini, J. P. Cerliani, M. Escoll, I. M. Antón, and F. Wandosell, "Cancer stem cell-like phenotype and survival are coordinately regulated by Akt/FoxO/bim pathway," *Stem Cells*, vol. 33, no. 3, pp. 646–660, 2014.
- [23] D. Kumar, S. Shankar, and R. K. Srivastava, "Rottlerin-induced autophagy leads to the apoptosis in breast cancer stem cells: molecular mechanisms," *Molecular Cancer*, vol. 12, no. 1, article 171, 2013.
- [24] Y. Lin, Y. Yang, W. Li et al., "Reciprocal regulation of Akt and Oct4 promotes the self-renewal and survival of embryonal carcinoma cells," *Molecular Cell*, vol. 48, no. 4, pp. 627–640, 2012.
- [25] M.-L. Wang, S.-H. Chiou, and C.-W. Wu, "Targeting cancer stem cells: emerging role of Nanog transcription factor," *Oncotargets and Therapy*, vol. 6, pp. 1207–1220, 2013.
- [26] Q.-W. Zhao, Y.-W. Zhou, W.-X. Li et al., "Akt-mediated phosphorylation of Oct4 is associated with the proliferation of stem-like cancer cells," *Oncology Reports*, vol. 33, no. 4, pp. 1621–1629, 2015.
- [27] S. Charoenrungruang, P. Chanvorachote, B. Sritularak, and V. Pongrakhananon, "Gigantol, a bibenzyl from *Dendrobium draconis*, inhibits the migratory behavior of non-small cell lung cancer cells," *Journal of Natural Products*, vol. 77, no. 6, pp. 1359–1366, 2014.
- [28] B. Sritularak, M. Anuwat, and K. Likhitwitayawuid, "A new phenanthrenequinone from *Dendrobium draconis*," *Journal of Asian Natural Products Research*, vol. 13, no. 3, pp. 251–255, 2011.
- [29] G. Fotakis and J. A. Timbrell, "In vitro cytotoxicity assays: comparison of LDH, neutral red, MTT and protein assay in hepatoma cell lines following exposure to cadmium chloride," *Toxicology Letters*, vol. 160, no. 2, pp. 171–177, 2006.
- [30] C. Foglieni, C. Meoni, and A. M. Davalli, "Fluorescent dyes for cell viability: an application on prefixed conditions," *Histochemistry and Cell Biology*, vol. 115, no. 3, pp. 223–229, 2001.
- [31] C. Kantara, M. O'Connell, S. Sarkar, S. Moya, R. Ullrich, and P. Singh, "Curcumin promotes autophagic survival of a subset of colon cancer stem cells, which are ablated by DCLK1-siRNA," *Cancer Research*, vol. 74, no. 9, pp. 2487–2498, 2014.
- [32] A. M. Martelli, C. Evangelisti, M. Y. Follo et al., "Targeting the phosphatidylinositol 3-kinase/Akt/mammalian target of rapamycin signaling network in cancer stem cells," *Current Medicinal Chemistry*, vol. 18, no. 18, pp. 2715–2726, 2011.

- [33] D. Hambardzumyan, O. J. Becher, M. K. Rosenblum, P. P. Pandolfi, K. Manova-Todorova, and E. C. Holland, "PI3K pathway regulates survival of cancer stem cells residing in the perivascular niche following radiation in medulloblastoma in vivo," *Genes and Development*, vol. 22, no. 4, pp. 436–448, 2008.
- [34] K. C. Davidson, A. M. Adams, J. M. Goodson et al., "Wnt/ β -catenin signaling promotes differentiation, not self-renewal, of human embryonic stem cells and is repressed by Oct4," *Proceedings of the National Academy of Sciences of the United States of America*, vol. 109, no. 12, pp. 4485–4490, 2012.
- [35] P. Xenopoulos, M. Kang, A. Puliafito, S. Di Talia, and A. K. Hadjantonakis, "Heterogeneities in nanog expression drive stable commitment to pluripotency in the mouse blastocyst," *Cell Reports*, vol. 10, no. 9, pp. 1508–1520, 2015.
- [36] S. Mora-Castilla, J. R. Tejedo, A. Hmadcha et al., "Nitric oxide repression of Nanog promotes mouse embryonic stem cell differentiation," *Cell Death and Differentiation*, vol. 17, no. 6, pp. 1025–1033, 2010.
- [37] E. M. Abdelalim and I. Tooyama, "NPR-A regulates self-renewal and pluripotency of embryonic stem cells," *Cell Death and Disease*, vol. 2, no. 3, article e127, 2011.
- [38] H. Korkaya, A. Paulson, E. Charafe-Jauffret et al., "Regulation of mammary stem/progenitor cells by PI3K/Akt/ β -catenin signaling," *PLoS Biology*, vol. 7, no. 6, Article ID e1000121, 2009.
- [39] T. Tada, H. Fukuda, K. Nakagawa et al., "Non-small cell lung cancer: radiation therapy for locoregional recurrence after complete resection," *International Journal of Clinical Oncology*, vol. 10, no. 6, pp. 425–428, 2005.
- [40] J. P. Sullivan, J. D. Minna, and J. W. Shay, "Evidence for self-renewing lung cancer stem cells and their implications in tumor initiation, progression, and targeted therapy," *Cancer and Metastasis Reviews*, vol. 29, no. 1, pp. 61–72, 2010.
- [41] M. A. Lawlor and D. R. Alessi, "PKB/Akt: a key mediator of cell proliferation, survival and insulin responses?" *Journal of Cell Science*, vol. 114, no. 16, pp. 2903–2910, 2001.
- [42] J. Qin, J. Ji, R. Deng et al., "DC120, a novel AKT inhibitor, preferentially suppresses nasopharyngeal carcinoma cancer stem-like cells by downregulating Sox2," *Oncotarget*, vol. 4, 4 pages, 2015.
- [43] Y. Wu and P. Y. Wu, "CD133 as a marker for cancer stem cells: progresses and concerns," *Stem Cells and Development*, vol. 18, no. 8, pp. 1127–1134, 2009.
- [44] H. Mizugaki, J. Sakakibara-Konishi, J. Kikuchi et al., "CD133 expression: a potential prognostic marker for non-small cell lung cancers," *International Journal of Clinical Oncology*, vol. 19, no. 2, pp. 254–259, 2014.
- [45] K. Okudela, T. Woo, H. Mitsui et al., "Downregulation of ALDH1A1 expression in non-small cell lung carcinomas—its clinicopathologic and biological significance," *International Journal of Clinical and Experimental Pathology*, vol. 6, no. 1, pp. 1–12, 2013.
- [46] M. Patel, L. Lu, D. S. Zander, L. Sreerama, D. Cocò, and J. S. Moreb, "ALDH1A1 and ALDH3A1 expression in lung cancers: correlation with histologic type and potential precursors," *Lung Cancer*, vol. 59, no. 3, pp. 340–349, 2008.
- [47] X. Zhang, Y. Lou, H. Wang et al., "Wnt signaling regulates the stemness of lung cancer stem cells and its inhibitors exert anticancer effect on lung cancer SPC-A1 cells," *Medical Oncology*, vol. 32, no. 4, 2015.
- [48] C. R. Jeter, B. Liu, X. Liu et al., "NANOG promotes cancer stem cell characteristics and prostate cancer resistance to androgen deprivation," *Oncogene*, vol. 30, no. 36, pp. 3833–3845, 2011.
- [49] M. Zhu, F. Yin, L. Yang et al., "Contribution of TIP30 to chemoresistance in laryngeal carcinoma," *Cell Death and Disease*, vol. 5, no. 10, article e1468, 2014.
- [50] C.-E. Huang, F.-W. Hu, C.-H. Yu et al., "Concurrent expression of Oct4 and Nanog maintains mesenchymal stem-like property of human dental pulp cells," *International Journal of Molecular Sciences*, vol. 15, no. 10, pp. 18623–18639, 2014.
- [51] E. M. Abdelalim and I. Tooyama, "Knockdown of p53 suppresses Nanog expression in embryonic stem cells," *Biochemical and Biophysical Research Communications*, vol. 443, no. 2, pp. 652–657, 2014.
- [52] Y.-D. Wang, N. Cai, X.-L. Wu, H.-Z. Cao, L.-L. Xie, and P.-S. Zheng, "OCT4 promotes tumorigenesis and inhibits apoptosis of cervical cancer cells by miR-125b/BAK1 pathway," *Cell Death and Disease*, vol. 4, no. 8, article e760, 2013.
- [53] S. Matsubara, Q. Ding, Y. Miyazaki, T. Kuwahata, K. Tsukasa, and S. Takao, "MTOR plays critical roles in pancreatic cancer stem cells through specific and stemness-related functions," *Scientific Reports*, vol. 3, article 3230, 2013.




Hindawi

Submit your manuscripts at
<http://www.hindawi.com>





Triclosan Potentiates Epithelial-To-Mesenchymal Transition in Anoikis-Resistant Human Lung Cancer Cells

Thidarat Winitthana¹, Somsong Lawanprasert¹, Pithi Chanvorachote^{1,2*}

¹ Department of Pharmacology and Physiology, Faculty of Pharmaceutical Sciences, Chulalongkorn University, Bangkok, Thailand, ² Cell-Based Drug and Health Product Development Research Unit, Faculty of Pharmaceutical Sciences, Chulalongkorn University, Bangkok, Thailand

Abstract

Alteration of cancer cell toward mesenchymal phenotype has been shown to potentiate tumor aggressiveness by increasing cancer cell metastasis. Herein, we report the effect of triclosan, a widely used antibacterial agent found in many daily products, in enhancing the epithelial-to-mesenchymal transition (EMT) in aggressive anoikis resistant human H460 lung cancer cells. EMT has been long known to increase abilities of the cells to increase migration, invasion, and survival in circulating system. The present study reveals that treatment of the cancer cells with triclosan at the physiologically related concentrations significantly increased the colony number of the cancer cells assessed by tumor formation assay. Also, the mesenchymal-like morphology and decrease in cell-to-cell adhesion were observed in triclosan-treated cells. Importantly, western blot analysis revealed that triclosan-treated cells exhibited decreased E-cadherin, while the levels of EMT markers, namely N-cadherin, vimentin, snail and slug were found to be significantly up-regulated. Furthermore, EMT induced by triclosan treatment was accompanied by the activation of focal adhesion kinase/ATP dependent tyrosine kinase (FAK/Akt) and Ras-related C3 botulinum toxin substrate 1 (Rac1), which enhanced the ability of the cells to migrate and invade. In conclusion, we demonstrated for the first time that triclosan may potentiate cancer cells survival in detached condition and motility via the process of EMT. As mentioned capabilities are required for success in metastasis, the present study provides the novel toxicological information and encourages the awareness of triclosan use in cancer patients.

Citation: Winitthana T, Lawanprasert S, Chanvorachote P (2014) Triclosan Potentiates Epithelial-To-Mesenchymal Transition in Anoikis-Resistant Human Lung Cancer Cells. PLoS ONE 9(10): e110851. doi:10.1371/journal.pone.0110851

Editor: Aamir Ahmad, Wayne State University School of Medicine, United States of America

Received: July 21, 2014; **Accepted:** September 24, 2014; **Published:** October 16, 2014

Copyright: © 2014 Winitthana et al. This is an open-access article distributed under the terms of the Creative Commons Attribution License, which permits unrestricted use, distribution, and reproduction in any medium, provided the original author and source are credited.

Data Availability: The authors confirm that all data underlying the findings are fully available without restriction. All relevant data are within the paper.

Funding: This research was supported by the Thailand Research Fund (to PC) (<http://www.trf.or.th>), Ratchadaphiseksomphot Endowment Fund of Chulalongkorn University (RES560530132-HR), the 90th Anniversary of Chulalongkorn University Fund (Ratchadaphiseksomphot Endowment Fund), and the Chulalongkorn University Graduate Scholarship to Commemorate the 72nd Anniversary of His Majesty King Bhumibol Adulyadej (<http://www.grad.chula.ac.th/eng/scholarships>). The funders had no role in study design, data collection and analysis, decision to publish, or preparation of the manuscript.

Competing Interests: The authors have declared that no competing interests exist.

* Email: pithi.c@chula.ac.th

Introduction

The well-known broad-spectrum anti-bacterial agent triclosan (2,4,4'-trichloro-2'-hydroxydiphenyl ether; TCS) (Figure 1A) has been commercially used in a variety of products to inhibit the growth of bacteria, fungi, and mildew [1,2]. TCS has been used under the regulation of the Food and Drug Administration (in cosmetics, deodorant, hand soaps, toothpaste) as well as the Environmental Protection Agency (in materials preservative incorporated into household plastics and textiles) [2,3]. The concentrations used of TCS in different products may vary; however, its levels in most personal care products range from 0.1–2% [1,3]. The fact that the significant levels of TCS are detectable in the plasma of TCS-exposed human at the concentration ranging from 0.02 and 20 µg/ml (0.069 and 69 µM) leads to the possible conception that this agent may possibly impact human physiology [4].

Focusing on cancer, up-to-date information has pointed out that TCS has insignificant effects on carcinogenesis and direct gene mutation [2,5,6]. However, considering that TCS is a substance that people can be exposed to for a long period in their life, it is important to fully understand the possible effects of this agent not only on carcinogenesis but also the possible impact on cancer cell

behaviors. Recent studies have indicated that the transition of cellular phenotype from epithelial to mesenchymal named epithelial-to-mesenchymal transition (EMT) is a critical factor in facilitating metastasis of many cancers [7–9]. EMT has received considerable attention in cancer-related researches and EMT has been recognized as a hallmark of cancer stemness as well as aggressiveness [10]. EMT process has resulted in the alteration of cell behaviors which, in most cases, enhances ability to metastasize, including potentiated migration of the cells from its primary tumor, and increased resistance to apoptosis [11–13].

Most evidence has suggested that the sub population of cancer cells that exhibit anoikis resistant property is the majority of cells undergoing successful metastasis [14–18]. Anoikis resistant cells are also known as circulating tumor cells (CTCs) [19]. In clinical practice, CTCs have been considered to be a potential biomarker that reflects cancer aggressiveness of many types of cancer including breast, prostate, colorectal, bladder, gastric, liver and lung cancers [20–24]. The presence and quantity of CTCs in peripheral blood are shown to correlate well with poor prognosis in cancer patients [19,20]. The population of CTCs exhibit heterogeneous cell phenotypes including epithelial, mesenchymal, and those phenotypes in a transitional state from epithelial to mesenchymal [20,24–27]. As the process of EMT resulted in the

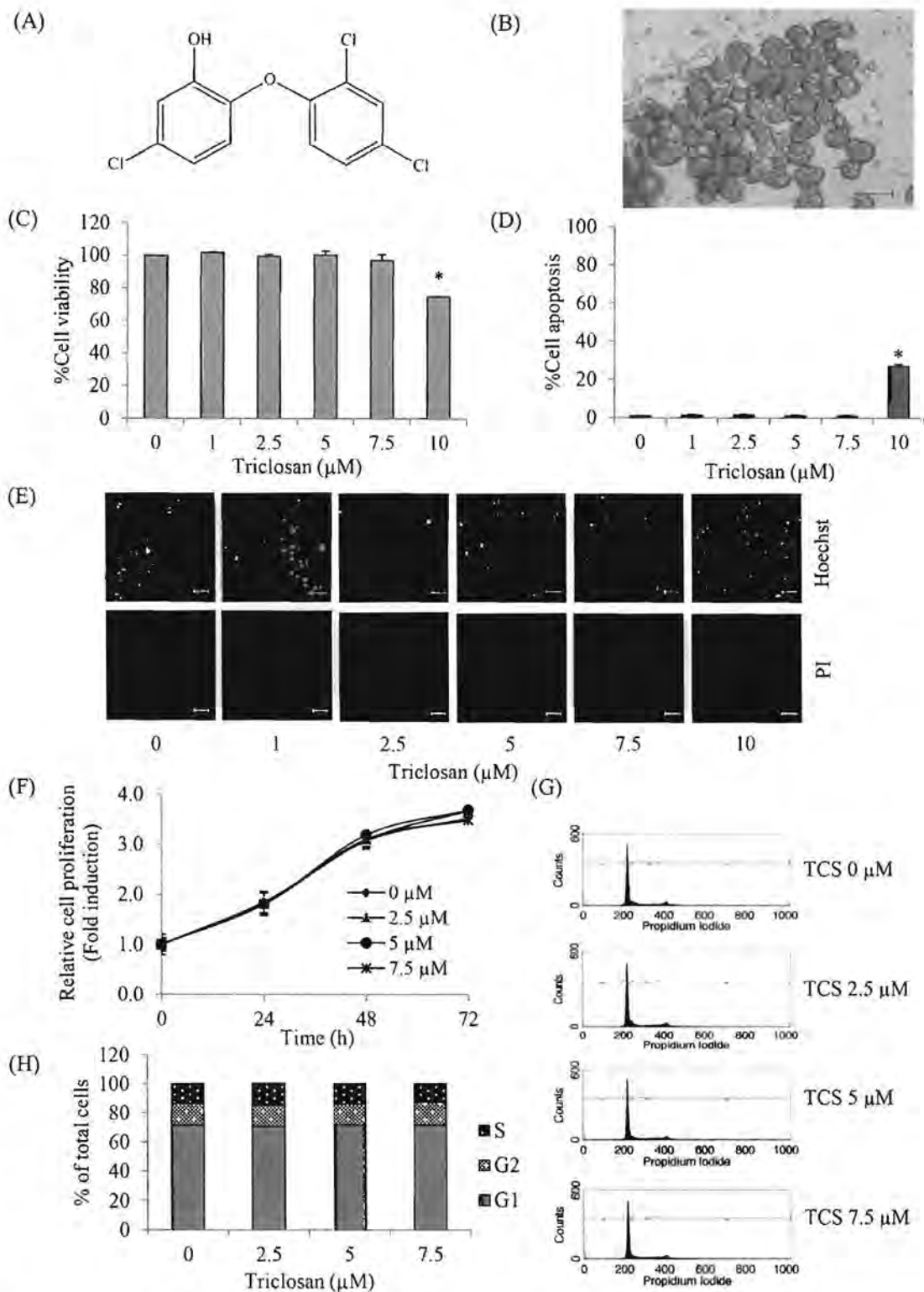


Figure 1. Cytotoxic effect and proliferative effect of TCS on anoikis resistant H460 cells. (A) The chemical structure of TCS. (B) Multicellular aggregation of anoikis resistant H460 cells. Scale bar is 1,000 μm . (C–D) After treatment with TCS (0–10 μM) for 24 h, the percentage of cell viability was determined by MTT assay and the percentage of apoptotic cells was detected by Hoechst33342 staining, respectively. Values are means of the three independent triplicate samples \pm SE. * $P < 0.05$ versus non-treated control. (E) After the indicated treatment, nuclear morphology of the cells was detected by Hoechst33342/PI co-staining assay and visualized under a fluorescence microscope. Scale bar is 50 μm . (F) Cells were treated with TCS (0–7.5 μM) for 24, 48 or 72 h. Cell viability was determined by MTT assay. The data represent the means of the three independent triplicate samples \pm SE. * $P < 0.05$ versus non-treated control at each indicated time. (G–H) Cells were treated with TCS (0–7.5 μM) for 48 h. Cell cycle of TCS-treated cells was determined by PI staining and flow cytometry. * $P < 0.05$ versus non-treated control. doi:10.1371/journal.pone.0110851.g001

mesenchymal phenotypes with increase metastasis potencies including anoikis resistance and invasive ability of cells [14,20,23] factors or stimuli that facilitate this EMT in CTCs may alter the phenotypes of CTCs population and affect the metastasis potentials of the cells. As CTCs are found in systemic circulation [19,24,28], the cells are likely to be exposed to several chemicals existing in the blood. Based on such a concern, several compounds have been investigated and reported to have an EMT-inducing property such as TGF- β [29,30], epidermal growth factor [31,32], celecoxib [33] gefitinib [34] and hexavalent chromium [35].

Although the presence of certain concentrations of TCS has been reported in human circulations, the information regarding effects of such an agent on EMT process of CTCs is still largely unknown. The present study aims to investigate the effects as well as the possible effects of this compound on the aggressive population of lung cancer cells. Better understandings obtained from this study may contribute to the safer use of TCS and provide new assessment approaches for cancer-related toxicity.

Materials and Methods

1. Cells and reagents

NCI-H460 was obtained from the American Type Culture Collection (ATCC, Manassas, VA, USA). The cancer cells were cultured in RPMI-1640 medium supplemented with 10% fetal bovine serum (FBS), 2 mM L-glutamine, 100 IU/ml penicillin, and 100 μ g/ml streptomycin (Life technologies, MD, USA) in 37°C with 5% CO₂ humidified incubator. Triclosan was obtained from Sigma (St. Louis, MO, USA). TCS was diluted with sterile medium to achieve the working concentrations with 0.1% DMSO in the final solution. As regards the sources of reagents, Hoechst33342, propidium iodide (PI), phalloidin tetramethylrhodamine B isothiocyanate, bovine serum albumin (BSA) and dimethylsulfoxide (DMSO) were purchased from Sigma (St. Louis, MO, USA). 3-(4,5-Dimethylthiazol-2-yl)-2,5-diphenyltetrazolium bromide (MTT) were purchased from Gibco (Life technologies, MD, USA). Matrigel was obtained from BD Biosciences, Inc. (Woburn, MA, USA). BCA assay kit and Supersignal west pico chemiluminescent was obtained from Thermo Scientific, Inc. (Rockford, IL, USA). Rabbit monoclonal antibodies for E-cadherin, N-cadherin, vimentin, slug, snail, Akt, phosphorylated Akt (S473), focal adhesion kinase (FAK), phosphorylated FAK (Y397), β -actin, peroxidase conjugated anti-rabbit IgG and peroxidase conjugated anti-mouse IgG were obtained from Cell Signaling (Denvers, MA, USA). Mouse monoclonal antibodies for Active Rac1-GTP and Active Rho-GTP were obtained from NewEast Biosciences (Malvern, PA, USA). Immobilon Western chemiluminescent HRP substrate was obtained from Millipore, Corp (Billerica, MA, USA) and Thermo Fisher Scientific Inc. (Rockford, IL, USA).

2. Anoikis resistant cells

Anoikis resistant cell culture was carried out according to method of Sakuma et al. [36] and Khongmancee et al. [37] with minor modifications. In brief, attached H460 cells were trypsinized when cells reached 80–90% confluence with 0.05% trypsin/0.02% EDTA. Then cells were cultured in ultralow attachment 6-well plate (Corning Costar, MA, USA) in RPMI-1640 medium while other conditions as described for attachment culture were maintained. Cells were cultured at a density of 2×10^5 cells/ml for 48 h. Suspended cells were then collected and prepared into a single cell suspension by 1 mM EDTA treatment. Then cells were washed with complete RPMI-1640 medium. Cell viability was

measured using automated cell counter. Viable cells were used for further experiments.

3. Cell viability assay and cell proliferation assay

Cells viability was determined by MTT assay. Cells were seeded at a density of 1×10^4 cells/well onto 96-well plate overnight. After that they were treated with various concentrations of TCS for 24 h. Following the treatment, the medium was then replaced with MTT solution (5.0 mg/ml in PBS) and incubated at 37°C for 4 h. Then the medium was replaced with 100 μ l DMSO to solubilize the formazan product and the intensity of the formazan product was measured at 570 nm using a microplate reader (Anthros, Durham, NC, USA). Cell viability was expressed as the percentage calculated from the optical density of treated cells relative to the controlled cells. Meanwhile, cell proliferative effect was determined also using MTT assay. Cells were seeded at a density of 2×10^3 cells/well in 96-well plate and incubated overnight. After that, the cells were treated with various concentrations of TCS for 0, 24, 48, and 72 h. Cell proliferation was measured by MTT assay as described in cell viability assessment.

4. Nuclear staining assay

Apoptotic and necrotic cell death were determined by Hoechst33342 and PI co-staining. Cells were seeded at a density of 1×10^4 cells/well onto 96-well plate and incubated overnight. Cells were then treated with TCS for 24 h. After specific treatments, cells were incubated with 10 μ g/ml of Hoechst33342 and 5 μ g/ml of PI for 30 min at 37°C. The apoptotic cells having condensed chromatin and/or fragmented nuclei and PI-positive necrotic cells were visualized and scored under a fluorescence microscope (Olympus IX51 with DP70, Olympus America Inc., Center valley, PA, USA).

5. Cell cycle analysis

After the treatment of the cells with TCS for 48 h, the cells were trypsinized and fixed with 70% absolute ethanol at -20°C overnight. the cells were then washed with cold PBS and incubated in PI solution containing 0.1% Triton-X, 1 μ g/ml RNase, and 1 mg/ml propidium iodide at 37°C for 30 min. DNA in whole cells were stained with PI and cell cycle profile was analyzed using flow cytometry (FACSort, Becton Dickinson, Rutherford, NJ, USA).

6. Colony formation assay

Upon treatment with TCS, anchorage-independent growth was examined via colony formation assay in accordance with the method of Koleske et al. [38] with minor modifications. Briefly, cells were treated with TCS at non-toxic concentrations for 24 h and then treated with 1 mM EDTA to prepare single cell suspension. The cells were suspended in RPMI-1640 containing 10% FBS and 0.33% agarose, then 250 μ l containing 1×10^3 cells were embedded as a second layer in a 24-well plate over a 500 μ l base layer containing 10% FBS and 0.5% agarose. The cells were fed every 3 days by adding 250 μ l of complete medium. After 7 and 10 days, the resulting colonies were photographed at $\times 4$ magnification. Colony number and colony size were determined on the 10th day of culture.

7. Filopodia characterization

Filopodia was characterized by phalloidin-rhodamine staining assay as described in Kowitdamrong et al. [39]. Cells were treated with TCS at non-toxic concentrations for 24 h in detach condition and seeded at a density of 2×10^3 cells/well onto 96-well plate for

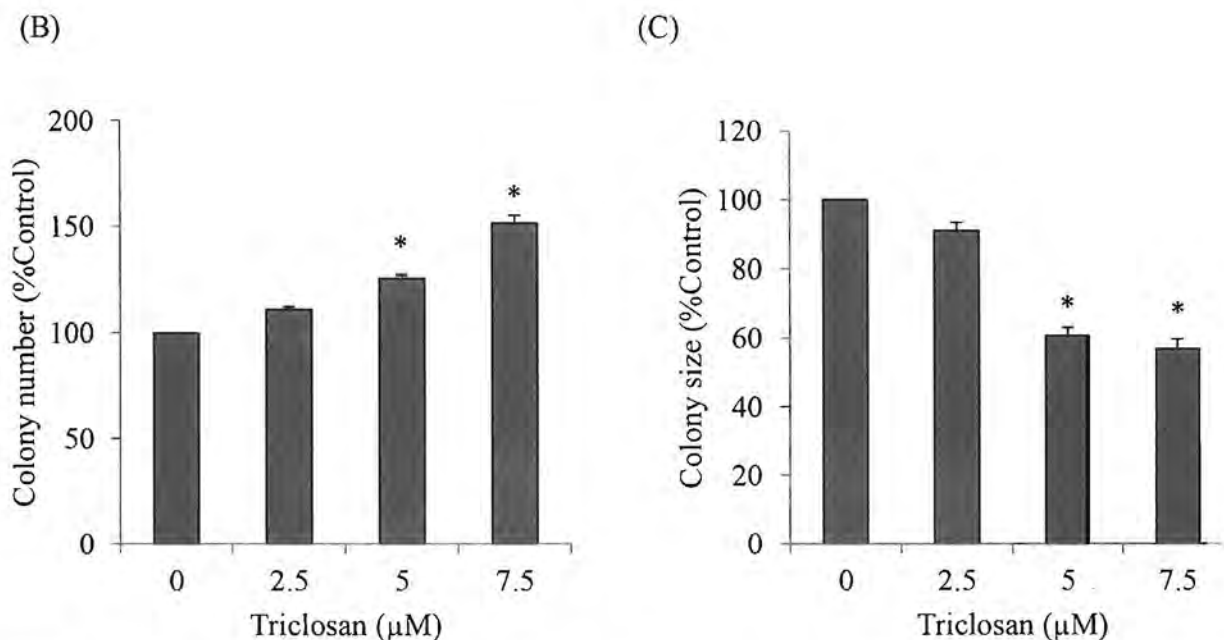
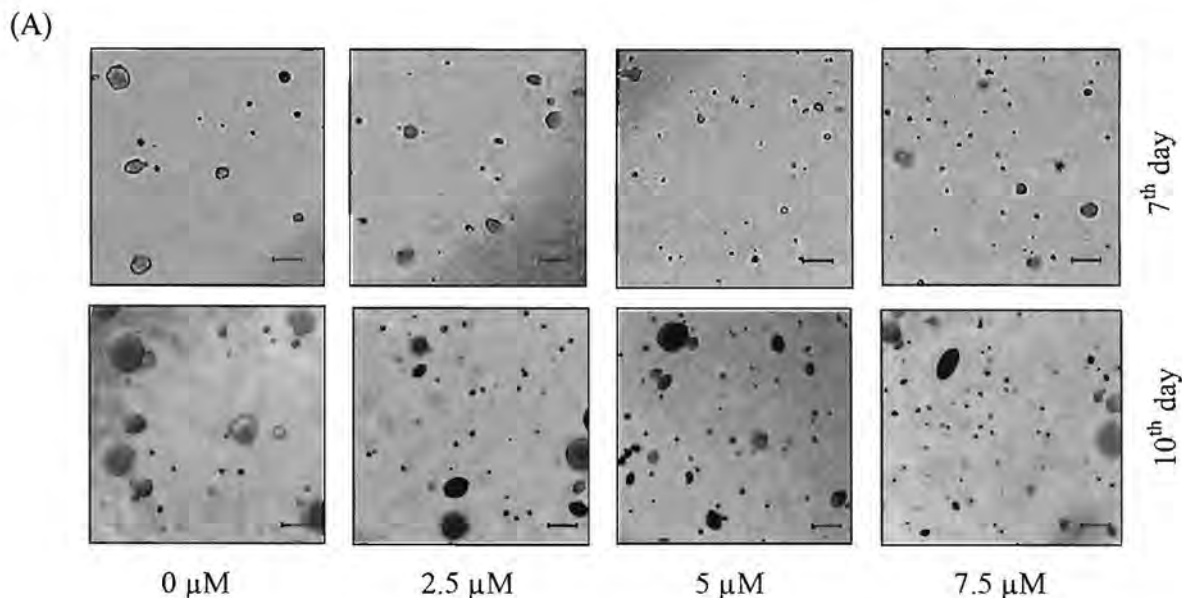


Figure 2. Effects of TCS on anchorage-independent growth of anoikis resistant H460 cells. (A) Cells were pretreated with TCS (0–7.5 μM) for 24 h and subjected to soft agar colony formation assay, as described in “Materials and Methods”. Representative fields from three independent experiments were photographed after the cells were cultured for 7 and 10 days. Scale bar is 1,000 μm . (B–C) Colony number and colony size were determined by image analyzer on the 10th day of culture. Values are means of the three independent triplicate samples \pm SE. * $P < 0.05$ versus non-treated control.

doi:10.1371/journal.pone.0110851.g002

4 h. The cells were then washed with PBS, fixed with 4% paraformaldehyde in PBS for 10 min at 37°C, permeabilized with 0.1% Triton-X100 in PBS for 4 min, and blocked with 0.2% BSA for 30 min. Following that, the cells were incubated with 1:100 phalloidin-rhodamine in PBS for 15 min and washed with PBS 3 times. Filopodia was then imaged by a fluorescence microscope (Olympus IX51 with DP70).

8. Migration assay

Migration was determined by Boyden chamber assay as previously as described in Kowitdamrong et al. [39]. Cells were pretreated with TCS at non-toxic concentrations for 24 h in detached condition. Then the cells were seeded at a density of 5×10^4 cells/well onto an upper 24-transwell plate of the transwell filter (8- μM pore) in the medium containing 0.1% serum and

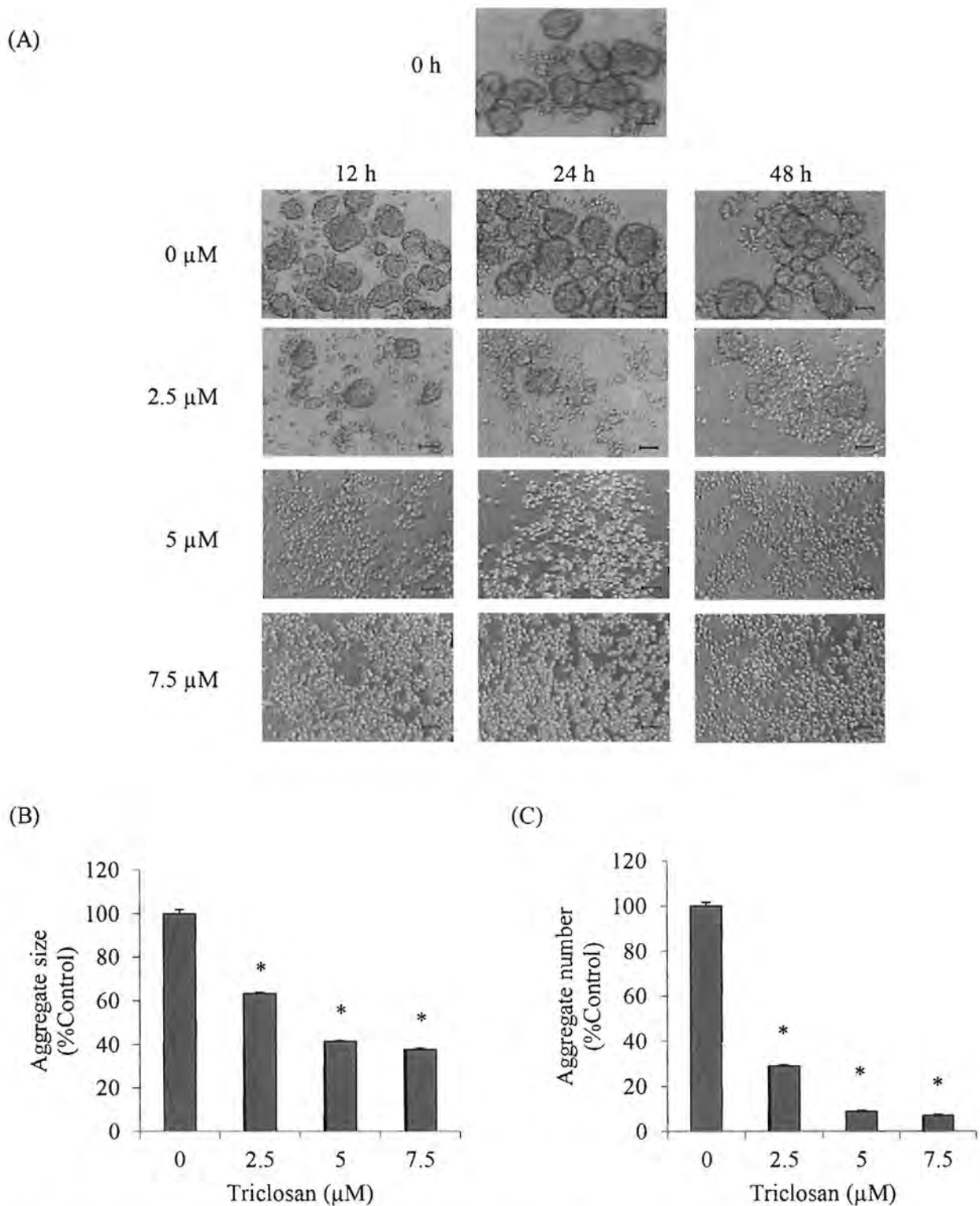
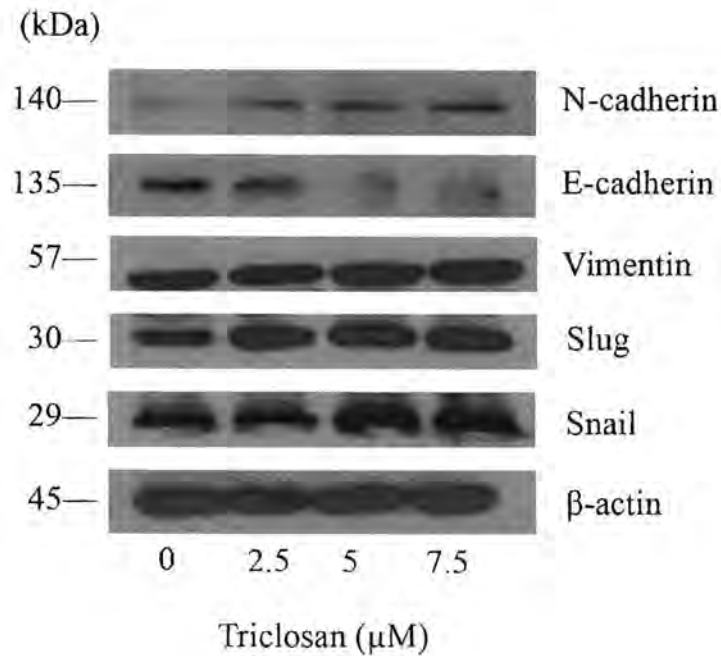


Figure 3. The effects of TCS on cell-cell interaction of anoikis resistant H460 cells. (A) Cells were treated with TCS (0–7.5 μM) for 12, 24 or 48 h in detached condition and cell-cell interaction was photographed. Scale bar is 1,000 μm . (B–C) After the treatment with TCS (0–7.5 μM) for 24 h in detached condition, aggregate size and aggregate number were determined by image analyzer. The data present means of the three independent triplicate samples \pm SE. * $P < 0.05$ versus non-treated control. doi:10.1371/journal.pone.0110851.g003

500 μl of complete medium was added to the lower chamber. After 24 h, the non-migrated cells in the upperside membrane were removed by cotton-swab wiping. The cells that migrated to

the underside of the membrane were stained with 10 $\mu\text{g/ml}$ Hoechst33342 for 30 min. The cells were then visualized and

(A)



(B)

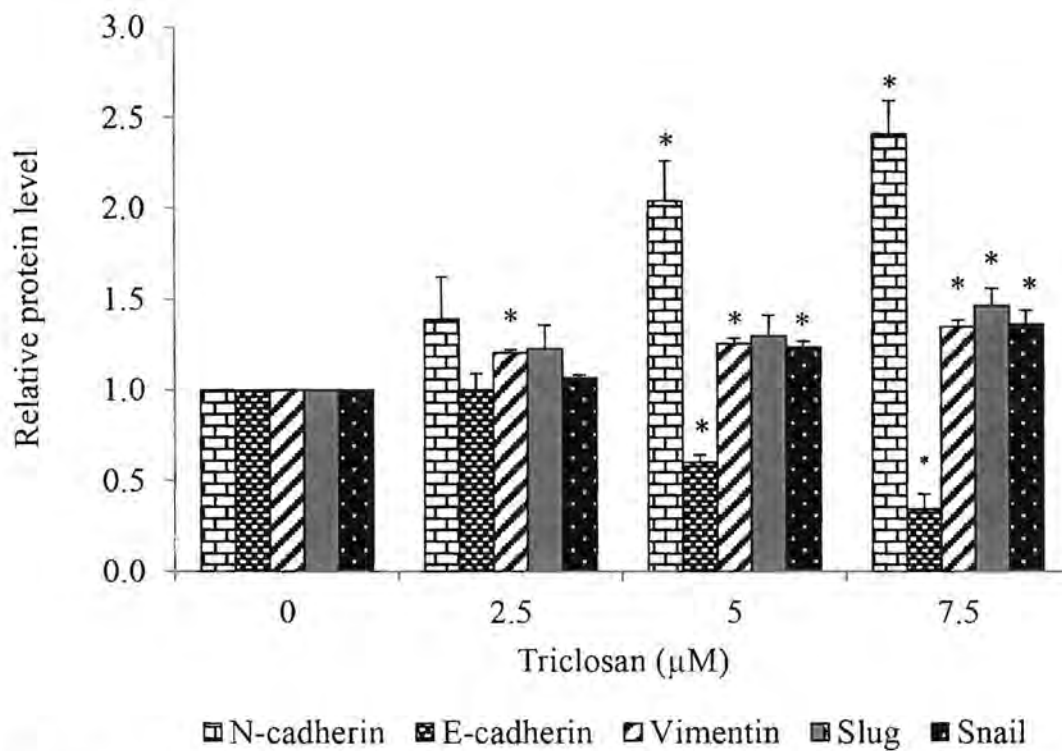


Figure 4. Effects of TCS on E-cadherin and EMT markers. (A) Anoikis resistant H460 cells were treated with TCS (0–7.5 μM) for 24 h in detached condition. The level of N-cadherin, E-cadherin, vimentin, slug and snail were determined by western blotting. Blots were reprobbed with β -actin to confirm equal loading. (B) The immunoblot signals were quantified by densitometry and mean data from independent experiments were normalized to the results. The data present means of the three independent triplicate samples \pm SE. * $P < 0.05$ versus non-treated control. doi:10.1371/journal.pone.0110851.g004

scored under a fluorescence microscope (Olympus IX51 with DP70).

9. Invasion assay

The invasion assay was carried out using 24-transwell chambers as previously as described in Kowitdamrong et al. [39]. Transwells

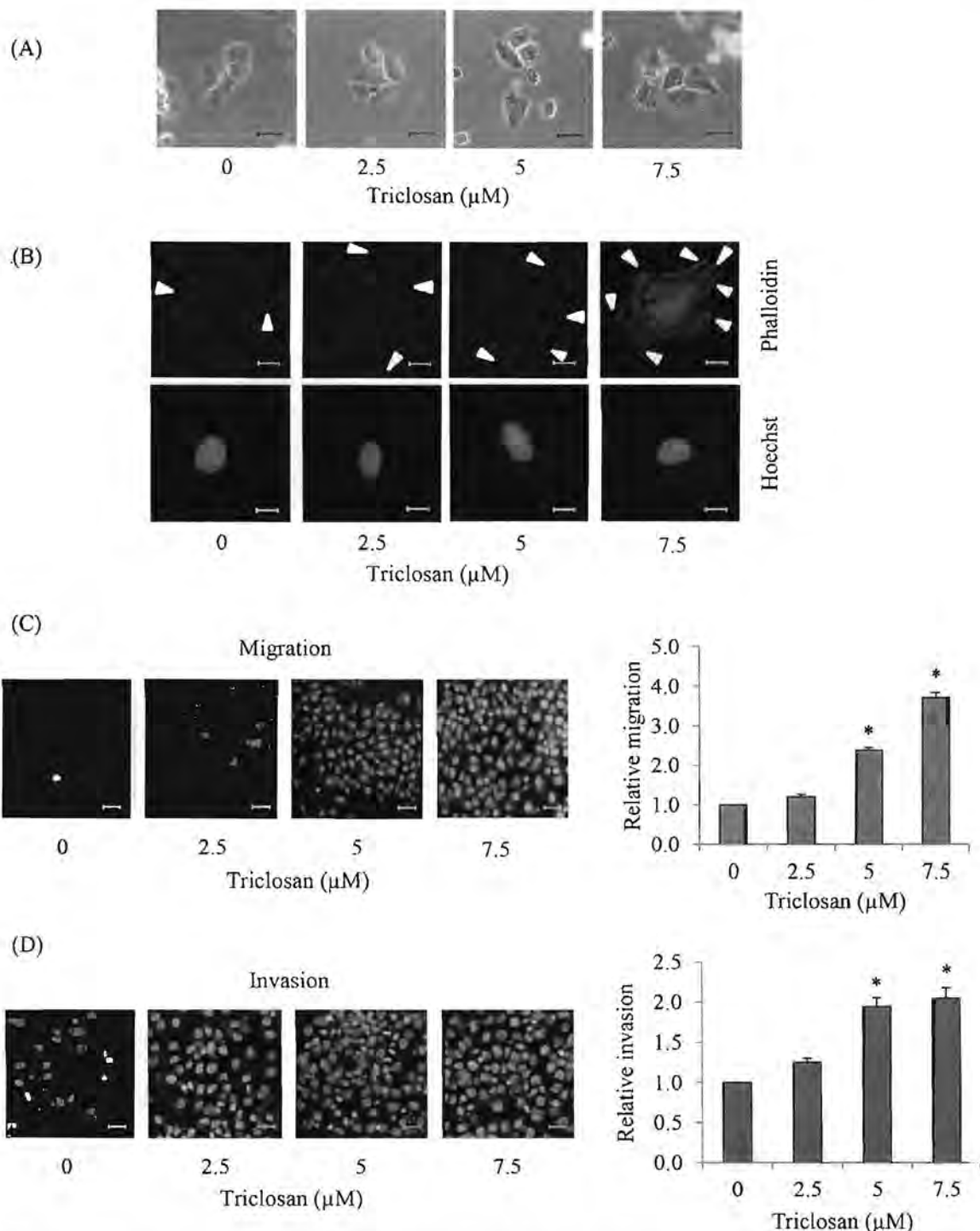
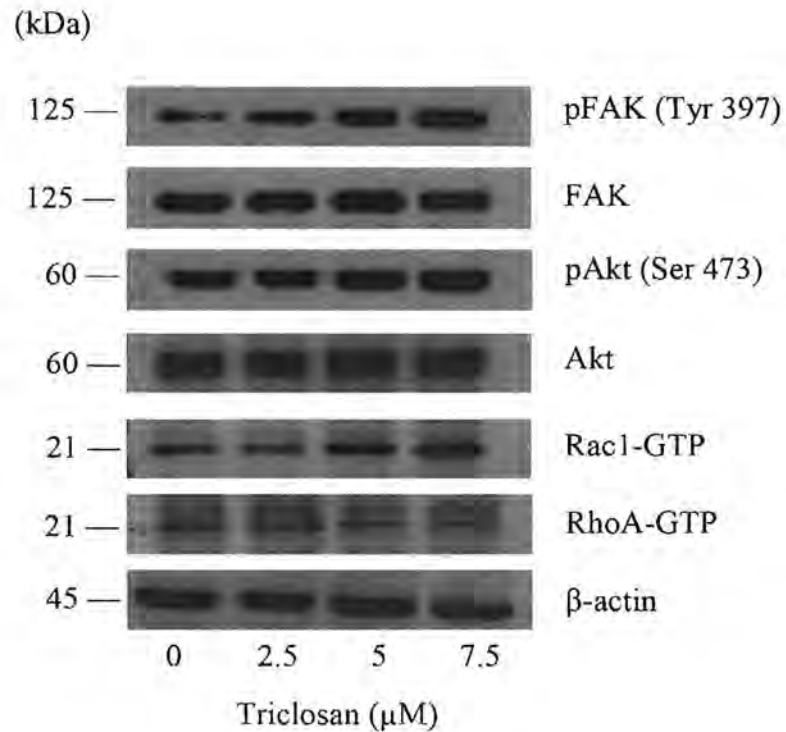


Figure 5. Effects of TCS-mediated EMT on migratory and invasive ability of anoikis resistant H460 cells. (A) Cells were treated with TCS at 0–7.5 μM for 24 h and then attached on conventional culture dishes for 4 h. Cell morphology was detected by phase contrast microscopy. Scale bar is 25 μm . (B) After the indicated treatment, filopodia and viable cells were detected by phalloidin-rhodamine or Hoechst33342 staining, respectively. Cells were visualized under fluorescence microscope. Filopodia protrusions of each treatment were indicated by arrows. Scale bar is 5 μm . (C) Cells were pretreated with TCS (0–7.5 μM) for 24 h. Transwell assay was used to investigate cell migration. Migratory cells at the basolateral side of membrane were stained with Hoechst33342 and visualized under fluorescence microscopy. Scale bar is 50 μm . The average numbers of migratory cells in each field at the basolateral side of membrane were plotted relative to the control group. Values are means of the three independent triplicate samples \pm SE. * $P < 0.05$ versus non-treated control. (D) After treatment with TCS (0–7.5 μM) for 24 h, cell invasion was evaluated using transwell coated with matrigel as described in "Materials and Methods". Invaded cells at the basolateral side of membrane were stained with Hoechst33342 and visualized under fluorescence microscopy. Scale bar is 50 μm . The average numbers of invaded cells in each field across the membrane were plotted relative to control group. Values are means of the three independent triplicate samples \pm SE. * $P < 0.05$ versus non-treated control.

doi:10.1371/journal.pone.0110851.g005

(A)



(B)

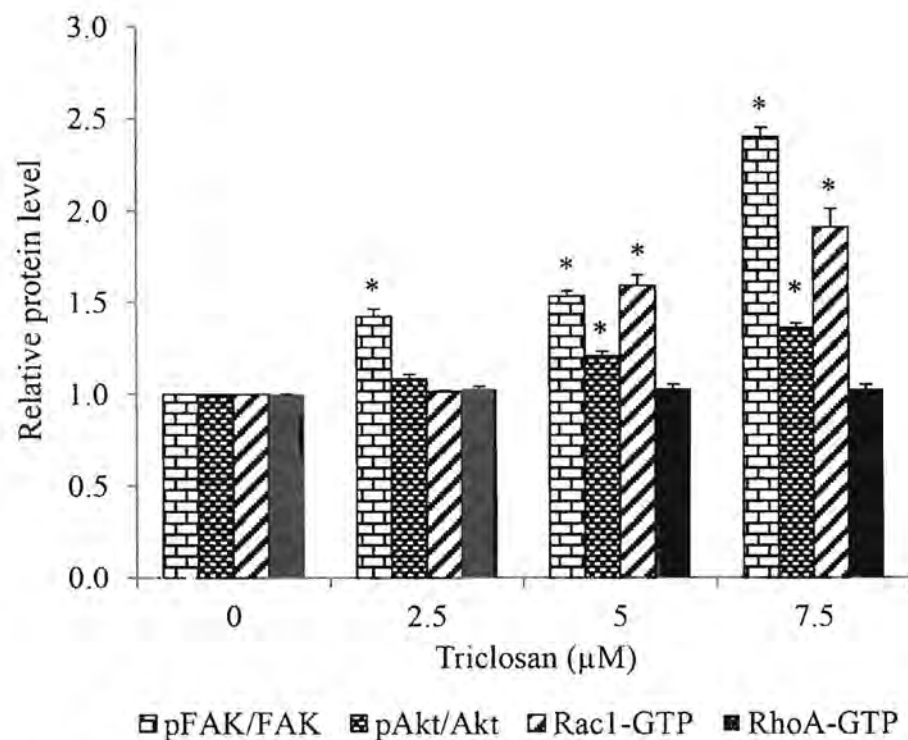


Figure 6. Effects of TCS-mediated EMT on migratory-related proteins. (A) Anoikis resistant H460 cells were treated with TCS at 0–7.5 μ M for 24 h in detached condition and then attached on conventional culture dishes for 4 h. The level of pFAK (Tyr 397), FAK, pAkt (Ser 473), Akt, activated Rac1 (Rac1-GTP) and activated RhoA (RhoA-GTP) were determined by western blotting. Blots were reprobbed with β -actin to confirm equal loading. (B) The immunoblot signals were quantified by densitometry and mean data from independent experiments were normalized to the results. Values are means of the three triplicate independent samples \pm SE, * $P < 0.05$ versus non-treated control. doi:10.1371/journal.pone.0110851.g006

were coated with 50 μ l of 0.5% matrigel on the upper surface of chamber and incubated overnight at 37°C in a humidified incubator. After treatment with TCS at non-toxic concentrations for 24 h in detached condition, cells were seeded at a density of 5×10^4 cells/well onto the upper chamber in medium containing 0.1% serum and 500 μ l of complete medium was added to the lower chamber. After 24 h, the non-invaded cells in the upper side of membrane were removed by cotton-swab wiping. Invaded cells at the basolateral side of membrane were fixed with cold absolute methanol for 10 min and stained with 10 μ g/mL Hoechst33342 for 30 min. Cells were then visualized and scored under a fluorescence microscope (Olympus IX51 with DP70).

10. Western blot analysis

After specific treatments, cells were incubated in a lysis buffer containing 20 mM Tris-HCl (pH 7.5), 1.5% Triton X-100, 150 mM sodium chloride, 10% glycerol, 1 mM sodium orthovanadate, 50 mM sodium fluoride, 1 mM phenylmethylsulfonyl fluoride, and a commercial protease inhibitor mixture (Roche Applied Science, Indianapolis, IN, USA) for 2 h on ice. Cell lysates were collected and protein content was determined using the Bradford method (Bio-Rad Laboratories, Hercules, CA). Equal amounts of protein from each sample were denatured by heating at 95°C for 5 min with loading buffer and subsequently loaded onto a 7.5% SDS-polyacrylamide gel electrophoresis for the detection of EMT markers and E-cadherin expression or 10% SDS-polyacrylamide gel electrophoresis for the detection of migratory-related protein expression. After separation, the proteins were transferred onto 0.45 μ m nitrocellulose membranes. The transferred membranes were blocked in 5% non-fat dry milk in TBST (25 mM Tris-HCl (pH 7.5), 125 mM NaCl, 0.05% Tween 20) for 1 h, and then incubated with a specific primary antibody (1:1,000 dilution) overnight at 4°C. The membranes were washed three times with TBST for 5 min and incubated with Horseradish peroxidase-coupled isotype-specific secondary antibodies (1:2,000 dilution) for 2 h at room temperature. The membranes were washed three times with TBST for 5 min and the immune complexes were detected by enhancement with a chemiluminescent substrate and quantified using analyst/PC densitometry software (Bio-Rad Laboratories, Hercules, CA, USA).

11. Statistical analysis

Data were obtained from three independent experiments and presented as means \pm standard error (SE). Statistical analyses were performed using one-way ANOVA and post hoc test (Turkey's test) at a significance level of P -values < 0.05. SPSS 17.0 was used for all statistical analyses.

Results

1. Effects of TCS on anoikis resistant H460 cells

Anoikis resistant cancer cells were used as a model for studying CTCs [36,37,40]. Anoikis resistant lung cancer cells were generated as described in Materials and Methods. It was found that detached H460 cells spontaneously formed multicellular aggregates after culture for 48 h (Figure 1B). To elucidate the possible effect of TCS on CTC lung cancer cells, cytotoxic effect of the compound on the cells was first characterized. TCS at the concentrations ranging from 0.069 and 69 μ M was found in the plasma of TCS-exposed subjects [4]. Therefore, the anoikis resistant cells were incubated with TCS at the concentrations of 0–10 μ M for 24 h and cell viability was assessed by MTT assay. Figure 1C shows that TCS treatment significantly decreased cell

survival at the dose of 10 μ M with approximately 80% of cells remaining viable, while treatment of the cells with TCS at 0–7.5 μ M caused no significant toxic effect. Hoechst33342/PI staining assay confirmed that apoptosis and necrosis were not detectable in the TCS-treated cells at 0–7.5 μ M. The apoptotic cells with fragmented or condensed nuclei were only detected in the cells treated with 10 μ M TCS (Figures 1D and E). Therefore, the concentrations of TCS at 0–7.5 μ M were used for following experiments.

Having shown the toxic effect of TCS on anoikis resistant cells, we next investigated the effects of TCS on cell proliferation and cell cycle. Cells were treated with non-toxic concentrations of TCS for 0–72 h and proliferation of the cells was determined as described in Materials and Methods. Proliferation response of anoikis resistant cells to TCS was shown in Figure 1F. TCS-treated cells showed no significant difference in terms of cell proliferation in comparison to the non-treated control cells. These results were confirmed by cell cycle analysis using PI and flow cytometry. The results indicated that TCS treatment caused no significant effects on the cell cycle (Figures 1G and 1H). Together, the results suggested that TCS possessed no proliferative effect on anoikis resistant H460 cells in normal culturing condition.

2. TCS promoting cell growth in anchorage-independent manner

Because anchorage-independent growth of the cancer cells has been shown to augment metastasis, we next investigated the effect of TCS on cancer cell growth in such condition. In doing this, anoikis resistant cells H460 were treated with TCS for 24 h before they were subjected to colony formation assay. The cells were then seeded in agarose layer to prevent cell-cell interaction and attachment. Colony number and colony size were obtained by photographing and counting after the cells were cultured for 7 and 10 days. The colony formation was shown in Figure 2A. Colony number and colony size of each treatment were calculated as a percentage of the control group and shown in Figure 2B and C, respectively. The results indicated that TCS at the concentrations of 5 and 7.5 μ M significantly increased colony formation of anoikis resistant H460 cells. However, TCS at both concentrations significantly reduced colony size in comparison to that of non-treated control group. Such observations indicated that TCS promoted anchorage-independent survival of the cells, but decreased the growth rate of the cells in detached condition. Our results consist with the previous findings that the increase in anchorage-independent survival with low proliferative ability has been observed in the cancer cells undergoing EMT [11,12,41,42].

3. TCS inhibiting cell-cell interaction

Loss of cell-cell adhesion was found in the cells during the process of EMT as a result from cadherin switching [7,8]. To examine the effect of TCS on cell-cell adhesion of anoikis resistant H460 cells, we seeded cells in 24-well low attach plate at the density of 1.5×10^5 cells/well and treated them with non-toxic concentrations of TCS. The cell-cell interaction was observed in formation of cell aggregation and photographed using a phase-contrast microscope. Aggregate size and number were determined and calculated relative to the non-treated control. Figure 3A shows that TCS treatment significantly altered the aggregate behavior of the cells to single cell suspension. Addition of TCS resulted in the significant reduction of both number and size of multi-cellular aggregates in a dose-dependent manner (Figure 3B and C). These results suggested that TCS promoted loss of cell-cell adhesion of anoikis resistant H460 cells which is a dominant characteristic of the cells undergoing EMT.

4. TCS increasing the expression of EMT markers

We next investigated the effect of TCS treatment on EMT markers including N-cadherin, vimentin, snail, and slug. Anoikis resistant H460 cells were treated with non-toxic concentrations of TCS for 24 h and EMT markers were evaluated by western blotting. Figures 4A and B show that the expression level of E-cadherin was significantly decreased in response to TCS treatment in a concentration-dependent manner. In addition, TCS significantly enhanced the increase of N-cadherin, vimentin, slug, and snail. The expression of snail was significantly enhanced by TCS treatment at 5 and 7.5 μM in a dose-dependent manner, while the expression of slug was only significantly induced by the treatment with TCS at 7.5 μM . These results suggested that TCS increased EMT phenotypes in these cells.

5. TCS-mediated EMT enhancing cells migration and invasion

An important hallmark of aggressive cancer cells is their high ability to migrate and invade [43,44]. EMT is recognized as an important factor facilitating cell motility [12,45]. Cells were treated with TCS at non-toxic concentrations for 24 h and the migration and invasion behaviors of the cells were determined as described in Materials and Methods. Figure 5A indicates that TCS-treated cells exhibited increased polarity and filopodia. Filopodia of the TCS-treated cells was stained with phalloidin-rhodamine as shown in Figure 5B. TCS-treated cells exhibited filopodia protrusions accumulating at the border of cells in a dose-dependent fashion. Additionally, migration and invasion assay revealed that TCS increased cell migration and invasion (Figures 5C and D). The above findings suggested that EMT induction upon TCS treatment promoted filopodia formation and potentiated migratory and invasive abilities of anoikis resistant H460 cells.

Furthermore, the down-stream effector proteins which are responsible for cell motility were determined using western blotting. The cells were treated with indicated concentrations of TCS for 24 h and subjected to western blot analysis. The expression levels of migratory-related proteins including activated FAK (phosphorylated FAK, Tyr 397), FAK, activated Akt (phosphorylated Akt, Ser 473), Akt, activated Rac1 (Rac1-GTP), and activated RhoA (RhoA-GTP) were investigated. Figures 6A and B show that TCS treatment significantly increased the level of phosphorylated FAK, activated Akt, and active Rac1-GTP. However, TCS possessed no significant effect on activated RhoA level. These results suggested that TCS-induced EMT promoted the motility of anoikis resistant H460 cells through the activation of FAK/Akt signaling pathway as well as Rac1 activation.

Discussion

Lung cancer has garnered most attentions in cancer research field since this type of cancers is considered as a major cause of cancer-related mortality [46]. Indeed, the high metastasis rate in such a cancer makes it the most life-threatening and in most cases metastasis is detected at the time of first diagnosis [47]. Because the ability of cancer cells to metastasize can be augmented by the process of EMT [9,12,48], the present study reporting the positive regulatory effect of TCS on the EMT of human cancer cells highlights the possible novel toxicity caused by this compound.

TCS has been widely used for over 30 years in health care products as well as in medical devices. TCS is readily and completely absorbed following oral administration. TCS has been identified in urine, plasma, and breast milk of humans with a wide range of levels depending upon the individual's daily intake, its the

concentration in the products as well as the route and frequency of administration [2,3]. The low and high concentrations of TCS in human plasma have been reported at 0.02 and 20 $\mu\text{g}/\text{ml}$ (0.069 and 69 μM) respectively [4]. Previous studies reported the possible effects of TCS in the induction of hepatocellular adenoma and carcinoma formations in rodent model [2]. Recently, Ma et al. (2013) found that TCS reduced global DNA methylation (GDM) in HepG2 cells and they proposed the reduction as the possible mechanism of TCS promoting tumor in rodents [49]. Since global DNA hypomethylation is associated with aberrant gene expression, loss of imprinting, chromosome instability and anomalies, it has been shown to play a key role in controlling EMT and cancer metastasis [50]. Thus, TCS induced global DNA hypomethylation raises a question whether TCS can promote cancer metastasis in the carcinogenesis safety aspect of this compound.

Anoikis resistant H460 cells were found to form multicellular aggregation in suspended condition and still express a high level of E-cadherin which is consistent with previous studies [36,40]. Together with this finding, the sub-population of CTCs was clinically found as multicellular aggregates with epithelial marker expression [25,51]. The transition of the cells towards mesenchymal phenotypes through EMT has been shown to enhance the ability of CTCs cells to be more aggressive in many cancers [14,20]. In this study, we employed anoikis resistant H460 cells as a model of CTCs and found that TCS enhanced EMT of such cells and promoted the ability of the cells to migrate and invade.

Our results indicated that TCS treatments significantly increased the cells' ability to survive in anchorage-independent condition (Figure 2) while decreased the proliferation rate of the cells. Such results were consistent with the previous study reporting that the cancer cells undergoing EMT possess the ability to survive in detached condition with decreased rate of growth [11,12,41,42]. The possible explanation on this phenomenon is that EMT-related transcription factors are responsible for the attenuation of cell proliferation through the impairment of cell cycle progression [41,42]. Cadherin switching from E-cadherin to N-cadherin is considered as the hallmark event of EMT [7,48,52]. Also, mesenchymal phenotypes of cells can be confirmed by the increased expression of vimentin which is a type-III intermediate filament highly expressed in mesenchymal cells [15,53] and the enhanced expression of snail and slug which are the transcription factors that regulate cadherin switching and that drive cells into EMT process [11,52,54,55]. In the present study, we found that treatment of the anoikis resistant cells with TCS significantly mediated cadherin switch and increased vimentin, snail, and slug (Figure 4). Because TCS was shown to decrease the level of GDM in cancer cells [49] and global DNA hypomethylation was related to EMT and stem-like phenotype [50], the possible mechanism of TCS to induce snail and slug expression in this case may be, at least in part, due to such effects of TCS on global DNA hypomethylation.

Several studies have reported that FAK plays an important role in dynamic turnover of focal adhesion of cells, increases filopodia formation and also modulates cell migration. FAK activation was reported to lead to the phosphorylation of Akt, which resulted in cell movement [39,56]. FAK/Akt phosphorylation also activated the GTP-binding of several Rho-family GTPases such as Rac1 and RhoA. Rac1 is essential to stimulate the formation of membrane ruffling, lamellipodia and focal-complex formation, while RhoA induces the formation of stress fibres and focal adhesion [56,57]. We found that TCS-induced EMT significantly promoted FAK/Akt activation as well as Rac1 activation. However, TCS possessed no effect on the level of RhoA-GTP. These results were consistent with previous reports that N-

cadherin and slug were able to activate Akt pathway involving in cell survival and migration [7,58]. In addition, N-cadherin increased steady-state levels of activated Rac1, which resulted in the increase of actin remodeling [7]. Moreover when cells undergo EMT, free p120-catenin in cytoplasm was recruited to N-cadherin on cell surface, which resulted in the activation of Rac1 and the subsequent inhibition of RhoA activation [59].

In summary, our findings highlighted the effects of TCS in inducing EMT process in anoikis resistant human lung cancer cells. TCS-treated cells exhibited increased EMT phenotypes including increased anchorage-independent survival, low cellular proliferation and loss of cell-cell adhesion. Importantly, TCS promoted the cadherin switch and increased vimentin, snail, and slug. In addition, we found that such TCS-mediated EMT enhanced the ability of the cells to migrate and invade through FAK/Akt and Rac1-dependent mechanisms. Consequently, such

findings show the potential effect of TCS in promoting EMT in CTCs which may result in cancer aggressiveness. Furthermore, this study provides some new toxicological information regarding TCS, which should lead to caution in the use of TCS in cancer patients.

Acknowledgments

The authors wish to thank Dr. Phisit Khemawoot for providing the reagent used for this research.

Author Contributions

Conceived and designed the experiments: PC. Performed the experiments: TW. Analyzed the data: TW PC. Contributed reagents/materials/analysis tools: PC. Contributed to the writing of the manuscript: PC TW SL.

References

- Jones RD, Jampani HB, Newman JL, Lee AS (2000) Triclosan: A review of effectiveness and safety in health care settings. *American Journal of Infection Control* 28: 184–196.
- Rodricks JV, Swenberg JA, Borzelleca JF, Maronpot RR, Shipp AM (2010) Triclosan: A critical review of the experimental data and development of margins of safety for consumer products. *Critical Reviews in Toxicology* 40: 422–484.
- Fang JL, Stingley RL, Beland FA, Harrouk W, Lumpkins DL, et al. (2010) Occurrence, efficacy, metabolism, and toxicity of triclosan. *Journal of Environmental Science and Health - Part C Environmental Carcinogenesis and Ecotoxicology Reviews* 28: 147–171.
- Henry ND, Fair PA (2013) Comparison of in vitro cytotoxicity, estrogenicity and anti-estrogenicity of triclosan, perfluorooctane sulfonate and perfluorooctanoic acid. *Journal of Applied Toxicology* 33: 265–272.
- Dayan AD (2007) Risk assessment of triclosan in human breast milk. *Food and Chemical Toxicology* 45: 125–129.
- Ciniglia C, Cascone C, Giudice RL, Pinto G, Pollio A (2005) Application of methods for assessing the geno- and cytotoxicity of Triclosan to *C. ehrenbergii*. *Journal of Hazardous Materials* 122: 227–232.
- Whelock MJ, Shintani Y, Maeda M, Fukumoto Y, Johnson KR (2008) Cadherin switching. *Journal of Cell Science* 121: 727–735.
- Under TT, Gupta PB, Mani SA, Yang J, Lander ES, et al. (2008) Loss of E-cadherin promotes metastasis via multiple downstream transcriptional pathways. *Cancer Research* 68: 3645–3654.
- Shi Y, Wu H, Zhang M, Ding L, Meng F, et al. (2013) Expression of the epithelial-mesenchymal transition-related proteins and their clinical significance in lung adenocarcinoma. *Diagnostic Pathology* 8: 1–8.
- Chunhacha P, Sriurapong V, Chanvorachote P (2013) Epithelial-mesenchymal transition mediates anoikis resistance and enhances invasion in pleural effusion-derived human lung cancer cells. *Oncology Letters* 5: 1043–1047.
- Nurwidya F, Takahashi F, Murakami A, Takahashi K (2012) Epithelial mesenchymal transition in drug resistance and metastasis of lung cancer. *Cancer Research and Treatment* 44: 151–156.
- Voulgari A, Pintzas A (2009) Epithelial-mesenchymal transition in cancer metastasis: Mechanisms, markers and strategies to overcome drug resistance in the clinic. *Biochimica et Biophysica Acta - Reviews on Cancer* 1796: 75–90.
- Klymkowsky MW, Savagner P (2009) Epithelial-mesenchymal transition: A cancer researcher's conceptual friend and foe. *American Journal of Pathology* 174: 1588–1593.
- Kim YN, Koo KH, Sung JY, Yun UJ, Kim H (2012) Anoikis resistance: An essential prerequisite for tumor metastasis. *International Journal of Cell Biology* 2012: 1–11.
- Guadamillas MC, Cerezo A, del Pozo MA (2011) Overcoming anoikis - pathways to anchorage-independent growth in cancer. *Journal of Cell Science* 124: 3189–3197.
- Chunhacha P, Chanvorachote P (2012) Roles of caveolin-1 on anoikis resistance in non-small cell lung cancer. *International Journal of Physiology, Pathophysiology and Pharmacology* 4: 149–155.
- Taddei ML, Giannoni E, Fiaschi T, Chiarugi P (2012) Anoikis: An emerging hallmark in health and diseases. *Journal of Pathology* 226: 380–393.
- Chiarugi P, Giannoni E (2008) Anoikis: A necessary death program for anchorage-dependent cells. *Biochemical Pharmacology* 76: 1352–1364.
- Liberko M, Kolostova K, Bobek V (2013) Essentials of circulating tumor cells for clinical research and practice. *Critical Reviews in Oncology/Hematology* 88: 338–356.
- Sun YF, Yang XR, Zhou J, Qiu SJ, Fan J, et al. (2011) Circulating tumor cells: Advances in detection methods, biological issues, and clinical relevance. *Journal of Cancer Research and Clinical Oncology* 137: 1151–1173.
- Paterlini-Brechot P, Benali NL (2007) Circulating tumor cells (CTC) detection: Clinical impact and future directions. *Cancer Letters* 253: 180–204.
- Franco R, Cantile M, Marino FZ, Pirozzi G (2012) Circulating tumor cells as emerging tumor biomarkers in lung cancer. *Journal of Thoracic Disease* 4: 438–439.
- Gorges TM, Pantel K (2013) Circulating tumor cells as therapy-related biomarkers in cancer patients. *Cancer Immunology, Immunotherapy* 62: 931–939.
- O'Flaherty JD, Gray S, Richard D, Fenell D, O'Leary JJ, et al. (2012) Circulating tumor cells, their role in metastasis and their clinical utility in lung cancer. *Lung Cancer* 76: 19–25.
- Hou JM, Krebs M, Ward T, Sloane R, Priest L, et al. (2011) Circulating tumor cells as a window on metastasis biology in lung cancer. *American Journal of Pathology* 178: 989–996.
- Armstrong AJ, Marengo MS, Oltean S, Kemeny G, Bitting RL, et al. (2011) Circulating tumor cells from patients with advanced prostate and breast cancer display both epithelial and mesenchymal markers. *Molecular Cancer Research* 9: 997–1007.
- Barriere G, Tartary M, Rigaud M (2012) Epithelial mesenchymal transition: a new insight into the detection of circulating tumor cells. *ISRN Oncol* 2012: 382010.
- Chaffer CL, Weinberg RA (2011) A perspective on cancer cell metastasis. *Science* 331: 1559–1564.
- Xu J, Lamouille S, Derynck R (2009) TGF-beta-induced epithelial to mesenchymal transition. *Cell Res* 19: 156–172.
- Kawata M, Koinuma D, Ogami T, Umezawa K, Iwata C, et al. (2012) TGF-beta-induced epithelial-mesenchymal transition of A549 lung adenocarcinoma cells is enhanced by pro-inflammatory cytokines derived from RAW 264.7 macrophage cells. *Journal of Biochemistry* 151: 205–216.
- Cheng J-C, Auersperg N, Lung PCK (2012) EGF-Induced EMT and Invasiveness in Serous Borderline Ovarian Tumor Cells: A Possible Step in the Transition to Low-Grade Serous Carcinoma Cells? *PLoS ONE* 7: e34071.
- Zhang S, Wang X, Iqbal S, Wang Y, Osunkoya AO, et al. (2013) Epidermal growth factor promotes protein degradation of epithelial protein lost in neoplasm (EPLIN), a putative metastasis suppressor, during epithelial-mesenchymal transition. *J Biol Chem* 288: 1469–1479.
- Wang ZL, Fan ZQ, Jiang HD, Qu JM (2013) Selective Cox-2 inhibitor celecoxib induces epithelial-mesenchymal transition in human lung cancer cells via activating MEK-ERK signaling. *Carcinogenesis* 34: 638–646.
- Rho JK, Choi YJ, Lee JK, Ryou BY, Na H, et al. (2009) Epithelial to mesenchymal transition derived from repeated exposure to gefitinib determines the sensitivity to EGFR inhibitors in A549, a non-small cell lung cancer cell line. *Lung Cancer* 63: 219–226.
- Ding SZ, Yang YX, Li XL, Michelli-Rivera A, Han SY, et al. (2013) Epithelial-mesenchymal transition during oncogenic transformation induced by hexavalent chromium involves reactive oxygen species-dependent mechanism in lung epithelial cells. *Toxicology and Applied Pharmacology* 269: 61–71.
- Sakuma Y, Yamazaki Y, Nakamura Y, Yoshihara M, Matsukuma S, et al. (2012) WZ4002, a third-generation EGFR inhibitor, can overcome anoikis resistance in EGFR-mutant lung adenocarcinomas more efficiently than Src inhibitors. *Laboratory Investigation* 92: 371–383.
- Khongmanee A, Lirdprapamoungkol K, Tit-ouu P, Chokchaichamankit D, Svasit J, et al. (2013) Proteomic analysis reveals important role of 14-3-3sigma in anoikis resistance of cholangiocarcinoma cells. *Proteomics* 13: 3157–3166.
- Koleske AJ, Baltimore D, Lisanti MP (1995) Reduction of caveolin and caveolae in oncogenically transformed cells. *Proceedings of the National Academy of Sciences of the United States of America* 92: 1381–1385.
- Kowidamrong A, Chanvorachote P, Sritularak B, Pongrakhananon V (2013) Moscatilin Inhibits Lung Cancer Cell Motility and Invasion via Suppression of Endogenous Reactive Oxygen Species. *BioMed Research International* 2013: 1–11.

40. Zhang Z, Han L, Cao L, Liang X, Liu Y, et al. (2008) Aggregation formation mediated anoikis resistance of BEL7402 hepatoma cells. *Folia Histochem Cytobiol* 46: 331–336.
41. Vega S, Morales AV, Ocaña OH, Valdés F, Fabregat I, et al. (2004) Snail blocks the cell cycle and confers resistance to cell death. *Genes & Development* 18: 1131–1143.
42. Tsai JH, Donaher JL, Murphy DA, Chau S, Yang J (2012) Spatiotemporal Regulation of Epithelial-Mesenchymal Transition Is Essential for Squamous Cell Carcinoma Metastasis. *Cancer cell* 22: 725–736.
43. Fidler IJ (2002) The organ microenvironment and cancer metastasis. *Differentiation* 70: 498–505.
44. Matilla PK, Lappalainen P (2008) Filopodia: molecular architecture and cellular functions. *Nat Rev Mol Cell Biol* 9: 446–454.
45. Friedl P, Wolf K (2003) Tumour-cell invasion and migration: Diversity and escape mechanisms. *Nature Reviews Cancer* 3: 362–374.
46. Siegel R, Naishadham D, Jemal A (2013) Cancer statistics, 2013. *CA: A Cancer Journal for Clinicians* 63: 11–30.
47. Herbst RS, Heymach JV, Lippman SM (2008) Lung Cancer. *New England Journal of Medicine* 359: 1367–1380.
48. Kalluri R, Weinberg RA (2009) The basics of epithelial-mesenchymal transition. *Journal of Clinical Investigation* 119: 1420–1428.
49. Ma H, Zheng L, Li Y, Pan S, Hu J, et al. (2013) Triclosan reduces the levels of global DNA methylation in HepG2 cells. *Chemosphere* 90: 1023–1029.
50. Wang Y, Shang Y (2013) Epigenetic control of epithelial-to-mesenchymal transition and cancer metastasis. *Experimental Cell Research* 319: 160–169.
51. Hou JM, Krebs M, Ward T, Morris K, Sloane R, et al. (2010) Circulating tumor cells, enumeration and beyond. *Cancers* 2: 1236–1250.
52. Peinado H, Portillo F, Cano A (2004) Transcriptional regulation of cadherins during development and carcinogenesis. *Int J Dev Biol* 48: 365–375.
53. Dauphin M, Barbe C, Lemaire S, Nawrocki-Raby B, Lagonotte E, et al. (2013) Vimentin expression predicts the occurrence of metastases in non small cell lung carcinomas. *Lung Cancer* 81: 117–122.
54. Thiery JP, Sleeman JP (2006) Complex networks orchestrate epithelial-mesenchymal transitions. *Nature Reviews Molecular Cell Biology* 7: 131–142.
55. Peinado H, Olmeda D, Cano A (2007) Snail, Zeb and bHLH factors in tumour progression: an alliance against the epithelial phenotype? *Nature Reviews Cancer* 7: 415–428.
56. Larsen M, Tremblay ML, Yamada KM (2003) Phosphatases in cell-matrix adhesion and migration. *Nat Rev Mol Cell Biol* 4: 700–711.
57. Mitra SK, Hanson DA, Schlaepfer DD (2005) Focal adhesion kinase: in command and control of cell motility. *Nat Rev Mol Cell Biol* 6: 56–68.
58. Fenouille N, Tichet M, Dufies M, Pottier A, Mogha A, et al. (2012) The epithelial-mesenchymal transition (EMT) regulatory factor SLUG (SNAI2) is a downstream target of SPARC and AKT in promoting melanoma cell invasion. *PLoS ONE* 7: 1–15.
59. Yilmaz M, Christofori G (2009) EMT, the cytoskeleton, and cancer cell invasion. *Cancer and Metastasis Reviews* 28: 15–33.

Review

Potential Anti-metastasis Natural Compounds for Lung Cancer

PITHI CHANVORACHOTE¹, SUPAKARN CHAMNI²,
CHUANPIT NINSONTIA¹ and PREEYAPORN PLAIMEE PHIBOONCHAIYANAN¹

¹Cell-Based Drug and Health Product Development Research Unit and Department of Pharmacology and Physiology, Faculty of Pharmaceutical Sciences, Chulalongkorn University, Bangkok, Thailand;

²Center for Bioactive Natural Products from Marine Organisms and Endophytic Fungi (BNPME), Department of Pharmacognosy and Pharmaceutical Botany, Faculty of Pharmaceutical Sciences, Chulalongkorn University, Bangkok, Thailand

Abstract. As lung cancer is the most common malignancy worldwide and high mortalities are the result of metastasis, novel information surpassing the treatment strategies and therapeutic agents focusing on cancer dissemination are of interest. Lung cancer metastasis involves increased motility, survival in circulation and ability to form new tumors. Metastatic cells increase their aggressive features by utilizing several mechanisms to overcome hindrances of metastasis, including epithelial to mesenchymal transition (EMT), increased in cellular survival and migratory signals. Sufficient amounts of natural product-derived compounds have been shown to have promising anti-metastasis activities by suppressing key molecular features upholding such cell aggressiveness. The knowledge regarding molecular mechanisms rendering cell dissemination together with the anti-metastasis information of natural product-derived compounds may lead to development of novel therapeutic strategies.

Lung cancer causes mortality in the estimated number of 1.5 million every year (1, 2). It has been widely accepted that in most aggressive malignancies, metastasis becomes the highlighted topic of research interests. In lung cancer, the metastasis-related death is found to be as high as 90% of all lung cancer mortality and approximately 70% of lung cancer patients are found with local lymph node metastasis or

distant spreading of cancer at the time of first diagnosis (3). According to such contexts, metastasis is an important impediment for the successful therapy of lung cancer and, thus, understanding of the underlying molecular basis in regulation of lung cancer dissemination may lead to discovery of novel effective targeted therapies.

Lung cancer is generated from normal lung epithelial cells that undergo multiple genetic damages and finally transform to uncontrolled proliferating cells with abnormal growth and aggressive behaviors in the airway of lungs. Lung cancer consists of two major types: non-small cell lung cancer ((NSCLC); 85% of all lung cancer cases) and small-cell lung cancer ((SCLC); about 15%) (4, 5). According to the histological classification, NSCLC can be divided into three major subtypes: squamous cell carcinoma, adenocarcinoma and large-cell carcinoma (4). The importance of classification is revealed to treatment strategy and prediction of cancer outcome. At the present day, surgery, radiation, chemotherapy and targeted therapy are used in lung cancer treatment; however, despite the fact that multiple approaches have been used for lung cancer treatment, the clinical outcomes of the current therapies are still not at satisfactory level.

Many widely prescribed chemotherapeutic agents have been discovered by investigating the potential compounds from plants, marine organisms, microorganisms and animals or developing from the natural product-derived lead compounds (6). In line with such a concept, several natural product-derived compounds have been currently evaluated and their anti-cancer activities have been focused on newly discovered mechanisms with the hope that they can be used or, at least, lead to better strategies against cancer (Table I).

Mechanism of Metastasis

Until now, the mechanism of metastasis of lung cancer is still not understood at a sufficient level. Although the appearance

This article is freely accessible online.

Correspondence to: Pithi Chanvorachote, Ph.D., Department of Pharmacology and Physiology, Faculty of Pharmaceutical Sciences, Chulalongkorn University, Phatumwan, Bangkok, 10330 Thailand. Tel: +66 812075039, Fax: +66 22188340, e-mail: pithi_chan@yahoo.com

Key Words: Lung cancer, metastasis, anti-metastasis, natural product, anti-cancer, review.

and phenotype of the metastatic cancer cells found in other parts of the body is similar to that of primary tumor cells, metastatic lung cancer cells have several different molecular features. With the same feature of certain proteins and chromosome defects found in original lung cancer cells, the metastatic cells possess specific signals that enhance their ability to metastasize. Such mechanisms allow the cells to disseminate from their original site. In general, lung cancer cell metastasis involves the common following steps as found in most solid tumors, which are (i) detachment from extracellular matrix (ECM), (ii) local migration and invasion, (iii) intravasation into blood or lymphatic systems, (iv) survival in circulatory system (resistant to anoikis), (v) extravasation at metastatic site and (vi) proliferation and formation of new tumor. The illustration of complicated processes of metastasis is shown in Figure 1.

The metastatic cells require special properties to overcome hindrances, with the most important being their ability to survive in detached conditions, invade and generate new tumors. Recent studies have shown that adaptive cell features changing from epithelial-like to mesenchymal phenotypes named "epithelial to mesenchymal transition" (EMT) (7-9) and cancer stem cells (CSCs) (8, 10-13) play critical roles in facilitating cancer cell dissemination. In addition, the augmentation of survival mechanisms, including Protein kinase B (AKT), ERK and anti-apoptotic protein members of the Bcl-2 family, have been intensively shown to increase metastasis ability of lung cancer cells (14-18).

Anoikis Regulatory Mechanism

Anoikis is the molecular event of programmed cell death triggered by the loss of appropriate cell contact to extracellular matrix or basement membrane. The process of anoikis involves the lack or diminishment of integrin-mediated survival signals (19). This death is found in most adherent cells, including solid tumor cells (20); therefore, anoikis has been recognized as a key impediment of cancer metastasis. Molecules like focal adhesion kinase (FAK), anti-apoptotic protein MCL-1 and caveolin-1 (CAV-1) have been shown to inhibit anoikis in lung cancer cells. Regarding FAK, it is a focal adhesion-associated protein, encoded by *PTK2* gene (protein tyrosine kinase). FAK acts as an essential early protein that co-localizes with integrins on the cytoplasmic domain and facilitates migration through transmission of integrin signaling. FAK is recruited and activated by signaling from integrin. The major phosphorylation site of FAK is identified as tyrosine 397 (Tyr 397). After FAK auto-phosphorylation, activated FAK forms a complex with SRC family kinases, which generate multiple downstream signaling through phosphorylation of other proteins to regulate cell survival (21). In lung cancer cells, FAK was shown to enhance cell survival in detached conditions via PI3K/AKT and MAPK-ERK pathways (22).

Recently, CAV-1 protein, a main component of caveolae, has been demonstrated to negatively control anoikis response in NSCLC cells (23, 24). In mechanistic detail, CAV-1 was shown to inhibit anoikis in lung cancer cells by its binding on and stabilizing of anti-apoptotic MCL-1 protein (25). The direct interaction of CAV-1 protects MCL-1 from ubiquitin-proteasomal degradation (25). Other possible mechanism of CAV-1 on anoikis resistance is that the protein can up-regulate the insulin-like growth factor-I receptors and enhance its downstream AKT signaling (26). Together with the facts that CAV-1 was shown to be highly expressed in metastatic and advanced stage cancer (27-29) and its expression was linked with poor prognosis (30, 31), suppressing this protein may be a potential way to overcome anoikis resistance and, as a consequence, inhibit metastasis.

Mounting evidence has demonstrated the activity of natural products in attenuation of cancer metastasis. Among several potential nature-derived compounds, curcumin [1], a compound isolated from the rhizome of turmeric (*Curcuma longa*), has garnered considerable attention over the past decade. Curcumin has been shown to sensitize anoikis in lung cancer cells by mediating Bcl-2 down-regulation (32). The study provided evidence that treatment of lung cancer cells with non-toxic concentrations of curcumin enhanced the degradation of Bcl-2 protein via ubiquitin-proteasomal degradation that, finally, resulted in the sensitization of anoikis (32).

The compound derived from *Angelica dahurica* root, imperatorin [2], was shown to increase anoikis response of lung cancer cells and inhibit anchorage-independent growth of lung cancer cells by down-regulation of MCL-1 protein (33). Likewise, artonin E [3], a compound obtained from *Artocarpus gomezianus*, and ecteinascidin 770 [ET-770, 4] isolated from marine tunicate *Ecteinascidia thurstoni*, were demonstrated to have anoikis sensitizing activity by decreasing the MCL-1 protein their non-toxic concentrations in NSCLC cells (34, 35). Recently, renieramycin M [RM, 5], a bistetrahydroisoquinolinequinone separated from marine blue sponge *Xestospongia* sp., was reported as a potential anti-metastatic agent by sensitizing anoikis-resistant lung cancer cells to anoikis by suppressing survival proteins p-ERK and p-AKT, along with anti-apoptotic proteins Bcl-2 and MCL-1 (36). Interestingly, ET-770 [4] and RM [5] consisted of similar chemical skeleton. The corresponding cytotoxicity and anti-cancer mechanism toward lung cancer potentially derived from the bistetrahydroisoquinoline core. A natural flavone isolated from the root of *Scutellaria baicalensis* known as Oroxylin A [6] was found to sensitize A549 cells to anoikis by inactivating the c-Src/AKT/HK II pathway (37). Furthermore, a mixture of flavonoids extracted from Korean *Citrus aurantium* was also reported to induce apoptosis of NSCLC (A549) cells involving protein cleaved caspase-3 and p-p53 (38).

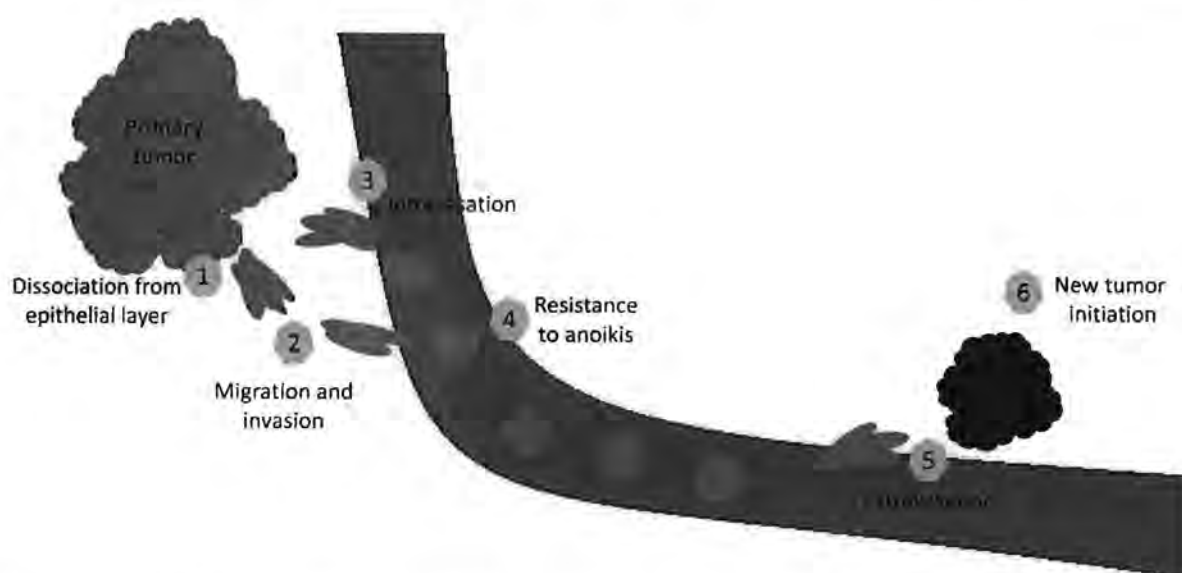


Figure 1. Cancer metastatic process. Metastasis is a complicated multistep process beginning with cancer cell detachment from extracellular matrix (ECM), migration, invasion and extravasation to the circulation. When the cancer cells reach secondary sites, they adhere, intravasate and begin dividing to form new tumors.

EMT and Migratory Suppression

EMT is a process of epithelial cells undergoing phenotypic change to mesenchymal cells. In general, EMT occurs during embryonic development, wound repair and pathological events, such as fibrosis and cancer (39).

EMT is classified into three different subtypes: 1) Type 1 EMT: This type occurs during embryonic development and organogenesis; 2) Type 2 EMT: This type associates with tissue repair and fibrosis; 3) Type 3 EMT: This type associates with cancer progression and metastasis.

EMT characteristics can be identified by the change of cell morphology and expression of EMT markers. During EMT, epithelial cells undergo remarkable morphological conversion from cobblestone-like epithelial morphology to elongated-like mesenchymal morphology. The crucial hallmark of EMT is the loss of E-cadherin, a cellular junction protein typically expressed in epithelial cells. In addition, EMT-phenotypic cells increase the expression of mesenchymal markers, such as N-cadherin and vimentin, as well as up-regulate transcriptional factors, namely Snail and Slug (39-42). The alteration of cell components, including adhesion molecules and cytoskeleton, makes the cells lose their polarity and acquired high migratory ability, thus facilitating cancer cell metastasis.

Focusing on cancer metastasis, accumulating evidences have indicated the roles of EMT in cancer aggressiveness and metastasis; EMT is being considered as the underlying cause of the high mortality rate of cancer (7-9). EMT elicits

distinct behaviors leading to cancer cell metastasis, including increased cell motility (migration and invasion) and anoikis resistance. Previous studies have demonstrated that loss of E-cadherin expression has been shown to decrease cell polarity and promote individual cell migration and invasion (43-46). Accordingly, the increased expression of N-cadherin results in a less stable cell-cell adhesion, which promotes cell motility and invasion by maintaining the steady-state level of active Rac1 (45, 46). Similar to N-cadherin, vimentin, type III intermediate filament protein, plays a predominant role in the changes in cell shape, adhesion and motility by maintaining FAK activity and Rac1 activation (47, 48).

During EMT process, lung cancer cells enhance their expression of mesenchymal transcription factors, such as, Slug, Snail and Twist. Besides, the increase of proteins like vimentin, fibronectin and alpha-smooth muscle actin (α -SMA), as well as the reduction of E-cadherin, have been shown to induce cell morphology change toward spindle shape and detachment of the cells from their basement. Focusing on cancer invasion, the augmented N-cadherin found in EMT cells encourages invasive and metastasis behaviors (49). EMT was also shown to increase cell invasive ability by triggering matrix metalloproteinases (MMPs), such as MMP-2, MMP-3 and MMP-9 (50). In NSCLC, the low vimentin level was found to be a predictor of better survival in primary NSCLC (51). EMT phenotypes in primary cells of lung cancer have been shown to link with anoikis and chemotherapeutic resistance (52, 53). Focusing on cancer cells and their environment interplays, EMT can be induced by several

Table 1. Natural product-derived compounds as potential anti-lung cancer agents.

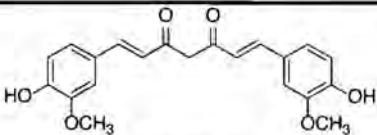
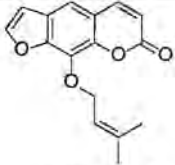
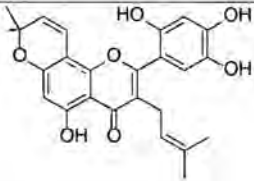
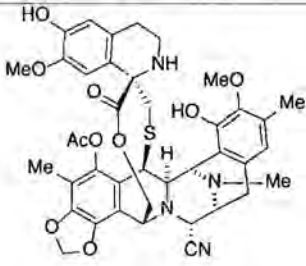
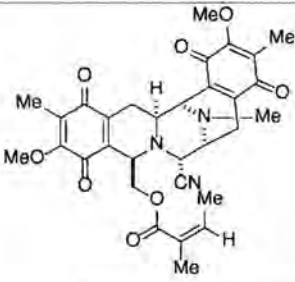
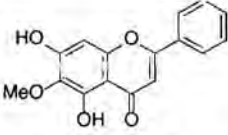
| Entry | Compound | Natural source | Origin/ Part use | Anti-lung cancer mechanism |
|-------|-------------------------------------------------------------------------------------------------------------|--------------------------------|-------------------------|-------------------------------|
| 1 |  Curcumin, 1 | <i>Curcuma longa</i> | Plant/ Rhizome | Anoikis sensitizing |
| 2 |  Imperatorin, 2 | <i>Angelica dahurica</i> | Plant/ Root | Anoikis sensitizing |
| 3 |  Artonin E, 3 | <i>Artocarpus gomezianus</i> | Plant/ Bark | Anoikis sensitizing |
| 4 |  Ecteinascidin 770, 4 | <i>Ecteinascidia thurstoni</i> | Tunicate/ Whole body | Anoikis sensitizing |
| 5 |  Renieramycin M, 5 | <i>Xestospongia</i> sp. | Sponge/ Whole body | Anoikis sensitizing |
| 6 |  Oroxylin A, 6 | <i>Scutellaria baicalensis</i> | Plant/root | Anoikis sensitizing |

Table 1. Continued

Table I. *Continued*

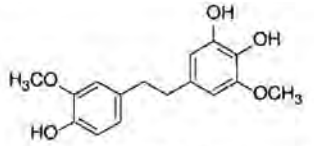
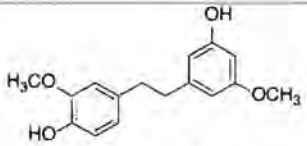
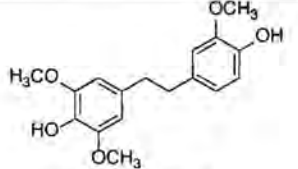
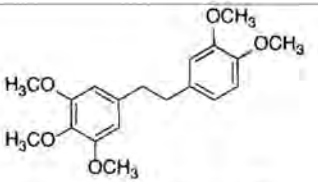
| Entry | Compound | Natural source | Origin/ Part use | Anti-lung cancer mechanism |
|-------|-------------------------------------------------------------------------------------------------------------------------------------------------|------------------------------------------------------------------------|-----------------------|-------------------------------------------------------------------------------------------------------|
| 7 |  <p>4,5,4'-Trihydroxy- 3,3'-dimethoxybibenzyl (TDB), 7</p> | <i>Dendrobium ellipsophyllum</i> | Plant/ Aerial part | EMT and migratory suppressing Anoikis sensitizing |
| 8 |  <p>Gigantol, 8</p> | <i>Dendrobium draconis</i> <i>Dendrobium pulchellum</i> | Plant/ Aerial part | EMT and migratory suppressing Anoikis sensitizing CSC phenotype suppressing |
| 9 |  <p>Moscatillin, 9</p> | <i>Dendrobium pulchellum</i> | Plant/ Aerial part | EMT and migratory suppressing Anoikis sensitizing |
| 10 |  <p>Chrysotobibenzyl, 10</p> | <i>Dendrobium pulchellum</i> | Plant Aerial part | EMT and migratory suppressing Anoikis sensitizing |

Table I. *Continued*

Table I. Continued

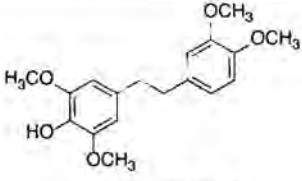
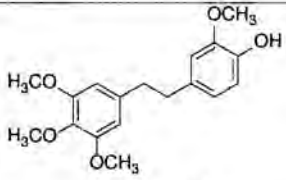
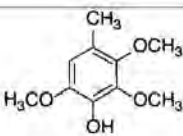
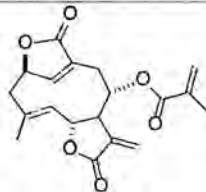
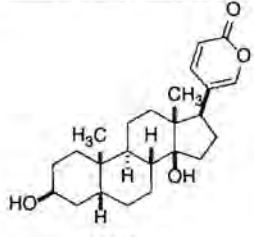
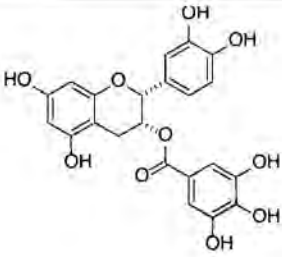
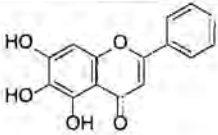
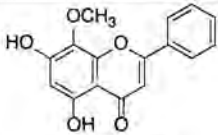
| Entry | Compound | Natural source | Origin/ Part use | Anti-lung cancer mechanism |
|-------|--------------------------------------------------------------------------------------------------------------------------------|----------------------------------------|---------------------------------------------------------------------------|-------------------------------------------------------------------|
| 11 |  <p>Chrysotoxine, 11</p> | <i>Dendrobium pulchellum</i> | Plant/ Aerial part | EMT and migratory suppressing Anoikis sensitizing |
| 12 |  <p>Crepidalin, 12</p> | <i>Dendrobium pulchellum</i> | Plant/ Aerial part | EMT and migratory suppressing Anoikis sensitizing |
| 13 |  <p>2,3,5-Trimethoxy-4-cresol (TMC), 13</p> | <i>Antrodia cinnamomea</i> | Fungus/ solid-state cultured mycelium | EMT and migratory suppression |
| 14 |  <p>Deoxyelephantopin, 14</p> | <i>Elephantopus scabe</i> | Plant/ Leaves | EMT and migratory suppression |
| 15 |  <p>Bufalin, 15</p> | <i>Bufo gargarizans</i> Chan Su | Animal/ Peptide from skin Traditional Chinese Medicine | EMT and migratory suppression |

Table I. Continued

Table I. Continued

| Entry | Compound | Natural source | Origin/ Part use | Anti-lung cancer mechanism |
|-------|-----------------------------------------------------------------------------------------------------------------------|------------------------------------|---------------------|-------------------------------------|
| 16 |  Epicatechin-3-gallate, 16 | <i>Camellia sinensis</i> | Plant/ leave | EMT and migratory suppression |
| 17 |  Baicalein, 17 | <i>Scutellaria baicalensis</i> | Plant/Root | EMT and migratory suppression |
| 18 |  Wogonin, 18 | <i>Scutellaria baicalensis</i> | Plant/Root | EMT and migratory suppression |

extracellular signals, including transforming growth factor- β 1 (TGF- β 1), interleukin-6 (IL-6) and nitric oxide, cancer-associated immune cells and fibroblasts (54-56).

As EMT phenotypes have been strongly linked to anoikis resistance and other aggressive behaviors of cancer cells, compounds that can suppress EMT is of interest for the development of anti-metastasis approaches. Several natural products have been shown to have abilities to suppress EMT in lung cancer cells. A bibenzyl 4,5,4'-trihydroxy-3,3'-dimethoxybibenzyl [TDB, **7**], isolated from *Dendrobium ellipsophyllum*, has been demonstrated to inhibit EMT and sensitize lung cancer cells to anoikis (57). Treatment of lung cancer cells with non-toxic concentrations of TDB significantly suppressed EMT markers, namely vimentin and Snail, while increased the level of E-cadherin. Also, such a decrease in EMT phenotypes was shown to induce anoikis and decrease cell growth in detached conditions by reduction of activated protein kinase B (p-AKT) and activated extracellular signal-regulated kinase (p-ERK) (57). Gigantol [**8**], extracted from *Dendrobium draconis*, and known bibenzyl compounds, including moscatilin [**9**], chrysobibenzyl [**10**], chrysoxine [**11**] and crepidatin [**12**], isolated from *Dendrobium pulchellum*,

have been demonstrated to suppress EMT in a lung cancer cell model and such suppression resulted in the induction of anoikis and decreased growth in an anchorage-independent manner (58, 59). The EMT inhibition of moscatilin [**9**] was recently described *via* mesenchymal cell markers' suppression, including vimentin, Slug and Snail (60). In addition, 2,3,5-trimethoxy-4-cresol [TMC, **13**], a substituted phenol obtained from Taiwanese edible fungus *Antrodia cinnamomea*, was reported as an effectively lung cancer migratory suppressing agent by reducing protein expression of AKT, MMP-2 and MMP-9 in conjugation with enhancing E-cadherin and TIMP-1 protein expression in A549 cancer cell line at subtoxic concentrations (61). Similar results were observed from the anti-metastatic study in A549 cells of deoxyelephantopin [**14**], a sesquiterpenelactone from *Elephantopus scabre*. This complex natural lactone suppressed the activation of p-ERK1/2 and p-AKT and exhibited down-regulation of NF- κ B, I κ B α MMP-2, MMP-9, uPA and uPAR. In addition, deoxyelephantopin [**14**] was associated with the up-regulation of TIMP2 without changing the TIMP1 protein level (62). Moreover, bufalin [**15**], a cardiotonic steroid originally isolated from serous fluid of Chinese toad, found as a component in Chan Su (a traditional

Chinese medicine), was recently investigated for its anti-metastasis effects on NCI-H460 lung cancer cells where suppression of MMP-2, MMP-9, MAPKs and NF- κ B was observed (63). Several natural flavonoids have been investigated as potential anti-metastasis agents toward various lung cancer cell lines. Epicatechin-3-gallate [16], a natural flavonoid found in green tea, was reported to reverse the TGF- β 1-induced EMT and up-regulated epithelial markers, such as E-cadherin (64). Moreover, flavone components in *Scutellaria baicalensis*, including baicalein [17] and wogonin [18], induced down-regulation of MMP-2 and MMP-9 in both A549 and H1299 cells (65).

Cancer Stem Cells (CSCs)

Accumulative evidence have pointed out the importance of small sub-populations within tumors with stem cell properties named "Cancer Stem Cells (CSCs)" on the process of carcinogenesis, cancer progression and metastasis (66). In lung cancer, the specific side-population has been isolated from lung cancer cell lines with CSC properties (67, 68).

The properties of CSCs are similar to those of normal stem cells within tissues. CSCs have the ability to self-renewal and can produce differentiated progeny through their pluripotency (69). It has been demonstrated that these CSCs in lung cancer resist to chemotherapeutic agents and have high tumorigenic potential (12, 70). Also, the lung CSCs were shown to have augmented ability to move to other tissues (8, 12, 71). The most important characteristic of CSCs is their ability to generate a new tumor. As a result of their self-renewal and differentiation capabilities, CSCs are believed to initiate tumor, as well as generate new tumors, at distant parts of the body. Nowadays, this new paradigm of CSCs has become the most interesting topic in research, clinical assessments and drug discovery and development, in particular, in lung cancer.

Due to their stem cell-like properties of tumorigenic potential and pluripotency, CSCs are believed to be key players of cancer metastasis and relapse (8, 10-13). Several CSC makers have been used to identify the CSC population in lung cancer, including cellular expression of CD44, CD133 and CD166 (67-71). Also aldehyde dehydrogenase (ALDH) activity and expression have been shown to indicate stemness in lung cancer (67-71). In NSCLC, the CD44-positive cells have been shown to have enhanced stem cell-like properties (72).

Currently, CSCs, as well as their behaviors, were shown to be regulated through the interaction with their microenvironment. In detail, the activity of self-renewal and differentiation can be modulated in response to the signals from environment (72). Focusing on lung cancer, evidence has shown that hypoxic conditions increased the population of CSCs through the activation of insulin-like growth factor 1 (IGF1) receptor (73). Also, the important biological

mediator nitric oxide was found to enhance stem cell-like phenotypes in NSCLC cells (56). The study by Yongsanguanchai *et al.* revealed that exposure of lung cancer cells with a long-term low dose of nitric oxide gradually increased the CSC makers and phenotypes in a time- and dose-dependent manner. Interestingly, this study demonstrated that induction of CSCs by nitric oxide is reversible. By withdrawal of nitric oxide after long-term treatment, the increase in CSCs was found to reverse to the baseline level comparable with the non-treated cells (56), thus suggesting the dynamic response of the CSCs to their environment.

In terms of molecular views, the molecular pathway found in normal stem cells, such as Wnt (74, 75), Notch (76, 77), Hedgehog (78) and PI3K/AKT, have been shown to regulate stem cell properties in lung cancer. The role of Wnt signal has been intensively elucidated in lung CSC regulation. Wnt was shown to control the expression of stem cell transcription factor Oct4 in lung CSCs (74). Also, the regulatory effect of Wnt has been demonstrated in several lung cancer cells, while the blockage of Wnt signal in lung CSCs was shown to inhibit growth and exhibit anti-cancer activity (79-81). For Notch signaling, its function was positively linked with the proliferation of CD133-positive lung CSCs (76). The inhibition of Notch in CD133-positive lung cancer cells resulted in growth halt and sensitive response to chemotherapy (76). Accordingly, cisplatin treatment of lung cancer cells resulted in enriched CD133-positive population through Notch signaling (82). The central cell survival signal AKT has been indicated as a principle regulator for stemness in lung CSCs. Studies in several NSCLC cell lines and primary human tumors grown in nude mice have shown that AKT is an essential upstream activator of Sox-2 in regulation of lung cancer stem-like phenotypes (83). Besides, the microRNA-31 was shown to inhibit lung CSCs through the suppression of PI3K/AKT (84). These evidences suggested the potential molecular targets for targeted therapy focusing on lung CSC.

In NSCLC, the plant-derived compound isolated from *Dendrobium draconis*, gigantol [8] was shown to reduce cancer stem cell-like phenotypes through AKT suppression (85). Gigantol at its non-toxic concentrations was shown to suppress CSC phenotypes and CSC makers CD133 and ALDH1A1 in lung cancer cells. Moreover, the suppressed CSC phenotypes were found as a consequence of AKT inhibition, which, in turn, decreased the cellular levels of pluripotency and self-renewal factors Oct4 and Nanog (85).

Conclusion

The current molecular technologies, as well as the discovery of new paradigms in cancer cell biology, have emphasized the potential of targeted therapy for treatment of cancers. Although several questions remain unanswered, including the key

pathways in controlling EMT and CSCs and the effect of environmental factors, the defined regulatory pathways underlying lung cancer metastasis form the critical basis for the development of novel strategies in overcoming lung cancer.

Nature has been long recognized as a very important and attractive source of new therapeutic compounds due to the chemical diversity found in plants, animals, marine organisms and microorganisms allowing us to select the compounds for our specific targets. This review concludes the currently focused molecular mechanisms in the area of lung cancer metastasis and provides information of potential natural derived compounds for anti-metastatic approaches. The provided information may support further investigations and development for using such compounds in cancer therapy.

Acknowledgements

This research is supported by the Thailand Research Fund (RSA780043).

References

- Jemal A, Bray F, Center MM, Ferlay J, Ward E and Forman D: Global cancer statistics. *CA Cancer J Clin* 61: 69-90, 2011.
- Youlten DR, Cramb SM and Baade PD: The International Epidemiology of Lung Cancer: Geographical distribution and secular trends. *J Thorac Oncol* 3: 819-831, 2008.
- Hirsch FR and Hansen HH: New techniques for early diagnosis of lung cancer. *Ugeskr Laeger* 163: 4321-4323, 2001.
- Goldstraw P, Ball D, Jett JR, Le Chevalier T, Lim E, Nicholson AG and Shepherd FA: Non-small-cell lung cancer. *The Lancet* 378: 1727-1740, 2011.
- van Meerbeeck JP, Fennell DA and De Ruyscher DK: Small-cell lung cancer. *Lancet* 378: 1741-1755, 2011.
- Kinghorn A. Drug discovery from natural products. *In: Foye WO, Lemke TL, Williams DA, editors. Foye's Principles of Medicinal Chemistry: Lippincott Williams & Wilkins; 2008. p. 12-25.*
- da Silva SD, Morand GB, Alobaid FA, Hier MP, Mlynarek AM, Alaoui-Jamali MA and Kowalski LP: Epithelial-mesenchymal transition (EMT) markers have prognostic impact in multiple primary oral squamous cell carcinoma. *Clin Exp Metastasis* 32: 55-63, 2015.
- Mehlen P and Puisieux A: Metastasis: A question of life or death. *Nat Rev Cancer* 6: 449-458, 2006.
- Tanaka Y, Terai Y, Kawaguchi H, Fujiwara S, Yoo S, Tsunetoh S, Takai M, Kanemura M, Tanabe A and Ohmichi M: Prognostic impact of EMT (epithelial-mesenchymal-transition)-related protein expression in endometrial cancer. *Cancer Biol Ther* 14: 13-19, 2013.
- Hermann PC, Huber SL, Herrler T, Aicher A, Ellwart JW, Guba M, Bruns CJ and Heeschen C: Distinct populations of cancer stem cells determine tumor growth and metastatic activity in human pancreatic cancer. *Cell Stem Cell* 1: 313-323, 2007.
- Merlos-Suarez A, Barriga FM, Jung P, Iglesias M, Cespedes MV, Rossell D, Sevillano M, Hernando-Mombona X, da Silva-Diz V, Munoz P, Clevers H, Sancho E, Manges R and Batlle E: The intestinal stem cell signature identifies colorectal cancer stem cells and predicts disease relapse. *Cell Stem Cell* 8: 511-524, 2011.
- Perona R, Lopez-Ayllon BD, de Castro Carpeno J and Beldan-Iniesta C: A role for cancer stem cells in drug resistance and metastasis in non-small-cell lung cancer. *Clin Transl Oncol* 13: 289-293, 2011.
- Scheel C and Weinberg RA: Cancer stem cells and epithelial-mesenchymal transition: concepts and molecular links. *Semin Cancer Biol* 22: 396-403, 2012.
- Liu B, Wu X, Liu B, Wang C, Liu Y, Zhou Q and Xu K: MiR-26a enhances metastasis potential of lung cancer cells via AKT pathway by targeting PTEN. *Biochim Biophys Acta* 1822: 1692-1704, 2012.
- McCubrey JA, Steelman LS, Chappell WH, Abrams SL, Wong EW, Chang F, Lehmann B, Terrian DM, Milella M, Tafuri A, Stivala F, Libra M, Basecke J, Evangelisti C, Martelli AM and Franklin RA: Roles of the Raf/MEK/ERK pathway in cell growth, malignant transformation and drug resistance. *Biochim Biophys Acta* 1773: 1263-1284, 2007.
- Roberts PJ and Der CJ: Targeting the Raf-MEK-ERK mitogen-activated protein kinase cascade for the treatment of cancer. *Oncogene* 26: 3291-3310, 2007.
- Ikegaki N, Katsumata M, Minna J and Tsujimoto Y: Expression of bcl-2 in small cell lung carcinoma cells. *Cancer Res* 54: 6-8, 1994.
- Anagnostou VK, Lowery FJ, Zolota V, Tzelepi V, Gopinath A, Liceaga C, Panagopoulos N, Frangia K, Tanoue L, Boffa D, Gettinger S, Detterbeck F, Homer RJ, Dougenis D, Rimm DL and Syrigos KN: High expression of BCL-2 predicts favorable outcome in non-small cell lung cancer patients with non squamous histology. *BMC Cancer* 10: 186, 2010.
- Boudreau NJ and Jones PL: Extracellular matrix and integrin signalling: the shape of things to come. *Biochem J* 339(Pt 3): 481-488, 1999.
- Frisch SM and Francis H: Disruption of epithelial cell-matrix interactions induces apoptosis. *J Cell Biol* 124: 619-626, 1994.
- Beausejour M, Noel D, Thibodeau S, Bouchard V, Harnois C, Beaulieu JF, Demers MJ and Vachon PH: Integrin/Fak/Src-mediated regulation of cell survival and anoikis in human intestinal epithelial crypt cells: selective engagement and roles of PI3-K isoform complexes. *Apoptosis* 17: 566-578, 2012.
- Liu G, Meng X, Jin Y, Bai J, Zhao Y, Cui X, Chen F and Fu S: Inhibitory role of focal adhesion kinase on anoikis in the lung cancer cell A549. *Cell Biol Int* 32: 663-670, 2008.
- Chanvorachote P, Pongrakhananon V and Halim H: Caveolin-1 regulates metastatic behaviors of anoikis resistant lung cancer cells. *Mol Cell Biochem* 399: 291-302, 2015.
- Halim H, Luanpitpong S and Chanvorachote P: Acquisition of anoikis resistance up-regulates caveolin-1 expression in human non-small cell lung cancer cells. *Anticancer Res* 32: 1649-1658, 2012.
- Chunhacha P, Pongrakhananon V, Rojanasakul Y and Chanvorachote P: Caveolin-1 regulates Mcl-1 stability and anoikis in lung carcinoma cells. *Am J Physiol Cell Physiol* 302: C1284-1292, 2012.
- Ravid D, Maor S, Werner H and Liscovitch M: Caveolin-1 inhibits cell detachment-induced p53 activation and anoikis by upregulation of insulin-like growth factor-1 receptors and signaling. *Oncogene* 24: 1338-1347, 2005.
- Ho CC, Huang PH, Huang HY, Chen YH, Yang PC and Hsu SM: Up-regulated caveolin-1 accentuates the metastasis capability of lung adenocarcinoma by inducing filopodia formation. *Am J Pathol* 161: 1647-1656, 2002.

- 28 Sloan KA, Marquez HA, Li J, Cao Y, Hinds A, O'Hara CJ, Kathuria S, Ramirez MI, Williams MC and Kathuria H: Increased PEA3/E1AF and decreased Net/Elk-3, both ETS proteins, characterize human NSCLC progression and regulate caveolin-1 transcription in Calu-1 and NCI-H23 NSCLC cell lines. *Carcinogenesis* 30: 1433-1442, 2009.
- 29 Ho CC, Kuo SH, Huang PH, Huang HY, Yang CH and Yang PC: Caveolin-1 expression is significantly associated with drug resistance and poor prognosis in advanced non-small cell lung cancer patients treated with gemcitabine-based chemotherapy. *Lung Cancer* 59: 105-110, 2008.
- 30 Moon KC, Lee GK, Yoo SH, Jeon YK, Chung JH, Han J and Chung DH: Expression of caveolin-1 in pleomorphic carcinoma of the lung is correlated with a poor prognosis. *Anticancer Res* 25: 4631-4637, 2005.
- 31 Yoo SH, Park YS, Kim HR, Sung SW, Kim JH, Shim YS, Lee SD, Choi YL, Kim MK and Chung DH: Expression of caveolin-1 is associated with poor prognosis of patients with squamous cell carcinoma of the lung. *Lung Cancer* 42: 195-202, 2003.
- 32 Pongrakhananon V, Nimmannit U, Luanpitpong S, Rojanasakul Y and Chanvorachote P: Curcumin sensitizes non-small cell lung cancer cell anoikis through reactive oxygen species-mediated Bcl-2 downregulation. *Apoptosis* 15: 574-585, 2010.
- 33 Choochuay K, Chunhacha P, Pongrakhananon V, Luechapudiporn R and Chanvorachote P: Imperatorin sensitizes anoikis and inhibits anchorage-independent growth of lung cancer cells. *J Nat Med* 67: 599-606, 2013.
- 34 Wongpankam E, Chunhacha P, Pongrakhananon V, Sritularak B and Chanvorachote P: Artonin E mediates MCL1 downregulation and sensitizes lung cancer cells to anoikis. *Anticancer Res* 32: 5343-5351, 2012.
- 35 Powan P, Saito N, Suwanborirux K and Chanvorachote P: Ecteinascidin 770, a tetrahydroisoquinoline alkaloid, sensitizes human lung cancer cells to anoikis. *Anticancer Res* 33: 505-512, 2013.
- 36 Sirimangkalakitti N, Chamni S, Suwanborirux K and Chanvorachote P: Renieramycin M sensitizes anoikis-resistant H460 lung cancer cells to anoikis. *Anticancer Res* 36: 1665-1671, 2016.
- 37 Wei L, Dai Q, Zhou Y, Zou M, Li Z, Lu N and Guo Q: Oroxylin A sensitizes non-small cell lung cancer cells to anoikis via glucose-deprivation-like mechanisms: c-Src and hexokinase II. *Biochim Biophys Acta* 1830: 3835-3845, 2013.
- 38 Park K-I, Park H-S, Kim M-K, Hong G-E, Nagappan A, Lee H-J, Yumnam S, Lee W-S, Won C-K, Shin S-C and Kim G-S: Flavonoids identified from Korean citrus aurantium L. inhibit non-small cell lung cancer growth *in vivo* and *in vitro*. *J Funct Foods* 7: 287-297, 2014.
- 39 Iwatsuki M, Mimori K, Yokobori T, Ishi H, Beppu T, Nakamori S, Baba H and Mori M: Epithelial-mesenchymal transition in cancer development and its clinical significance. *Cancer Sci* 101: 293-299, 2010.
- 40 Yang J and Weinberg RA: Epithelial-mesenchymal transition: at the crossroads of development and tumor metastasis. *Dev Cell* 14: 818-829, 2008.
- 41 Thiery JP, Acloque H, Huang RY and Nieto MA: Epithelial-mesenchymal transitions in development and disease. *Cell* 139: 871-890, 2009.
- 42 De Craene B and Berx G: Regulatory networks defining EMT during cancer initiation and progression. *Nat Rev Cancer* 13: 97-110, 2013.
- 43 Onder TT, Gupta PB, Mani SA, Yang J, Lander ES and Weinberg RA: Loss of E-cadherin promotes metastasis via multiple downstream transcriptional pathways. *Cancer Res* 68: 3645-3654, 2008.
- 44 Wong AS and Gumbiner BM: Adhesion-independent mechanism for suppression of tumor cell invasion by E-cadherin. *J Cell Biol* 161: 1191-1203, 2003.
- 45 Nieman MT, Prudoff RS, Johnson KR and Wheelock MJ: N-cadherin promotes motility in human breast cancer cells regardless of their E-cadherin expression. *J Cell Biol* 147: 631-644, 1999.
- 46 Wheelock MJ, Shintani Y, Maeda M, Fukumoto Y and Johnson KR: Cadherin switching. *J Cell Sci* 121: 727-735, 2008.
- 47 Mendez MG, Kojima S and Goldman RD: Vimentin induces changes in cell shape, motility, and adhesion during the epithelial to mesenchymal transition. *Faseb J* 24: 1838-1851, 2010.
- 48 Havel LS, Kline ER, Salgueiro AM and Marcus AI: Vimentin regulates lung cancer cell adhesion through a VAV2-Rac1 pathway to control focal adhesion kinase activity. *Oncogene* 34: 1979-1990, 2015.
- 49 Hazan RB, Phillips GR, Qiao RF, Norton L and Aaronson SA: Exogenous expression of N-cadherin in breast cancer cells induces cell migration, invasion, and metastasis. *J Cell Biol* 148: 779-790, 2000.
- 50 Thiery JP and Sleeman JP: Complex networks orchestrate epithelial-mesenchymal transitions. *Nat Rev Mol Cell Biol* 7: 131-142, 2006.
- 51 Al-Saad S, Al-Shibli K, Donnem T, Persson M, Bremnes RM and Busund LT: The prognostic impact of NF-kappaB p105, vimentin, E-cadherin and Par6 expression in epithelial and stromal compartment in non-small-cell lung cancer. *Br J Cancer* 99: 1476-1483, 2008.
- 52 Chunhacha P, Sriuranpong V and Chanvorachote P: Epithelial-mesenchymal transition mediates anoikis resistance and enhances invasion in pleural effusion-derived human lung cancer cells. *Oncol Lett* 5: 1043-1047, 2013.
- 53 Huang RY, Wong MK, Tan TZ, Kuay KT, Ng AH, Chung VY, Chu YS, Matsumura N, Lai HC, Lee YF, Sim WJ, Chai C, Pietschmann E, Mori S, Low JJ, Choolani M and Thiery JP: An EMT spectrum defines an anoikis-resistant and spheroidogenic intermediate mesenchymal state that is sensitive to e-cadherin restoration by a src-kinase inhibitor, saracatinib (AZD0530). *Cell Death Dis* 4: e915, 2013.
- 54 Yadav A, Kumar B, Datta J, Teknos TN and Kumar P: IL-6 promotes head and neck tumor metastasis by inducing epithelial-mesenchymal transition via the JAK-STAT3-SNAIL signaling pathway. *Mol Cancer Res* 9: 1658-1667, 2011.
- 55 Ko H: Geraniin inhibits TGF-beta1-induced epithelial-mesenchymal transition and suppresses A549 lung cancer migration, invasion and anoikis resistance. *Bioorg Med Chem Lett* 25: 3529-3534, 2015.
- 56 Yongsanguanchai N, Pongrakhananon V, Mutirangura A, Rojanasakul Y and Chanvorachote P: Nitric oxide induces cancer stem cell-like phenotypes in human lung cancer cells. *Am J Physiol Cell Physiol* 308: C89-100, 2015.
- 57 Chaotham C, Pongrakhananon V, Sritularak B and Chanvorachote P: A Bibenzyl from *Dendrobium ellipsophyllum* inhibits epithelial-to-mesenchymal transition and sensitizes lung cancer cells to anoikis. *Anticancer Res* 34: 1931-1938, 2014.
- 58 Unahabhokha T, Chanvorachote P and Pongrakhananon V: The attenuation of epithelial to mesenchymal transition and induction

- of anoikis by gigantol in human lung cancer H460 cells. *Tumour Biol*. 2016.
- 59 Chanvorachote P, Kowitdamrong A, Ruanghirun T, Sritularak B, Mungmee C and Likhirwitayawuid K: Anti-metastatic activities of bibenzyls from *Dendrobium pulchellum*. *Nat Prod Commun* 8: 115-118, 2013.
- 60 Busaranon K, Plaimee P, Sritularak B and Chanvorachote P: Moscatilin inhibits epithelial-to-mesenchymal transition and sensitizes anoikis in human lung cancer H460 cells. *J Nat Med* 70: 18-27, 2016.
- 61 Lin CC, Chen CC, Kuo YH, Kuo JT, Senthil Kumar KJ and Wang SY: 2,3,5-Trimethoxy-4-cresol, an anti-metastatic constituent from the solid-state cultured mycelium of *Antrodia cinnamomea* and its mechanism. *J Nat Med* 69: 513-521, 2015.
- 62 Farha AK, Dhanya SR, Mangalam SN and Remani P: Anti-metastatic effect of deoxyelephantopin from *Elephantopus scaber* in A549 lung cancer cells *in vitro*. *Nat Prod Res* 29: 2341-2345, 2015.
- 63 Wu SH, Hsiao YT, Kuo CL, Yu FS, Hsu SC, Wu PP, Chen JC, Hsia TC, Liu HC, Hsu WH and Chung JG: Bufalin inhibits NCI-H460 human lung cancer cell metastasis *in vitro* by inhibiting MAPKs, MMPs, and NF-kappaB pathways. *Am J Chin Med* 43: 1247-1264, 2015.
- 64 Huang SF, Horng CT, Hsieh YS, Hsieh YH, Chu SC and Chen PN: Epicatechin-3-gallate reverses TGF-beta1-induced epithelial-to-mesenchymal transition and inhibits cell invasion and protease activities in human lung cancer cells. *Food Chem Toxicol* 94: 1-10, 2016.
- 65 Gong WY, Wu JF, Liu BJ, Zhang HY, Cao YX, Sun J, Lv YB, Wu X and Dong JC: Flavonoid components in *Scutellaria baicalensis* inhibit nicotine-induced proliferation, metastasis and lung cancer-associated inflammation *in vitro*. *Int J Oncol* 44: 1561-1570, 2014.
- 66 Bonnet D and Dick JE: Human acute myeloid leukemia is organized as a hierarchy that originates from a primitive hematopoietic cell. *Nat Med* 3: 730-737, 1997.
- 67 Ho MM, Ng AV, Lam S and Hung JY: Side population in human lung cancer cell lines and tumors is enriched with stem-like cancer cells. *Cancer Res* 67: 4827-4833, 2007.
- 68 Shi Y, Fu X, Hua Y, Han Y, Lu Y and Wang J: The side population in human lung cancer cell line NCI-H460 is enriched in stem-like cancer cells. *PLoS One* 7: e33358, 2012.
- 69 Zakaria N, Yusoff NM, Zakaria Z, Lim MN, Baharuddin PJ, Fakiruddin KS and Yahaya B: Human non-small cell lung cancer expresses putative cancer stem cell markers and exhibits the transcriptomic profile of multipotent cells. *BMC Cancer* 15: 84, 2015.
- 70 Liu J, Xiao Z, Wong SK, Tin VP, Ho KY, Wang J, Sham MH and Wong MP: Lung cancer tumorigenicity and drug resistance are maintained through ALDH(hi)CD44(hi) tumor initiating cells. *Oncotarget* 4: 1698-1711, 2013.
- 71 Nolte SM, Venugopal C, McFarlane N, Morozova O, Hallett RM, O'Farrell E, Manoranjan B, Murty NK, Klurfan P, Kachur E, Provias JP, Farrokhyar F, Hassell JA, Marra M and Singh SK: A cancer stem cell model for studying brain metastases from primary lung cancer. *J Natl Cancer Inst* 105: 551-562, 2013.
- 72 Castano Z, Fillmore CM, Kim CF and McAllister SS: The bed and the bugs: interactions between the tumor microenvironment and cancer stem cells. *Semin Cancer Biol* 22: 462-470, 2012.
- 73 Murakami A, Takahashi F, Nurwidya F, Kobayashi I, Minakata K, Hashimoto M, Nara T, Kato M, Tajima K, Shimada N, Iwakami S, Moriyama M, Moriyama H, Koizumi F and Takahashi K: Hypoxia increases gefitinib-resistant lung cancer stem cells through the activation of insulin-like growth factor I receptor. *PLoS One* 9: e86459, 2014.
- 74 Zhang Y, Zhang X, Huang J and Dong Q: Wnt signaling regulation of stem-like properties in human lung adenocarcinoma cell lines. *Med Oncol* 32: 157, 2015.
- 75 Jiang HL, Jiang LM and Han WD: Wnt/beta-catenin signaling pathway in lung cancer stem cells is a potential target for the development of novel anticancer drugs. *J Buon* 20: 1094-1100, 2015.
- 76 Liu J, Mao Z, Huang J, Xie S, Liu T and Mao Z: Blocking the NOTCH pathway can inhibit the growth of CD133-positive A549 cells and sensitize to chemotherapy. *Biochem Biophys Res Commun* 444: 670-675, 2014.
- 77 Hassan KA, Wang L, Korkaya H, Chen G, Maillard I, Beer DG, Kalemkerian GP and Wicha MS: Notch pathway activity identifies cells with cancer stem cell-like properties and correlates with worse survival in lung adenocarcinoma. *Clin Cancer Res* 19: 1972-1980, 2013.
- 78 Zhang S, Wang Y, Mao JH, Hsieh D, Kim IJ, Hu LM, Xu Z, Long H, Jablons DM and You L: Inhibition of CK2alpha down-regulates Hedgehog/Gli signaling leading to a reduction of a stem-like side population in human lung cancer cells. *PLoS One* 7: e38996, 2012.
- 79 Teng Y, Wang X, Wang Y and Ma D: Wnt/beta-catenin signaling regulates cancer stem cells in lung cancer A549 cells. *Biochem Biophys Res Commun* 392: 373-379, 2010.
- 80 Zhang X, Lou Y, Wang H, Zheng X, Dong Q, Sun J and Han B: Wnt signaling regulates the stemness of lung cancer stem cells and its inhibitors exert anticancer effect on lung cancer SPC-A1 cells. *Med Oncol* 32: 95, 2015.
- 81 Zhang X, Lou Y, Zheng X, Wang H, Sun J, Dong Q and Han B: Wnt blockers inhibit the proliferation of lung cancer stem cells. *Drug Des Devel Ther* 9: 2399-2407, 2015.
- 82 Liu YP, Yang CJ, Huang MS, Yeh CT, Wu AT, Lee YC, Lai TC, Lee CH, Hsiao YW, Lu J, Shen CN, Lu PJ and Hsiao M: Cisplatin selects for multidrug-resistant CD133+ cells in lung adenocarcinoma by activating Notch signaling. *Cancer Res* 73: 406-416, 2013.
- 83 Singh S, Trevino J, Bora-Singhal N, Coppola D, Haura E, Altiock S and Chellappan SP: EGFR/Src/Akt signaling modulates Sox2 expression and self-renewal of stem-like side-population cells in non-small cell lung cancer. *Mol Cancer* 11: 73, 2012.
- 84 Hou C, Sun B, Jiang Y, Zheng J, Yang N, Ji C, Liang Z, Shi J, Zhang R, Liu Y, Ye C and Zuo P: MicroRNA-31 inhibits lung adenocarcinoma stem-like cells *via* down-regulation of MET-PI3K-Akt signaling pathway. *Anticancer Agents Med Chem* 16: 501-518, 2016.
- 85 Bhummaphan N and Chanvorachote P: Gigantol suppresses cancer stem cell-like phenotypes in lung cancer cells. *Evid Based Complement Alternat Med* 2015: 836564, 2015.

Received August 15, 2016

Revised September 1, 2016

Accepted September 2, 2016

Cisplatin at Sub-toxic Levels Mediates Integrin Switch in Lung Cancer Cells

ARNATCHAI MAIUTHED¹ and PITHI CHANVORACHOTE^{1,2}

¹Cell-based Drug and Health Products Development Research Unit,
Faculty of Pharmaceutical Sciences, Chulalongkorn University, Bangkok, Thailand;

²Department of Pharmacology and Physiology, Faculty of Pharmaceutical Sciences,
Chulalongkorn University, Bangkok, Thailand

Abstract. *Background:* Resistance to chemotherapeutic agents, as well as enhanced metastasis, have been frequently reported in lung cancer. *Materials and Methods:* Cytotoxicity and proliferative effects of cisplatin on H460 lung cancer cells were evaluated by the MTT assay. Migration capacity was evaluated by the wound healing assay. The number of filopodia per cell were detected by rhodamine-phalloidin staining assay. The changes of protein levels of integrins, and migration-related proteins in response to cisplatin at sub-toxic concentrations were determined by western blotting. *Results:* Herein we demonstrate for the first time that exposure to low concentrations of cisplatin results in increase of cell motility with the alteration of integrin expression. Cisplatin-treated cells exhibited a significant increase in the number of filopodia per cell in correlation with enhanced migration. Migration regulatory proteins, namely activated forms of focal-adhesion kinase (FAK) and ATP-dependent tyrosine kinase (AKT), were found to significantly be up-regulated in cisplatin-treated cells in comparison to those of the non-treated control. Active Rho A-GTP and Rac-GTP were found to be increased in accordance with activation of FAK/AKT signals. Furthermore, we found that such migration enhancement may be in part due to the integrin switch mediated by cisplatin treatment. Cisplatin induced a dramatic alteration in the integrin expression pattern by up-regulating integrin α_4 , α_v , β_1 , and β_5 which were previously reported to increase cell motility, while it had no effect on integrin α_5 , and β_3 . *Conclusion:* As the integrin switch is a hallmark of highly aggressive cancer, these findings may

provide insights for better understanding of cancer cell adaptation after exposure to cisplatin.

The incidence as well as mortality rates of patients with lung cancer have increased annually. The main causes of cancer-related death in lung cancer are chemotherapeutic resistance and metastasis (1). Evidence suggests that certain cancer cells receiving chemotherapeutic agents alter their behaviors towards a more aggressive phenotype (2, 3). Moreover, studies indicate that chemotherapeutic drugs enhance the metastatic capacity of cancer cells (4, 5). Among well-known chemotherapeutic agents, cisplatin, a cis-diamminechloroplatinum (II) is a potent cytotoxic compound for the treatment of many solid tumors, including lung cancer (6). Although this drug has been shown to be highly effective in certain patients, cancer relapse and metastasis are frequently observed (1). A better understanding of the molecular basis of these phenomena, as well as of the possible effects of cisplatin on cisplatin-resistant lung cancer cells, may help improve strategic uses of cisplatin.

Interestingly, numerous studies have revealed that the metastatic potential of cancer cells can be potentiated by the distinct expression pattern of adhesion molecules named integrins (7-9). An integrin molecule is composed of two non-covalently transmembrane glycoprotein subunits termed α and β (8). Integrins are important biological molecules that help maintain firm adhesion of the cell to extracellular matrix and such adhesion provides fundamental survival signals to the cells (10). It is widely accepted that an increase of certain integrins, especially integrin α_4 , α_5 , α_v , and β_1 , enhances motility of cancer cells.

So far, the effect of low concentrations of cisplatin on integrin switch in lung cancer cells is largely unknown. We, thus, investigated the effect of this widely prescribed chemotherapeutic agent on integrin expression pattern in non-small cell lung cancer cells. The knowledge gained from the present study may benefit better understanding of cancer cell biology and adaptive response of the cell during chemotherapy.

Correspondence to: Pithi Chanvorachote, Department of Pharmacology and Physiology, Faculty of Pharmaceutical Sciences, Chulalongkorn University, Pathumwan, Bangkok, Thailand 10330. Tel: +662 2188344, Fax: +662 2188340, e-mail: pithi_chan@yahoo.com

Key Words: Integrin, lung cancer, migration, cisplatin, metastasis.

Materials and Methods

Cells and reagents. Human lung cancer epithelial H460 cells were obtained from the American Type Culture Collection (Manassas, VA, USA), and culture in RPMI-1640 medium containing 10% fetal bovine serum, 2 mM L-glutamine and 100 units/ml of penicillin/streptomycin (Gibco, Gaithersburg, MA, USA) at 37°C with 5% CO₂ in a humidified incubator. Cisplatin, dimethyl sulfoxide (DMSO), 3-(4,5-dimethylthiazol-2-yl)-2,5-diphenyltetrazoliumbromide (MTT), Hoechst 33342, propidium iodide (PI), phalloidin-tetramethylrhodamine B isothiocyanate, and bovine serum albumin (BSA) were obtained from Sigma Chemical, Inc. (St. Louis, MO, USA). Antibodies for integrins α_4 , α_5 , α_v , β_1 , β_3 and β_5 , ATP-dependent tyrosine kinase (AKT), phosphotyrosine kinase (p-AKT) (S473), focal adhesion kinase (FAK), phosphotyrosine kinase (p-FAK) (Y397), β -actin and peroxidase-labeled secondary antibodies were obtained from Cell Signaling Technology, Inc. (Danvers, MA, USA) and Rho-GTP, Rac-GTP were obtained from NewEast Bioscience, (King of Prussia, PA, USA).

Cell viability assay. Cell viability was determined by MTT colorimetric assay. Initially, cells were seeded at a density of 10⁴ cell/well in 96-well overnight. After that, cells were treated with different concentrations of cisplatin for 24 h. The medium was replaced with 500 μ g/ml of MTT for 4 h at 37°C. The supernatant was then removed and 100 μ l DMSO was added to solubilize the formazan product and the intensity of formazan product was measured by spectrophotometry at 570 nm using an ELISA reader (Anthros, Durham, NC, USA). The percentage cell viability was calculated as the absorbance of cisplatin-treated cells relative to control cells.

Apoptosis assay. Cells were seeded at a density of 10⁴ cells/well onto 96-well plate and incubated overnight for cell attachment. After the indicated treatments of cisplatin (0.25-10 μ M), cell were washed and incubated with 10 μ g/ml Hoechst33342 and 5 μ g/ml propidium iodide (PI) for 30 min. Nuclear condensation and DNA fragmentation of apoptotic cells and PI-positive necrotic cells were visualized by fluorescence microscopy (Olympus IX51 with a DP70 digital camera system, Tokyo, Japan).

Proliferation assay. Cells were exposed to cisplatin at indicated concentrations (0.25-1 μ M) and were subjected to the cell proliferation assay after 0, 24, 48, and 72 h. Cells were seeded at a density of 2x10³ cell/well in a 96-well plate. Cell proliferation was determined through incubation with 500 μ g/ml MTT for 4 h, and the absorbance of formazan product which was dissolved by DMSO was measured by spectrophotometry at 570 nm using an enzyme-linked immunosorbent assay reader (Anthros, Durham, NC, USA).

Migration determination. Migration was determined by wound-healing assays. For the wound-healing assay, a monolayer of cells was cultured in a 96-well plate, and a wound was made with a 1-mm-wide tip. After rinsing with PBS, the cell monolayers were treated with cisplatin (0.25-1 μ M) and allowed to migrate for 24 h. Micrographs were taken under a phase contrast microscope (Olympus IX51 with a DP70 digital camera system, Tokyo, Japan), and the wound spaces were measured using Olympus DP controller software. Quantitative analysis of cell migration was performed using an average wound space from random fields of view, and the percentage of change in the wound space was calculated using the

following formula: % change=(average space at time 0 h)-(average space at time 24 h)/(average space at time 0 h)×100. Relative cell migration was calculated by dividing the percentage change in the wound space of treated cells by that of the control cells in each experiment.

Morphological characteristics of cancer cells. Cell morphology was investigated using phalloidin-rhodamine assay. After treated with cisplatin at indicated concentration, the cells were fixed with 4% paraformaldehyde in PBS for 10 min at 37°C, permeabilized with 0.1% Triton-X100 in PBS for 5 min, rinsed with PBS and then blocked for unspecific binding by incubation with 0.2% BSA in PBS for 30 min. The fixed cells were then incubated with a 1:100 dilution of phalloidin-rhodamine in PBS for 20 min, then rinsed with PBS three times and mounted with 50% glycerol in PBS. The cell morphology was captured using a Nikon eclipse Ti-U fluorescence microscope, Nikon Corporation, Tokyo, Japan.

Western blot analysis. After specific treatments, cells were incubated in lysis buffer containing 20 mM Tris-HCl (pH 7.5), 1% Triton X-100, 150 mM sodium chloride, 10% glycerol, 1 mM sodium orthovanadate, 50 mM sodium fluoride, 100 mM phenylmethylsulfonyl fluoride, and a protease inhibitor cocktail (Roche Molecular Biochemicals, Mannheim, Germany) for 40 min on ice. The cell lysates were collected, and the protein content was determined using the Bradford method (Bio-Rad Laboratories). Equal amounts of proteins from each sample were denatured by heating at 95°C for 5 min with Laemmli loading buffer and subsequently loaded onto a 10% sodium dodecyl sulfate polyacrylamide gel electrophoresis (SDS-PAGE). After separation, proteins were transferred onto 0.45 μ M nitrocellulose membranes (Bio-Rad). The transferred membranes were blocked for 1 h in 5% nonfat dry milk in TBST (25 mM Tris-HCl pH 7.5, 125 mM NaCl, and 0.05% Tween 20) and incubated with the appropriate primary antibodies (anti-integrin α_4 , α_5 , α_v , β_1 , β_3 and β_5 , AKT, p-AKT (S473), FAK, p-FAK (Y397), Rho-GTP, Rac-GTP and β -actin) at 4°C overnight. The membranes were washed twice with TBST for 10 min and incubated with horseradish peroxidase-labeled isotype-specific secondary antibodies for 2 h at room temperature. The immune complexes were detected by enhancement with chemiluminescence substrate (Supersignal West Pico; Pierce) and quantified using analysis/PC densitometry software (Bio-Rad).

Statistical analysis. All data are expressed as the mean±S.E.M. from three or more independent experiments. Multiple comparisons were examined for significant differences of multiple groups, using analysis of variance (ANOVA), followed by individual comparisons with the Scheffe's *post-hoc* test. Statistical significance was set at $p < 0.05$.

Results

Effect of cisplatin on the viability of the H460 human lung cancer cell line. We first determined the cytotoxic effect of cisplatin on H460 human lung cancer cell line. The cells were cultured in the presence or absence of cisplatin (0-50 μ M) for 24 h, and cell viability was determined by the MTT assay. Figure 1A shows that when cells were treated with cisplatin at concentrations ranging 0.1-2 μ M, neither cytotoxicity nor proliferative effects were observed. A significant decrease in

terms of cell viability was first detected in cells treated with 5 μM , with approximately 90% of the cells remaining viable.

Consistent with the above findings, apoptosis and necrotic cell death determined by Hoechst33342/PI assay were not found in response to 0-1 μM cisplatin treatment. Significant apoptotic nuclei exhibiting condensed/fragmented nuclei were detected in cells treated with 10 μM (Figure 1 C-E). To investigate the effect of cisplatin on cell proliferation, H460 cells were treated with sub-toxic concentrations of cisplatin (0.25-1 μM) for 24 h, then the treated cells were seeded in 96-well plate and were determined for proliferation at 0, 24, 48, and 72 h (Figure 1B). A significant decrease in cell proliferative capacity was detected at 48, and 72 h in cells treated with 1 μM of cisplatin.

Effect of cisplatin on H460 migration. To investigate the effect of cisplatin on cell migration, we performed scratch wound-healing assays. Cells were exposed to non-toxic concentrations of cisplatin (0.25-1 μM) for 24 h and were subjected to migration assay for a further 24 and 48 h. Figure 2A shows that treatment with cisplatin enhanced migration of the cells in a dose-dependent manner compared to the H460 control cells. Treatment with 0.5 and 1 μM cisplatin significantly potentiated the migration of the cells at 24 h, while treated with 0.25 μM cisplatin significantly enhanced motility of cell at 48 h of the assay (Figure 2B). Treatment with cisplatin 1 μM increased the migration of cells by approximately 1.5- and 2.5-fold compared to that of the non-treated cells in the 24 and 48 h assays, respectively. These results indicate that sub-toxic concentrations of cisplatin enhance migration behavior of these cells.

Cisplatin enhanced filopodia formation in H460 lung cancer cells. Filopodia, cellular protrusions at the edge of motile cells, are produced by actin polymerization and rearrangement of actin filaments, and the formation of filopodia has been shown to play an essential role in cell movement (11). To confirm the enhancement effect of cisplatin treatment on cell motility, cells were treated with non-toxic concentrations of cisplatin for 24 h as previously described, and the filopodia were determined using a phalloidin-rhodamine staining assay. Figure 3 shows that cisplatin-treated cells exhibited a significant increase in filopodia protrusions accumulating at the cellular edge in a dose-dependent manner as compared with the H460 control cells.

Cisplatin mediates integrin switch and activates migration signaling pathways. The switching in the expression pattern of integrins towards increasing the level of integrins α_4 , α_5 , α_v , and β_1 was shown to enhance motility in cancer cells. Together with the above observations demonstrating the potentiating effect of cisplatin exposure on lung cancer cell

movement, we next examined the underlying mechanisms by evaluating migration regulatory proteins as well as integrins. Cells were treated with cisplatin for 24 h, and the expression of proteins including phosphorylated FAK (Tyr 397), phosphorylated AKT (Ser 473), RhoA-GTP, Rac-GTP, and integrins α_4 , α_5 , α_v , β_1 , β_3 and β_5 were evaluated by western blot analysis. Figure 4 shows that treatment with cisplatin caused a significant increase of activated FAK, RhoA-GTP, Rac-GTP, and activated AKT in dose-dependent manner as compared to those of non-treated control cells.

Figure 5 shows that cisplatin caused substantial up-regulation of integrins α_4 , β_1 and β_5 . Importantly, the expression of integrin α_v was found to be dramatically increased in response to cisplatin treatment. However, such cisplatin exposure had no effect on integrins α_5 , and β_3 . Our results not only confirm the previous findings indicating that the up-regulation of these integrins α_4 , α_v and β_1 enhance motility of cancer cells, but also provide evidence indicating that treatment with cisplatin can mediate such an integrin switch, leading to increased migratory activity of lung cancer cells.

Discussion

Most lung cancer deaths are attributed to cancer metastasis and resistance to chemotherapeutic agents (12). Increasing evidence has suggested that among the many steps of cancer metastasis, movement of the cancer cells from their original tumors and their motility during the process of cancer dissemination are an important hallmark for the successful cancer spread. However, information regarding the possible inducing factors and mediators that potentiate the migratory activities of cancer cells remains largely unknown. Certain cancer cells develop mechanisms to overcome the death signals provided by anticancer agents and such a population remains after chemotherapy (13). These chemoresistant cancer cells have frequently been shown to be a key player in metastasis as well as in cancer relapse (14-16). This concept led us to the hypothesis of whether chemotherapeutic agents such as cisplatin could increase the metastatic potential of lung cancer cells. Previously, we demonstrated that sub-toxic concentrations of cisplatin conferred resistance to anoikis in human lung cancer cells (5). Herein, we provide further information regarding the effect of such sub-toxic concentrations of cisplatin on migration of lung cancer cells.

Integrins are a family of transmembrane glycoprotein receptors that mediate cell-matrix and cell-cell interactions which play a pivotal role in cell behavior, such as cellular adhesion and cellular movement. Integrins consist of α and β subunits; there are 18 α and eight β subunits, which provides heterodimerization at least distinct 24 subtypes (17). In cancer biology, an increase in the expression of integrin α_4 , α_5 , α_v and β_1 are correlated with more aggressiveness

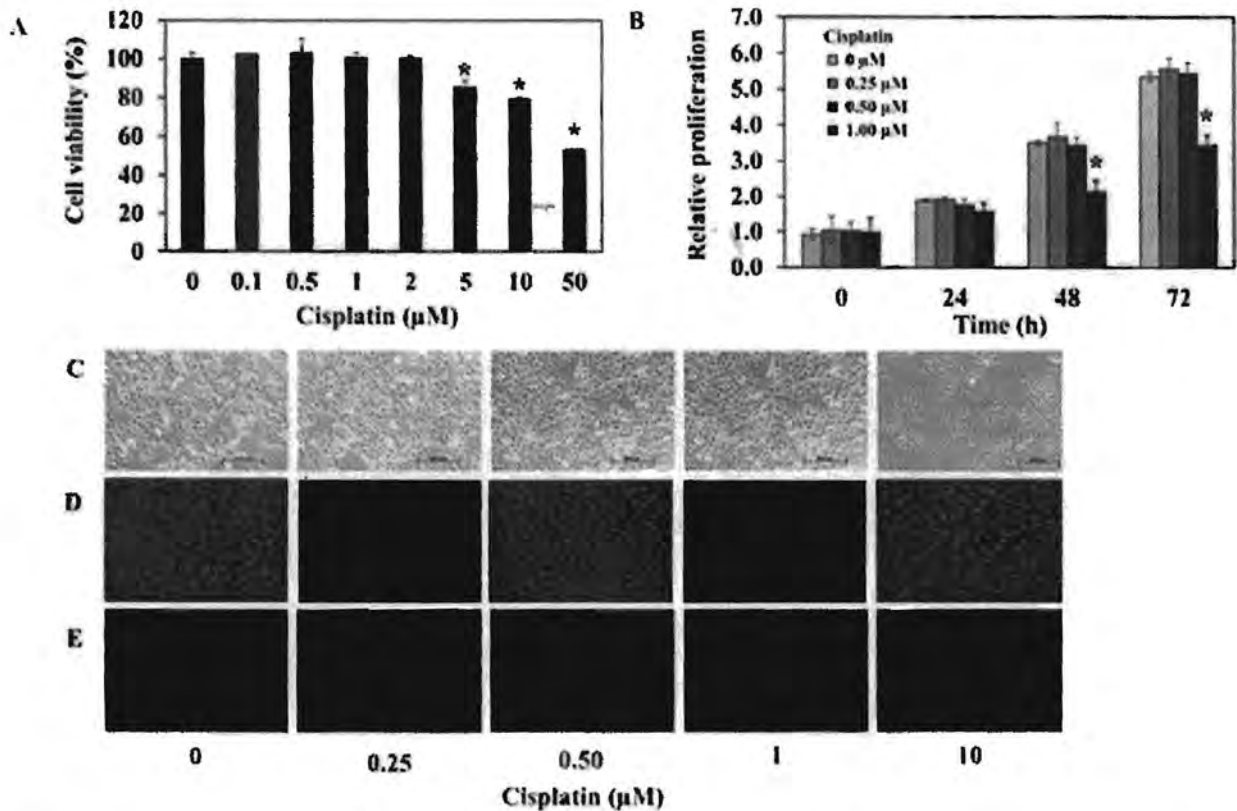


Figure 1. Cytotoxicity of cisplatin on H460 human lung cancer cell line. A: Cells were treated with different concentrations of cisplatin (0-50 μM) for 24 h. B: Proliferation of the cells treated with cisplatin (0-1 μM) for 24 h determined at 0, 24, 48, and 72 h. C: After the indicated treatment for 24 h, phase-contrast images were captured. D: After indicated treatment for 24 h, apoptosis cell death was examined by Hoechst33342 staining assay. E: After indicated treatment for 24 h, necrosis cell death was examined by PI stained assay. Data represent the mean±SD (n=3). *p<0.05 versus non-treated control cells.

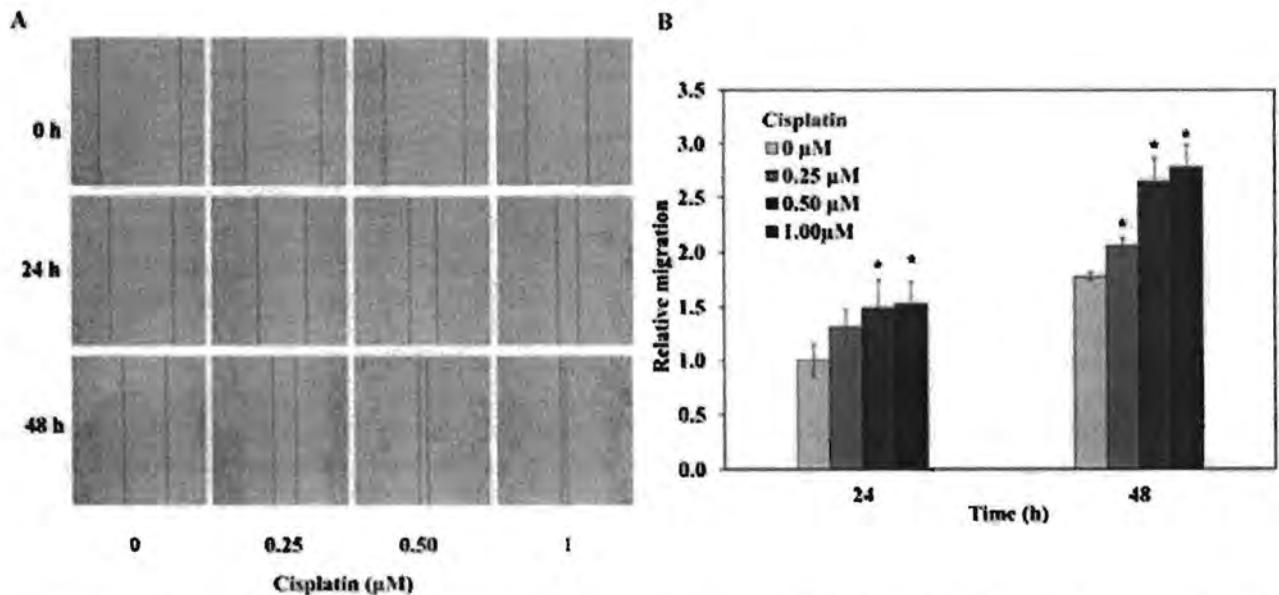


Figure 2. Effects of cisplatin on H460 cell migration. A: After treatment with cisplatin (0-1 μM) for 24 h, the confluent monolayer of H460 was wounded using a 1-mm width tip and cultured with complete medium for the indicated times. B: Wound space was analyzed and presented as relative migration levels. Data represent the mean±SD (n=3). *p<0.05 versus non-treated control cells.

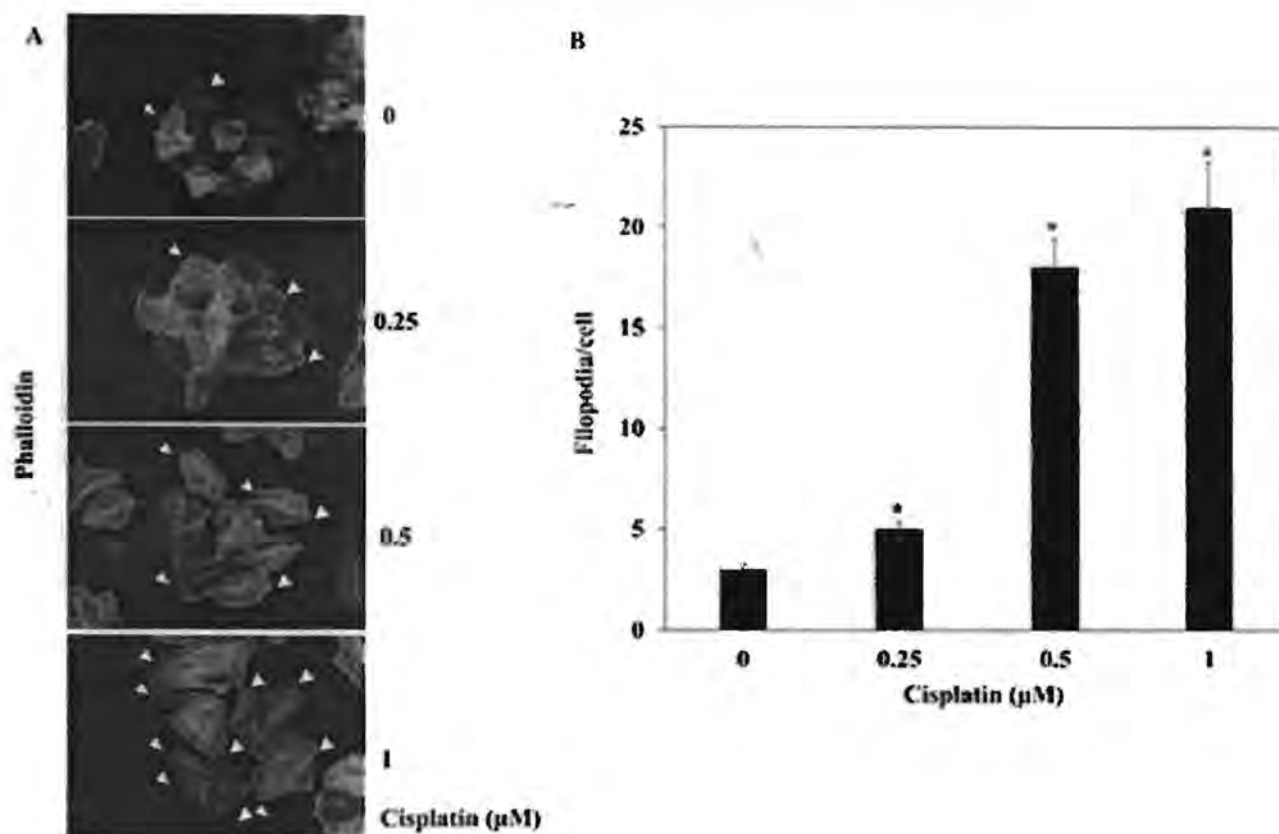


Figure 3. Filopodia formation in H460 cells treated with cisplatin. A: Cells were treated with 0-1 μM cisplatin for 24 h. The cells were stained with phalloidin-rhodamine and visualized under fluorescence microscopy. Filopodia are indicated by arrowheads. B: The number of filopodia per cisplatin-treated cell was analyzed and compared to that of non-treated control cells. Data represent the mean \pm SD (n=3). * p <0.05 versus non-treated control cells.

behavior of cancer cells (18-22). Studies of human cancer pathogenesis revealed that integrin subtype was altered with tumor stage (23) and switches in integrin expression frequently enhance the aggressive behavior of cancer cells (24, 25).

Evidence has indicated that molecules such as FAK and AKT play important roles in triggering cell movement (26, 27). In motile cells, FAK at the edge of cells incorporating integrin is activated by phosphorylation at Tyr 397 (26, 28). The active form of FAK in turn activates AKT, leading to actin polymerization and filopodia formation. Accordingly, we found that treatment with cisplatin enhanced activation of FAK-AKT signals (Figure 4) in correlation with increased filopodia in cells (Figure 3). For downstream regulation of cell migration, the role of small GTPase Rac and RhoA on actin rearrangements have been demonstrated in a number of studies (29-32). The active form of Rac (Rac-GTP) induces plasma membrane protrusion and regulates lamellipodia formation (33). In addition, active RhoA (RhoA-GTP) promotes stress fiber accumulation and induces new focal adhesions (34). We

also observed the involvement of these downstream signals in cisplatin-treated cells. Both active forms of Rac and Rho A were found to be significantly increased in cisplatin-treated cells in a dose-dependent manner (Figure 4).

Collectively, the present study reveals the possible adaptive mechanisms of cancer cells exposed to low or insufficient doses of cisplatin. The cisplatin-treated cancer cells adapted themselves toward increased expression of migratory-related integrins, namely integrins α_4 , α_v , β_1 , β_5 and in combination with activation of the migratory proteins FAK, AKT, Rho A, and Rac. The information gained from this study raises concerns regarding the awareness of such adaptation to inadequate cisplatin concentrations, as well as the need for better strategic use for chemotherapy for highly metastatic cancer.

Conflicts of Interest

The Authors declare that there are no conflicts of interest regarding this research.

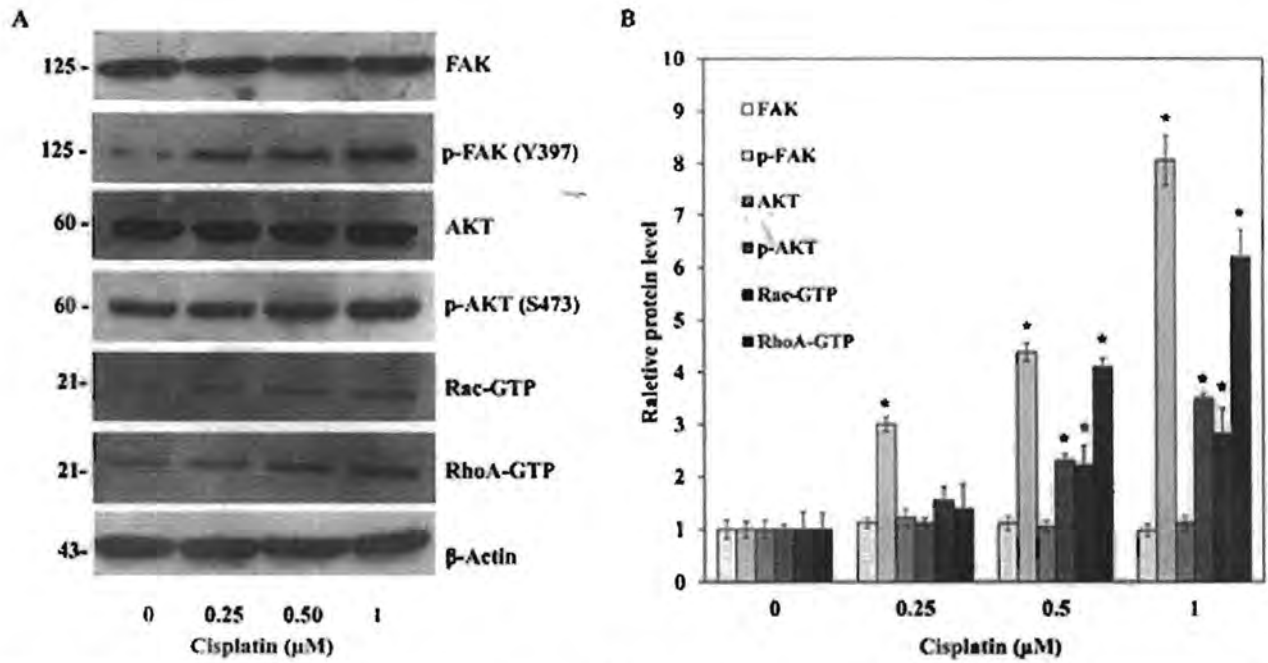


Figure 4. Cisplatin exposure activates the focal-adhesion kinase/ATP-dependent tyrosine kinase (FAK/AKT)-associated migration pathway. A: After treating H460 cells with cisplatin for 24 h, the expression levels of phosphorylated FAK, phosphorylated AKT, Rac-GTP, and RhoA-GTP were determined by western blot analysis. To confirm equal loading of the protein samples, the blots were re-probed with β -actin antibody. B: The immunoblot signals were quantified by densitometry. Data represent the mean \pm SD (n=3). *p<0.05 versus non-treated control cells.

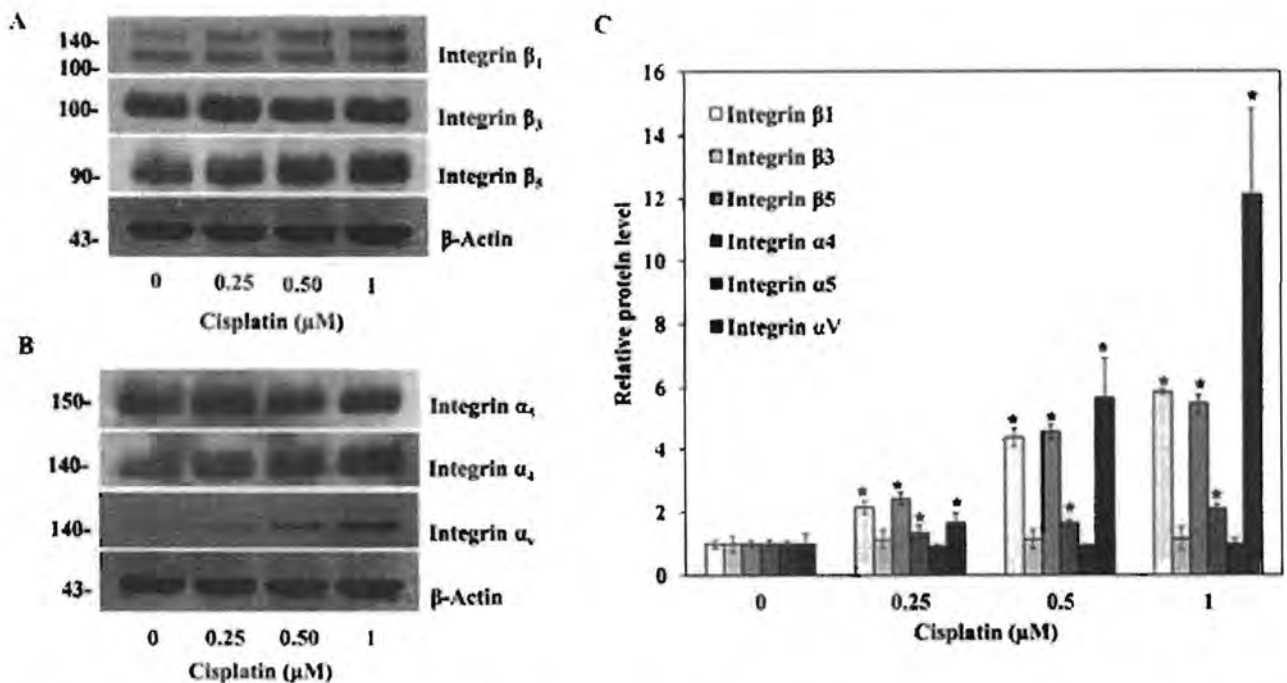


Figure 5. Effects of cisplatin on integrin expression. A and B: After treating cells with cisplatin for 24 h, the expression levels of integrins α_4 , α_5 , α_v , β_1 , β_3 and β_5 were determined by western blotting. β -Actin was used as loading control to confirm equal loading of the samples. C: The protein signals were quantified by densitometry. Data represent the mean \pm SD (n=3). *p<0.05 versus non-treated control cells.

Acknowledgements

This research is supported by grants from the Thailand Research Fund (RSA5780043).

References

- Siegel R, Naishadham D and Jemal A: Cancer statistics, 2012. *CA Cancer J Clin* 62(1): 10-29, 2012.
- El Sharouni SY, Kal HB and Battermann JJ: Accelerated regrowth of non-small-cell lung tumours after induction chemotherapy. *Br J Cancer* 89(12): 2184-2189, 2003.
- Bourhis J, Wilson G, Wibault P, Janot F, Bosq J, Armand JP, Luboinski B, Malaise EP and Eschwege F: Rapid tumor cell proliferation after induction chemotherapy in oropharyngeal cancer. *Laryngoscope* 104(4): 468-472, 1994.
- Latifi A, Abubaker K, Castrechini N, Ward AC, Liongue C, Dobill F, Kumar J, Thompson EW, Quinn MA, Findlay JK and Ahmed N: Cisplatin treatment of primary and metastatic epithelial ovarian carcinomas generates residual cells with mesenchymal stem cell-like profile. *J cell Biochem* 112(10): 2850-2864, 2011.
- Songserm T, Pongrakhananon V and Chanvorachote P: Sub-toxic cisplatin mediates anoikis resistance through hydrogen peroxide-induced caveolin-1 up-regulation in non-small cell lung cancer cells. *Anticancer Res* 32(5): 1659-1669, 2012.
- Gütz S: Chemotherapy in cancer of the lung. *MMW Fortschr Med* 148(22): 33-34, 2006.
- Moschos SJ, Drogowski LM, Reppert SL and Kirkwood JM: Integrins and cancer. *Oncology* 21(9 Suppl 3): 13-20, 2007.
- Desgrosellier JS, Cheresh DA: Integrins in cancer: biological implications and therapeutic opportunities. *Nat Rev Cancer* 10(1): 9-22, 2010.
- Huttenlocher A and Horwitz AR: Integrins in cell migration. *Cold Spring Harb Perspect Biol* 3(9): a005074, 2011.
- Stupack DG: The biology of integrins. *Oncology* 21(9 Suppl 3): 6-12, 2007.
- Xue F, Janzen DM and Kuecht DA: Contribution of Filopodia to Cell Migration: A Mechanical Link between Protrusion and Contraction. *Int J Cell Biol* 507821, 2010.
- D'Antonio C, Passaro A, Gori B, Del Signore E, Migliorino MR, Ricciardi S, Fulvi A and de Marinis F: Bone and brain metastasis in lung cancer: recent advances in therapeutic strategies. *Ther Adv Med Oncol* 6(3): 101-114, 2014.
- Gottesman MM: Mechanisms of cancer drug resistance. *Annu Rev Med* 53: 615-627, 2002.
- Ceppi P, Mudduluru G, Kumarswamy R, Rapa I, Scagliotti GV, Papotti M and Allgayer H: Loss of miR-200c expression induces an aggressive, invasive, and chemoresistant phenotype in non-small cell lung cancer. *Mol Cancer Res* 8(9): 1207-1216, 2010.
- Acharyya S, Oskarsson T, Vanharanta S, Malladi S, Kim J, Morris PG, Manova-Todorova K, Leversha M, Hogg N, Seshan VE, Norton L, Brogi E and Massagué J: A CXCL1 paracrine network links cancer chemoresistance and metastasis. *Cell* 150(1): 165-178, 2012.
- Dong X, Lin D, Low C, Vucic EA, English JC, Yee J, Murray N, Lam W, Ling V and Lam S: Elevated expression of BIRC6 protein in non-small-cell lung cancers is associated with cancer recurrence and chemoresistance. *J Thorac oncol* 8(2): 161-170, 2013.
- Hynes RO: Integrins: versatility, modulation, and signaling in cell adhesion. *Cell* 69(1): 11-25, 1992.
- Holzmann B, Gossler U and Bittner M: alpha 4 integrins and tumor metastasis. *Curr Top Microbiol Immunol* 231: 125-141, 1998.
- Sawada K, Mitra AK, Radjabi AR, Bhaskar V, Kistner EO, Tretiakova M, Jagadeeswaran S, Montag A, Becker A, Kenny HA, Peter ME, Ramakrishnan V, Yamada SD and Lengyel E: Loss of E-cadherin promotes ovarian cancer metastasis via alpha 5-integrin, which is a therapeutic target. *Cancer Res* 68(7): 2329-2339, 2008.
- Takayama S, Ishii S, Ikeda T, Masamura S, Doi M and Kitajima M: The relationship between bone metastasis from human breast cancer and integrin alpha(v)beta3 expression. *Anticancer Res* 25(1a): 79-83, 2005.
- Wewer UM, Shaw LM, Albrechtsen R and Mercurio AM: The integrin alpha 6 beta 1 promotes the survival of metastatic human breast carcinoma cells in mice. *Am J Pathol* 151(5): 1191-1198, 1997.
- Shibue T and Weinberg RA: Integrin beta1-focal adhesion kinase signaling directs the proliferation of metastatic cancer cells disseminated in the lungs. *Proc Natl Acad Sci USA* 106(25): 10290-10295, 2009.
- Lu X, Lu D, Scully M and Kakkar V: The role of integrins in cancer and the development of anti-integrin therapeutic agents for cancer therapy. *Perspect Medicin Chem* 2: 57-73, 2008.
- Roman J, Ritzenthaler JD, Roser-Page S, Sun X and Han S: alpha5beta1-integrin expression is essential for tumor progression in experimental lung cancer. *Am J Respir Cell Mol Biol* 43(6): 684-691, 2010.
- Schaffner F, Ray AM and Dentenwill M: Integrin alpha5beta1, the Fibronectin Receptor, as a Pertinent Therapeutic Target in Solid Tumors. *Cancers* 5(1): 27-47, 2013.
- Schlaepfer DD, Mitra SK and Ilic D: Control of motile and invasive cell phenotypes by focal adhesion kinase. *Biochim Biophys Acta* 1692(2-3): 77-102, 2004.
- Xue G and Hemmings BA: PKB/Akt-dependent regulation of cell motility. *J Natl Cancer Inst* 105(6): 393-404, 2013.
- Sieg DJ, Hauck CR, Schlaepfer DD: Required role of focal adhesion kinase (FAK) for integrin-stimulated cell migration. *J Cell Sci* 112(Pt 16): 2677-2691, 1999.
- Spiering D and Hodgson L: Dynamics of the Rho-family small GTPases in actin regulation and motility. *Cell Adh Migr* 5(2): 170-180, 2011.
- O'Connor K and Chen M: Dynamic functions of RhoA in tumor cell migration and invasion. *Small GTPases* 4(3): 141-147, 2013.
- Parri M, Chiarugi P: Rac and Rho GTPases in cancer cell motility control. *Cell Commun Signal* 8: 23, 2010.
- Yamazaki D, Kurisu S and Takenawa T: Regulation of cancer cell motility through actin reorganization. *Cancer Sci* 96(7): 379-386, 2005.
- Nobes CD and Hall A: Rho, rac, and cdc42 GTPases regulate the assembly of multimolecular focal complexes associated with actin stress fibers, lamellipodia, and filopodia. *Cell* 81(1): 53-62, 1995.
- Burridge K and Chrzanowska-Wodnicka M: Focal adhesions, contractility, and signaling. *Annu Rev Cell Dev Biol* 12: 463-518, 1996.

Received July 17, 2014

Revised September 3, 2014

Accepted September 9, 2014